Sourcing and Characterising Cells: Constructing Foundations for Successful Tissue Engineering Strategies

UNIVERSITY OF LIVERPOOL

Thesis submitted in accordance with the requirements of The University of Liverpool for the degree of Doctor in Philosophy

By

Steven Gerard Thompson

October 2010

Steven Gerard Thompson
Sourcing and Characterising Cells: Constructing Foundations for Successful Tissue Engineering Strategies

Abstract

Tissue engineering and regenerative medicine strategies have the potential to treat numerous chronic degenerative conditions that are a significant burden on health services worldwide. At present, many groups are attempting to regenerate damaged organs and tissues using phenotypically diverse cell types with intricately designed biomaterials. Given the restricted proliferative capacity of terminally differentiated cells, stem and progenitor cells, capable of high levels of proliferation and guided lineage differentiation, have become of significant interest.

In order to assess populations heterogeneously from four diverse niches, adherent cells from human bone marrow, dental pulp, peripheral blood and umbilical cord were isolated using various isolation methods: Bone marrow-derived populations, termed Mesenchymal Stem Cells (MSCs), were purchased from Lonza; Peripheral blood cells were isolated using Histopaque and RosetteSep commercial isolation strategies; Umbilical cord-derived populations were isolated either by the plating of Wharton's jelly on tissue culture plastic or, alternatively, the mechanical and enzymatic digestion of the entire cord; finally, Dental pulp-derived populations were isolated via mechanical and enzymatic digestion of the pulp tissue.

Following isolation, adherent populations were maintained in basal culture conditions until required. Bone marrow-derived populations demonstrated an inability to maintain phenotype and proliferation following progressive *in vitro* culture, in particular following a sixth passage. This is most likely attributable to the rapid *in vitro* aging of the population, as demonstrated by the quickly reducing length of telomeres.

Peripheral blood cells isolated using both Histopaque and RosetteSep methods demonstrated little cross-phenotypic variance. Adherent cells displayed an ability to form CFU-Fs and CFU-GMs upon semi-solid culture and, furthermore, a capacity to undertake adipogenic, chondrogenic and osteogenic differentiation following appropriate stimulation. However, they could not be cultured beyond an initial passage, a severe limitation from a tissue engineering perspective.

Umbilical cord cells isolated by plating Wharton's jelly or whole cord digestion exhibited morphologically dissimilar but phenotypically similar profiles. However, whilst demonstrating an ability to undertake neuronal lineage differentiation, populations showed a similar proliferative and phenotypic demise following increasing *in vitro* culture as that of bone marrow-derived MSCs.

Dental pulp-derived populations demonstrated stable phenotype and proliferation rates regardless of *in vitro* culture time, likely due to the lengths of their telomeres being maintained or reducing at a rate similar to that of those observed *in vivo*. Cells cultured in semi-solid media demonstrated the ability to generate CFU-Fs and CFU-GMs, and therefore an ability to undertake diverse differentiation including adipogenic, chondrogenic, osteogenic, neuronal and hepatic lineages. However, given their heterogeneous expression of plasticity maintaining proteins Sox2 and Oct4, whilst furthermore expressing proteins associated with early embryonic development and those of the neuronal and retinal pigmental epithelium lineage, such differentiation may represent just a part of their lineage potential. Purification of populations based upon Hoechst33342 produced cells capable of forming microvascular-like structures following appropriate semi-solid culture. However, comparable to purification based upon surface antigens, the sorted population re-established a heterogeneous phenotype following allowance of proliferation, therefore suggesting either the incorporation of impurities when utilising such selection criteria or, alternatively, an innate ability of cells to re-establish the heterogeneous niche post-purification. Assuming the former, novel cell purification strategies based upon Stem Cell Conserved Domains (SCCD) were devised, potentially allowing for the homogeneous selection of stem and progenitor subsets.

In conclusion, whilst populations isolated from each niche demonstrated multilineage potential, the limitations of bone marrow-, peripheral blood- and umbilical cord-derived populations must be addressed if these cells are to be utilised clinically. However, the homogeneous selection of dental pulp subpopulations using SCCD purification strategies may provide a population on which to base future regenerative strategies.

Acknowledgements

There are many people that I would like to thank for their continued help and support during my PhD thesis, and, for those who I have not mentioned, I urge them to contemplate ways in which they could have been of more assistance. However, since I am unlikely to undertake another PhD in the future, it is likely that your boat has sailed with regards getting an acknowledgment. Nevertheless, to the successful helpers, I would like to extend my thanks, starting with my supervisors John Hunt and Nick Rhodes, who provided continued support, thought provoking ideas and practical help throughout the project. Other members of the STEPS project, which is greatly acknowledged for providing three years of funding, are also thanked.

I would also like to especially thank Jude Curran for here continued response to the persistent harassment for varying types of help. This is also applicable to Fan Rong Pu and Sandra Fawcett, who are greatly appreciated for their fantastic help with blood/cord work and SEM work respectively. The three aforementioned names are further thanked for their witty banter and maintained sarcasm throughout three years of tea breaks, for which Nick Bryan, Katie Nixon, Victoria Kearns, Sandra Portugal, Fiona Lewis and Kirstie Andrews must also be thanked. However, whilst in addition to providing help, support and biscuits during tea breaks, each of these people must be thanked for their additional input during my thesis: Nick Bryan for his continued help and support in both a scientific and alcohol-associated manner. He is especially thanked for his continued help with chemically-defined media-based investigations; Katie Nixon for her maintained ability to radically change topics of conversation; Victoria Kearns for her handy hints and tips with regards Microsoft in general and also tennis; Sandra Portugal for her maintained chirpiness, scientific help, port tips and Portuguese cream cakes; Fiona Lewis for her help/hindrance with Western blotting; and finally Kirstie Andrews, who was of great help in all neuronal related studies. Katie Smith, Joanne Convrey and Melba are also thanked for their input to the highly enjoyable tea breaks. A massive thank you to you all. I would further like to thank Dan Jones, who further substantiated my hypothesis that all Irishmen are horse racing fans. Further appreciation goes to Mick Loughran and Rui Chen for not getting mad at my continual raids into Jude's office for help. Finally at UK-TE I would like to thank Shirley Rawlings, firstly for her help in placing my many orders but more importantly her persistent friendliness and willingness to chat whilst I leaned against the radiator.

To the Physiology department and I would especially like to thank John Quinn for his continued help and advice. I would also like to thank Greg Jacobson, Kate Haddley, Stuart Gilles and Jill Bubb for their help with the SCCD project.

From ophthalmology I would like to thank Carl Sheridan and David Pattwell, without whom the RPE-associated studies would not have been possible. Carl Sheridan is also thanked along with Barry Campbell and Stuart Wood for their continued support and willingness to play football and go to the pub.

Finally, and most importantly however, I would like to thank my Mum, Dad and Vicky for their continued help and support during not only my PhD but also the preceding years. I would therefore like to dedicate this to them.

Contents

List of Figures

List of Tables

Abbreviations

AFP – Alpha Fetoprotein
AGM – Aorta-Gonad-Mesonephros
ALDH – Aldehyde Dehydrogenase
BFU-E – Burst Forming Unit-Erythroid
BFU-Meg – Burst Forming Unit-Megakaryocyte
CCSP – Clara cell marker
CD – Cluster of Differentiation
CFU-Bas – Colony Forming Unit-Basophile
CFU-E – Colony Forming Unit-Erythroid
CFU-Eo – Colony Forming Unit-Eosinophil
CFU-G – Colony Forming Unit-Granulocyte
CFU-GEMM – Colony Forming Unit-Granulocyte-Erythrocyte-Monocyte-Megakaryocyte
CFU-GM – Colony Forming Unit-Granulocyte-Monocyte
CFU-M – Colony Forming Unit-Monocyte
CFU-Mast – Colony Forming Unit-Mast Cell
CFU-Meg – Colony Forming Unit-Megakaryocyte
CHOP – C/EBP Homologous Protein
CLP – Common Lymphoid Progenitor
CMP – Common Myeloid Progenitor
CNC – Cranial Neural Crest
CNS – Central Nervous System
DAPI – 4', 6'-Diamidino-2-phenylindole
DMEM – Dulbecco's Modified Eagle's Medium
DNA – Deoxyribose Nucleic Acid
ECs – Endothelial Cells
EC Cell – Embryonal Carcinoma Cell
ECM – Extracellular Matrix
ECR – Evolutionary Conserved Region
EG Cell – Embryonic Germ Cell
ELISA – Enzyme-Linked Immunosorbent Assay
EPC – Endothelial Progenitor Cell
ES Cell – Embryonic Stem Cell
FCS – Fetal Calf Serum
GFP – Green Fluorescent Protein
GMP – Granulocyte/Macrophage progenitor
GVHD – Graft Versus Host Disease
HDAC – Histone Deacetylase
HSC - Hematopoietic Stem Cell
ICM – Inner Cell Mass
IPS – Induced Pluripotent Stem Cell
IVF – *In vitro* Fertilisation
LIF – Leukaemia Inhibitory Factor
LTC-IC – Long-term Culture Initiating Cell Assay
LB – Lysogeny Broth
MEP – Megakaryocyte/Erythrocyte Progenitor
MBT – Midblastula Transition
MESF – Molecules of Equivalent Soluble Fluorochrome

MHC – Major Histocompatibility Complex
MPC – Multipotent Progenitor Cell
MPP – Multipotent Progenitor
MSC – Mesenchymal Stem Cell
NGF – Neural Growth Factor
NGFR – Neural Growth Factor Receptor
NK – Natural Killer Cell
NOD-SCID – Non-Obese Diabetic-Severe Combined Immunodeficient Mouse
PBS – Phosphate Buffered Saline
PGC – Primordial Germ Cell
PNA – Poly Nucleic Acid
PNS – Peripheral Nervous System
PPAR – Peroxisome Proliferator Activated Receptor
RBC – Red Blood Cell
REST – RE-1 Silencing Transcription Factor
RNA – Ribose Nucleic Acid
RPE – Retinal Pigment Epithelial
RT-PCR – Reverse Transcription-Polymerase Chain Reaction
SA – Serum Albumin
SCCD – Stem Cell Conserved Domain
SCID – Severe Combined Immunodeficient Mouse
SCNT – Somatic Cell Nuclear Transfer
SEM – Scanning Electron Microscope
SP-C – Pro-surfactant protein C
SSEA – Stage-Specific Embryonic Antigen
SVP – Synaptic Vesicle Protein
TBR – T-box Brain Gene
TC – Tissue Culture
TRF – Telomere Restriction Fragment
VCAM – Vascular Cell adhesion Molecule
VPA – Valproic Acid
YFP - Yellow Fluorescent Protein

1. Introduction

1.1 Overview of Tissue Engineering

1.1.1 Fundamentals of Tissue Engineering

Neurodegenerative disorders, cardiovascular disease, musculoskeletal abnormalities, macular degeneration, diabetes and cancer are diseases typically caused by aging or trauma, which subsequently prevent cells from undertaking reparative maintenance. Obstruction of these pathways can result in cellular malfunction or cellular senescence, consequentially causing erroneous protein production or tissue necrosis respectively. These diseases place excessive burden upon health services worldwide. With operations a time consuming process and donated organs and tissues in significant shortage, treatment of an ever-ageing population is becoming problematic. Given these facts, cell and molecular biologists, biochemists, engineers, pharmacologists and physicians have undertaken collaboration in an attempt to devise tissue-engineering strategies capable of providing ready supplies of organs and tissues[1-28].

The concept of a tissue-engineered approach evolves from the ability of adult humans to undertake limited regeneration throughout their lifespan. For example, blood and skin are continually restored, and liver, bone, muscle, and blood vessels maintain a limited capacity for self-repair. However, it is important to emphasise that, whilst tissues are repaired following injury, the replacement tissue is often a non-functional scar tissue[29-31]. Tissue engineering thereby endeavours to induce regeneration in situations where naturally-occurring regeneration will no longer take place[3,32-35].

1.1.2 Strategic Approaches to Tissue Engineering

Approaches that attempt to invoke tissue regeneration have been devised along three strategies: (i) acellular matrices to invoke *in situ* tissue regeneration; (ii) implantation of primary isolated or cultured cells; (iii) implantation of tissues assembled *in vitro* via a combination of cells and scaffolds[36-38].

Acellular matrices, where unseeded polymers are implanted within a patient, are dependent on the natural ability of the body to undertake regenerative processes when exposed to precise temporal and spatial signals. Acellular tissue matrices are generally prepared via the removal of cellular components from tissues using mechanical and chemical manipulation, thereby producing collagen-rich matrices. These matrices undergo deliberate degradation upon implantation and are generally substituted with ECM proteins secreted by cells growing inwardly[4,39-42].

Autologous and allogeneic implantation of cells has thus far yielded promising yet inconclusive results. Clinical benefit has been observed following the intravenous (IV) administration of heterogeneous populations of mesenchymal stem cells (MSCs) in patients exhibiting a range of clinical abnormalities including osteogenesis imperfecta, myocardial infarction and acute graft-versus-host disease[43-50]. However, despite the encouraging results achieved, significant questions remain. Fundamentally we must consider methods of cell delivery, understand the intricate networks of adhesion molecules and chemokines and the guidance of cells to sites of injury, and finally the mechanisms that improve clinical prognosis[51]. Combining various cell types with biomaterials has the potential to overcome many of these problems, although such strategies possess a host of other problems. The engineering of semi-artificial and transplantable tissue requires research into the biocompatibility of materials seeded with various cell types. Furthermore, the issues of adhesion, nutrition, proliferation and differentiation *in vivo* must be rigorously studied. However, combining a given cell type with the correct biomaterial would undoubtedly give rise to numerous products with key applications in tissue engineering[52-57].

Undoubtedly each of these tissue-engineering strategies exhibits individual benefits relevant to multiple therapeutic applications. However, this thesis will largely focus upon cellular-mediated approaches to tissue engineering, for which reproducible isolation and comprehensive characterisation are required. Given that terminally-differentiated somatic cell types have severe proliferation and trans-differentiation limitations, stem cells have attracted considerable interest as a potential cell source for tissue-engineering strategies.

1.2 The Potential of Stem Cells for Tissue Engineering Strategies

1.2.1 The Stem Cell: Concepts of Plasticity

Stem cells are unspecialised precursors with a unique ability to self-renew whilst maintaining the capacity to differentiate along multiple lineages when exposed to appropriate cytokines and growth factors. The stem cell population self-maintains by, on average, each stem cell division generating one replacement stem cell (*i.e.* a clone) and one transit-amplifying cell (*i.e.* a lineage-committed cell). This is known as asymmetric division. Alternatively, consistency within the population can be achieved through symmetrical divisions, provided that each time a given stem cell generates two transit-amplifying cells, one other produces two daughter stem cells (*Figure 1.1*)[9,58-59].

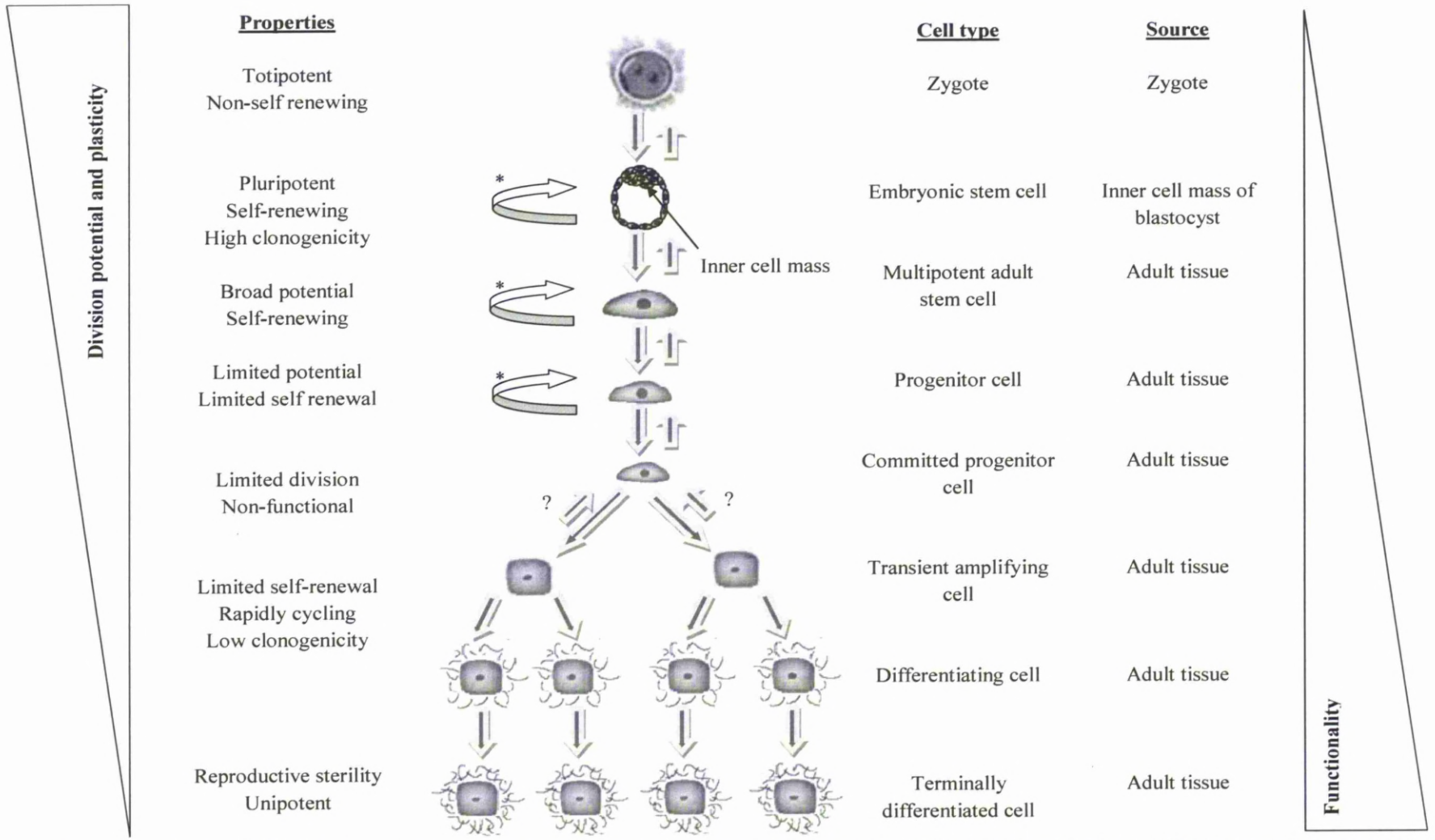

Figure 1.1 - **Hierarchal differentiation pathway. Plastic cells (totipotent, pluripotent, multipotent stem cells) generate progenitor and further restricted committed progenitor cells, which give rise to transit-amplifying cells exhibiting limited division potential and increased proliferation. Under appropriate conditions, progenitor cells can revert to a stem cell phenotype (multipotent cell). Terminal differentiation is generally associated with reproductive sterility and imminent apoptotic cell death.**

Plasticity implies the ability of a stem cell to differentiate along multiple lineages when exposed to defined environmental cues, although the degree of plasticity appears to vary between stem cell populations. Elementary developmental theories depict distinct lineages emerging from pluripotent cells throughout early embryogenesis, with progressively more restricted, less plastic cells generating specialised precursors that make up preparatory material for organs and tissues. It was therefore assumed that cells rigidly follow the theory of the central dogma, progressing in a unidirectional manner along defined differentiation pathways with an inability to modify fates[60-61]. Consequently the concept of plasticity was given solely to cells associated with early stages of development. However, numerous studies in recent years have challenged this pre-conception, suggesting that many tissue-specific stem cells in embryos and adults may in fact possess a plastic potential, allowing them to differentiate towards cell types of an unrelated lineage if transferred to an appropriate environment[62-83]. These alternative environments, many of which have been created *in vitro* through the utilisation of growth factors, reprogram the cell to generate daughter cells consistent with this new environment.

1.2.2 Identification of Underlying Mechanisms Governing Stem Cell Plasticity

Following the discovery of more plasticity than initially anticipated, exhaustive investigations attempting to understand pluripotency in stem cells at the molecular level have been pursued to elucidate their fundamental properties and processes of cellular reprogramming. It seems that plasticity is a property conveyed to cells during the early stages of embryogenesis, a cocktail of as yet unidentified factors present within the blastocyst pre-programming the genome to invoke a capacity for self-renewal and pluripotent differentiation. Validation of these factors have been demonstrated through several elaborate studies, initially when somatic cells were reprogrammed by transferring their nuclear contents into oocytes or by fusion with embryonic stem cells[84-89]. Identification of factors responsible for this transferral of pluripotency have been partially established through an investigation demonstrating nuclear reprogramming of permeabilised human cells using extracts from *Xenopus laevis* eggs and early embryos. Digitonin and non-digitonin permeabilised 293T kidney cells and primary isolated leukocytes have been cultured in the presence of *Xenopus* egg extracts. Permeabilised cells exhibited an upregulation of pluripotency-

associated genes, though surprisingly, non-permeabilised cells also demonstrated an upregulation, albeit at a reduced level. However, reprogrammed leukocytes had a limited lifespan and did not express surface antigens associated with pluripotent cells, suggesting that reprogramming was incomplete. Interestingly, the ability of egg extract to infer plasticity varied with different stages of *Xenopus* embryogenesis. Upregulation of pluripotency-associated genes was detected with extracts prepared from eggs and fertilised embryos at stage 4 (8 cell) and stage 5 (16 cell) but lost at blastula stage 9, thereby suggesting that reprogramming activity is lost at midblastula transition (MBT) and the initiation of zygotic transcription in *Xenopus* embryos. Furthermore, late blastula-stage extracts were not only inactive but also inhibited reprogramming. Immunodepletion screening of egg extracts identified the chromatin remodelling protein ATPase BRG1 as a key regulator inferring pluripotent competence in cells[90]. It is surmised that BRG1 works in alliance with other chromatin-remodelling ATPases, including ISWI-1[91], to achieve nuclear reprogramming. ISWI-I is a member of the ISWI remodelling complex, which is distinct from the SWI-SNF complex. ISWI-D is mandatory for the specific release of TATA binding factor from adult nuclei incubated with *Xenopus* oocyte extracts, which accompanies chromatin decondensation and protein exchange. It is therefore likely that ATPase-dependent remodelling occurs in conjunction with transcriptional regulators such as Oct4, Sox2 and Nanog to achieve pluripotency.

Recent identification of Oct4 transcriptional targets has revealed an interaction between Oct4, Sox2 and Nanog which provide a framework for core transcriptional circuitry that maintains pluripotency through a series of feedback and feedforward loops[92]. Sox2 seemingly represents the foundation of this regulatory pathway, synergistically functioning with Oct4 to activate Oct-Sox enhancers that in turn regulate the expression of Nanog, Oct4 and Sox2 itself[93]. Concomitant expression of these regulatory genes represents the apex of a hierarchical pathway of plasticity, seemingly regulating numerous pathways involved in the maintenance of plasticity[92,94-102] and multilineage differentiation. Predictably, null mutations of Sox2, Oct4 or Nanog result in early embryonic lethality due to an inability to maintain pluripotency and subsequent guided differentiation within cells[100,103-104].

Understanding pathways involved in maintaining plasticity is required if stem cells are to become therapeutically viable, allowing controlled differentiation towards desired lineages to address numerous debilitating illnesses. Thus far, embryonic stem (ES) cells have provided an ideal model for investigating such intricate networks, allowing rapid identification of pathways involved in maintaining and suppressing plasticity. However, whilst representing ideal candidates with respect to studying developmental pathways, their therapeutic value remains fundamentally questionable, although ongoing investigations utilising induced pluripotent stem (iPS) cell technologies are attempting to overcome such ethical and technical issues (see 1.3.3)

1.3 Embryonic Stem Cells

1.3.1 The History of Embryonic Stem Cell Research

ES cell research and its accompanying ethical and legal dilemmas are vehemently debated amongst the media, general public, politicians and academics of numerous disciplines. Whilst this is predictable considering their potential therapeutic benefits but difficult moral issues, it is perhaps surprising that the vast majority of discussions perceive ES cells as an innovatively discovered cell source, whilst in actual fact recent developments are based on previous research efforts. Indeed, research on teratocarcinomas and embryonic stem cells undertaken throughout the previous half century have passed through several distinct phases (*Figure 1.2*), inevitably influenced by available technologies, contemporary scientific interest and social demands. Comparatively reticent interest during the 1950s and 1960s increased significantly in the 1970s, corresponding to curiosity in mammalian developmental biology and cell differentiation. The identification of mouse ES cells in the early 1980s prompted supposition for their utilisation as a vehicle for introducing targeted genetic modifications into the germ line, thereby highlighting embryonic stem cells as a potential tool for gene function analysis. Ultimately the isolation of human ES cells and their potential application in regenerative medicine cumulatively resulted in both the scientific community and general public envisaging ideal regeneration strategies, effectively supplying off-the shelf replacements for irreparable organs and tissues[105-106].

Although investigations probing mouse and human ES cells proceeded along corresponding experimental pathways, advances using mouse cells generally superseded their human counterparts by approximately a decade. In recent years, however, human and mouse models have been used simultaneously in comparative experiments, though it is apparent that research undertaking human ES cell experiments profited substantially from the underpinning advances achieved using mouse cells. Furthermore, concurrent experiments using mouse and human cells quickly demonstrated that, despite numerous similarities, results obtained with mouse cells are not necessarily directly applicable to human cells[105].

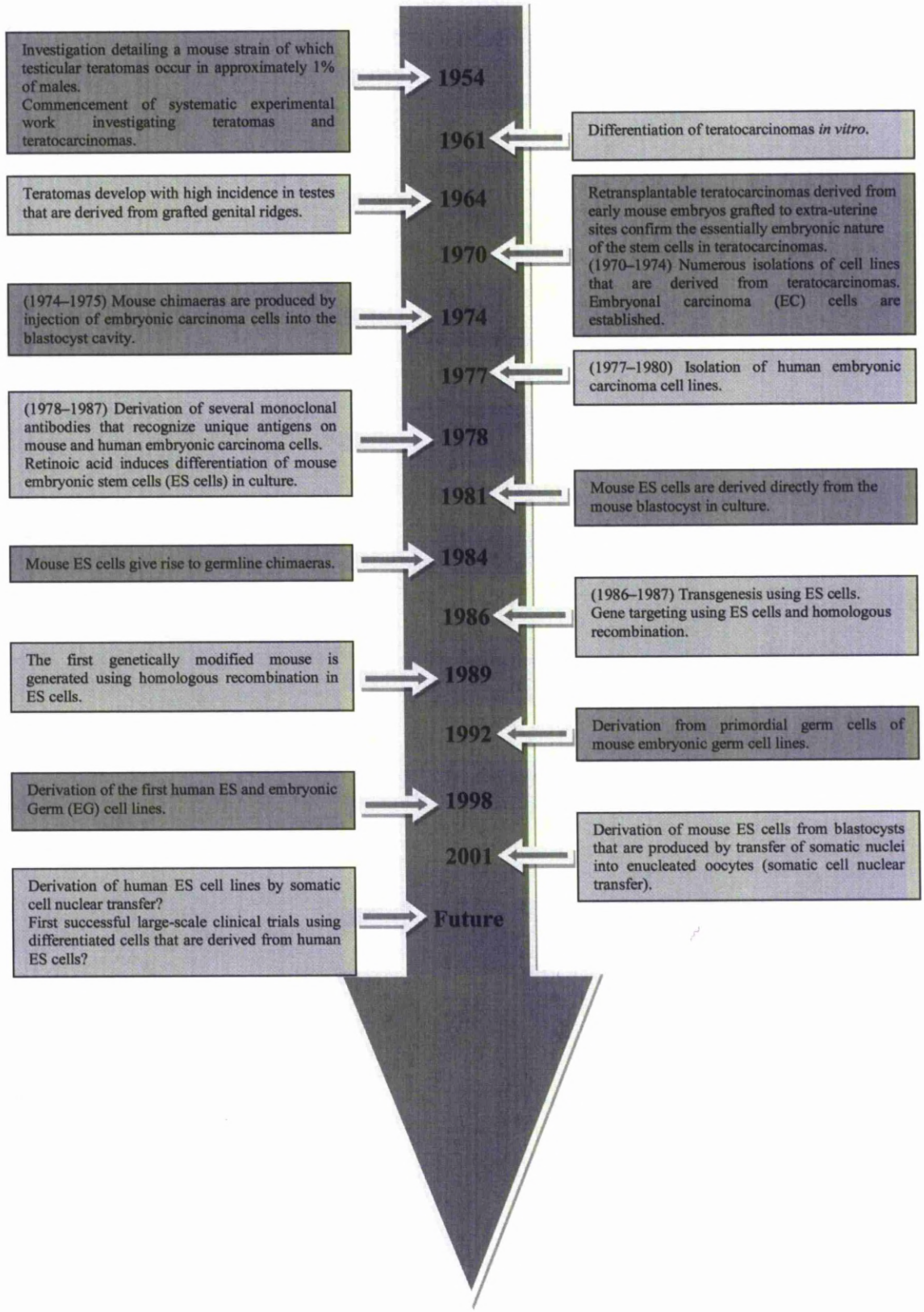

Figure 1.2 **- ES cell timeline - The history of embryonic stem cell research[105].**

1.3.2 The Embryonic Stem Cell Niche

ES cells are derived from the inner cell mass (ICM) of the early embryo (blastocyst) and demonstrate a pluripotent capacity allowing them to differentiate into any cell type present within the three germ layers (endoderm, mesoderm and ectoderm) in addition to germ cells[107-112]. However, ES cells cannot differentiate to form extraembryonic tissues and therefore are considered pluripotent as opposed to totipotent.

The potential plasticity of neonatal-derived stem cells can largely be hypothesised by considering the early stages of embryogenesis. Shortly after fertilisation, the haploid nuclei of the oocyte and sperm amalgamate to generate a single nucleus containing the diploid number of chromosomes. Following zygotic division, the resulting progeny undertake several rounds of further division to form a compact ball of cells called the morula. Each of the 32-128 cells in the morula is totipotent and can therefore generate all cell types of the embryo in addition to all extraembryonic tissues necessary for implantation in the uterine wall. This remarkable totipotent ability allows the sacrifice of one or more cells of the morula without impairment, a phenomenon on which the foundations of genetic testing are based. Preimplantation genetic diagnosis, used in fertilisation treatments, is a technique in which a totipotent morula cell is drawn into a micropipette and subjected to a sensitive PCR assay using cDNA primers, and is now available for an increasing number of genetic disorders in order to screen for potential disease-associated mutations. This technology allows physicians to inform parents of the health of the embryo prior to implantation of the still-viable morula into the uterus.

Whilst travelling along the oviduct, cells of the morula continue to proliferate to form a hollow sphere called the blastocyst (or blastula). During concluding days in the oviduct and primary days in the uterus, a small number of cells delaminate from the surface layer of the blastula to generate an ICM within the cavity (*Figure 1.3*). This cluster of cells represents the source of ES cells which can be dissociated from the ICM and cultured *in vitro* using techniques first developed more than 20 years ago for the manipulation of mouse embryos. However, it is imperative to emphasise that the ICM forms prior to implantation, with blastocysts generated *in vitro*

containing an ICM despite the fact that the embryo was created and maintained in a test tube[113].

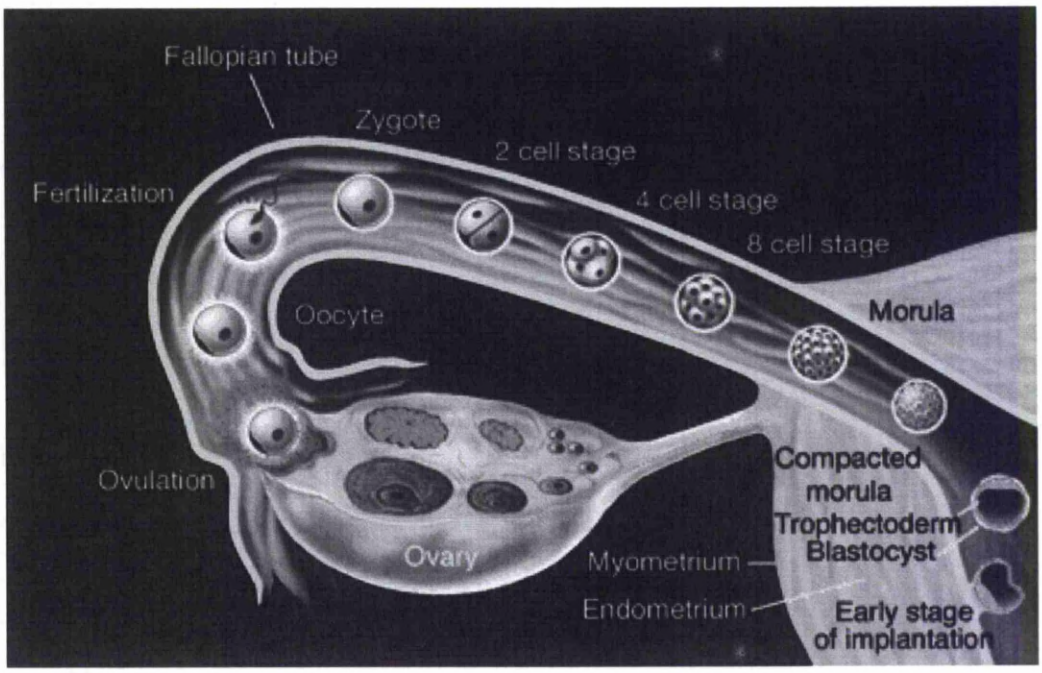

***Figure 1.3* - From zygote to blastula: early stages of human development[113].**

The time from fertilisation to implantation in the uterine wall is approximately 14 days in humans. Shortly after implantation, the blastocyst invaginates, initiating a crucial succession of cell motilities known as gastrulation. This key event results in the formation of the three germ layers of the developing embryo: ectoderm, endoderm, and mesoderm. Formation of the three germ layers begins the rudimentary outline of the human body as numerous cellular fates are determined: the endoderm gives rise to vasculature and blood-forming organs; the mesoderm produces muscle; and the ectoderm generates the skin and nervous system (*Figure 1.4, Figure 1.5*).

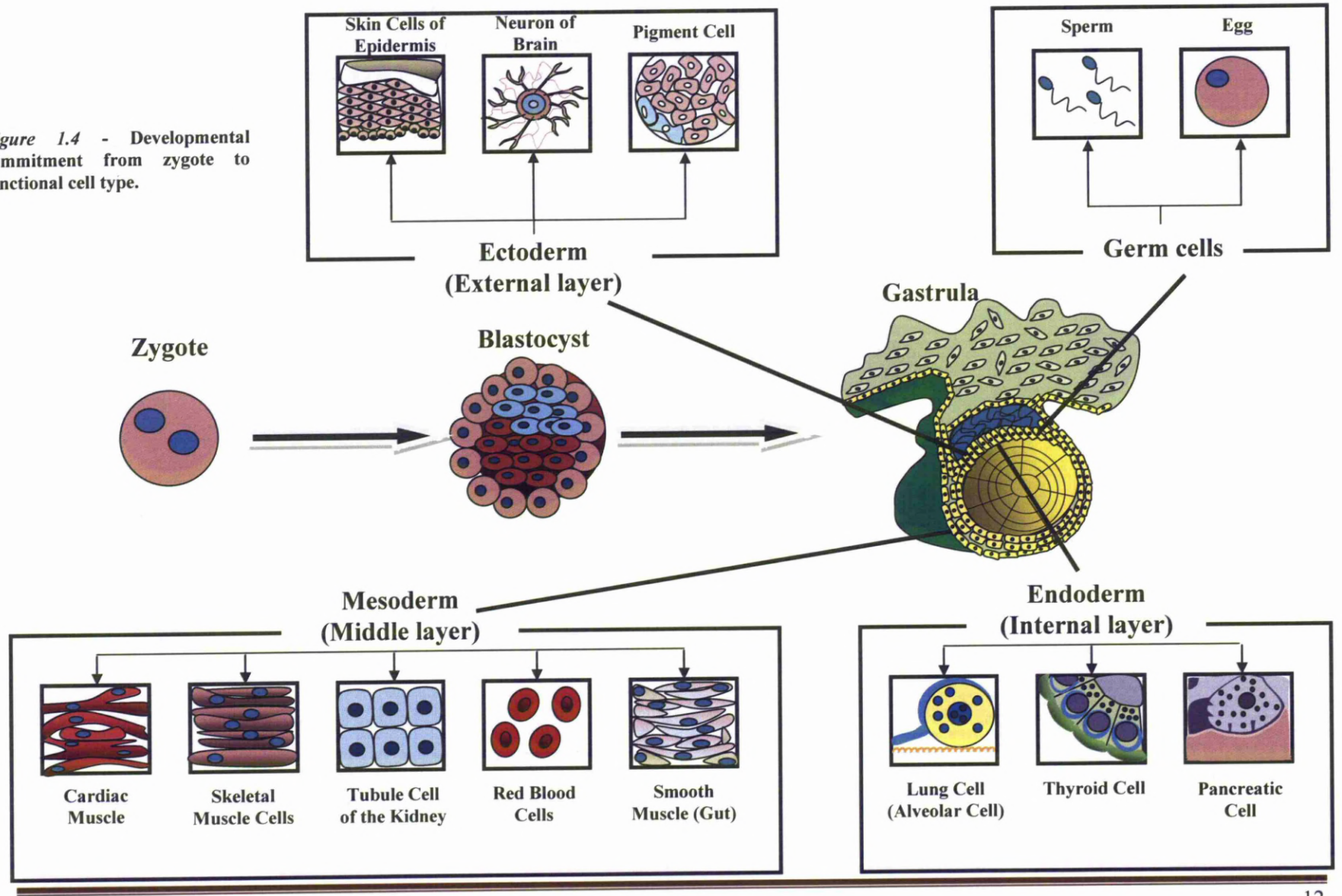

Figure 1.4 - **Developmental commitment from zygote to functional cell type.**

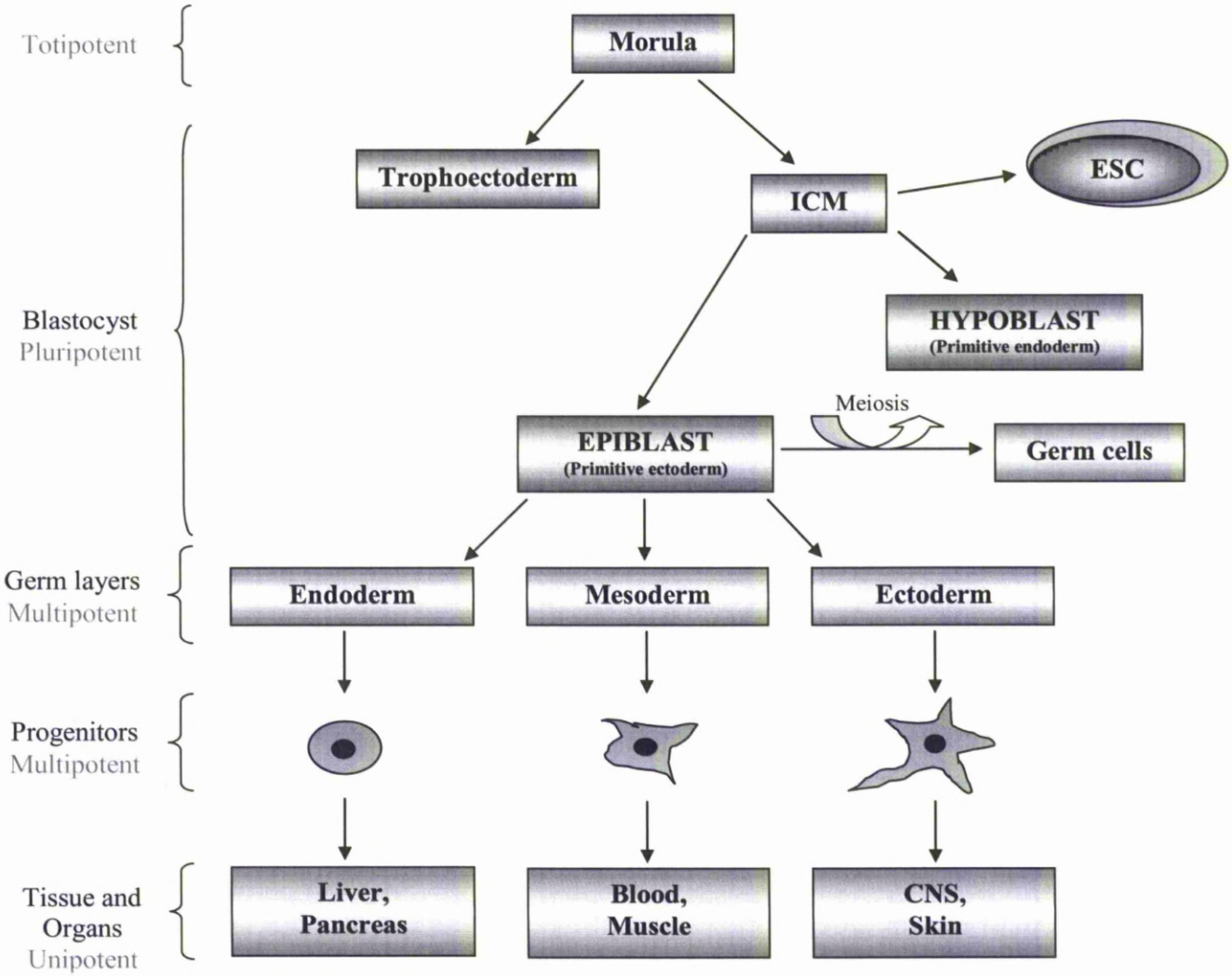

Figure 1.5 **- From totipotent to unipotent; Progressive cellular commitment of trophic germ layers[114].**

1.3.3 Isolation of Embryonic Stem Cells

The derivation of the first human ES cell lines and human embryonic germ (EG) cell lines lagged significantly behind their murine counterparts. Considering that isolation techniques were comparable and the necessary markers to identify human ES and EC cells were readily available, it is probable that such delays were attributable to difficulties involved in obtaining suitable human embryonic material and the understandable reluctance of many investigators to work in a field fraught with potential legal problems, combined with political and moral dilemmas[113,115-126]. However, despite such obstacles, detailed reports of isolated human ES and EG cells were published in 1998. The first publication described the successful isolation of ES cell lines from human blastocysts[108]. In this study, fresh or frozen cleavage stage

human embryos, generated by *in vitro* fertilisation (IVF) for clinical purposes, were obtained. Embryos were cultured to the blastocyst stage and the trophoectoderm removed by immunosurgery[127] using a rabbit anti-human spleen cell antiserum followed by exposure to guinea pig complement. Fourteen intact inner cell masses were isolated from lysed trophoectoderm and plated on mouse embryonic fibroblasts. Following culture, a central mass of cells was removed from epithelial outgrowths and, following gentle dissociation with a micropipette, replated on mouse embryonic fibroblasts. Following further culture, colonies with a morphology resembling ES cells were selected and expanded. Individual cells were selected by micropipette, establishing the isolation of five ES cell lines originating from five separate embryos, and cultured on mouse embryonic fibroblasts. The resulting cells demonstrated a high ratio of nucleus to cytoplasm, prominent nucleoli, and colony morphology similar to that observed previously with rhesus monkey ES cells. Three cell lines had a normal XY karyotype, two displayed a normal XX karyotype, and four of the cell lines were successfully cryopreserved and thawed following 5 to 6 months of continuous undifferentiated proliferation. The other cell line was reported to have retained a normal XX karyotype following 6 months of culture. However, whilst this study failed to identify any karyotypic abnormalities following prolonged *in vitro* culture, studies examining mouse ES cells have reported karyotype modifications[128-129] which may be translatable to human ES cells. Thus, before human ES cells are considered for therapeutic application, investigations must comprehensively demonstrate that such abnormalities do not arise.

Cells isolated from human blastocysts expressed high levels of telomerase activity. Telomerase is a ribonucleoprotein responsible for the addition of telomere repeats to ends of chromosomes, a mechanism responsible for the maintenance of replicative life-span and hypothesised to regulate aging in all species[130]. Furthermore, the blastocyst-derived ES cells expressed cell surface markers associated with undifferentiated non-human primate ES and human EC cells, including SSEA3, SSEA4, Tra-1-60, Tra-1-81 and alkaline phosphatase. The pluripotency regulator Oct4 was highly expressed in undifferentiated ES cells, and thus unsurprisingly human ES cell lines demonstrated the potential to form derivatives of all three embryonic germ layers, with all five aforementioned cell lines producing teratomas following injection into severe combined immunodeficient (SCID) beige mice. Each

teratoma contained epithelium (endoderm); cartilage, bone, smooth muscle and skeletal muscle (mesoderm); and neural epithelium, embryonic ganglia and skeletal squamous epithelium (ectoderm). *In vitro*, the ES cells differentiated when cultured in the absence of a mouse embryonic feeder layer, both in the presence and absence of human leukaemia inhibitory factor (LIF). Additionally, when grown to confluence and allowed to form multiple layers, ES cells spontaneously differentiated despite the presence of the feeder cells[108].

Concurrent with the isolation of ES cells from the human blastocyst, in 1998 Shamblott *et al.* detailed the isolation of EG cells from primordial germ cells (PGCs) via the mechanical and enzymatic digestion of gonadal ridges and mesenteries from 5 to 9 week post-fertilisation human embryos. Following isolation and culture on mouse embryonic fibroblasts, human EG cells demonstrated many of the features observed with ES cells including high levels of alkaline phosphatase and a pluripotent capacity for differentiation[131]. However, whilst EG cells again demonstrated potential clinical value, they are plagued with the same ethical and technical dilemmas tarnishing ES cell research.

Whilst ES and EG cells derived from both the blastocyst and fetal gondal tissues respectively demonstrate differentiation capacities with enormous clinical promise, a major drawback of using such cells is the issue of histocompatibility, a principle lying at the heart of many failed clinical attempts. Somatic cell nuclear transfer (SCNT) techniques have attempted to overcome such problems, with the underlying principles extrapolating from studies demonstrating that in amphibians, nuclei transferred from human keratinocytes established in culture support development to the juvenile tadpole stage[132-133]. However, it is important to stress that whilst this re-programming involves differentiation of cells into complex tissues and organs, no development to the adult stage was reported, leaving open to question whether complete re-programming of somatic cell nuclei was possible. Nevertheless, further investigations demonstrated the birth of live lambs following nuclear transfer from cultured ES cells, although it was required to induce cellular quiescence within the donor cells, essentially inducing the cell to exit the growth phase, a period which causes modifications to chromatin structure that facilitate re-programming of gene expression. This breakthrough was followed by the demonstration that cells derived

from fetal or adult-derived tissue were also capable of generating full-term lambs when induced to exit the growth cycle and enter the G_0 phase of the cell cycle (*Figure 1.6*) prior to nuclear transfer.

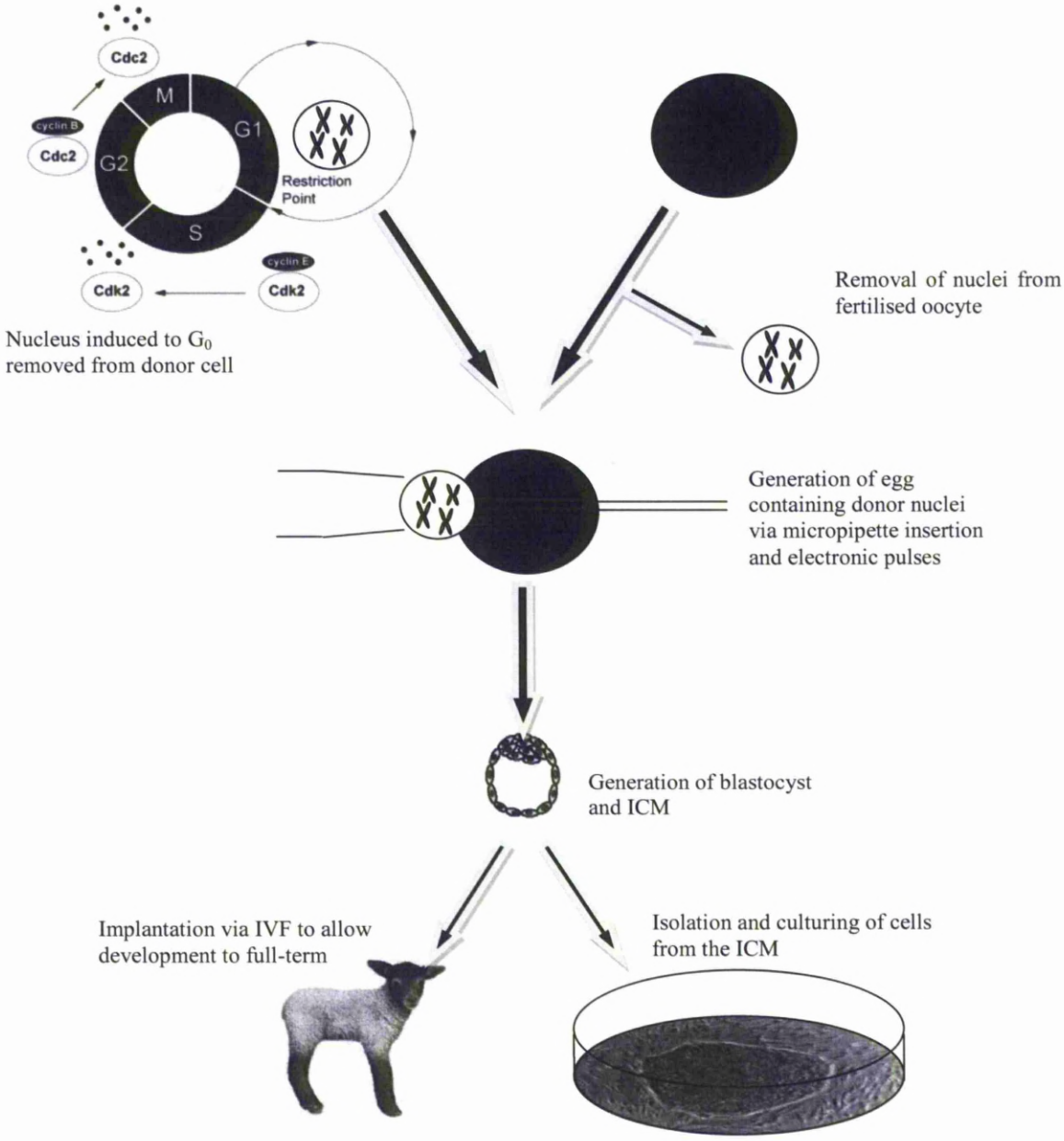

***Figure 1.6* - Diagrammatic representation of SCNT.**

Three populations of cells were synthesised for the experiment: those derived from: (i) a day-9 embryo; (ii) a day 26 fetus; and (iii) mammary gland of a 6 year old ewe in the last trimester of pregnancy. Whilst ultrasound scanning detected 21 single fetuses 50-60 days post oestrus, 62% of the fetuses aborted, a significantly greater number than the 6% that had been predicted following results obtained from natural mating studies[134]. Following approximately 110 days of pregnancy, 4 fetuses were dead, all from embryo-derived cells, with post-mortems indicating liver failure as the cause of two of the abortions, although no reason could be attributed to the remaining two. Following full-term, eight ewes gave birth to live lambs representing all three cell cloned populations. One weak lamb, derived from fetal fibroblasts, died shortly after birth, although a post-mortem failed to identify any abnormality or infection. However, at 12.5%, perinatal loss was not dissimilar to that occurring in a large study of commercial sheep, when 8% of lambs died within 24 hours of birth[135]. In all cases lambs exhibited morphological characteristics attributable to the breed used to derive the nucleus donors and not that of the oocyte donor. Furthermore microsatellite analysis confirmed that each lamb was derived from the cell population used as the nuclear donor. Thus the lamb born from the somatic-derived nucleus demonstrated that terminally differentiated cells can be reprogrammed to generate all three germ layers, subsequently leading to much controversial interest[136].

Understandably progression towards human based SCNT was undertaken, and in 2001 Cibelli *et al.* published findings detailing the first transfer of a human somatic cell and subsequent progression to pronuclear and early embryonic development. However, claims of early embryonic growth following SCNT seem premature given that the most advanced embryo reached only the 6-cell stage. Moreover, such was the consternation generated by these preliminary data that three members of the editorial board of the publishing journal felt the need to resign[137]. Thus, whilst SCNT may in future lead to promising regenerative technologies via the generation of autologous organs and tissues, at present methods for acquiring them are primitive and raise many ethical questions. Furthermore almost all previously cloned animals exhibit one or more abnormalities[138-139]. Unsurprisingly therefore human reproductive cloning, in which embryos generated by SCNT are allowed to develop to full term, is illegal in most countries.

Fllowing results obtained using SCNT techniques, investigators attempted to re-induce such plasticity in a synthetic manner, essentially recreating the genetic reprogramming conditions found within the developing egg. An elegant study hypothesised that enforced expression of a limited number of genes associated with maintenance of plasticity may allow direct reprogramming of somatic cells[84]. To evaluate this hypothesis, investigators introduced a mini-library of 24 candidate reprogramming factors into mouse embryonic fibroblasts containing a fusion of the β-galactosidase and neomycin-resistance genes expressed from the Fbx15 locus, which is expressed in mouse ES cells and early embryos, although it is non-essential for the maintenance of plasticity. Fundamental principles of this system encompass the ability of the activated Fbx15 gene to generate resistance to the antibiotic G418. Mouse embryonic fibroblasts infected with all 24 candidate genes, cultured on feeder cells in G418 containing-ES cell media, generated drug resistant colonies with a proportion exhibiting an ES-like morphology, including a round shape, large nucleoli, and negligible cytoplasm. Following an intricate elimination process, the transcription factors Oct4, Sox2, Klf4 and c-Myc were acknowledged as capable of inducing pluripotency, though curiously Nanog was evidently dispensable.

However, despite reports detailing similarities between the iPS cells and primary isolated murine ES cells, key differences were noted, including the inability of iPS cells to achieve germline transmission in blastocyst complementation assays. Furthermore, iPS cells exhibited a gene expression profile similar but not identical to that of murine ES cells. Subsequently, several groups have attempted to progress direct reprogramming techniques with a view to generating cells identical to primary isolated ES cells from a given species. Interestingly, direct reprogramming was achieved using the same quartet of factors in rhesus macaque and human cells[140-141], indicating that fundamental transcriptional machinery governing plasticity is conserved across species (*Table 1.1*). Further investigations have demonstrated a redundancy for c-Myc during reprogramming[142-143], a result of significant clinical benefit considering that c-Myc reactivation can predispose cells to malignant transformation of iPS derivatives[144].

Factor combination	Overview of achievements
Mouse	
KLF4, c-Myc, Oct4, Sox2	Initial report generating iPS cells from mouse embryonic and adult fibroblasts. IPS cells exhibited morphological and growth characteristics associated with ES cells, furthermore expressing ES associated markers. Subcutaneous transplantation into nude mice resulted in tumour formation containing tissues composing all three germ layers. Following injection into blastocysts, iPS cells contributed towards mouse embryonic development. No germline transmission was achieved in chimeric mice[84].
KLF4, c-Myc, Oct4, Sox2	Following iPS induction and Nanog-based purification, germline competent cells exhibiting increased ES-cell-like gene expression and DNA methylation patterns compared with Fbx15 iPS cells were obtained. The four transgenes were strongly silenced in Nanog iPS cells. Adult chimeras were obtained from several Nanog iPS cell clones, with one clone transmitting through the germline to the next generation. Approximately 20% of the offspring developed tumours attributable to the reactivation of the c–Myc transgene[141].
KLF4, Oct4, Sox2	Generation of murine and human iPS cells in the absence of the c-Myc retrovirus. Generated from adult dermal fibroblasts, iPS cells exhibited many ES cell characteristics. Mice derived from generated iPS cells did not develop tumours[145].
KLF4, c-Myc, Oct4, Sox2	Synthesis of mouse iPS cells exclusive of viral vectors. Repeated transfection of two expression plasmids, one containing Oct4, Sox2 and KLF4 cDNAs, the other incorporating c-Myc cDNA, into mouse embryonic fibroblasts resulted in iPS cells without evidence of plasmid integration[146].
KLF4, c-Myc, Oct4, Sox2	Reprogramming of mouse fibroblasts and liver cells using a non-integrating adenovirus transiently expressing Oct4, Sox2, KLF4, and c-Myc. Adenoviral iPS cells exhibited DNA methylation patterns associated with reprogrammed cells, expressed endogenous pluripotency genes, formed teratomas, and contributed to multiple tissues, including the germline, in chimeric mice[147].
KLF4, Oct4, Sox2	Reprogramming efficiency increased via the utilisation of methyltransferase and Histone deacetylase (HDAC) inhibitors. In particular, valproic acid (VPA), an HDAC inhibitor, improved reprogramming efficiency more than 100 fold without the introduction of the oncogene c-Myc[148].
Oct4	Reprogramming of murine adult neuronal stem cells with Oct4 (one factor iPS) generated cells resembling ES cells *in vitro* and vivo, efficiently differentiating into neurons, cardiomyocytes, and germ cells *in vitro*, whilst capable of teratoma development and germ line transmission *in vivo*[149].
Rhesus macaque	
KLF4, c-Myc, Oct4, Sox2	Generation of iPS cells via retrovirus-mediated introduction of specified transcription factors[142].
Human	
KLF4, c-Myc, Oct4, Sox2 hTERT, SV40 large T	Derivation of iPS cells from fetal, neonatal and adult human primary cells, including dermal fibroblasts. IPS cells resembled ES cells with regards morphology and gene expression and in

	their ability to generate teratomas within immune-deficient mice[150].
Oct4, Sox2, Nanog, Lin28	Reprogramming of human somatic cells generated pluripotent human cells exhibiting a normal karyotype, expressing telomerase and ES cell-associated surface markers and genes, and maintaining a developmental capacity capable of generating advanced derivatives of all three primary germ layers[143].
KLF4, c-Myc, Oct4, Sox2	iPS cells generated from human adult dermal fibroblasts exhibited similar morphological, proliferative, phenotypic, gene expression and epigenetic parameters as human ES cells, and could furthermore differentiate into cell types of the three germ layers *in vitro* and in teratomas[151].
KLF4, Oct4, Sox2	See murine desciption[145].
Oct4, Sox2	See murine desciption[148].

Table 1.1 **- Investigations detailing reprogramming of cells from numerous species using combinatorial arrays of transcription factors[144].**

Whilst the ability to reprogramme cells has generated much excitement with regards potential clinical and technical outcomes, much concern has been voiced with regards the oncogenicity of factors utilised in reprogramming and the potential for insertional mutagenesis consequential to integrating retroviral or lentiviral vectors. Primary reports detailing generation of germline competent iPS cells further noted that approximately 20% of chimeric mice succumbed to tumours that were attributable to the reactivation of the c-Myc proviral transgene that had spontaneously integrated into the host genome[141]. Whilst many groups have achieved successful reprogramming in the absence of c-Myc, the percentage of cells undertaking an iPS cell phenotype was greatly reduced in comparison with reprogramming in the presence of c-Myc. Thus, whilst c-Myc does not appear to be critical to the reprogramming of cells, results would suggest that c-Myc instead acts as a reprogramming catalyst, increasing the speed of the stochastic events reinstating pluripotency. Given the low reprogramming efficiency in the absence of c-Myc and the residual risk inherent to integrating gene transfer vectors, alternative approaches to reprogramming have been undertaken, including the use of small molecule chemicals in conjunction with genetic factors[148], the use of adult stem cells as a starting population for reprogramming and non-integrating gene transfer systems to deliver required reprogramming genes[146]. Should these alternative approaches prove a stable and efficient method of reprogramming following intensive studies, a clinical use for iPS cells must surely await.

1.4 Human Adult Stem Cells

1.4.1 Human Adult Stem Cell Niches

Whilst developmentally primitive cells such as ES and EG cells have demonstrated impressive capacities for lineage induced differentiation, ethical and technical issues have and will continue to inhibit clinical advances. It is therefore hoped that understandings of plasticity and mechanisms of differentiation gained via the study of these controversial cells can accelerate research concerning cells derived from adult tissues. Throughout recent years numerous publications have challenged the dogma that organ specific, somatic stem cells do not integrate into unrelated organs and consequently adopt phenotypic or functional characteristics[73,78,152-163]. This ability to undertake transdifferentiation could yield immense promise for clinical applications incorporating adipose[164], bone[165], cartilage[166], neural[167], tooth[168] and numerous other regenerative approaches. Thus cells isolated from numerous adult tissues (*Figure 1.7*) are currently being assessed for their ability to undertake such multilineage differentiation.

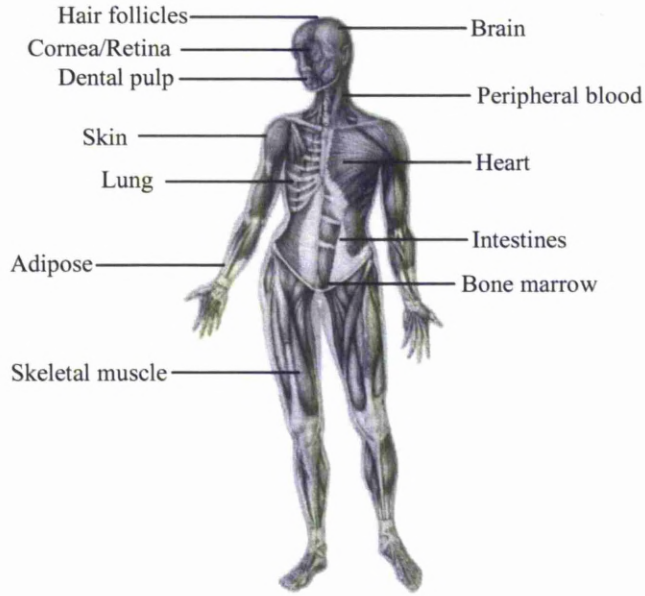

***Figure 1.7* - Regions of known stem cell residence facilitating potential isolation.**

1.4.2 Hematopoietic Stem Cells

Hematopoietic stem cells (HSCs) are a well-characterised population of self-renewing cells that produce progenitors capable of differentiating into every type of mature blood cell in a comprehensively defined hierarchy (*Figure 1.8*). Developmentally, HSCs are derived from the mesoderm, with morphological studies hypothesising the hemangioblast as the common mesodermal precursor for both the endothelial and hematopoietic lineages. In non-mammalian vertebrate embryos, several distinct tissues independently specify hematopoietic fate, for example the yolk sac generates a transient ephemeral embryonic hematopoietic system, whilst the region of the dorsal aorta generates the adult hematopoietic system[169-171]. Within the mammalian embryo, original theories depicted adult HSCs acquiring their phenotypic fate within the blood islands of the yolk sac during midgestational stages and subsequently migrating and colonising the fetal liver and progressively the adult bone marrow, their eventual niche of residence[172]. However, recent investigations have suggested that the aorta-gonad-mesonephros (AGM) regions, and more specifically the midgestation dorsal aorta, as the initial area in which adult-repopulating HSCs are generated[173-175]. However, like many areas of developmental biology, alternative theories appear plausible and consequently studies investigating the origin of adult HSCs in mammals are continually being undertaken. Furthermore, several recent studies concentrating on the mouse embryo have implicated numerous other tissues as reservoirs for, and perhaps even producers of, adult HSCs[176]. Unfortunately however, due to the *in utero* development of mammalian embryos and subsequent lack of optimal assay systems, identification and characterisation of human HSCs and procuring lineage mapping has proved somewhat difficult.

In vitro assays investigating both murine and human hematopoiesis are sufficient to demonstrate clonal myelo-erythroid, B-, NK- (Natural Killer) and dendritic cell but not T cell, proliferation and differentiation. However, whilst competitive *in vivo* repopulating studies in mice have demonstrated a sustained self-renewal and multipotent differentiation capacity of murine HSCs, in addition to T cell development from HSCs and committed progenitors, such assays cannot be performed in humans due to obvious ethical considerations. Thus throughout previous years studies have attempted to generate surrogate assays. Long-term

culture initiating cell assays (LTC-IC) are useful for the identification of primitive or primarily quiescent progenitors *in vitro*, demonstrating a capacity for self renewal or multilineage differentiation. However, to investigate human HSCs *in vivo* two essential prerequisites need to be met: Primarily the host should not eliminate the xenografts via an immune response, and secondly provide a permissive microenvironment for engraftment and multilineage differentiation of donor cells. Spontaneously occurring immunodeficient mouse strains partially meet these criteria and have been manipulated in order to enhance their model function, generating mouse models such as NOD-SCID (NonObese Diabetic Severe Combined Immunodeficient), β2 microglobulin knockout, NOD-RAG1 knockout, NOD/SCID/γc triple-mutant, and RAG2/common cytokine receptor γ chain double mutant. In contrast to murine xenotransplantation models, a large animal transplantation allowing the introduction of human HSCs intraperitoneally into unconditioned, early gestational sheep fetuses can be undertaken. In this model low numbers of selected progenitors can engraft, allowing myelo-erythroid as well as T and B lymphoid numbers to be monitored over several years[177-178]. Thus through numerous replicate models understanding of hematopoiesis has steadily progressed, with results from respective studies enhancing perception of hierarchal hematopoietic pathways. Current theories depict the HSC residing as a pluripotent stem cell, giving rise to: myeloid stem cells capable of generating erythrocytes, platelets, neutrophils, monocytes and subsequently macrophages, eosinophils, basophils, and mast cells; B stem cells differentiating to form B cells and subsequently plasma cells; and T stem cells committed towards the T cell lineage (*Figure 1.8*)[179]. In addition to B- and T-lymphoid stem cells, an additional myeloid precursor cell (not shown in *Figure 1.8*) generates NK cells. Furthermore, recent studies have suggested that both lymphoid and myeloid precursors are implicated in the generation of dendritic cells *in vivo*[180-182]. Perhaps most striking with regards to this current model of hematopoiesis is the association of HSCs with pluripotency. Whilst demonstrating an ability to differentiate towards all blood lineages, such abilities do not strictly fulfil the terminology of pluripotency. However, recent investigations examining HSC plasticity have reported expression of pluripotent-associated markers[183] and non-blood related differentiation, thereby indicating a potential pluripotent aspect[184-186].

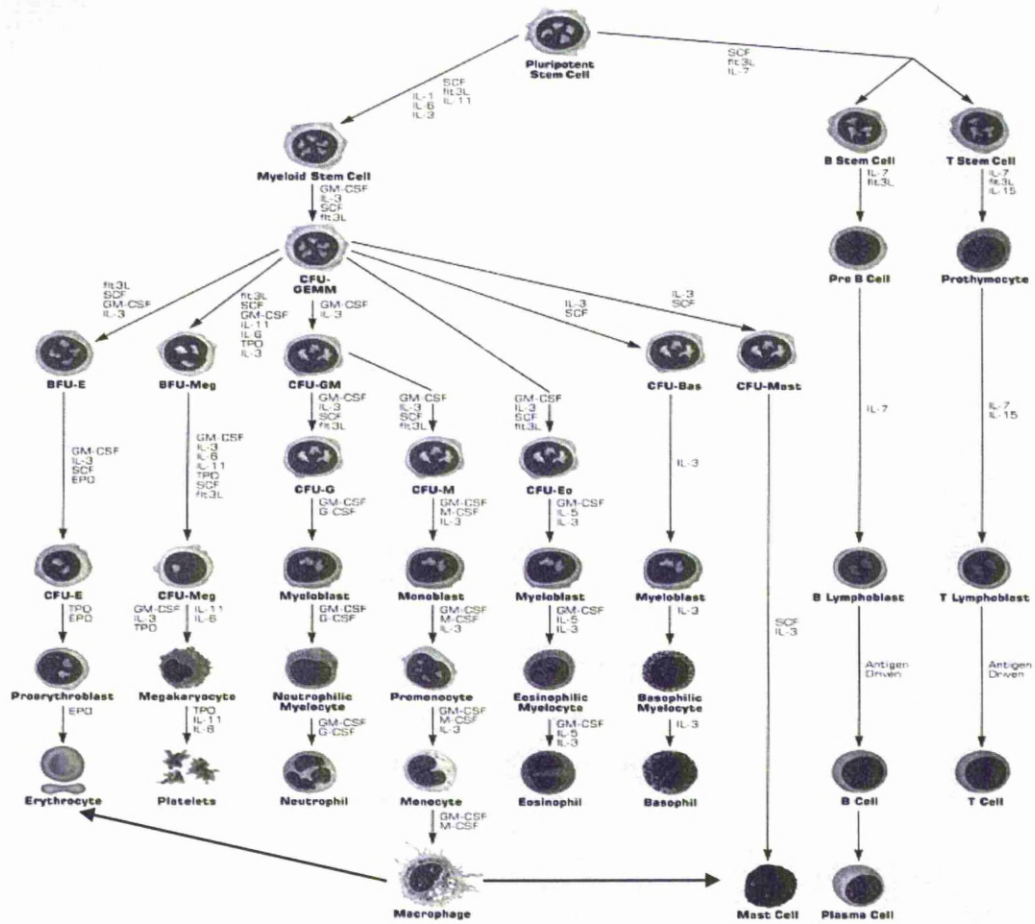

Figure 1.8 - **Differentiation cascade of HSCs. NK lineage pathway is not shown[179]. CFU-GEMM – Colony Forming Unit-Granulocyte-Erythrocyte-Monocyte-Megakaryocyte; BFU-E – Burst Forming Unit-Erythroid; CFU-E – Colony Forming Unit-Erythroid ; BFU-Meg – Burst Forming Unit-Megakaryocyte; CFU-Meg – Colony Forming Unit-Megakaryocyte; CFU-GM – Colony Forming Unit-Granulocyte-Monocyte; CFU-G – Colony Forming Unit-Granulocyte; CFU-M – Colony Forming Unit-Monocyte; CFU-Eo – Colony Forming Unit-Eosinophil; CFU-Bas – Colony Forming Unit - Basophile; CFU-Mast – Colony Forming Unit-Mast Cell.**

Given their blood regenerative capacity and potential further lineage commitment, the isolation of HSCs for therapeutic application could obviously yield immense therapeutic results. In addition to bone marrow, HSCs have been found in numerous other adult tissues including peripheral[187] and umbilical cord blood[183], and following successful heterogeneous cell isolation, the homogeneous isolation of HSCs is imperative for therapeutic progression. Unlike purification of numerous cell types, the generation of monoclonal antibodies against CD34 almost two decades ago has enabled high purification of HSC and progenitor populations, though fails to comprehensively distinguish between the two. Furthermore, among non-hematopoietic tissues, CD34 is expressed on endothelial cells (ECs). Therefore a

surface profile comprising combinatorial antigen expression is utilised to purify the desired stem, progenitor and functional hematopoietic populations from various tissues in both mice (*Figure 1.9*) and humans (*Table 1.2*). However, whilst numerous results achieved via the study of hematopoiesis in mice are translatable to humans, many of the surface marker profiles of HSCs and progenitor cells differ (*Figure 1.10*). Furthermore, it is still acknowledged that, despite purification using a combinatorial array of surface markers, murine and human HSC populations remain heterogeneous with regards multipotentiality.

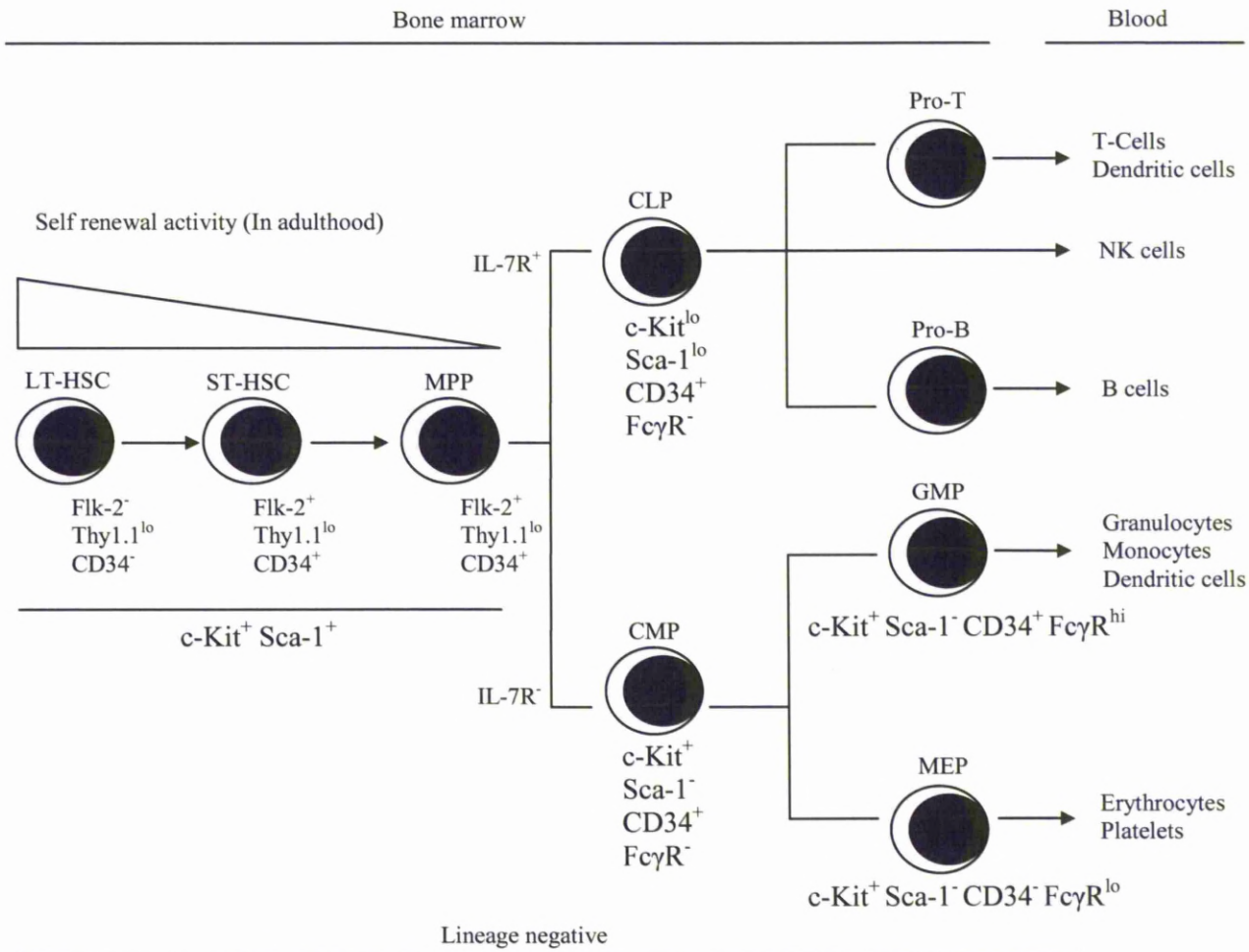

***Figure 1.9* - Conceptual hematopoietic hierarchies in adult mice. Long-term hematopoietic stem cells (LT-HSC) self-renew for life, whereas their downstream short-term (ST)-HSC self-renew for six to eight weeks. Further downstream progenitors have been prospectively isolated to phenotypic, functional, and for the more mature cells, gene expression profile homogeneity. MPP - multipotent progenitor; CLP - common lymphoid progenitor; CMP - common myeloid progenitor; GMP - granulocyte/macrophage progenitor; MEP - megakaryocyte/erythrocyte progenitor[178,188].**

Tissue	Surface marker profile	Read out	Assay
Candidate HSC			
FBM	$Lin^- CD34^+ Th\text{-}1^+$	T/B/myeloid	SCID-hu
FBM	$CD34^+ CD38^- HLA\text{-}DR^+$	Clonal B/myeloid	CFU
CB	$CD34^+ CD38^{lo} CD10^- CD19^-$	Clonal B/myeloid	Liquid culture
CB	$CD34^+ CD38^- CD33^- CD10^-$	Clonal B/myeloid	CFU
CB/BM	$Lin^- CD34^+ CD38^-$	Clonal B/NK/myeloid	NOD-SCID
CB	$Lin^- CD34^- CD38^-$	B/T/myeloid	NOD-SCID
BM	$Lin^- CD34^-$	T/myeloid	Fetal sheep
CB	$Lin^- CD34^+ CD38^- CD33^+$	B/myeloid	NOD-SCID
Candidate lymphoid progenitors			
FBM/BM	$Lin^- CD34^+ CD38^+ CD10^+$	Clonal B/NK/DC	Stroma culture
FBM/BM	$CD45RA^+ Thy\text{-}1^- HLA\text{-}DR^+$	T cells	SCID-hu
CB	$CD34^+ CD38^- CD7^+ IL\text{-}7R\alpha^-$	Clonal B/NK/DC	Stroma culture
Candidate myeloid progenitors			
BM	$CD34^+ CD45RO^-$	CFU-GM enriched	Methylcellulose
BM	$CD34^+ CD45RO^+$	BFU-E enriched	Methylcellulose
CB/BM/PB	$CD34^+ CD45RA^+$	CFU-GM enriched	Methylcellulose
CB/BM/PB	$CD34^+ CD45RA^-$	BFU-E enriched	Methylcellulose
Fetal BM/BM	$CD34^+ CD64^- M\text{-}CSFR^{hi}$	CFU-G/M/GM enriched	Methylcellulose
Fetal BM/BM	$CD34^+ CD64^+ M\text{-}CSFR^{hi}$	CFU-M enriched	Methylcellulose
Fetal BM/BM	$CD34^+ CD64^- M\text{-}CSFR^{lo}$	CFU-G enriched	Methylcellulose
FL/CB/MPB	$CD34^+ IL\text{-}3R^{lo}$	All myeloid colonies	Methylcellulose
FL/CB/MPB	$CD34^+ IL\text{-}3R^+$	CFU-GM enriched	Methylcellulose
FL/CB/MPB	$CD34^+ IL3R^-$	BFU-E enriched	Methylcellulose
CB/BM	$CD34^+/Flt\text{-}3^+$	CFU-GEMM/GM enriched	Methylcellulose
CB/BM	$CD34^+/Flt\text{-}3^-$	BFU-E enriched	Methylcellulose
CB	$CD34^+/CCR1^+$	CFU-GM enriched	Methylcellulose
CB	$CD34^+/CCR1^+$	BFU-E enriched	Methylcellulose

Table 1.2 - **Surface marker expression on candidate human hematopoietic stem and progenitor cells. FL – Fetal liver; FBM – Fetal bone marrow; CB – Cord blood; BM – Bone marrow; PB – Peripheral blood; MPB – Mobilised peripheral blood.**

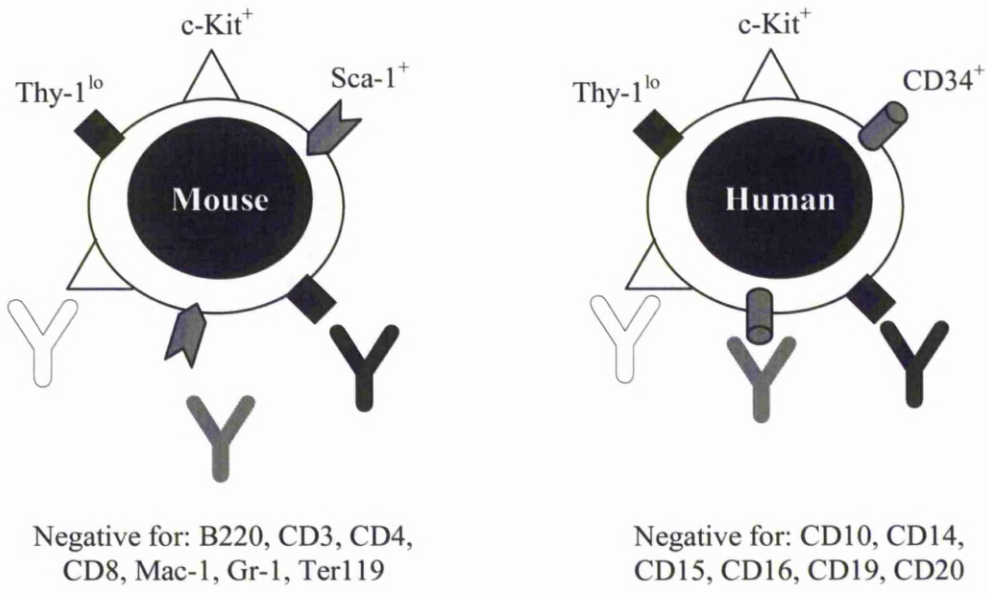

***Figure 1.10* - Candidate HSC surface markers in murine and human cell populations.**

Despite fundamental purification issues of HSCs and progenitors of varying differentiation capacity, the selection of populations based upon surface marker profiles has sufficed in allowing translation towards clinical applications. At present, the common clinical application of hematopoietic cell transplantation (HCT) treats patients with malignancies, bone marrow failure states, and immunodeficiencies via autologous or allogeneic means. Patients receiving autologous grafts receive such treatments due to an underlying malignancy comprising either a high risk of relapse or a pre-failure post standard chemotherapy. Thus, the therapeutic principle underpinning autologous transplantation denotes an ability to administer significantly increased doses of radiation and/or chemotherapy in order to maximise tumour eradication, with the dose-limiting toxicity, detrimental to the hematopoietic organ, rescued by the HCT. Conversely, allogeneic transplantation differs in that HSCs are obtained from an appropriately matched HLA-donor. Such allogeneic HCTs not only infer an ability to rescue patients who undergo myeloablative radiation combined with or without chemotherapy, but the allogeneic graft can also confer an effect that has been termed graft-versus-tumour[189]. However, a significant complication of allogeneic transplantation using an unmodified graft is the consequential graft-versus-host disease (GVHD)[190], in which mature T cells that develop following implantation identify host antigens as foreign bodies and subsequently mount an immune attack against the host organs. Whilst numerous efforts are underway in an

attempt to reduce the morbidity and mortality of GVHD, the current method of repression requires that patients undertake systemic post-transplant immunosuppressive therapy for the remainder of their lives. Studies have demonstrated that T cell depletion of bone marrow results in significantly increased incidences of graft failure, whilst further studies observed an increased loss or reduction of graft-versus-tumour activity following T cell diminution[178]. Purification of HSCs destined for T cell lineage and comprehensive study may therefore generate methods for modification or removal of T cells alleviating immunogenic responses against the host.

Considering HSCs within the whole, remarkable advances throughout the previous decade have allowed their utilisation within a clinical setting. However, issues regarding regulation of self-renewal and capacity for differentiation of varying HSC stem and progenitor subpopulations require further clarification. Should fundamental knowledge addressing these issues be attained, HSCs and their progenitor counterparts may be able to be used in numerous clinical treatments.

1.4.3 Bone Marrow-derived Mesenchymal Stem Cells

In addition to HSCs residing within the bone marrow, MSCs represent a co-inhabiting *in vitro* adherent population capable of proliferative expansion with a finite lifespan of 15-50 cell population doublings. The first successful isolation of fibroblast-like colonies from bone marrow were detailed almost four decades ago, with the isolation protocol based upon the adherence of fibroblast-like cells to the plastic substrate of the cell culture plate and a concomitant lack of adherence of co-isolated HSCs[191]. To date, this procedure is considered a standard protocol to isolate bone marrow MSCs[192-194], with isolation and characterisation of MSCs from numerous vertebrate species, including human[75,83,195], murine[192,194,196], lapine[197], canine[198], ovine[199], avian, porcine[200], equine[201] and bovine[202], founded on this pioneering isolation technique. However, MSCs isolated in this manner are exceedingly heterogeneous, likely incorporating osteoblasts and their precursors, adipocytes, fibroblasts, reticular cells, macrophages, endothelial cells, and a fraction of blood cells and HSCs[203-204]. Thus numerous approaches have been, and continue to be, investigated in an attempt to prepare bone marrow-derived MSCs

encapsulating increased homogeneity[75,83,195,203,205-211], predominantly via selection based upon surface antigen expression profiles. MSCs can be defined in their undifferentiated state via the extracellular antigen expression pattern $CD13^{+}$, $CD29^{+}$, $CD44^{+}$, $CD54^{+}$, $CD73^{+}$, $CD90^{+}$, $CD105^{+}$, $CD106^{+}$, $CD166^{+}$, $CD271^{+}$, SSEA-4^{+}, $SH2^{+}$, $SH3^{+}$, $SH4^{+}$, frizzled-9^{+}, $CD3^{-}$, $CD11a^{-}$, $CD14^{-}$, $CD19^{-}$, $CD31^{-}$, $CD34^{-}$, $CD38^{-}$, $CD45^{-}$ and $CD66b^{-}$[205,212]. This phenotypic profile does however modify with prolonged *in vitro* culture, perhaps signifying a reduction or cessation of multipotentiality. Alternatively, modified surface expression may indicate lineage commitment or differentiation of cells within the population, with spontaneous differentiation of MSCs in culture being demonstrated in studies of bone marrow-derived MSCs in rat[213]. Perhaps more accurate assessment of the global cellular phenotype can therefore be ascertained by the assessment of intracellular proteins associated with maintenance of plasticity or guided differentiation. At present, antigens such as STRO-1 represent the most widely used markers for MSC identification[214-215], and whilst some antigens are undoubtedly capable of yielding a population of greater homogeneity following sorting, they fail to distinguish between stem cells and committed progenitors of lesser plasticity. The stem cell proliferation marker nucleostemin is a protein found in the nucleoli of ES cells, adult CNS stem cells, primitive cells in the bone marrow and cancer cells, and is hypothesised to regulate cell cycle progression in stem and cancer cells[216-217]. However, nucleostemin once again encompasses the problems associated with STRO-1 with regards to progenitor impurity. Investigations are therefore ongoing in an attempt to identify a marker specific to MSCs which is lost immediately following lineage commitment. However, due to the innate ability of stem cells to undertake multilineage differentiation, if antigen-based selection is to be used for homogeneous cell isolation, it is likely that no sole antigen will identify non-committed MSCs, and that subsequently an array of surface markers will be required to identify such populations.

The ability of bone marrow-derived cells to differentiate designate them a stem cell containing population, however their mechanisms of plasticity remain fervently debated. The expression of Oct4, a crucial mediator of plasticity in ES cells, has been reported to be both positively and negatively expressed within bone marrow-derived MSCs[218-220]. A study investigating Oct4 function within murine-derived somatic

stem cells revealed that Oct4 is dispensable for both cellular self-renewal and maintenance[221], suggesting that somatic stem cells mediate plasticity by alternative mechanisms. However, numerous studies have documented Oct4 expression within bone marrow-derived MSCs, also noting its interaction with other ES-associated proteins. In addition to similar gene targeting, studies have suggested that Oct4 expression in MSCs promotes expression of MSC-specific genes and regulates cell cycle progression[222]. Investigations have also suggested expression of other hypothesised co-regulators of plasticity including Sox2 and Nanog[222-224], although the expression and location of all of these proteins appears to vary dependent on the antibodies utilised within the study[220]. It is therefore imperative that, if comprehensive characterisation of given cells is to be achieved, a known standard antibody must be utilised in all studies in order to allow comparative expression.

MSCs demonstrate the ability to undertake numerous lineage commitments *in vitro*, capable of generating adipocytes, chondrocytes, osteoblasts, astrocytes, oligodendrocytes, neurons, tenocytes and myocytes following exposure to appropriate chemical stimuli[75,225]. This innate differentiation ability does however, along with their proliferative capabilities, decrease with increasing *in vitro* passage. This rapid aging of MSCs following *in vitro* culture is thought be the result of quickly decreasing telomere lengths[226-233], a mechanism which may have significant clinical impacts.

Whilst homogeneous *in vitro* characterisation of bone marrow-derived MSCs and residing subpopulations remains elusive, many *in vivo* applications using these cells have, perhaps in many cases prematurely, been undertaken. Progression of MSC research to *in vivo* trials is further scrutinised when we consider that very little is known with regards the extent to which MSCs are responsible for normal growth and maintenance throughout development and adulthood. Nevertheless, non-manipulated bone marrow-derived MSCs have been applied to numerous clinical models with varying success, including attempted regeneration of skeletal muscle, cardiac muscle, liver, skin, GI tract, lung, pancreas, kidney, and central nervous system[156].

1.4.4 Isolation of MSC-like Cells from Numerous Other Adult tissues

Evolving from the understanding that bone marrow-derived MSCs possess a capacity to elicit multilineage differentiation surpassing previously held concepts, investigations attempting to isolate cells of such potentiality from alternative adult tissue sources have been undertaken. Utilising an array of continually evolving isolation methods, cells exhibiting varying levels of plasticity have been isolated from numerous tissues including hair follicles[234], brain tissue[235-236], cornea[237-240] and retina[241-244], dental pulp[245-246], lung[247], peripheral blood[248-251], heart[252], intestines[253-256], adipose[155,257-264], skeletal muscle[74,265-268] and skin[162,269-273] from many species including humans. Furthermore, in addition to cells isolated from adult tissues, populations derived from embryo/adult adjoining tissues such as placenta and umbilical cord cells have also demonstrated multipotentiality (*Table 1.3*), although the origin of the populations, disputably embryo or adult generated, remains unconfirmed.

The isolation of cells exhibiting plasticity from numerous adult tissues has raised hopes of developing tissue engineered devices incorporating adult- derived cells, potentially overcoming the ethical dilemmas and intensive technical issues encountered with ES cells. However, many studies fail to identify the fundamental properties of isolated cells, characterising the heterogeneous phenotype rather than comprising subpopulations. Whilst surface markers have allowed partial purification of subpopulations to enable studies of increased homogeneity, partitioning of cells encapsulating varying plasticity and lineage commitment remains elusive. Thus, whilst numerous reports have documented phenotypic profiles, differentiation capacities and *in vitro* proliferation of cells isolated from numerous tissues, it is important to emphasise that such analysis incorporates globally isolated cell populations, failing to attribute a given phenotype, differentiation induction or proliferative ability to individual cells. Whilst many perceive this as trivial with regards their utilisation clinically, the presence of lineage committed progenitors has the potential to generate undesirable tissues following implantation. However, when using such therapies as a last resort, many patients may decide that the potential gain far outways this risk.

Tissue of isolation	Global expression patterns	Demonstrated lineage potential
Adipose[155,257-264,274]	$CD14^-$ $CD29^+$ $CD31^-$ $CD34^-$ $CD44^+$ $CD45^-$ $CD73^+$ $CD90^+$ $CD105^+$ $CD106^+$ $CD133^-$ $CD146^+$ $CD166^+$ STRO-1^+	Adipogenic, Chondrogenic, Osteogenic
Brain[235,275]	$PDGF^+$ $ALDH^+$ $Nestin^+$ $Sox2^+$	Neuronal, Macroglial
Cornea[237-240,276]	$CD11b^+$ $CD34^+$ $CD45^+$ $EGFR^+$ $HLA\text{-}DR^+$ Integrin $\beta1^+$ $K3^+$ $K19^+$ $Involucrin^+$ Connexin 43^+	Epithelial
Dental pulp[245-246,277]	$CD13^+$ $CD29^+$ $CD31^+$ $CD34^-$ $CD43^-$ $CD45^-$ $CD44^+$ STRO-1^+ $Nanog^+$ $Oct4^+$ SSEA-3^+ SSEA-4^+ Tra-1-60^+ Tra-1-81^+	Adipogenic, Chondrogenic, Osteogenic Neuronal, Smooth and Skeletal muscle
Hair follicles[234,278]	$CD34^+$ $CD45^{+/-}$ $CD133^{+/-}$ $CD146^{+/-}$ Ki-67^+	Epithelial, Neuronal
Heart[252]	$CD117^+$ $CSps^+$ $isl1^+$ Sca-1^+	Cardiomyogenic
Intestine[254-256,279]	BMPR1α^+ $DCAMKL1^+$ $Lgr5^+$ $Telomerase^+$	Epithelial
Lung[247,279-280]	$CD31^-$ $CD34^+$ $CD45^-$ $AT2^+$ SC-C^+ $CCSP^+$ Sca-1^+	Epithelial
Peripheral blood[248-250,281]	$CD14^+$ $CD15^+$ CD29+ $CD31^{+/-}$ $CD34^{+/-}$ $CD40^+$ CD41- $CD45^+$ $CD105^+$ $CD117^-$ $CD133^-$ $CD144^+$	Adipogenic, Chondrogenic, Osteogenic, Angiogenic, Myogenic, Neuronal
Placenta/Amniotic fluid[282-285]	$CD4^-$ $CD8^-$ $CD34^-$ $CD133^-$ $Oct4^+$ $SSEA4^+$ $Desmin^-$ $Vimentin^+$ Tra-1-60^- Tra-1-80^-	Adipogenic, Chondrogenic, Osteogenic, Endothelial, Hepatic, Myogenic, Neuronal
Retina[241-244,286-287]	DCX^+ Flk-1^+ $Hes1^+$ $Musashi^+$ $Nestin^+$	Neuronal – Photoreceptors, amacrine and horizontal cells, RPE, rod bipolar, Muller glia, retinal ganglion cells

Skeletal muscle[74,265-268]	$CD10^+$ $CD13^+$ $CD34^{+/-}$ $CD45^-$ $CD56^+$ Bcl-2^+ Sca-1^+	Adipogenic, Chondrogenic, Osteogenic, Hematopoietic, Neuronal, Skeletal muscle
Skin[162,269-273 288]	$CD34^+$ Keratin19^+	Adipogenic, Neuronal, Smooth muscle cells
Umbilical cord[289-290]	$CD29^+$ $CD31^-$ $CD44^+$ $CD45^-$ $CD51^+$ $CD105^+$ $SH2^+$ $SH3^+$ $Oct4^+$ $Sox2^+$	Adipogenic, Chondrogenic, Osteogenic Cardiogenic
Umbilical cord blood[80,183,291-293]	$CD34^+$ $CD38^+$ $CD133^+$ HLA-DR^+ Oct4	Adipogenic, Chondrogenic, Osteogenic, Neuronal

Table 1.3 - **Expression profiles and differentiation potential of cells isolated from numerous adult tissues. A fundamental issue with regards transferability of characterisation data is evident when examining numerous reports; whilst some investigators report positive expression of a given antigen/protein, others detail negative expression. This is probably attributable to the utilisation of antibodies purchased from alternative suppliers. Thus it would be clinically beneficial if a world standard produce for cell characterisation be put forward. Furthermore, the formation of a database accessible to registered scientific users would allow rapid collaboration of results and evolve a mutual understanding of cell types.**

$^{+/-}$ - Reports detailing both positive and negative expression; ALDH – Aldehyde dehydrogenase; SP-C – Pro-surfactant protein C; CCSP – Clara cell marker; RPE – Retinal Pigment Epithelial.

1.5 Aims

1.5.1 Aims of the study

Investigations demonstrating the innate plasticity of cells residing in numerous adult tissues have raised hopes for rapid generation of numerous tissue engineered devices addressing a range of debilitating illnesses. However, whilst isolation of populations exhibiting multilineage potential has been documented for numerous adult tissues, detailed characterisation of homogeneous subpopulations have yet to be refined. Whilst adult-derived stem cells have, to some extent, distanced themselves from the ethical and technical dilemmas associated with embryonic-derived stem cells or synthetically modified iPS cells, they encompass many technical issues of their own, not least their inability to maintain phenotype following *in vitro* culture. It is therefore imperative that, prior to clinical commencement, complete understandings of individual subpopulations are ascertained, detailing their potential to maintain phenotype, differentiation ability, proliferation capacity, karyotype, and a capability to contribute to teratoma formation *in vivo*. This study, therefore, endeavours to assess the characteristics of cells derived from human bone marrow, peripheral blood, umbilical cord, and dental pulp *in vitro*, detailing fundamental aspects of the populations incorporating heterogeneous and increasingly homogeneous assessment. However, since it is likely that isolated cells will be heterogeneous, likely incorporating stem and progenitor cells of varying plasticity and developmental commitment, it is difficult to hypothesise with any great purpose the type of subpopulations we expect to obtain from each respective tissue. This issue is complicated further by findings detailing the potential plasticity of HSCs[183], thus questioning, if attained, which cells (MSC-like cells, HSCs, progenitor cells, etc.) are responsible for observed differentiation. And whilst it is plausible that increased homogeneity may be facilitated via optimisation of isolation techniques, it is likely that isolated cells will require purification post culture. However, it is largely accepted that purification via positive or negative antibody exclusion fails to adequately isolate homogeneous populations, novel strategies of purification may need to be developed. In the first instance, however, isolated populations will be assessed in a heterogeneous manner in an attempt to identify the subpopulations present, the phenotypic and proliferative stability of the population following *in vitro*

culture, and finally the capacity of the population to undertake lineage differentiation. Following this heterogeneous assessment, attempts will be made to homogeneously isolate subpopulations hypothesised to be present following heterogeneous characterisation.

It is foreseen that by comprehensively characterising the stability and potential of cells isolated from numerous sources, informative decisions can be made allowing the selection of an optimal cell type for a given therapeutic application. Thus it is hoped that the study will provide comprehensive characterisations on which to advance the utilisation of these cells for therapeutic applications, whilst also providing a template detailing characterisation requirements on which future cell assessment can be based. Investigations will therefore attempt to:

1. Optimise methods for the isolation of adherent cells from human peripheral blood, dental pulp and umbilical cord. Each varying isolation procedure will be scored for its ability to isolate populations exhibiting homogeneous characteristics whilst being able to maintain a stable undifferentiated phenotype when cultured in basal conditions *in vitro* and when subjected to freeze-thaw cycles.

2. Phenotypically characterise each isolated cell population using an array of antibodies to compose a surface antigen profile of the heterogeneous populations, potentially indicating the phenotypes of subpopulations present within the culture. Cell populations will be subjected to such analysis at each passage and following freeze-thaw cycling to assess the effects of *in vitro* culture and cryopreservation on the cells, whilst bone marrow-derived cells purchased from Lonza will also be characterised at each passage. With respect to cells isolated from peripheral blood and dental pulp, for which information regarding the donor will be available, the phenotype of populations from each donor will be compared.

3. Investigate expression of plasticity regulatory proteins within each respectively isolated population throughout increasing *in vitro* basal culture and following cryopreservation. Expression of proteins such as Oct4 and

Sox2 would indicate a population capable of undertaking multilineage differentiation, and thus the effects of prolonged *in vitro* culture and cryopreservation upon each respective cell type and subsequently their ability to maintain an undifferentiated phenotype can be addressed via monitoring the expression of such proteins.

4. Assess the proliferation capacities of each isolated cell type throughout *in vitro* culture and following cryopreservation. Should the given cell type be utilised within a clinical setting, it is likely that large numbers, and hence prolonged *in vitro* passage and possible cryopreservation, will be required, and thus it is imperative that the population can reproducibly generate mass numbers of daughter cells.

5. Establish numbers of hematopoietic and non-hematopoietic progenitor subpopulations within each passage of respective culture using colony forming unit (CFU) assays. Such CFU assays will enable quantification of the number of hematopoietic and non-hematopoietic progenitor cells within each heterogeneously isolated population. The number of CFUs can therefore be monitored and compared across passage number and donor.

6. Assess impacts of *in vitro* culture upon the aging of cells through the monitoring of telomere lengths within each population. Furthermore, in the case of peripheral blood and dental pulp cells, for which donor information is available, compare telomere lengths and respective regulation in donors of varying age and sex. Telomere degradation within cells is known to be a key regulator of the aging process and thus comparing telomere lengths within each population will enable the effects of *in vitro* culture to be assessed.

7. Investigate lineage potential of each isolated population at varying passages and following cryopreservation when induced using commercially available and chemically-defined differentiation media. The ability of isolated populations to reproducibly undertake differentiation towards desired lineages represents the underpinning of many tissue engineering and regenerative medicine approaches, and thus it is imperative that cultures are assessed for their lineage potential.

8. Homogeneously isolate subpopulations exhibiting varying phenotypic surface antigen expression and, following purification, characterise cells as detailed above for heterogeneous populations. However, should antibody- based purification strategies prove to be ineffective for the homogeneous isolation of desired subpopulations, novel approaches to cell sorting will be considered.

2. Materials and Methods

2.1 Isolation of Adherent Cell Populations

2.1.1 Mesenchymal Stem Cells Derived from Human Bone Marrow

Cryopreserved passage 2 human mesenchymal stem cells (MSCs) were purchased from Lonza (Cat#PT-2501). When required, 750,000 (1 vial) of these cells were thawed and seeded into 2 x T-75 tissue culture plastic flasks in MSCGM™ Mesenchymal Stem Cell Growth Media (Lonza; Cat#PT-3001), thereby changing into passage 3 cells. Cells were obtained from the posterior iliac crest of healthy males and non-pregnant females aged between 18 and 45 years. Harvested cells were tested for purity using flow cytometry and for their ability to undertake adipogenic, chondrogenic and osteogenic lineages. They were positive for surface antigens CD29, CD44, CD105 and CD166, and exhibited negative expression of CD14, CD34 and CD45. In this thesis, the MSCs were maintained in MSCGM™ Mesenchymal Stem Cell Growth Media (Lonza; Cat#PT-3001).

2.1.2 Isolation of Mononuclear Cells from Human Peripheral Blood using Histopaque Density Centrifugation

Human peripheral blood was isolated from the median cubital vein of donors using a 21-gauge SURFLO® winged needle infusion set (Terumo®; Cat#SV-21BL). Heparin (Sigma-Aldrich; Cat#H4784) was added to 20ml of isolated blood at a final concentration of 0.5µg/ml to prevent coagulation. To isolate mononuclear cells, 5ml of blood were layered onto 3ml of Histopaque® -1077 (Sigma-Aldrich; Cat#H8889) in 4 x 15ml Falcon tubes (BD Biosciences; Cat#352096). Samples were spun at 2700 x g for 20 minutes at 20°C with the absence of brakes. Following centrifugation the lymphocyte/monocyte layer was harvested, initially through scraping cells from the side of the tubes using the tip of a pipette prior to harvesting the entire contents. The resulting isolates of two harvested lymphocyte/monocyte layers were combined in one 30ml universal. 20ml of PBS/1mM EDTA (4°C) were added and solutions centrifuged at 2300 x g for 10 minutes at 4°C. Following discarding of the supernatant, pelleted cells were resuspended in PBS/1mM EDTA (4°C) and spun at

2000 x g for 10 minutes at 4°C. Centrifuged cells were resuspended in PBS/1mM EDTA (4°C) and spun for at 1300 x g for 15 minutes at 4°C. Finally, pelleted cells were resuspended in 10ml of DMEM (Low glucose) (GIBCO; Cat#10567014) containing 10% (v/v) FCS and 1% (v/v) 10,000U/ml of penicillin and 10mg/ml of streptomycin in 0.9% (w/v) sodium chloride (Sigma-Aldrich; Cat#S7653), prior to plating into 2 wells of a 6 well pre-coated fibronectin (20µg/ml) plate. Media was replaced after 72 hours, thereby removing the non-adherent lymphocytes.

2.1.3 Isolation of Mononuclear Cells from Human Peripheral Blood using RosetteSep® Human Monocyte Enrichment Cocktail

Peripheral blood from donors was withdrawn as described in 2.1.2. To isolate mononuclear cells, EDTA was added to 10ml whole blood at a final concentration of 1mM in 2 x 15ml Falcon tube (BD Biosciences; Cat#352096). 500µl of RosetteSep® Human Monocyte Enrichment Cocktail (StemCell Technologies; Cat#15028) were added to 10ml of whole blood and vortexed. Following 20 minutes incubation at room temperature, samples were diluted with 10ml of PBS with 2% (v/v) FCS and 1mM EDTA and agitated gently. Diluted samples were layered on top of 15ml Ficoll-Paque® (StemCell Technologies; Cat#07907) and centrifuged for 20 minutes at 2600 x g at room temperature with the absence of brakes. Cells were harvested from the Ficoll-Paque® plasma interface and washed twice with PBS containing 2% (v/v) FCS. Cells were resuspended in 10ml of DMEM (Low glucose) (GIBCO; Cat#10567014) containing 10% (v/v) FCS and 1% (v/v) 10,000U/ml of penicillin and 10mg/ml of streptomycin in 0.9% (w/v) sodium chloride (Sigma-Aldrich; Cat#S7653), prior to plating into 2 wells of a 6 well pre-coated fibronectin (20µg/ml) plate. Media was replaced after 72 hours, removing the non-adherent lymphocyte layer.

The underlying principle of the RosetteSep® protocol is founded on the ability of the antibody cocktail to crosslink unwanted human cells in human whole blood to multiple RBCs, forming immunorosettes (*Figure 2.1*). This increases the density of the unwanted (rosette) cells, such that they are pelleted along with the free RBCs when centrifuged over a buoyant density media such as Ficoll-Paque®. Crucially, mononuclear cells cease to be labelled with antibody and are therefore readily

identified and harvested as a highly enriched population at the interface between the plasma and the buoyant density media.

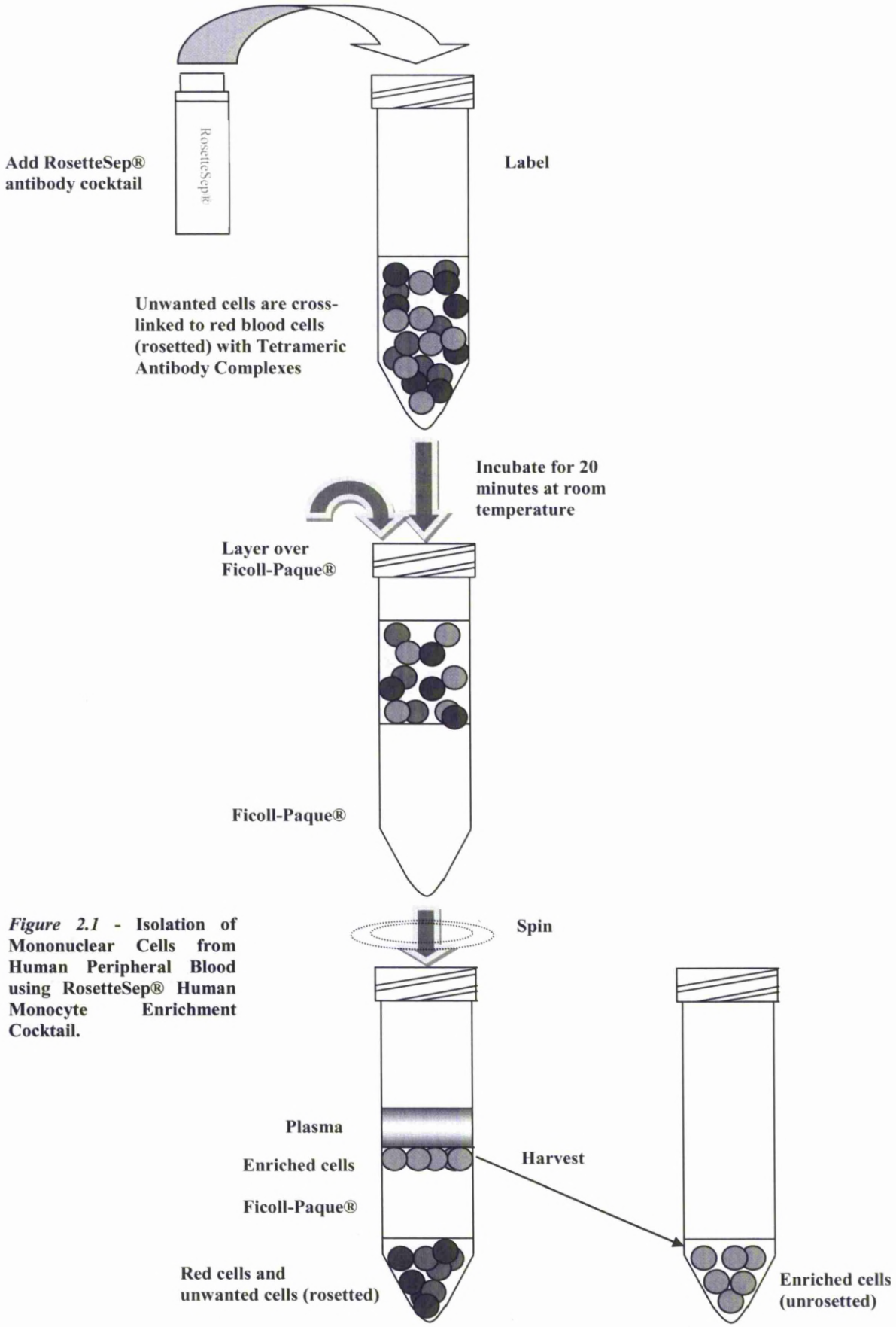

Figure 2.1 - **Isolation of Mononuclear Cells from Human Peripheral Blood using RosetteSep® Human Monocyte Enrichment Cocktail.**

2.1.4 Isolation of Cells from Human Umbilical Cord Following Blood Vessel Removal and Plating of Wharton's Jelly on Tissue Culture Plastic

Fresh human umbilical cords were obtained with informed consent following birth and stored in Hanks' balanced salt solution for 1-24 hours prior to tissue processing. To obtain multipotent cells from Wharton's jelly, cords were washed in PBS/1mM EDTA (4°C) prior to the removal of blood vessels. Following blood vessel removal, Wharton's jelly was plated directly onto untreated tissue culture plastic of a 6 well plate. Plated Wharton's jelly dissections were soaked in DMEM (Low glucose) (GIBCO; Cat#10567014) containing 15% (v/v) FCS and 1% (v/v) 10,000U/ml of penicillin and 10mg/ml of streptomycin in 0.9% (w/v) sodium chloride (Sigma-Aldrich; Cat#S7653). Following cell adherence and proliferation, dissected Wharton's jelly was removed from the culture and cells maintained in fresh basal media.

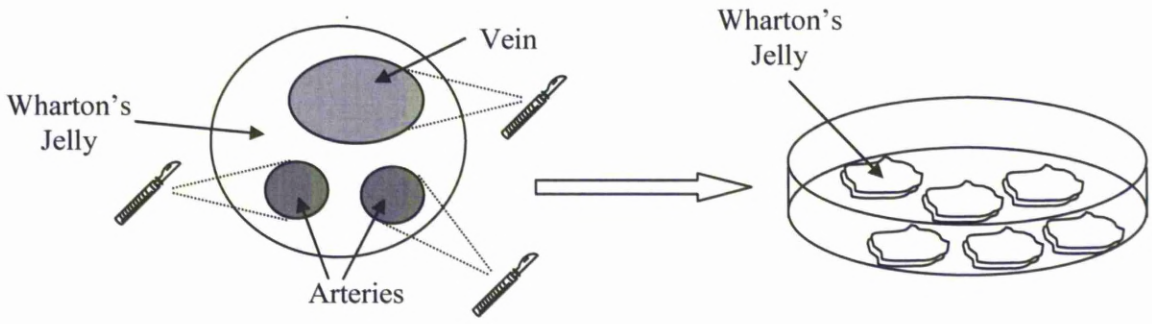

***Figure 2.2* - Isolation of cells from Wharton's jelly following blood vessel removal.**

2.1.5 Isolation of Cells from Human Umbilical Cord by Whole Cord Digestion

Fresh cords stored in Hanks' balanced salt solution for 1-24 hours were washed in PBS/1mM EDTA (4°C). Whole cords were mechanically disassembled into fractions approximately 50mm^2 in size. Dissected cords were enzymatically digested by incubation in a solution containing 2% (w/v) Dispase I (Sigma-Aldrich; Cat#4818) and 2% (w/v) Collagenase type II (Invitrogen; Cat# 17101015) overnight at 37°C with gentle agitation. Digested cords were centrifuged at 2000 x g for 5 minutes at 20°C. Pelleted substrates were resuspended in DMEM (Low glucose) (GIBCO; Cat#10567014) containing 10% (v/v) FCS and 1% (v/v) 10,000U/ml of penicillin and 10mg/ml of streptomycin in 0.9% (w/v) sodium chloride (Sigma-Aldrich;

Cat#S7653), prior to filtration using a 0.2μM filter to remove debris. Following filtration, cells were seeded into wells of a 6 well plate at a concentration of 50,000 cells per well.

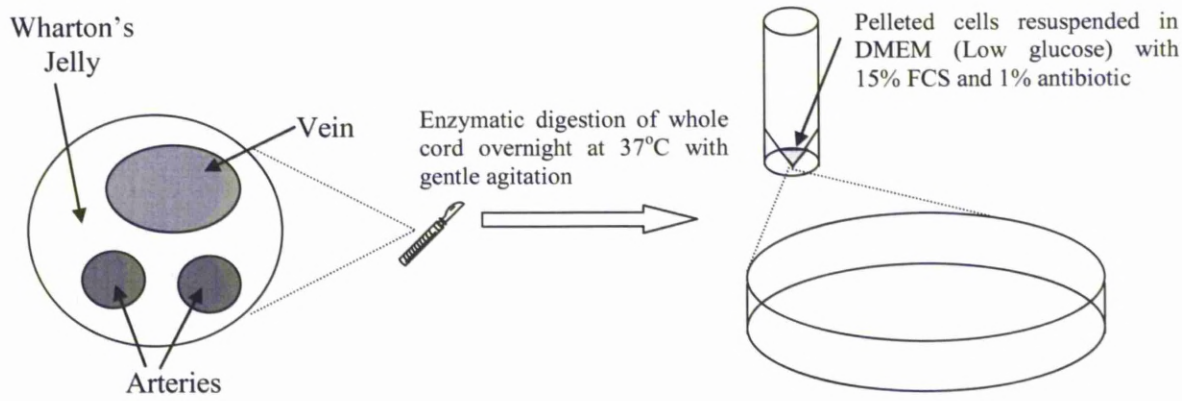

***Figure 2.3* - Isolation of cells from umbilical cord following whole cord digestion.**

2.1.6 Isolation of Cells from Human Dental Pulp

Teeth were acquired following informed consent after dental procedures or loss of deciduous teeth. Received teeth were stored in 199 Media (GIBCO; Cat#12350039) containing 5% (v/v) FCS and 1% (v/v) 10,000U/ml of penicillin and 10mg/ml of streptomycin in 0.9% (w/v) sodium chloride (Sigma-Aldrich; Cat#S7653) until delivered to the laboratory for pulp isolation. Upon arrival, teeth were treated in a gentamicin solution (Invitrogen; Cat#15710-049) (20μg/ml) for 5 minutes at room temperature to eradicate any residing infection. To isolate pulp, teeth were sheered at the dentine interface (*Figure 2.4*) and pulp removed. Following mechanical dissection using forceps and scalpel, pulp was enzymatically digested in a solution composing 2% (w/v) Dispase I (Sigma-Aldrich; Cat#4818) and 2% (w/v) Collagenase type II (Invitrogen; Cat# 17101015) for 8 hours at 37°C with gentle agitation. Digested pulp was centrifuged at 2000 x g for 5 minutes at 4°C and pelleted cells resuspended in 199 Media containing 5% (v/v) FCS and 1% (v/v) 10,000U/ml of penicillin and 10mg/ml of streptomycin in 0.9% (w/v) sodium chloride (Sigma-Aldrich; Cat#S7653). The resuspended solution was filtered through a 0.2μM filter to remove debris and cells seeded in 1 well of an uncoated 6 well plate.

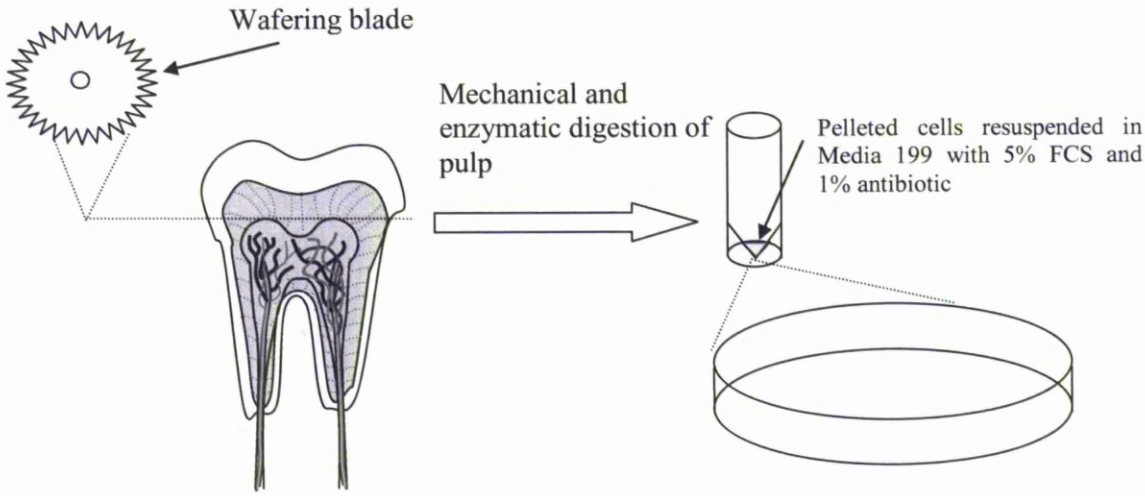

Figure 2.4 - **Isolation of multipotent progenitor cells from human dental pulp.**

2.1.7 Cell Culture Techniques

Cells were maintained on conventional tissue culture polystyrene plastic unless otherwise stated (Scientific Laboratory Supplies, UK). Cells requiring passage were initially washed in PBS following removal of redundant media and enzymatically dissociated using a solution comprising 5g porcine Trypsin, 2g EDTA in 100mL of 0.9% (w/v) sodium chloride (Sigma-Aldrich; Cat#6567) diluted to a working concentration of 10% (v/v) using PBS. Cells were trypsinised at 37°C for 15 minutes and the enzymatic reaction subsequently neutralised via the addition of an equal volume of serum-containing basal media. Detached cells were pelleted by centrifugation at 2000 x g for 5 minutes at 4°C and resuspended in an appropriate volume of corresponding basal media. Resuspended cells were seeded in a given culture vector and incubated at 37°C with 5% CO_2. Cell culture media was replenished every 4 days. The basal media used for culture was dependent on the isolated cell type. Cells were subcultured at a ratio of 1:3, although dental pulp could be subcultured up to 1:10.

2.1.8 Freezing and Thawing of Cells

Cultured cells were enzymatically dissociated using Trypsin as detailed in 2.1.7. Pelleted cells were resuspended in 1ml of a solution consisting of 90% (v/v) FCS and 10% (v/v) DMSO (Sigma-Aldrich; Cat#C6164). Suspended cells were transferred to a cryo-vial and placed into a commercially available freezing box containing isopropanol, which cools at 1°C per minute, and stored at -80°C for 24 hours, after which vials were transferred to liquid nitrogen storage. To thaw, frozen vials were heated at 37°C and resuspended in 1ml of pre-warmed basal media. Resuspended cells were transferred to relevant tissue culture plasticware.

2.2 Flow Cytometry-based Phenotyping

2.2.1 Phenotypic Analysis of Cells using Flow Cytometry

Cultured cells were enzymatically dissociated using Trypsin and pelleted by centrifugation at 2000 x g for 5 minutes at 4°C. Pelleted cells were resuspended in PBS and 100µl containing approximately 1 x 10^5 cells added to each of the required number of flow cytometry sample tubes. 10µl of antibody (1:10 working dilution) (*Table 2.1*) or their appropriate isotype (1:10 working dilution) (*Table 2.2*) were added to the cell suspension and samples incubated for 15 minutes at 4°C in the absence of light. Cells incubated in the absence of antibodies were used as an additional control. Following incubation, 180µl of BD FACSFlow™ (BD Biosciences; Cat#342003) were added to each sample. Cells were processed to a count of 3 x 10^4 per sample using a Becton Dickinson FACSort with Cell Quest software.

Antibody (Conjugate) (Clonality)	Host Species	Target Species	Cross Reactivity	Working Dilution	Isotype	Supplier	Catalogue Number
CD9 (FITC) (M)	Mouse	Human	Horse, Bovine, Rabbit, Rhesus Monkey, Dog, Cat, Pig	1:10	Mouse IgG2b (FITC)	Serotec	MCA469F
CD14 (FITC) (M)	Mouse	Human	None reported	1:10	Mouse IgG1, k (FITC)	BD Biosciences	347493
CD15 (FITC) (M)	Mouse	Human	None reported	1:10	Mouse IgM (FITC)	Serotec	MCA2458F
CD29 (PE-Cy5) (M)	Mouse	Human	None reported	1:10	Mouse IgG1, k (PE-Cy5)	BD Biosciences	559882
CD30 (FITC) (M)	Mouse	Human	None reported	1:10	Mouse IgG2a (FITC)	Serotec	MCA2319F
CD31 (PE) (M)	Mouse	Human	None reported	1:10	Mouse IgG1, k (PE)	BD Biosciences	555446
CD34 (Class II) (FITC) (M)	Mouse	Human	Cynomolgus monkey, Rhesus Monkey	1:10	Mouse IgG1 (FITC)	Serotec	MCA547F
CD34 (Class III) (FITC) (M)	Mouse	Human	Cynomolgus monkey	1:10	Mouse IgG2a (FITC)	Serotec	MCA1578F
CD41a (PE) (M)	Mouse	Human	None reported	1:10	Mouse IgG1, k (PE)	BD Biosciences	555467
CD44 (PE) (M)	Mouse	Human	None reported	1:10	Mouse IgG2b, k (PE)	BD Biosciences	555479
CD45 (FITC) (M)	Mouse	Human	None reported	1:10	Mouse IgG1, k (FITC)	BD Biosciences	555482
CD50 (FITC) (M)	Mouse	Human	None reported	1:10	Mouse IgG1 (FITC)	Serotec	MCA2358F
CD56 (FITC) (M)	Mouse	Human	None reported	1:10	Mouse IgG2a (FITC)	Serotec	SFL2046F
CD62E (FITC) (M)	Mouse	Human	None reported	1:10	Mouse IgG2a (FITC)	Serotec	MCA1969F
CD73 (PE) (M)	Mouse	Human	None reported	1:10	Mouse IgG1, k (PE)	BD Biosciences	550257
CD81 (FITC) (M)	Mouse	Human	Chimpanzee	1:10	Mouse IgG1 (FITC)	Serotec	MCA1847F
CD90 (FITC) (M)	Mouse	Human	Cynomolgus monkey, Monkey	1:10	Mouse IgG1 (FITC)	Serotec	MCA90F
CD105 (FITC) (M)	Mouse	Human	None reported	1:10	Mouse IgG1 (FITC)	Serotec	MCA1557F
CD106 (PE) (M)	Mouse	Human	None reported	1:10	Mouse IgG1, k (PE)	BD Biosciences	555647
CD117 (PE) (M)	Mouse	Human	None reported	1:10	Mouse IgG1, k (PE)	BD Biosciences	555714
CD133 (PE) (M)	Mouse	Human	None reported	1:10	Mouse IgG1 (PE)	Miltenyi Biotech	130-090-826
CD135 (FITC) (M)	Mouse	Human	None reported	1:10	Mouse IgG1 (FITC)	Serotec	MCA1843F
CD146 (FITC) (M)	Mouse	Human	None reported	1:10	Mouse IgG1 (FITC)	Serotec	MCA2141F
CD166 (PE) (M)	Mouse	Human	None reported	1:10	Mouse IgG1, k (PE)	BD Bioscience	559263
HLA-ABC (FITC) (M)	Mouse	Human	None reported	1:10	Mouse IgG2a (FITC)	Serotec	MCA116F
HLA-DR (FITC) (M)	Rat	Human	None reported	1:10	Rat IgG2a (FITC)	Serotec	MCA71F
STRO-1 (PE) (M)	Mouse	Human	Murine	1:10	Goat IgM (PE)	Santa-Cruz	sc-47733
VWF (FITC) (P)	Sheep	Human	None reported	1:10	Polyclonal IgG (FITC)	Serotec	AHP062F
NGFR5 (FITC) (M)	Mouse	Human	None reported	1:10	Mouse IgG1, k (FITC)	Cedarlane	CL10013F

Table 2.1 - **Flow cytometry antibodies for phenotypic analysis by flow cytometry. Clonality: M – Monoclonal; P – Polyclonal.**

Isotype control	Working Dilution	Supplier	Catalogue Number
Goat IgM (PE)	1:10	Santa-Cruz	sc-2082
Mouse IgG1 (FITC)	1:10	Serotec	MCA928F
Mouse IgG1 (PE)	1:10	Miltenyi Biotech	130-092-212
Mouse IgG1, k (FITC)	1:10	BD Biosciences	555748
Mouse IgG1, k (FITC)	1:10	Cedarlane	CLCMG101
Mouse IgG1, k (PE)	1:10	BD Biosciences	340761
Mouse IgG1, k (PE-Cy5)	1:10	BD Biosciences	555750
Mouse IgG2a (FITC)	1:10	Serotec	MCA929F
Mouse IgG2b (FITC)	1:10	Serotec	MCA1423F
Mouse IgG2b, k (PE)	1:10	BD Biosciences	555743
Mouse IgM (FITC)	1:10	Serotec	MCA692F
Polyclonal IgG (FITC)	1:10	Serotec	AAC10F
Rat IgG2a (FITC)	1:10	Serotec	MCA1125F

***Table 2.2* - Flow cytometry isotype controls.**

2.2.2 Phenotypic Association of Surface Antigens

Ready availability of purified antibodies and simultaneous advances in flow cytometric techniques have allowed numerous surface antigens to be attributed to a given cell type (*Table 2.3*), thereby hypothetically allowing homogeneous characterisation of subpopulations following cell isolation. Surface antigens listed in *Table 2.1* were selected to generate surface marker profiles of cells isolated from bone marrow, peripheral blood, umbilical cord and dental pulp over increasing passage *in vitro*. Assembling such detailed phenotypic characteristics allowed the effects of prolonged *in vitro* culture to be assessed and furthermore suggested potential classification of the numerous subpopulations within the culture.

Antibody (Conjugate) (Clonality)	Surface antigen associated cell type and functional capacity
CD9 (FITC) (Monoclonal)	CD9 is a 244kD glycoprotein expressed by platelets, endothelial cells, monocytes and pre-B cells. A high level of CD9 mRNA is expressed in undifferentiated ES cells, although expression decreases significantly following introduction of differentiation stimuli. Addition of LIF to differentiating ES cells re-establishes mRNA expression of CD9 coinciding with reinstated plasticity. Addition of anti-CD9 antibodies to culture blocks ES cell colony formation and reduces cell viability, thus indicating that CD9 may facilitate a regulatory role in LIF-mediated maintenance of undifferentiated ES cells[294].
CD14 (FITC) (Monoclonal)	CD14 is present on the majority of normal peripheral blood monocytes and functions within the activation of cells through the binding of lipopolysaccharide (LPS)[295].
CD15 (FITC) (Monoclonal)	Also known as Lewis X and SSEA-1 (Stage-specific embryonic antigen I), CD15 is a carbohydrate antigen which functions as a mediator of phagocytosis, bactericidal activity and chemotaxis. CD15 is expressed predominantly by peripheral blood granulocytes, including neutrophils and eosinophils, and to a varying extent by monocytes, though not by lymphocytes, basophils or dendritic cells. CD15 was initially identified in the early 1980s and readily demonstrated its ability to highlight myeloid differentiation. CD15 also serves as a marker of mouse ES cells and MSCs, whilst also demonstrating expression in a subset of human medulloblastomas[296].
CD29 (PE-Cy5) (Monoclonal)	CD29 is the beta1 subunit, a member of the integrin gene superfamily that function as a receptor for cell adhesion molecules of the extracellular matrix. Porcine integrin beta1 subunit is involved in rejection of pig-to-human tissue xenografts as target of the natural antibodies present in the human serum. Moreover since CD29, as part of the beta1 integrins very late antigen 4 (VLA-4) and VLA-6, is involved in homing and differentiation of haematopoietic progenitor cells, its characterization in pig is critical to study the interaction of porcine adhesion molecules with human ligands in the induction of donor-specific tolerance toward porcine antigens, a process extremely desirable to prevent rejection of xenogeneic organs. CD29 also exacerbates a broad tissue distribution including surface expression on leukocytes, endothelia, epithelia, and oocytes. Furthermore, cells exhibiting multipotential characteristics isolated from numerous adult tissues, such as bone marrow-derived MSCs, express high levels of CD29[297].

CD30 (FITC) (Monoclonal)	CD30 is a member of the tumour necrosis factor receptor (TNF) superfamily with a restricted pattern of tissue distribution, demonstrating expression only in immune cells, decidual tissue, and human embryonal carcinoma. In keeping with characteristics associated with other embryonal carcinoma markers, CD30 is expressed within foci of cells in a subpopulation of seminomas. CD30 exerts pleiotrophic effects on normal and malignant lymphoid cells including apoptosis and necrosis, differentiation and cell division. Investigations probing cultured cell lines derived from human embryonal carcinomas and yolk sac carcinomas demonstrated CD30 expression within embryonal carcinomas only, with CD30 expression down-regulated during stem cell differentiation *in vitro*[298].
CD31 (PE) (Monoclonal)	Also known as PECAM-1 (Platelet Endothelial Cell Adhesion Molecule-1), CD31 is a 130kDa integral membrane protein, a member of the immunoglobulin superfamily, which mediates cell-to-cell adhesion. CD31 is expressed constitutively on the surface of adult and embryonic endothelial cells and is also expressed on numerous peripheral leukocytes and platelets at low levels. It has also been detected on bone marrow-derived hematopoietic stem cells and ES cells. Functionally CD31 is involved in the transendothelial emigration of neutrophils, highlighted by the down regulation of neutrophil PECAM-1 following extravasation into inflamed tissues. Multiple alternatively spliced isoforms are detected during early post-implantation embryonic development; this alternative splicing is fundamental in the regulation of ligand specificity, with CD31-mediated endothelial cell-cell interactions key for progression of angiogenesis[299].
CD34 (Class II) (FITC) (Monoclonal)	Expression of the stem cell antigen CD34 is a defined characteristic of HSCs and their progenitor subsets. CD34 is therefore used as a marker for the enumeration, isolation and manipulation of HSCs. CD34 class II homologue is a 110kD glycoprotein and is predictably expressed on the surface of HSCs and capillary endothelial cells. Interestingly, a 2001 study identified that CD34 class III epitopes are more diversely projected on $CD34^+$ HSCs than CD34 Class II epitopes, and furthermore that a null expression of CD34 class II is observed in $CD34^+$ HSCs at a late stage of myeloid development[300].
CD34 (Class III) (FITC) (Monoclonal)	CD34 Class III is a 105kD glycoprotein expressed by HSCs and endothelial cells.
CD41a (PE) (Monoclonal)	CD41a reacts with a calcium-dependent complex of CD41/CD61 expressed on normal platelets and megakaryocytes. CD41/CD61 complex acts as a receptor for fibrinogen, fibronectin and von Willebrand factor, whilst furthermore regulating platelet adhesion and aggregation.

CD44 (PE) (Monoclonal)	CD44 is an 80-95kD glycosylated type I transmembrane protein which is also known as phagocytic glycoprotein-1 (Pgp-1). CD44 represents a receptor for hyaluronic acid and is expressed on leukocytes, erythrocytes, epithelial cells and to lesser extent platelets. CD44 is also called extracellular matrix receptor type III and demonstrates functional capacities with cell migration, lymphocyte homing and adhesion during hematopoiesis and lymphocyte activation. However, the ability of CD44 to act as a receptor for hyaluronic acid is a key regulator within the maintenance of plasticity, with hyaluronic acid binding inducing the upregulation of the Nanog, Stat-3-mediated MDR1 gene[301].
CD45 (FITC) (Monoclonal)	Contains 180kD, 190kD, 205kD and 200kD isoforms which are expressed on all human leukocytes including lymphocytes, monocytes, granulocytes, eosinophils, and thymocytes, though are absent from circulating erythrocytes, platelets, or mature erythroid cells of bone marrow and non-hematopoietic tissues. Functionally CD45 modulates signals emanating from integrin and cytokine receptors, whilst recent studies have focused on regulation of CD45 expression and alternative splicing, isoforms-specific differences in signal transduction, and regulation of phosphatise activity. Resultant from studies, a model is emerging in which CD45 affects cellular responses by modulating the relative threshold of sensitivity to external stimuli. Perturbation of this function may impact significantly within autoimmunity, immunodeficiency and malignancy[302].
CD50 (FITC) (Monoclonal)	CD50 comprises 110kD glycoprotein also known as ICAM-3, a transmembrane glycoprotein containing five immunoglobulin-like C2-type domains and a ligand for LFA-1. CD50 is expressed on a diverse range of leukocytes and demonstrates a functional capacity within leukocyte adhesion whilst additional acting as a signalling and co stimulatory molecule on T-lymphocytes.
CD56 (FITC) (Monoclonal)	CD56 is a single gene which is spliced to form numerous isoforms, most notably the 140kD isoform neural cell adhesion molecule (NCAM) present on natural killer (NK) lymphocytes. CD56 is expressed on approximately 10-25% of peripheral blood leukocytes, therefore in essence on all resting and activated $CD16^{+}$ NK lymphocytes and approximately 5% of CD3+ peripheral blood lymphocytes. Recent studies have demonstrated that NCAM is involved in multiple adhesive interactions with several classes of ligands present on the cell surface and in the extracellular matrix. One such ligand is fibroblast growth factor receptor (FGFR), which is expressed on neural cells. An investigation probing NCAM/FGFR interactions concluded that CD56 oversees within a functional capacity the interaction between NK cells and T cells[303].
CD62E (FITC) (Monoclonal)	Additionally known as E-selectin or endothelial-leukocyte adhesion molecule-1 (ELAM-1), CD62E is hypothesised to be involved in the regulation of neutrophils with inflamed endothelium, subsequent to experiments illustrating high levels of expression on cytokine-stimulated endothelium but to a significantly lower level on non-stimulated endothelium.

CD73 (PE) (Monoclonal)	CD73 is a glycosyl phosphatidylinositol (GPI)-anchored lymphocyte adhesion molecule possessing an ecto-5' nucleotidase enzyme activity. CD73 is expressed on subsets of T and B lymphocytes, follicular dendritic cells, epithelial cells and endothelial cells, cardiomyocytes, osteoblasts, trophoblasts, and MSCs[304]. CD73 lymphocyte expression increases significantly during T and B cell development, and engagement of CD73 increases lymphocyte binding to endothelial cells in an LFA-1-dependent manner[305].
CD81 (FITC) (Monoclonal)	CD81 is a 26kD cell surface antigen also named TAPA-1, and a member of the tetraspanin family. CD81 is widely expressed on human leukocytes and is hypothesised to function in numerous cellular processes, including adhesion, activation, proliferation and differentiation. Furthermore, CD81 is expressed on the surface of neural progenitor cells[306].
CD90 (FITC) (Monoclonal)	CD90 is a 25kD glycoprotein originally identified in mice and also known as Thy-1. However, proteins similar to Thy-1 are present in many species although the distribution of the antigen amongst hematopoietic cells varies considerably. In humans CD90 is expressed by some early T and B lymphocytes, fibroblasts, HSCs and MSCs, keratinocyte precursor cells[307]. However, whilst CD90 has been identified on numerous human cells, its functional relevance remains a mystery, although in mice CD90 functions as an adhesion molecule and has also been shown to initiate numerous neural signalling pathways in mice, particularly the inhibition of neurite outgrowth in mature astrocytes.
CD105 (FITC) (Monoclonal)	CD105 is a cell surface antigen consisting of a glycoprotein homodimer comprising 95kD subunits. Also known as endoglin, CD105 is expressed by endothelial cells, hMSCs, activated monocytes and some leukaemia cells. CD105 is an accessory receptor for members of the TGF-β superfamily, and a study in 2001 reported that during the differentiation of murine ES cells *in vitro*, hematopoietic commitment within $Flk1^+$ mesodermal precursor populations is characterised by expression of CD105. In particular, CD105 is expressed during the progression from the Flk^+CD45^- to $Flk\text{-}CD45^+$ stage. Thus, the developmentally regulated expression of CD105 suggests that it may contribute significantly during early hematopoiesis from $Flk1^+$ precursors[308].
CD106 (PE) (Monoclonal)	CD106 is a 110kD glycoprotein also known as vascular adhesion molecule-1 (VCAM-1), and is expressed at high levels on the surface of cytokine-stimulated endothelium, and at contrastingly minimal levels on unstimulated endothelium. VCAM-1 functions as a ligand for the leukocyte integrins α4β1 (CD49/CD29 complex). Furthermore, a recent study has highlighted VCAM-1 as a potential regulator of MSC migration in the context of wound healing[309].
CD117 (PE) (Monoclonal)	Also known as c-Kit, CD117 is a 145kD cell surface glycoprotein with tyrosine kinase activity. CD117 is expressed on HSC subsets, thymocytes, mast cells, hepatocytes and histiocytes, and functions as a cytokine receptor for stem cell factor (SCF), with this interaction fundamental to hematopoiesis, mast cell differentiation, melanogenesis, and germ cell development. Interestingly, CD117 is not expressed in cells expressing the pluripotent maintaining protein Oct4[310].

CD133 (PE) (Monoclonal)	CD133 is a 120kD glycosylated protein containing five transmembrane domains, and may provide an alternative to CD34 for selection of HSCs. Recent studies have demonstrated that CD133 is not limited to primitive blood cells, but instead defines unique cell populations in non-hematopoietic tissues. Interestingly, CD133+ progenitor cells from peripheral blood can be induced to differentiate into endothelial cells *in vitro*. More recently, CD133 has been used to positively select for neural progenitors derived from ES cells.[311]
CD135 (FITC) (Monoclonal)	CD135 is a 155-165kD, class III tyrosine kinase receptor which is structurally related to the receptors for PDGF, SCF-1 and kit ligand. CD135 is expressed on multipotent myelomonocytic and primitive B-cell progenitors, and highly primitive hematopoietic progenitor cells express low levels of CD135 as a functioning growth factor receptor.
CD146 (FITC) (Monoclonal)	Member of immunoglobulin superfamily, CD146 is a 118kD cell surface glycoprotein expressed by all endothelial cells and melanoma cells. Also known as MUC18, CD146 is a 118kD surface glycoprotein which has been used to isolate multipotent cells from bone marrow capable of adipogenic, chondrogenic and osteogenic differentiation[312].
CD166 (PE) (Monoclonal)	100-105kD transmembrane glycoprotein also known as leukocyte cell adhesion molecule (ALCAM), CD166 is composed of an immunoglobulin-like extracellular domain, a transmembrane region and a short cytoplasmic tail. CD166 belongs to the Ig superfamily and is expressed on neurons, activated T cells, activated monocytes, epithelial cells and fibroblasts, mediating adhesion interactions between thymic epithelial cells and $CD166^{+}$ cells during intrathymic T-cell development. Whilst exhibiting high levels of expression in MSCs derived from bone marrow, CD166 is present at significantly lower levels in freshly isolated adipose tissue-derived cells[313].
HLA-ABC (FITC) (Monoclonal)	HLA-ABC is also known as HLA-B27 and is detected on peripheral blood lymphocytes, precipitating cell surface molecules of 43kD and 12kD which correspond to the MHC-Class I heavy chain and beta 2 microglobulin. MHC-Class I impacts significantly in activating immune responses and is expressed on a range of cells including bone marrow-derived MSCs as well as multipotent cells derived from alternative sources[314].
HLA-DR (FITC) (Monoclonal)	HLA-DR is also known as MHC-Class II and is expressed by B lymphocytes, activated T cells and monocytes.
STRO-1 (PE) (Monoclonal)	STRO-1 is a surface glycoprotein and is widely used for the purification of multipotent cells from bone marrow and other tissues, with the frequency of CFU-F enriched approximately 100-fold following STRO-1 purification. $STRO\text{-}1^{+}$ enriched subsets are able to differentiate into mesenchymal lineages including hematopoiesis-supportive stromal cells with a vascular smooth muscle phenotype, adipocytes, chondrocytes and osteoblasts.

VWF (FITC) (Polyclonal)	VonWillebrand Factor (VWF) is a multimeric plasma glycoprotein synthesised by endothelial cells and megakaryocytes. In plasma, VWF circulates as multimers which range from dimmers of approximately 500kD to multimers of 20000kD, and functions as a transporter for Factor VIII and is a mediator of initial platelet adhesion to subendothelium and platelet-platelet interaction. Platelets bind to VWF via the platelet GPIb/IX and GPIIb/IIIa complexes. Abnormalities within VWF give rise to vonWillebrand disease (VWD) which generates a variety of bleeding conditions[315]
NGFR5 (FITC) (Monoclonal)	Nerve Growth Factor Receptor is the low affinity NGFR (LNGFR) which binds NGF and other neurotrophins. NGFR p75 is a transmembrane glycoprotein predominantly expressed in Schwann cells and neurons, regulating neuronal growth, migration, differentiation and cell death during development of the central and peripheral nervous system.

Table 2.3 - **Associated expression and functional comparison of surface markers used for phenotypic characterisation by flow cytometry.**

2.2.3 Processing of Raw Flow Cytometry Data using WinMDI Version 2.8

Following cell processing, acquired data was analysed using WinMDI Version 2.8. To calculate the percentage of cells demonstrating positive expression of a given antigen within the population, raw fluorescence binding values for the given antibody were compared with the corresponding isotype for that particular antibody within a histogram (*Figure 2.5*). Positive expression was calculated as fluorescence shifted to the right of the isotype control and quantified by assigning a marker to subtract fluorescence attributable to the isotype control and thereby homogeneously gate cells exhibiting positive expression. The number of events demonstrating positive expression was plotted.

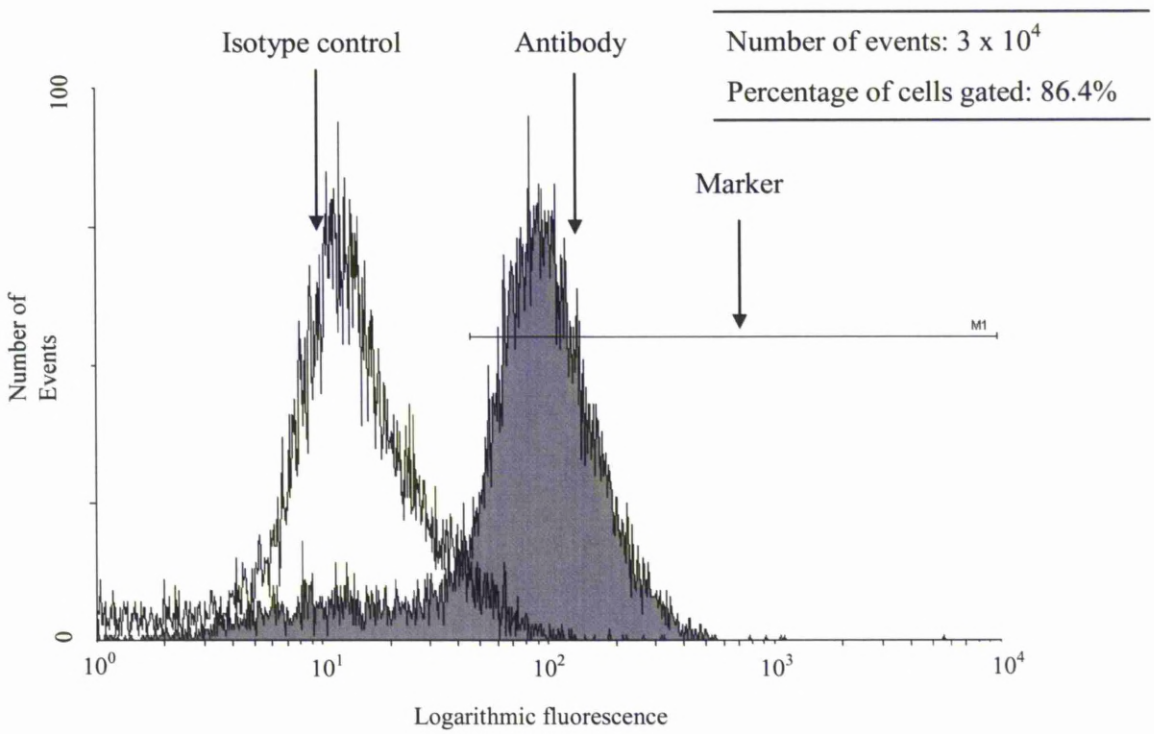

***Figure 2.5* - Calculation of positive expression of a given antigen within a cell population using WinMDI following analysis by flow cytometry.**

2.3 Cell Proliferation

2.3.1 Assessment of Proliferation using CyQUANT® Cell Proliferation Assay

Cells were assessed for their proliferation capacity over a defined culture period using CyQUANT® Cell Proliferation Assay Kit (Invitrogen; Cat#C7027). The underlying principle for the CyQUANT® kit is the utilisation of a proprietary green fluorescent dye, CyQUANT® GR, which exhibits strong fluorescence enhancement when bound to cellular nucleic acids. To carry out proliferative studies, cells were cultured as described in 2.1.7. Then, at the relevant time points, culture media was removed and cells washed with PBS prior to freezing at -80°C within the plastic culture vial until required. In order to generate controls for the proliferation study, cells identical to those required for analysis were enzymatically dissociated using Trypsin and pelleted as described in 2.1.7. Cells were resuspended in PBS and counted using a haemocytometer. Defined cell numbers were aliquoted into eppendorfs and centrifuged at 2000 x g for 5 minutes. The resultant supernatant was carefully discarded and pelleted cells frozen at -80°C until required.

On the day of the experiment, the concentrated cell-lysis buffer stock solution provided (Component B) was diluted 20-fold with distilled water to generate a 1x solution. Shortly before carrying out the experiment, the CyQUANT® GR stock solution (Component A) was diluted 80-fold in 1 x cell-lysis buffer to create a 5x solution.

To analyse frozen samples and controls, cells previously counted and subsequently frozen were thawed at room temperature. Counted cells were resuspended in 200µl of CyQUANT® GR/cell-lysis buffer solution via brief vortexing and transferred to an RNase-free 96 well microplate (Bio-Rad; Cat#223-9441). Cells were incubated for 5 minutes at room temperature in the absence of light and analysed using an FL_x800 microplate fluorescence reader in conjunction with a KC Junior operating platform (BIO-TEK Instruments). In order to generate a standard curve, fluorescent values for control samples of known cell number were plotted, generating a baseline on which to calculate cells present in given samples based on fluorescence.

2.4 Antibody-based Cell Purification

2.4.1 Mo-Flow High-speed Cell Sorting for the Purification of Cell Populations based on Surface Marker Expression or Emission of Hoechst 33342 Dye

Following phenotypic evaluation described in 2.2, cells were sorted based on their surface marker expression. Cells were removed from culture and labelled as described in 2.2.1. In addition, Hoechst 33342 (Invitrogen, Cat#H3570) was also used as a marker for the isolation of a residing side population (SP). In this case, cells were pelleted and resuspended as in 2.2.1. Hoechst 33342 was added to a final concentration of 5µg/ml and vortexed. Samples were incubated at 37°C for 90 minutes and agitated every 15 minutes, after which cells were centrifuged at 2000 x g for 5 minutes at 4°C and the pellet resuspended in a fresh 100µl volume of PBS. Cells stained with Hoechst or antibodies detailed in *Table 2.1* were analysed using a Mo-Flow high speed cell sorter (*Figure 2.6*). Selected populations were retained in pre-warmed basal media and transferred to a T-25 TC plastic flask containing basal media. Sorted cells were cultured at 37°C until required for further analysis.

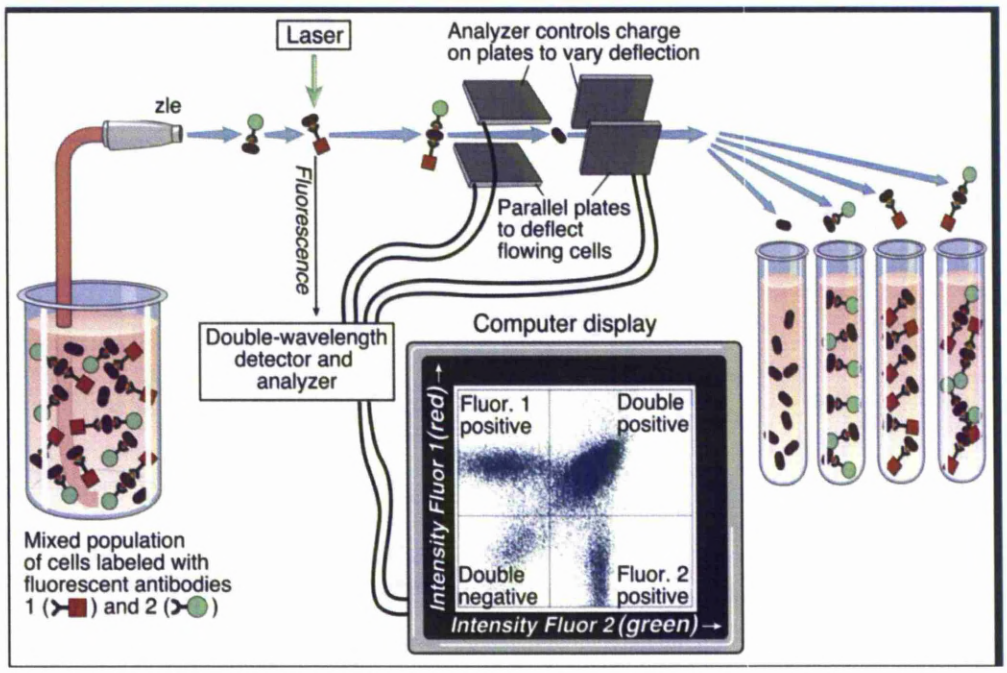

Figure 2.6 **- Diagrammatic representation of High-speed cell sorting using Mo-Flow. Image courtesy of Dr N. M. Ponzio, UMDNJ.**

2.5 Colony-Forming Unit Assays

2.5.1 Introduction

Within the adult human, hematopoietic and non-hematopoietic progenitor cells reside within numerous tissues. Such cells represent highly proliferative subpopulations capable of differentiation towards numerous lineages. With regards to hematopoietic progenitors, such cells differentiate into all mature blood cells. Non-hematopoietic progenitors have been demonstrated to form numerous functional cell types including adipocytes, chondrocytes, osteoblasts and tenocytes. *In vitro* assay systems have been developed to quantify hematopoietic and non-hematopoietic multi-potential progenitors and lineage restricted progenitors. Colony Forming Unit – Granulocyte Monocyte (CFU-GM) assays identify progenitors of the erythrocyte, granulocyte, monocyte-macrophage and megakaryocyte myeloid cell lineages, and Colony Forming Unit – Fibroblast (CFU-F) assays those of non-hematopoietic potential. Such assays represent semi-solid media with appropriate stimuli capable of inducing individual progenitors known as CFUs to proliferate and subsequently form discrete cell clusters or colonies. CFU assays were therefore undertaken using the methylcellulose-based Complete MethoCult media range, utilising CFU-GM (Stem Cell Technologies; Cat#28404) and CFU-F (Stem Cell Technologies; Cat#28374) assays accordingly.

2.5.2 Human Colony-Forming Cell Assays Using MethoCult®

When required, volumes of aliquoted CFU-GM or CFU-F MethoCult® media were thawed overnight under refrigeration (2-8°C). Culture dishes were prepared by placing two 35mm Petri dishes with lids inside a 100mm Petri dish with a lid. A third 35mm Petri dish without a lid was added containing distilled water in order to maintain humidity. This set of dishes represented one duplicate assay. Cultured cells were enzymatically dissociated using Trypsin and pelleted by centrifugation at 2000 x g for 5 minutes at 4°C. Pelleted cells were counted using a Haemocytometer and resuspended in IMDM media (GIBCO; Cat#21980065) with 2% (v/v) FCS and 1% (v/v) 10,000U/ml of penicillin and 10mg/ml of streptomycin in 0.9% (w/v) sodium chloride (Sigma-Aldrich; Cat#S7653) at 10x the concentration required for plating.

0.3ml of cell suspension was added to 3ml of pre-thawed MethoCult® media and the contents vortexed vigorously. Following a 5 minute incubation to allow dissipation of bubbles, 1.1ml of the cell containing methylcellulose solution was dispensed into each 35mm Petri dish. Media was distributed uniformly across each plate by gently tilting and rotating the dish to allow the meniscus to attach to the wall of the dish on all sides. 35mm Petri dishes were placed into the 100mm Petri dish and incubated at 37°C with 5% CO_2 and greater than 95% humidity for 14 days.

To establish CFU formation, cultures were monitored on a daily basis and imaged using transmitted light microscopy, with the number of colonies in 50 random image frames counted. The average number of colonies within an area of 250μM x 680μM were then ascertained and recorded.

2.6 Telomere Length Analysis

2.6.1 Assessment of Telomere Length by Flow Cytometry using Fluorescent *In Situ* Hybridisation and a Fluorescein-conjugated Peptide Nucleic Acid (PNA) Probe

The Telomere PNA Kit/FITC for Flow Cytometry (DAKO; Cat#K5327) provides an expedient method for detection of the telomeric sequences present in nucleated cells from vertebrates. The probes of this kit cease to recognise subtelomeric sequences, and in contrast to traditional telomere restriction fragment (TRF) measurements, the DAKO kit, therefore, allows an estimation of the telomere length without inclusion of subtelomeres. The kit is deliberately designed to ensure that post-hybridisation treatments are kept to a minimum and formaldehyde washes are avoided. The probe of the kit recognises telomeric repeats, although intrachromosomal TTAGGG repeats are also measured within the fluorescent signal. However, examination of the literature demonstrates that whilst prevalence of non-telomeric TTAGGG sequences varies, they were found to be few and short using the sensitive Q-FISH method with a PNA probe. These data, in conjunction with closely correlated Southern blotting, support the idea that intrachromosomal telomere sequences are of minimal significance for the total hybridisation signal detected by flow cytometry.

In order to assess telomere lengths, cultured cell populations were washed with PBS and enzymatically dissociated via incubation with Trypsin for 15 minutes at 37°C. Following centrifugation at 2000 x g for 5 minutes at 4°C, cells were counted using a Haemocytometer. For each sample, 2 x 10^6 test cells and 2 x 10^6 control cells were aliquoted into two 30ml universal tubes. 6ml of PBS were added to each tube and resuspended cells divided into 4 x 1.5ml aliquots (1 x 10^6 cells) and placed into 1.7ml microcentrifuge tubes. Cells were centrifuged at 500 x g for 5 minutes and the supernatant discarded. To the control cells, 300µl of Hybridisation solution were added, whilst 300µl of Telomere PNA Probe/FITC solution were added to the test cells and vortexed. The four solutions were placed in a pre-warmed heating block at 82°C for 10 minutes. Cells were vortexed and incubated at room temperature overnight in the absence of light. Post-incubation, 1ml of Wash Solution (1:10 dilution) was added to each of the four tubes and vortexed. Tubes were placed in a pre-warmed heating block at 40°C for 10 minutes and vortexed. Following centrifugation at 500 x g for 5 minutes and decanting of the supernatant, 1ml of Wash Solution (1:10 dilution) was added to each tube and vortexed. Tubes were again incubated in a pre-warmed heating block at 40°C for 10 minutes and vortexed prior to centrifugation at 500 x g for 5 minutes. Following discarding of the supernatant, samples were treated in a 2mg/ml Propidium iodide solution for 15 minutes at 4°C. Samples were then spun at 500 x g for 5 minutes at 4°C and resuspended in 100µl of PBS. Samples were transferred to flow cytometry analysis tubes and vortexed prior to incubation for 5 hours at 4°C in the absence of light. Post-incubation, samples were analysed using a Becton Dickinson FACSort with Cell Quest software. Quantum FITC MESF beads (Bangs Laboratories; Cat#824), which allowed for the direct quantification of FITC content within a sample in terms of number of molecules or equivalent soluble fluorochrome (MESF), were used as quantitative controls.

2.6.2 Analysis of DNA Labelled using Fluorescent *In Situ* Hybridisation and a Fluorescein-conjugated PNA Probe

Following cell processing, acquired data was analysed using WinMDI Version 2.8. Generation of a standard curve by plotting the MESF (y-axis) against the peak channel (x-axis) for each of the four fluorescence intensity populations provided in

the Quantum FITC MESF beads kit allowed a baseline on which to quantify telomere lengths. To analyse results obtained using the PNA/FITC probes, all cells not cycling within the $G_{0/1}$-phase of the cell cycle were excluded as to ensure analysis assessed single copy DNA possessing cells only. Fluorescence projecting above that detected in the sample containing hybridisation solution without the PNA probe, a solution which essentially provided an isotype, was noted. Positive fluorescence and MESF values were noted and Bangs QuickCal software (Bangs Laboratories) used to calculate telomere lengths.

2.7 Lineage Induction of Cell Populations

2.7.1 Differentiation of Cells towards Committed Lineages using Commercially Available Media

For differentiation of hMSCs, umbilical cord and dental pulp-derived cells, cultured cells were enzymatically dissociated from the tissue culture polystyrene and centrifuged at 2000 x g for 5 minutes at 4°C. Pelleted cells were resuspended in a lineage induction media at a seeding density dependent on cell type for 28 days. For hMSCs and umbilical cord-derived cells, a density of 5 x 10^4 cells per well of a 24 well plate TC plastic plate were seeded. For dental pulp, a seeding density of 3 x 10^3 cells was used within the same substrate. For differentiation of peripheral blood-derived cells, populations isolated as described in 2.1.2/2.1.3 were cultured in basal media for approximately 7 days. Upon attaining 70-80% confluence, induction media was added to the culture and maintained for 28 days.

To induce adipogenic differentiation, cells were cultured for 10 days in pre-adipocyte growth media (Promocell; Cat#C-27410) with supplement (Promocell; Cat#C-39425) comprising 0.4% (v/v) ECGS/H, 5% (v/v) FCS, 10ng/ml Epidermal growth factor and 1µg/ml hydrocortisone. After 10 days, cells were transferred to pre-adipocyte differentiation media (Promocell; Cat#C-27436) with supplement (Promocell; Cat#C-39436) containing 8µg/ml d-Biotin, 0.5µg/ml bovine Insulin, 400ng/ml dexamethasone, 44µg/ml IBMX, 9µg/ml L-Thyroxine and 3µg/ml ciglitazone. Following 72 hours in pre-adipocyte differentiation media, cells were maintained for 15 days in adipocyte nutrition media (Promocell; Cat#C-27438)

containing 0.003% (v/v) FCS, 8µg/ml d-Biotin, 0.5µg/ml recombinant human Insulin and 400ng/ml dexamethasone.

For chondrogenic lineage induction, cells were resuspended in DMEM (High glucose) (GIBCO; Cat#10313039) supplemented with 1% (v/v) ITS premix (contains 0.5mg/ml Insulin from bovine pancreas, 0.5mg/ml human transferrin and 0.5µg/ml sodium selenite) (Biotrace; Cat#354351), 100mM Ascorbate-2-Phosphate, 100nM dexamethasone, 1% (v/v) FCS and 10mg/ml TGF-β1 (R&D Systems; Cat#240-B-002/CF).

For osteogenic differentiation, cells were cultured in DMEM (Low glucose) (GIBCO; Cat#10567014) supplemented with 10% (v/v) FCS, 100mM Ascorbate-2-Phosphate, 100nM dexamethasone and 10mM β-glycerophosphate.

To induce neural differentiation, cells were resuspended in basal media supplemented with 1% (v/v) retinoic acid (Sigma-Aldrich; Cat# R2625).

2.7.2 Differentiation of Cells towards Committed Lineages using Chemically Defined Media

Cultured cells were dissociated from culture and pelleted as described in 2.7.1. On this occasion, however, cells were cultured in serum-free, chemically-defined media synthesised specifically to generate conditions for the maintained proliferation of cells in an undifferentiated state (basal media) or differentiation towards adipogenic, chondrogenic, osteogenic, neuronal and hepatic phenotypes.

2.7.3 Differentiation of Hoechst SP Sorted cells Towards an Endothelial Lineage using Human Plasma-based Gels

Cells isolated based on Hoechst 33342 (Invitrogen; Cat#H3570) expression, as described in section 2.4.1, were seeded on a human plasma based gel. Gels were synthesised following the isolation of human peripheral blood from the median cubital vein of donors and subsequent prevention of coagulation using 10% (v/v) 10mM sodium citrate, which inhibited clotting by chelation of Ca^{2+}. Anticoagulated

blood samples were incubated at room temperature for 2 hours prior to a further incubation overnight at 4°C. This overnight incubation caused separation of the blood cells and blood plasma to generate two distinct fractions. Blood fractionation was further enhanced by centrifugation at 700 x g for 10 minutes at 4°C. Following collection of the supernatant, the blood pellet was discarded and the retained supernatant subjected to a further centrifugation at 700 x g for 5 minutes at 4°C in order to ensure complete removal of residual red blood cells, white blood cells and platelets. Purified plasma was frozen at -20°C until required.

When required, frozen plasma was thawed at room temperature and subsequently pre-warmed to 37°C. At the same time culture media, which would replenish the chelated Ca^{2+} content and therefore re-establish conversion of prothrombin (factor II) to thrombin (factor I) and subsequently production of fibrin, was prepared and pre-warmed to 37°C. In this case, DMEM (High glucose) (GIBCO; Cat#10313039) was combined with 1% (v/v) 10,000 U/ml penicillin and 10mg/ml streptomycin in 0.9% (w/v) sodium chloride (Sigma-Aldrich; Cat#S7653). DMEM was used as a basal media for the routine culture and maintenance of human cells using the hydrogel system. The blood plasma fraction was added to the basal media at a concentration of 10% (v/v) and returned to 37°C, in a humidified atmosphere, containing 5% CO_2. After approximately 3-5 minutes of incubation a stable hydrogel formed as a result of combination of the two solutions. Gels were generally cast 3mm in thickness unless gels of a greater thickness were required for a particular investigation.

Cultured Hoechst 33342 side populations were trypsinised and pelleted as described in section 2.1.7. Cells were then introduced to the plasma in one of two ways: (i) Trypsinised cells were transferred to the fluid plasma and vortexed. The cell seeded plasma was distributed among the desired culture vials and incubated at 37°C until solidified; (ii) Plasma was distributed directly into culture vessels and allowed to solidify at 37°C. Cells were resuspended in a culture media and administered to the surface of the gel. In this case, cells were cultured in 199 Media (GIBCO; Cat#12350039). Cells were cultured at 37°C for 28 days.

2.8 Immunohistochemistry

2.8.1 Controls for Immunofluorescent Staining

In order to establish a positive control for immunofluorescent investigations and furthermore optimise staining, cells known to express a given protein were stained with serial dilutions of the primary and secondary antibody (*Figure 2.7*). Cells known not to express the given protein were also stained in order to establish a negative control. Controls to assess the extent of non-specific binding and hence fluorescence of secondary antibodies were carried out by replacing primary antibodies with PBS.

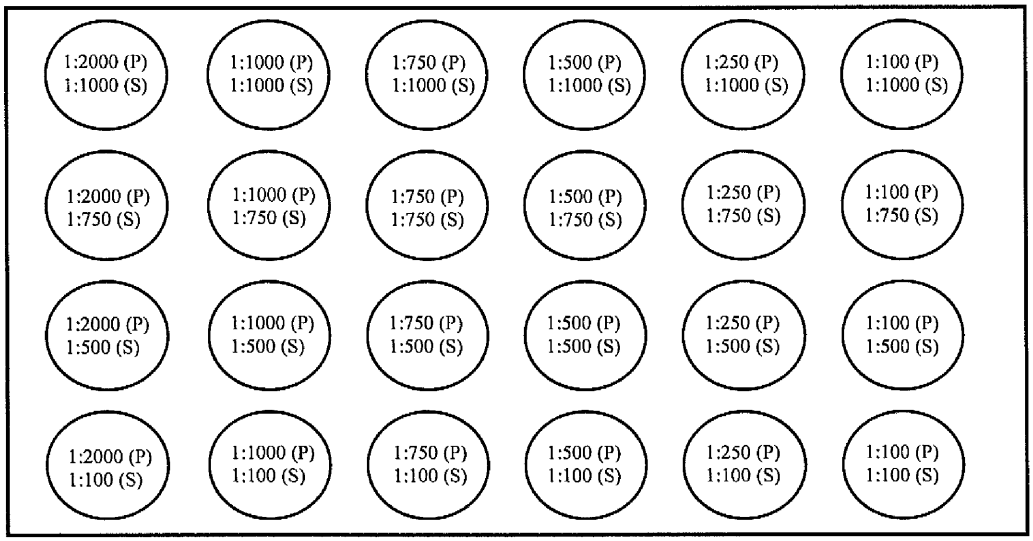

***Figure 2.7* – Serial dilution assay of primary/secondary antibody with cells known to express (positive control) or not to express (negative control) a given protein. P – Primary antibody; S – Secondary antibody.**

2.8.2 Immunofluorescent Staining of Differentiated and Undifferentiated Cells

Samples cultured on 13mm TC polystyrene coverslips (Sarstedt; Cat#83.1840.002) were fixed through incubation with a solution containing 4% (v/v) formaldehyde and 2% (w/v) sucrose for 15 minutes at 37°C. Post-fixation, samples were washed in PBS and seeded cells permeabilised by exposure to a 0.005% (v/v) solution of Triton-X100 (Sigma-Aldrich; Cat#X-100) for 5 minutes at 4°C. Following a rinse in PBS at room temperature, the primary antibody (*Table 2.4, Table 2.5*), diluted accordingly with 1% (w/v) BSA, was added to the sample and incubated for 1 hour at 37°C. Post-

incubation samples were rinsed with a 0.1% (v/v) Tween-20 (Sigma-Aldrich; Cat#P9416) solution for 5 minutes at room temperature and incubated with a corresponding secondary antibody (diluted accordingly with 1% (w/v) BSA) (*Table 2.6*) for 1 hour at 37°C. Stained samples were washed with a 0.1% (v/v) Tween-20 solution and incubated with Oregon Green® 488 Phalloidin (Invitrogen; Cat#O7466) (diluted to appropriate working concentration with distilled water) for 30 minutes at 4^0C, after which samples were washed in PBS for 5 minutes and mounted using Vector Shield with DAPI (Vector Laboratories; Cat#H-1200) or Vector Shield (Vector Laboratories; Cat#H-1000) with TO-PRO-3 (Invitrogen; Cat#T3605) added at a concentration of 0.001% (v/v). Mounted samples were imaged using laser-scanning confocal microscopy.

For particular applications, a second primary antibody raised within a different species to the first was added to illustrate combined expression of two distinct proteins in a given cell. In such instances, the incubation of samples with Oregon Green® 488 Phalloidin was discarded and samples were instead washed with 0.1% (v/v) Tween-20 solution and subjected to 1 hour incubation at 37°C with the second primary antibody diluted accordingly with 1% (w/v) BSA. Following a rinse with 0.1% (v/v) Tween-20 solution, samples were incubated with a corresponding secondary antibody presenting an alternative fluorochrome than the initial stain (diluted accordingly with 1% (w/v) BSA) and incubated for 1 hour at 37°C.

1° Antibody (Unconjugated) (Clonality)	Host Species	Target Species	Cross Reactivity	Working Dilution	Supplier	Catalogue Number
Adiponectin (M)	Mouse	Human	Mouse	1:500	Abcam	ab22554
α-feto-protein (M)	Mouse	Human	None reported	1:100	Abcam	ab3980
Aggrecan (M)	Mouse	Human	Cow	1:500	Abcam	ab3778
Beta-III-Tubulin (M)	Mouse	Human	Mouse, Rat	1:1000	Abcam	ab77060
CBFA-1 (M)	Mouse	Human	None reported	1:1000	R&D Systems	MAB2006
CHOP (M)	Mouse	Human	None reported	1:500	Alexis Biochemicals	ALX-804-551
CD31 (M)	Mouse	Human	Mouse, Rat	1:100	Abcam	ab24590
Collagen I (M)	Mouse	Human	Rat, Cow, Dog, Pig, Rabbit Rhesus Monkey	1:2000	Abcam	ab6308
Collagen II (M)	Mouse	Human	None reported	1:1000	Serotec	2150-0040
Collagen X (M)	Mouse	Human	Rat, Cow, Dog, Pig, Rabbit	1:500	Abcam	ab6308
Cripto-1 (P)	Rabbit	Human	Mouse	1:500	Abcam	ab19917
GFAP (M)	Mouse	Human	None reported	1:500	Abcam	ab7806
KLF4 (M)	Mouse	Human	None reported	1:500	Abcam	ab56542
Leptin (P)	Rabbit	Human	None reported	1:1000	Abcam	ab9826
Nestin (M)	Mouse	Human	None reported	1:500	Abcam	ab22035
Neurofilament (M)	Mouse	Human	Rat, Chicken	1:1000	Abcam	ab24573
NGF (P)	Sheep	Human	Mouse, Rat, Bird	1:500	Abcam	ab24486
Nucleostemin (M)	Rat	Human	Mouse, Rat	1:500	R&D Systems	AF1638
MITF (M)	Mouse	Human	Mouse, Rat	1:1000	Abcam	ab12039
Oct4 (P)	Goat	Human	Mouse	1:500	Abcam	ab27985
Osteocalcin (M)	Mouse	Human	None reported	1:1000	R&D Systems	MAB1419
p75 (M)	Mouse	Human	Cat, Pig	1:500	Abcam	ab10495
Pax6 (P)	Rabbit	Human	Mouse, Rat, Sheep	1:1000	Abcam	ab51358
Perilipin (P)	Rabbit	Human	Mouse	1:250	Abcam	ab3572
PPAR-γ (M)	Mouse	Human	None reported	1:500	Abcam	ab52270
REST4 (M)	Mouse	Human	None reported	1:750	Abcam	ab52850
S100 (M)	Mouse	Human	Mouse, Rat, Cow, Pig	1:500	Abcam	ab7852
Serum Albumin (P)	Rabbit	Human	None reported	1:100	Abcam	ab2406
Sox2 (P)	Rabbit	Human	Mouse, Rat, Chicken	1:500	Abcam	ab15830
STRO-1 (M)	Mouse	Human	None reported	1:1000	R&D Systems	MAB1038
Substance P (M)	Mouse	Human	Rat, Guinea pig	1:500	Abcam	ab14184
Synaptic Vesicle Protein2 (M)	Mouse	Human	None reported	1:1000	Novocastra Laboratories	NCL-SV2
Synaptophysin (M)	Mouse	Human	Mouse, Rat, Cow, Hamster	1:500	Abcam	ab8049
TBR2 (M)	Mouse	Human	None reported	1:1000	Millipore	MAb5668
Tra-1-81 (M)	Mouse	Human	None reported	1:1000	Abcam	ab16289
VE-Cadherin (M)	Mouse	Human	None reported	1:250	Abcam	ab7047

Table 2.4 **- Primary antibodies used for immunofluoresence. Clonality: M – Monoclonal; P – Polyclonal.**

1° Antibody (Unconjugated) (Clonality)	Mechanistic function and cell associated expression
Adiponectin (Monoclonal)	30kD protein transcribed from Acrp30 gene, adiponectin is a circulating protein secreted exclusively by terminally differentiated adipocytes. Transcribing mRNA is induced more than 100 fold during adipogenesis, with generated adiponectin enhancing the ability of insulin to suppress glucose production at sub physiological levels, thereby associating adipose tissue to whole body glucose regulation. Adiponectin production is regulated by phosphatidylinositol-3-kinase and is significantly down-regulated within the adipose tissue of obese patients prescribing type II diabetes. Adiponectin spontaneously self-associates into larger structures. Initially three adiponectin molecules combine forming a heterotrimer, with the resulting trimers continuing self-association and consequentially generating hexamers or dodecamers. Whilst the full role of physiologically active forms of adiponectin and methods of regulation is at present vague, it is known that adiponectin exerts some weight regulatory activities via neurological means[316-319].
α-feto-protein (Monoclonal)	Encoded by the AFP gene, α-feto-protein is a plasma protein produced in the fetal yolk sac and liver and is hypothesised to be the fetal counterpart of serum albumin. Positioned on chromosome 4, α-feto-protein is present in monomeric, dimeric and trimeric forms, and binds copper, nickel, fatty acids and bilirubin. Post-natally α-feto-protein levels progressively decline and achieve levels found within adults by 8 to 12 months post birth. Levels of α-feto-protein within normal adults are low though are detectable, although peculiarly exerts no function, with higher levels in adults associated with hepatocellular carcinoma and endodermal sinus tumours. However, hereditary persistence of α-feto-protein has also been detected in individuals displaying no apparent pathology. Within normal fetuses, α-feto-protein binds the hormone estradiol, and levels within amniotic fluid of pregnant women are closely monitored as a screening test for a subset of developmental abnormalities, with high levels principally associated with open neural tube defects and omphalocoele. Lower levels of α-feto-protein are commonly a marker of Down's syndrome[320-324]. A recent investigation has reported the expression of α-feto-protein in bone marrow-derived MSCs induced towards a hepatic lineage[325].
Aggrecan (Monoclonal)	Highly expressed within articular cartilage, Aggrecan is a proteoglycan consisting of 2316 amino acids which can be expressed as numerous isoforms due to alternative splicing. Aggrecan is composed of three major domains, namely G1, G2 and G3. Residing within the G1 and G2 domains is an interglobulin region which acts as a major site of cleavage by specific proteases such as metalloproteinase and aggrecanase, with such cleavage being associated with numerous diseases including rheumatoid arthritis and osteoarthritis. Aggrecan is therefore indicative of chondrogenic differentiation[326].

Beta-III-Tubulin (Monoclonal)	Abundant within central and peripheral nervous systems (CNS and PNS), beta-III-tubulin is prominently expressed during fetal and postnatal development. As exemplified in cerebellar and sympathoadrenal neurogenesis, distribution of beta-III-tubulin is neuron-associated, exhibiting temporospatial gradients according to the regional neuroepithelia of origin. However, transient expression of beta-III-tubulin is also observed within the subventricular regions of the CNS comprising putative neuronal and/or glial precursor cells[327-332].
CBFA-1 (Monoclonal)	Transcription factor fundamental within osteogenesis and skeletal morphogenesis, CBFA-1 is a member of the RUNX family of transcription factors and contains a Runt DNA-binding domain. CBFA-1 essentially acts as a scaffold for nucleic acids and regulatory factors involved within skeletal gene expression[333-335] and recent studies have suggested that this master regulator of osteogenesis may act as a repressor of early stem cell markers such as hTERT, thereby influencing resulting cellular fate[336].
CHOP (Monoclonal)	C/EBP homologous protein (CHOP) is responsible for the repression of adipogenesis *in vitro*. Contrarily CHOP is also responsible for the induction of osteogenesis, with CHOP null mice exhibiting decreased bone formation and impaired osteoblastic function. CHOP proteins contain a highly conserved DNA binding domain and a leucine zipper dimerisation domain, allowing the formation of homo- and hetero-dimers capable of binding specific sequence motifs. CHOP is expressed in numerous cell types including adipocytes and osteoblasts, within the latter interacting with CBFA-1 to activate osteocalcin activity[337].
CD31 (Monoclonal)	See Table 6.
Collagen I (Monoclonal)	Collagen I, a transcriptional product of Col1A1 or Col1A2, is the most abundant collagen present within the adult human, predominantly expressed in tendons, skin, artery walls, endomysium of myofibrils, fibrocartilage, and the organic sections of bones and teeth. Irregular expression levels can result in conditions such as osteogenesis imperfecta, Ehlers-Danlos syndrome and infantile cortical hyperostosis. MSCs induced towards a chondrogenic lineage express high levels of collagen I during initial stages of chondrogenesis, although collagen I production is replaced with collagen II during the latter stages of differentiation [338-340].
Collagen II (Monoclonal)	Collagen II denotes a fibrillar collagen located within cartilage and vitreous humor of the eye, and is essential for normal embryonic development of the skeleton, in particular for linear growth and allowing cartilage to exhibit an ability to resist highly compressive forces. Mutations within Col2A1, the gene transcribing Collagen II, are associated with achondrogenesis, chondrodysplasia, early onset family osteoarthritis, SED congenita, Langer Saldino achondrogenesis, Kniest dysplasia, Stickler syndrome type I, and spondyloepimetaphyseal dysplasia. During *in vitro* induction of chondrogenesis of MSCs, collagen II production coincides with ceasing of collagen I expression[341-343].

Collagen X (Monoclonal)	Highly expressed by hypertrophic chondrocytes during endochondral ossification. Mutations within the collagen X gene are associated with Schmid type metaphyseal chondrodysplasia (SMCD) and Japanese type spondylometaphyseal dysplasia (SMD).
Cripto-1 (Polyclonal)	Epidermal growth factor which performs an obligatory role as co-receptors for the TGF-β family of proteins during embryogenesis. Expression of Cripto-1 is increased in several human cancers with overexpression associated with the development of mammary tumours in mice. More recently, the Cripto-1 translating gene CR-1 has been identified as a direct target within a canonical Wnt/β-catenin/Tcf signalling pathway, a pathway fundamental within the promotion of stem cell renewal, pluripotency and guided differentiation[344].
GFAP (Monoclonal)	Glial Fibrillary Acidic Protein (GFAP) is a member of the class III intermediate filament family of proteins which synthesise networks alleviating support and strength to cells. GFAP is highly expressed in astrocytes and certain other astroglia within the central nervous system (CNS), in satellite cells within the peripheral ganglia, and non-myelinating Schwann cells in peripheral nerves. Furthermore, neural stem cells frequently express high levels of GFAP. Although its specific function is not fully understood, GFAP is hypothesised to be involved within regulation of morphology, motility, and function of astroglial cells, whilst also functioning within cell communication and regulation of the blood-brain barrier.
KLF4 (Monoclonal)	Kruppel-like factor 4 is a transcription factor that is proposed to function within the differentiation of epithelial cells and may also regulate progression of kidney and skeletal development. KLF4 has roles as both an oncogene and a tumour repressor and introduction into terminally differentiated cells has demonstrated it possesses a capacity to induce iPS[150,345-346].
Leptin (Polyclonal)	Expressed in adipocytes, leptin is an adipocyte hormone that functions as the afferent signal in a negative feedback loop regulating overall body weight. Furthermore, leptin forms a key link between nutrition and the function of most, if not all other physiologic systems. Defects within leptin production induce severe hereditary obesity in rodents and humans. In addition to its role within maintenance of body weight, leptin incorporates a variety of other functions, including regulation of hematopoiesis, angiogenesis, neurogenesis, wound healing, and the immune and inflammatory responses[347-350].
MiTF (Monoclonal)	Microphthalmia-associated Transcription Factor (MiTF) is reported to play a crucial role in regulating the differentiation of pigment cells such as melanocytes and RPE via modulating the expression of major melanogenic proteins such as tyrosinase and the tyrosinase-related proteins TRP1 and TRP2. Mice bearing null alleles of the MiTF gene display complete loss of neural crest-derived melanocytes, deafness and a failure of RPE differentiation[351,352].

Nestin (Monoclonal)	Nestin is a Class VI intermediate filament expressed in dividing cells within the developing central nervous system (CNS), PNS and in myogenic and other tissues. Upon differentiation, nestin is downregulated and replaced by tissue-specific intermediate filament proteins such as GFAP. Expression is further associated with neuronal stem and progenitor cells, glioma cells, and tumour endothelial cells in the mammalian CNS.
Neurofilament (Monoclonal)	Neurofilaments usually detail three intermediate filament proteins: L and M (160kD), and H (200kD), which are involved in the maintenance of neuronal caliber. 200kD neurofilament preserves an important role within mature thick and thin axons, and also some dendrites such as basket cell dendrites, that are not subserved by the two smaller proteins.
NGF (Polyclonal)	Nerve growth factor (NGF) is a member of a neurotrophin family which induce survival and proliferation of neurons. *In vitro*, NGF induces the formation of neurite projections and, *in vivo*, may stimulate the innervations of tissues. Furthermore, NGF functions within the repair, regeneration, and projection of neurons, and could therefore represent a therapeutic agent within neurodegenerative disorders such as Alzheimer's disease[353].
Nucleostemin (Monoclonal)	Nucleostemin is a protein concentrated in the nucleolus of the majority of stem cells and also in numerous tumour cells, being implicated in cell-cycle progression owing to its ability to modulate p53. Targeted deletion of nucleostemin within the mouse results in developmental arrest at the implantation stage, indicating that nucleostemin is crucial for early embryogenesis[354-356].
Oct4 (Polyclonal)	The POU homeodomain transcription factor Oct4 (Pou5f1) is an essential mediator of plasticity, lineage specific differentiation, adult stem cell identity, and cancer, functioning via combinatorial activation of genes required to maintain self-renewal and pluripotency while concomitantly repressing genes which facilitate lineage specific differentiation. Initial thoughts that this protein was restricted to undifferentiated ES and EG cells have been challenged subsequent to reports detailing its expression in adult-derived stem cells[92,94,97,183,222,277,357].
Osteocalcin (Monoclonal)	A non-collagenous protein constituting 1-2% of total bone protein, osteocalcin is a 49 amino acid single chain vitamin K dependent protein secreted by osteoblasts, Post translational modification by vitamin K dependent carboxylase generates three gamma carboxyglutamic acid residues at positions 17, 21 and 24, inducing a high affinity for calcium and apatite and thereby facilitating a fundamental role within mineralisation and calcium ion homeostasis. In 2007 it was reported that osteocalcin acts as a hormone, stimulating beta cells in the pancreas to upregulate insulin synthesis which concomitantly directs adipose cells the generate adiponectin, thereby increasing insulin sensitivity[358].

P75 (Monoclonal)	Also known as Nerve Growth Factor Receptor (NGFR) p75 is a receptor for the neurotrophins NFG, Brain-Derived Neurotrophic Factor (BDNF), Neurotrophin-3 (NT-3) and Neurotrophin-4/5 (NT-4/5). P75 is predominantly expressed in Schwann cells and neurons although has been detected in non-neuronal cells. Whilst the absence of an inherent enzyme activity within the cytoplasmic domain of the molecule has hindered characterisation of p75 signalling, it is thought that p75 plays a fundamental role within the regulation of neuronal growth, migration, differentiation and cell death during development of the CNS and PNS. Within rat Schwann cells, NGF association with p75 has been demonstrated to activate NF-κB, possibly modulating Schwann cell migration during nerve development. Furthermore p75 expression has been detailed in murine MSCs[359-362].
Pax6 (Polyclonal)	Transcription factor fundamental within developmental regulation of the eye, nose, central nervous system and pancreas. Activated by Six3, Pax6 regulates the earliest stages of mammalian lens induction, with mutations in Pax6 giving rise to disorders such as human aniridia, Peter's anomaly, and congenital cataracts [363-364].
Perilipin (Polyclonal)	Predominantly located at the surfaces of lipid droplets in adipocytes, members of the perilipin family are also found in steroidogenic cells. The predominant perilipin isoform, perilipin A, increases the triacylglycerol content of cells via formation of a barrier that reduces the access of soluble lipases to store lipids, thereby inhibiting triacylglycerol hydrolysis[365].
PPARγ (Monoclonal)	Peroxisome proliferators are non-genotoxic carcinogens which are purported to infer functionality within cells via their interaction with Peroxisome Proliferator-Activated Recptors (PPARs). PPARα, PPARβ and PPARγ have thus far been identified and, via alternative splicing, PPARγ transcribes into three distinct forms: PPARγ1 which is expressed in virtually all tissues including heart, muscle, colon, kidney, pancreas, and spleen; PPARγ2 which is expressed in adipose tissue, though is 30aa longer than PPARγ1; PPARγ3 which is expressed in macrophages, large intestine, and white adipose. The PPARγ2 isoform appears to be induced within the premature stages of differentiation in numerous adipocyte cell lines, and is hypothesised to be a dominant regulator of the murine P2 (aP2) gene which encodes an intracellular lipid binding protein expressed solely within adipocytes. Alike numerous other hormone receptors, PPARγ2 heterodimerisers with RXRα, with defects in PPARγ potentially resulting in type-II-insulin resistant diabetes and hypertension, whilst furthermore perhaps contributing towards genetic predispositions to obesity.
REST4 (Monoclonal)	RE1 silencing transcription factor, also known as neuron-restrictive silencing factor (NRSF), is a key regulator of neuron-specific gene expression, essentially silencing neuron-associated genes in non-neuronal tissues. Within neuronal cells, a truncated, neuronal specific REST/NRSF isoform, REST4, is hypothesised to inactivate the neuronal silencing properties of REST/NRSF via competitively binding the BDNF promoter, a major silencing target for REST/NRSF, and thereby allowing neuronal induction following exposure to appropriate stimuli[366-368].

S100 (Monoclonal)	The S100 family of calcium binding proteins contains approximately 16 members each of which exhibits a unique pattern of cell associated expression. Predominantly expressed within the nervous system, S100 proteins are predominantly expressed within neuronal cells, with *in vitro* reports detailing cytoplasmic and nuclei expression within astrocytes, Schwann cells, ependymomas and astrogliomas. The originating members of the S100 family, S100α and S100β, function diversely, alleviating roles in cell-cell communication, cell growth, cell structure, energy metabolism, contraction and intracellular transduction[369-371].
Serum Albumin (Polyclonal)	The most abundant protein in human blood plasma, serum albumin is produced by hepatocytes and is functionally responsible for maintenance of osmotic pressure required for accurate distribution of body fluids. Serum albumin further functions as a plasma carrier via non-specifically binding several hydrophobic steroid hormones, and as a transport protein for hemin and fatty acids. Serum albumin is initially synthesised as preproalbumin which has an N-terminal peptide that is cleaved subsequent to release of the nascent protein through the endoplasmic reticulum. The product, proalbumin, is in turn leaved within the Golgi vesicles to generate secreted serum albumin.
Sox2 (Polyclonal)	Sox2 is a co-regulator within maintenance of plasticity in both developing embryo and adult stem cells, functioning in collaboration with other factors such as Oct4 and Nanog to prevent lineage commitment of cells. Sox2 is hypothesised to synergistically function with Oct4 to generate Oct-Sox enhancers that regulate numerous pluripotent maintaining and lineage inducing pathways. Predictably null mutations of Sox2 result in embryonic lethality due to an inability to maintain pluripotency and subsequent guided differentiation. With regards iPS cells, Sox2 is a key inducing agent required for reprogramming of somatic cells, further indicating its requirement to establish and maintain plasticity[84,93-94,96,104,141,143,147,149-151,346,372-376].
STRO-1 (Monoclonal)	STRO-1 is widely used for the purification of stem cell populations, being expressed by numerous stem and progenitor populations. Whilst little is known with regards its function, cells expressing STRO-1 are often capable of differentiating into numerous mesenchymal lineages[203,214,377-378].
Substance P (Monoclonal)	A member of the tachykinin neuropeptide family, substance P (SP) is hypothesised to function as a transmitter of pain information to the CNS, although is also thought to play key roles within cellular growth *in vitro*, regulation of vasodilatation, and promotion of wound healing. SP is expressed in neuronal cells, although reports have also detailed expression in articular chondrocytes and platelets, functioning via interactions with the NK1 receptor in autocrine and paracrine manners[379-382].
Synaptic Vesicle Protein 2 (Monoclonal)	Synaptic vesicle protein 2 (SV2) is a membrane glycoprotein expressed exclusively within the secretory vesicles of neural and endocrine cells. It appears to be unique to vertebrates, suggesting that it represents a key regulator of complex signalling systems. In mammals, three SV2 genes have been identified, denoted A, B and C, and although the regulatory functions of the corresponding proteins are unclear, it is hypothesised that SV2 proteins modulate synaptic networks by ensuring that low-frequency neurotransmission is faithfully conveyed.

Synaptophysin (Monoclonal)	A synaptic vesicle glycoprotein, synaptophysin is present within the membrane of neuroendocrine cells and virtually all neurons in the brain, spinal cord and retina, vesicles of adrenal medulla, and neuromuscular junctions. Although the exact function of synaptophysin remains questionable, recent findings suggest that it may function within regulating activity-dependent synapse formation[383].
TBR2 (Monoclonal)	TBR2 is expressed by neural progenitor cells and functions intricately within regulation of hippocampal neurogenesis. It is also hypothesised that TBR2 functions within a similar manner with regards neurogenesis in the adult subgranular zone (SGZ) as in the embryonic cerebral cortex[384].
Tra-1-81 (Monoclonal)	Tra-1-81 is expressed on human ES, EG and EC cells but not their mouse counterparts, and although is accepted as a marker of pluripotency, its functional role is unknown.
VE-Cadherin (Monoclonal)	Cadherins are calcium dependent cell adhesion proteins and preferentially interact with themselves in a homophilic manner. VE Cadherin is proposed to function purposely within endothelial cells via the cohesion and organisation of intracellular junctions, furthermore associating with catenin to generate a relationship with the cytoskeleton. Further studies have defined an interaction of VE Cadherin with fibrin, a cohesion which may contribute to the mechanism through which fibrin induces angiogenesis[385].

Table 2.5 - **Associated expression and function of proteins used for phenotypic characterisation by immunofluorescent techniques.**

Antigen	Host	Reactivity	Conjugate	Working Dilution	Supplier	Catalogue Number
IgG	Chicken	Rabbit	Alexa Fluor 488	1:100	Invitrogen	A21441
IgG	Chicken	Rabbit	Alexa Fluor 594	1:100	Invitrogen	A21442
IgG	Chicken	Mouse	Alexa Fluor 488	1:100	Invitrogen	A21200
IgG	Donkey	Sheep	Alexa Fluor 594	1:100	Invitrogen	A11016
IgG	Goat	Rabbit	Alexa Fluor 568	1:100	Invitrogen	A11011
IgG	Goat	Mouse	Alexa Fluor 488	1:100	Invitrogen	A21042
IgG	Goat	Rabbit	Texas Red	1:100	Invitrogen	T2767
IgG	Goat	Mouse	Rhodamine	1:500	MP Biochemicals	55527
IgG	Rabbit	Goat	Alexa Fluor 594	1:100	Invitrogen	A11080

***Table 2.6* - Secondary antibodies used for immunofluorescence.**

2.9 Histological staining

2.9.1 Identification of Lipids using Oil Red O Staining

Prior to staining, a 0.5% (w/v) Oil red O solution was prepared. To generate this, 0.5g of Oil Red O (Sigma-Aldrich; Cat#O0625) were dissolved in 100ml of concentrated 1, 2-Propanediol (Sigma-Aldrich; Cat#398039) and heated to 95°C with gentle agitation. Whilst still warm, 0.5% (w/v) Oil Red O solution was filtered through coarse filter paper and incubated overnight at room temperature. Following incubation, the solution was passed through a media fritted glass filter and stored at room temperature until required.

To stain cells with Oil Red O, cultured cells were air dried for 30 minutes prior to fixation in a formaldehyde-sucrose solution for 15 minutes at 37°C. Samples were rinsed in three changes of distilled water. In order to avoid transfer of water into the Oil Red O, samples were incubated for 5 minutes in absolute 1, 2-Propanediol. Pre-prepared 0.5% (w/v) Oil Red O solution was added and samples incubated at 60°C for 8 minutes. Samples were rinsed in 85% (v/v) 1, 2-Propanediol solution and washed in distilled water prior to staining with Gill's number 1 Hematoxylin solution (Sigma-Aldrich; Cat#GHS-1) for 30 seconds at room temperature. Stained samples were washed in running water for 3 minutes and rinsed in two changes of distilled water prior to mounting with aqueous mounting media. Samples were imaged using transmitted light microscopy.

2.9.2 Identification of Glycosaminoglycans using Alcian Blue Staining

Prior to staining, two solutions were prepared. To produce a 1% (w/v) Alcian blue solution, 1g of Alcian blue 8GX (Sigma-Aldrich; Cat#A5268) was dissolved in 100ml of 3% (v/v) glacial acetic acid. Nuclear Fast Red solution was produced by dissolving 0.1g of Nuclear Fast Red (Sigma-Aldrich; Cat#N3020) in 100ml of 5% (w/v) aluminium sulphate solution and adding 0.1g of thymol.

Following fixation of cells with a formaldehyde-sucrose solution for 15 minutes at 37°C, samples were washed in 3% (v/v) glacial acetic acid solution for 3 minutes at room temperature. Samples were transferred to a 1% (v/v) Alcian blue solution and incubated for 30 minutes. Stained samples were washed in running water for 2 minutes and further rinsed in distilled water prior to counterstaining with Nuclear Fast Red solution for 5 minutes. Following 3 washes with distilled water, samples were dehydrated by successive incubations in 70% (v/v), 80% (v/v), 90% (v/v) and 100% (v/v) ethanol for 5 minutes periods. Samples were mounted using DPX and imaged using transmitted light microscopy.

2.9.3 Identification of Collagen using Van Geison Staining

Samples were fixed using a formaldehyde-sucrose solution and washed in distilled water prior to treatment with Celestine blue (Sigma-Aldrich; Cat#206342) for 30 minutes at room temperature. Samples were rinsed in distilled water and cells differentiated by brief exposure to 1% (v/v) acid alcohol. Following a wash in distilled water, samples were stained with Van Geison solution (Sigma-Aldrich; Cat#HT254) for 5 minutes and blotted using filter paper. Dried samples were dehydrated by successive incubations in 70% (v/v), 80% (v/v), 90% (v/v) and 100% (v/v) ethanol for 5 minutes periods. Samples were mounted using DPX and imaged using transmitted light microscopy.

2.9.4 Identification of Extracellular Matrix Calcification using Von Kossa Staining

Samples fixed using formaldehyde-sucrose were washed in 3 changes of distilled water for 5 minutes and incubated in 1% (w/v) silver nitrate solution for 60 minutes under the presence of ultraviolet light. Following 3 x 5 minute rinses in distilled water, samples were treated with a 2.5% (w/v) sodium thiosulphate solution for 5 minutes at room temperature. Samples were washed in 3 changes of distilled water for 5 minutes and counterstained in Harris' Hematoxylin solution (Sigma-Aldrich; Cat#HHS16) for 10 minutes at room temperature. Following washing in alkaline water for 5 minutes, samples were differentiated with brief exposure to 1% (v/v) acid alcohol and dehydrated by successive incubations in 70% (v/v), 80% (v/v), 90% (v/v) and 100% (v/v) ethanol for 5 minutes periods. Dehydrated samples were mounted using DPX and imaged using transmitted light microscopy.

2.10 SEM imaging

2.10.1 Critical Point Drying Preparation of Samples for Imaging using Scanning Electron Microscopy

Cells required for imaging using scanning electron microscopy were cultured on sterile glass coverslips. To process cells for imaging, cells were subjected to critical point drying. Samples were initially fixed with a solution containing 4% (v/v) formaldehyde and 2% (w/v) sucrose for 15 minutes at 37°C prior to undertaking critical point drying. Anhydrous samples were imaged using Scanning Electron Microscopy.

2.11 RT-PCR analysis

2.11.1 Isolation of RNA for RT-PCR analysis

Before isolating RNA, the following solutions were prepared in addition to those provided within the Qiagen RNeasy Mini Kit (Qiagen; Cat#74104): (i) 10µl of 1M β-

Mercaptoethanol (Sigma Aldrich; Cat#M3148) were added to 1ml of buffer RLT. (ii) 44ml of 100% ethanol were added to 6ml of buffer RPE.

To isolate RNA, adherent cells in a 24 well plate were subjected to three 5 minute washes in PBS followed by treatment with 350µl of buffer RLT. Following 5 minutes incubation at room temperature, cell lysate was transferred to a QIAshredder column and centrifuged at 13500 x g for 2 minutes. Eluted supernatant was diluted with 250µl of 100% ethanol and transferred to an RNeasy mini column prior to centrifugation at 13500 x g for 15 seconds, after which 500µl of buffer RW1 were added to the column and incubated for 5 minutes at room temperature. Following a further 15 second centrifugation at 13500 x g, 500µl of buffer RPE were added to the column followed by centrifugation for 15 seconds at 13500 x g. Finally, a further 500µl of buffer RPE were added and columns centrifuged at 13500 x g for 2 minutes. To elute the RNA, the column was placed into a fresh 1.5ml RNase free eppendorf tube to which 30µl of RNase-free dH_2O were added. Following 10 minutes incubation at room temperature, columns were centrifuged at 13500 x g for 1 minute. Suspended RNA was collected and frozen at -80°C until required.

2.11.2 Reverse Transcription of RNA to Generate cDNA

Prior to reverse transcription, the following solutions were prepared: (i) Stock solution 1 comprising 1µl 50uM $Oligo(dT)_{20}$, 1µl 10mM dNTP cocktail and 9µl RNase-free dH_2O. (ii) Stock solution 2 was generated via combining 4µl 5X first-strand buffers, 1µl 0.1M DTT, 1µl RNaseOUT recombinant RNase inhibitor (40 U/µl) and 1µl Superscript III RT (200U/µl). These stock solutions were sufficient for reverse transcription of one sample (2µl) of RNA generated from 2.11.1 (15-200µg/ml total RNA) and were scaled up accordingly to accommodate larger sample volumes. 2µl of RNA solution were added to stock solution 1 and incubated at 65°C for 5 minutes to initiate denaturation and then immediately transferred to a -20°C environment for 1 minute. Samples were subsequently treated with stock solution 2 and incubated for 40 minutes at 50°C, after which they were heated for a further 15 minutes at 70°C. Resultant cDNA was stored at 4°C until required for analysis. Unless otherwise stated, solutions were components of the Superscript™ III CellsDirect cDNA Synthesis System (Invitrogen; Cat#18080-200).

2.11.3 RT-PCR Analysis of Isolated cDNA

Generation of RT-PCR reactions comprised 2µl of cDNA synthesised in 2.11.2 diluted 100 fold using molecular biology grade dH_2O (Invitrogen; Cat#10977015), 0.5µl of sense primer (100µM) (Sigma Aldrich), 0.5µl antisense primer (100µM) (Sigma Aldrich), 7.5µl SYBR green single tube real time PCR master mix (Bio-Rad; Cat#172-5100) and 4.5µl of molecular grade dH_2O. Stated volumes were adjusted accordingly when required.

Reactions were synthesised in RNase-free 96 well plates (Bio-Rad; Cat#223-9441) with a total reaction volume of 15µl. Pipetting was undertaken using RNase-free pipette tips. Controls were generated by replacing template cDNA with an equal volume of dH_2O in order to identify potential DNA contaminants. PCR reactions (*Table 2.7*) were carried out using a Bio-Rad i-cycler (Bio-Rad).

Step	Temperature	Time	Number of cycles
Initial denaturation	95°C	3 minutes	1
Denaturation	95°C	1 minute	40
Annealing	Variable	30 seconds	40
Amplification	95°C	30 seconds	40
Final amplification	95°C	30 seconds	1
Soak	4°C	Indefinite	1

***Table 2.7* - RT-PCR reaction conditions. Annealing temperature was dependent upon optimised conditions for each primer detailed in *Table 2.8*.**

C_t values were calculated at the point at which fluorescence generated as a result the SYBR green molecule binding double stranded DNA during amplification passed a threshold value (Excitation 497nm, Emission 520nm when bound to dsDNA). Post-amplification, melt curve analysis of the product was performed via subjecting plates to an increase in temperature at an increment of 1°C per second commencing at 55°C and terminating at 95°C, allowing quantification of the decrease in fluorescence as a result of the dsDNA becoming denatured, the two strands dissociating and thus the SYBR green emission decreasing. The variation in dsDNA melting temperature was

an indicator of the similarity of the amplification product base composition compared to the target product for a given primer.

Target gene	Accession number	Sense primer (5' – 3')	Antisense primer (3' – 5')	Ta Opt (°C)
Adiponectin	EU420013	ATATGAAGGATGTGAAGGTC	CAGCATAGAGTCCATTACG	54.1
Aggrecan	BC036445	GTCTACCTCTACCCTAACC	TCTTGCTCTGATGGATGG	56.3
Alkaline Phosphatase	X55958	GGCATCCCAGTACCAGTTG	CCAAGAAAGCAGGAAAGTCAG	55.3
α-SMA	AL157394	TCCACCTTCCAGCAGATG	CCACAGGACATTCACAGTTG	53.6
β-Actin	NM001101	GGACCTGACTGACTACCTC	GCCATCTCTTGCTCGAAG	53.9
β-III-tubulin	BC003021	AGGTGCGTGAGGAGTATC	GAAGCAGATGTCGTAGAGC	56.9
CBFA1/RUNX2	AH005498	GGCAGTTCCCAAGCATTTC	GCAGGTAGGTGTGGTGTG	54.5
Chondroadherin	AF371328	TTATCTACTTGTACCTGTCC	AAGATGAAGAGGTTGACC	54.9
Collagen I	NM000088	GCCACTCCAGGTCCTCAG	CCACAGCACCAGCAACAC	54.5
Collagen II	NM000582	GAGCAGCAAGAGCAAGGAGAAG	TGGACAGCAGGCGTAGGAAG	54.3
D7-Fib	AX772981	AGGAACAGAGCACAGGCCTTAGTG	AAGACCCCTCCCAGATAGATGG	55.0
Elastin	AH007100	GAGTTGGTGCTGGTGTTC	AGGTGCTGAGAGGAGGAG	56.2
Fibrillin-1	AB177803	AGGCTGTGTAGATGAGAATGAATG	GGCACTCGTCCTGGTTGG	56.5
Fibronectin	U42594	TCATCCGTGGTTGTATCAG	GTCTCAGTCTTGGTTCTCC	54.2
GAPDH	NM002046	GAAGGTGAAGGTCGGAGT	CATGGTGGAATCATGTTGGAA	53.5
Laminin	Z15008	ACTATTGCCTCATATTGTCCTCTG	CCAACACTGCTCACTTCTTCC	52.9
Osteonectin	BC008011	GCTGGATGATGAGAACAACAC	AAGAAGTGGCAGGAAGAG	53.4
Osteopontin	NM000582	GCGAGGCGTTGAATGGTG	CTTGTGGCTGTGGGTTTC	53.9
Osterix	AF477981	CCACAAACTCTCATCTCAG	GGACAGCAGGAAATAAGC	54.1
Nerve Growth Factor	BC032517	GCAGACCCGCAACATCACTG	ATCTCCAACCCAACACACTGACA	61.0
Nestin	NM005517	GGAAAGTCAAAGGAATCTG	CTTCTCCACCGTATCTTC	53.7
Neurofilament	NM006158	CTTCCAGAAGCCAAGACTCCAG	GAAGCAGATGTCGTAGAGC	55.0
PPARγ	NM005037	GACCACTCCCACTCCTTTG	GTGAATGGAATGTCTTCGTAATG	50.7
REST	BC017822	GCATCACATCAGTGTTCACAG	CAGCGGTCACAGCGAATG	54.5
Smoothelin	Y13492	GAGTCCATGACCGATGTG	TCTCTTGAGCCACTGTTG	55.9
Sox9	X65665	CTACTCCACCTTCACCTAC	TGTGTAGACGGGTTGTTC	52.6
Substance P	NM013996	TTCTTGTCTCCACTCAGC	GAATCAGCATCCCGTTTG	54.2
Topoisomerase-III	D87012	N/A	N/A	60.0

Table 2.8 **- Primers used in RT-PCR experiments. Topoisomerase-III was purchased pre-synthesised from** www.primerdesigns.co.uk.

2.12 Enzyme-Linked Immunosorbent Assay (ELISA)

2.12.1 Isolation of Protein for ELISA

Cells differentiated towards a hepatic lineage as detailed in section 2.7.2 were washed 3 times in PBS following removal of the culture media. Cells were treated with 1% (w/v) sodium-dodecyl sulphate for 5 minutes at room temperature and the subsequent lysate transferred to an eppendorf. Lysate samples were denatured via treatment at 95°C for 5 minutes and stored at -20°C until required.

2.12.2 Assessment of Human Serum Albumin Production using ELISA

Human serum albumin production was detected using a Human serum ELISA quantitation assay kit (Bethyl Laboratories; Cat#E80-129). Prior to undertaking the assay, the following solutions were prepared: (i) Coating buffer containing 0.05M sodium bicarbonate, pH9.6. (ii) Wash solution comprising 50mM Tris, 0.14M NaCl, 0.05% (v/v) Tween 20, pH8.0. (iii) Blocking solution containing 50mM Tris, 0.14M NaCl and 1% (w/v) bovine serum albumin, pH8.0. (iv) Sample diluent, prepared by combining 50mM Tris, 0.14M NaCl, 1% (w/v) bovine serum albumin and 0.05% (v/v) Tween 20, pH8.0.

On the day of the experiment, the required numbers of 96 well plates were coated with 100µl of coating solution supplemented with 10µg/ml of goat anti-human albumin antibody. Samples were incubated at room temperature for 1 hour after which samples were washed 3 times in 200µl of wash solution. Following washing, the antibody associated substrata was blocked via the addition of 200µl of blocking solution and incubation at room temperature for 5 minutes, after which cells were subjected to 3 further washes with wash solution. In order to generate a calibration curve from which unknown serum albumin concentrations could be extrapolated, defined standard concentrations of human serum albumin were produced using human serum with a previously elucidated concentration of serum albumin. Human serum albumin was serially diluted with sample diluent such that the final concentrations of serum albumin used as standards were $1.0x10^4$, 400, 200, 100, 50, 25, 12.5, 6.25, 3.12 and 1.6ng/mL. Experimental samples comprising cell lysates and

media aspirates were diluted based upon predicted serum albumin concentrations using sample diluent (1:10). 100µl of calibration controls and associated samples were added to appropriately pre-coated wells and incubated for 1 hour at room temperature. Post-incubation, samples were washed 5 times with 200µl of wash buffer. Controls were included in which samples were replaced with identical volumes of dH_2O to identify non-specific binding. Horseradish peroxidise conjugate was diluted $1:7.5x10^4$ using sample diluent and 100µl transferred to each well. Following 1 hour incubation at room temperature, samples were washed 5 times in 200µl of wash buffer. Immediately prior to use, enzyme substrate 3, 3', 5, 5'-tetramethylbenzidine (TMB) was prepared by combining equal volumes of the two provided substrate reagents, and 100µl added to each sample. Following 30 minutes incubation at room temperature, the reaction was terminated by exposure to 100µl of 2M H_2SO_4. Samples were analysed using a µQuant microwell plate reader with associated KC Junior operating platform (BIO-TEK Instruments). Final concentrations of target protein in the experimental samples were calculated by reference to an equation based on the curvature of the calibration curve: y = 0.3279Ln(x) + 0.0602, re-expressed as x = e^[(y-0.0602)/0.039] where y is the absorbance and x is the target protein concentration.

2.12.3 Assessment of Human Transferrin Production using ELISA

Human transferrin production was detected using a Human transferrin ELISA quantitation assay kit (Assaypro; Cat#ET3105). Prior to undertaking the experiment, the following solutions were prepared: (i) Sample diluent was produced by diluting the provided 10X diluent concentrate 10 fold using dH_2O. (ii) Wash buffer was prepared by diluting the provided 10X concentrate 10 fold using dH_2O. Control standards were generated by serial dilution of a provided 1mg/ml standard solution of human apo-transferrin providing final concentrations for standard curve generation of 750, 375, 118, 59, 29, 15, 7.5, 3.8, 1.9, 1.0, 0.5 and 0.25ng/mL. Experimental samples comprising cell lysates and media aspirates were diluted based upon predicted serum albumin concentrations using sample diluent (1:10). 50µl of standards and samples were aliquoted into a 96 well plate pre-coated with polyclonal goat anti-human apo-transferrin antibody and incubated at room temperature for 2 hours. Controls were included in which samples were replaced by an identical

volume of dH_2O to identify non-specific binding. Post-incubation, samples were washed 5 times with 200µl of wash buffer and subjected to 1 hour incubation at room temperature in the presence of 50µl of an 80X solution of biotinylated polyclonal goat anti-human transferrin antibody diluted accordingly with diluent. Following incubation, samples were washed 5 times with 200µl of wash buffer and subjected to a 30 minute incubation at room temperature in the presence of 50µl of 100X Streptavidin-Peroxidase conjugate diluted accordingly using diluent solution. Samples were subjected to 5 further washes using 200µl of wash buffer and treated with 50µl of 3, 3', 5, 5'-tetramethylbenzidine for 10 minutes at room temperature. Reacting vessels were terminated using 0.5M HCl and analysed using a µQuant microwell plate reader with associated KC Junior operating platform (BIO-TEK Instruments). Final concentrations of target protein in the experimental samples were calculated by reference to an equation based on the curvature of the calibration curve: $y = 0.1521\text{Ln}(x) + 0.0716$ and transposed such that x becomes the subject:
$x = e^{[(y-0.0716)/0.1521]}$ where y is the absorbance and x is the target protein concentration. The absorbance for unknown samples was then used to calculate the resultant concentration of human apo-transferrin.

2.13 Construction of Stem Cell Conserved Domain (SCCD) Reporter Constructs

2.13.1 Synthesis of Primers for Amplification of Selected SCCDs

Genes known to exhibit a functional aspect within a desired cell phenotype were examined using the Evolutionary Conserved Region (ECR) browser (http://ecrbrowser.dcode.org), an on-line program allowing comparative bioinformatics detailing evolutionary conservation of genomes across numerous species. Regions upstream of the selected genes were assessed for the presence of highly conserved intronic DNA sequences conserved throughout numerous species, thereby signifying an important functional aspect. Transcription factor binding sites present within conserved intronic regions were examined and the potential functionality of the sequence noted. These regions were termed Stem Cell Conserved Domains (SCCDs) (*Figures 2.8-2.10*) and primers were designed (*Table 2.9*) in order to amplify selected SCCD regions (*Table 2.10*) for eventual cloning.

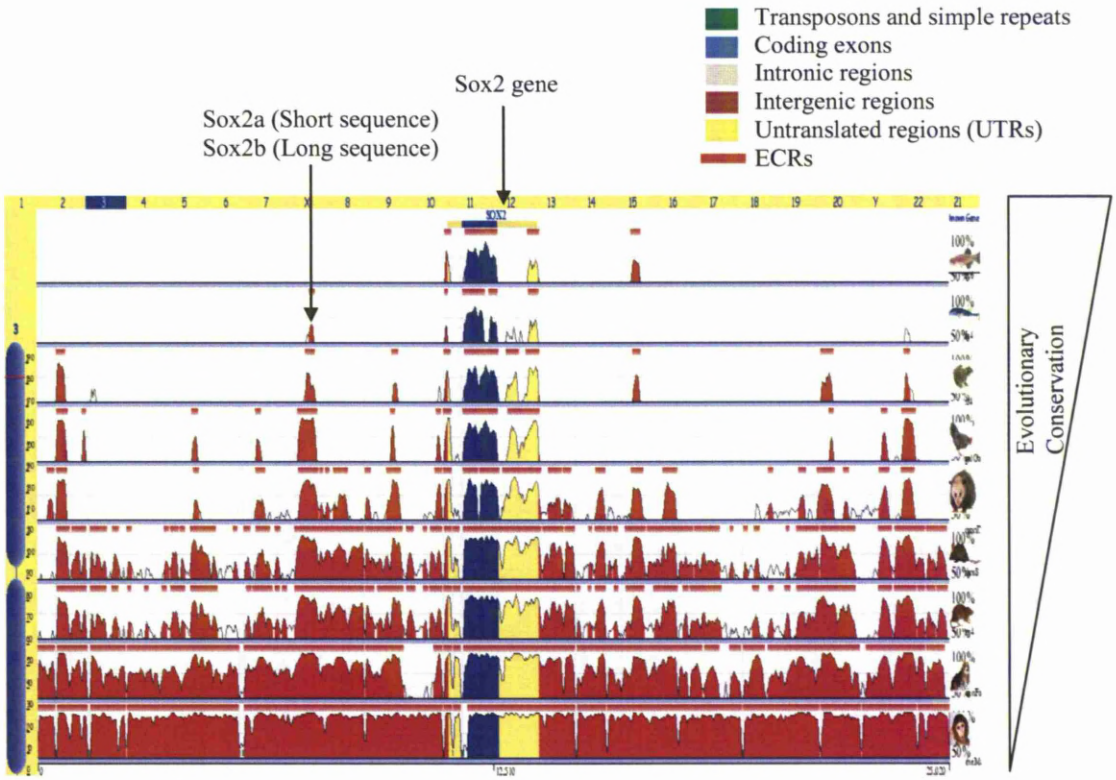

Figure 2.8 **- SCCDs residing upstream of the Sox2 gene – potential for identification and purification of cells exhibiting varying levels of plasticity.**

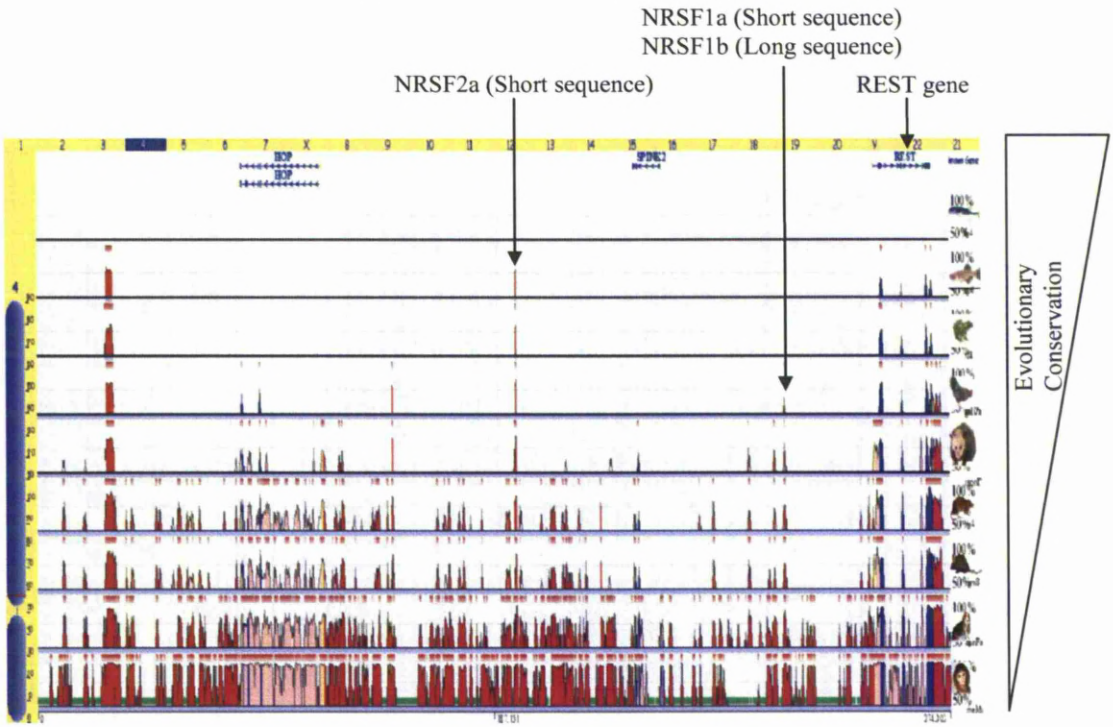

Figure 2.9 **- SCCDs residing upstream of the REST (NRSF) gene – potential for the identification and purification of neuronal progenitor cells.**

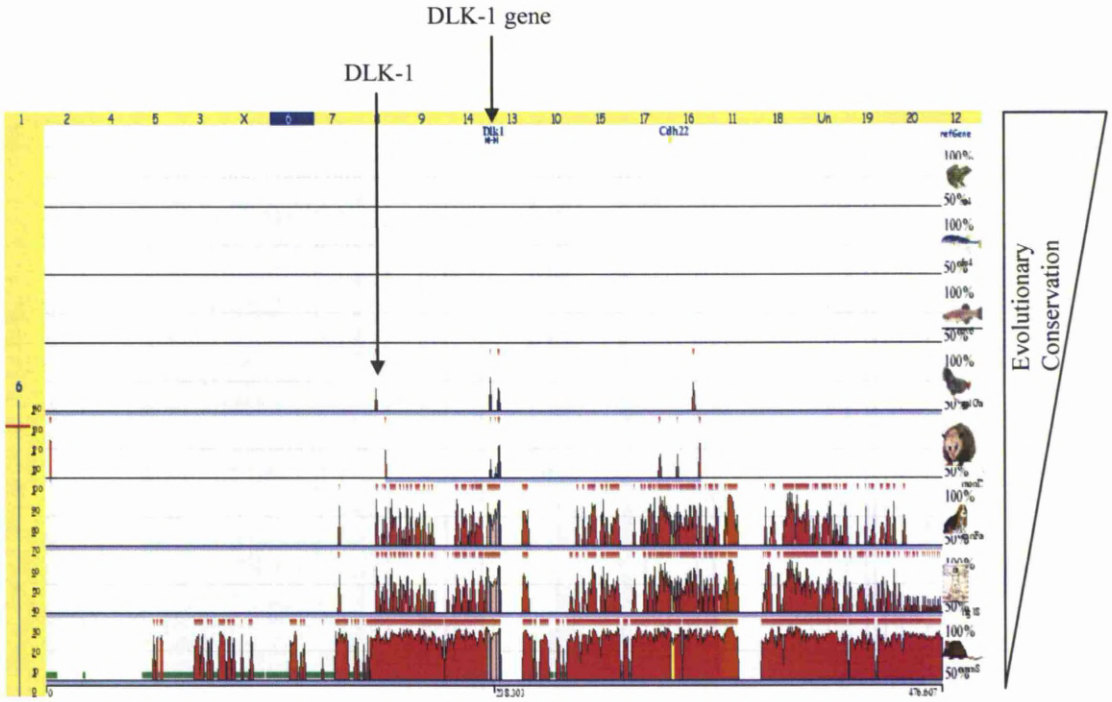

Figure 2.10 **- SCCDs residing upstream of the DLK-1 gene – potential for the identification and purification of adipogenic progenitor (Pre-adipocyte) cells.**

2.13.2 PCR Amplification of Identified SCCD Regions

PCR was utilised in order to amplify selected SCCD regions identified in 2.13.1. To generate PCR reactions, a 50µl reaction comprising 5µl PFU polymerase 10x buffer (Promega; Cat#M776A), 1µl dNTP mixture (Promega; Cat#U1511), 5µl sense primer (100µM) (MWG), 5µl antisense primer (100µM) (MWG) (*Table 2.9*), 1µl human genomic DNA (Promega; Cat#G3041), 0.4µl PFU polymerase (Promega; Cat#M7741) and 32.6µl nuclease free water, was prepared. Reactions were performed (*Table 2.10*) using a PxE 0.2 thermal cycler (Thermo Electron Corporation).

SCCD	Sense primer (5' – 3')	Antisense primer (3' – 5')	Ta Opt (°C)
Sox2a	AAACGCGTGCAATGCTGAGAAATTCC	AACTCGAGCTCAAGTATTATATCTGAAACC	62°C
Sox2b	AAACGCGTGACCACATCTGGCTGCTTG	AACTCGAGCTCCTAAAGTCTCCTCAGCAC	62°C
NRSF1a	AAACGCGTGATATTCTGAGTGACTGCCTC	AACTCGAGGGCACCGCTGATACTGAG	62°C
NRSF1b	AAACGCGTGCAGATGCTGCTTTGCTG	AACTCGAGAGTTCCCCTAGCTCACAGTG	62°C
NRSF2a	AAACGCGTACTATATATGAATTAAAATCAATCTCTTC	AACTCGAGAAACTGCTGCTCTTTCACTTC	62°C
DLK-1	AAACGCGTCTACAGAGGACGAAACTTTCAG	AACTCGAGGCTGTTGAGAATTTCTTAATTCC	62°C

***Table 2.9* - Primer sequences with accompanying restriction enzyme sequences for amplification of selected SCCD regions.**

MluI restriction enzyme site (Forward) XhoI restriction enzyme site (Reverse)

Step	Temperature	Time	Number of cycles
Initial denaturation	95°C	1 minute	1
Denaturation	95°C	30 seconds	35
Annealing	Variable	30 seconds	35
Amplification	72°C	1 minute	35
Final amplification	72°C	5 minutes	1
Soak	4°C	Indefinite	1

***Table 2.10* - Reaction conditions for amplification of SCCD regions.**

2.13.3 Purification of Synthesised PCR Product

PCR products generated in 2.13.2 were purified using QIAquick PCR Purification kit (Qiagen; Cat#28106). To purify, 5 volumes of Buffer PB were added to 1 volume of the PCR sample, applied into the QIAquick column and centrifuged for 1 minute at 13500 x g. The flow-through was discarded and the column washed by adding 750µl of PE buffer prior to centrifugation for 1 minute at 13500 x g. Following discarding of flow-through, the column was re-centrifuged for an additional 1 minute at 13500 x g to completely remove residual ethanol present within buffer PE. The column was placed into a fresh 1.5ml eppendorf tube, and the DNA eluted by adding 30µl of nuclease-free water to the centre of the column, incubated for 5 minutes at room temperature, and finally centrifuged for 2 minutes at 13500 x g.

2.13.4 Enzymatic Digestion of Purified PCR Product and pGL3p Reporter Construct

In order to generate restriction sites to allow cloning of SCCD sequences into the pGL3P luciferase reporter construct (Promega; Cat#E1761), purified PCR products generated in 2.13.2/2.13.3 and the pGL3P reporter construct were subjected to enzymatic digestion. Products and construct were initially digested with MluI restriction enzyme (Promega; Cat#R6381) (*Table 2.11*), then, following purification using QIAquick PCR Purification Kit (Qiagen; Cat#28106), digested with XhoI restriction enzyme (Promega; Cat#R6165) (*Table 2.12*).

Component	PCR product digestion	pGL3P Digestion
Product/Construct	15µl	2µl
10x buffer D (Promega; Cat#R9921)	2µl	2µl
10x BSA	2µl	2µl
MluI enzyme	1µl	0.5µl
Nuclease free water	0µl	13.5µl
Total	20µl	20µl
*Incubated for 4 hours at 37°C		

***Table 2.11* - MluI restriction digests of SCCD PCR product and pGL3P construct.**

Component	PCR product digestion	pGL3P Digestion
Product/Construct	15µl	2µl
10x buffer D (Promega; Cat#R9921)	2µl	2µl
10x BSA	2µl	2µl
XhoI enzyme	1µl	0.5µl
Nuclease free water	0µl	13.5µl
Total	20µl	20µl

*Incubated for 4 hours at 37°C

***Table 2.12* - XhoI restriction digests of SCCD PCR product and pGL3P construct.**

2.13.5 Analysis of Digested Products using Agarose Gel Electrophoresis

Digested products and constructs generated in 2.13.4 were analysed using agarose gel electrophoresis. 1-2% (w/v) multi-purpose agarose (Bioline; Cat#BIO-41025) was combined with 0.5 x TBE buffer and heated until fully dissolved, at which point 5µl of ethidium bromide were added (10mg/ml aqueous solution) (Sigma Aldrich; Cat#E-5134). The resulting solution was poured into 12 x 14cm or 20.5 x 10cm casting trays and, following insertion of appropriate combs, allowed to solidify at room temperature. The cast gels were submerged in horizontal gel electrophoresis tanks containing 0.5 x TBE buffer. 10µl of samples generated in 2.13.4 were combined with 2µl of 6 x loading buffer (Promega; Cat#G1881) and subsequently loaded into the wells. The size of the PCR or construct digest was determined by loading either a 100bp DNA ladder (Promega; Cat#G2891), 1kb ladder (Promega; Cat#G7541), or Mass ruler (Fermentas; Cat#SM0403). In general, gels were run for 3 hours at 60V. The electrophoretically separated DNA was visualised using an Evenscan broadband dual wavelength transluminator (Alpha Innotech Corporation), encapsulated within a MultiImageII Light Cabinet (Alpha Innotech Corporation), at a wavelength of 302nm.

2.13.6 Recovery of Digested DNA from Agarose Gels

Digested products separated by electrophoresis in 2.13.5 were assessed and DNA corresponding to the desired fragment sizes excised from the gel using a scalpel

blade following visualisation with long wave UV translumination. DNA was recovered from the excised gel using QIAquick Gel Extraction Kit (Qiagen; Cat#28706) following the manufacturers instructions. Briefly, 3 volumes of buffer QG were added to 1 volume of pre-weighed gel extract and incubated for 10 minutes at 50°C to allow the gel fragment to dissolve. One gel volume of 100% isopropanol was added and the sample vortexed prior to transfer to a QIAquick spin column, which was subsequently placed into a 2ml collection tube and centrifuged at 13500 x g for 1 minute. Following discarding of the flow-through, the column was washed via the addition of 750µl of PE buffer and centrifuged for 1 minute at 13500 x g. Initial flow-through was discarded and the column subjected to a second centrifugation to ensure complete removal of residual ethanol present within buffer PE. The column was placed into a fresh 1.5ml eppendorf tube and the DNA eluted via the addition of 30µl of nuclease free water to the centre of the column, incubation for 5 minutes at room temperature, and finally centrifugation at 13500 x g for 2 minutes.

2.13.7 Ligation of Digested PCR Products and Reporter Construct

Ligation of purified digests was undertaken using LigaFast™ Rapid DNA Ligation System (Promega; Cat#M8225). For each ligation, insert: vector molar ratios were varied, ranging from 1:1 to 3:1 ratios of molar ends. To calculate the required volumes of digested products and construct required for each ligation, the following calculation was performed:

$$\frac{\text{Ng Vector x kb size of insert}}{\text{Kb size of vector}} \quad \text{x insert: vector ratio} = \text{ng of insert required}$$

A ligation reaction was performed with 100ng of digested vector DNA (pGL3P), calculated amount of digested insert, 5µl of 2 x Rapid ligation buffer, 3 units (Weiss units) of T4 DNA Ligase, and nuclease free water to a final volume of 10µl. Synthesised ligation reactions were incubated for 5 minutes at room temperature.

2.13.8 Transformation of Ligated Reporter Plasmids into Chemically Competent *E. coli* Cells

Reporter plasmids generated in 2.13.7 were transformed into strains of competent *E. coli* (DH5-α) (Invitrogen; Cat#18265-017). To initiate transformations, a 50µl aliquot of competent cells was defrosted on ice, and the 10µl ligation reaction generated in 2.13.7 added to the thawed cells. Following 30 minutes incubation on ice, samples were subjected to a heat-shock at 42°C for 45 seconds prior to re-transferral to ice for 2 minutes. 950µl of pre-warmed LB broth were added to the transformations, and the cultures incubated at 37°C for 1 hour with agitation at 225rpm. 50-200µl of cultured transformations was spread onto LB agar plates supplemented with 100µg/ml ampicillin, and cultured overnight at 37°C. Following overnight incubation, formed colonies were selected using a sterile pipette tip, and transferred to a universal tube containing 5ml of LB broth culture media supplemented with 100µg/ml ampicillin. Isolated colonies were cultured overnight at 37°C with agitation at 225rpm. Post-culture, glycerol stocks containing 750µl of culture and 750µl of 80% (v/v) glycerol were mixed and frozen at -80°C until required. 1ml of culture was taken and subjected to mini-preparation for subsequent analysis to confirm uptake of the correct insert.

2.13.9 Mini-Preparation of Plasmid DNA

A small scale preparation of up to 20µg of plasmid DNA was purified for screening using QIAprep Spin Miniprep Kit (Qiagen; Cat#27106). 1ml of transformed cells taken from overnight cultures was centrifuged at 2600 x g for 5 minutes at 4°C. Following discarding of the supernatant, cells were resuspended in 250µl of buffer P1 and transferred to a 1.5ml eppendorf tube. To the suspension, 250µl of buffer P2 were added and mixed thoroughly via inverting the tubes 4-6 times. 350µl of buffer N3 were added to the solution and mixed by a repeat inversion. Following centrifugation for 10 minutes at 13500 x g, the resultant supernatants were applied to a QIAprep spin column and centrifuged for 60 seconds at 13500 x g. Following discarding of flow-through, columns were washed with 0.5ml of buffer PB and centrifuged for 60 seconds at 13500 x g. Flow-through was discarded and columns subjected to a second wash with 0.75ml of buffer PE followed by centrifugation for

60 seconds at 13500 x g. Following discarding of the supernatant, columns were re-centrifuged to remove residual wash buffer, after which the QIAprep column was placed into a clean 1.5ml eppendorf tube. To elute DNA, 50µl of buffer EB were added to the centre of each column then, post 5 minutes incubation at room temperature, centrifuged at 13500 x g for 5 minutes.

2.13.10 Test Digest of Plasmid DNA

Purified plasmid DNA generated in 2.13.9 was subjected to restriction enzyme digestion to confirm the presence and correct location of the insert. Plasmid DNA was initially digested with ACC65I (Promega; Cat#R6921) restriction enzyme (*Table 2.13*), then, following purification using QIAquick PCR Purification Kit (Qiagen; Cat#28106), digested with BGLII restriction enzyme (Promega; Cat#R6807) (*Table 2.13*).

Component	ACC65I Digestion	BGLII Digestion
Product/Construct	15µl	15µl
10x buffer D (Promega; Cat#R9921)	2µl	2µl
10x BSA	2µl	2µl
Restriction enzyme	1µl	1µl
Nuclease free water	0µl	0µl
Total	20µl	20µl
*Incubated for 4 hours at 37°C		

***Table 2.13* - ACC65I and BGLII restriction digests of Plasmid DNA construct.**

Purified fragments generated following restriction digest were analysed using two methods. Firstly, fragments were subjected to agarose gel electrophoresis as detailed in 2.13.5 and fragment sizes assessed. Following identification of correct fragment sizes, purified fragments were sent for sequencing to The Sequencing Service (School of Life Sciences, University of Dundee) using Applied Biosystems Big-Dye Version 3.1 chemistry on an Applied Biosystems model 3730 automated capillary sequencer.

2.13.11 Maxi-Preparation of Plasmid DNA

Following demonstration of the correct sequence insertion into the construct, QIAfilter Plasmid Maxi Kit (Qiagen; Cat#12263) was utilised for the isolation of up to 500µg of plasmid DNA. 200µl of glycerol stocks of plasmid generated in 2.13.8 were added to 100ml of LB broth media supplemented with 100µg/ml ampicillin and cultured for 12 hours at 37°C with agitation at 225rpm. Following incubation, cells were harvested by centrifugation at 2600 x g for 15 minutes at 4°C and the pellet resuspended in 10ml of buffer P1. To this suspension, 10ml of buffer P2 were added and, following mixing by 4-6 inversions of the tube, was incubated at 20°C for 5 minutes. Post-incubation, 10ml of chilled buffer P3 were added to the lysate and, following mixing by inversion, the solution transferred to a QIAfilter cartridge and incubated for 10 minutes at room temperature. During this incubation, a Qiagen-tip 500 was equilibrated via the addition of 10ml of buffer QBT, which was subsequently allowed to empty from the column via gravity flow. Following incubation, the cap of the QIAfilter cartridge outlet nozzle was removed and a plunger inserted, allowing the cell lysate to enter the previously equilibrated Qiagen-tip by gravity flow, which was washed twice with 30ml buffer QC. DNA was eluted by washing with 15ml of buffer QF, and precipitated by adding 10.5ml of isopropanol, mixing, and centrifuging at 13500 x g for 30 minutes at 4°C. Post-centrifugation, the supernatant was carefully decanted and the pellet washed with 5ml of 70% (v/v) ethanol. Following centrifugation at 13500 x g for 10 minutes, the supernatant was again carefully discarded and the pellet air-dried for 10 minutes. DNA was dissolved in a suitable volume of TE buffer (pH 8.0).

2.13.12 Quantification of DNA Concentration by Spectrophotometry

DNA concentration of purified plasmids was determined using a UV spectrophotometer (Jenway Genova Life Science Analyser). Calibration of the spectrophotometer was achieved using 100µl of dH_2O. Following calibration, DNA diluted 100 fold was analysed, with the DNA concentration determined using the following formula: Original concentration = O.D. value (wavelength 260nm) x 50ng/ml x dilution factor, where 1 O.D. at 260nm for double stranded (ds) DNA

equals 50ng/ml of dsDNA[386]. Quantified plasmids were stored at -20°C until required for transfection.

2.14 Transfection of SCCD Reporter Constructs

2.14.1 Transfection of Cells using Amaxa Human MSC Nucleofector® Kit

Human MSC Amaxa Nucleofector® technology (Amaxa; Cat#VPE-1001) was used to transfect synthesised constructs into cultured cells. When approximately 85% confluent, cells were harvested as described in 2.1.7. Pelleted cells were resuspended in PBS and counted using a haemocytometer. The desired number of cells (10^5 cells per nucleofection sample) was transferred to an eppendorf and centrifuged at 200 x g for 10 minutes in a microcentrifuge. Following discarding of the supernatant, the pellet was resuspended in Human MSC Nucleofector Solution at a final concentration of 4 x 10^5 cells/100µl. 2µg of construct DNA synthesised in section 2.13 or associated pGL3P (Promega; Cat# E1761) or pGL3C (Promega; Cat#E1741) control were added to the 100µl cell suspension. 0.1µg of Renillin internal control were also added to non-control samples, and solutions transferred to an Amaxa certified cuvette, taking care to avoid air bubbles whilst pipetting. The cuvettes were transferred to an Amaxa Nucleofector and subjected to the U-23 program, which initiates high Transfection efficiency. To the treated cells, 500µl of pre-warmed culture media were added and the entire contents transferred to pre-prepared culture plates containing media at 37°C using the pipettes provided. Cells were incubated at 37°C and assessed for post-nucleofection viability after 2 hours by assessment of the GFP control (below). Cells were cultured for a further 22 hours and analysed as described in 2.14.3.

To establish a positive control additional to the pGLP3P and pGLP3C constructs and Renillin, pmaxGFP from *Potellina sp.* was transfected into one cell-containing well and observed using laser scanning confocal microscopy to assess transfection efficiency.

To generate a negative control, cells were treated with DNA and transfection solutions without induction using the U-23 program. As a second control, cells

without DNA were treated with these solutions and induced with the Amaxa Nucleofector.

2.14.2 Transfection of Cells using Qiagen Effectene® Transfection Reagent

Cells seeded within a 24 well plate and cultured in basal and defined differentiation media as described in 2.7.2 were transfected using a Qiagen Effectene Transfection Kit (Qiagen; Cat#301427). On the day of transfection, 1µg of DNA synthesised in 2.12 or appropriate pGLP3P or pGLP3C control was diluted to a concentration of 0.2µg/ul with DNA-condensation buffer (Buffer EC) to a total volume of 60µl for each proposed transfection. 0.1µg of Renillin were added to non-control containing samples. To this solution, 1.6µl of Enhancer were added and the resulting product vortexed for 1 second. Following incubation at room temperature for 5 minutes, samples were briefly centrifuged to remove solution from the top of the eppendorf. To this solution, 5µl of Effectene Transfection Reagent were added and mixed via gentle pipetting. Samples were incubated for 10 minutes at room temperature to allow formation of the transfection complex. Whilst complex formation was ongoing, culture media was aspirated from each well and the cells washed with PBS. 350µl of desired media were added to the cells. Following formation of the transfection complex, 350µl of the same media were added to the solution. Mixing was achieved by gentle pipetting and the solution was immediately added drop-wise onto the cells culturing within the 24 well plates. Plates were smoothly rotated to ensure uniform distribution of the transfection complexes. Cells were incubated at 37°C and assessed for post-nucleofection viability after 2 hours by the assessment of the GFP positive control as described 2.14.1. Cells were cultured for a further 22 hours and analysed as described in 2.14.3. pGLP3P, pGLP3C and Renillin were used as positive controls. To generate a negative control, cells were transfected in the absence of synthesised DNA constructs.

2.14.3 Analysis of Cells Transfected with Synthesised Constructs

Quantification of luciferase protein production conveyed from transfected plasmids was estimated using the Dual Luciferase Assay kit (Promega; Cat#E1500). Briefly, transfected cells were washed twice with PBS prior to the addition of 70µl of 1 x

passive lysis buffer to each well and incubation for 15 minutes at room temperature with gentle agitation. 20µl of the acquired lysate were added to wells of a 96 well plate (Bio-Rad; Cat# Cat#223-9441) and the plate transferred to a Glomax 96 microplate luminometer Quantificat. 100µl of Firefly luciferase and 100µl of sea Renilla luciferase substrate were injected into each well to calculate luminescence intensity. Renilla luciferase substrate solution determined production of the internal control Renillin, and thereby allowed normalisation for transfection efficiency.

2.15 Statistics

2.15.1 Statistical Analysis of Quantitative Results

Flow cytometry, CyQuant Proliferation, Telomere Length, and ELISA experiments were each performed in duplicate and repeated 4 times (n = 4). For SCCD transfection studies, each experiment was carried out in triplicate (n = 4). Following data collection, Microsoft Excel was used to calculate the mean average and standard deviation of results. To assess the statistical significance of results, a two tail student t-test was employed where necessary.

3. Human Bone Marrow as a Potential Source of Multipotent Adult Stem/Progenitor Cells

3.1. Introduction

3.1.1 Bone Marrow-derived MSCs

Following the discovery that the bone marrow niche harbours multipotent cells in addition to the well characterised HSC population, investigators have striven to characterise these cells both *in vitro* and *in vivo*. Isolated MSCs have been combined with numerous chemical and topographical stimuli attempting to maintain cells in an undifferentiated state or induce lineage specific differentiation[44,154,387-390]. At present however, subpopulations capable of maintaining plasticity or undertaking directed lineage differentiation have yet to be homogeneously isolated. Furthermore, whilst expression of plasticity-associated markers such as Oct4 have been demonstrated within bone marrow-derived MSCs, expression profiles vary between laboratories, perhaps attributable to differing culture conditions or antibodies used for characterisation[220]. Conversely, reports describing the absence of Oct4 expression may be correct given findings suggesting that Oct4 is not required for self-renewal of mouse somatic stem cells[221]. An alternative theory regarding this absence of Oct4 expression is that bone marrow-derived cells, thought to be exhibiting multipotential abilities, in fact do not. Instead, the bone marrow niche may represent a residence accommodating numerous committed progenitor subpopulations, capable of unipotent differentiation subsequent to appropriate stimuli, thereby not requiring expression of Oct4. This hypothesis is further substantiated when we consider their limited capacity for proliferation *in vitro*[391], thought to be attributable to rapidly decreasing telomeres[233], a demise not usually associated with stem cells, in particular ES cells, which express telomerase and can be cultured for prolonged periods *in vitro*. However, it must be noted that characteristics observed *in vitro* do not necessarily correlate with functional capabilities *in vivo*, and the phenotypic degeneration may be attributable to a lack of knowledge with regards current *ex vivo* culture protocols. Regardless of whether isolated bone marrow cells possess a multipotent stem cell population, it is almost certain that the heterogeneously isolated population will contain numerous progenitor subpopulations. It is therefore

imperative that each subpopulation and, if present, stem cell population is homogeneously isolated and assessed for their differentiation capacity both *in vitro* and *in vivo*. Furthermore, homogenous isolation of individual subpopulations may facilitate the optimisation of culture conditions to maintain phenotypes of each subpopulation *in vitro*, allowing prolonged *ex vivo* expansion generating large numbers of cells, a substantial benefit if bone marrow-derived cells are to be utilised clinically.

Whilst it is likely that bone marrow contains numerous lineage progenitors, each of which could excel when applied homogeneously within a given restorative application, many investigators insist that adult cell-based regenerative approaches require a multipotent stem cell based foundation. At present, STRO-1 is widely used for the purification of hypothesised multipotent cells from bone marrow[203], although in addition to the obvious diverse potential of STRO-1^+ selected populations, which exhibit an ability to generate cells including adipocytes, chondrocytes, osteoblasts and neuronal cells, STRO-1^- cell populations have demonstrated capacities for potential therapeutic application, exhibiting an innate ability to support hematopoietic engraftment *in vivo*[392]. This potential of STRO-1^- populations to be used for therapeutic applications highlights the heterogeneity of the bone marrow niche, and encourages purification methods generating greater homogeneity to be tailored. However, given that significant advancements in purification are required in order to homogeneously isolate subpopulations of varying plasticity, it is essential in the first instance to establish the potential of bone marrow-derived cells, in addition to cells isolated from alternative tissues (Chapters 4 to 6), in a heterogeneous manner. Lonza purchased MSCs have demonstrated an ability to undertake adipogenic, chondrogenic and osteogenic differentiation following exposure to appropriate stimuli and, whether such observed lineage commitment is undertaken by a stem (mesenchymal or hematopoietic) or progenitor subpopulation, the population as a whole clearly demonstrates a potential for clinical use. It is therefore imperative that Lonza MSCs are assessed for their ability to heterogeneously maintain phenotype and proliferative capacities throughout *in vitro* culture, issues addressed within this chapter.

3.1.2 Aims of this Chapter

This investigation into bone marrow-derived cells therefore aims to use flow cytometry to assess potential subpopulations present at each respective passage whilst furthermore assessing the phenotypic stability of the population. In addition, the ability of the population to maintain proliferation throughout *in vitro* culture will be addressed. Previous studies have described phenotypic and proliferation instability of bone marrow-derived cells and have attributed this to rapidly reducing telomere lengths *in vitro*[233], seemingly causing the population to age more rapidly than *in vivo*. The telomere lengths of these bone marrow cells will also therefore be assessed. Overall, this chapter aims to confirm previously obtained data for bone marrow-derived cells and establish a base on which to compare cells isolated from other tissues.

3.2 Phenotyping of Bone Marrow Cells using Flow Cytometry

3.2.1 Phenotypic Analysis of Bone Marrow Cells throughout Prolonged *In Vitro* Culture using Flow Cytometry

Adherent fibroblast-like cells (*Figure 3.1*) isolated from bone marrow and demonstrating *in vitro* differentiation capacities are termed MSCs, although this collective description fails to emphasise the heterogeneity of the population. Nevertheless, this population forms the basis of much stem cell related research, predominantly using cells of low passage number due to their stability with regards proliferation and differentiation. However, whilst this is acceptable for small scale *in vitro* experiments, clinical utilisation of any cell type is likely to require abundant numbers of cells, and thus cells of greatly increased passage are likely to be required. It is therefore surprising that comprehensive characterisation of MSC phenotypes throughout prolonged *in vitro* culture have failed to be comprehensively studied, with only a handful of studies examining modifications of cell phenotype, proliferation and differentiation capacities at varying passage[393]. It is therefore uncertain the extent to which the MSC phenotype modifies *in vitro*. Furthermore, it is imperative that observed modifications in surface phenotype can be directly

correlated to differing regulation of transcription factors controlling plasticity, differentiation and proliferation.

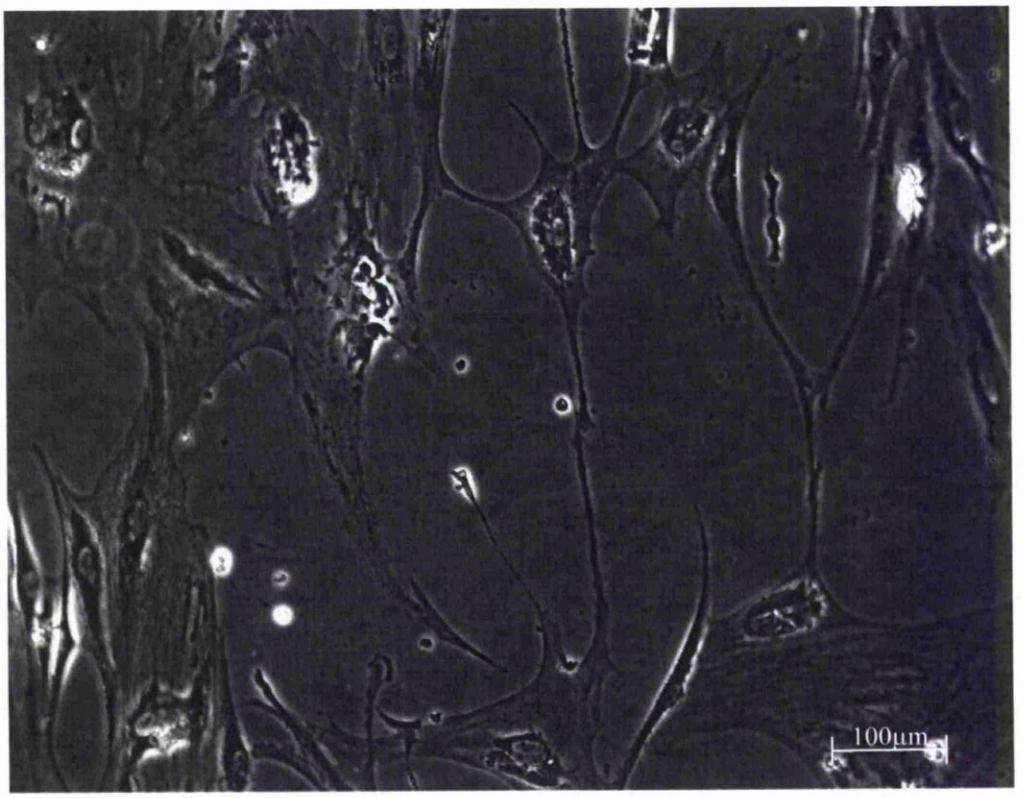

Figure 3.1 **- Adherent Lonza-purchased bone marrow-derived cells cultured in basal media (Passage 4).**

In an attempt to ascertain the effects of prolonged *in vitro* culture on cellular phenotype, bone marrow-derived MSCs were cultured in commercial basal media and their surface phenotype at passages 4 - 9 assessed using flow cytometry. Antibodies were selected to probe an array of surface antigens associated with MSCs, HSCs and endothelial cells, and ES and progenitor cells.

Throughout passages 4 and 5 the bone marrow-derived population maintained consistently high expression of MSC-associated markers (*Figure 3.2*). CD29 was expressed by approximately 95.2% of the population at passage 4, reducing to 89.5% and 88.7% at passages 5 and 6 respectively. However, expression reduced to 59.0%, 54.0% and 34.6% at passages 7, 8 and 9 respectively (*Figure 3.3*). This fate was mirrored by other MSC-associated markers including CD44 which, following expression of 76% - 88% throughout passages 4 - 6 decreased to 40% at passage 7

and 23.0% and 13.5% at passages 8 and 9 respectively. The population expressed CD117 in a similar manner, with 91.7%, 84.0% and 81.0% expression at passages 4, 5 and 6 reducing to 12.8%, 2.3% and 1.9% at passages 7 - 9.

Whilst CD29, CD44 and CD117 exhibited stable expression within the population throughout passages 4 - 6, alternative MSC markers displayed instability following passage 5. CD73 was expressed by 78.2% and 73.7% of cells at passages 4 and 5, but only 59.8%, 23.4%, 17.6% and 11.5% at passages 6, 7, 8 and 9 respectively. CD90 incorporated similar phenotypic modifications following *in vitro* culture, with 94.2% and 86.3% expression at passages 4 and 5 reducing to 55.5%, 12.4%, 6.3% and 2.6% at passages 6 - 9. TGF-β receptor CD105 was expressed by 87.0% and 83.8% of the population at passages 4 and 5, reducing to 55.8%, 7.4%, 1.4% and 0.8% at passages 6 - 9 respectively. CD146 is hypothesised to represent a marker of MSCs, and was expressed within 81.7% and 73.6% of the population at passages 4 and 5. However, at passages 6 - 9 only 11.6%, 9.0%, 1.4% and 1.3% of cells respectively expressed CD146. Passages 6 - 9 also resulted in downregulation of CD166, with expression levels of 74.9% and 69.3% at passages 4 and 5 reducing to 20.1%, 13.9%, 1.3% and 1.1% at passages 6 - 9 respectively.

HLA-ABC, also known as MHC class I, was expressed by 29.8% and 26.7% of cells during passages 4 and 5 but only 7.4%, 2.5%, 0.9% and 0.9% at passages 6 - 9. HLA-DR, the second class of MHC antigen, was expressed by 4.9% and 4.8% of cells at passages 4 and 5 but reduced to 1.4%, 0.9%, 0.6% and 0.4% at passages 6 - 9 respectively.

CD106 has been proposed to act as key regulator of MSC migration *in vivo* and 2.5%, 2.9% and 7.5% of cells respectively expressed CD106 at passages 4, 5 and 6. However, at passages 7, 8 and 9 only 0.4%, 0.4% and 1.0% expressions were observed. STRO-1 was expressed by 2.2% of the population at passage 4, reducing to 1.3%, 0.6%, 0.3% and 0.6% at passages 5 - 9 respectively. Interestingly however, no passage 9 cells expressed STRO-1, suggesting that hypothesised stem cell subpopulations are lost following prolonged culture should STRO-1 represent its proposed function.

Phenotyping of the bone marrow-derived population demonstrated disconcerting downregulation of hypothesised MSC markers following 5 - 6 passages of culture. Whilst the functional aspect of many of these markers remains questionable, the absence of markers such as CD105, which acts as a receptor for the chondrogenesis-inducing growth factor TGF-β, would suggest that the population demonstrates a reduced capacity to undertake differentiation following prolonged *in vitro* culture. It is therefore suggested that studies investigating the differentiation potential of bone marrow-derived MSCs utilise early passage cells, and thereby ascertain accurate results with regards the differentiation capacity of the population. However, whilst this may facilitate gaining further understanding of the population, the lack of scope for phenotypically stable proliferation limits their potential with regards clinical application, for which large numbers of cells are likely to be required. It is possible that results describing downregulation of MSC-associated markers can provide a platform on which to tailor culture conditions in order to maintain phenotypic characteristics of the population. Conversely, the downregulation of MSC-associated antigens may be a reflection of their ability to differentiate into different tissue phenotypes.

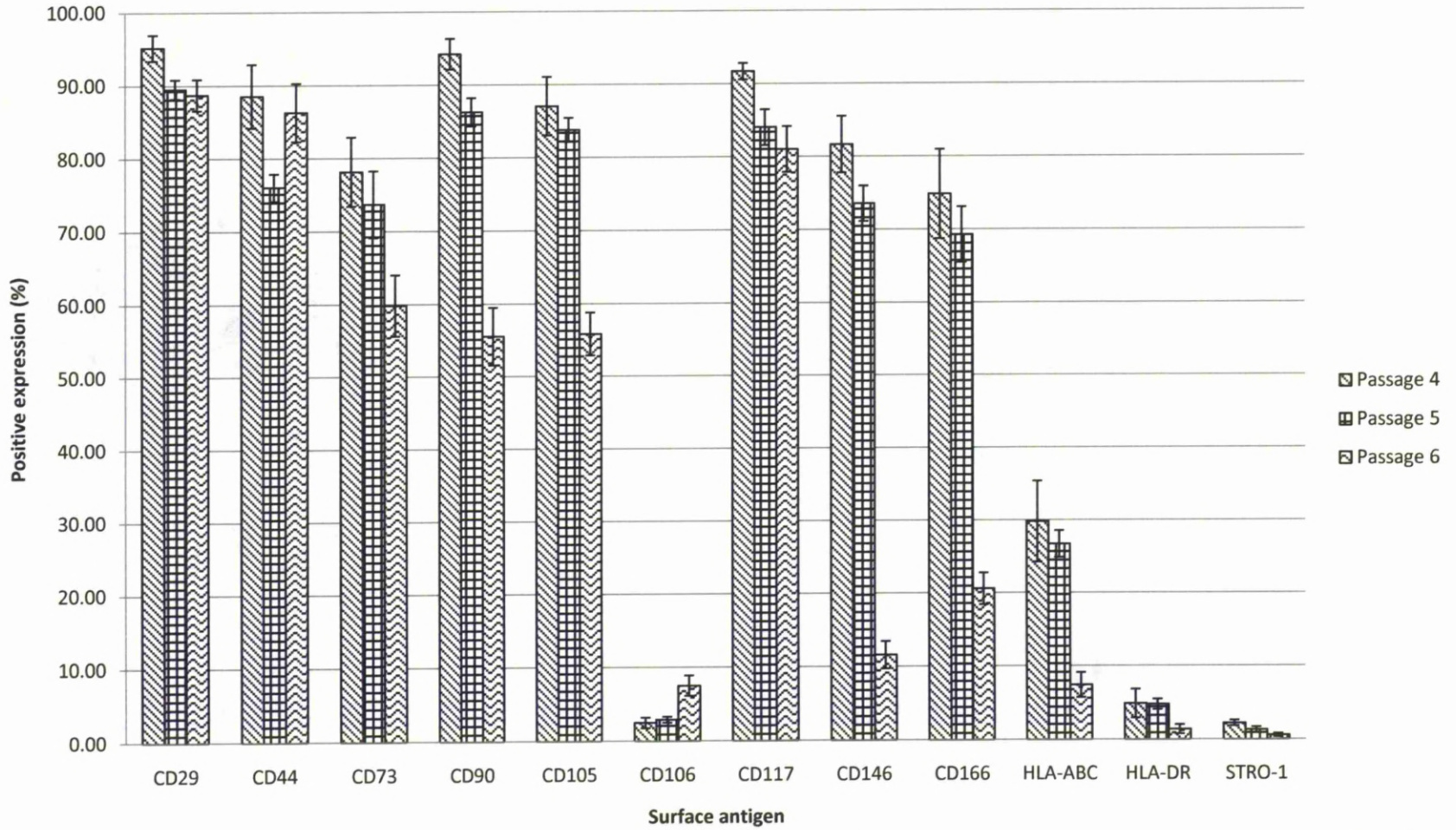

Figure 3.2 - **MSC-associated marker phenotyping of Lonza bone marrow-derived MSCs passages 4 - 6 cultured in commercial media (1 x Freeze-Thaw cycles). Values represent mean positive expression as observed by flow cytometry (n = 4). Error bars correspond to Standard Deviations.**

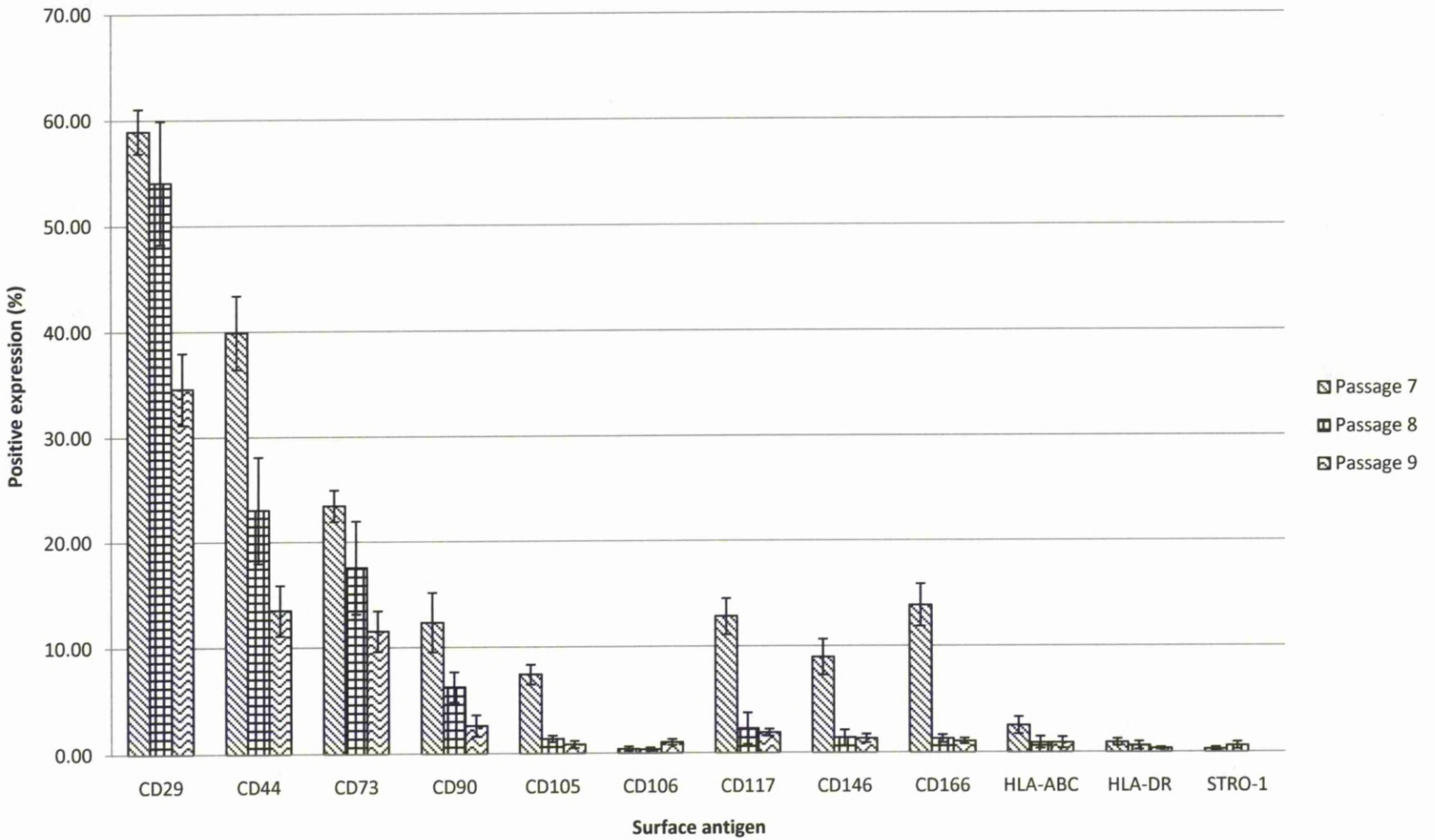

Figure 3.3 - **MSC-associated marker phenotyping of Lonza bone marrow-derived MSCs passages 7 - 9 cultured in commercial media (1 x Freeze-Thaw cycles). Values represent mean positive expression as observed by flow cytometry (n = 4). Error bars correspond to Standard Deviations.**

In addition to probing the bone marrow-derived population for the expression of MSC-associated markers, cells were further examined for their expression of surface antigens associated with HSCs and endothelial cells (*Figures 3.4* and *3.5*). CD9 is predominantly expressed by endothelial cells, platelets and megakaryocytes[394], although expression has also been reported in undifferentiated ES cells. CD9 was expressed by 18.7%, 19.1% and 15.7% of cells at passages 4, 5 and 6 respectively, but reduced to 1.8%, 0.3% and 0.03% passages 7 - 9. HSC and endothelial cell-associated marker CD31 was expressed by 0.9%, 0.9%, 0.04% and 0.6% of cells at passages 4 - 7, though interestingly increased to 20.0% and 23.8% at passages 8 and 9 respectively. CD34 class II was expressed by 0.75% of the population at passage 4 and gradually increased to 2.7% at passage 9. Alternative splice variant CD34 class III was expressed by 2.8% - 5.9% of the population throughout passages 4 - 9.

Von Willebrand factor receptor CD41a was expressed by 0.09% of cells at passage 4, increasing to 1.8% at passage 9. CD45 exhibited similar expression, with 0.3% expression at passage 4 increasing to 2.8% at passage 9. CD50 was expressed by 0.3%, 0.6% and 0.9% of the population at passages 4, 5 and 6 respectively, increasing to 3.1%, 2.4% and 3.4% at passages 7 - 9. CD62E maintained minimal expression throughout *in vitro* culture, with between 0.2% and 0.9% expression at passages 4 - 9. Finally, CD133 exhibited progressively increasing expression, with 0.1% at passage 4 increasing to 2.9% at passage 9.

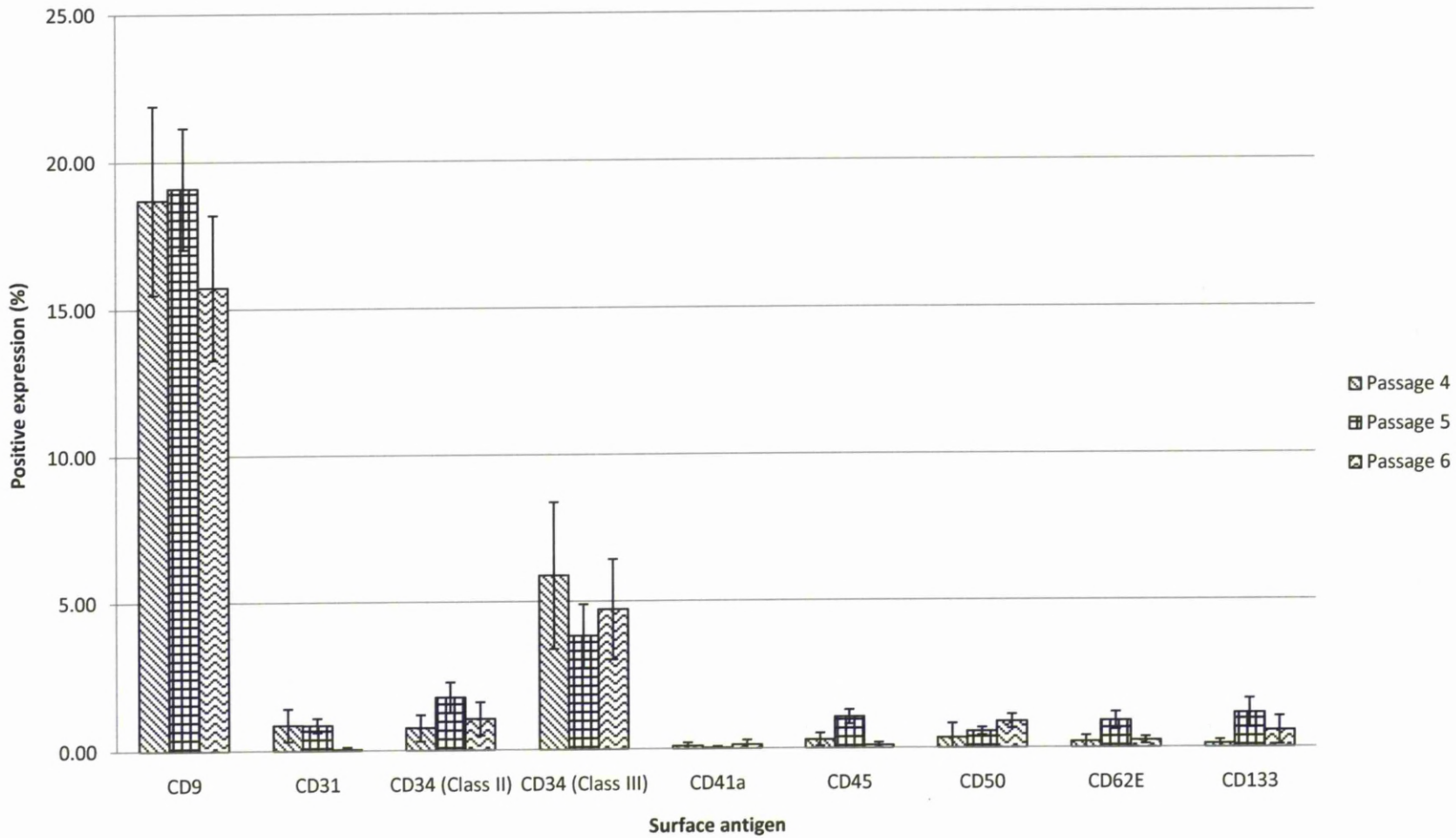

Figure 3.4 - **HSC and endothelial-associated marker phenotyping of Lonza bone marrow-derived MSCs passages 4 - 6 cultured in commercial media (1 x Freeze-Thaw cycles). Values represent mean positive expression as observed by flow cytometry (n = 4). Error bars correspond to Standard Deviations.**

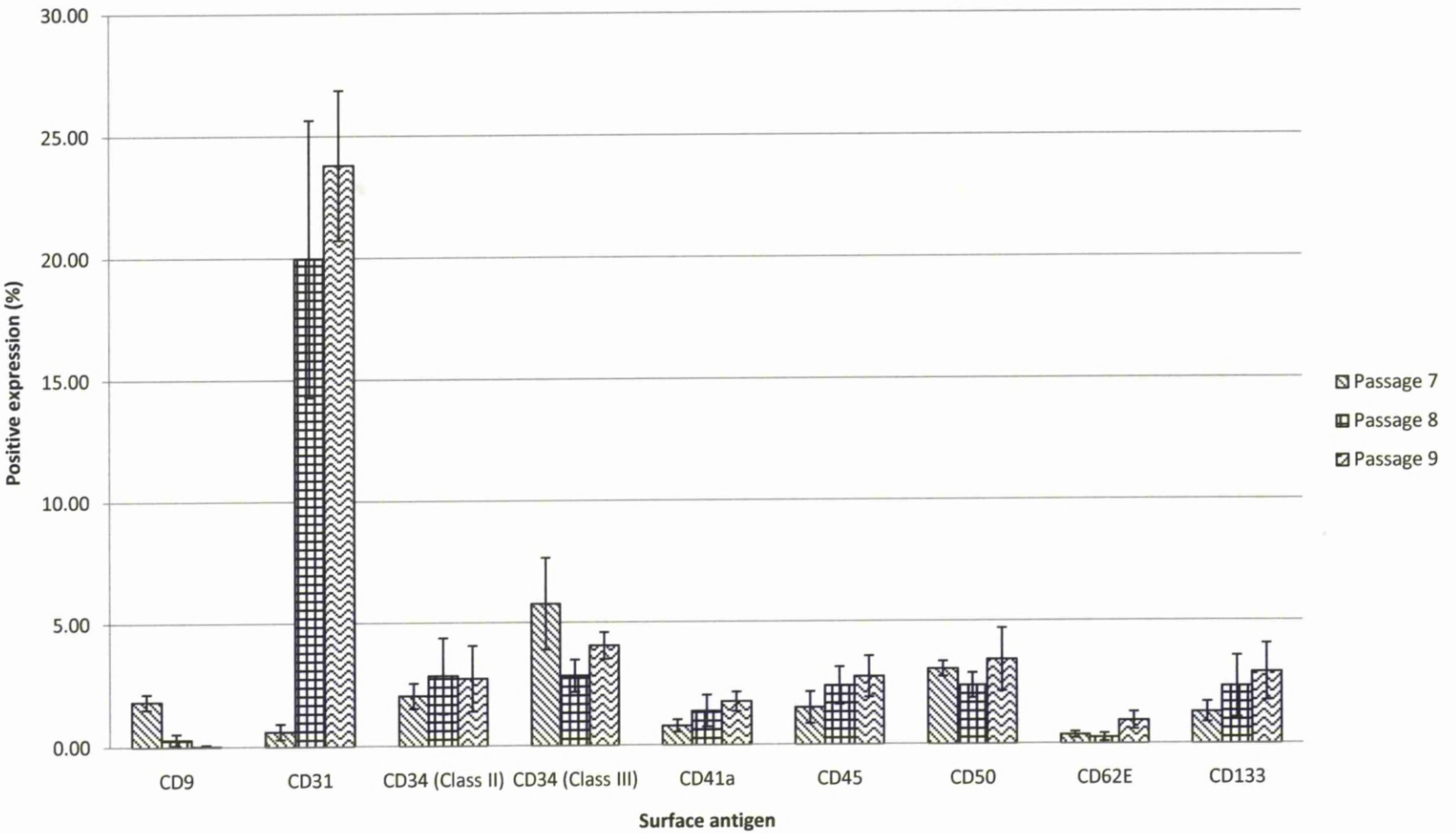

Figure 3.5 - **HSC and endothelial-associated marker phenotyping of Lonza bone marrow-derived MSCs passages 7 - 9 cultured in commercial media (1 x Freeze-Thaw cycles). Values represent mean positive expression as observed by flow cytometry (n = 4). Error bars correspond to Standard Deviations.**

Bone marrow-derived populations were further probed for surface antigens associated with ES cells and progenitors of varying commitment (*Figures 3.6* and *3.7*). Whilst CD15 is highly expressed in mouse MSCs, only 0.03% - 0.6% of human MSCs demonstrated expression. CD30 is highly expressed in embryonal carcinoma cells and, interestingly, the bone marrow population exhibited 20.1% - 31.7% expression throughout passages 4 - 9. CD56 was expressed by 0.4%, 1.1% and 0.01% of cells throughout passages 4 - 6, increasing to 2.6%, 3.5% and 5.1% at passages 7, 8 and 9 respectively. CD135 was expressed by 3.4%, 2.6% and 2.5% at passages 4, 5 and 6 respectively, reducing to 0.9% at passages 7 - 9.

Phenotypic profiling of bone marrow-derived cells demonstrated significant modifications following *in vitro* culture. Surface antigens hypothesised to be associated with MSCs, HSCs and endothelial cells, and ES and progenitor cells were up- and down- regulation at varying passage, indicating variability within subpopulations comprising the heterogeneous population. However, in order to understand the effects of *in vitro* on isolated cells, it will be necessary to correlate transcriptional profiling, proliferation and differentiation capacities with a surface expression phenotype.

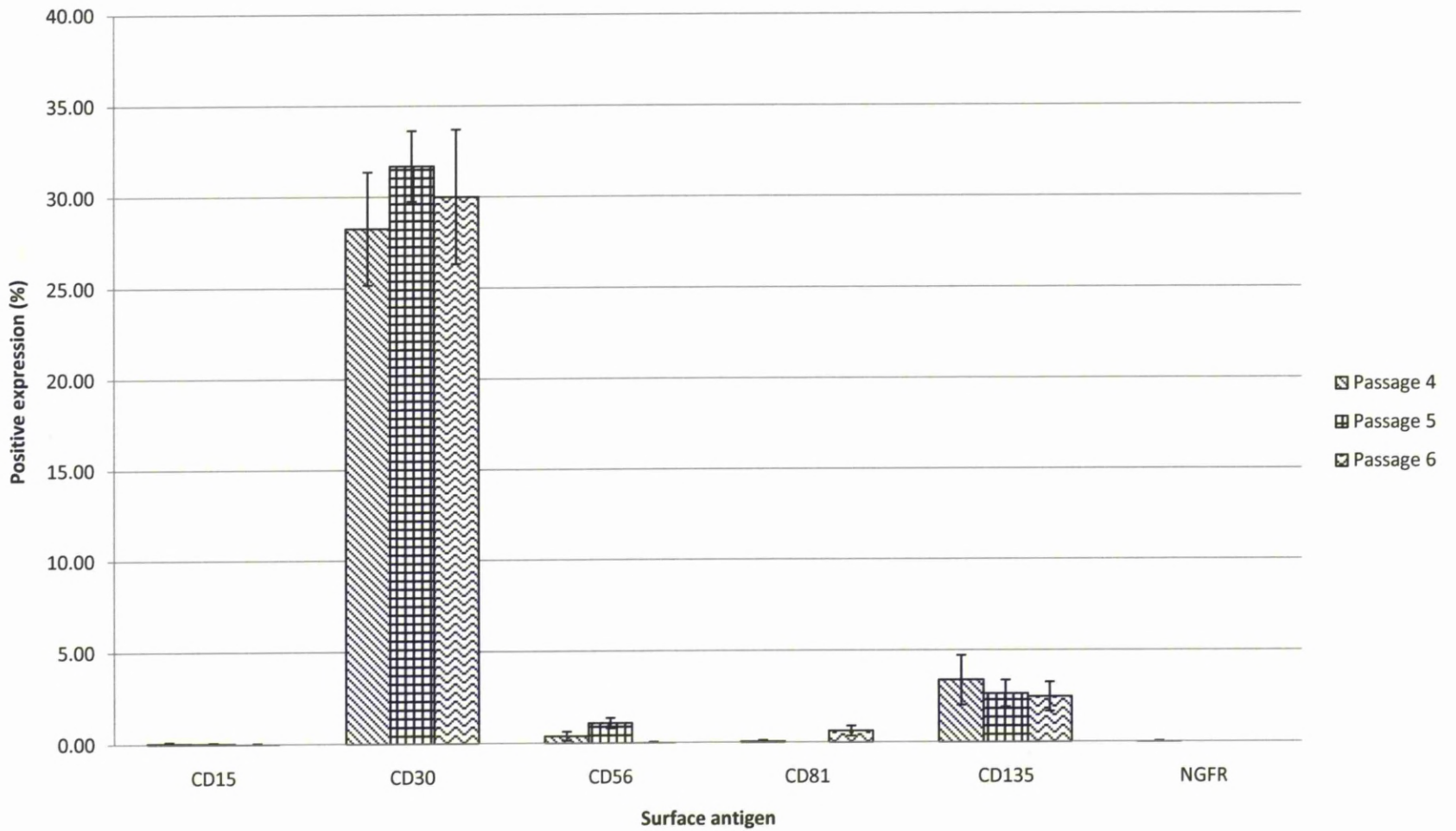

Figure 3.6 - **ES and progenitor-associated marker phenotyping of Lonza bone marrow-derived MSCs passages 4 - 6 cultured in commercial media (1 x Freeze-Thaw cycles). Values represent mean positive expression as observed by flow cytometry (n = 4). Error bars correspond to Standard Deviations.**

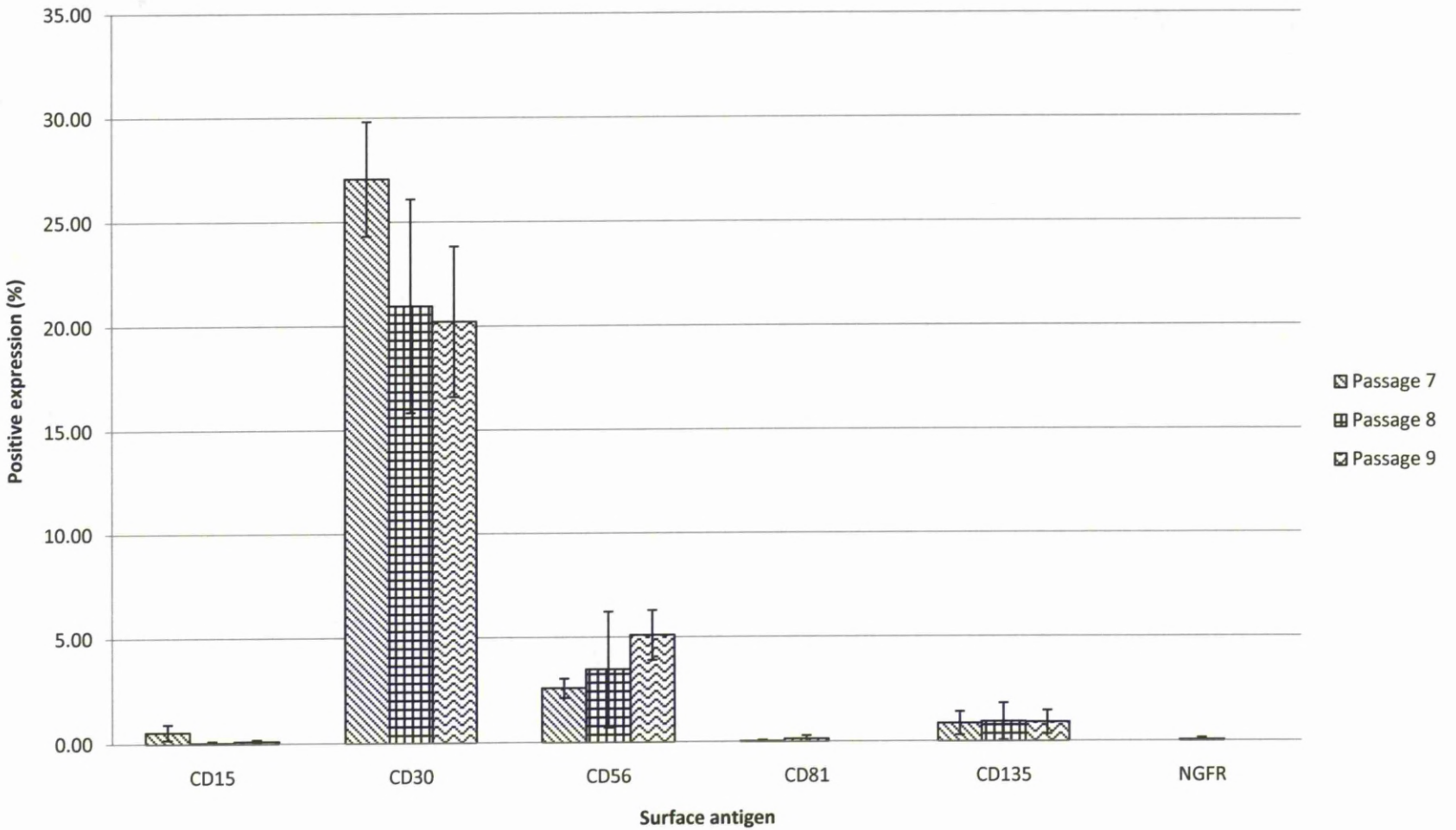

Figure 3.7 - **ES and progenitor-associated marker phenotyping of Lonza bone marrow-derived MSCs passages 7 - 9 cultured in commercial media (1 x Freeze-Thaw cycles). Values represent mean positive expression as observed by flow cytometry (n = 4). Error bars correspond to Standard Deviations.**

3.3 Proliferation Capacity of Bone Marrow Cells

3.3.1 Proliferation Capacities of Bone Marrow Cells throughout Prolonged *In Vitro* Culture using CyQUANT Analysis

In order to further demonstrate phenotypic transformation following prolonged *in vitro* culture, the proliferative capacity of MSCs was assessed at passages 4 - 9 (*Figure 3.8*). 1 x 10^4 bone marrow-derived cells were seeded per well of a 24 well culture plate and maintained in basal media for 7 days, with the total cell number per well counted at days 1, 3 and 7. Following 24 hours of culture, passage 4 cells had proliferated to generate 1.7 x 10^4 cells. Passage 5 cells generated a slightly reduced number of cells following 24 hours of culture, with approximately 1.5 x 10^4 cells. Prolonged *in vitro* culture resulted in further reduced proliferation rates, with 1.3-, 1.1-, 1.0- and 1.0- x 10^4 cells observed following 24 hours of culture at passages 6, 7, 8 and 9 respectively.

Whilst reduced proliferation was observed following 24 hours of basal culture, increased quiescence within the population was further pronounced when examining cells cultured for 72 hours. Whilst passage 4 and 5 cultures generated 3.1- and 2.8- x 10^4 cells respectively at day 3, succeeding passages demonstrated reduced levels of proliferation, with passage 6 - 9 cultures generating approximately 1.4-, 1.7-, 1.2- and 1.2- x 10^4 respectively.

Following 7 days of culture, passages 4 and 5 indicated further proliferation within the population, attaining cell numbers of approximately 4.4 x 10^4 in both passages. Cells cultured for prolonged *in vitro* periods continued to demonstrate a reduced capacity for proliferation, with 2.4-, 2.0-, 1.4- and 1.2 x 10^4 cells at passages 5, 6, 7 and 9 respectively post 7 days of basal culture.

Assessment of MSC proliferation *in vitro* demonstrated their progressively reduced ability to undertake cell division, in particular post passage 5. This reduction coincides with the downregulation of MSC-associated surface antigens observed in 3.2.1, and poses significant problems if these cells are to be used clinically. It is

therefore required that culture conditions are optimised to ensure that cells are able to proliferate to Hayflicks limit of 70 cell passages[395].

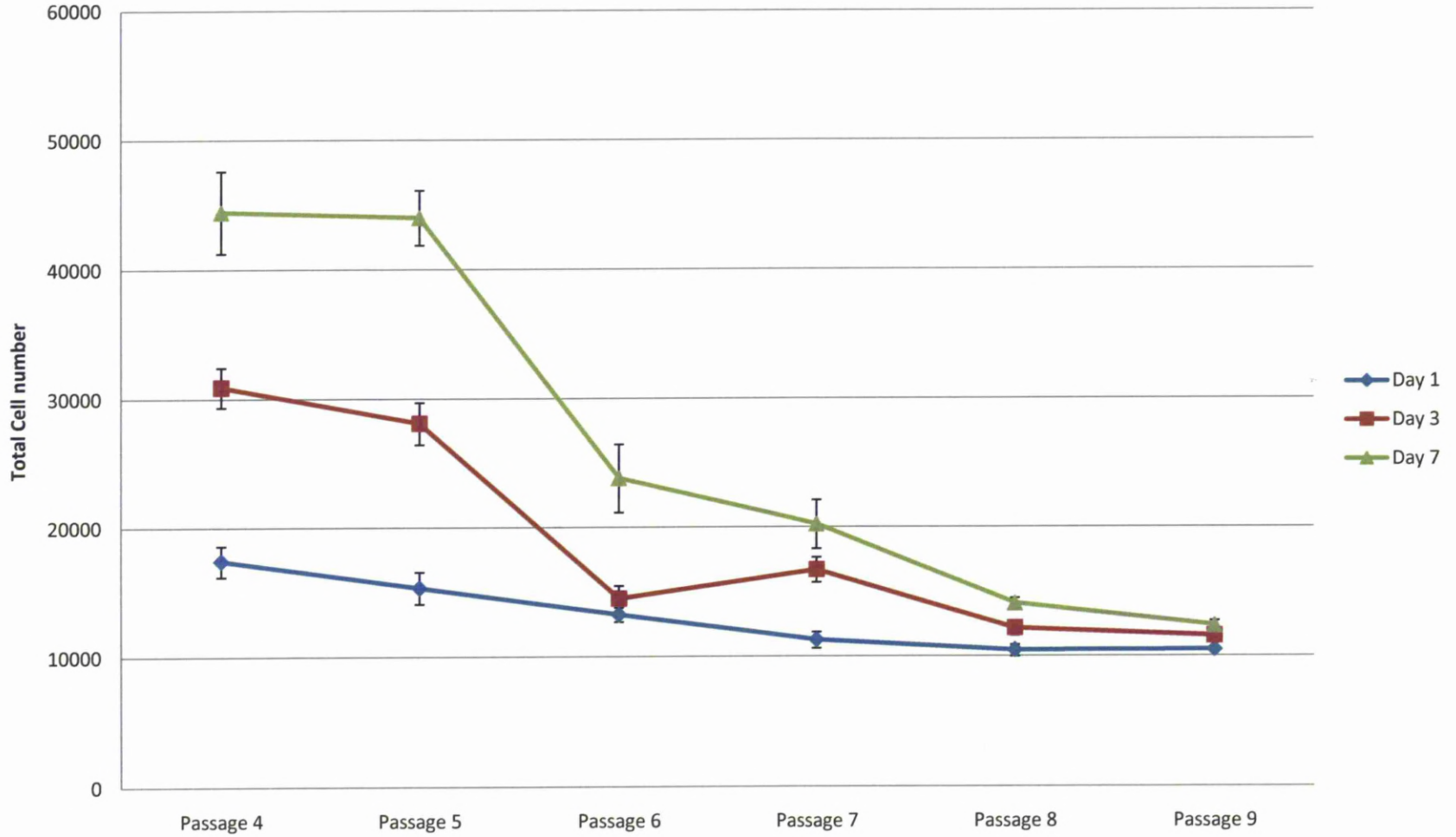

Figure 3.8 - **Proliferation capacity of Lonza bone marrow-derived MSCs passages 4 - 9 (1 x Freeze-thaw cycle) cultured in basal media for 7 days. Initial seeding density 1 x 10^4 cells. Values represent mean numbers of total cells counted per well at days 1, 3 and 7 for each respective passage (n = 4). Error bars correspond to Standard Deviations.**

3.4 Telomere Length Assessment of Bone Marrow Cells

3.4.1 Telomere Length Regulation of Bone Marrow Cells throughout Prolonged *In Vitro* Culture using DAKO Telomere Length Analysis

Telomeres represent specialised structures present at the ends of eukaryotic chromosomes and are proposed to control the underlying mechanistic pathways governing cell replicative lifespan and possibly the aging process. Such structures may therefore represent attractive markers for assessing the impact of cell culture on the population, potentially allowing modification of culture media to reduce degradation of or even retain telomere length. However, in order to maintain telomere length, the base generating enzyme telomerase must be activated, and whilst this can conceivably overcome reducing telomere length, its activation can often be associated with cancer. *In vivo*, humans demonstrate an average telomere loss of approximately 17 bases per annum[233], although cells have been demonstrated to age more rapidly *in vitro*.

Bone marrow-derived MSCs were cultured in commercially available basal media on tissue culture polystyrene and assessed for their respective X chromosome telomere length following varying periods of culture (*Figure 3.9*). Passage 4 cells globally exhibited a mean X chromosome telomere length of 10721 bases, which reduced subsequent to further culture. Passage 5 cells exhibited an average telomere length of 10655 bases, reducing to 10549, 10431, 10330 and 10188 base lengths at passages 6, 7, 8 and 9 respectively. The results demonstrated a reduced telomere length of approximately 100 - 150 bases per passage, significantly greater than the proposed 17 base loss per annum observed *in vivo*. It is likely therefore that this rapid reduction in telomere lengths impact significantly on cellular phenotype, causing the modifications of phenotype and reduced proliferation observed in MSC cultures. Culture conditions should therefore be tailored to reduce this rapid aging of cells *in vitro*, with maintenance of telomeres inducing a more stable phenotype, proliferation rate and differentiation capacity, all of which are key parameters if these cells are to be utilised clinically.

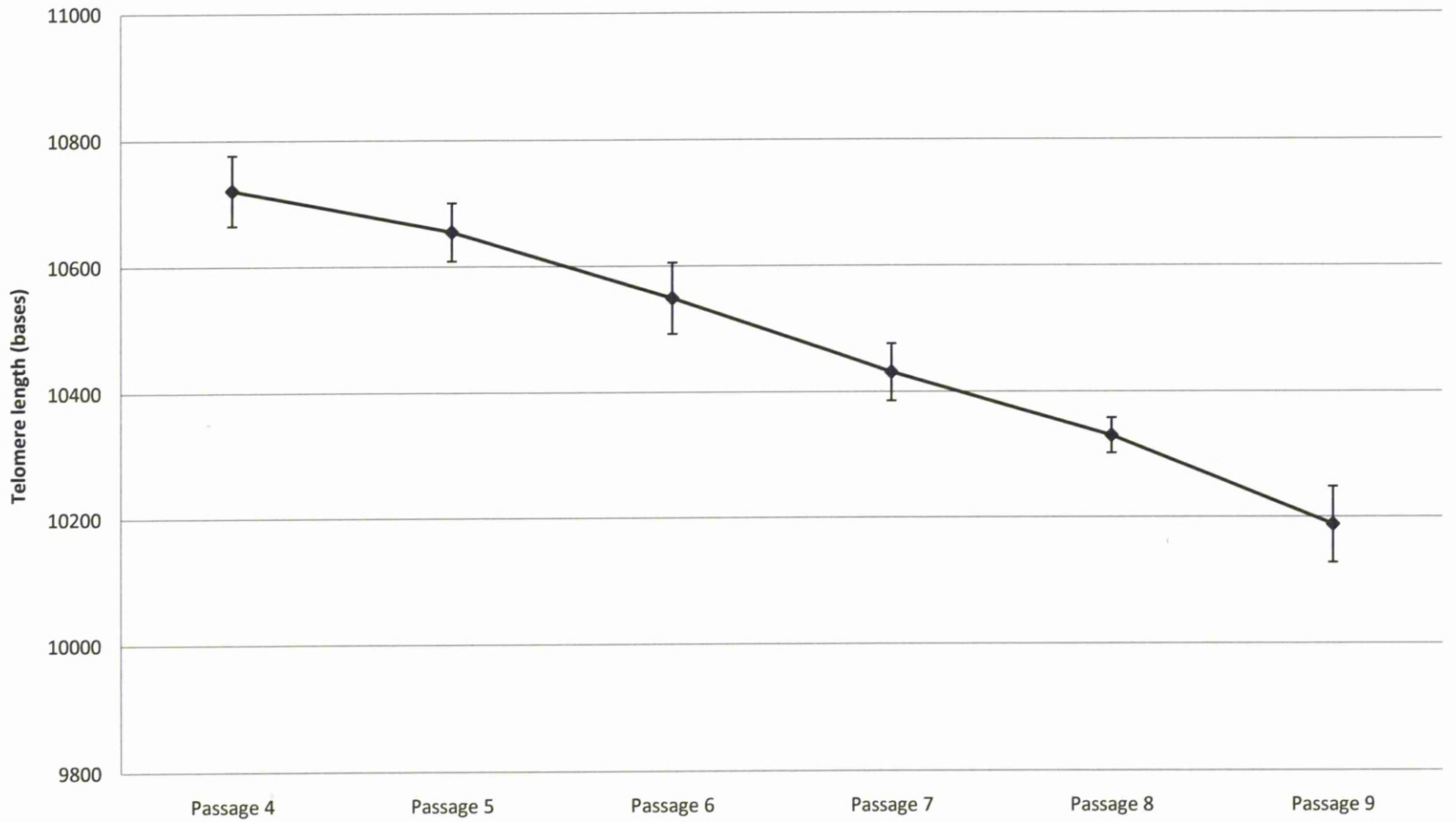

Figure 3.9 **- Mean telomere lengths (n = 4) of Lonza bone marrow-derived MSCs cultured in basal commercial media (1 x Freeze-thaw cycles) passages 4 - 9. Error bars correspond to Standard Deviations.**

3.5 Conclusion

3.5.1 Bone marrow as a Niche for the Isolation of Clinically Desirable Cells

Bone marrow-derived cells represent the most comprehensively studied cell type to date and have already been utilised in numerous *in vivo* applications. However, flow cytometry data presented within this chapter suggests significant heterogeneity within the population, expressing antigens associated with MSCs, HSCs and endothelial cells, and ES and alternative progenitor subsets. However, the heterogeneic phenotype varied significantly during prolonged *in vitro* culture and this raises concerns with regards their potential clinical utilisation, especially given that maintained passage of adherent cells is likely to be required in order to generate the cell numbers needed for regenerative applications. Furthermore, the modification of surface phenotype with increasing *in vitro* culture coincided with a reduced capacity to undertake proliferation, both of which are likely attributable to the rapid aging of the population as demonstrated by telomere length regulation studies.

Following observation of this apparent aging of the population *in vitro*, modification of *ex vivo* culture conditions may provide an environment capable of maintaining the natural *in vivo* phenotype. It is therefore hoped that results obtained in this study can infer a baseline on which to compare alternative culture conditions, in particular the telomere length study which, given the apparent rapid aging the population *in vitro*, can represent an attractive marker with which to compare *in vitro* with *in vivo* conditions. Furthermore, upon attaining a consistent *in vitro* phenotype following prolonged culture, homogeneous isolation of individual subpopulations present within adherent bone marrow cultures may allow the application of bone marrow-derived cells within numerous clinical applications, given that the population is likely to contain cells of varying plasticity and lineage commitment in addition to terminally differentiated, essentially clinically redundant cells. This homogeneous isolation is reuired if bone marrow-derived populations are to be utilised in any clinical setting, given that progenitor subsets of undesirable lineage commitment are likely to hinder, or potentially prove detrimental, to a regenerative strategy.

In conclusion the bone marrow can be regarded as a niche of significant interest, potentially allowing for the isolation of cells of varying potential. Further studies must now concentrate upon developing optimised culture conditions and isolation strategies to facilitate the prolonged *ex vivo* culture of clinically useful cells without modifications of phenotype or reduction of proliferations rates which are likely attributable to rapid aging of cells. Furthermore, in order to facilitate their purification and assess the differentiation potential of cells isolated from varying donors, functional characteristics must be associated with their surface antigen profiles, allowing rapid assessment and homogeneous isolation of desired subpopulations post initial isolation from each donor.

3.5.2 Response to Chapter Aims

Results gained within this chapter address the aims set out in 3.1.1 by hypothesising potential subpopulations following analysis by flow cytometry, although it was noted that this phenotype, along with proliferation rate, modified following *in vitro* culture. Rapidly reducing telomere lengths have previously been hypothesised to be responsible for this, and such rapid aging was undertaken by Lonza bone marrow cells. Given the data obtained, this chapter has provided a base on which to compare cells isolated from other adult tissues.

4. Human Peripheral Blood as a Potential Source of Multipotent Adult Stem/Progenitor Cells

4.1 Human Peripheral Blood Cells

4.1.1 Introduction

Human peripheral blood represents an attractive niche for the isolation of cells, being a renewable source with straightforward and relatively non-invasive methods of isolation. However, whilst methods for the isolation of cells from peripheral blood are well documented, the populations of adherent cells present remains open to discussion.

Initial theories of the central dogmaa refuted the presence of endothelial progenitor cells (EPCs) and the corresponding vasculogenesis within the adult human, insisting that such cells are limited to presence within the early embryo in order to induce development of the circulatory system. However, following the discovery of EPCs in 1997[396], policies of the central dogma have been repeatedly challenged, with researchers hypothesising that transplantation of EPCs may augment vasculogenesis, potentially allowing therapeutic strategies for the treatment of ischemic diseases to be developed, with many preliminary studies already exhibiting palpable clinical benefit[397-398]. EPCs demonstrate an impressive capacity to undertake proliferation and furthermore can develop into mature endothelial cells (ECs), principles fundamental to their clinical potential. However, at present their origin within peripheral blood populations remains unclear, with numerous groups articulating differing opinions with regards EPC derivation. $CD14^+$ cells, which are typically $CD34^-$, have been suggested as the source of EPCs[399], with this monocyte enriched population displaying an ability to undertake an EC-like phenotype *in vitro*. Interestingly, however, this population also expresses dendritic cell antigens, suggesting that monocytes can differentiate into macrophages, dendritic cells, or ECs depending on environmental cues. Furthermore, data obtained from this study demonstrated that the EPCs, also known as angioblasts, are of increased abundance within peripheral blood than previously hypothesised. And whilst this study adequately assessed capabilities of a purified $CD14^+/CD34^-$ subpopulation, it was

interesting to note the results obtained from the transplantation of $CD34^-$ and $CD14^+/CD34^-$ into ischemic mice. Whilst both subpopulations grafted within the endothelium of murine blood vessels, this was only observed following the co-injection of $CD34^+$ cells, suggesting that leukocyte-leukocyte interactions perform a critical role governing angioblast behaviour *in vivo*. Conversely, other groups have demonstrated that $CD34^+$ cells, of which a subset represent EPCs according to one study[396], differentiate along the monocyte/macrophage lineage *in vitro*[400], casting further doubt on the origin of EPCs. This uncertainty has resulted in a theory depicting two distinct populations of EPCs, the first co-expressing monocyte/macrophage and EC markers, with the second expressing EC-associated markers only and subsequently demonstrating an impressive capacity for proliferation[401-402]. At present, however, no methodologies exist to homogeneously purify populations based upon their functional capacities, and thus the origin of EPCs remains illusive[403].

To further complicate matters regarding adherent subpopulations present within human peripheral blood, a recent study has suggested the presence of a multipotent cell population exhibiting many characteristics associated with ES cells[404]. Proposed Multipotent Progenitor Cells (MPCs) were isolated from healthy donors following the administration of granulocyte colony stimulating factor. Small clusters of adherent proliferating cells demonstrated expression of ES cell-associated transcription factors Nanog, Oct4, c-Myc and KLF-4, and furthermore established lineage progression towards neurons, glial cells, hepatocytes, cardiomyocytes, endothelial cells and osteoblasts following exposure to appropriate chemical stimuli. However, whilst this innate differentiation capacity potentially offers a potent source of functional cell types, it is fundamental that this MPC population is homogeneously assessed. Considering chemotactic summoning of cells post trauma, it is likely that the blood contains numerous stem and progenitor subsets in addition to EPCs, trafficking towards sites of injury in order to provide functional repair. This hypothesised MPC population could in fact therefore represent an array of stem and progenitor cells, each with a differing lineage potential. The aim of this chapter is therefore to identify potential adherent subpopulations present within human peripheral blood isolated from four donors using Histopaque and RosetteSep methodologies through antigen-based phenotypic profiling. Furthermore,

alternatively isolated populations will be assessed for their ability to generate CFU-Fs and CFU-GMs to hypothesise residing numbers of multipotent and hematopoietic progenitor subsets respectively. Finally, peripheral blood cells will be induced using adipogenic, chondrogenic and osteogenic differentiation conditions in order to assess the capability of the population to undertake such lineage commitment.

4.1.2 Aims of this Chapter

This investigation aims to assess human peripheral blood as a niche for the isolation of clinically desirable cells, comparing those isolated using Histopaque and RosetteSep methods from four donors. Respectively isolated populations will be analysed using flow cytometry to hypothesise residing subpopulations present and this phenotype, along with their proliferation rate, monitored throughout *in vitro* culture. Should similar phenotype and proliferation modifications as those seen in bone marrow-derived cells be observed, telomere length analysis will be undertaken. CFU assays will be undertaken to quantify the number of CFU-Fs and CFU-GMs present in each population, and their ability to undertake adipogenic, chondrogenic and osteogenic differentiation assessed. Following these investigations, it is hoped that an optimal method for the isolation of cell from human peripheral blood can be identified, yielding populations of multipotent cells maintaining a stable phenotype and proliferation rate following *in vitro* culture.

4.2 Isolation of Cells from Human Peripheral Blood

4.2.1 Isolation of Cells from Human Peripheral Blood using Histopaque and RosetteSep Purification

Human peripheral blood was isolated from the median cubital vein of both male and female donors representing varying ages (*Table 4.1*). Cells were isolated either by Histopaque density centrifugation or RosetteSep purification so as to assess the phenotypic capacities of cells isolated by these two techniques. Pelleted lymphocyte/monocyte layers isolated using the respective isolation strategies were resuspended in DMEM (Low glucose) supplemented with 10% (v/v) FCS and 1% (v/v) 10,000U/ml of penicillin and 10mg/ml of streptomycin in 0.9% (w/v) sodium

chloride (Sigma-Aldrich; Cat#S7653) and seeded onto fibronectin-coated tissue culture polystyrene plates.

Peripheral blood donor	Donor age (Years)	Donor sex
1	23	Male
2	41	Male
3	31	Female
4	39	Female

***Table 4.1* - Peripheral blood donors.**

Cells isolated using both Histopaque and RosetteSep methodologies isolated adherent cells with a small, rounded morphology from all donors 24 hours post isolation (*Figures 4.1* and *4.2*). Following 72 hours of culture, the media was replaced in order to remove non-adherent cells. Interestingly, RosetteSep cultures demonstrated a reduced number of non-adherent cells compared with Histopaque isolation independent of donor. However, following 7 - 10 days of further basal culture, both populations yielded adherent cells displaying a fibroblastic-like phenotype (*Figures 4.3* and *4.4*). Regardless of donor, adherent cells isolated using each methodology displayed limited capacity for cell division, failing to proliferate following passage post initial confluence.

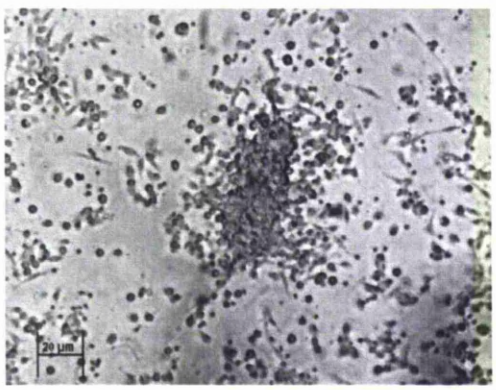

***Figure 4.1* - Blood donor 2 cells isolated using Histopaque density centrifugation and cultured on fibronectin coated plates for 24 hours in basal media.**

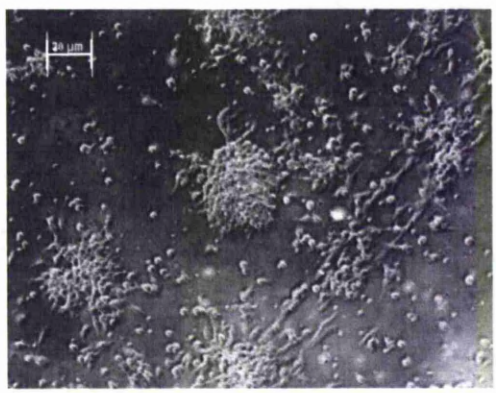

***Figure 4.2* - Blood donor 3 cells isolated using RosetteSep and cultured on fibronectin coated plates for 24 hours in basal media.**

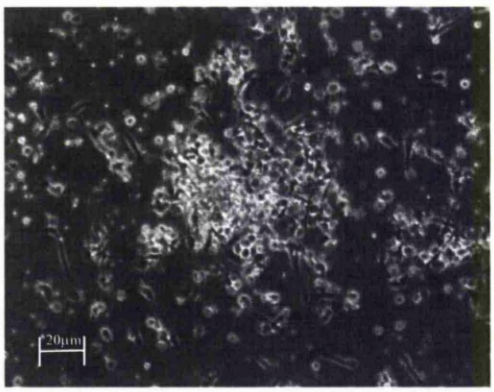

Figure 4.3 - **Blood donor 2 cells isolated using Histopaque density centrifugation and cultured on fibronectin coated plates for 7 days in basal media.**

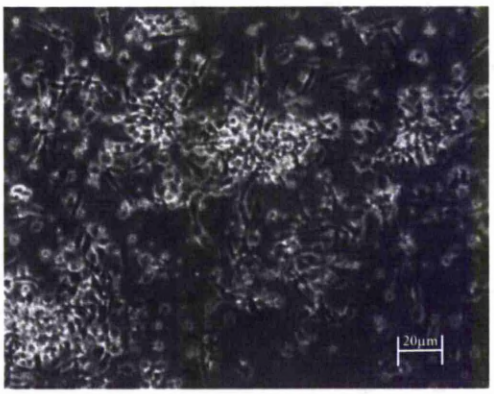

Figure 4.4 - **Blood donor 3 cells isolated using RosetteSep and cultured on fibronectin coated plates for 7 days in basal media.**

4.3 Phenotyping of Peripheral Blood Cells using Flow Cytometry

4.3.1 Phenotypic Analysis of Peripheral Blood Cells throughout Prolonged *In Vitro* Culture using Flow Cytometry

Whilst Histopaque and RosetteSep isolation of cells from each donor generated no observable variations with regards morphology and proliferation capacity, comprehensive assessment of adherent cells was facilitated by surface antigen profiling using flow cytometry. Adherent cells cultured for 7 days in commercial basal media were enzymatically dissociated from the surface prior to analyysis using an array of MSC-associated markers revealed comparable expression in cells from all donors isolated using Histopaque and RosetteSep methodologies (*Figures 4.5* and *4.6*).

CD29 is expressed by leukocytes and proposed MSCs, and cells isolated from all donors using both Histopaque and RosetteSep purification methods demonstrated high levels of expression. Histopaque-isolated cells demonstrated 82.1%, 78.2%, 74.4% and 86.5% expression following 7 days of basal culture from the blood of donors 1, 2, 3 and 4 respectively. Equivalent expression was observed within cells isolated using RosetteSep, exhibiting 76.8%, 90.5%, 85.7% and 81.9% from blood donors 1 - 4.

CD44 is also expressed by leukocytes whilst furthermore demonstrating high levels of expression in bone marrow-derived cells detailed in 3.2.1. Histopaque-isolated cells exhibited 82.7%, 78.3%, 77.8% and 77.9% expression from blood donors 1 - 4 respectively, whilst RosetteSep-isolated equivalents exhibited similar expression levels, generating 78.5%, 84.7%, 85.6% and 87.1%.

CD73 exhibits a broad expression profile including high expression on endothelial cells and MSCs. Both Histopaque and RosetteSep-isolated cells from all blood donors exhibited positive CD73 population expression of approximately 73% - 84%, indicating potential residence of endothelial and/or MSC-like cells within the adherent population.

Both HSCs and MSCs are hypothesised to express the CD90 surface antigen, and blood-derived cells from donors 1 - 4 demonstrated high levels of expression within the adherent population. Histopaque-isolated cells from donors 1 - 4 exhibited 76.1%, 83.5%, 72.8% and 78.9% expression respectively, with RosetteSep-isolated cells demonstrating similar expression of 83.8%, 90.5%, 89.3% and 90.0%.

CD105 is presented on the surface of numerous cell types including endothelial cells, MSCs and activated monocytes, and populations derived from human peripheral blood therefore predictably demonstrated high levels of expression. Histopaque-isolated cells exhibited 80.8%, 83.4%, 84.4% and 80.0% expression in donor cells 1 to 4 respectively with RosetteSep-isolated cells exhibiting positive expression in 91.5%, 86.5%, 87.7% and 86.7% of cells.

Also known as VCAM-1, CD106 has been proposed as a chemotactic regulator of MSCs post trauma. Within peripheral blood populations isolated using Histopaque density centrifugation, donors 1 through 4 demonstrated consistent levels of CD106 expression, with 65.6%, 69.8%, 63.5% and 62.8% of cells respectively. RosetteSep-isolated cells demonstrated fractionally lower expression within the population, exhibiting 59.7%, 54.8%, 54.8% and 49.2% expression in donor cells 1 - 4.

Histopaque-isolated cells exhibited 69.9%, 70.9%, 72.1% and 72.4% expression of the primitive HSC-associated marker CD117 in blood donors 1 - 4 respectively

following 7 days of basal culture. RosetteSep-isolated cells demonstrated slightly increased expression at 76.7%, 77.0%, 74.0% and 84.3%.

CD146 currently represents a marker for isolating populations of cells capable of undertaking multilineage differentiation, and the Histopaque populations from donors 1 through 4 demonstrated 76.1%, 74.8%, 67.6% and 74.3% expressions respectively. RosetteSep-isolated cells exhibited marginally increased levels of CD146, with 74.2%, 79.5%, 87.4% and 85.2%. CD166 functions as a transmembrane glycoprotein and is expressed on MSCs and activated monocytes. Within peripheral blood cells, populations isolated using Histopaque exhibited surprisingly low levels, with only 16.3%, 14.5%, 18.7% and 20.2%. RosetteSep isolations gave similar results, with 13.7%, 18.7%, 21.0% and 16.6%.

HLA-ABC is a key antagonist within the immune response and is highly expressed on MSCs. Peripheral blood cells derived using Histopaque demonstrated 53.1%, 49.4%, 42.8% and 50.6% expressions, with RosetteSep-derived populations exhibiting a similar phenotype, demonstrating 59.5%, 52.4%, 48.5% and 50.5%. Interestingly the MHC class II marker HLA-DR, which is expressed at low levels in bone marrow-derived cells, was highly expressed in peripheral blood-derived populations. Histopaque-isolated cells demonstrated 59.1%, 54.9%, 42.6% and 31.5% expression, whilst RosetteSep-isolated populations produced similar expression, with 55.7%, 63.0%, 54.7% and 51.6%.

STRO-1 expression within the peripheral blood populations was comparable to levels observed within bone marrow-derived cells, with cells isolated from blood donors 1 - 4 using Histopaque exhibiting 0.6%, 0.3%, 0.4% and 0.4% expression respectively. RosetteSep-isolated cells also demonstrated STRO-1 expression similar to bone marrow-derived populations, with 0.3%, 0.7%, 0.4% and 0.3%.

Considering MSC-associated surface antigen expression of peripheral blood-derived cells isolated using both Histopaque and RosetteSep, it is apparent that, whilst not exhibiting morphological or proliferative similarities, the population contains subpopulations of cells phenotypically similar to those present within bone marrow-derived populations at low passage, displaying comparable if slightly decreased

levels of CD29, CD44, CD90, CD117, CD146 and STRO-1. These cells may therefore incorporate the hypothesised MPC population. Furthermore, CD73 and CD105 were comparably expressed within the two populations, although peripheral blood cells demonstrated marginally higher expression. MSC chemotaxic regulator CD106 exhibited significantly increased expression within peripheral blood populations, probably attributable to its function of guiding MSCs to sites of injury, a capacity not required whilst residing within the bone marrow niche. Surprisingly CD166, which is highly expressed within early passage bone marrow populations, demonstrated much lower expression within peripheral blood cells. However, most significant was the increased expression of MHC classes I and II, which demonstrated considerably higher expression within peripheral blood populations compared with bone marrow-derived counterparts, an expression which could impact significantly with regards allogeneic transplantations of such cells.

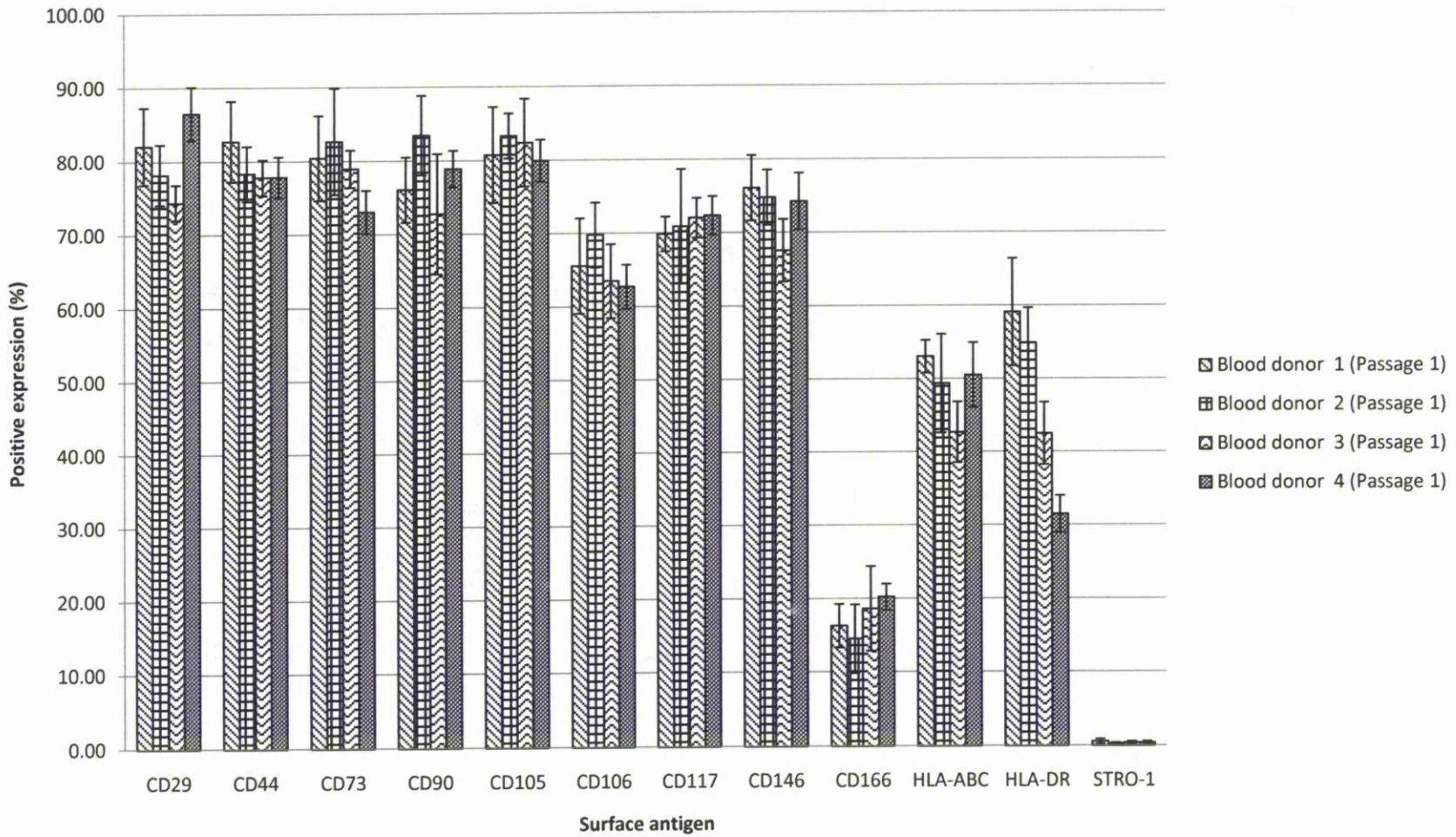

Figure 4.5 - **MSC-associated marker phenotyping of peripheral blood-derived cells isolated by Histopaque density centrifugation cultured for 7 days in basal media. Values represent mean positive expression as observed by flow cytometry (n = 4). Error bars correspond to Standard Deviations.**

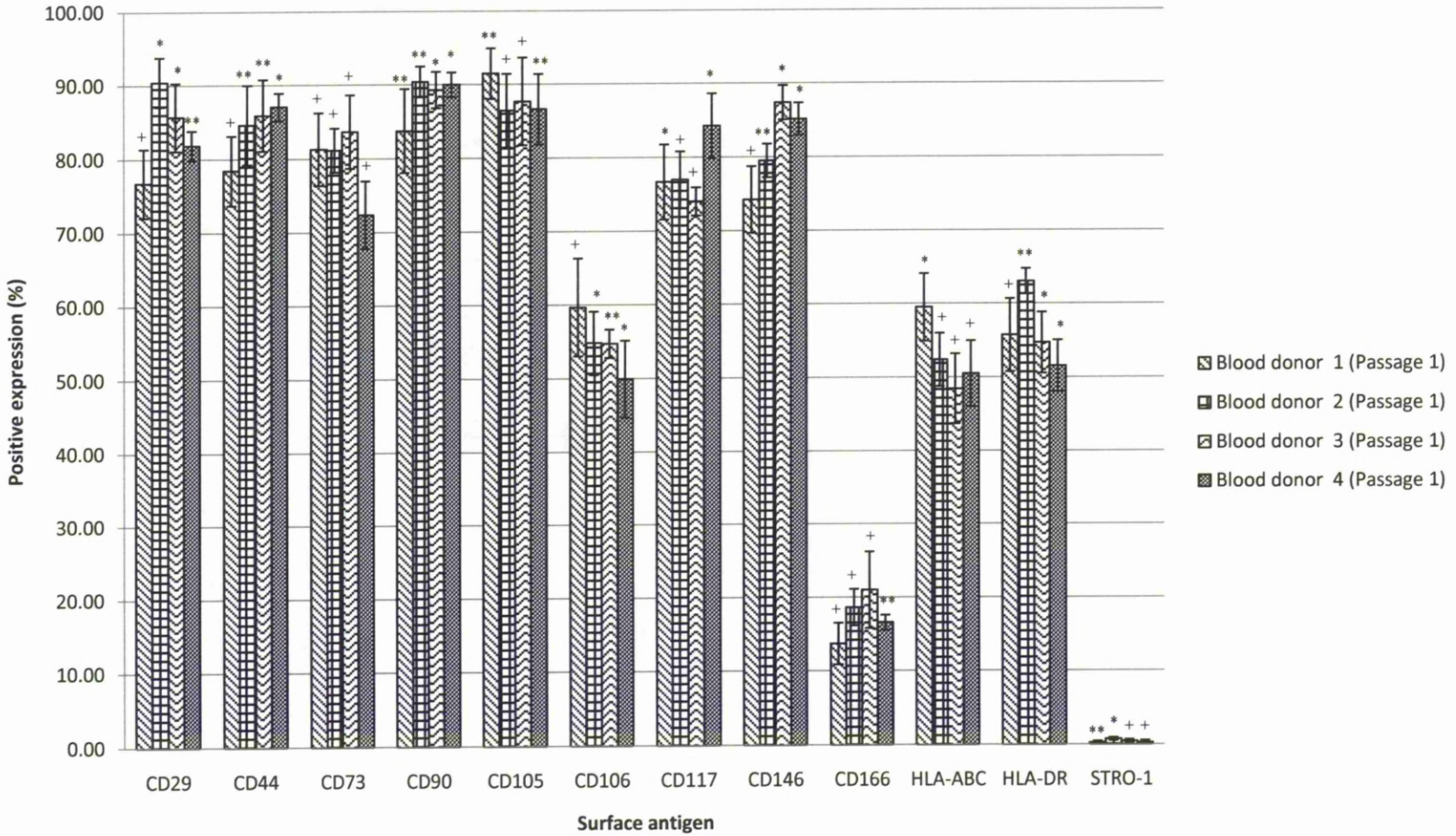

Figure 4.6 **- MSC-associated marker phenotyping of peripheral blood-derived cells isolated by RosetteSep cultured for 7 days in basal media. Values represent mean positive expression as observed by flow cytometry (n = 4). Error bars correspond to Standard Deviations. Student *t*-test indicated that there were significant (*$p \leq 0.001$) (**$p \leq 0.05$) and non-significant (+$p \geq 0.05$) antigen expression differences between cells isolated using Histopaque and RosetteSep from donors 1-4.**

Furthering MSC-associated surface antigen profiling, peripheral blood cells were investigated for their expression of hematopoietic and endothelial cell-associated antigens (*Figures 4.7* and *4.8*). The monocyte, endothelial and platelet-associated antigen CD9 exhibited expression within 17.2%, 13.7%, 17.4% and 16.9% of cells isolated from donors 1 - 4 respectively using Histopaque and 18.8%, 15.1%, 20.9% and 14.4% with RosetteSep isolation.

CD14 has been proposed as a key marker of EPCs, and cells isolated using Histopaque from donors 1 - 4 demonstrated 69.5%, 66.5%, 75.7% and 60.1% positive expression respectively. RosetteSep isolation produced similar CD14 expression, with 65.9%, 59.7%, 58.6% and 57.2%. The endothelial-associated marker CD31 was similarly expressed by cells isolated using both Histopaque and RosetteSep methodologies, with 56% - 68% having expression in blood donors 1 - 4.

Following previous studies attempting to identify EPCs within peripheral blood, numerous hypotheses have been generated with regards to their surface expression patterns. Whilst almost all perceive that EPCs express CD14, the expression of CD34 on EPCs remains questionable. Histopaque-isolated cells from donors 1 - 4 demonstrated 11% - 18% expression of the CD34 class II variant, with RosetteSep-isolated cells exhibiting similar expression. However, CD34 class III demonstrated considerably greater expression within both the Histopaque and RosetteSep purified cells of 51% - 65%.

CD41a is predominantly expressed on platelets and megakaryocytes and was therefore predictably expressed by low numbers of the population, indicating that the majority of such cells were removed during Histopaque and RosetteSep isolations. CD45 is expressed by numerous blood cells including monocytes and was highly expressed by cells isolated using Histopaque, with 84.1%, 85.6%, 87.0% and 88.1% from donors 1 - 4. RosetteSep-isolated cells exhibited similar expression with 89.4%, 86.8%, 82.0% and 92.1% respectively. CD50 represents a leukocyte-associated antigen and is highly expressed within donor populations isolated using Histopaque and RosetteSep, with 83% - 91% of the population demonstrating positive expression. Interestingly, leukocyte adhesion molecule CD62E demonstrated expression using Histopaque and RosetteSep of 11% - 25% positive expression,

suggesting the presence of cytokine-stimulated endothelial cells within the population. Finally, hematopoietic and non-hematopoietic progenitor subset-associated marker CD133 demonstrated 29% - 51% positive expression in both isolation techniques, indicating the presence of progenitor subsets exhibiting endothelial and alternative lineage potentials.

Hematopoietic and endothelial-associated antigen expression within all peripheral blood donors isolated demonstrated similar expression profiles. The expression of CD14, respective classes of CD34 and CD133 suggests the presence of endothelial progenitor subsets within the population, with their isolation and homogeneous characterisation offering significant clinical potential. However, purification using each individual surface antigen is unlikely to allow homogeneous isolation of EPCs since CD14 and CD133 are likely to be expressed on progenitors of alternative lineage and CD34 of alternative hematopoietic progenitors. Furthermore, whilst purification based upon combined expression of these three markers may result in greater homogeneity, it is likely that alternative progenitor impurities would persist and thus alternative sorting methods should be developed.

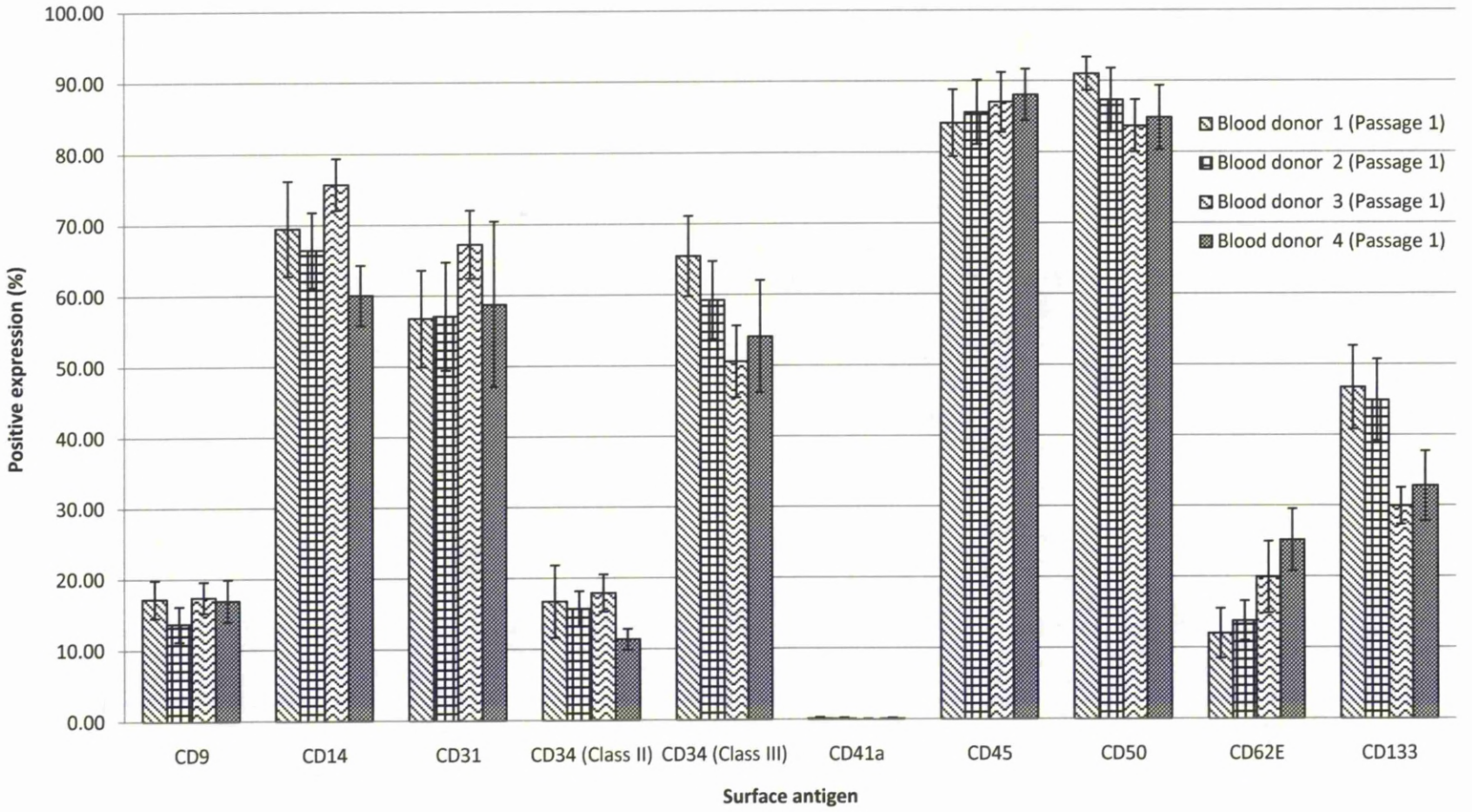

Figure 4.7 - **HSC and endothelial-associated marker of peripheral blood-derived cells isolated by Histopaque density centrifugation cultured for 7 days in basal media. Values represent mean positive expressions as observed by flow cytometry (n = 4). Error bars correspond to Standard Deviations.**

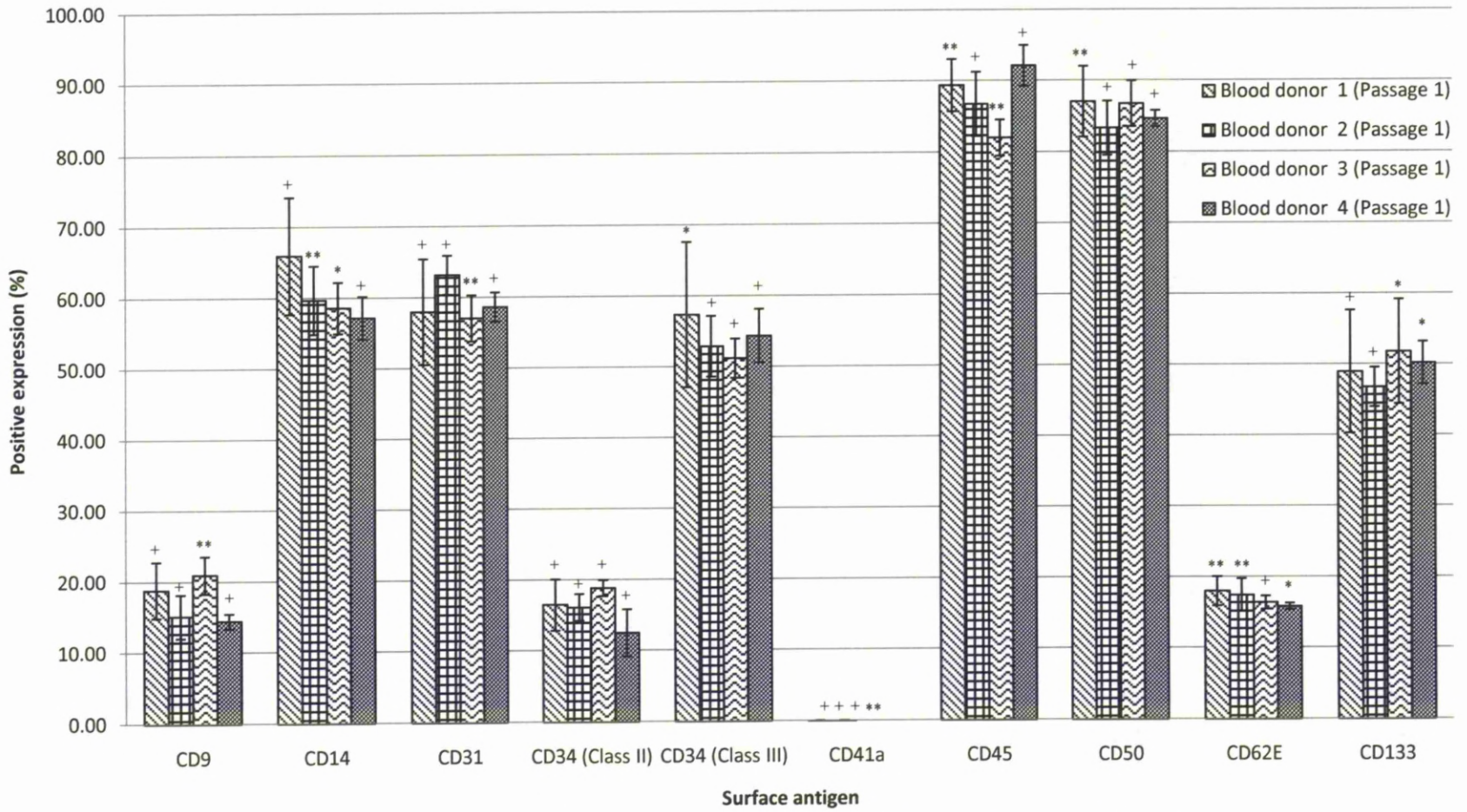

Figure 4.8 - **HSC and endothelial-associated marker phenotyping of peripheral blood-derived cells isolated by RosetteSep cultured for 7 days in basal media. Values represent mean positive expressions as observed by flow cytometry (n = 4). Error bars correspond to Standard Deviations. Student *t*-test indicated that there were significant (*$p \leq 0.001$) (**$p \leq 0.05$) and non-significant (+$p \geq 0.05$) antigen expression differences between cells isolated using Histopaque and RosetteSep from donors 1-4.**

Peripheral blood-derived populations were finally investigated for their expression of ES and alternative lineage progenitor-associated surface antigens (*Figures 4.9* and *4.10*). CD15 is a marker associated with monocytes and murine ES and MSCs, although it was not expressed by bone marrow-derived populations. Since peripheral blood-derived cells exhibit significant comparability with bone marrow-derived populations when probed with MSC-associated antigens, high levels of expression observed in peripheral blood-derived populations are likely to be attributable to monocytes. Histopaque-isolated cells exhibited 54.4%, 48.6%, 46.9% and 62.4% positive expression in donors 1 - 4 respectively, whilst RosetteSep isolation demonstrated 52.5%, 53.5%, 43.5% and 42.4% respectively.

CD30 is expressed in early embryonic cells in addition to immune-associated cells, and both Histopaque and RosetteSep peripheral blood-derived populations exhibited 0.5% - 1.7% cell specific expression within donor populations 1 - 4. Whilst this population may represent a subset of undesired immunogenic cells, they may in fact represent an immature cell population exhibiting high proliferation and differentiation capacity, and thus their isolation and homogeneous characterisation would be of significant interest.

CD56 is known to be expressed on approximately 10% - 25% of peripheral blood leukocytes although it is also thought to be expressed by more primitive progenitor subsets, and thus its 1% - 3% expression within isolated populations is of interest, with homogeneous isolation of subsets of cells expressing CD56 perhaps producing cells with multidifferentiation potential.

CD81 represents a surface antigen associated with neural progenitor subsets and is expressed by 0.5%, 0.2, 0.1% and 0.1% of cells isolated using Histopaque from donors 1 - 4 respectively. RosetteSep isolations generated 0.1% positive expression within donor 1 cells, although donor 2, 3 and 4 populations failed to demonstrate CD81 expression, and it may be that the proposed increased monocyte purification of RosetteSep isolation discriminates against this cell type. NGFR represents a surface antigen expressed by more committed neuronal phenotypes, and Histopaque isolations from donors 1 - 4 exhibited 0.5%, 0.2%, 0.1% and 0.1% expression respectively. Interestingly, RosetteSep isolations demonstrated 0.1% upregulation in

donor 1 cells only, furthering the hypothesis that RosetteSep may discriminate against these cells.

CD135 represents a primitive marker of ES cells and HSCs, and was expressed within 9.0%, 6.9%, 3.3% and 2.1% of cells isolated from donors 1 - 4 respectively using Histopaque. RosetteSep isolations, however, produced higher levels with 9.6%, 18.4%, 4.6% and 7.1% expression.

Surface antigen profiling of peripheral blood-derived populations has determined that variations in donor age or sex yields insignificant differences with regards phenotype of adherent populations, with cells displaying consistent levels of MSC, HSC, EPC, monocyte and alternative lineage progenitor markers. Furthermore, varying methods of isolation produce little difference with regards population surface expression, with differences probably attributable to environmental volatility of blood donors, unavoidable parameters such as time of isolation (morning or afternoon), diet and recent activity of the donor undoubtedly resulting in varying numbers of each cell population being present within the peripheral blood circulation. However, regardless of accompanying parameters, peripheral blood undoubtedly contains cells of varying lineage potential and, considering its relatively non-invasive isolation, could represent a readily available and renewable source for autologous clinical applications, although allogeneic utilisation must first overcome the high levels of MHC class expression. It is therefore suggested that each individual subpopulation is homogeneously isolated and assessed for differentiation capacity, potentially providing a source of clinically useful cells on tap.

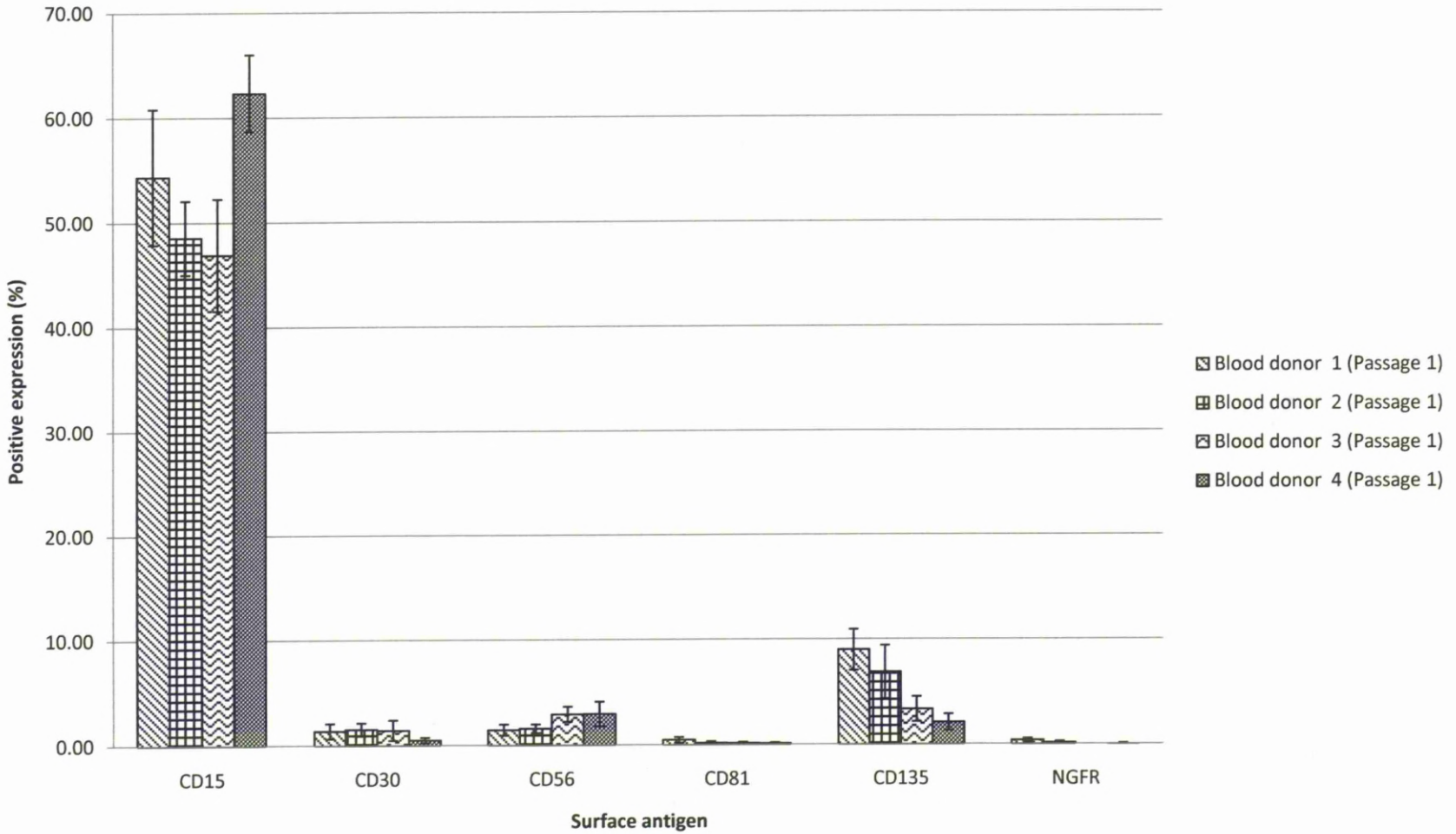

Figure 4.9 **- ES and progenitor-associated marker of peripheral blood-derived cells isolated by Histopaque density centrifugation cultured for 7 days in basal media. Values represent mean positive expressions as observed by flow cytometry (n = 4). Error bars correspond to Standard Deviations.**

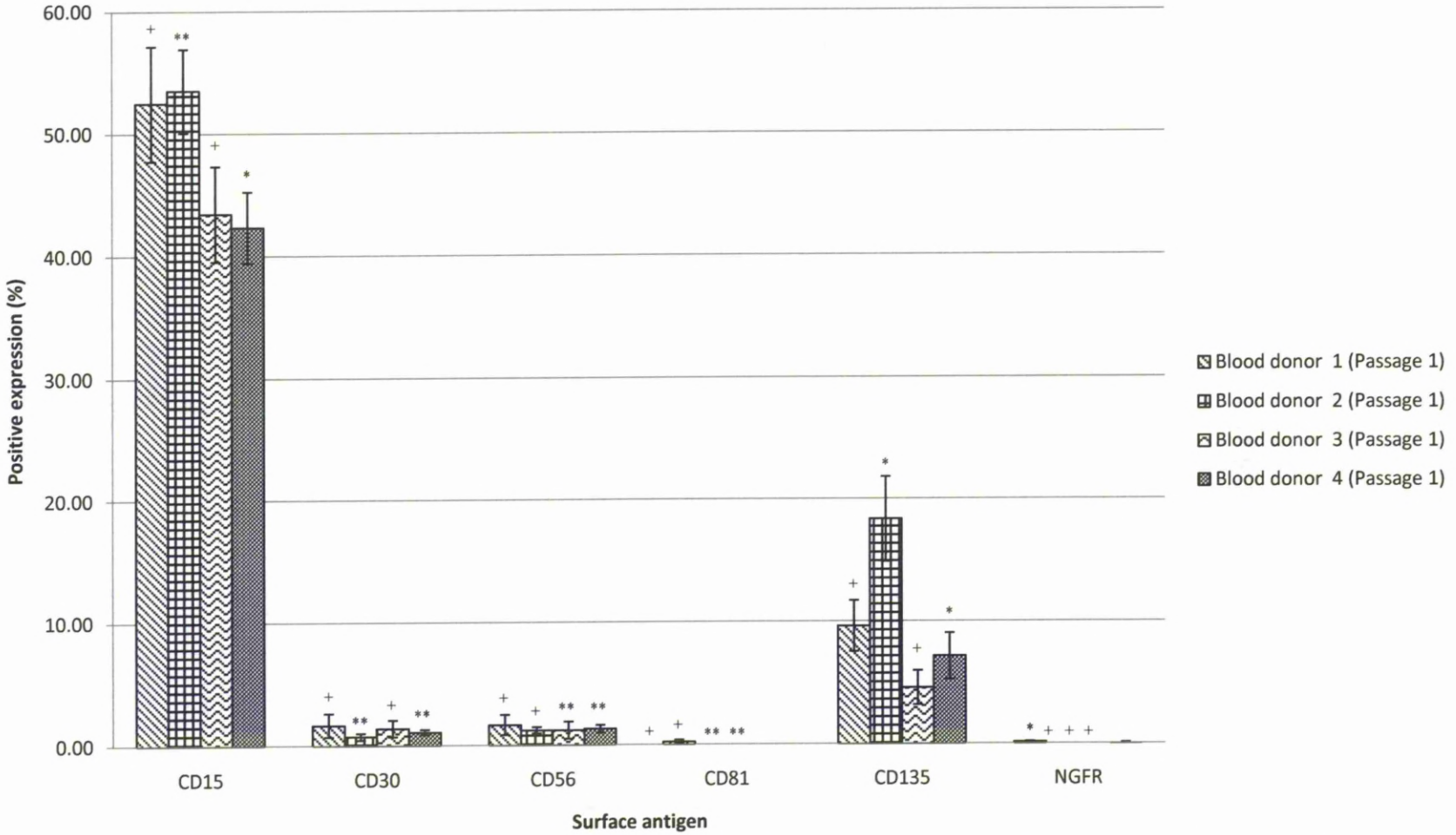

Figure 4.10 **- ES and progenitor-associated marker phenotyping of peripheral blood-derived cells isolated by RosetteSep cultured for 7 days in basal media. Values represent mean positive expressions as observed by flow cytometry (n = 4). Error bars correspond to Standard Deviations. Student *t*-test indicated that there were significant (*$p \leq 0.001$) (**$p \leq 0.05$) and non-significant (+$p \geq 0.05$) antigen expression differences between cells isolated using Histopaque and RosetteSep from donors 1-4.**

4.4 CFU Analysis of Peripheral Blood Cells

4.4.1 CFU-Fibroblast Analysis of Peripheral Blood-derived Cells

Given the expression of surface antigens associated with MSCs and lineage progenitors observed by flow cytometry, CFU-F assays were performed on peripheral blood-derived cells to establish the number of non-hematopoietic multipotent progenitors present. Following initial confluence, 1 x 10^6 isolated cells were seeded for CFU-F analysis and the number of colonies (*Figures 4.11* and *4.12*) counted following 12 days of culture. Blood donor 1 cells isolated using Histopaque generated an average of 74.5 colonies per 35mm^2 culture dish, similar to the 78.5 colonies achieved with RosetteSep. Blood donors 2, 3 and 4 isolated using Histopaque generated similar numbers of colonies following 12 days of culture, with respective populations generating 66.8, 69.8 and 68.3 colonies per 35mm^2 culture dish. RosetteSep-isolated cells for these respective donors generated 82.3, 70.8 and 53.3 (*Figure 4.13*). Interestingly, these data suggest that, despite 75% - 90% of cells expressing the hypothesised MSC-associated marker CD146, the actual number of cells within the population exhibiting CFU-F capacities, and therefore associated stem/progenitor characteristics, is much smaaller. In fact, less than 0.007% of cells exhibited the capacity to generate CFU-Fs, suggesting that the remainder of cells may represent more terminally committed progenitor subsets. STRO-1 was expressed on 0.2% - 0.8% of the population, and whilst this number correlates more accurately with the number of cells exhibiting CFU-F capacity compared with alternative MSC markers such as CD90 and CD146, the number of STRO-1$^+$ cells within the population are too plentiful for each to represent a CFU-F forming cell. Therefore, it may be that STRO-1 allows partial purification of progenitor subsets, though still incorporating cells demonstrating increased commitment.

Regarding donor variation, results obtained suggest minimal differences in the number of CFU-Fs present within each donor population, with differences again likely to be attributable to environmental factors discussed previously. Furthermore, Histopaque and RosetteSep isolations resulted in cells capable of generating similar numbers of CFU-Fs, supplementing the phenotype data achieved in 4.3.

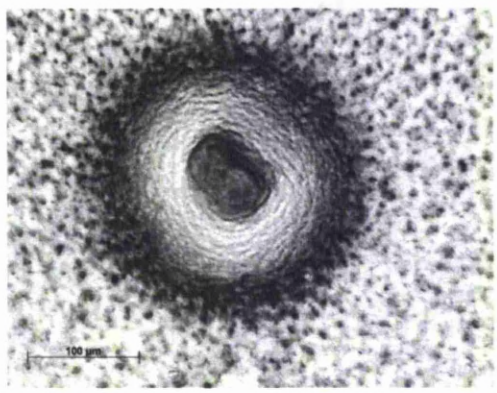

Figure 4.11 - **CFU-F formation by adherent blood donor 1 cells isolated using Histopaque and cultured for 12 days in MethoCult media.**

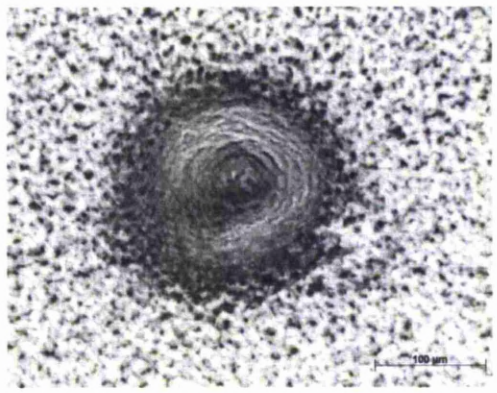

Figure 4.12 - **CFU-F formation by adherent blood donor 1 cells isolated using RosetteSep and cultured for 12 days in MethoCult media.**

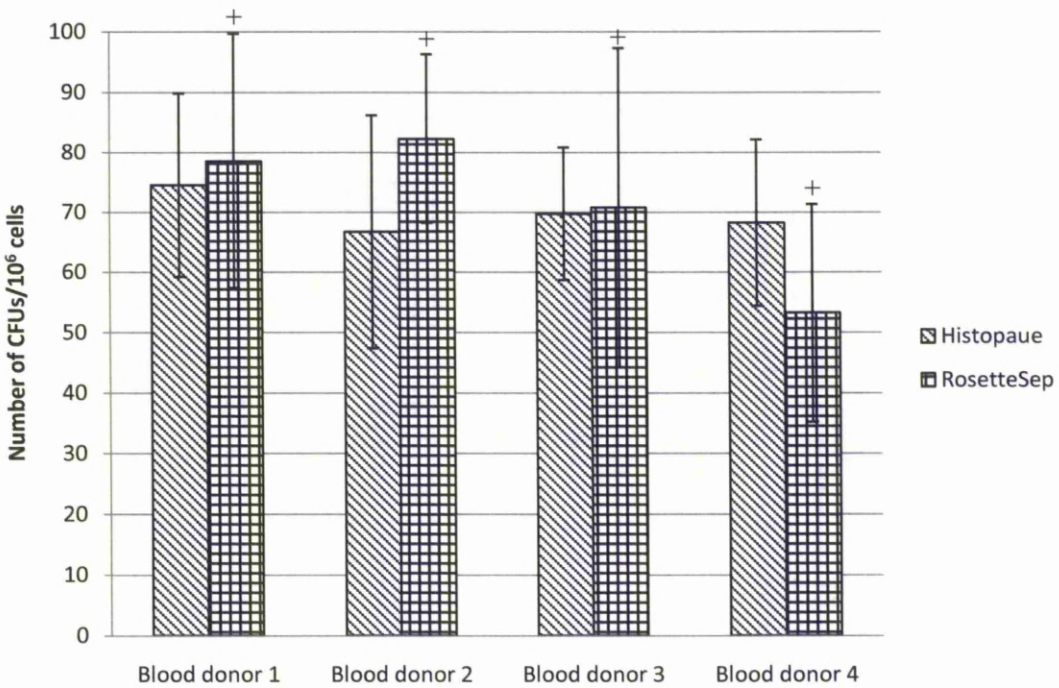

Figure 4.13 - **CFU-F formation per 1 x 10^6 cells isolated from human peripheral blood donors 1 - 4 using Histopaque and RosetteSep isolation methods following 12 days of MethoCult culture. Values represent mean number of cells observed per 35mm^2 culture dish for each donor and isolation technique (n = 4). Error bars correspond to Standard Deviations. Student *t*-test indicated that there were no significant differences in the number of CFU-Fs generated in donors 1-4 isolated using RosetteSep compared with corresponding Histopaque isolations (+$p \geq 0.05$).**

4.4.2 CFU-Granulocyte/Monocyte Analysis of Peripheral Blood-derived Cells

Peripheral blood-derived cells demonstrated positive expression of surface markers associated with hematopoietic progenitors and subsequently were assessed for their capacity to generate CFU-GMs. CFU-GM assays allow the quantification of hematopoietic progenitors within cell populations. Peripheral blood cells isolated from donors 1 - 4 using Histopaque and RosetteSep were cultured to confluency and 1 x 10^6 cells seeded in MethoCult stimulation media. Following 12 days of culture, seeded populations had generated visible colonies (*Figures 4.14* and *4.15*). Histopaque-isolated cells generated an average of 69.3, 60.1, 55.3 and 57.5 colonies per 35mm^2 culture dishes, compared to 62.3, 61.0, 64.5 and 49.3 colonies generated following RosetteSep isolation (*Figure 4.16*). However, these results once again cast doubt on the exact phenotype of cells exhibiting HSC and EPC surface antigens. CD14 represents a hypothesised EPC marker, and was expressed by 57% - 76% of donor cells. However, the number of colonies generated by 1 x 10^6 cells suggests that again less than 0.007% of cells within the population are capable of generating CFU-GMs. Thus it is likely that the majority of cells expressing HSC and EPC markers such as CD14, CD34 classes II and III, CD45 and CD133 are progenitors incapable of generating CFU-GM, suggesting a more committed phenotype.

Considering comparative cell profiling of the peripheral blood populations, variation in blood donor age or sex revealed no significant variation regarding the number of CFU-GM forming cells within the populations, with differences likely to be due to environmental variance. This echoes variation due to method of isolation: no significant differences were observed in number of CFU-GM forming cells isolated using the two methods. Considering the minimal variation observed with regards surface phenotype and number of CFU-Fs/CFU-GMs generated following Histopaque and RosetteSep isolations, Histopaque may represent a more attractive technology for isolation of cells for clinical application given its reduced cost. Therefore the remainder of this chapter will concentrate upon assessing cells isolated using Histopaque density centrifugation.

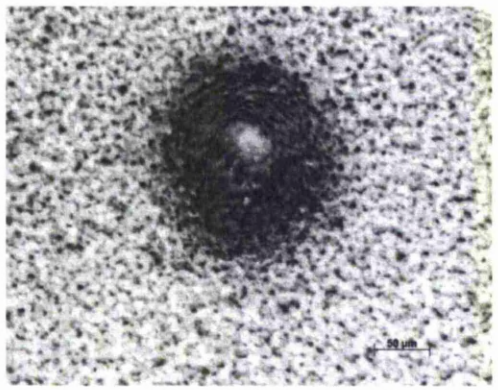

Figure 4.14 - **CFU-GM formation by adherent blood donor 1 cells isolated using Histopaque and cultured for 12 days in MethoCult media.**

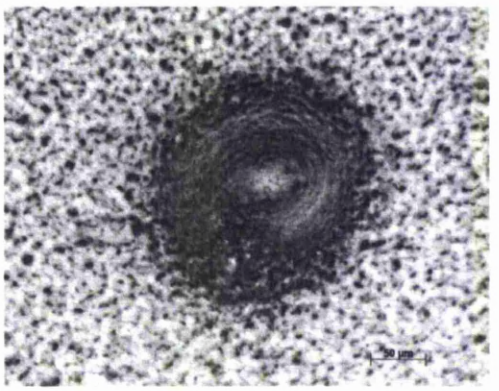

Figure 4.15 - **CFU-GM formation by adherent blood donor 1 cells isolated using RosetteSep and cultured for 12 days in MethoCult media.**

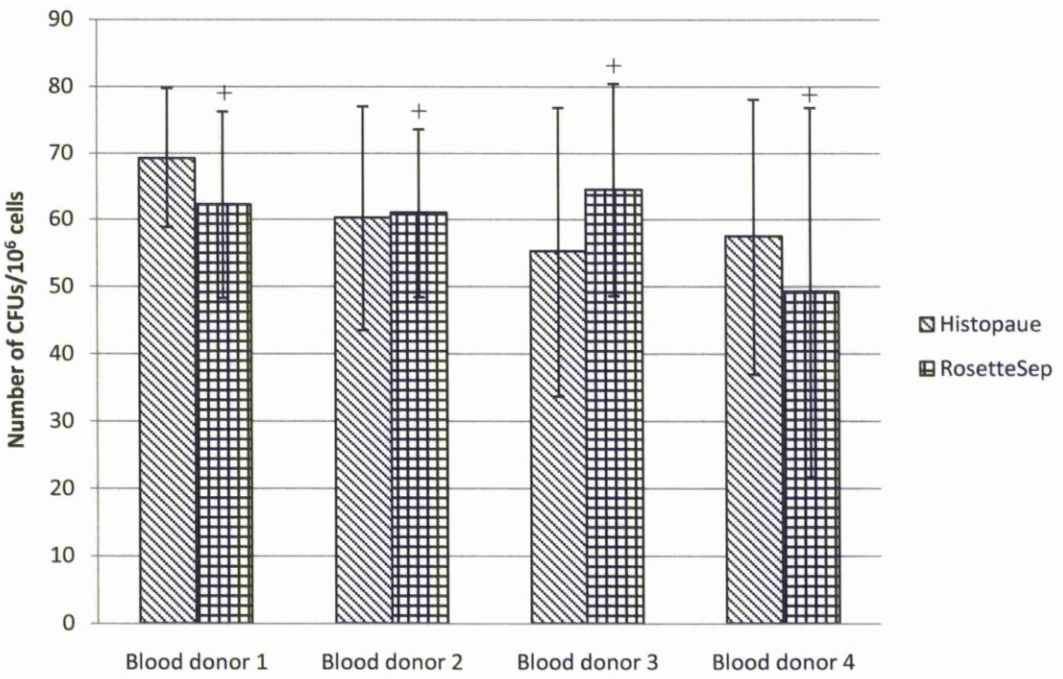

Figure 4.16 - **CFU-GM formation per 1 x 10^6 cells isolated from human peripheral blood donors 1 - 4 using Histopaque and RosetteSep isolation methods following 12 days of MethoCult culture. Values represent mean number of cells observed per 35mm^2 culture dish for each donor and isolation technique (n = 4). Error bars correspond to Standard Deviations. Student *t*-test indicated that there were no significant differences in the number of CFU-GMs generated in donors 1-4 isolated using RosetteSep compared with corresponding Histopaque isolations (+$p \geq 0.05$).**

4.5 Differentiation of Peripheral Blood Cells

4.5.1 Adipogenic Differentiation of Peripheral Blood-derived Cells using Commercial Differentiation Media

Peripheral blood-derived cells demonstrated expression of multipotent-associated markers and furthermore a small number were able to generate CFU-Fs following appropriate stimulation, an intrinsic property associated with highly proliferative and plastic cells. To assess differentiation potential within peripheral blood populations, cells isolated from donors 1 - 4 using Histopaque were subjected to differentiation stimuli. To ascertain capabilities of the population to undertake adipogenic differentiation, adherent cells were cultured in basal media for 7 days, at which point media was replaced with commercial pre-adipocyte growth media. Following 10 days of culture, pre-adipocyte differentiation media was added to the cells for 72 hours, after which cultures were maintained for 15 days in adipocyte nutrition media. Following 21 days of culture, populations from donors 1 - 4 heterogeneously expressed the adipocyte-specific circulatory protein adiponectin (*Figure 4.17*), and the key adipogenesis regulator PPARγ (*Figure 4.18*) within approximately 50% of cells. Furthermore, following 21 days of adipogenic induction, approximately 20% of the population demonstrated lipid production as observed by positive staining with Oil Red O (*Figures 4.19* and *4.20*).

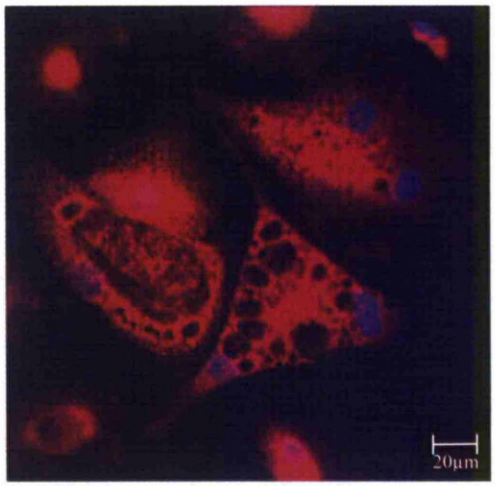

Figure 4.17 - **Peripheral blood donor 2 cells (Passage 1) isolated using Histopaque cultured in commercial adipogenic differentiation media for 21 days stained with Hoechst 33258 (blue) and adiponectin antibody (red). Approximately 50% of adherent blood cells exhibited positive adiponectin expression.**

Figure 4.18 - **Peripheral blood donor 2 cells (Passage 1) isolated using Histopaque cultured in commercial adipogenic differentiation media for 21 days stained with Hoechst 33258 (blue) and PPARγ antibody (red). Approximately 50% of adherent blood cells exhibited positive PPARγ expression.**

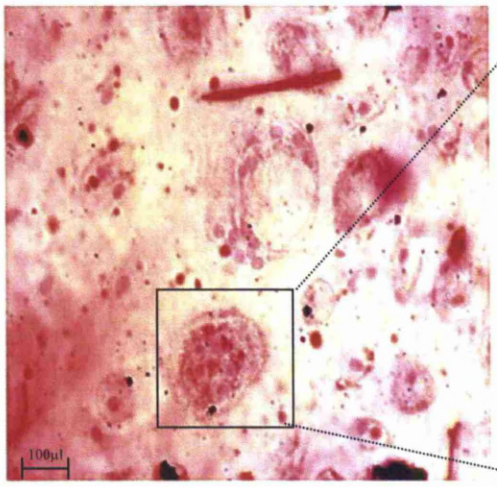

Figure 4.19 - **Peripheral blood donor 2 cells (Passage 1) isolated using Histopaque cultured in commercial adipogenic differentiation media for 21 days stained Oil Red O (red). Approximately 20% of adherent blood cells exhibited positive Oil Red O expression.**

Figure 4.20 - **Peripheral blood donor 2 cells (Passage 1) isolated using Histopaque cultured in commercial adipogenic differentiation media for 21 days stained Oil Red O (red) (Magnified version of *Figure 4.19*). Approximately 20% of adherent blood cells exhibited positive Oil Red O expression.**

4.5.2 Chondrogenic Differentiation of Peripheral Blood-derived Cells using Commercial Differentiation Media

Furthering demonstration of adipogenic differentiation, isolated peripheral blood cells cultured for 7 days in basal media post Histopaque isolation were induced with chondrogenic stimulation media, which was replenished every 3 days throughout the 28 day culture period. Peripheral blood cells isolated from donors 1 - 4 demonstrated chondrogenic lineage progression following 21 days of culture, expressing the chondrogenic-associated protein Collagen II (*Figure 4.21*) and the hypertrophic cartilage protein Collagen X (*Figure 4.22*) in approximately 70% of the population.

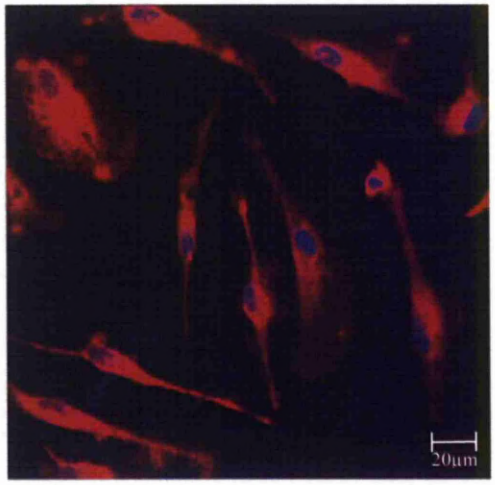

Figure 4.21 **- Peripheral blood donor 2 cells (Passage 1) isolated using Histopaque cultured in commercial chondrogenic differentiation media for 21 days stained with Hoechst 33258 (blue) and collagen II antibody (red). Approximately 70% of adherent blood cells exhibited positive collagen II expression.**

Figure 4.22 **- Peripheral blood donor 2 cells (Passage 1) isolated using Histopaque cultured in commercial chondrogenic differentiation media for 21 days stained with Hoechst 33258 (blue) and collagen X antibody (red). Approximately 70% of adherent blood cells exhibited positive collagen X expression.**

4.5.3 Osteogenic differentiation of Peripheral Blood-derived Cells using Commercial Differentiation Media

Histopaque-isolated cells from peripheral blood donors 1 - 4 were further assessed for their ability to undergo non-associated lineage differentiation by assessing their capability to generate osteoblasts. Adherent cells cultured for 7 days post isolation were induced with commercial osteogenic differentiation media which was subsequently replenished every 3 days throughout the culture. Following 21 days of

stimulated culture, cells exhibited expression of the osteogenesis master regulator CBFA-1 (*Figure 4.23*) and the mineralisation co-ordinator osteocalcin (*Figure 4.24*) within approximately 70% of the population, demonstrating the capacity of subpopulations within peripheral blood-derived cells to undertake osteogenic differentiation.

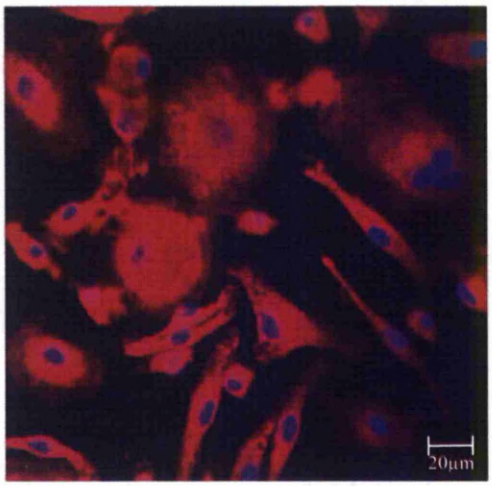

***Figure 4.23* - Peripheral blood donor 2 cells (Passage 1) isolated using Histopaque cultured in commercial osteogenic differentiation media for 21 days stained with Hoechst 33258 (blue) and CBFA-1 antibody (red). Approximately 70% of adherent blood cells exhibited positive CBFA-1 expression.**

***Figure 4.24* - Peripheral blood donor 2 cells (Passage 1) isolated using Histopaque cultured in commercial osteogenic differentiation media for 21 days stained with Hoechst 33258 (blue) and osteocalcin antibody (red). Approximately 70% of adherent blood cells exhibited positive osteocalcin expression.**

4.6 Conclusion

4.6.1 Peripheral Blood as a Niche for the Isolation of Clinically Desirable Cells

Cells isolated from peripheral blood of donors comprising varying sex and age demonstrated little morphological or phenotypic differences regardless of isolation methodology. Adherent populations demonstrated heterogeneous surface antigen expression associated with a diverse range of cell types; CD14, hypothesised to be expressed by EPCs, was expressed by approximately 65% of cells and, following results obtained in previous studies hypothesising that there may in fact be two distinct EPC populations, comprising a $CD14^+/CD34^-$ and $CD14^+/CD34^+$ phenotype, the expression of CD34 class II and CD34 class III antigens within approximately 15% - 60% of cells respectively, further substantiated this hypothesis. Furthermore,

the expression of CD9 and CD105 within subsets of the population suggested the presence of EPCs within peripheral blood populations.

In addition to expressing both classes of CD34 antigen, which are expressed by both HSCs and EPCs, hematopoietic antigens CD90, CD105 and CD135 were also expressed, indicating the presence of a HSC subpopulation within peripheral blood-derived cells. The presence of HSC-like cells was also signified by the ability of 0.007% of cells to generate CFU-GMs, although this confirmed that not all HSC antigen expressing cells are of hematopoietic lineage.

A comparable number of peripheral blood-derived cells also demonstrated the ability to undertake stimulated CFU-F formation, and the presence of potential MPCs was further suggested by the heterogeneous expression of CD29, CD44, CD73, CD90, CD105, CD146, CD166 and STRO-1. However, given the expression of ES and progenitor-associated antigens CD15, CD30, CD56 and CD135, it could be that progenitor subsets were responsible for the formation of these observed CFU-Fs.

Given the heterogeneous nature of adherent peripheral blood cells, and furthermore the hypothesised capability of HSCs to undertake non-hematopoietic multilineage differentiation, it is difficult to hypothesise which cell type is responsible for the observed adipogenic, chondrogenic and osteogenic differentiation. However, at present methods to purify cells exhibiting MPC, ES cell-like or progenitor, HSC and EPC phenotypes are unavailable, thus restricting investigations attempting to identify the responsible cell type.

Whilst peripheral blood appears to contain a heterogeneous array of cells exhibiting MPC, ES cell-like and committed progenitor, HSC and EPC-asscoiated characteristics, the inability of cells to proliferate following initial passage infers significant clinical boundaries which must be addressed via tailoring of culture conditions. Perhaps therefore homogeneous isolation of individual subpopulations would allow both the identification of cells exhibiting varying capabilities and subsequent tailoring of *in vitro* culture conditions to allow prolonged proliferation of such cell types, highlighting peripheral blood as a self-renewing source of MPC, progenitor, HSC and EPC subsets with numerous clinical applications.

4.6.2 Response to Chapter Aims

Results presented within this chapter largely address aims detailed in 4.1.1, with cells isolated from four different donors using Histopaque and RosetteSep methods characterised by surface phenotype expression, CFU-F and GM capabilities, and an ability to undertake multilineage differentiation. However, given the limited self-renew capacity of adherent cells, no quantifiable data could be gained with regards phenotypic and proliferative stability or telomere length regiulation. Nevertheless, it was apparent that cells isolated from the four donors using Histopaque and RosetteSep methods yielded phenotypically similar cells, and studies should now attempt to optimise culture conditions to prolong their *in vitro* lifespan.

5. Human Umbilical Cord as a Potential Source of Multipotent Adult Stem/Progenitor Cells

5.1 Introduction

5.1.1 Umbilical Cord Cells

The umbilical cord is a connecting structure allowing passage of key nutrients from the mother to the residing embryo or fetus, developing from the yolk sac in the 5th week of development. Interestingly, the cord is not directly connected to a mother's circulatory system, and instead interacts with the placenta which permits transfer of materials to and from the mother's blood without concomitant interaction. Structurally the cord consists of two umbilical arteries and one umbilical vein encapsulated within a layer of Wharton's jelly, a glutinous material predominantly composed of mucopolysaccharides. The umbilical vein functions as a passage for the transportation of oxygenated, nutrient rich blood to the fetus, with the two arteries facilitating the removal of deoxygenated, nutrient depleted blood from the embryo.

Interaction of the developing embryo with the umbilical cord is undertaken within three weeks post-fertilisation, facilitated by a connecting stalk. Following 28 days of development the fully formed yolk sac, present at the levels of the anterior wall of the embryo, is restrained to a vitelline duct which is surrounded by a primitive umbilical cord ring. Post 5 weeks of development this ring contains numerous fundamental structures. Firstly, in addition to containing the established umbilical vein and two arteries, the ring houses an internal connecting stalk which bypasses the allantois or primitive excretory duct. Additionally, the ring structure contains the vitelline duct or yolk sac stalk, and furthermore a canal which connects the intra- and extra- embryonic coelomic cavities. Following a further 5 weeks of development, the gastrointestinal tract has fully developed and subsequently protrudes through the umbilical cord ring to generate a physiologically normal herniation within the umbilical cord, concurrently replacing the yolk sac duct. Following 3 months of development these loops of bowel regress into the peritoneal cavity and become the cord as is observed post-natally.

Within the developing fetus the generated umbilical cord interacts via the abdomen, an area which post-natally becomes the umbilicus or naval. Within the fetus, the umbilical cord vein projects towards the transverse fissure of the liver at which point it splits into two individual branches: the left progression adjoins with the hepatic portal vein, with the right branch, known as the ductus venosus, functioning to permit approximately 80% of incoming blood to bypass the liver and flow via the left hepatic vein into the inferior vena cava, which subsequently transports blood towards the heart. The two umbilical arteries bypass each side of the urinary bladder and interact with the internal iliac arteries[405].

The developmental immaturity and functional interaction with embryonic tissues identifies umbilical cords as a potential niche for the isolation of both primitive and adult cells of various lineage committment. At present the hyaluronic acid preserved network of glycoprotein microfibrils and collagen fibres present within Wharton's jelly has been used for the isolation of fibroblastic-like cells. These adherent cells display many of the characteristics associated with bone marrow-derived cells, including the expression of MSC-associated markers CD29, CD44 and CD105, although do not express hematopoietic markers such as CD34 and CD45. Furthermore, the population demonstrates the capacity to undertake adipogenic, chondrogenic and osteogenic differentiation[290]. However, like bone marrow-derived populations, these adherent cells represent a heterogeneous population, highlighted by the identification of myofibroblasts via ultrastructural characterisation[406].

The umbilical cord therefore represents an attractive tissue for the isolation of both adult and embryonic-like cells, with both potentially offering significant clinical potential. However, at present, Wharton's jelly remains the most studied component of the cord, with investigations neglecting many other regions. This is surprising since it is likely that the cord contains primitive cell types derived from the developing fetus, given it is known that nutrient and cell exchange between mother and fetus is a two way transferral, with fetal derived cells being present within the peripheral blood of pregnant women[407]. Thus it is perplexing that populations have not been probed for ES and primitive progenitor- associated markers, with the homogeneous assessment of individual ES and adult-derived subpopulations residing within the cord potentially allowing for the isolation and banking of mother and child

cells from this redundant organ, providing autologous cells with potential for use in later life.

5.1.2 Aims of this Chapter

The aim of this chapter is therefore to phenotypically hypothesise subpopulations present within alternatively isolated cord populations, with cells being isolated either by plating of Wharton's jelly or digestion of the whole cord. Given the interactive purpose of the tissue, it is likely that the cord will contain both adult and ES-like cells. Furthermore, the proliferative and phenotypic stability of both populations will be assessed following prolonged *in vitro* culture and also following freeze-thawing, an important issue if cord cells are to be successfully banked for future regenerative strategies. Finally, given that Wharton's jelly-derived cord cells have previously demonstrated an ability to undertake adipogenic, chondrogenic and osteogenic lineages following exposure to appropriate stimuli, cells isolated via both methodologies will be assessed for their capacity to undertake neuronal differentiation, thereby further assessing the plasticity of the populations.

5.2 Isolation of Cells from Human Umblical Cord

5.2.1 Isolation of Cells from Human Umbilical Cord by Plating of Wharton's Jelly or Whole Cord Digestion

Fresh whole umbilical cords were obtained following the birth of four separate children and stored in Hanks' balanced salt solution for up to 24 hours. No information was obtained with regards the age of the mother, sex of the unborn infant or duration of the pregnancy, restricting comparative studies of isolated cells. Umbilical cords were approximately 50cm in length and 2cm in diameter, allowing the isolation of high numbers of cells. Furthermore, the length of the cord facilitated an attempt at varying isolation methods in order to compare adherent cells obtained. Cells were isolated from cords using two different methods: (i) Umbilical cords were mechanically dissected and the two umbilical arteries and one umbilical vein removed. Wharton's jelly was then carefully removed and plated onto tissue culture plastic in the presence of basal media and cultured at 37°C; (ii) Whole umbilical

cords were mechanically dissembled to generate small fractions approximately 50mm^2. Subsequently these cuttings were enzymatically digested via incubation in a solution containing 2% (w/v) Dispase I and 2% (w/v) Collagenase type II overnight at 37°C with gentle agitation. Following centrifugation, pelleted cells were resuspended in basal media and, following filtration to remove non-cellular debris, seeded onto tissue culture substrate and cultured at 37°C.

Regardless of donor or isolation technique, cells adhered following 24 hours of culture, though initially whole cord digestion cultures produced a greater number of adherent cells. Nevertheless, cells isolated from different donors using both techniques became confluent within the 10 days following isolation, although the morphology of Wharton's jelly and whole cord cultures varied considerably, with cells isolated from Wharton's jelly exhibiting a fibroblastic morphology and generating obvious colonies (*Figures 5.1* and *5.2*), compared with the smooth muscle-like morphology observed in whole cord cultures (*Figures 5.3* and *5.4*). Interestingly, despite their apparent morphological differences, both populations expressed the stem cell proliferation marker nucleostemin within approximately 30% of the population (*Figure 5.5*) throughout passages 3 - 5, although no expression was observed in any cells following this passage (*Figure 5.6*).

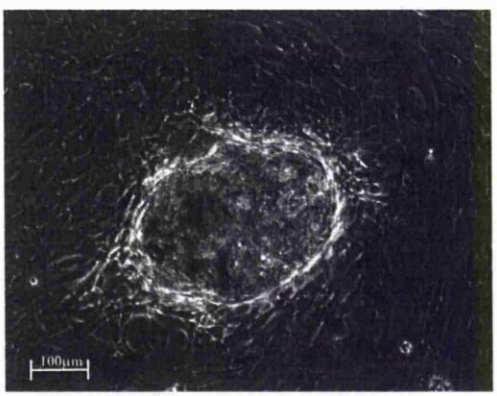

Figure 5.1 **- Umbilical cord donor 1 cells isolated from Wharton's jelly and cultured in basal media for 10 days.**

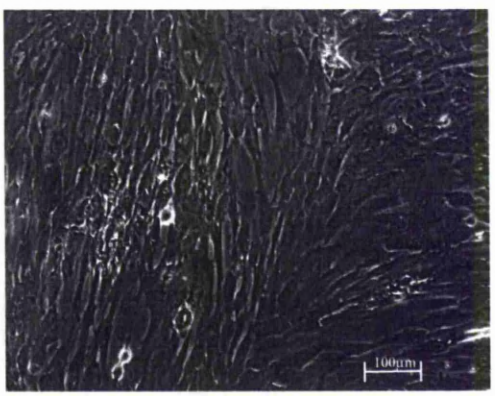

Figure 5.2 **- Umbilical cord donor 2 cells isolated from Wharton's jelly and cultured in basal media for 8 days.**

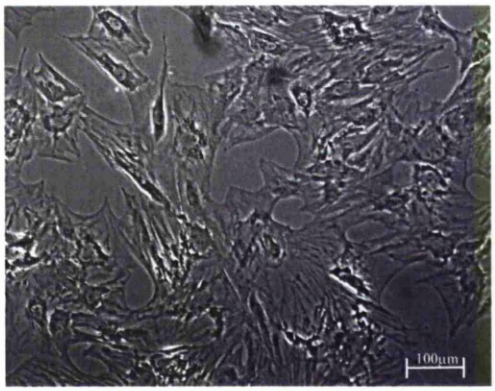

Figure 5.3 - **Umbilical cord donor 1 cells isolated via whole cord digestion and cultured in basal media for 10 days.**

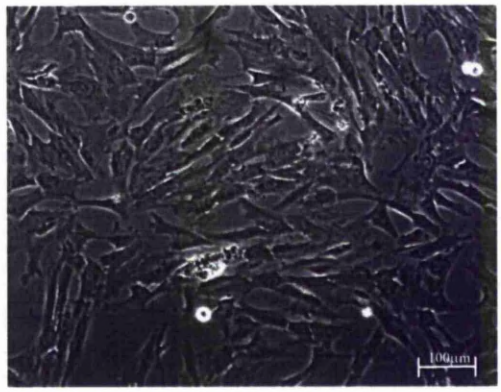

Figure 5.4 - **Umbilical cord donor 2 cells isolated via whole cord digestion and cultured in basal media for 9 days.**

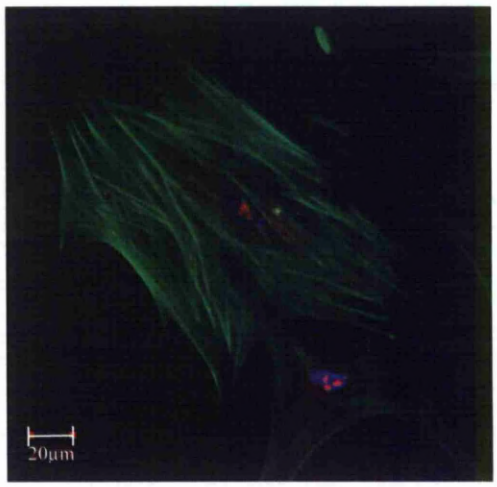

Figure 5.5 - **Umbilical cord donor 1 cells isolated from Wharton's jelly and cultured in basal media (Passage 4; 0 x Freeze-thaw cycles) stained with Hoechst 33342 (blue), Oregon green (green) and nucleostemin antibody (red). Approximately 30% expressed nucleostemin at passages 3 to 5.**

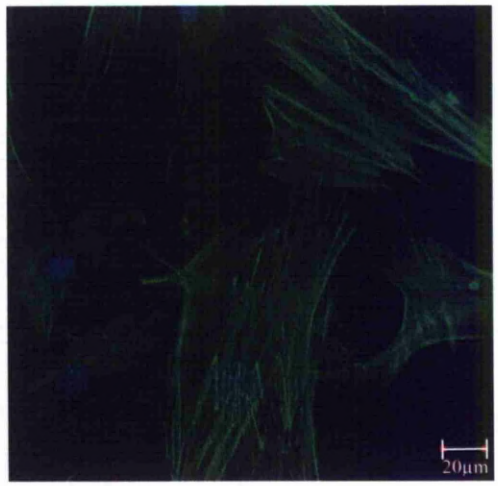

Figure 5.6 - **Umbilical cord donor 1 cells isolated from Wharton's jelly and cultured in basal media (Passage 7; 0 x Freeze-thaw cycles) stained with Hoechst 33342 (blue), Oregon green (green) and nucleostemin antibody (red). No cells expressed nucleostemin post a sixth passage of *in vitro* culture.**

5.3 Phenotyping of Umbilical Cord Cells using Flow Cytometry

5.3.1 Phenotypic Analysis of Umbilical Cord-derived Cells, Isolated by Plating Wharton's Jelly or Whole cord Digestions, Throughout Prolonged *In Vitro* Culture using Flow Cytometry

Adherent cells isolated from four separate cords demonstrated obvious morphological differences. However, in order to identify potential subpopulations residing within the cultures, passage 3 and further cultures were phenotypically

assessed using flow cytometry. However, due to the anonymity of cord donors regarding age of the mother, sex of the baby and term of the pregnancy, phenotyping and subsequent experiments were undertaken using only cord donor 1 cells isolated by each methodology.

Interestingly, despite their apparent morphological differences, umbilical cord 1 cells derived either by plating of Wharton's jelly or whole cord digestion displayed similar phenotypic profiles. Concerning a subset of MSC-associated surface antigens, both Wharton's jelly and whole cord digest-derived populations displayed consistently high levels of expression throughout passages 3 - 5 (*Figures 5.7* and *5.8*). CD29 demonstrated high expression within Wharton's jelly-derived cells, exhibiting 88.4%, 87.1% and 83.0% at passages 3, 4 and 5 respectively. This expression was comparable with cells isolated by whole cord digestion, which expressed 90.5%, 92.0% and 85.3%. Alternative MSC-associated markers demonstrated similar expression within each isolated population, with CD44, CD73, CD90 and CD117 expressed by 82% - 93% of cells in each population at passages 3 - 5. Furthermore, the cells demonstrated similar levels of STRO-1 expression with those observed in bone marrow, exhibiting 0.4% - 0.8% expressions at passages 3 - 5. CD106 also exhibited comparable expression levels for each isolation method and with bone marrow-derived cells.

However, whilst numerous MSC-associated markers within alternatively isolated cord populations demonstrated expression levels comparable with those observed in bone marrow-derived cells, other markers had reduced expression. CD105 was expressed by approximately 87% of passage 4 bone marrow cells, but 56% - 70% expression in cord cells throughout passages 3 - 5. CD146 and CD166 displayed lower expression in comparison with bone marrow-derived cells. Wharton's jelly-derived cells displayed 33.6%, 45.4% and 47.4% CD146 expression at passages 3, 4 and 5 respectively, slightly higher than the 35.2%, 37.2% and 39.0% observed within whole cord digests. CD166 demonstrated reduced expression in cord cells compared with bone marrow-derived equivalents, with Wharton's jelly-derived populations demonstrating 37.3%, 39.4% and 33.7% expression at passages 3 - 5 respectively, and whole cord digests 14.8%, 16.3% and 18.3%.

Wharton's jelly- derived populations exhibited 47.0%, 40.9% and 33.7% expression of HLA-ABC at passages 3, 4 and 5 respectively, whilst furthermore demonstrating 42.2%, 32.4% and 25.9% expression of HLA-DR. However, HLA-ABC was expressed by 13% - 16% of whole cord digestion-isolated cells, which also exhibited 11% - 28% HLA-DR expression, a downregulation which could have significant impact with regards implant rejection should umbilical cord cells be required for allogeneic transplantation.

However, whilst umbilical cord-derived cells demonstrated alternative regulation of MSC-associated surface antigens compared with bone marrow-derived cells, cord populations isolated by respective methods demonstrated a similar inability to maintain phenotype, with passages 6 - 8 demonstrating progressively reduced downregulation of MSC-associated surface antigens (*Figures 5.9* and *5.10*).

CD29 demonstrated downregulation within the population following a sixth passage, with Wharton's jelly isolated cells demonstrating 42.0%, 30.2% and 16.4% expression at passages 6, 7 and 8 respectively. Whole cord isolates mirrored this CD29 downregulation, with 46.0%, 25.0% and 8.7% expression.

MSC-associated antigen CD44 exhibited downregulation at passage 6 onwards in both isolated cord populations. Wharton's jelly-isolated cells demonstrated progressive downregulation at passages 6 - 8, the population demonstrating 59.9%, 30.5% and 6.0% CD44 expression. Adherent cells isolated by whole cord digestion also exhibited progressive CD44 downregulation, with populations exhibiting 37.1%, 15.6% and 3.4% expression at passages 6 - 8. CD73 was also downregulated, with Wharton's jelly-derived cells demonstrating 39.1%, 27.1% and 13.4% expression at passages 6 – 8 and whole cord digests 37.1%, 11.4% and 12.8%.

CD90 demonstrated reduced upregulation within both isolated cord populations at passage 6 onwards, with 52.0%, 28.3% and 6.3% expression at passages 6 - 8 of Wharton's jelly-derived cells, whilst whole cord digests demonstrated 41.5%, 24.3% and 5.8%. CD105 mirrored CD90 expression within both populations, with 34.3%, 23.0% and 2.5% of Wharton's jelly derivatives demonstrating expression at passages 6 to 8 respectively. Whole cord digests also demonstrated reduced expression of

CD105, with passage 6 - 8 cultures demonstrating 29.0%, 15.6% and 1.7% expression respectively. Stem cell factor cytokine receptor CD117 demonstrated reduced global upregulation within both isolated populations. Wharton's jelly-derived cells progressively downregulated CD117 within the population, exhibiting 68.5%, 18.1% and 3.5% expression at passages 6 - 8 respectively. Adherent cells isolated by whole cord digestions displayed similar regulatory expression, with passages 6 - 8 respectively demonstrating 52.4%, 8.6% and 5.0% expression.

CD166 demonstrated differential expression between isolated cord populations and when compared with bone marrow-derived cells. Wharton's jelly-derived cultures displayed progressive global downregulation of CD166, with passages 6, 7 and 8 populations exhibiting 22.0%, 16.6% and 0.9% expressions. Interestingly, whole cord digestion isolation maintained expression at passage 6, with 21.0% of cells exhibiting positive expression. However, passages 7 and 8 resulted in downregulation of CD166, with 12.4% and 1.1% positive expression.

HLA-ABC and HLA-DR demonstrated contrasting expression within differently isolated populations during passages 3 - 5, although both populations exhibited progressive downregulation of these MHC antigens throughout passages 6 - 8, resulting in less than 1% of cells expressing either antigen at passage 8, regardless of isolation methodology. STRO-1 was also downregulated at increasing passage in each isolated culture, with passage 8 populations failing to demonstrate positive expression.

Interestingly CD146, whilst expressed at lower levels within each cord population than bone marrow-derived cells, maintained expression until passage 7, at which point each population demonstrated reduced expression. This expression was further downregulated at passage 8, at which point approximately 1% of the population expressed CD146.

In conclusion, adherent cord cells derived by different methodologies displayed similar MSC-associated phenotypic characteristics, with the notable exceptions of CD166 and both MHC antigens. However, as with bone marrow-derived populations, each cord-derived population demonstrated an inability to maintain

expression of MSC-associated markers following a sixth passage of *in vitro* culture, an issue which must be addressed if these cells are to be utilised clinically.

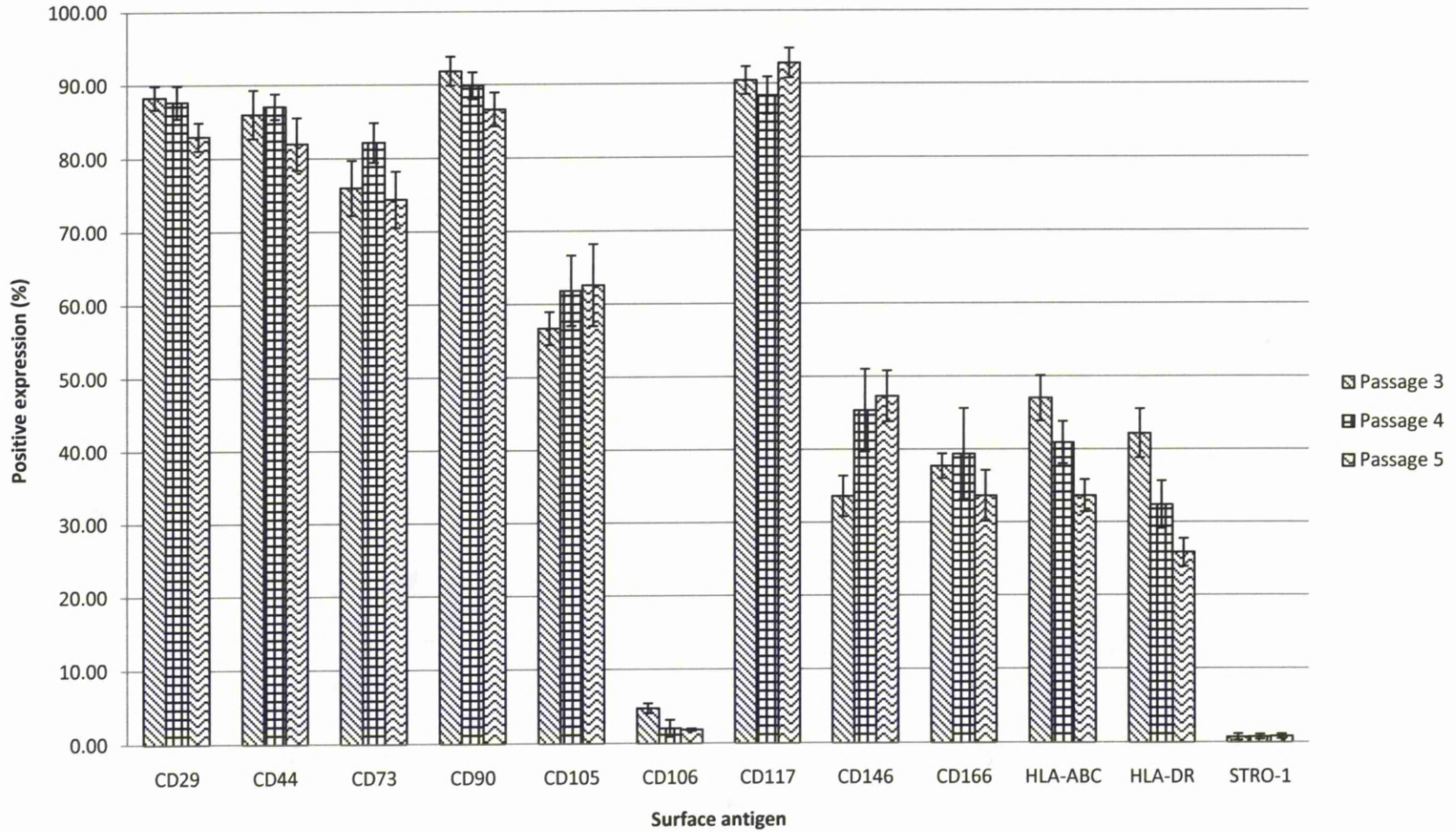

Figure 5.7 - **MSC-associated marker phenotyping of umbilical cord donor 1 cells (Passages 3 - 5; 0 x Freeze-thaw cycles) isolated by plating Wharton's jelly. Values represent mean positive expression as observed by flow cytometry (n = 4). Error bars correspond to Standard Deviations.**

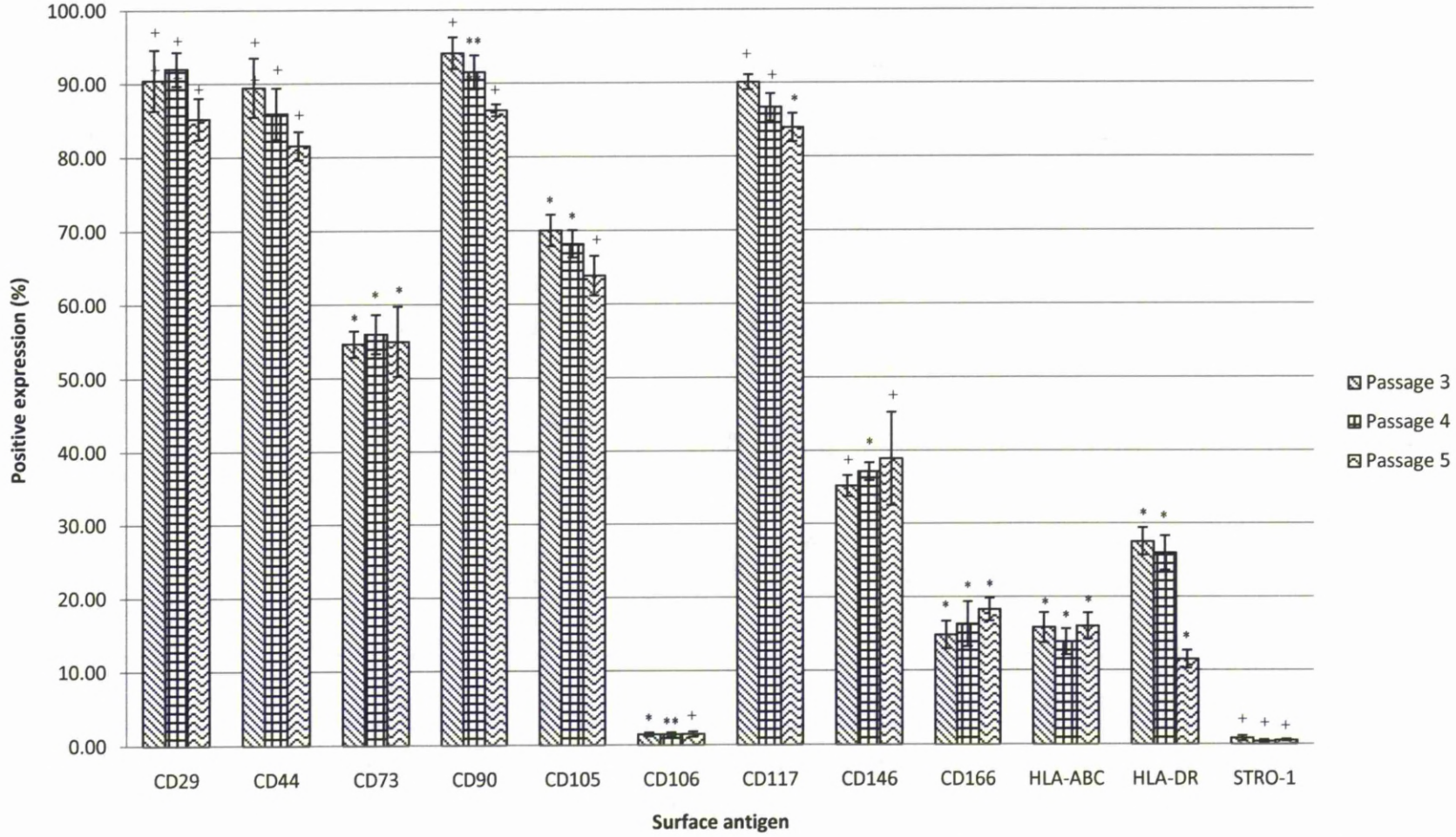

Figure 5.8 - **MSC-associated marker phenotyping of umbilical cord donor 1 cells (Passages 3 - 5; 0 x Freeze-thaw cycles) isolated by whole cord digestion. Values represent mean positive expression as observed by flow cytometry (n = 4). Error bars correspond to Standard Deviations. Student *t*-test indicated that there were significant (*$p \leq 0.001$) (**$p \leq 0.05$) and non-significant (+$p \geq 0.05$) antigen expression differences when comparing cells isolated by whole cord digestion with those isolated from plating Wharton's jelly at corresponding passages.**

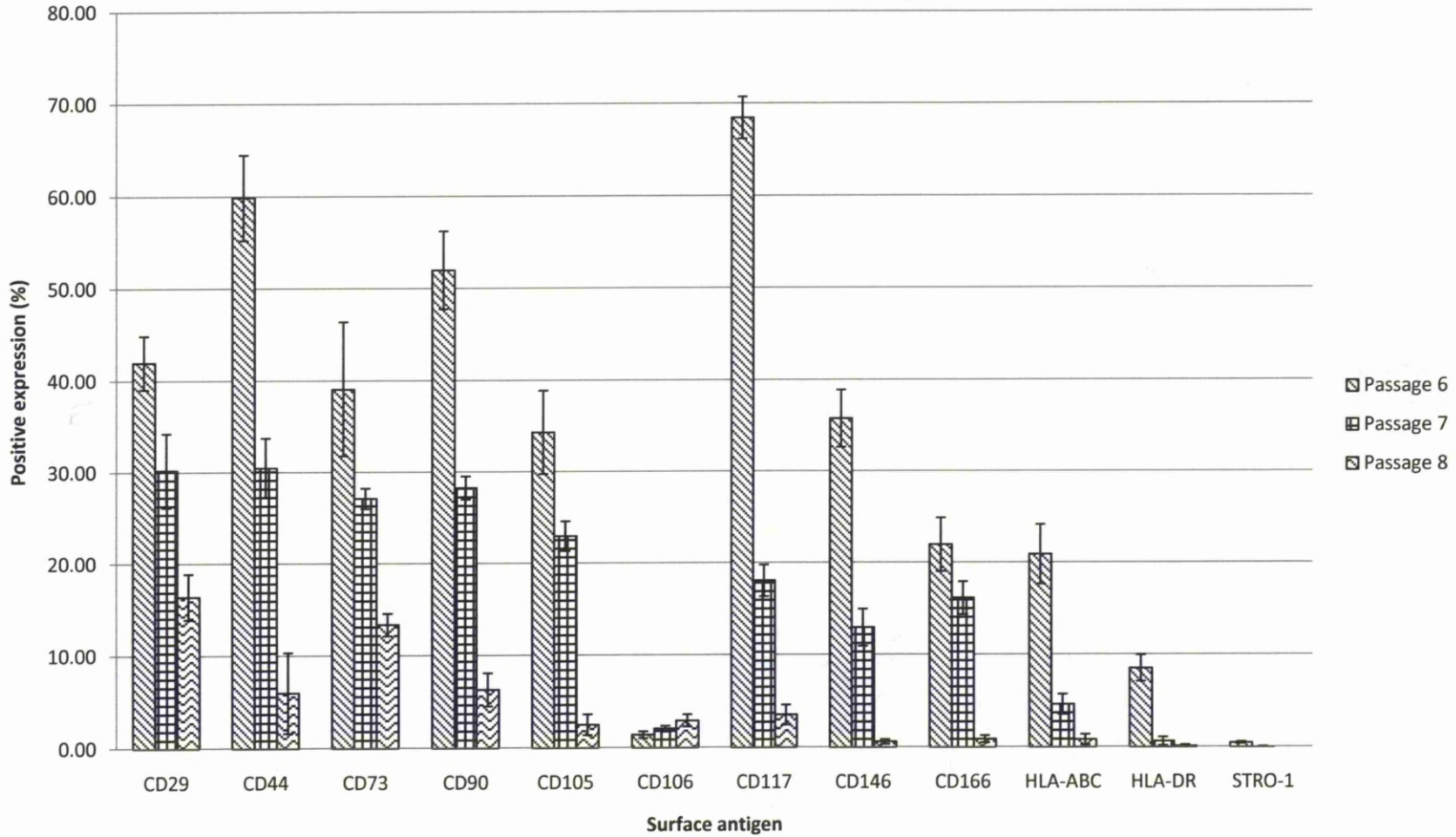

Figure 5.9 - **MSC-associated marker phenotyping of umbilical cord donor 1 cells (Passages 6 - 8; 0 x Freeze-thaw cycles) isolated by plating Wharton's jelly. Values represent mean positive expression as observed by flow cytometry (n = 4). Error bars correspond to Standard Deviations.**

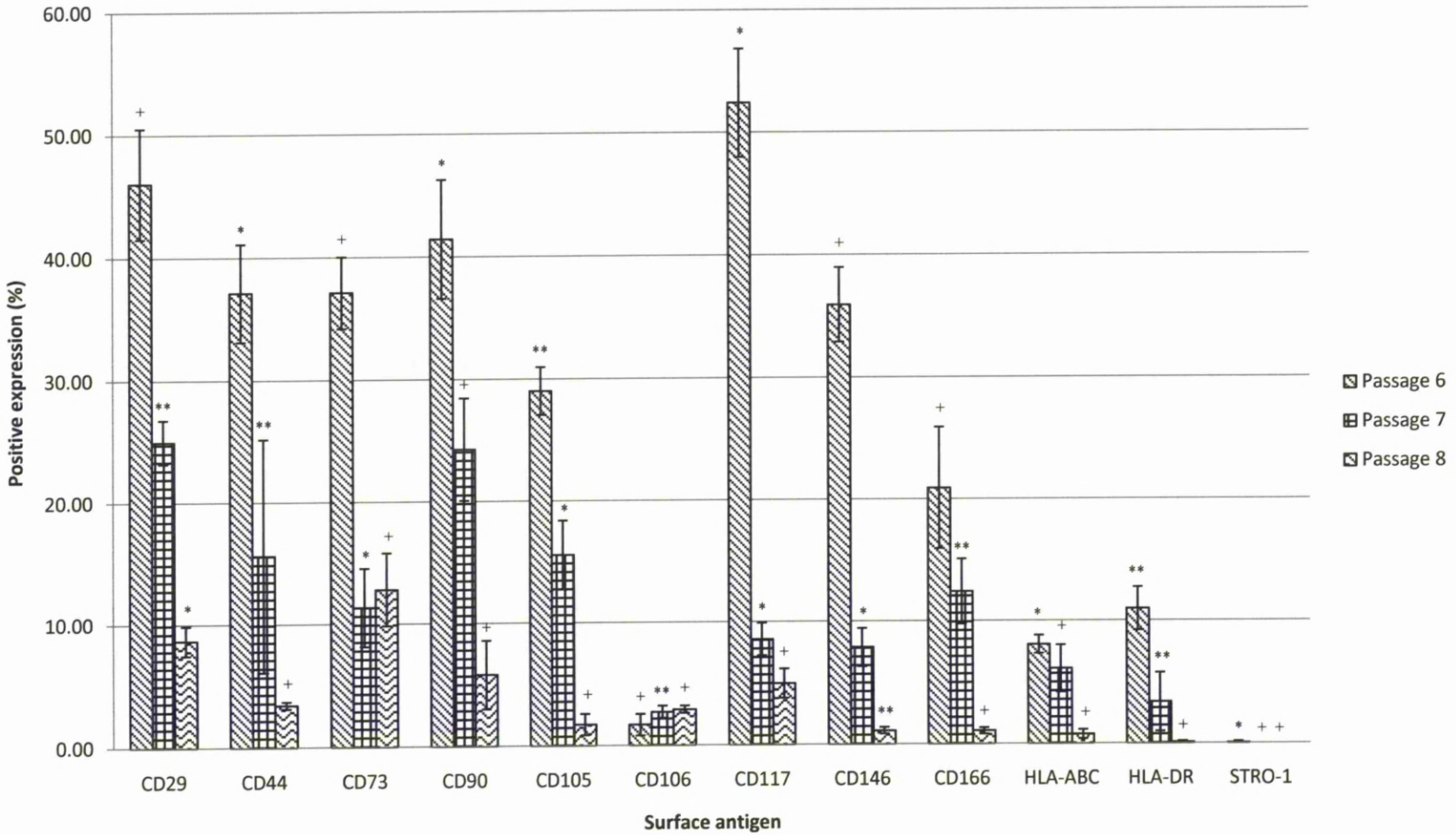

Figure 5.10 - **MSC-associated marker phenotyping of umbilical cord donor 1 cells (Passages 6 - 8; 0 x Freeze-thaw cycles) isolated by whole cord digestion. Values represent mean positive expression as observed by flow cytometry (n = 4). Error bars correspond to Standard Deviations. Student *t*-test indicated that there were significant (*$p \leq 0.001$) (**$p \leq 0.05$) and non-significant (+$p \geq 0.05$) antigen expression differences when comparing cells isolated by whole cord digestion with those isolated from plating Wharton's jelly at corresponding passages.**

Following assessment of the populations for expression of MSC-associated surface antigens, isolated cord populations were assessed for their global expression of HSC and endothelial-associated surface antigens at passages 3 - 5 (*Figures 5.11* and *5.12*) and 6 - 8 (*Figures 5.13* and *5.14*). Endothelial-associated antigens CD31 and CD133 maintained low levels of expression throughout passages 3 - 5 of Wharton's jelly and whole cord-derived cultures, with less than 1.0% of cells demonstrating expression. However, following passage 6, each isolated population exhibited progressive upregulation of CD31 and CD133, perhaps indicating, given the simultaneous downregulation of MSC-associated markers, endothelial differentiation of cells previously exhibiting a plastic phenotype. Interestingly, endothelial and ES-associated antigen CD9 was expressed by 28% - 43% of cells isolated by the different methodologies at passages 3 - 5. However, CD9 demonstrated progressively reduced global expression at passages 6 - 8, culminating in approximately 1% of Wharton's jelly and whole cord-derived cells exhibiting expression at passage 8. Perhaps, therefore, CD9 is expressed predominantly by EPCs, and subsequently downregulates due to spontaneous differentiation of these cells a consequence of *in vitro* culture. Alternatively, given that CD9 is proposed to be expressed by ES cells, perhaps a subset of CD9 cells may represent a population derived from the developing fetus. It would therefore be interesting to purify $CD9^{+}$ cells in a combinatorial manner, co-staining and sorting using additional ES/endothelial antigens, thereby potentially isolating populations of ES or endothelial specificity.

HSC-associated surface antigen CD34 class II was expressed by 10.2% and 10.6% of Wharton's jelly-derived cells at passages 3 and 4 respectively. However, following a fifth passage, CD34 class II was downregulated, demonstrating 3.8%, 2.8%, 2.1% and 0.9% expression at passages 5 - 8. CD34 class III demonstrated increased expression within the Wharton's jelly-derived population, with 20.1%, 20.3%, 21.2% and 19.2% expression at passages 3, 4, 5 and 6 respectively. However, following a seventh passage Wharton's jelly-derived cells demonstrated reduced CD34 class III expression, with passages 7 and 8 exhibiting 7% and 3% expression respectively. Interestingly, whole cord digestions yielded populations exhibiting reduced levels of CD34 class II expression, with 1.6%, 1.5%, 2.2%, 5.0% and 2.3% of cells demonstrating expression at passages 3 - 7 respectively. Following an eighth passage, however, CD34 class II demonstrated 0.5% expression. CD34 class III was

also expressed by reduced numbers of whole cord digest cells compared with their Wharton's jelly counterparts, with 18.2%, 16.6%, 16.7% and 14.5% expression at passages 3 - 6 respectively. However, subsequent passages demonstrated reduced upregulation, with 3.7% and 1.6% expression at passages 7 and 8 respectively.

CD50 was expressed by both Wharton's jelly and whole cord digest populations, demonstrating maintained expression of 10% - 22% throughout passages 3 - 6. However, following a seventh passage Wharton's jelly and whole cord-derived cells demonstrated reduced CD50 expression of less than 3%. Further suggesting of spontaneous differentiation within each population was the progressive upregulation of CD41a, CD45 and CD62E upon increasing passage, suggesting non-induced endothelial differentiation within subsets of the population.

Following assessment of cord cells using HSC and endothelial-associated antigens, it appears that the umbilical cord contains subpopulations phenotypically similar to HSCs and EPCs, both of which could represent therapeutically useful tools. Furthermore CD9, which is hypothesised to be expressed by both EPCs and primitive ES cells, could represent a marker which, if used along side additional ES or HSC-associated antigens, could facilitate the purification of populations exhibiting differing lineage potential. However, the persistent inability of culture conditions to maintain the phenotype of either cord population represents the initial challenge which must be addressed.

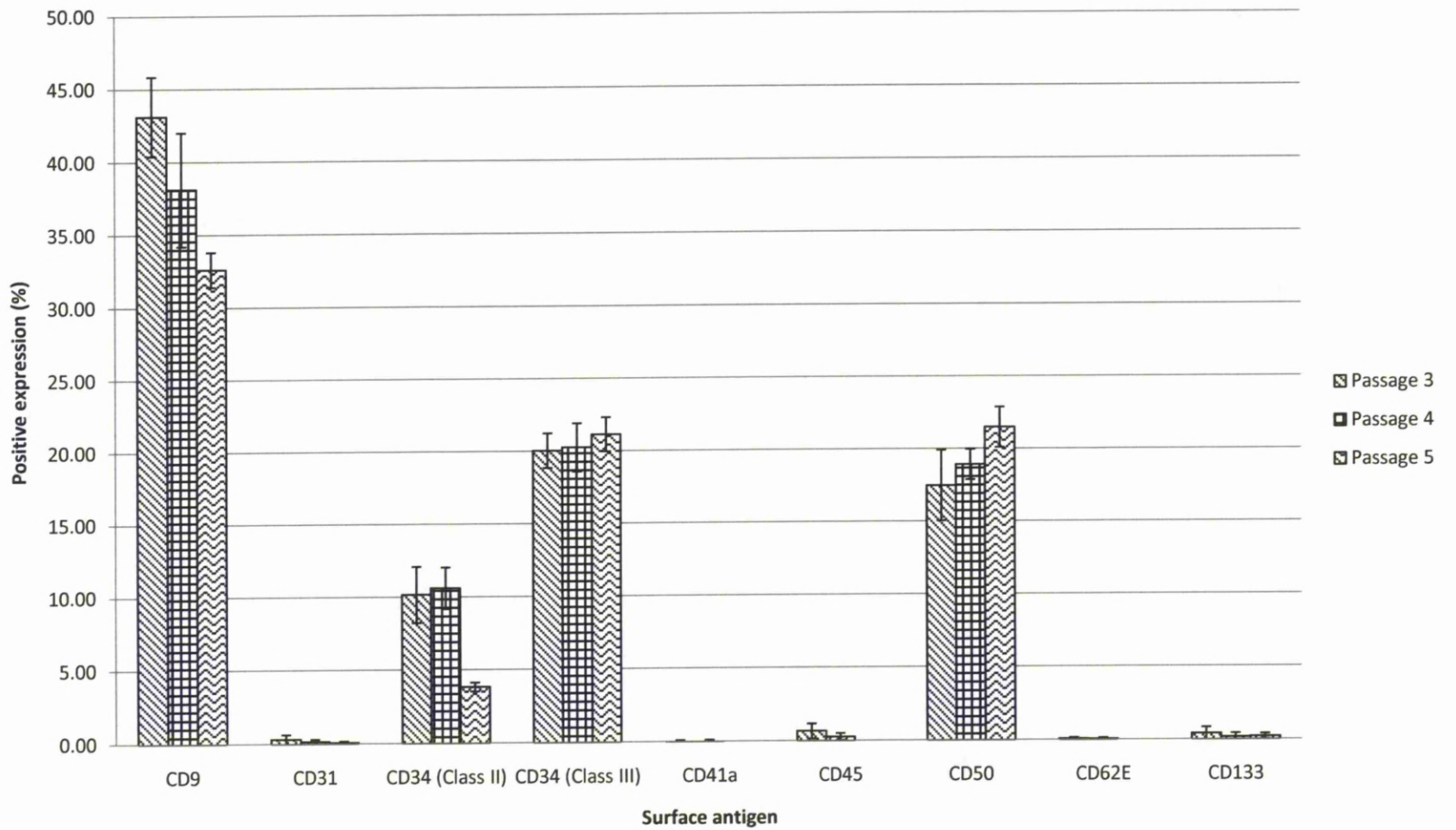

Figure 5.11 - **HSC and endothelial-associated marker phenotyping of umbilical cord donor 1 cells (Passages 3 - 5; 0 x Freeze-thaw cycles) isolated by plating Wharton's jelly. Values represent mean positive expression as observed by flow cytometry (n = 4). Error bars correspond to Standard Deviations.**

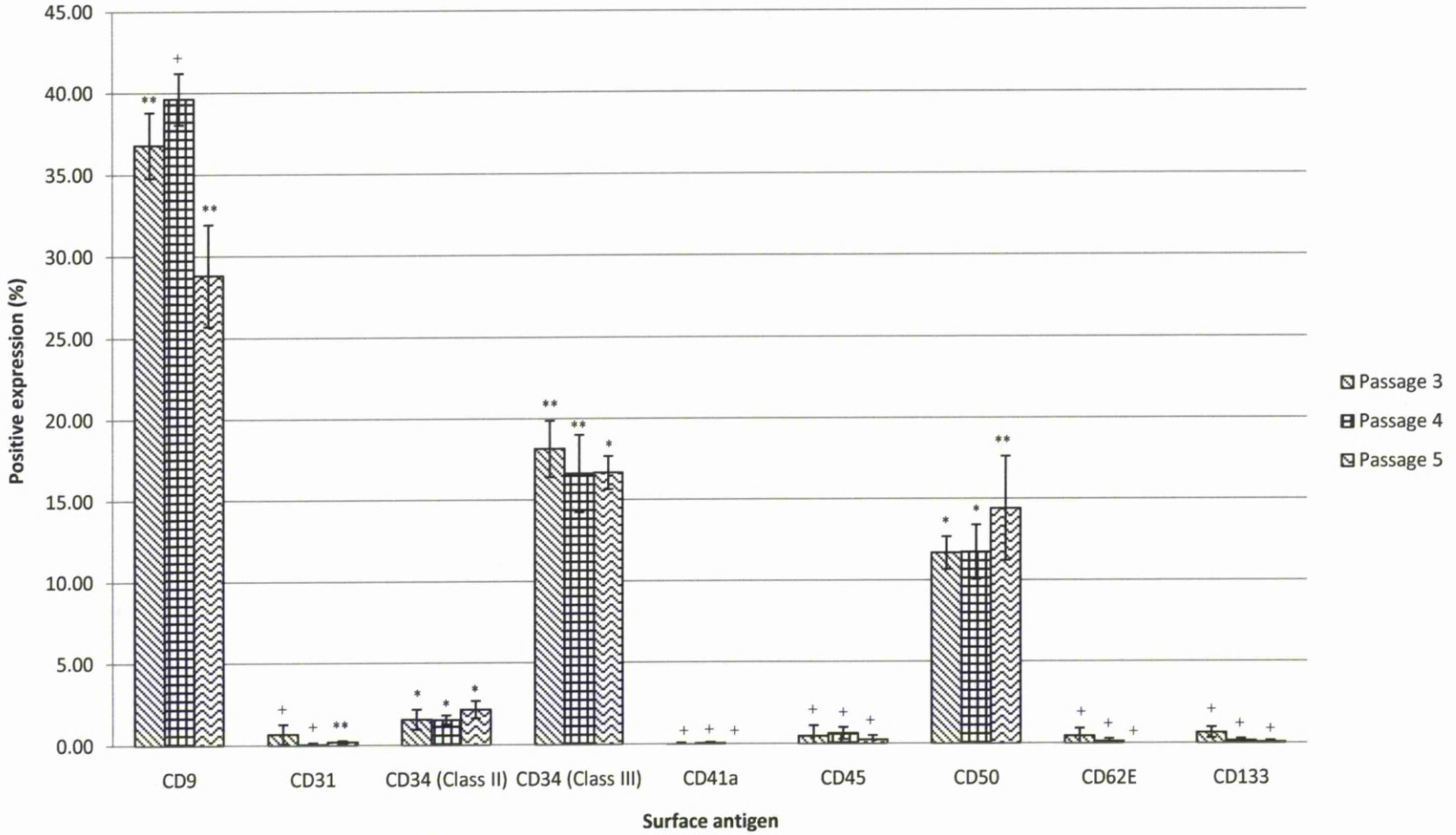

Figure 5.12 - **HSC and endothelial-associated marker phenotyping of umbilical cord donor 1 cells (Passages 3 - 5; 0 x Freeze-thaw cycles) isolated by whole cord digestion. Values represent mean positive expression as observed by flow cytometry (n = 4). Error bars correspond to Standard Deviations. Student *t*-test indicated that there were significant (*$p \leq 0.001$) (**$p \leq 0.05$) and non-significant (+$p \geq 0.05$) antigen expression differences when comparing cells isolated by whole cord digestion with those isolated from plating Wharton's jelly at corresponding passages.**

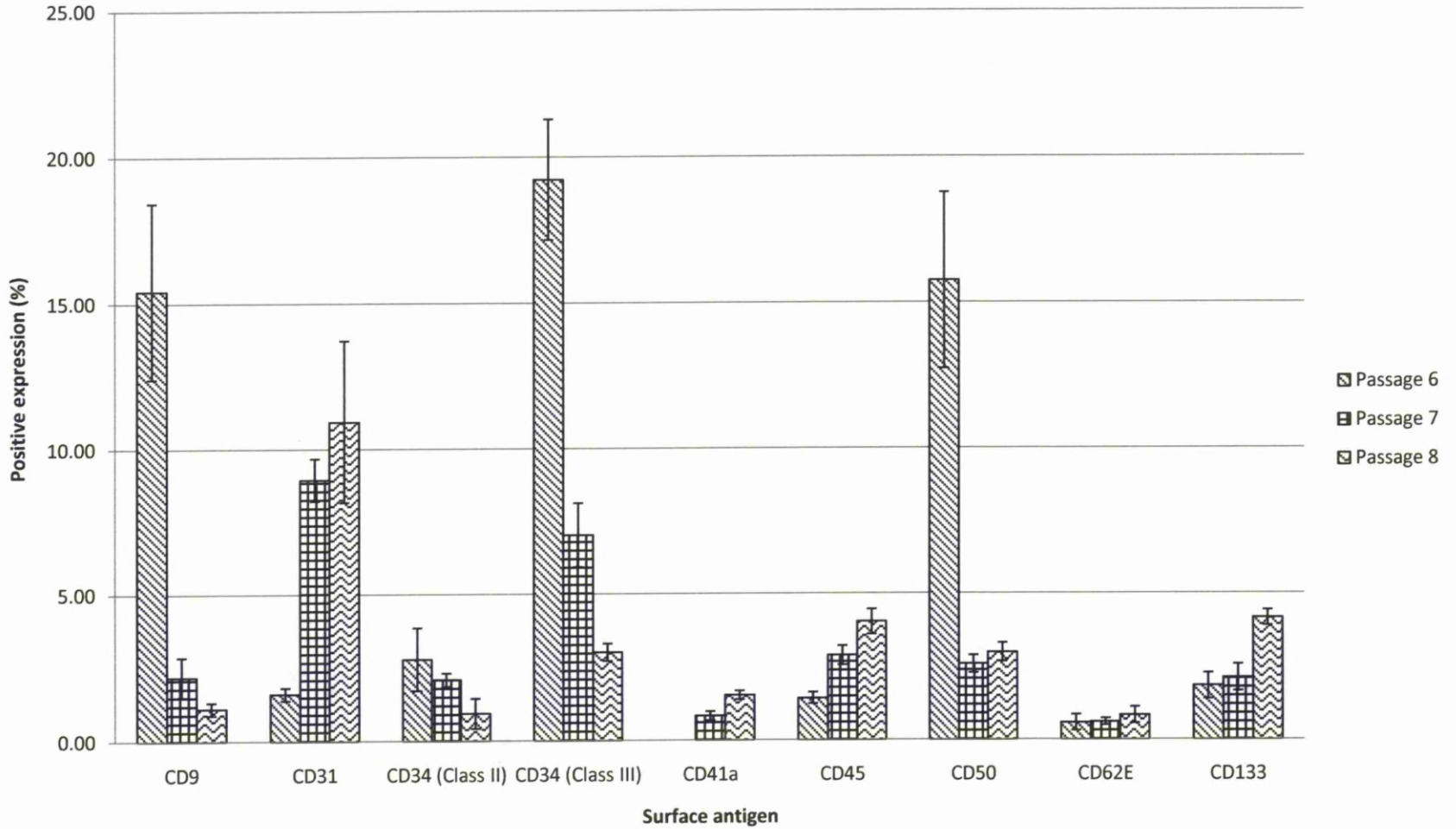

Figure 5.13 - **HSC and endothelial-associated marker phenotyping of umbilical cord donor 1 cells (Passages 6 - 8; 0 x Freeze-thaw cycles) isolated by plating Wharton's jelly. Values represent mean positive expression as observed by flow cytometry (n = 4). Error bars correspond to Standard Deviations.**

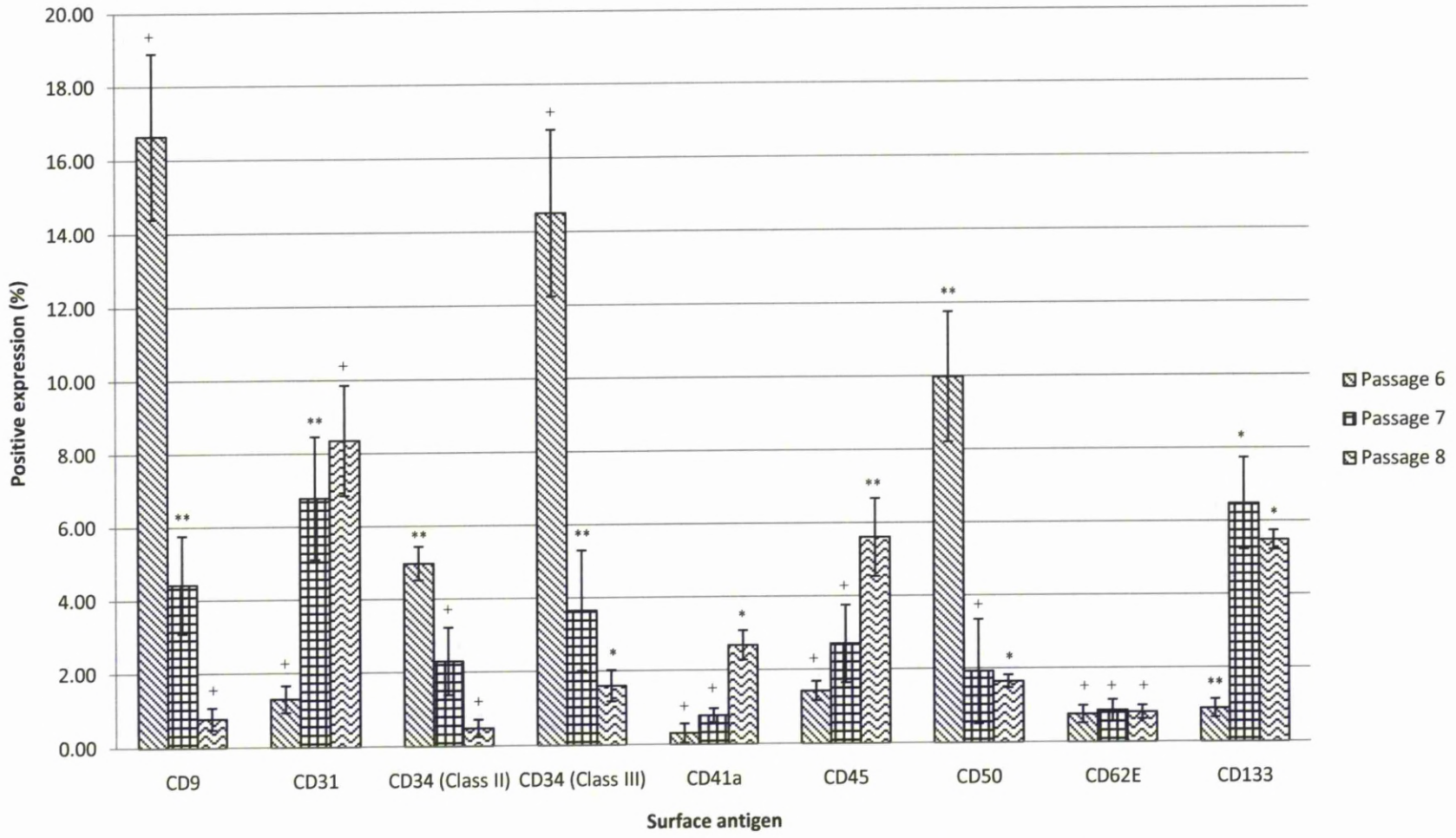

Figure 5.14 - **HSC and endothelial-associated marker phenotyping of umbilical cord donor 1 cells (Passages 6 - 8; 0 x Freeze-thaw cycles) isolated by whole cord digestion. Values represent mean positive expression as observed by flow cytometry (n = 4). Error bars correspond to Standard Deviations. Student *t*-test indicated that there were significant (*$p \leq 0.001$) (**$p \leq 0.05$) and non-significant (+$p \geq 0.05$) antigen expression differences when comparing cells isolated by whole cord digestion with those isolated from plating Wharton's jelly at corresponding passages.**

Umbilical cord-derived populations were finally assessed for their expression of ES and progenitor-associated surface antigens at passages 3 - 5 (*Figures 5.15* and *5.16*) and 6 - 8 (*Figures 5.17* and *5.18*). ES cell-associated antigen CD30 was expressed by 68.1%, 62.5% and 49.4% of Wharton's jelly-derived cells at passages 3 - 5 respectively, marginally higher than the expression observed in whole cord digest isolated cells, which demonstrated 41.4%, 42.3% and 33.2% expression. However, cord cells isolated by each method exhibited progressively reduced expression at passages 6 - 8, with Wharton's jelly-derived cells exhibiting 15.3%, 12.5% and 5.8% expression respectively, and whole cord digests 8.9%, 12.2% and 4.5%. CD56 and CD135 were expressed similarly to CD30, although whilst CD135 demonstrated reduced expression following a sixth passage, CD56 global downregulation was less extreme, with expression maintained by 19.5% and 17.5% of passage 8 populations isolated from Wharton's jelly and whole cord digests respectively. Interestingly CD15, which is expressed by murine ES cells, displayed little or no expression within passages 3 - 5 of Wharton's jelly or whole cord-derived cells, though was progressively upregulated at higher passages.

CD81 and NGFR are surface antigens related to neuronal lineages, and displayed differing levels of expression within contrastingly isolated populations. Whilst Wharton's jelly-derived cultures exhibited little or no expression, whole cord digests displayed 0.2% - 0.3% positive expression throughout passages 3 - 5, although no expression was observed at passages beyond this, suggesting that cultures failed to maintain this immature neuronal phenotype. However, the purification of this subpopulation could yield cells with a capacity for neuronal differentiation. In fact, the cord appears to contain ES and progenitor-like subpopulations which, whether mother or fetus derived, could offer a source of clinically useful cells isolated non-invasively.

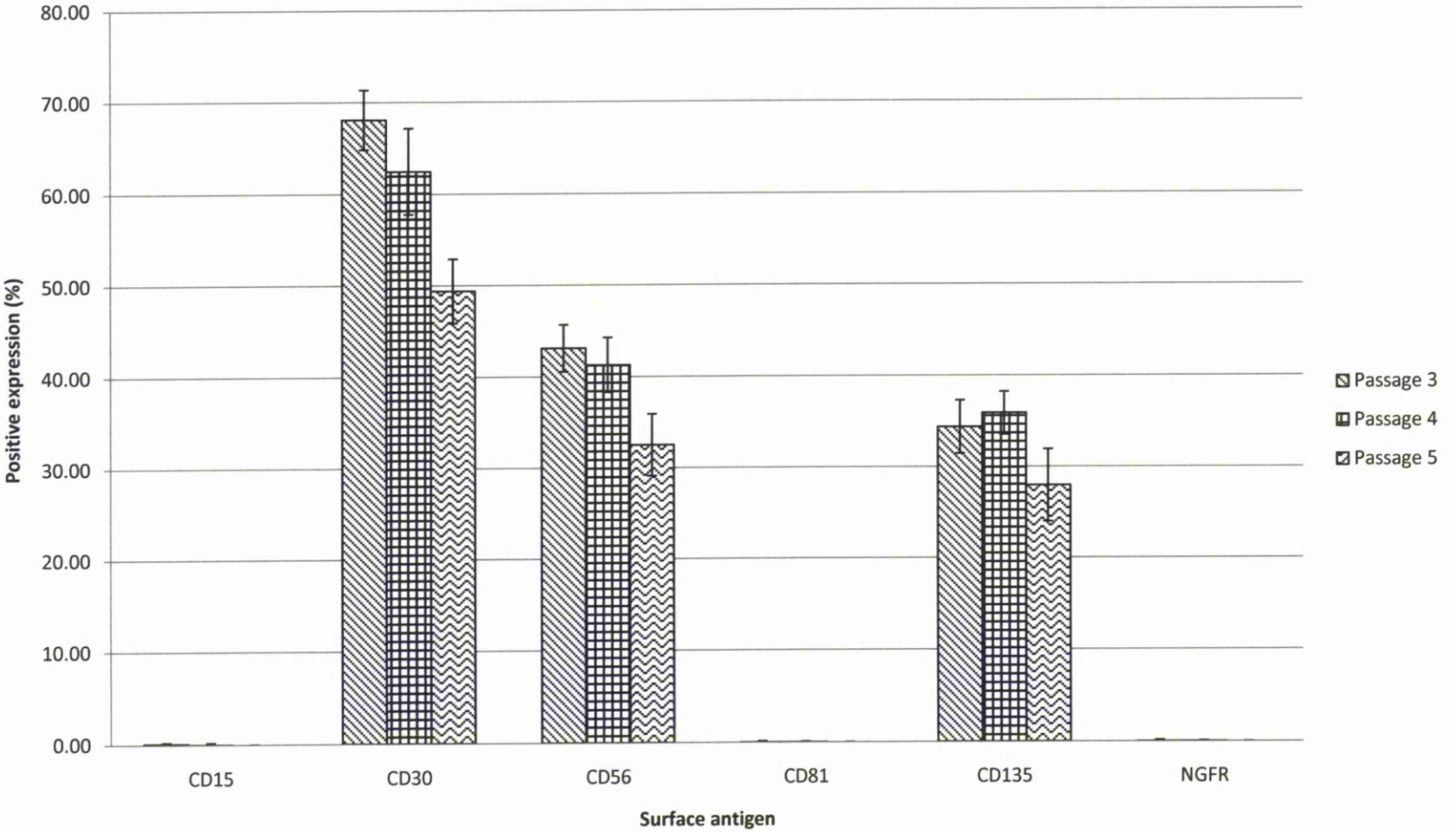

Figure 5.15 - **ES and progenitor-associated marker phenotyping of umbilical cord donor 1 cells (Passages 3 - 5; 0 x Freeze-thaw cycles) isolated by plating Wharton's jelly. Values represent mean positive expression as observed by flow cytometry (n = 4). Error bars correspond to Standard Deviations.**

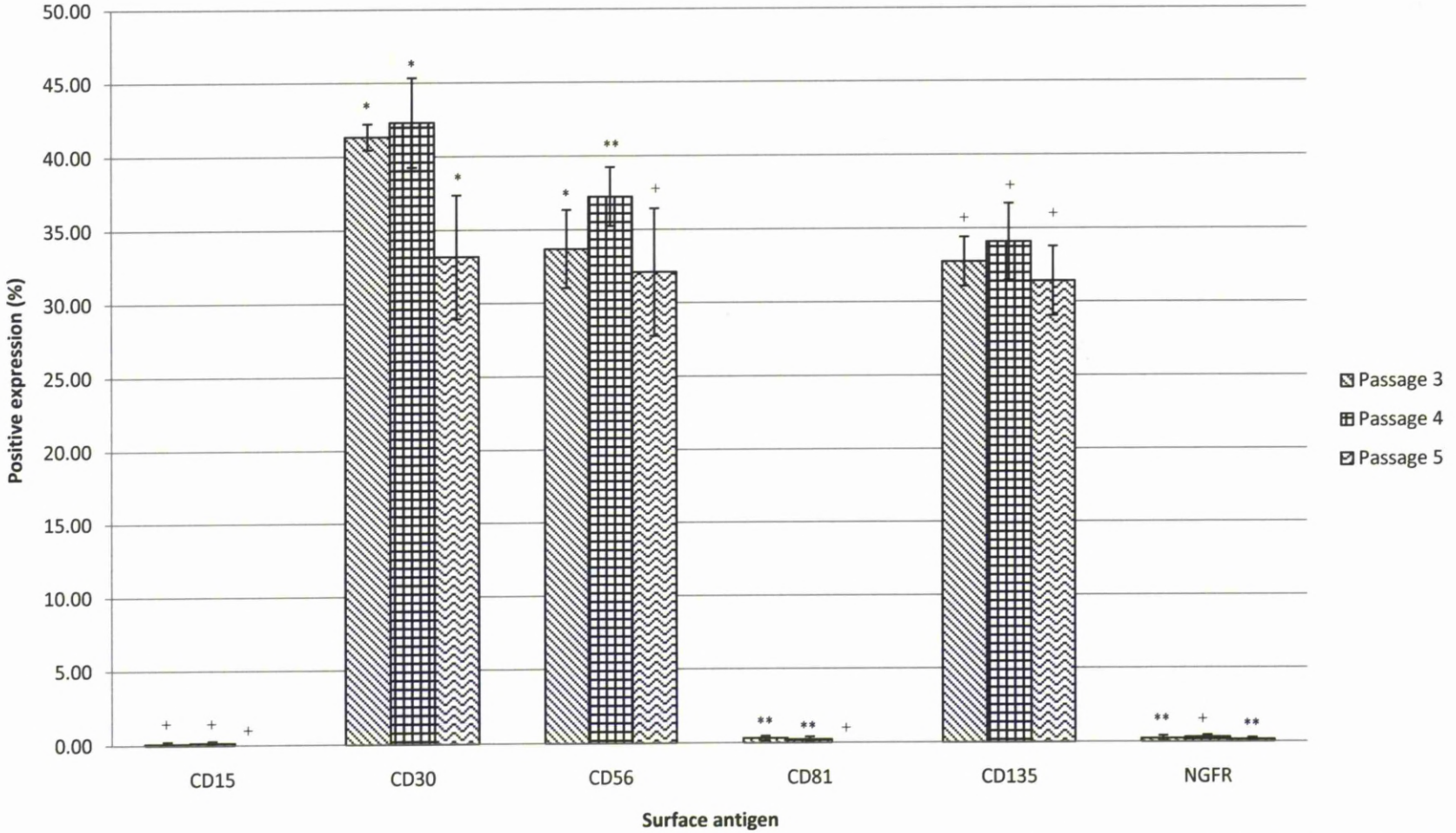

Figure 5.16 - **ES and progenitor-associated marker phenotyping of umbilical cord donor 1 cells (Passages 3 - 5; 0 x Freeze-thaw cycles) isolated by whole cord digestion. Values represent mean positive expression as observed by flow cytometry (n = 4). Error bars correspond to Standard Deviations. . Student *t*-test indicated that there were significant (*$p \leq 0.001$) (**$p \leq 0.05$) and non-significant (+$p \geq 0.05$) antigen expression differences when comparing cells isolated by whole cord digestion with those isolated from plating Wharton's jelly at corresponding passages.**

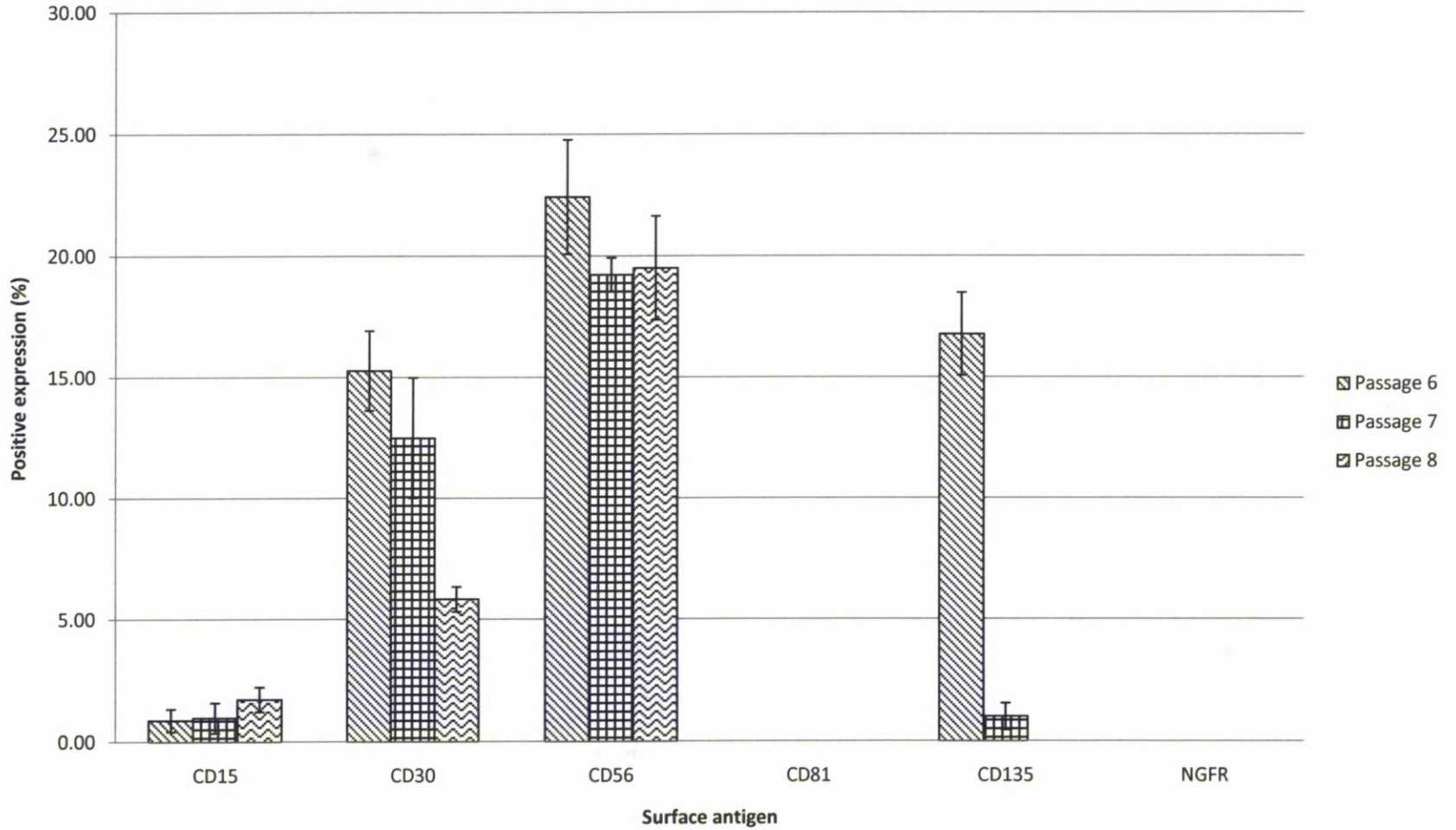

Figure 5.17 - **ES and progenitor-associated marker phenotyping of umbilical cord donor 1 cells (Passages 6 - 8; 0 x Freeze-thaw cycles) isolated by plating Wharton's jelly. Values represent mean positive expression as observed by flow cytometry (n = 4). Error bars correspond to Standard Deviations.**

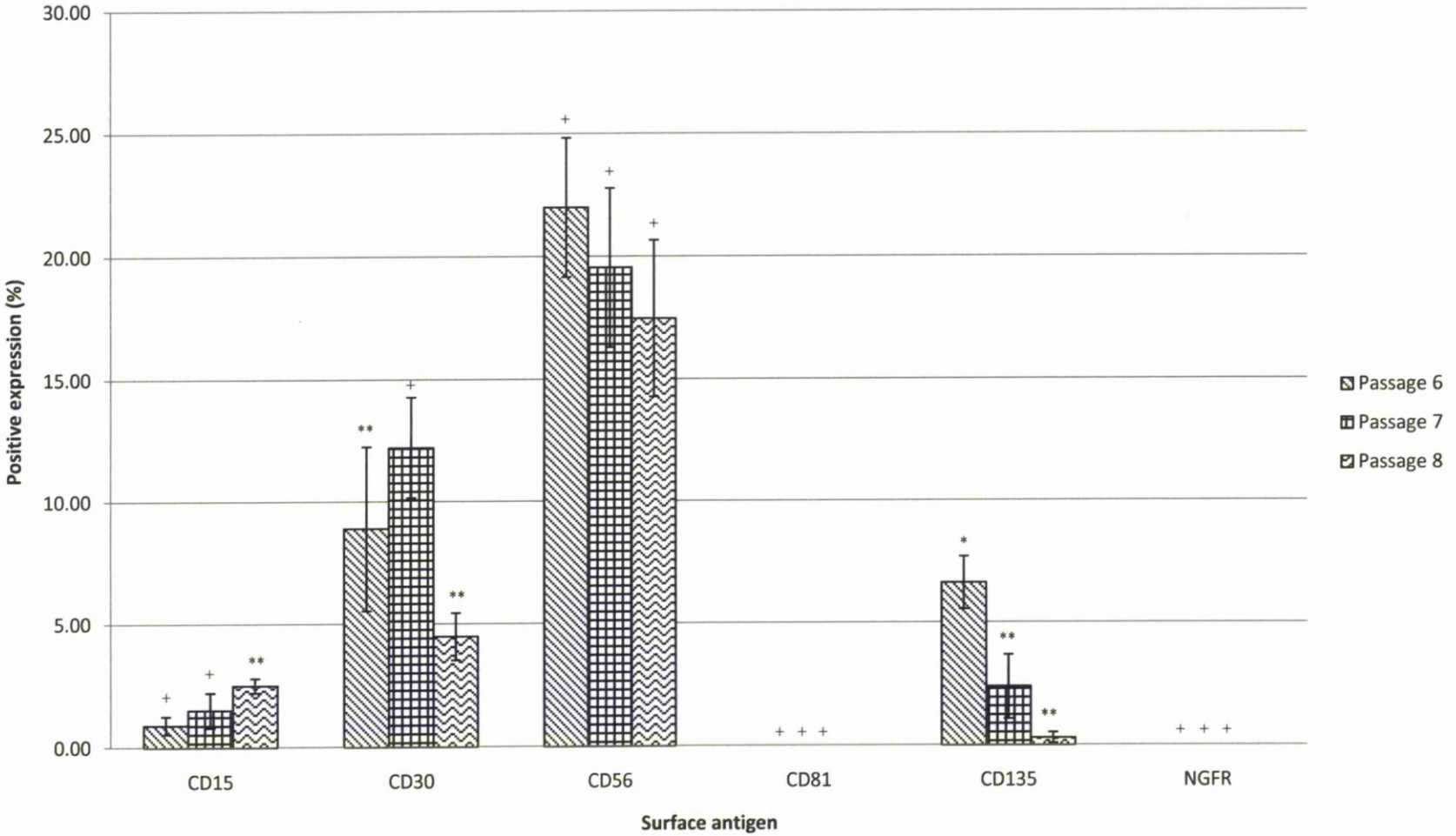

Figure 5.18 - **ES and progenitor-associated marker phenotyping of umbilical cord donor 1 cells (Passages 6 - 8; 0 x Freeze-thaw cycles) isolated by whole cord digestion. Values represent mean positive expression as observed by flow cytometry (n = 4). Error bars correspond to Standard Deviations. . Student *t*-test indicated that there were significant (*$p \leq 0.001$) (**$p \leq 0.05$) and non-significant (+$p \geq 0.05$) antigen expression differences when comparing cells isolated by whole cord digestion with those isolated from plating Wharton's jelly at corresponding passages.**

If umbilical cord-derived populations are to be utilised clinically, it is imperative that isolated cells can be freeze-stored for prolonged periods without modification to their phenotype, proliferation or differentiation capacity. Cord cells isolated by varying methodologies were therefore frozen at -80°c at passage 4. Following 30 days at -80°c, cells were thawed and resuspended in basal media. Freeze-thawed and non-freeze-thawed passage 5 cells from each isolation were assessed for their expression of MSC- (*Figure 5.19*), HSC- and endothelial- (*Figure 5.20*), and ES- and progenitor- (*Figure 5.21*) associated surface antigens.

MSC-associated surface antigens displayed downregulation within populations subjected to a freeze-thaw cycle compared with those which remained in culture, regardless of isolation method. CD29 was expressed by 83.0% of passage 5 Wharton's jelly-derived populations, though following a freeze-thaw cycle, equivalent passage cells exhibited 57.5% expression. Whole cord digestion cells, which demonstrated 85.3% expression at passage 5, also exhibited severely reduced upregulations following a freeze-thaw cycle, with only 46.0% expression. CD44, CD73, CD90, CD105, CD106, CD117, CD146, HLA-ABC and HLA-DR also demonstrated similarly reduced expression following freeze-thawing, although perhaps most signficant was the reduction in STRO-1 expression post freeze-thawing. CD166 expression was reduced following freezing of Wharton's jelly-derived populations, from 33.7% expression in passage 5 cells not subjected to freezing to 14.6% post-freeze-thawing. Interestingly whole cord digest isolates demonstrated no downregulation of CD166, exhibiting 18.3% and 18.4% in non-freeze-thaw and freeze-thaw cultures respectively.

HSC and endothelial-associated surface antigens displayed, with the exception of CD9, little or no downregulation within either isolated population following a freeze-thaw cycle. CD9 however demonstrated reduced expression in both populations, from 32.6% expression in passage 5 Wharton's jelly-derived cells reducing post-freezing to 11.4%. Whole cord digest isolated cells, of which 28.8% exhibited expression following passage 5, demonstrated reduced expression of CD9 post freezing, with only 8.7% expression.

Concerning ES- and progenitor-associated surface antigen expression following freeze-thawing of cells, numerous markers exhibited reduced expression compared with their continually cultured counterparts. Passage 5 Wharton's jelly-derived cells exhibited 49.4% expression of CD30, though following a freeze-thaw cycle only 17.5% of the population demonstrated expression. Whole cord digest populations demonstrated similar expression of CD30, with the 33.5% expression observed within non-freeze-thaw populations decreasing post freeze-thaw cycling, with the population demonstrating 13.1% expression. CD56 and CD135 expression within both respectively isolated populations demonstrated similar downregulation post freeze-thawing, whilst CD15, CD81 and NGFR were not expressed by any passage 5 populations.

Following phenotyping with an array of surface antigens, it is hypothesised that Wharton's jelly and whole cord-derived cord populations contain MSC-like stem and progenitor cells, HSCs and EPCs, and more primitive ES-like cells. However, it is apparant that freeze-thaw cycling results in modified expression of many of these surface antigens, and it would therefore be of significant interest to investigate telomere lengths within cells subjected to freeze-thaw cycling and compare them with those in non-freeze-thawed populations in order to ascertain whether cells rapidly age following cryopreservation. Telomere length studies could therefore again represent a key analytical tool to determine effects of optimised freeze-thaw protocols, since it is imperative that isolated cells can be frozen until required for therapeutic utilisation without phenotypic modifications.

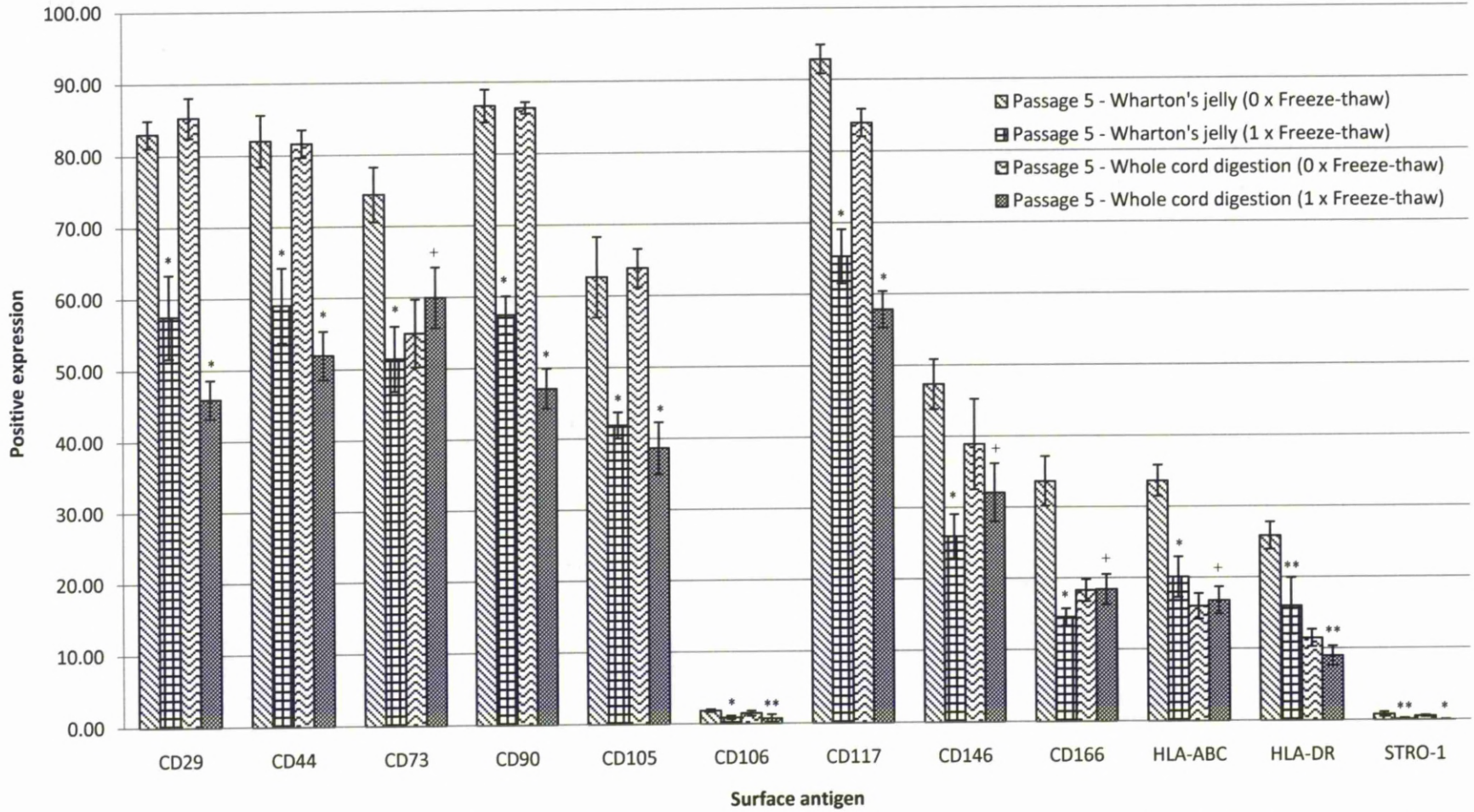

Figure 5.19 - **MSC-associated marker phenotyping of umbilical cord donor 1 cells isolated by plating Wharton's jelly or whole cord digestion (Passage 5; 0/1 x Freeze-thaw cycles). Values represent mean positive expression as observed by flow cytometry (n = 4). Error bars correspond to Standard Deviations. Student *t*-test indicated that there were significant (*$p \leq 0.001$) (**$p \leq 0.05$) and non-significant (+$p \geq 0.05$) antigen expression differences when comparing cells isolated by whole cord digestion and those isolated from plating Wharton's jelly before and after 1 x freeze-thawing.**

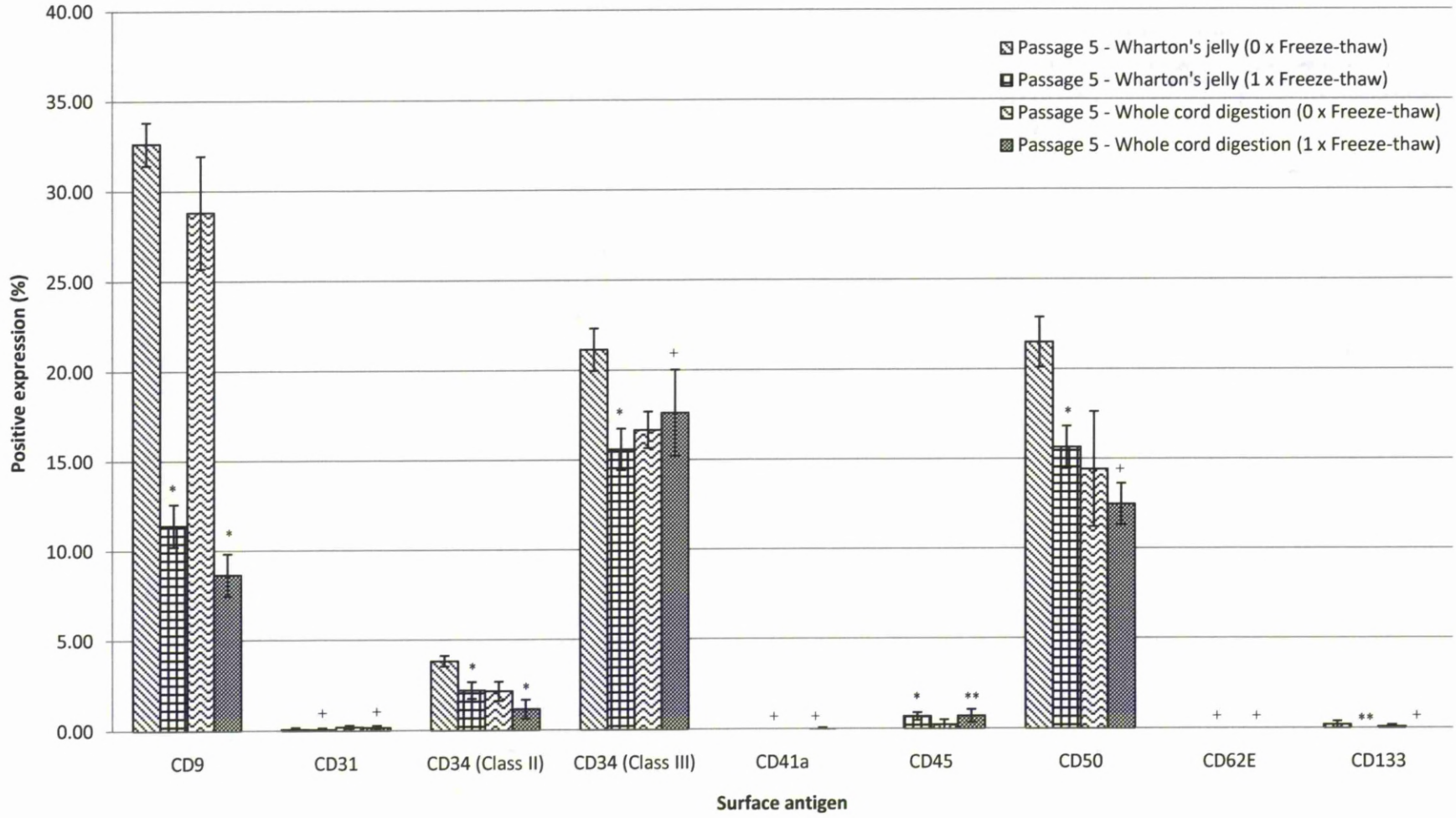

Figure 5.20 - **HSC and endothelial-associated marker phenotyping of umbilical cord donor 1 cells isolated by plating Wharton's jelly or whole cord digestion (Passage 5; 0/1 x Freeze-thaw cycles). Values represent mean positive expression as observed by flow cytometry (n = 4). Error bars correspond to Standard Deviations. Student *t*-test indicated that there were significant (*$p \leq 0.001$) (**$p \leq 0.05$) and non-significant (+$p \geq 0.05$) antigen expression differences when comparing cells isolated by whole cord digestion and those isolated from plating Wharton's jelly before and after 1 x freeze-thawing.**

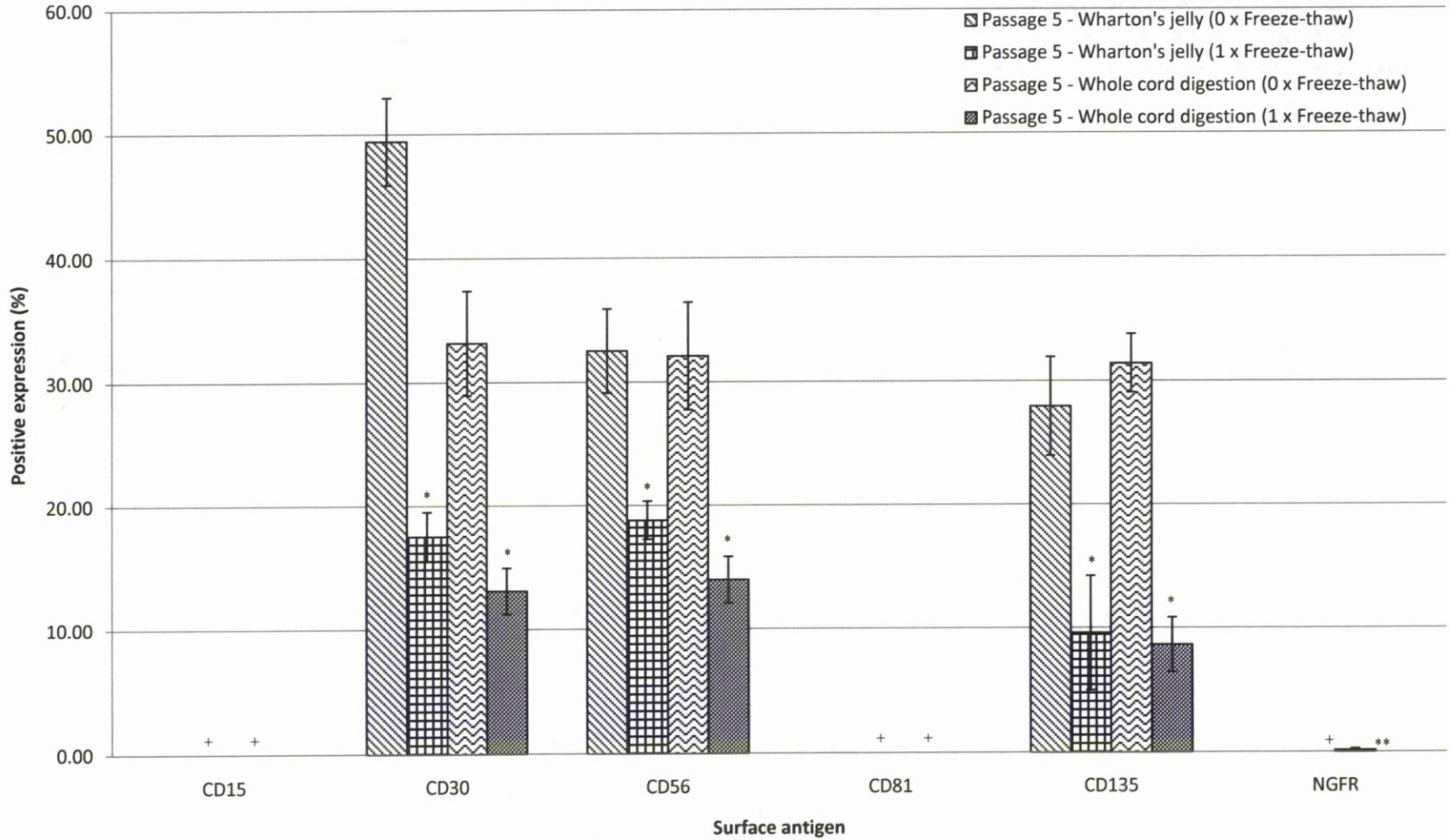

Figure 5.21 - **ES and progenitor-associated marker phenotyping of umbilical cord donor 1 cells isolated by plating Wharton's jelly or whole cord digestion (Passage 5; 0/1 x Freeze-thaw cycles). Values represent mean positive expression as observed by flow cytometry (n = 4). Error bars correspond to Standard Deviations. Student *t*-test indicated that there were significant (*$p \leq 0.001$) (**$p \leq 0.05$) and non-significant (+$p \geq 0.05$) antigen expression differences when comparing cells isolated by whole cord digestion and those isolated from plating Wharton's jelly before and after 1 x freeze-thawing.**

5.4 Proliferation Capacity of Umbilical Cord Cells

5.4.1 Proliferation Capacities of Differently Isolated Umbilical Cord Cells throughout Prolonged *In Vitro* Culture using CyQUANT Analysis

Further to the demonstration that isolated umbilical cord populations fail to maintain a stable phenotype following prolonged *in vitro* culture, adherent cells were assessed for their proliferative capacity over time (*Figures 5.22* and *5.23*). Following the seeding of 1 x 10^4 cells, passage 3 - 5 cultures of varyingly isolated populations displayed similar proliferative capacities, with total cell numbers of approximately 2 x10^4, 3.2 x 10^4 and 4.7 x 10^4 at days 1, 3 and 7 respectively. However, following a sixth passage each Wharton's jelly and whole cord-derived cells displayed reduced capacities to undertake proliferation, with passage 6 cells generating 1.5 x 10^4, 2.5 x 10^4 and 3.2 x 10^4 at days 1, 3 and 7 respectively. Whilst passage 7 cells derived from Wharton's jelly displayed a similar proliferative capacity to passage 6 cells, passage 7 whole cord digest cells exhibited reduced proliferation compared with passage 6 cells, generating 1 x 10^4 fewer cells following 7 days of basal culture. However, following an eighth passage both isolated cell populations displayed severe limitations to undertake proliferation compared with early passage cells, generating approximately 1.5 x 10^4 cells following 7 days of culture.

Proliferation assays examining Wharton's jelly and whole cord-derived cells revealed reduced capacities of the population to undertake cell divisions following prolonged *in vitro* culture. In fact, as with their phenotypic profiles, each isolated cord population undertakes this reduced capacity following a sixth passage, simultaneous to the global downregulation of perceived MSC antigens. Whilst no telomere studies were performed with umbilical cord-derived cells, given their similarity to bone marrow-derived populations, it is likely that these cells undertake rapid aging *in vitro*, and it is therefore imperative that culture conditions are optimised to prevent this rapid telomere demise and subsequent reduction in proliferation and modification of phenotype.

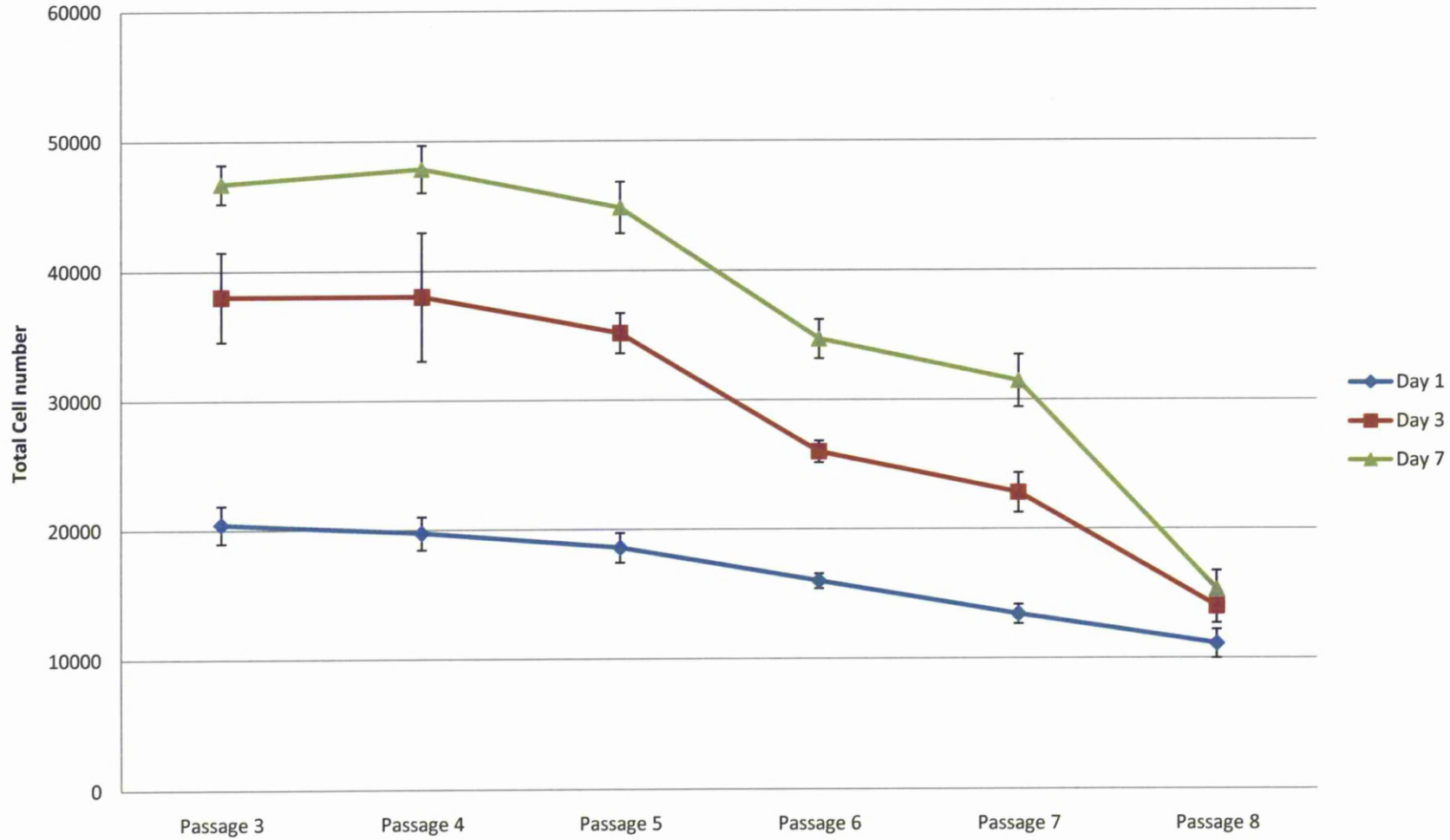

Figure 5.22 - **Proliferation capacity of Wharton's jelly-derived cells from umbilical cord donor 1 passages 3-8 (0 x Freeze-thaw cycle) cultured in basal media for 7 days. Initial seeding density 1 x 10^4 cells. Values represent mean numbers of total cells counted at days 1, 3 and 7 for each passage (n = 4). Error bars correspond to Standard Deviations.**

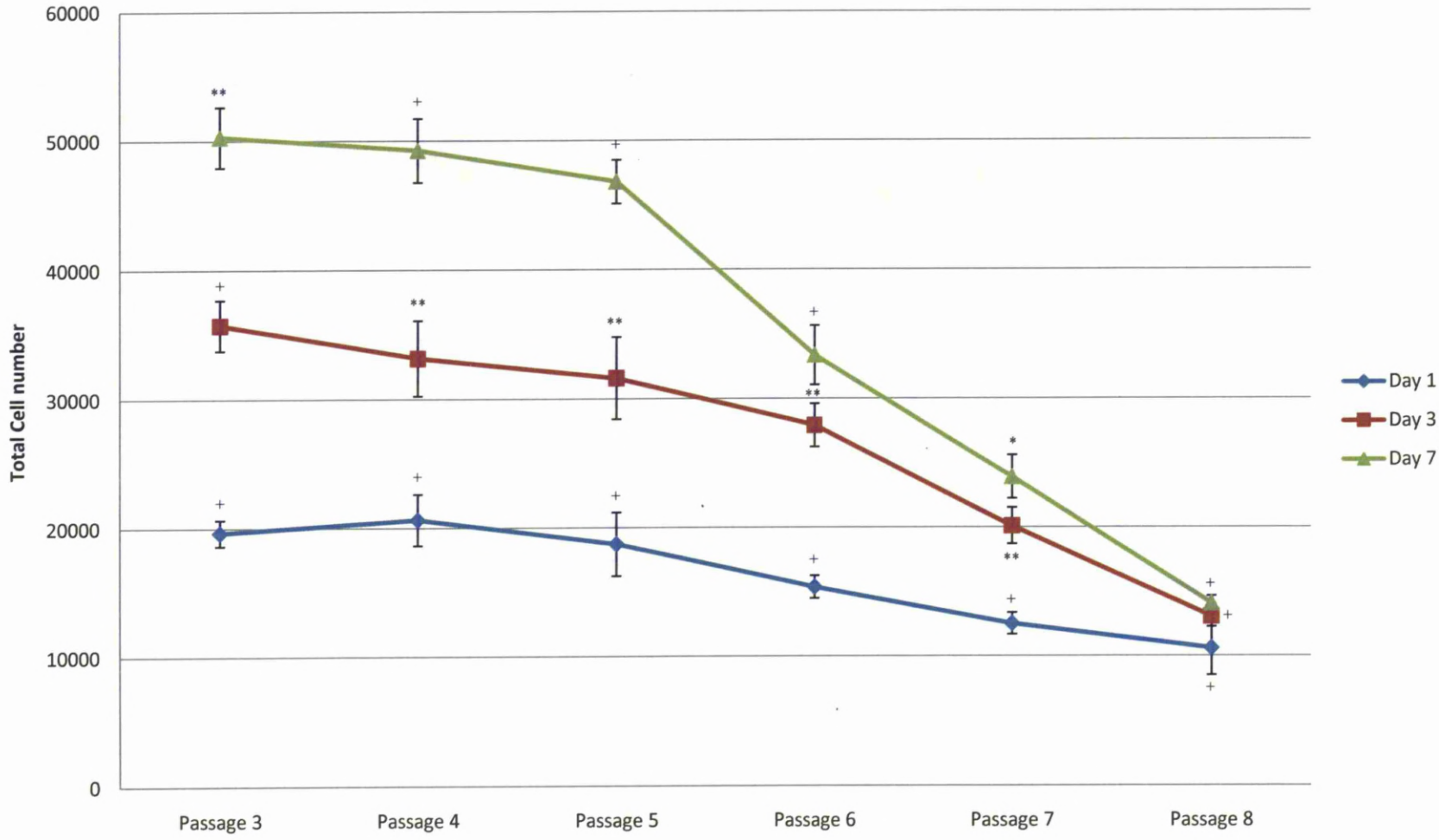

Figure 5.23 - **Proliferation capacity of whole cord digest-derived cells from umbilical cord donor 1 passages 3-8 (0 x Freeze-thaw cycle) cultured in basal media for 7 days. Initial seeding density 1 x 10^4 cells. Values represent mean numbers of total cells counted at days 1, 3 and 7 for each passage (n = 4). Error bars correspond to Standard Deviations. Student *t*-test indicated that there were significant (*$p \leq 0.001$) (**$p \leq 0.05$) and non-significant (+$p \geq 0.05$) differences in proliferation when comparing cells isolated by whole cord digestion and those isolated from plating Wharton's jelly at specific day and passage *e.g.* Passage 3 Whole cord digest-derived total cell number at day 3 of culture compared with Passage 3 Wharton's jelly derived total cell number at day 3 of culture.**

5.5 Neural Differentiation of Umbilical Cord Cells

5.5.1 Neuronal Differentiation of Umbilical Cord-derived Cells Isolated from Wharton's jelly and Cultured in Commercial Differentiation Media

Following phenotypic profiling using surface antigens, it was apparent that Wharton's jelly and whole cord-derived cell populations exhibited a heterogeneic phenotype potentially containing MSC- and progenitor-like cells, HSCs and EPCs, and more primitive ES-like cells. Given that Wharton's jelly-derived cells reporting a similar phenotype to that observed within this investigation have previously demonstrated an ability to differentiate towards adipogenic, chondrgenic and osteogenic lineages[290,408-411], isolated populations were assessed for their ability to progress along a neuronal lineage. To achieve this, passage 4 cells derived from Wharton's jelly and whole cord digestions were cultured in conditions known to induce neuronal differentiation. Following 28 days of induction, adherent cells displayed morphological (*Figures 5.24* and *5.25*) and phenotypic characteristics associated with terminally differentiated neuronal cells. Whilst neural progenitor-associated protein nestin was expressed by approximately 40% of induced cells at day 21 (*Figure 5.26*), expression had ceased at day 28 (*Figure 5.27*) and was replaced by proteins associated with terminally differentiated neuronal cell types. The expression of nestin within 40% of the population was, however, particularly interesting given that less than 0.5% of cells expressed neuronal progenitor-associated antigens CD81 and NGFR, thereby indicating that a non-committed stem cell population had undergone differentiation to a neuronal progenitor cell expressing nestin. These subpopulations appeared to further commit towards a mature neuronal phenotype following further induction, with the neuronal-associated proteins Beta-III-tubulin (*Figure 5.28*), neurofilament (*Figure 5.29*), S100 (*Figure 5.30*) and synaptophysin (*Figure 5.31*) expressed by approximately 40% of induced cord cells following 28 days, although interestingly the population also expressed Schwann-cell-associated proteins GFAP (*Figure 5.32*) and p75 (*Figure 5.33*) by approximately 5% of cells. This ability of umbilical cord-derived cells to undertake neuronal differentiation upon exposure to differentiation stimuli could offer immense clinical benefit. Interesting to note, however, is the heterogeneous differentiation of the population, with varying subpopulations from both cord niches exhibiting phenotypic

characteristics associated with Schwann and neuronal lineages. However the stem or progenitor subsets from which each terminally differentiated cell originates is unclear, with $CD81^+$, $NGFR^+$, MSC-like, ES-like or even HSC associated antigen expressing cells perhaps responsible for the differentiation.

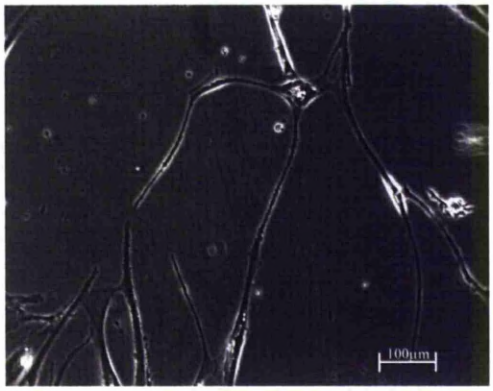

Figure 5.24 **- Umbilical cord donor 1 cells isolated from Wharton's jelly (Passage 4; 0 x freeze-thaw) and cultured in neuronal differentiation media for 28 days.**

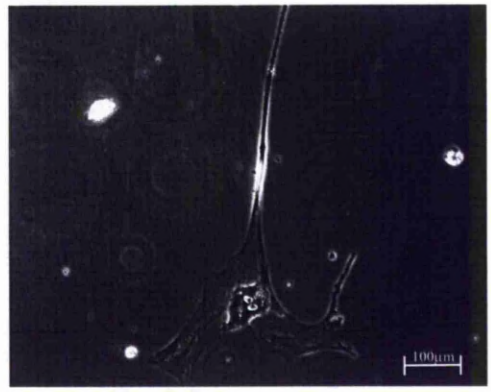

Figure 5.25 **- Umbilical cord donor 1 cells isolated via whole cord digestion (Passage 4; 0 x freeze-thaw) and cultured in neuronal differentiation media for 28 days.**

Figure 5.26 **- Umbilical cord donor 1 cells isolated from Wharton's jelly (Passage 4; 0 x freeze-thaw) and cultured in neuronal differentiation media for 21 days stained with Hoechst 33342 (blue), Oregon green (green) and nestin antibody (red). Approximately 40% of umbilical cord cells exhibited positive nestin expression following 21 days of induction.**

Figure 5.27 **- Umbilical cord donor 1 cells isolated from Wharton's jelly (Passage 4; 0 x freeze-thaw) and cultured in neuronal differentiation media for 28 days stained with Hoechst 33342 (blue), Oregon green (green) and nestin antibody (red). No umbilical cord cells exhibited positive nestin expression following 28 days of induction.**

Figure 5.28 - **Umbilical cord donor 1 cells isolated via whole cord digestion (Passage 4; 0 x freeze-thaw) and cultured in neuronal differentiation media for 28 days stained with Hoechst 33342 (blue), Oregon green (green) and beta-III-tubulin antibody (red). Approximately 40% of umbilical cord cells exhibited positive beta-III-tubulin expression.**

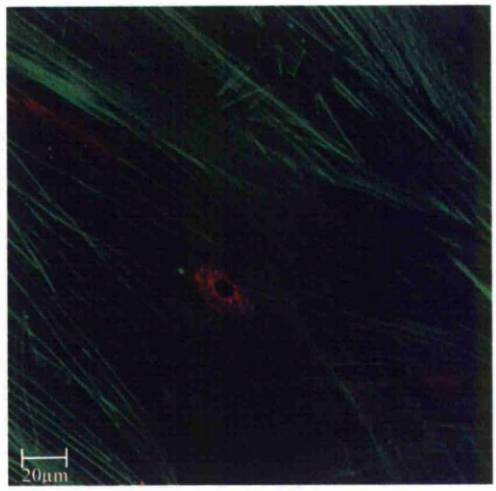

Figure 5.29 - **Umbilical cord donor 1 cells isolated from Wharton's jelly (Passage 4; 0 x freeze-thaw) and cultured in neuronal differentiation media for 28 days stained with Hoechst 33342 (blue), Oregon green (green) and neurofilament antibody (red). Approximately 40% of umbilical cord cells exhibited positive neurofilament expression.**

Figure 5.30 - **Umbilical cord donor 1 cells isolated via whole cord digestion (Passage 4; 0 x freeze-thaw) and cultured in neuronal differentiation media for 28 days stained with Hoechst 33342 (blue), Oregon green (green) and S100 antibody (red). Approximately 40% of umbilical cord cells exhibited positive S100 expression.**

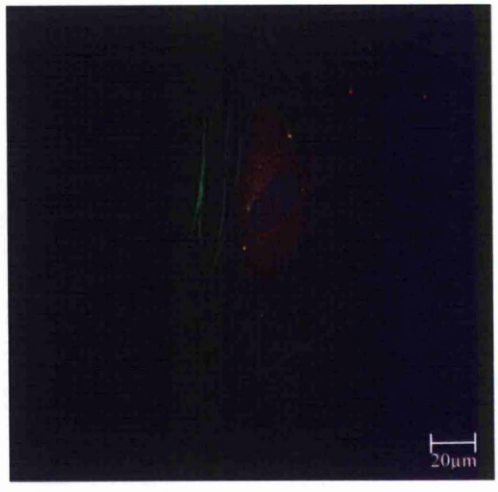

Figure 5.31 - **Umbilical cord donor 1 cells isolated from Wharton's jelly (Passage 4; 0 x freeze-thaw) and cultured in neuronal differentiation media for 28 days stained with Hoechst 33342 (blue), Oregon green (green) and synaptophysin antibody (red). Approximately 40% of umbilical cord cells exhibited positive synaptophysin expression.**

Figure 5.32 - **Umbilical cord donor 1 cells isolated from Wharton's jelly (Passage 4; 0 x freeze-thaw) and cultured in neuronal differentiation media for 28 days stained with Hoechst 33342 (blue), Oregon green (green) and GFAP antibody (red). Approximately 5% of umbilical cord cells exhibited positive GFAP expression.**

Figure 5.33 - **Umbilical cord donor 1 cells isolated from Wharton's jelly (Passage 4; 0 x freeze-thaw) and cultured in neuronal differentiation media for 28 days stained with Hoechst 33342 (blue), Oregon green (green) and p75 antibody (red). Approximately 5% of umbilical cord cells exhibited positive p75 expression.**

5.6 Conclusion

5.6.1 Umbilical Cord as a Niche for the Isolation of Clinically Desirable Cells

Umbilical cords represent an attractive organ for the isolation of cells originating from both the mother and the unborn fetus, potentially allowing isolation of cells exhibiting innate capacities for multilineage differentiation. Wharton's jelly or whole cord digestion isolations yielded morphologically dissimilar yet phenotypically comparable cells, displaying similar phenotypic surface expression composed of markers associated with bone marrow-derived MSCs, alternative non-hematopoietic progenitor lineages, HSCs and EPCs, and ES cells. However, this heterogeneic phenotype, like that observed in bone marrow-derived populations, failed to be maintained following *in vitro* culture. In fact, numerous cells appeared spontaneously differentiate following a sixth passage, as observed by a decrease in plasticity-associated antigens and an increase in those associated with terminally differentiated phenotypes, in particular CD31 and CD133, which are largely associated with functional endothelial cells. Such terminal differentiation could be the result of MSC-like cells, primitive fetal-derived cells or EPCs undertaking such spontaneous

lineage induction. Furthermore, Wharton's jelly and whole cord-derived cells displayed surface phenotype modifications following freeze-thaw cycling, another issue which must be addressed if this cell source is to be utilised within a clinical setting. In addition to this phenotypic instability, proliferative capacities of the populations were reduced upon increasing passage.

Given that previous reports have detailed the isolation of phenotypically comparable cells from Wharton's jelly capable of differentiating towards adipogenic, chodrogenic and osteogenic lineages, isolated cord cells were differentiated towards a neuronal lineage to demonstrate a further capacity of differentiation. However, whilst neuronal differentiation was observed within approximately 40% of the population, and furthermore Schwann cell lineage induction within 5% of cells, it is difficult to associate this differentiation with one specific cell phenotype given the heterogeneity of the population. However, given that less that 0.5% of cells expressed the neuronal progenitor-associated proteins CD81 and NGFR, it is likely that MSCs or a more primitive cell undertook differentiation given that approximately 40% of cells expressed nestin following 21 days of neuronal induction and further differentiated towards a mature neuronal lineage after 28 days.

In conclusion, if umbilical cord-derived populations are to be used as a cell source for clinical application, several issues must be addressed. Primarily, homogeneous subpopulations present within the heterogeneously isolated adherent population should be purified in order to facilitate banking of fetal and mother-derived cells of varying potential. And whilst Wharton's jelly and whole cord-derived populations exhibited similar phenotypic profiles, given the expression, albeit minimal, of neuronal progenitor antigens, and furthermore the slightly reduced expression of MHC class antigens, it may be that whole cord digests represent a more suitable base material for undertaking purification strategies. Achieving purification of such subpopulations may resolve the second issue, potentially allowing tailoring of culture and freeze-thaw cycling conditions to maintain the mother and fetal subpopulations in a desired phenotypic state. Should these issues be addressed, the umbilical cord will undoubtedly provide a therapeutically useful reservoir for the isolation of cells for autologous utilisation within mother and fetus in later life.

5.6.2 Response to Chapter Aims

Results obtained within this chapter address the aims set out in 5.1.1 by phenotypically characterising Wharton's jelly and whole cord-derived cells using flow cytometry. Furthermore, the ability of isolated populations to maintain phenotype and proliferation following *in vitro* culture and freeze-thaw cycling was investigated, results of significant interest from a clinical viewpoint. Finally, results describing the ability of these cord cells to differentiate towards a neuronal phenotype not only addressed the aims set out 5.1.1, but complemented previously published results describing adipogenic, chondrogenic and osteogenic differentiation of phenotypically similar cells.

6. Human Dental Pulp as a Potential Source of Pluripotent Adult Stem/Progenitor Cells

6.1. Introduction

6.1.1 Dental pulp cells

The vertebrate neural crest is a pluripotent cell population derived from the lateral ridges of the neural plate during early stages of embryogenesis. Neural crest cells disperse from the dorsal surface of the neural tube and migrate extensively throughout the embryo, subsequently generating an array of differentiated cell types. Throughout recent years, understanding of neural crest cell establishment within the early embryo and subsequent lineage segregation, differentiation and functional contribution to a given cell type, mediated by genetic and epigenetic mechanisms, have been elucidated.

During craniofacial development, neural crest cells migrate ventrolaterally due to populating of the branchial arches. The proliferative activity of these cells generates the discrete swellings that demarcate each branchial arch. The subsequent migration of these ectodermally-derived cells makes an extensive contribution to the formation of mesenchymal structures within the head and neck. Studies monitoring cell migration have further demonstrated that neuroectoderm cells of rhombomeres 1 - 4 (r1 - 4), located in the forming posterior midbrain and anterior hindbrain, transform into cranial neural crest (CNC) cells, which migrate into the first branchial arch and thereafter reside within the maxillary and mandibular prominences. Residing CNC cells contribute significantly to tooth morphogenesis, migrating, proliferating and differentiating into odontoblasts, cementoblasts, fibroblasts, osteoblasts and chondroblasts or their precursor representatives.

In addition to CNC cells, non-CNC cells have also been demonstrated to reside within the developing tooth, although their tissue of origin remains unaccounted for. Transplantation of wild-type tooth germ into the kidney of *lacZ*-transgenic mice demonstrated localisation of host *lacZ* expressing cells and RBCs within the transplanted tooth. *LacZ* expressing cells were located near or inside blood vessels,

demonstrating that circulating cells are capable of invading the dental pulp via blood vessel angiogenic mechanisms and consequentially circulating cells could be the origin of non-CNC cells within the dental pulp. However, whilst this study hypothesises a potential migratory pathway for the presence of non-CNC cells, it fails to identify the tissue from which the circulating cells originated[412-414].

Subsequent to the demonstration that dental pulp could yield numerous stem and progenitor cells of CNC and non-CNC association, numerous studies were undertaken attempting to isolate pluripotent cells hypothesised to reside within the tissue. Thus far studies have isolated cells reserving an MSC-like morphology and phenotype, similarly possessing a multipotent ability to differentiate along adipogenic, chondrogenic, osteogenic and neural phenotypes, although maintaining negative aspects such as reduced proliferative and differentiation capacities following prolonged *in vitro* culture[245-246]. Studies isolating cells from deciduous teeth from children aged 5 - 7 years noted the expression of Oct4, Nanog, SSEA-3, SSEA-4, Tra-1-60 and Tra-1-81 throughout the 25 passage culture[277]. However, no investigation has yet reported that this expression of embryonic associated markers and ability to undertake lineage differentiation extends to cells isolated from adult teeth. Furthermore, and perhaps more importantly from a clinical perspective, no studies have yet identified cells responsible for these observed results, failing to attribute expression firstly to CNC or non-CNC cells, and subsequently to which stem or progenitor subsets within the given cell family. Considering developmental studies which have noted that CNC cells partially and terminally differentiate to form odontoblasts, cementoblasts, fibroblasts, osteoblasts and chondroblasts or their precursor representatives, it is fundamental that sustained proliferation and differentiation potential, surface phenotype and karyotype stability and consequently clinical applicability, be assessed. Whist this may seem cumbersome to many clinically associated representatives, the ability of numerous committed progenitor subsets within heterogeneous cell populations to spontaneously generate life threatening tissues must not be underestimated. Therefore dental pulp cells derived from deciduous and adult teeth should be homogeneously segregated in order to generate individual subpopulations of differing potential which can be rigorously characterised. Initially however, this chapter will investigate the types of cells present within heterogeneously isolated populations using flow cytometry to probe

surface antigen expression and immunofluorescent staining to investigate intrinsic proteins. The stability of this heterogeneic phenotype and also the proliferative capacity of the population will be assessed throughout increasing *in vitro* culture and also following freeze-thaw cycling, whilst CFU-F and CFU-GM assays will be undertaken to establish the number of non-hematopoietic and hematopoietic progenitors present respectively. Assuming the hypothesised presence of stem or progenitor subsets following aforementioned analysis, populations will be differentiated along varying lineages in order to establish multipotentiality of dental pulp populations. If subsequent to this analysis we hypothesise the presence of varying stem and progenitor subpopulations of interest, the cells will be isolated using surface antigen purification methodologies and characterised upon a basis of greater homogeneity.

6.1.2 Aims of this Chapter

This investigation aims to characterise adherent cell populations from the dental pulp of donors of varying age, sex and tooth condition. Isolated cells will be characterised using flow cytometry to identify CNC and non-CNC subpopulations, and this phenotype, as well as proliferation, assessed for stability throughout *in vitro* culture and following freeze-thaw cycling. Given their potentially immature phenotype, pulp-derived cells will be investigated for the presence of proteins associated with maintenance of plasticity and early lineage commitment, particularly towards that of the neuronal progenitor. CFU assays will be undertaken to quantify the number of CFU-Fs and CFU-GMs present in each population and cells will be induced towards adipogenic, chondrogenic, osteogenic, neuronal and hepatic lineages in order to assess their multipotentiality. Each of these characterisation steps will be carried out at increasing *in vitro* passage and following freeze-thaw cycling, and telomere length assays will be undertaken to identify the aging rate of the population. In the assumption that adherent cells will be heterogeneous, populations will be purified based on surface antigen expression and these cells characterised as detailed above.

6.2 Isolation of Cells from Human Dental Pulp

6.2.1 Isolation of Cells from Human Dental Pulp by Enzymatic Digestion

Teeth were attained following consented dental extractions or loss of milk teeth and stored in 199 Media with 5% (v/v) FCS and 1% (v/v) 10,000U/ml of penicillin and 10mg/ml of streptomycin in 0.9% (w/v) sodium chloride until pulp isolation. Pulp was extracted from teeth and enzymatically digested prior to plating in one well of a 6-well plate. Adult and deciduous incisors, canines, pre-molars and molars (*Figure 6.1*) of differing conditions were received from donors of varying age and sex (*Table 6.1*). *Table 6.1* identifies tooth position using a tooth numbering system detailed in *Figure 6.1*, and attributes a score of 1-10 (1 – Poor; 10 – Excellent) qualitatively dependent on condition of tooth. Cells adhered to the uncoated tissue culture plastic following 4 to 10 days of incubation and began rapid proliferation, attaining a state of confluence approximately 7 days after initial adherence.

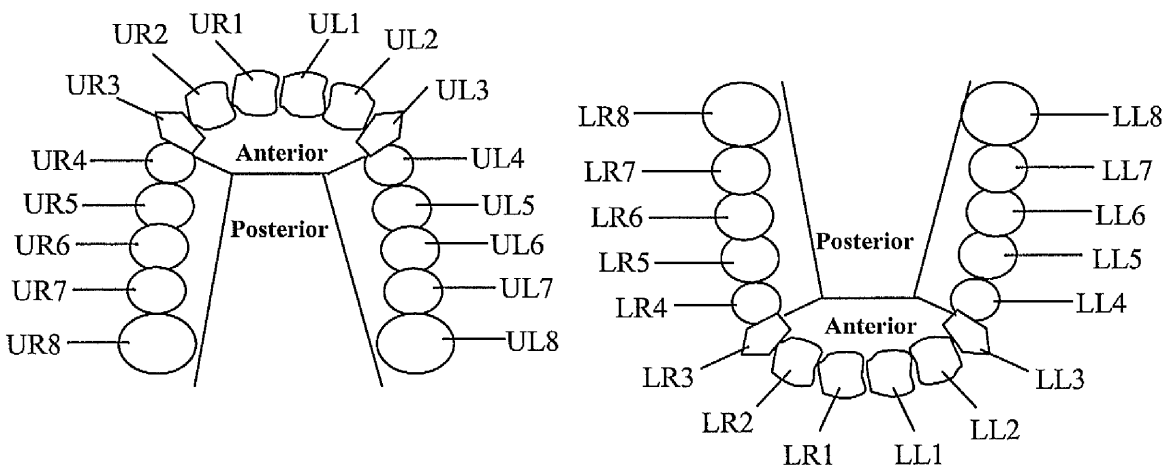

***Figure 6.1* - Diagrammatic representation of tooth numbering system; UL – Upper Left; UR – Upper right; LL – Lower left; LR – Lower right.**

Dental pulp cells were isolated from 23 of the 31 donors, adhering following a minimum of 4 days of culture and a maximum of 10. No correlation could be devised to associate number of days for cell adherence with age, sex, tooth position or condition of tooth, although none of the received teeth attaining a condition score of 1 allowed for the isolation of adherent cells. In such teeth, pulp was no longer a morphologically soft tissue, and instead portrayed a hard, black appearance which

could not be mechanically or enzymatically digested. No explanation could be devised to suggest possible reasons why cells could not be isolated from teeth of good condition, with no observable correlation to donor age, sex or tooth position.

Adherent cells from all donors exhibited a heterogeneous fibroblastic-like morphology, although numerous other morphologically dissimilar cells were observed in all populations (*Figures 6.2* to *6.10*). Adherent cells proliferated rapidly, attaining confluence within one well of a 6 well plate after a minimum of 5 days post-adherence and a maximum of 18 days. Due to their variance in donor age, sex, condition of tooth and the position from which it was extracted, donors 1 - 4 were subjected to further analysis as detailed below. The remaining adherent cells were subcultured up to 3 passages to attain a greater cell number and subsequently frozen until required.

Dental pulp Donor	Donor age (Years)	Donor sex	Tooth numbering system Position	Condition of Tooth	Primary adherence period (Days)	Primary confluence period (Days)
1	15	Male	UR5	9	4	13
2	15	Female	UL3	7	7	16
3	79	Female	LL7	5	7	12
4	69	Male	UR4	2	10	18
5	12	Female	UR4	6	8	15
6	37	Male	LL3	5	8	16
7	67	Female	LR5	4	N/A	N/A
8	67	Female	UR8	1	N/A	N/A
9	71	Male	LL4	1	N/A	N/A
10	71	Male	UR6	2	6	15
11	15	Male	LL7	5	8	19
12	15	Male	LR7	5	10	17
13	10	Male	UR4	10	8	18
14	28	Female	UR4	4	N/A	N/A
15	40	Female	UL7	2	N/A	N/A
16	53	Male	LL4	4	N/A	N/A
17	54	Female	LR6	1	N/A	N/A
18	16	Male	LR3	5	7	15
19	16	Male	LL5	7	9	22
20	40	Female	UR8	4	10	28
21	51	Female	UR6	2	6	14
22	?	Male	LL4	1	N/A	N/A
23	14	Female	UL5	4	9	17
24	14	Female	UR5	7	8	17
25	14	Female	LL2	8	7	12
26	7	Male	UR1	10	5	15
27	26	Male	LL4	5	6	14
28	59	Male	LL4	3	9	20
29	54	Male	UR7	5	7	18
30	16	Male	UR7	4	4	12
31	17	Female	LL6	5	6	14

Table 6.1 - **Details of dental pulp donors, tooth numbering position (See *Figure 6.1*), condition of tooth (1 – Poor; 10 – Excellent), number of days required for adherence and subsequent attainment of confluence. N/A denotes tooth samples from which cells were unobtainable.**

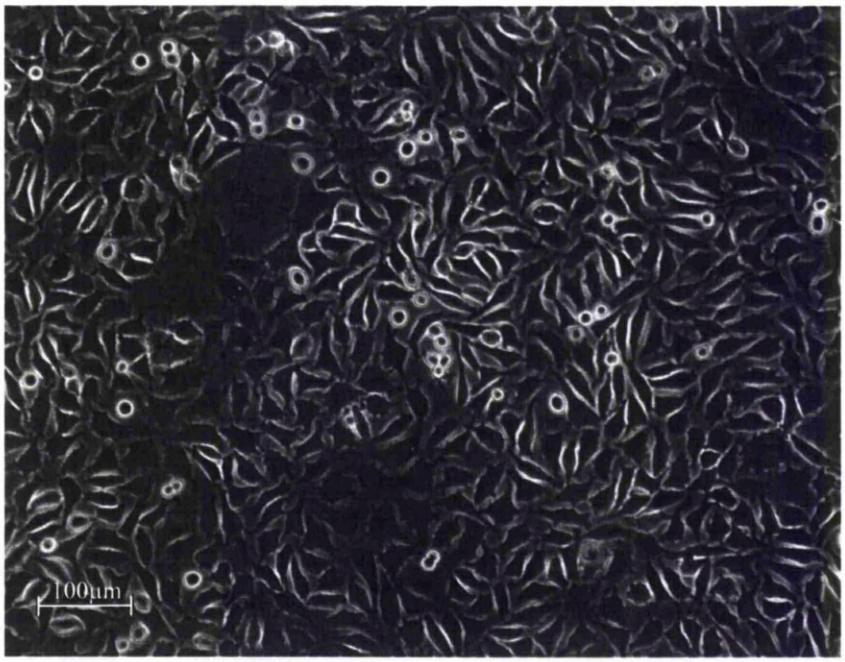

Figure 6.2 - **Cells isolated from pulp donor 1 following 9 days of primary culture.**

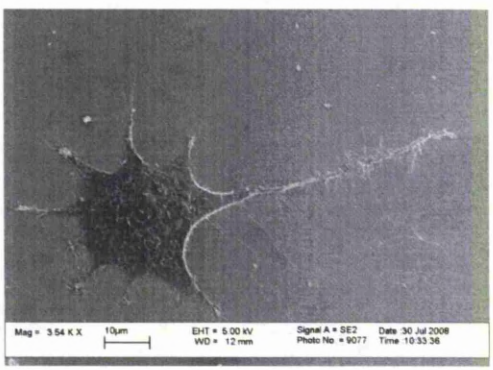

Figure 6.3 - **SEM image of pulp donor 1 cells (Passage 5, 1 x freeze-thaw cycles) cultured in commercial basal media.**

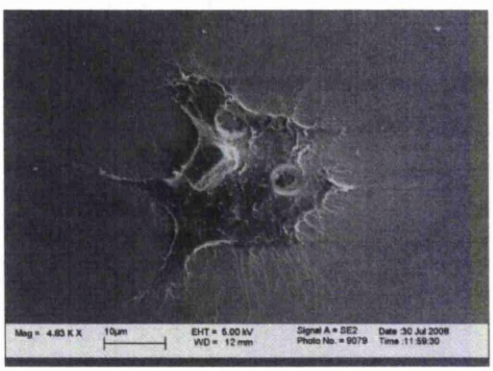

Figure 6.4 - **SEM image of pulp donor 1 cells (Passage 5, 1 x freeze-thaw cycles) cultured in commercial basal media.**

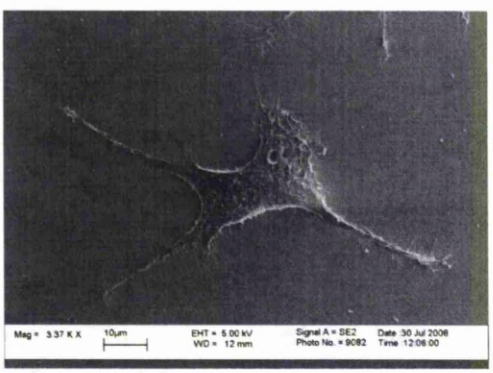

Figure 6.5 - **SEM image of pulp donor 2 cells (Passage 5, 1 x freeze-thaw cycles) cultured in commercial basal media.**

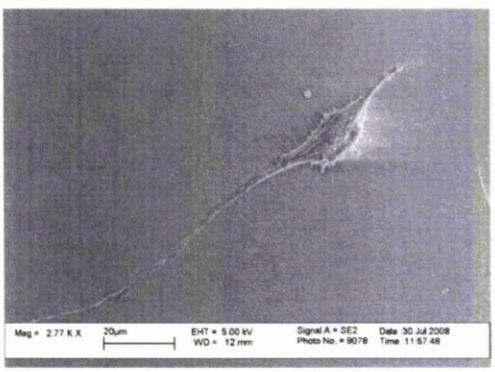

Figure 6.6 - **SEM image of pulp donor 2 cells (Passage 5, 1 x freeze-thaw cycles) cultured in commercial basal media.**

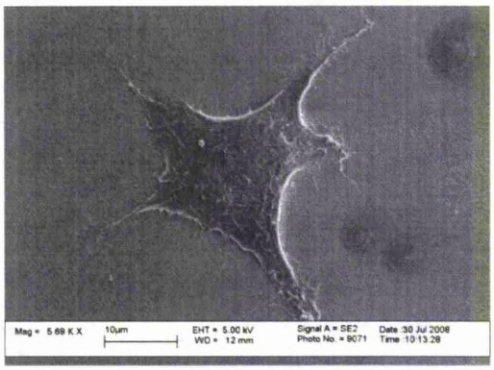

Figure 6.7 - **SEM image of pulp donor 3 cells (Passage 5, 1 x freeze-thaw cycles) cultured in commercial basal media.**

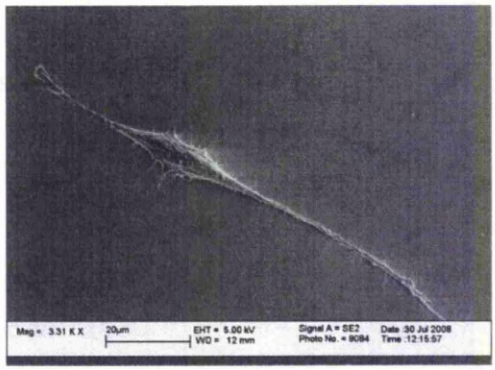

Figure 6.8 - **SEM image of pulp donor 3 cells (Passage 5, 1 x freeze-thaw cycles) cultured in commercial basal media.**

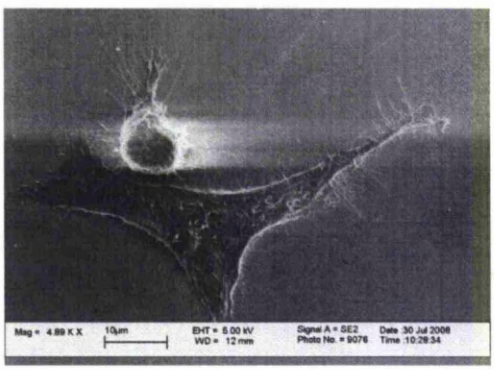

Figure 6.9 - **SEM image of pulp donor 4 cells (Passage 5, 1 x freeze-thaw cycles) cultured in commercial basal media.**

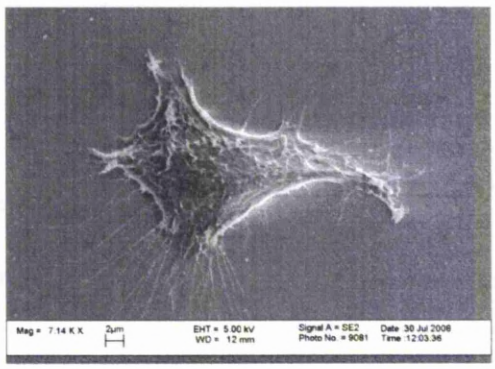

Figure 6.10 - **SEM image of pulp donor 4 cells (Passage 5, 1 x freeze-thaw cycles) cultured in commercial basal media.**

6.3 Phenotyping of Dental Pulp Cells

6.3.1 Phenotypic Analysis of Dental Pulp Cells throughout Prolonged *In Vitro* Culture using Flow Cytometry

Phenotypic analysis of cell populations derived from bone marrow and umbilical cord demonstrated the inability of such populations to maintain a stable phenotype following maintained periods of *in vitro* culture. This spontaneous modification of phenotype is both concerning and limiting with regards their potential utilisation within a clinical setting, given that the reduced expression of stem cell-associated antigens is accompanied by a reduced, and ultimately deceased, capacity to undertake proliferation and differentiation *in vitro*. Thus it is probable that therapeutic strategies utilising such cells will largely focus upon early passage cells

given their increased proliferative and differentiation capacities. However, it is likely that many clinical applications will require significantly large numbers of cells, and thus the ability of the selected cell type to be readily cultured *in vitro* without variation of phenotype will be preferable in order to generate large cell numbers without taking large biopsies from donors. Therefore, in order to assess the capabilities of dental pulp-derived cells to maintain a constant phenotype over increasing passage *in vitro*, cells derived from donors 1 - 4 were subjected to phenotypic analysis during each passage. Furthermore, cells were assessed for phenotypic variance following freeze-thaw cycling, a key feature if the cells are to be used clinically, in particular for cells which are being isolated and 'banked'. At present, cells derived from umbilical cord and umbilical cord blood are popular tissues for the isolation and freezing of cells which maybe used autologously should the newly born child or, given the likely presence of adult cells the mother, require any medical treatment in their later years. Dental pulp, and in particular that derived from spontaneously extracting deciduous teeth, may offer an alternative cell source from which autologous cells can be isolated, particularly if they can maintain a stable phenotype following long-term freeze storage.

Isolated cells were cultured up to 3 passages at which point a suitable cell number had been attained in order to assess the population by flow cytometry. Adherent cells from each donor were assessed for their expression of MSC-, HSC- and endothelial-, and ES- and progenitor- associated surface antigens at passages 3 to 9 and passage 30. Cells were also assessed for their ability to sustain phenotype following freeze-thawing. Finally, cells were cultured for prolonged periods in chemically-defined basal media which could potentially overcome many of the ethical and technical dilemmas associated with serum-containing commercial media.

Whilst little phenotypic difference was observed between varying donors within blood and cord derived populations, the inability of blood-derived cells to maintain proliferation and that of cord cells to maintain a stable phenotype or proliferation rate following prolonged *in vitro* culture or freeze-thaw cycling presents significant hurdles from a therapeutic viewpoint. Therefore, of significant interest with regards dental pulp-derived populations is that, whilst displaying little or no variability between differing donors, they are capable of maintaining a phenotype throughout

prolonged *in vitro* culture and post freeze-thaw cycling at passage 5/6 (*Figures 6.11* to *6.40*).

Concerning MSC-associated surface antigen expression (*Figures 6.11*, *6.14*, *6.17*, *6.20*, *6.23*, *6.26*, *6.29*, *6.32*, *6.35* and *6.38*), dental pulp donors displayed similar expression of all antigens and maintained this phenotype throughout prolonged *in vitro* culture. Cells from each donor were cryopreserved at passage 5 and, following 30 days at -80°C, were resuspended in commercial or chemically-defined basal media. Following two further passages in commercial or chemically-defined culture conditions, passage 8 cells were assessed for their MSC-associated profile. Cells subjected to freeze-thaw and cultured in commercial or chemically-defined culture conditions demonstrated no phenotypic difference between each other or continually cultured cells (*Figures 6.35* and *6.38*), highlighting dental pulp-derived cells as a cell source capable of being cryopreserved until required for therapeutic application.

Phenotypically, cell populations demonstrated approximately 90% expression of CD29 and CD117 at each passage, though interestingly alternative MSC-associated antigens exhibited lower expression. Hyaluronic acid plasticity regulator CD44 was expressed by approximately 20% of cells, whilst CD90 and CD105 exhibited 25% - 35% expression. MSC-associated antigen CD73 demonstrated approximately 30% - 50% expression. Multipotent- and endothelial-associated antigen CD146 was consistently expressed by 20% - 30% of donor cells, though interestingly CD166 demonstrated little or no expression within the populations. MHC class I antigen HLA-ABC consistently demonstrated 20% - 30% expression within the population, whilst MHC class II antigen HLA-DR exhibited approximately 5%. Whilst CD106 exhibited little or no expression within the populations, STRO-1 expression within the populations was maintained at approximately 0.5% - 1.5%.

HSC- and endothelial- associated antigens (*Figures 6.12*, *6.15*, *6.18*, *6.21*, *6.24*, *6.27*, *6.30*, *6.33*, *6.36* and *6.39*) were also maintained on cells from varying donor and passage. Furthermore, cells subjected to freeze-thaw cycling and cultured in chemically-defined basal media also demonstrated conserved expression of HSC and endothelial antigens. ES- and monocyte- associated surface antigen CD9 demonstrated approximately 10% - 20% expression, although since it is unlikely that

monocytes would be present within the dental pulp, it is hypothesised that $CD9^+$ cells may represent primitive subpopulations of endothelial or ES-like cells. Endothelial-associated antigens CD31 and CD133 were expressed by few or no cells within the populations, although conversely cytokine-stimulated endothelial antigen CD62E was consistently expressed by approximately 5% - 20%. Whilst CD41a and CD45 were expressed by minimal or no cells, approximately 10% - 20% demonstrated expression of the leukocyte antigen CD50, although given the niche, it is perhaps more feasible that this antigen is expressed by alternative cell types. Concerning HSC-associated markers, populations demonstrated approximately 5% - 10% expression of CD34 class II antigen, whilst CD34 class III was expressed by 20% - 30% of cells.

Dental pulp-derived populations furthermore maintained antigens associated with ES- and progenitor- cell types throughout prolonged passage and following freeze-thaw cycling (*Figures 6.13*, *6.16*, *6.19*, *6.22*, *6.25*, *6.28*, *6.31*, *6.34*, *6.37* and *6.40*). Whilst cells exhibited little or no expression of murine ES marker CD15, a number of other ES-associated antigens were consistently expressed within the populations. CD30 was expressed by approximately 25% - 40%, whilst progenitor antigens CD56 and CD135 demonstrated maintained expression of approximately 20% - 40%. Unsurprisingly given its developmental derivation from the neural crest, populations exhibited approximately 5% CD81 and NGFR expression, a potential subpopulation of neuronal progenitor cells.

In conclusion, dental pulp-derived populations displayed an array of MSC-, HSC-, ES- and progenitor- associated antigens which could represent attractive subpopulations of cells for a diverse range of therapeutic utilisations. Furthermore, the ability of heterogeneously isolated populations to maintain this phenotype following prolonged passage, freeze-thaw cycling and culture in serum-free media, highlights this cell source as an attractive proposition for future regenerative strategies, allowing for the culture of large numbers of cells which can be cryopreserved until required. It is of extreme interest, therefore, to homogeneously isolate and characterise each individual subpopulation, assessing its capacity to undertake lineage specific differentiation, with phenotype assaying suggesting the presence of cells capable of attaining a number of terminal lineages following

appropriate stimulation, thereby providing a potent clinical cell source for numerous applications.

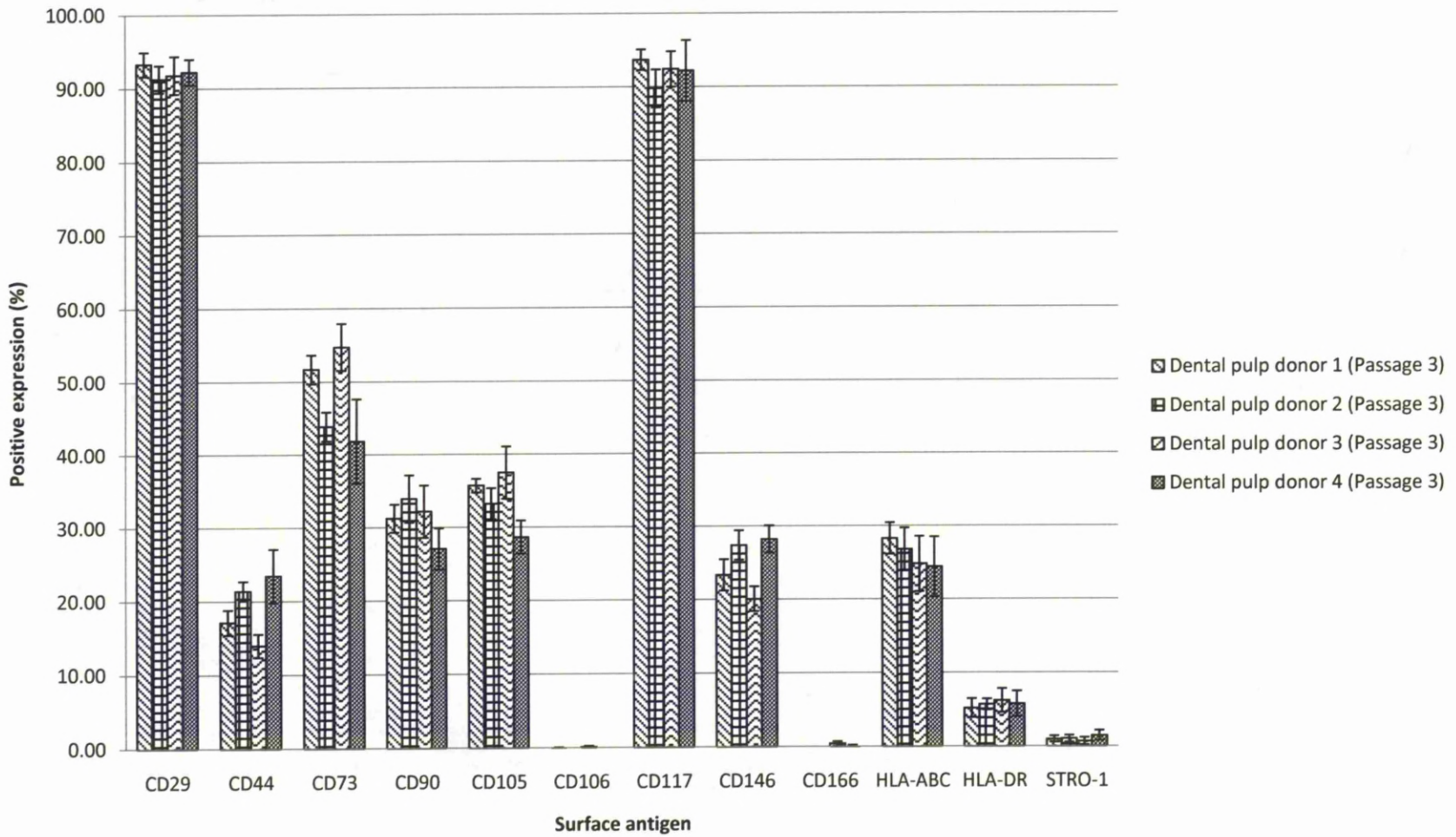

Figure 6.11 - **MSC-associated surface marker phenotyping of passage 3 dental pulp cells derived from donors 1-4 cultured in basal commercial media (0 x Freeze-Thaw cycles). Values represent mean positive expression as observed by flow cytometry (n = 4). Error bars correspond to Standard Deviations.**

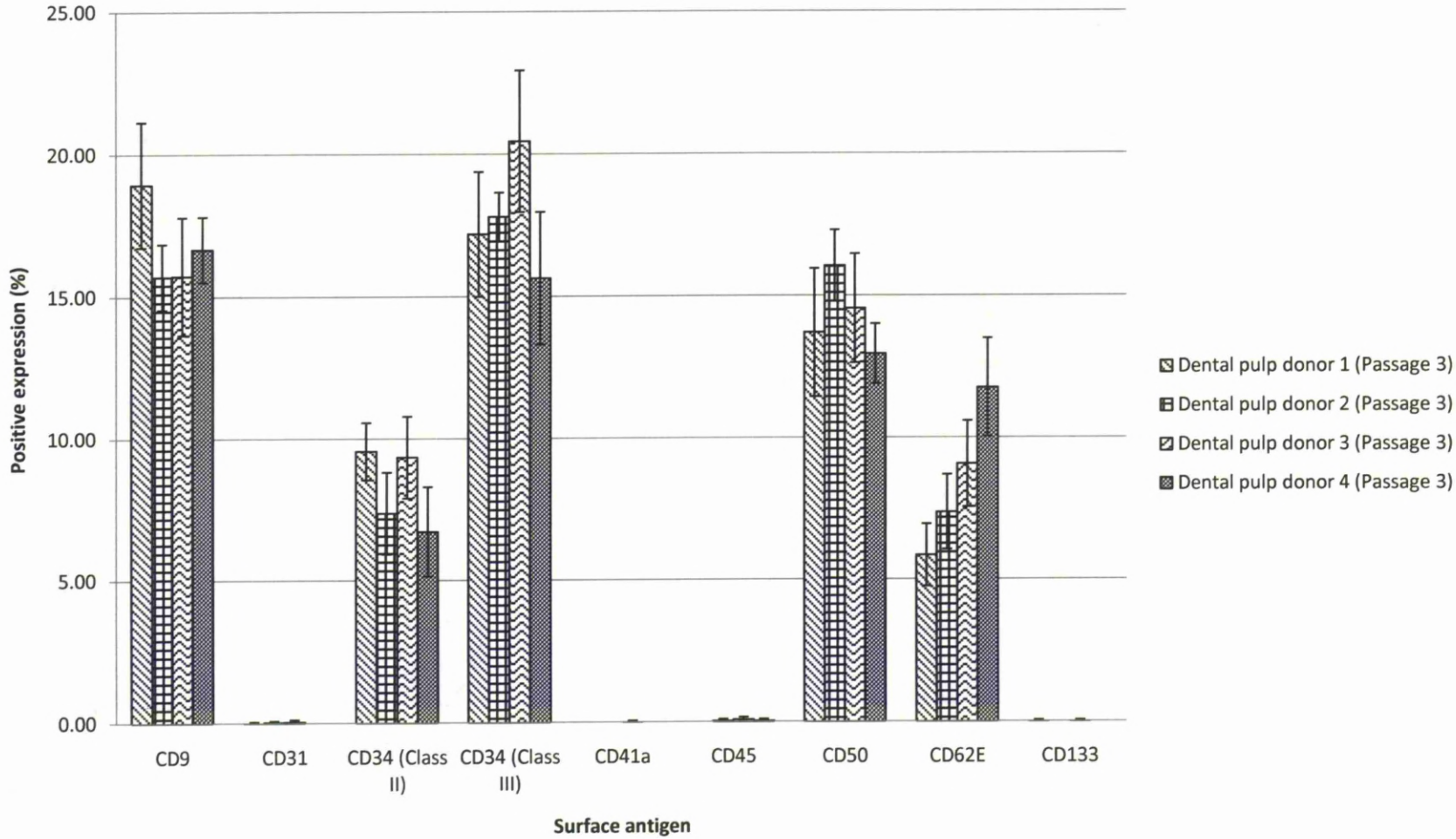

Figure 6.12 **- HSC and endothelial-associated surface marker phenotyping of passage 3 dental pulp cells derived from donors 1-4 cultured in basal commercial media (0 x Freeze-Thaw cycles). Values represent mean positive expression as observed by flow cytometry (n = 4). Error bars correspond to Standard Deviations.**

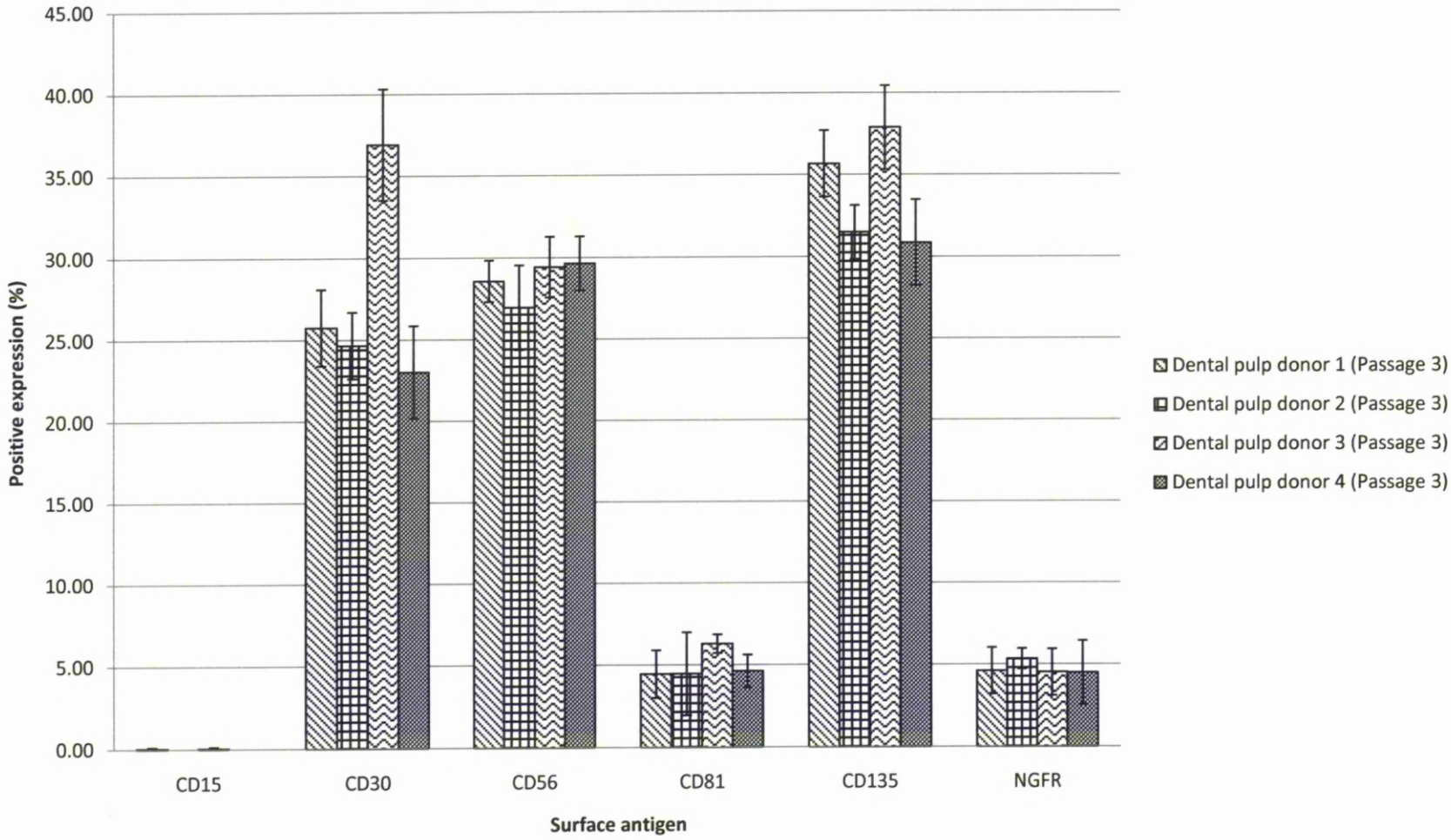

Figure 6.13 - **ES cell and Progenitor-associated surface marker phenotyping of passage 3 dental pulp cells cultured in basal commercial media derived from donors 1-4 (0 x Freeze-Thaw cycles). Values represent mean positive expression as observed by flow cytometry (n = 4). Error bars correspond to Standard Deviations.**

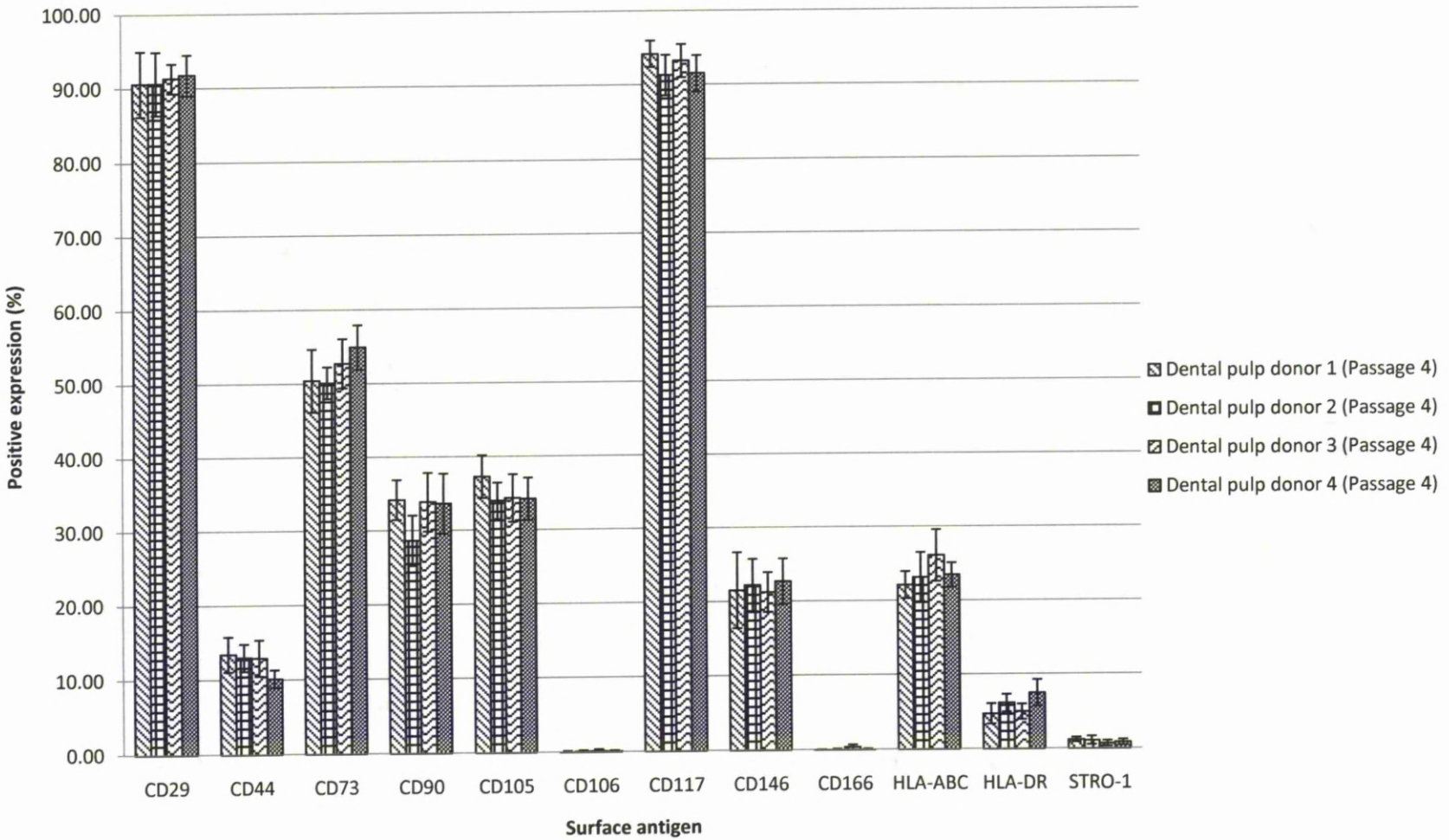

Figure 6.14 - **MSC-associated surface marker phenotyping of passage 4 dental pulp cells derived from donors 1-4 cultured in basal commercial media (0 x Freeze-Thaw cycles). Values represent mean positive expression as observed by flow cytometry (n = 4). Error bars correspond to Standard Deviations.**

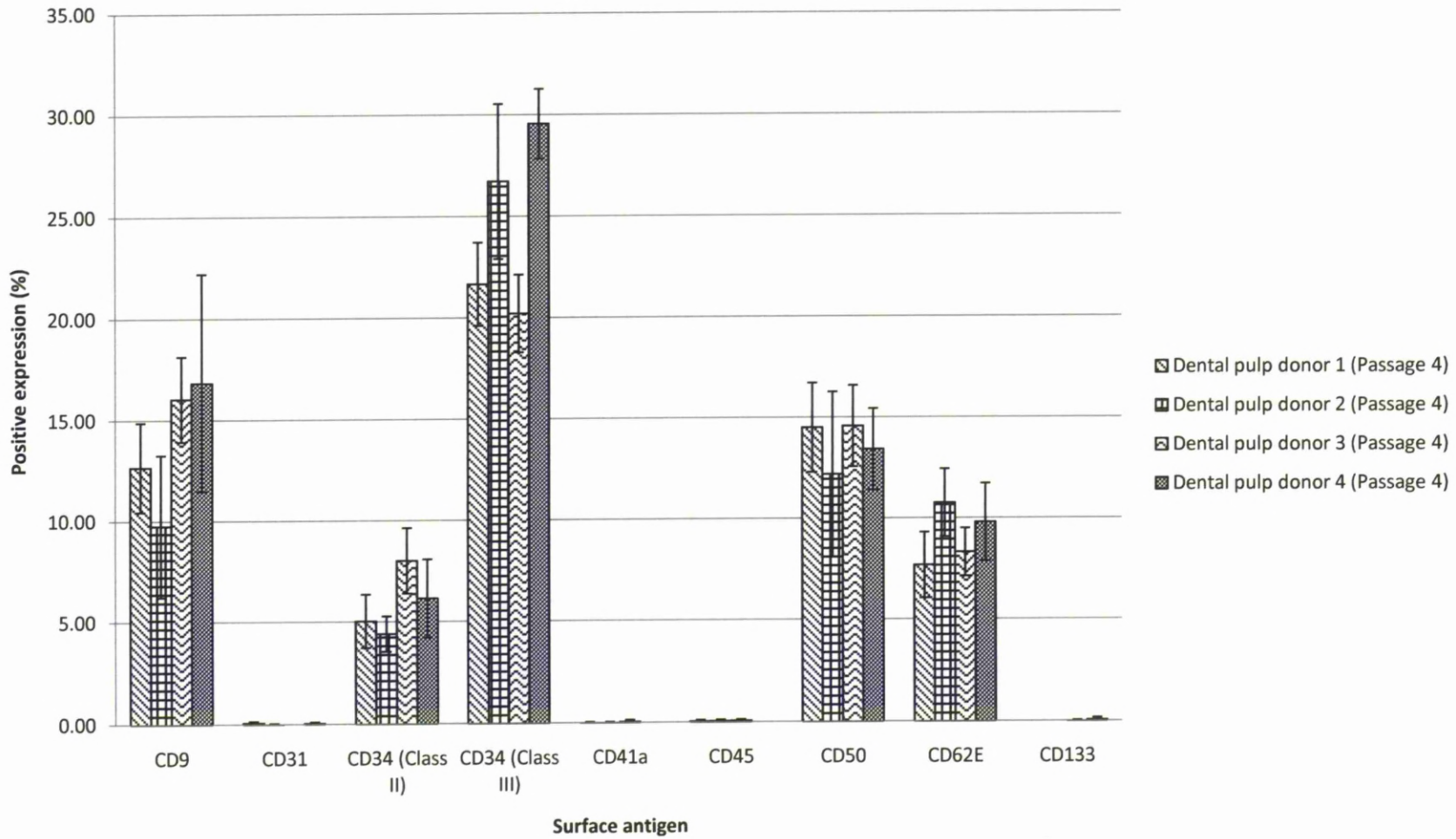

Figure 6.15 - **HSC and endothelial-associated surface marker phenotyping of passage 4 dental pulp cells derived from donors 1-4 cultured in basal commercial media (0 x Freeze-Thaw cycles). Values represent mean positive expression as observed by flow cytometry (n = 4). Error bars correspond to Standard Deviations.**

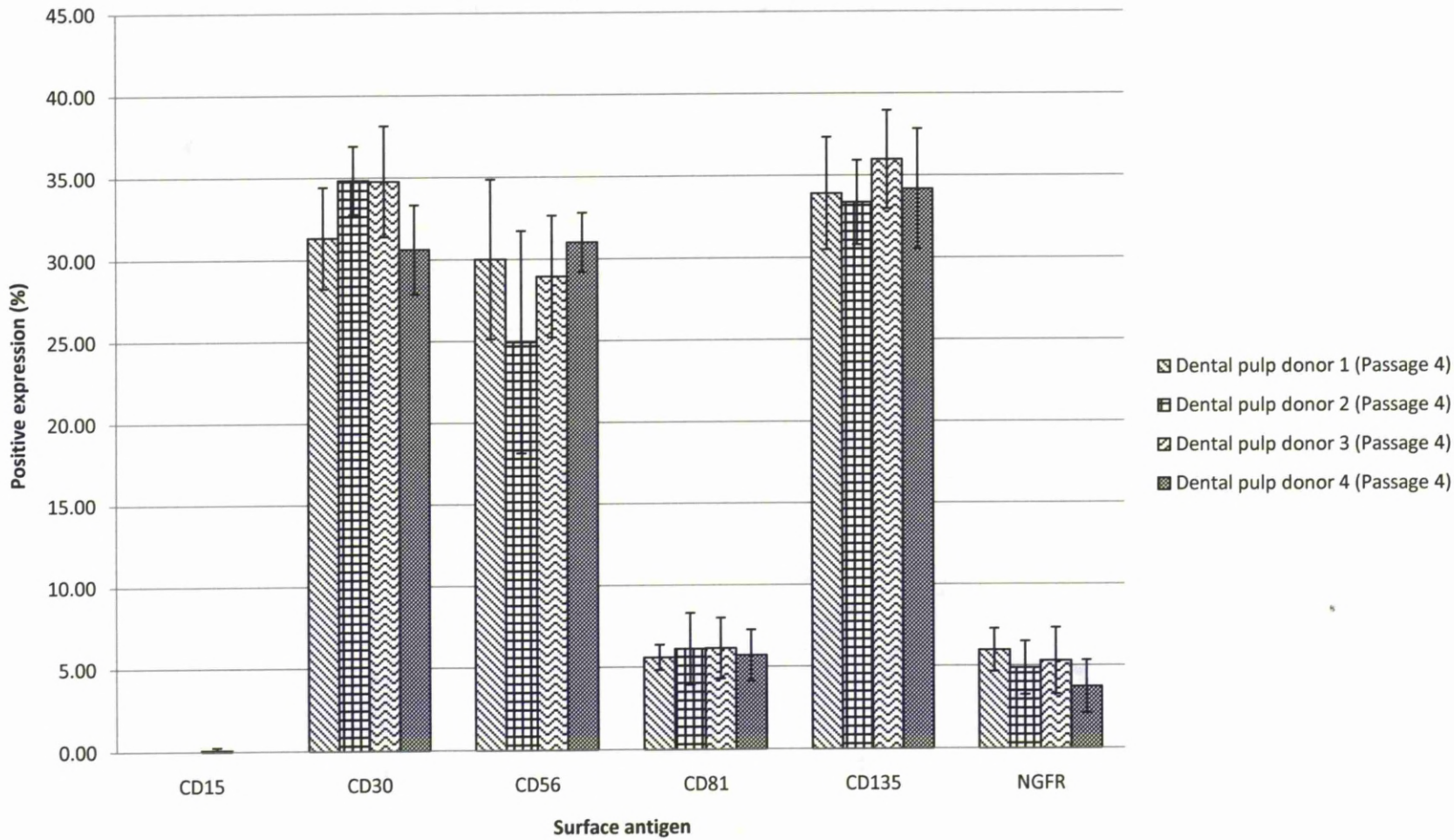

Figure 6.16 - **ES cell and Progenitor-associated surface marker phenotyping of passage 4 dental pulp cells derived from donors 1-4 cultured in basal commercial media (0 x Freeze-Thaw cycles). Values represent mean positive expression as observed by flow cytometry (n = 4). Error bars correspond to Standard Deviations.**

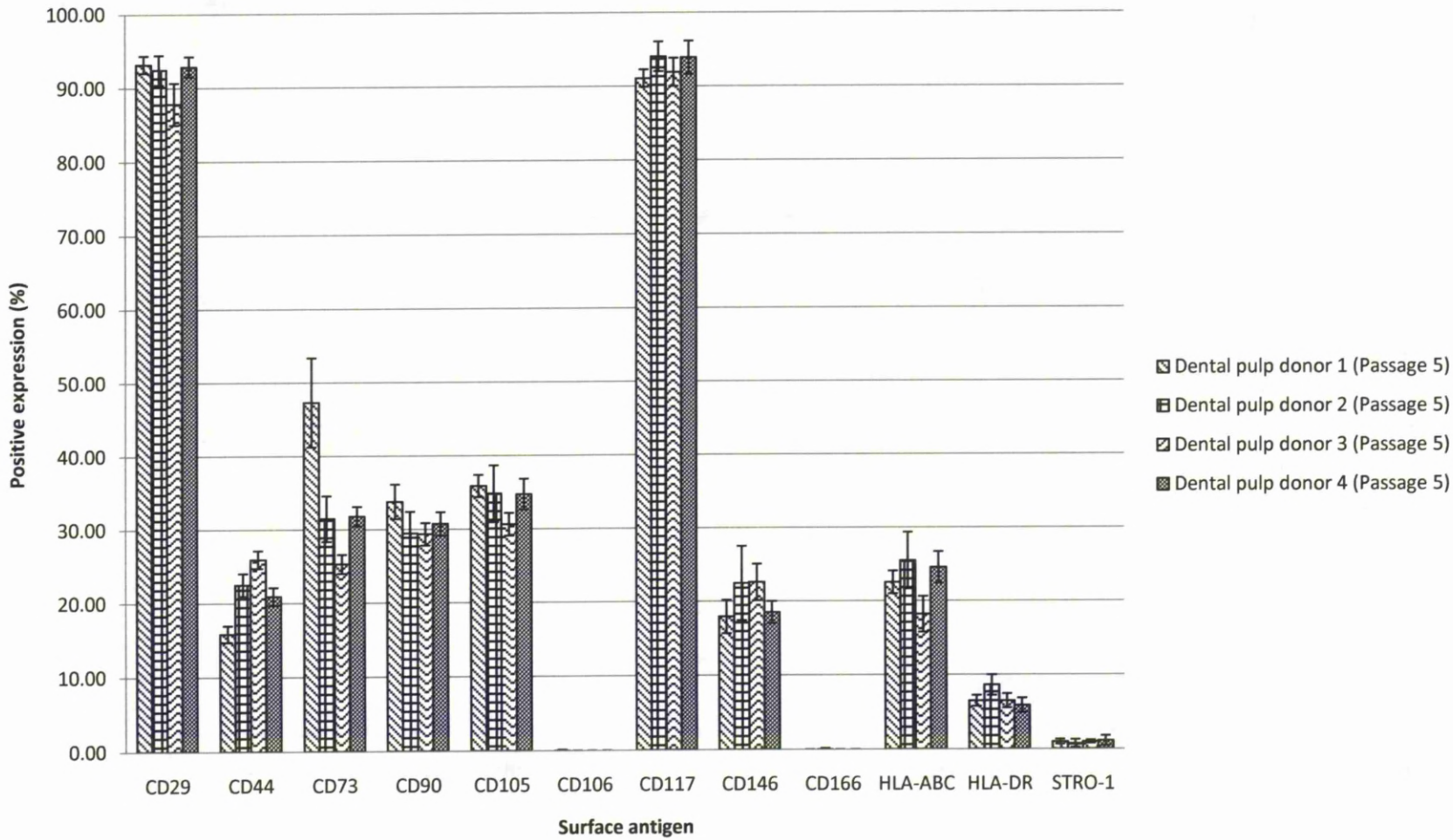

Figure 6.17 - **MSC-associated surface marker phenotyping of passage 5 dental pulp cells derived from donors 1-4 cultured in basal commercial media (0 x Freeze-Thaw cycles). Values represent mean positive expression as observed by flow cytometry (n = 4). Error bars correspond to Standard Deviations.**

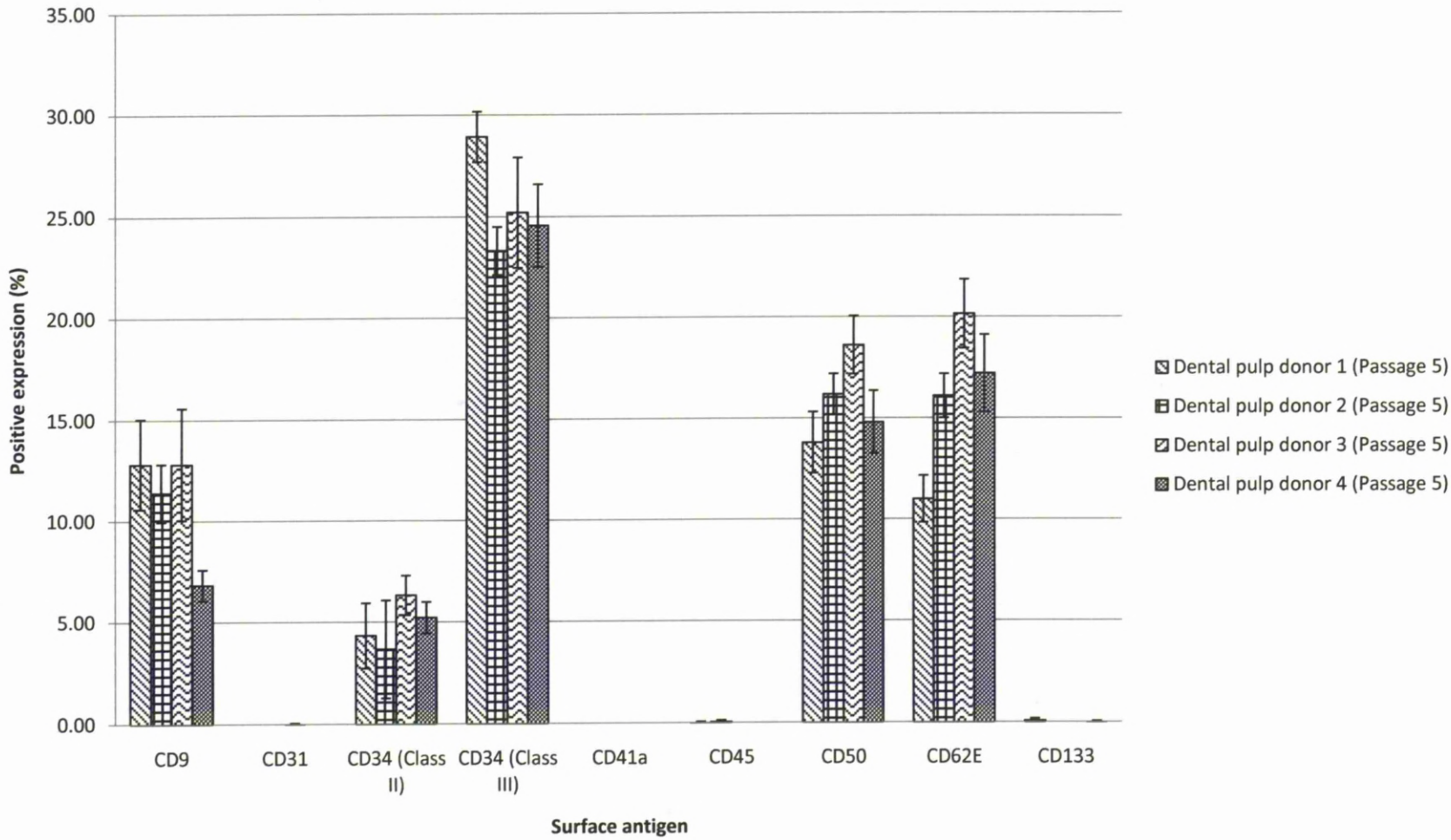

Figure 6.18 **- HSC and endothelial-associated surface marker phenotyping of passage 5 dental pulp cells derived from donors 1-4 cultured in basal commercial media (0 x Freeze-Thaw cycles). Values represent mean positive expression as observed by flow cytometry (n = 4). Error bars correspond to Standard Deviations.**

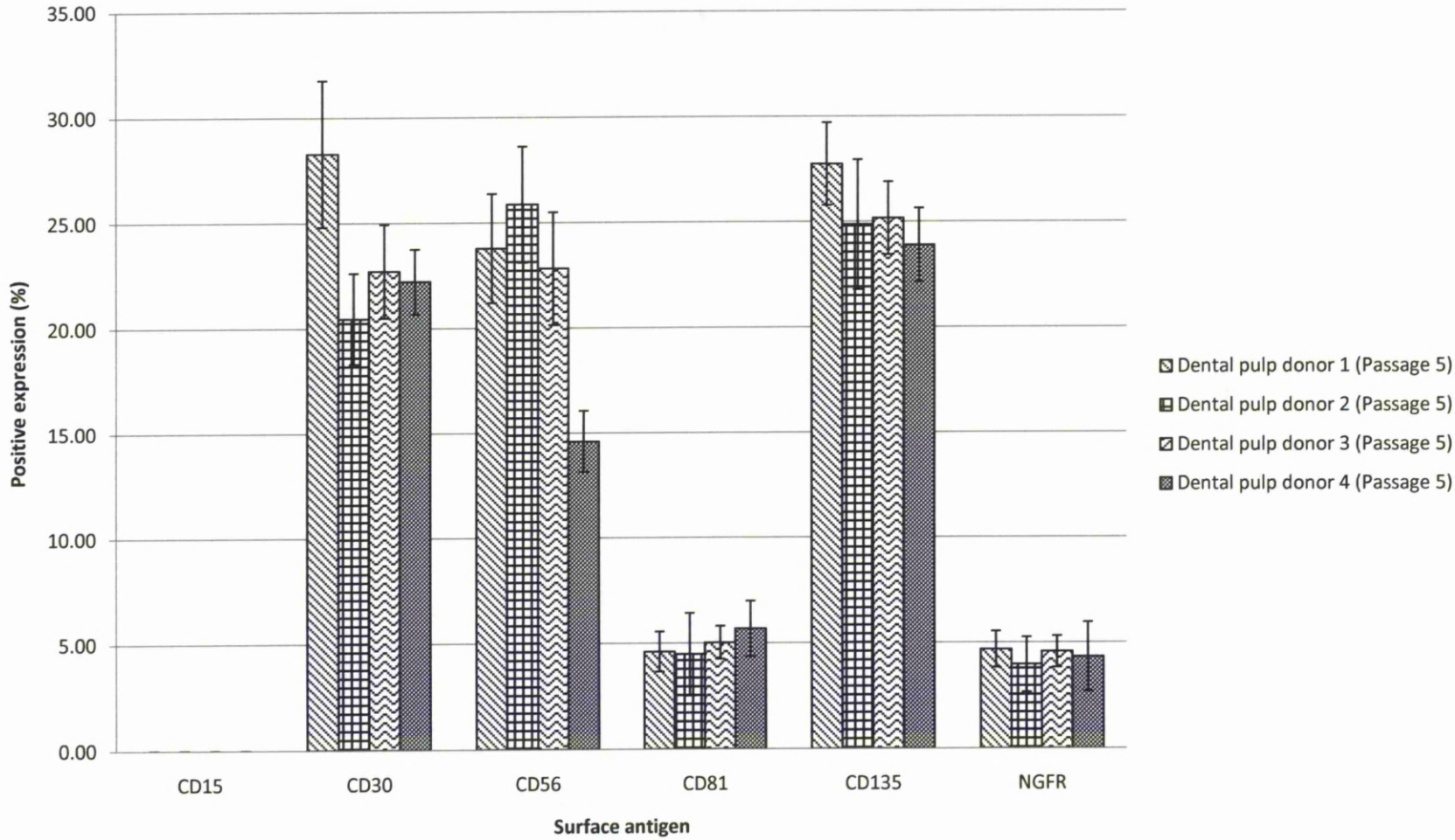

Figure 6.19 **- ES cell and Progenitor-associated surface marker phenotyping of passage 5 dental pulp cells derived from donors 1-4 cultured in basal commercial media (0 x Freeze-Thaw cycles). Values represent mean positive expression as observed by flow cytometry (n = 4). Error bars correspond to Standard Deviations.**

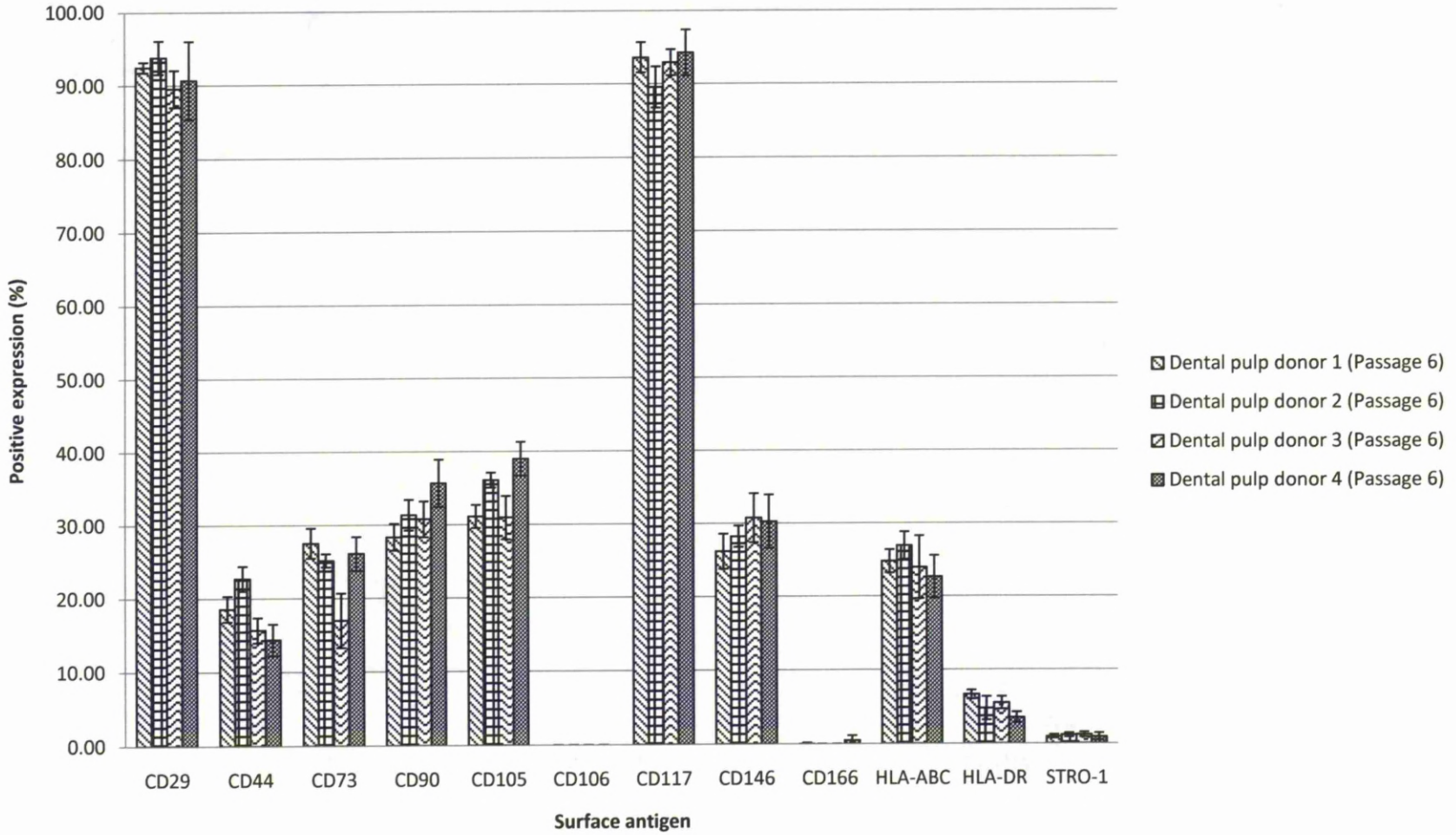

Figure 6.20 - **MSC-associated surface marker phenotyping of passage 6 dental pulp cells derived from donors 1-4 cultured in basal commercial media (0 x Freeze-Thaw cycles). Values represent mean positive expression as observed by flow cytometry (n = 4). Error bars correspond to Standard Deviations.**

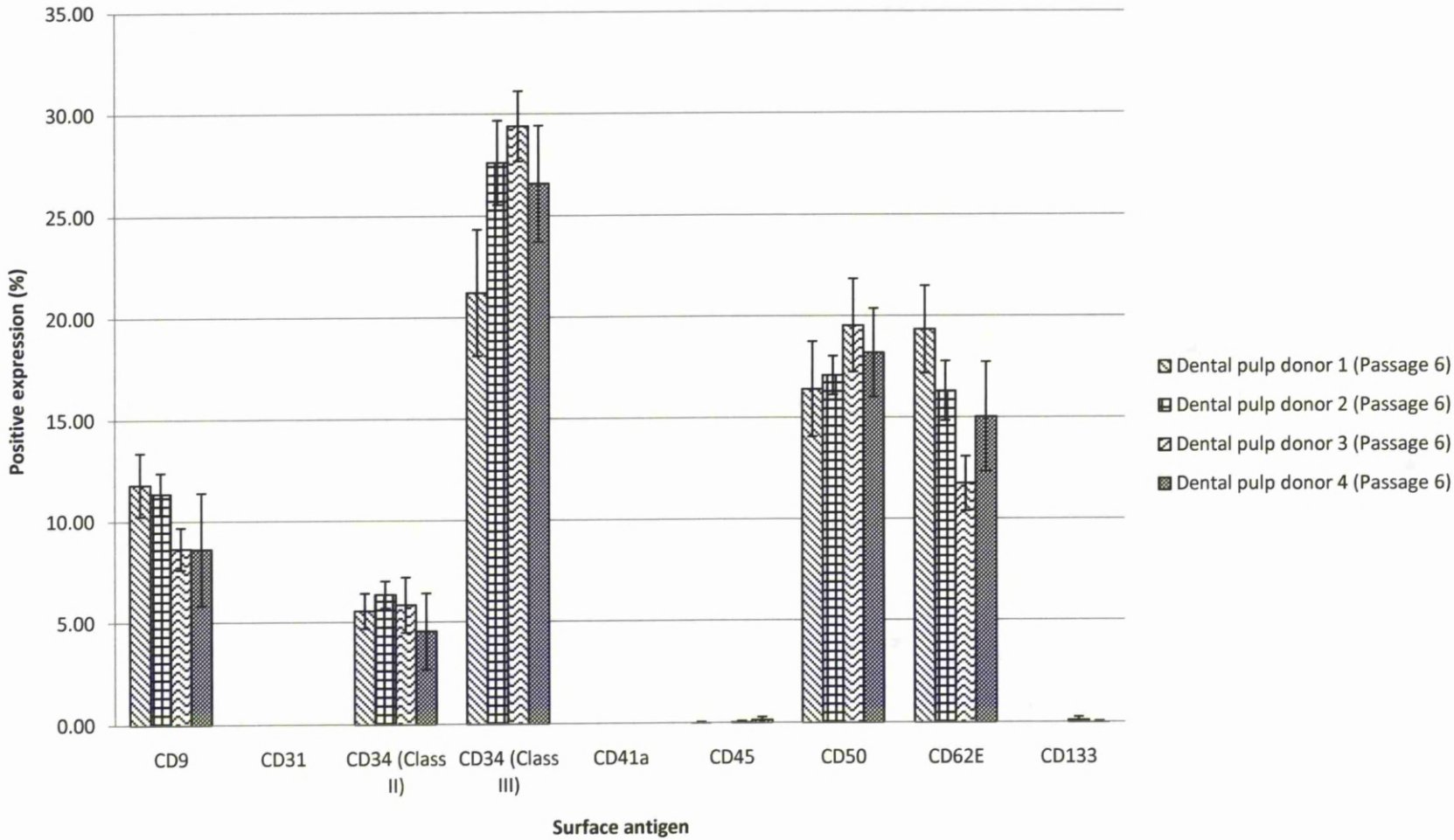

Figure 6.21 - **HSC and endothelial-associated surface marker phenotyping of passage 6 dental pulp cells derived from donors 1-4 cultured in basal commercial media (0 x Freeze-Thaw cycles). Values represent mean positive expression as observed by flow cytometry (n = 4). Error bars correspond to Standard Deviations.**

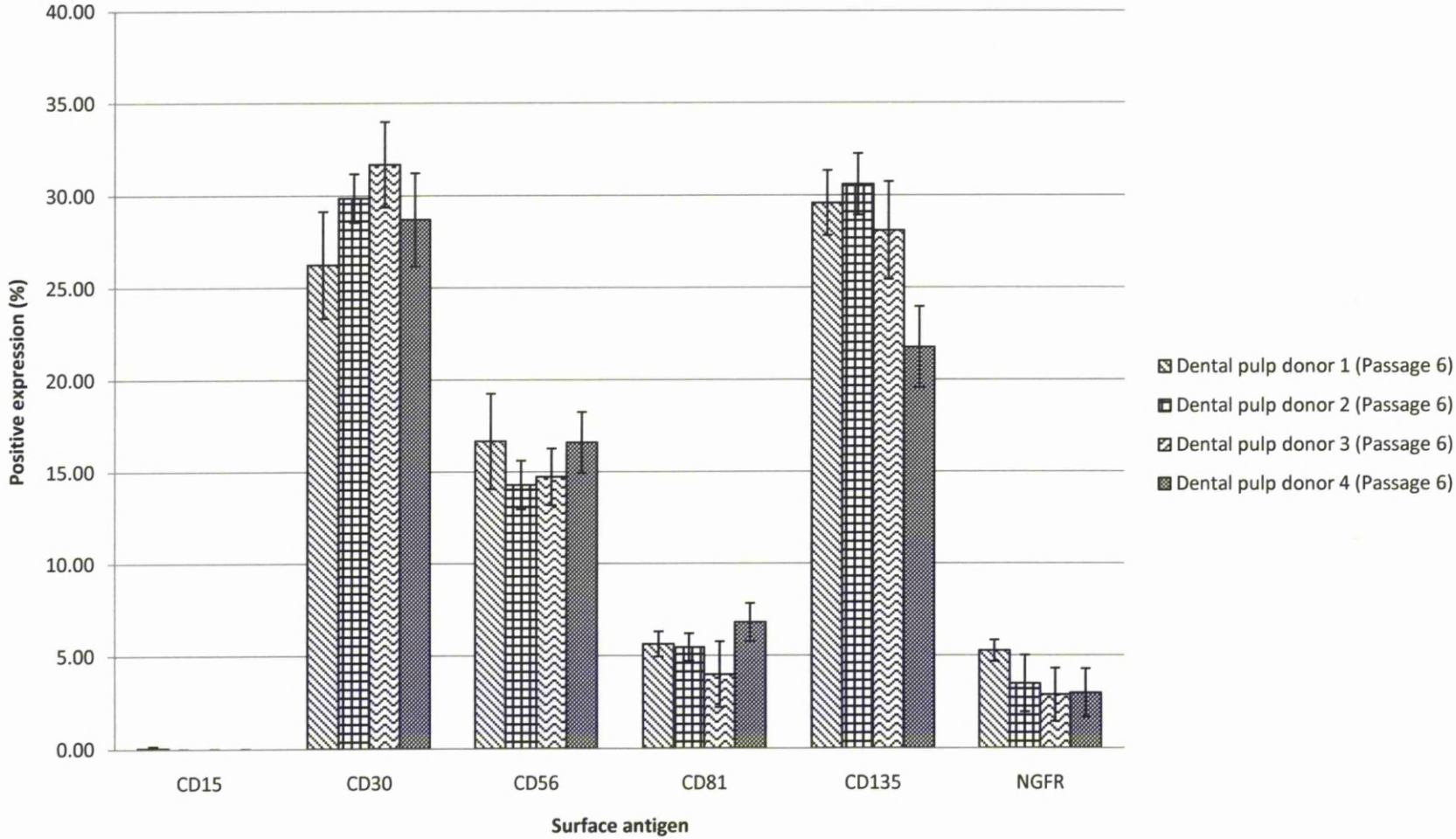

Figure 6.22 **- ES cell and Progenitor-associated surface marker phenotyping of passage 6 dental pulp cells derived from donors 1-4 cultured in basal commercial media (0 x Freeze-Thaw cycles). Values represent mean positive expression as observed by flow cytometry (n = 4). Error bars correspond to Standard Deviations.**

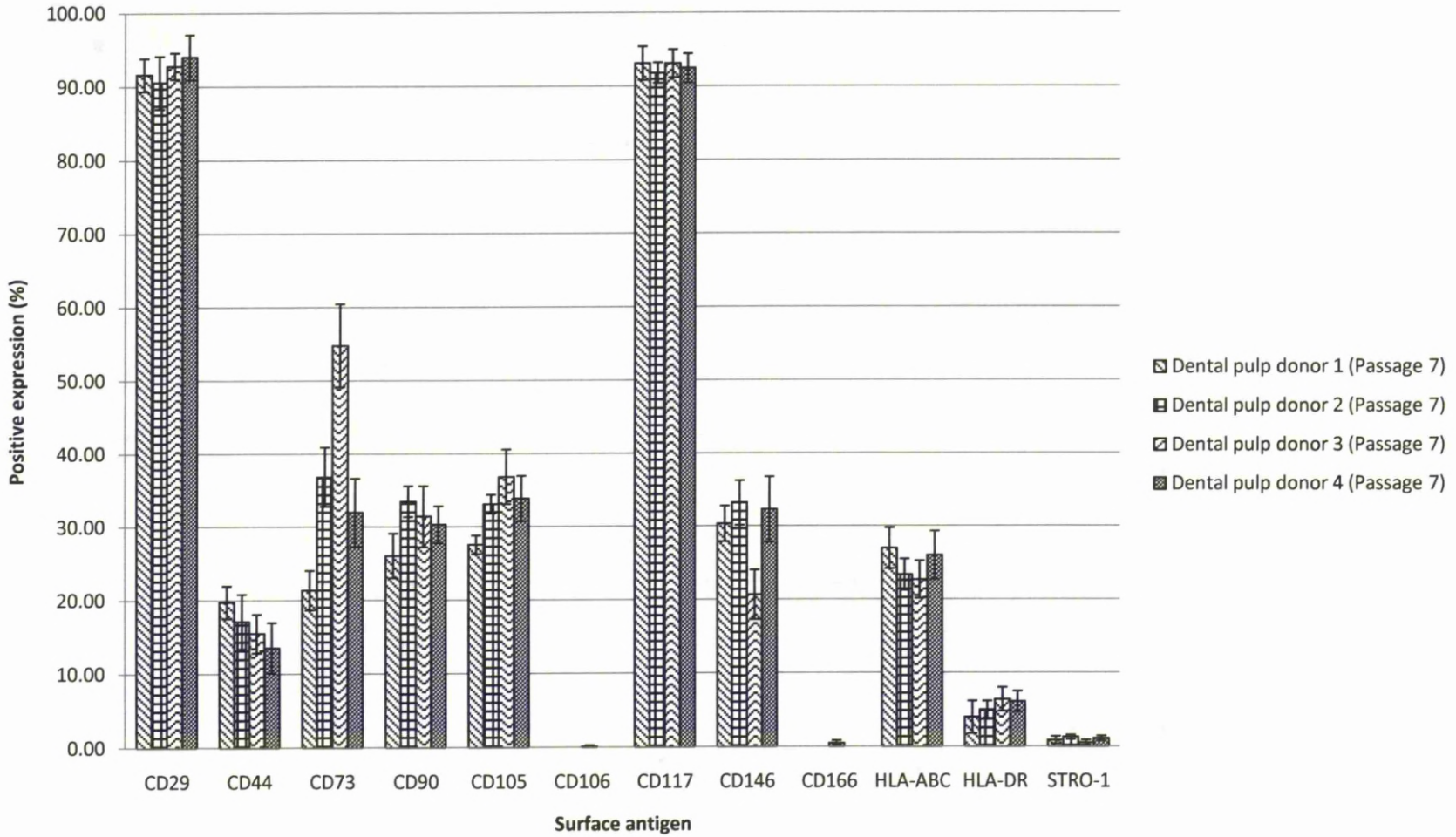

Figure 6.23 - **MSC-associated surface marker phenotyping of passage 7 dental pulp cells derived from donors 1 - 4 cultured in basal commercial media (0 x Freeze-Thaw cycles). Values represent mean positive expression as observed by flow cytometry (n = 4). Error bars correspond to Standard Deviations.**

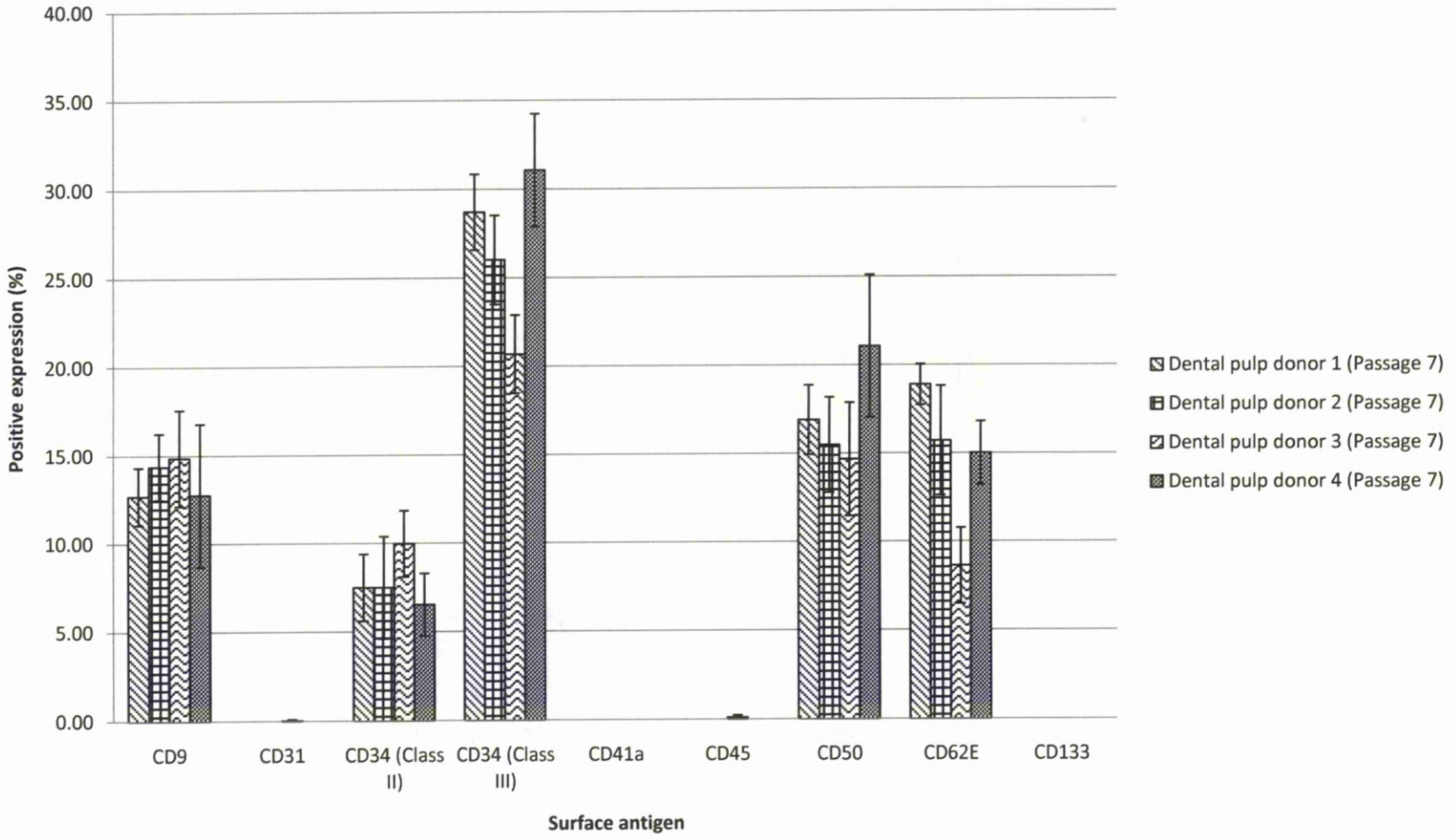

Figure 6.24 - **HSC and endothelial-associated surface marker phenotyping of passage 7 dental pulp cells derived from donors 1-4 cultured in basal commercial media (0 x Freeze-Thaw cycles). Values represent mean positive expression as observed by flow cytometry (n = 4). Error bars correspond to Standard Deviations.**

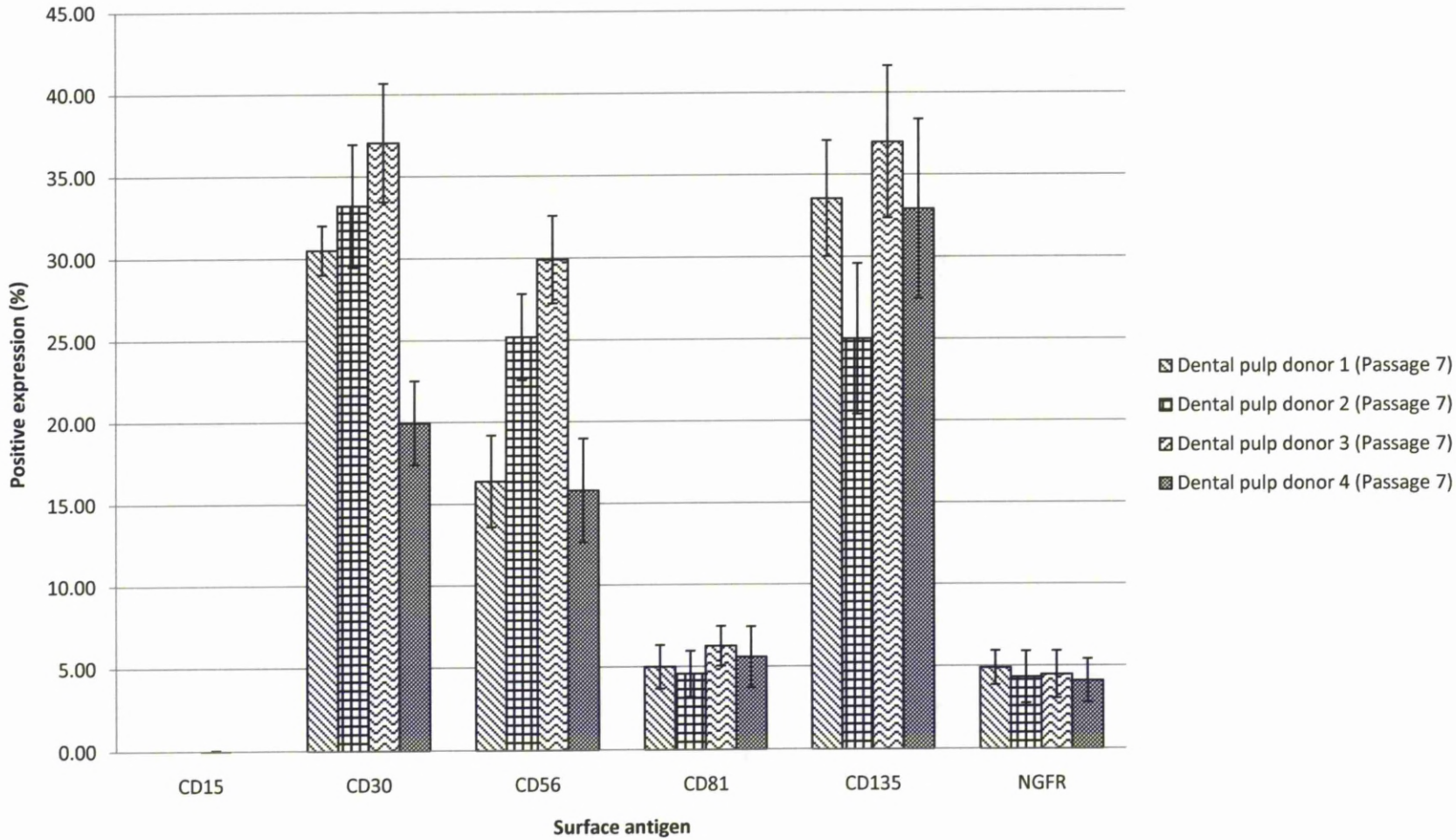

Figure 6.25 **- ES cell and Progenitor-associated surface marker phenotyping of passage 7 dental pulp cells derived from donors 1-4 cultured in basal commercial media (0 x Freeze-Thaw cycles). Values represent mean positive expression as observed by flow cytometry (n = 4). Error bars correspond to Standard Deviations.**

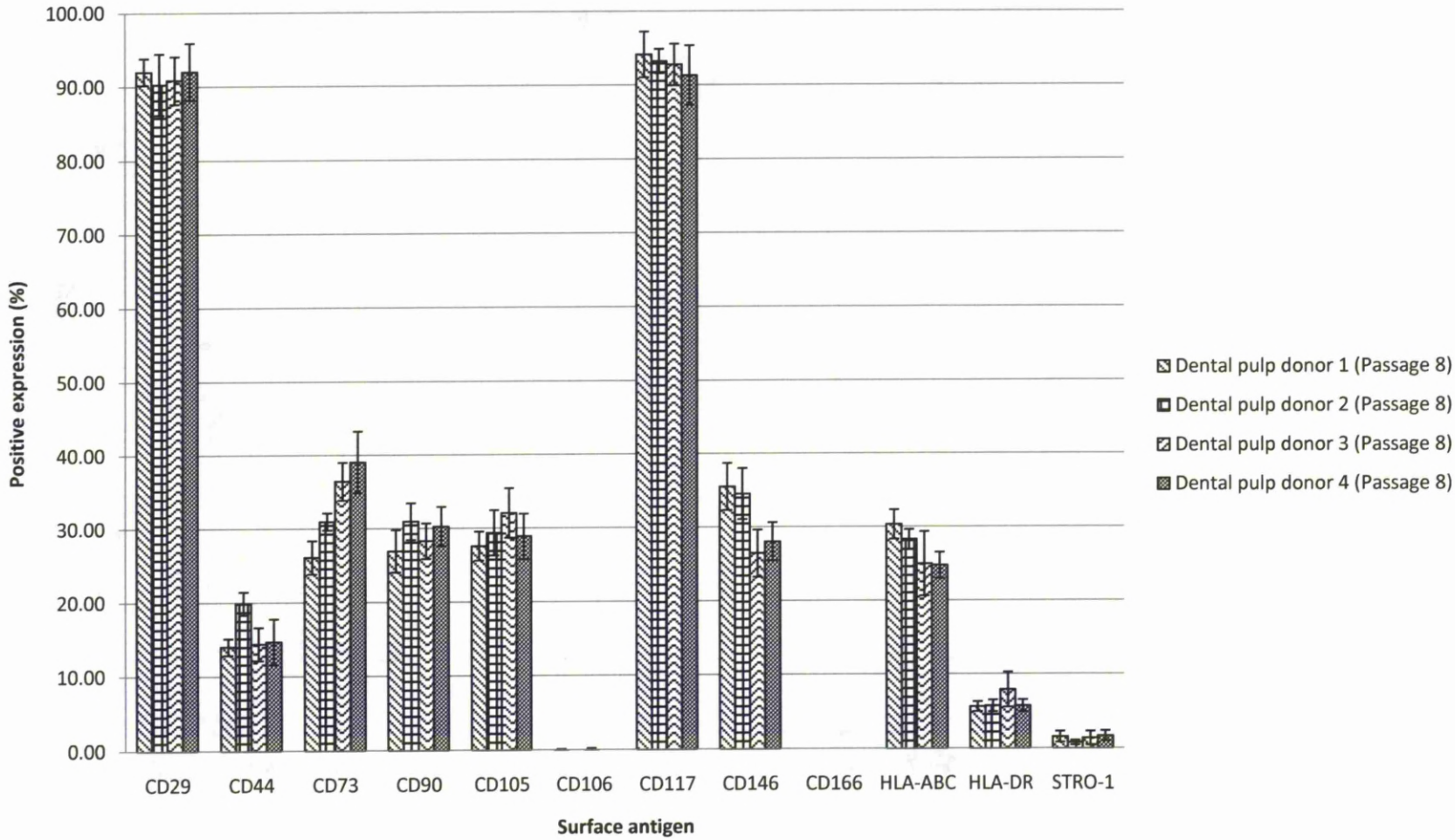

Figure 6.26 - **MSC-associated surface marker phenotyping of passage 8 dental pulp cells derived from donors 1-4 cultured in basal commercial media (0 x Freeze-Thaw cycles). Values represent mean positive expression as observed by flow cytometry (n = 4). Error bars correspond to Standard Deviations.**

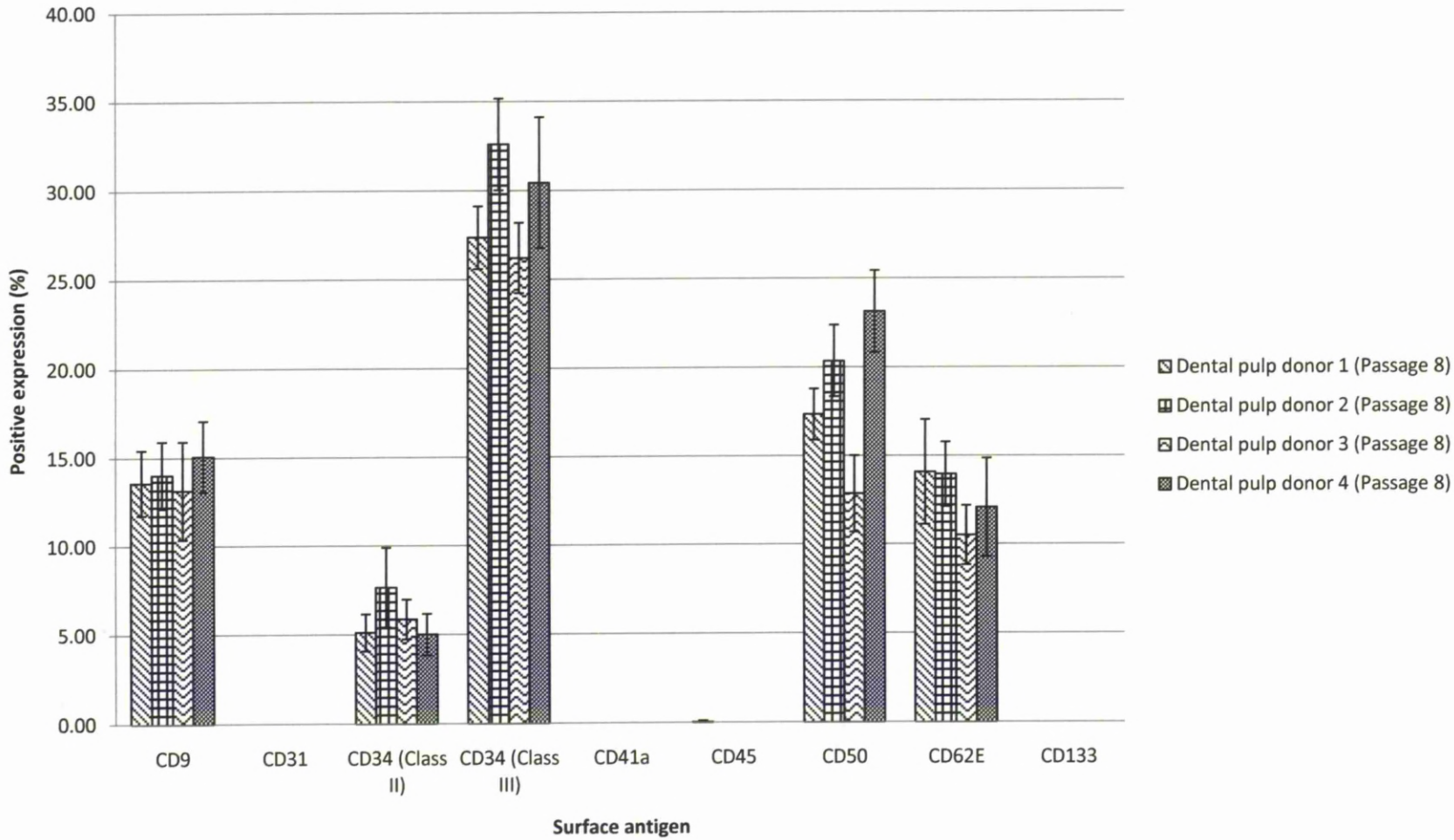

Figure 6.27 **- HSC and endothelial-associated surface marker phenotyping of passage 8 dental pulp cells derived from donors 1-4 cultured in basal commercial media (0 x Freeze-Thaw cycles). Values represent mean positive expression as observed by flow cytometry (n = 4). Error bars correspond to Standard Deviations.**

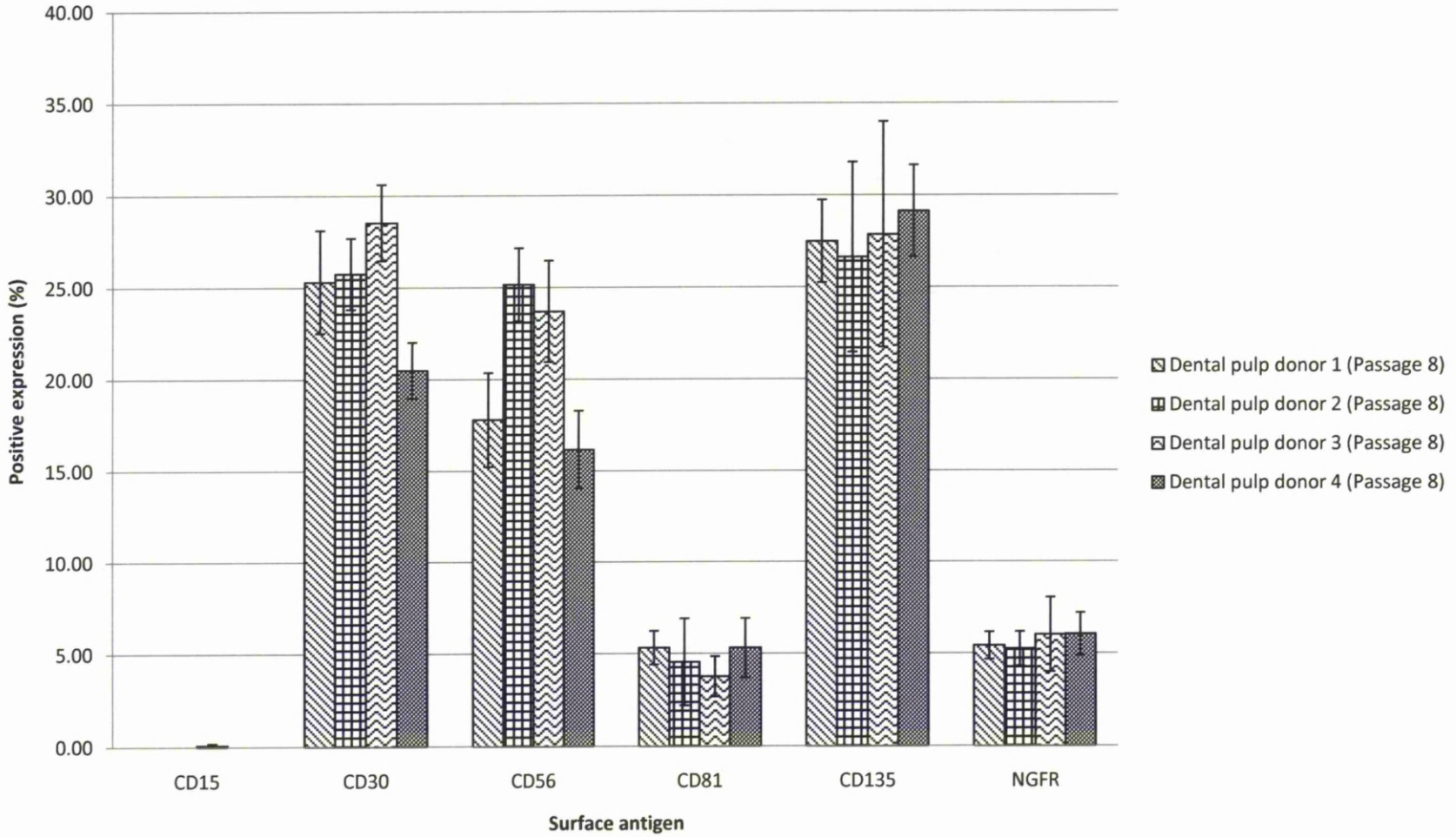

Figure 6.28 - **ES cell and Progenitor-associated surface marker phenotyping of passage 8 dental pulp cells derived from donors 1-4 cultured in basal commercial media (0 x Freeze-Thaw cycles). Values represent mean positive expression as observed by flow cytometry (n = 4). Error bars correspond to Standard Deviations.**

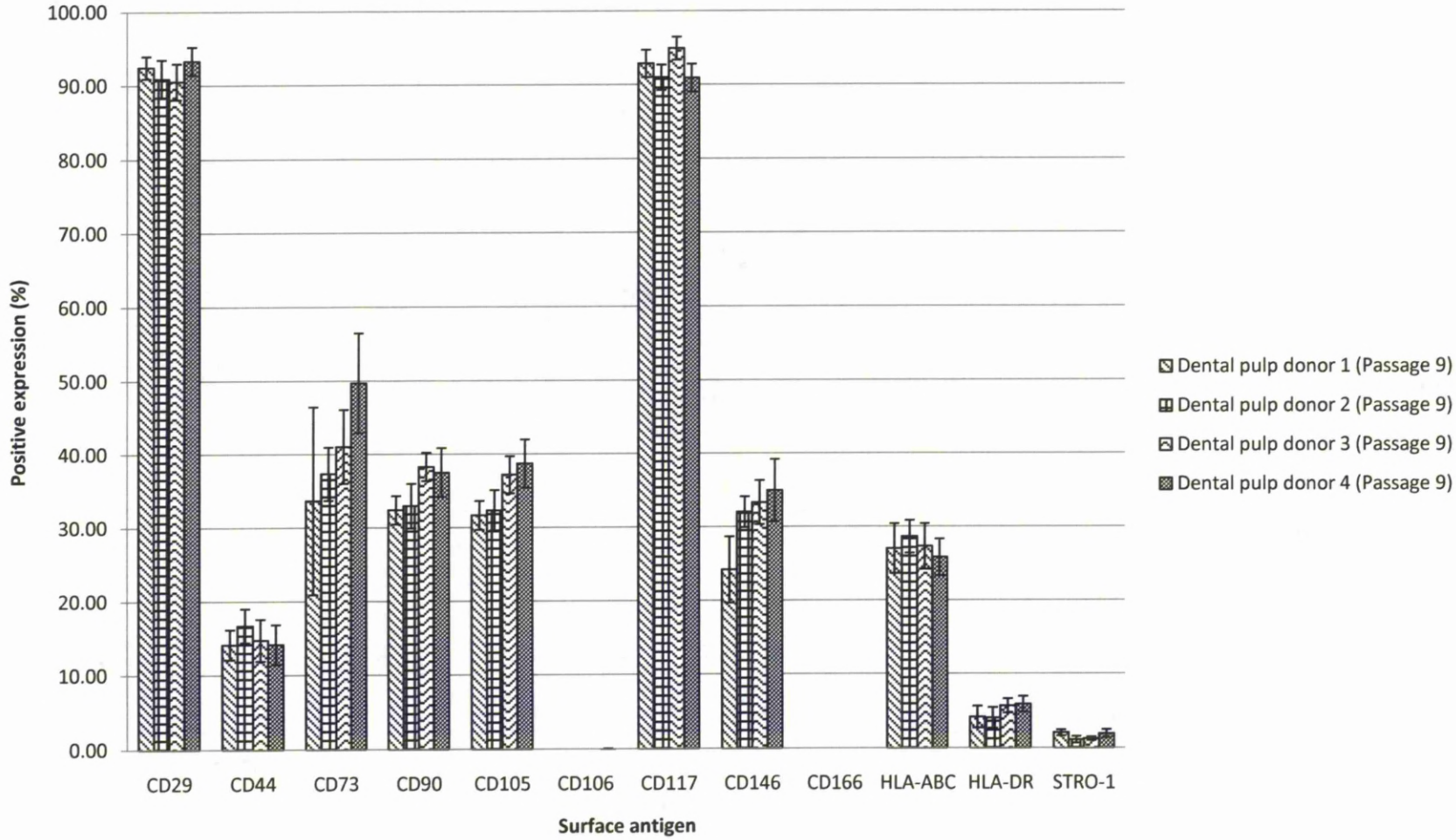

Figure 6.29 - **MSC-associated surface marker phenotyping of passage 9 dental pulp cells derived from donors 1-4 cultured in basal commercial media (0 x Freeze-Thaw cycles). Values represent mean positive expression as observed by flow cytometry (n = 4). Error bars correspond to Standard Deviations.**

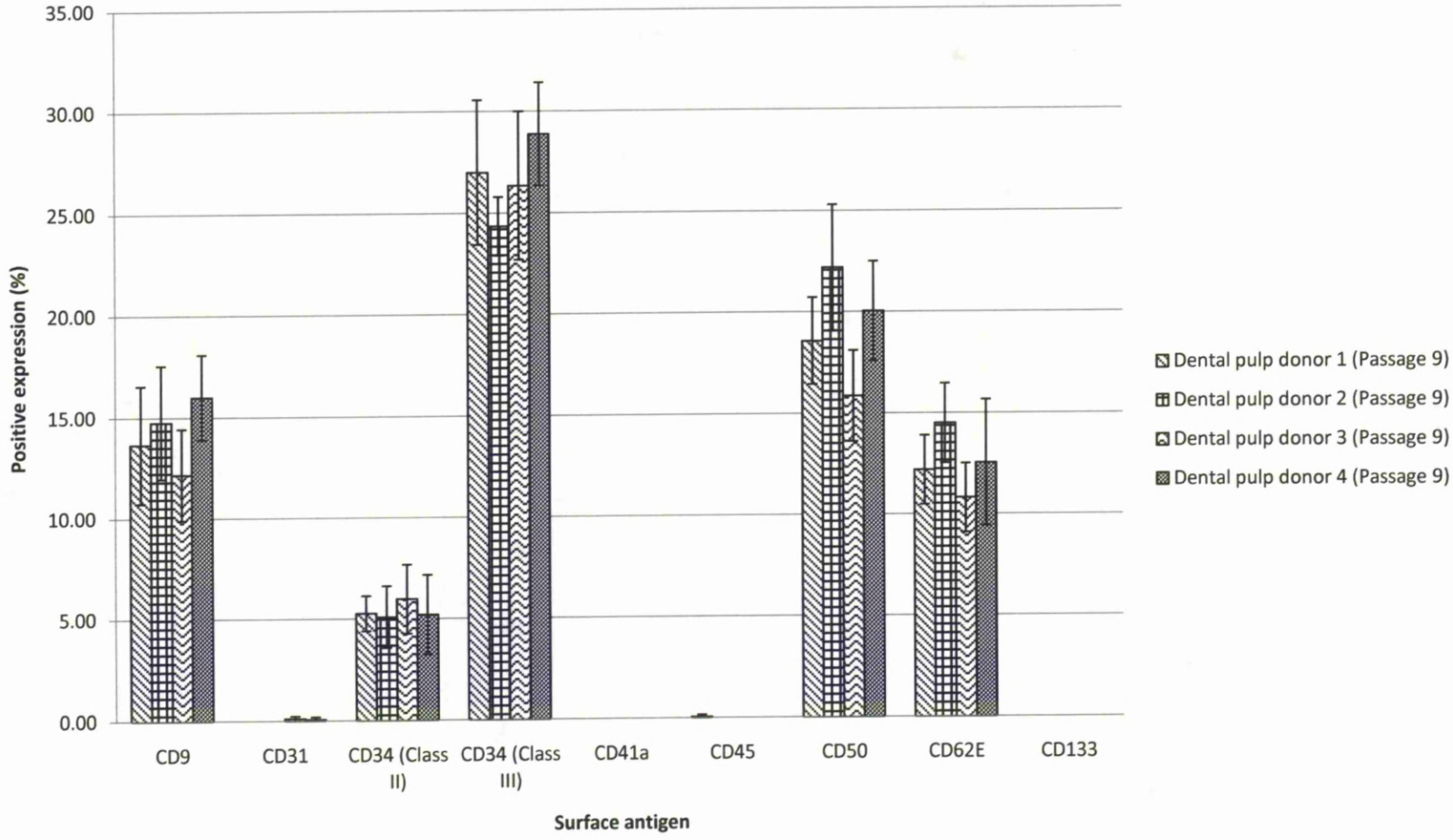

Figure 6.30 - **HSC and endothelial-associated surface marker phenotyping of passage 9 dental pulp cells derived from donors 1-4 cultured in basal commercial media (0 x Freeze-Thaw cycles). Values represent mean positive expression as observed by flow cytometry (n = 4). Error bars correspond to Standard Deviations.**

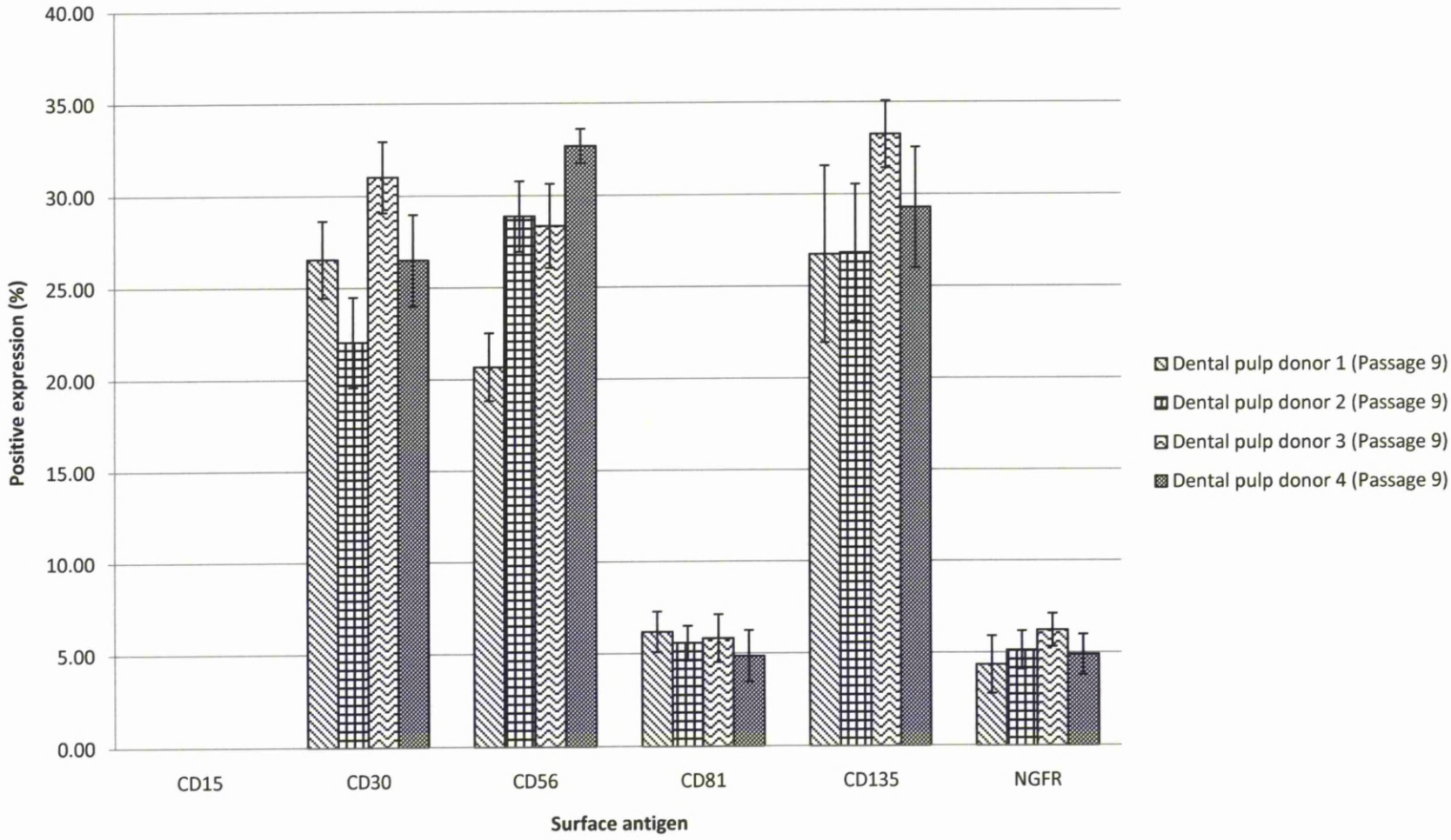

Figure 6.31 **- ES cell and Progenitor-associated surface marker phenotyping of passage 9 dental pulp cells derived from donors 1-4 cultured in basal commercial media (0 x Freeze-Thaw cycles). Values represent mean positive expression as observed by flow cytometry (n = 4). Error bars correspond to Standard Deviations.**

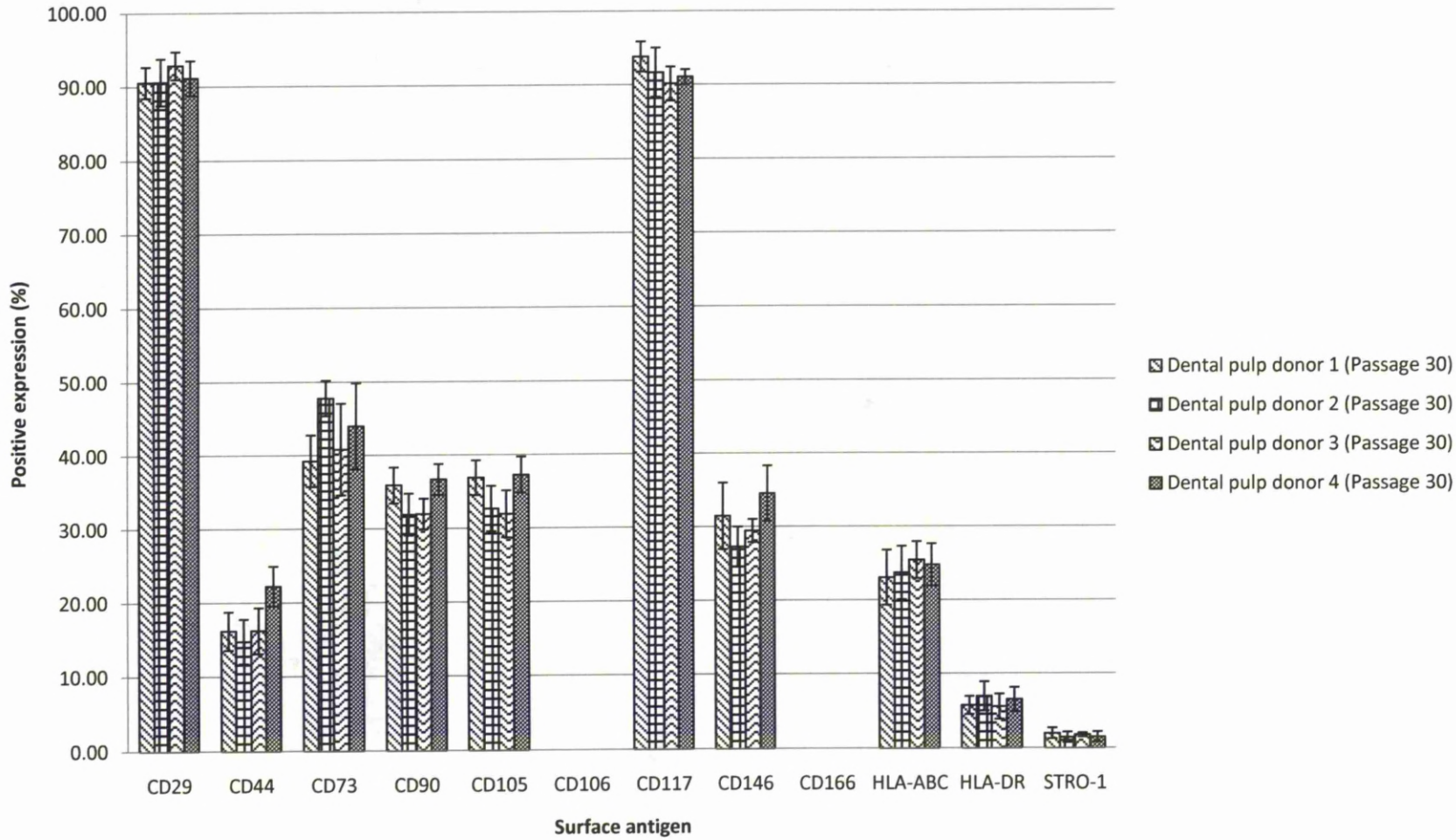

Figure 6.32 - **MSC-associated surface marker phenotyping of passage 30 dental pulp cells derived from donors 1-4 cultured in basal commercial media (0 x Freeze-Thaw cycles). Values represent mean positive expression as observed by flow cytometry (n = 4). Error bars correspond to Standard Deviations.**

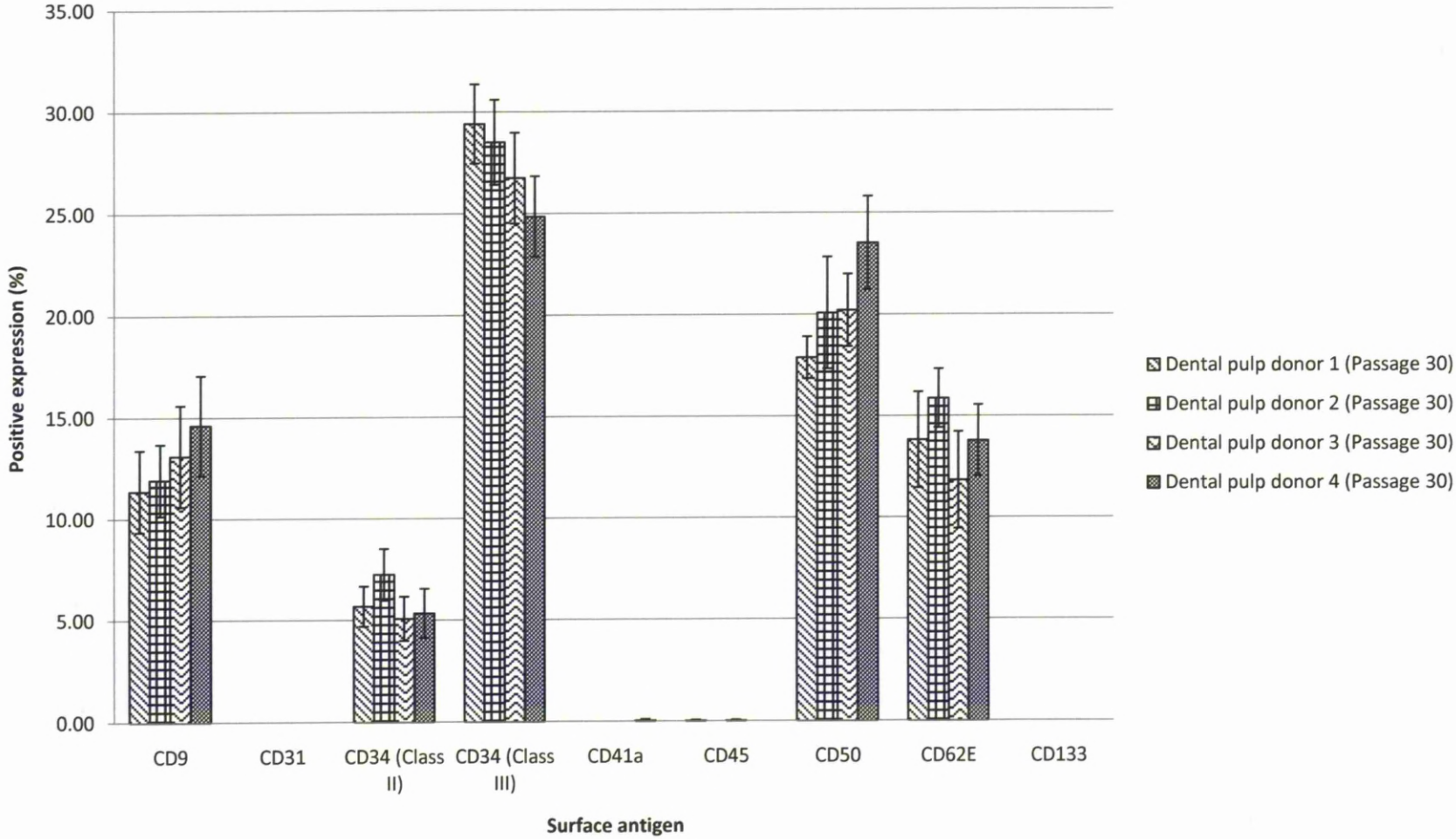

Figure 6.33 - **HSC and endothelial-associated surface marker phenotyping of passage 30 dental pulp cells derived from donors 1-4 cultured in basal commercial media (0 x Freeze-Thaw cycles). Values represent mean positive expression as observed by flow cytometry (n = 4). Error bars correspond to Standard Deviations.**

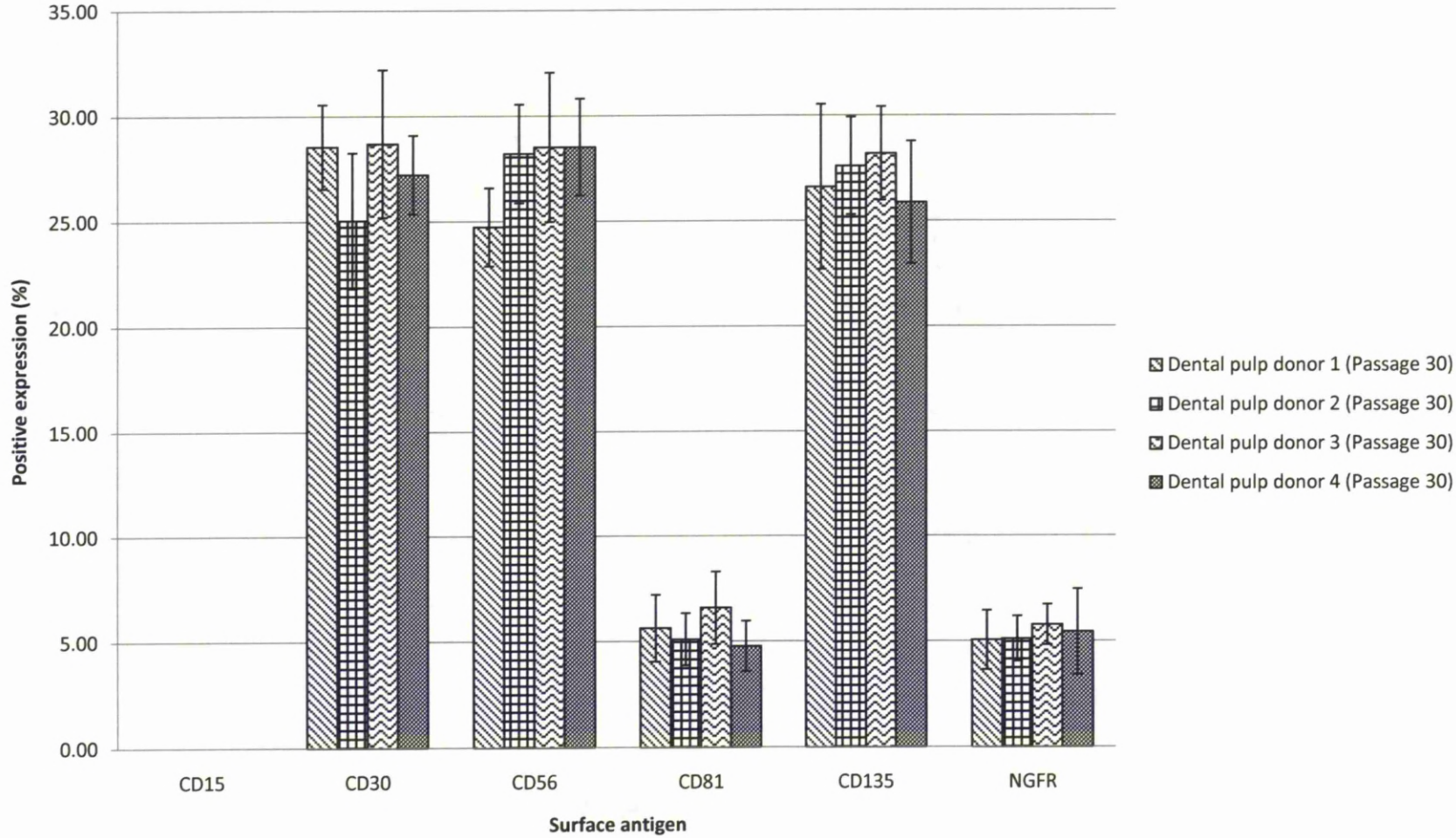

Figure 6.34 **- ES cell and Progenitor-associated surface marker phenotyping of passage 30 dental pulp cells derived from donors 1-4 cultured in basal commercial media (0 x Freeze-Thaw cycles). Values represent mean positive expression as observed by flow cytometry (n = 4). Error bars correspond to Standard Deviations.**

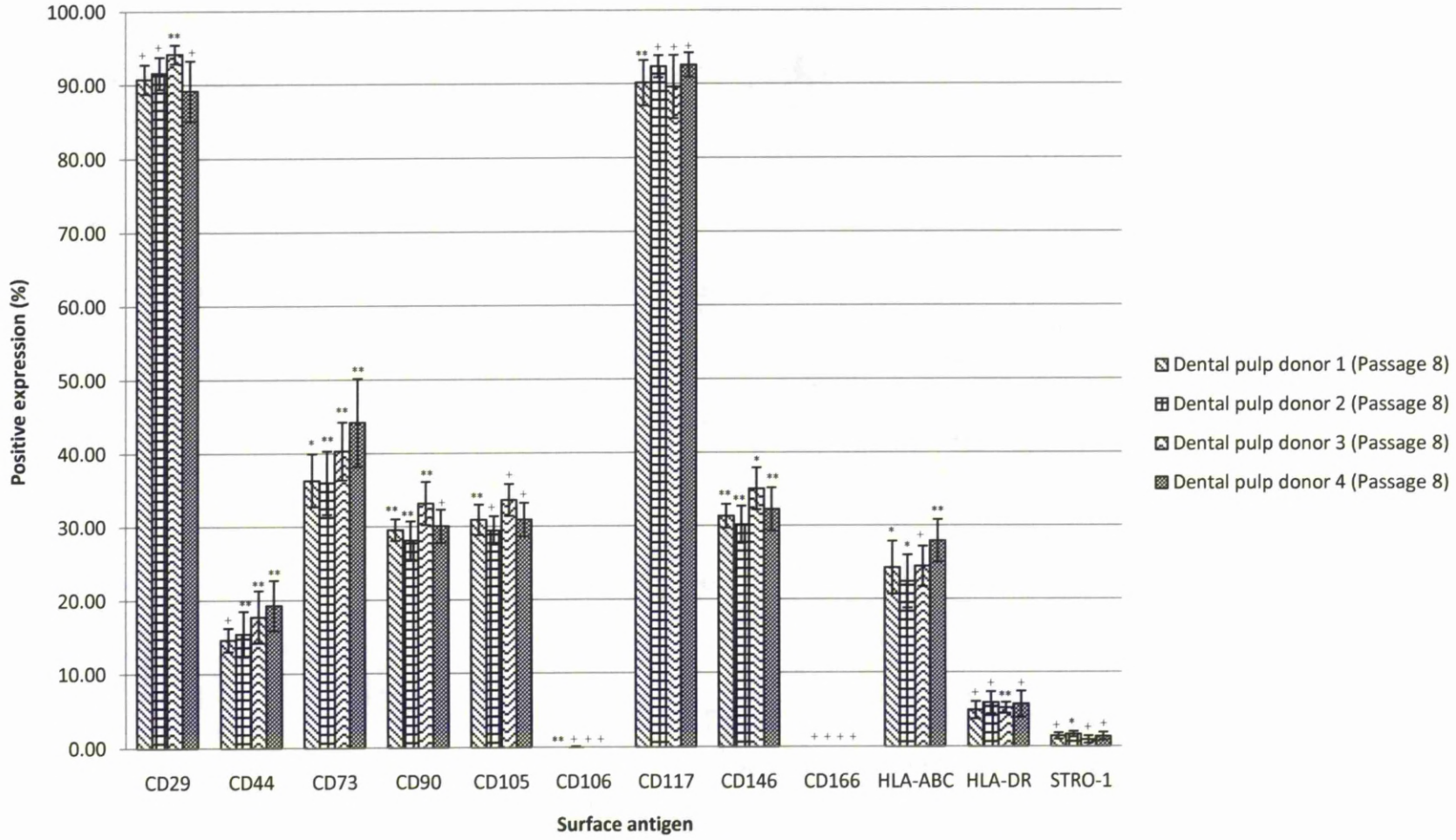

Figure 6.35 **- MSC-associated surface marker phenotyping of passage 8 dental pulp cells derived from donors 1-4 cultured in basal commercial media (1 x Freeze-Thaw cycles). Values represent mean positive expression as observed by flow cytometry (n = 4). Error bars correspond to Standard Deviations. Student *t*-test indicated that there were significant (*$p \leq 0.001$) (**$p \leq 0.05$) and non-significant (+$p \geq 0.05$) antigen expression differences when comparing passage 8 cells from each donor which have undergone 1 freeze-thaw cycle with those which have not been freeze-thawed (*Figure 6.26*, Page 209).**

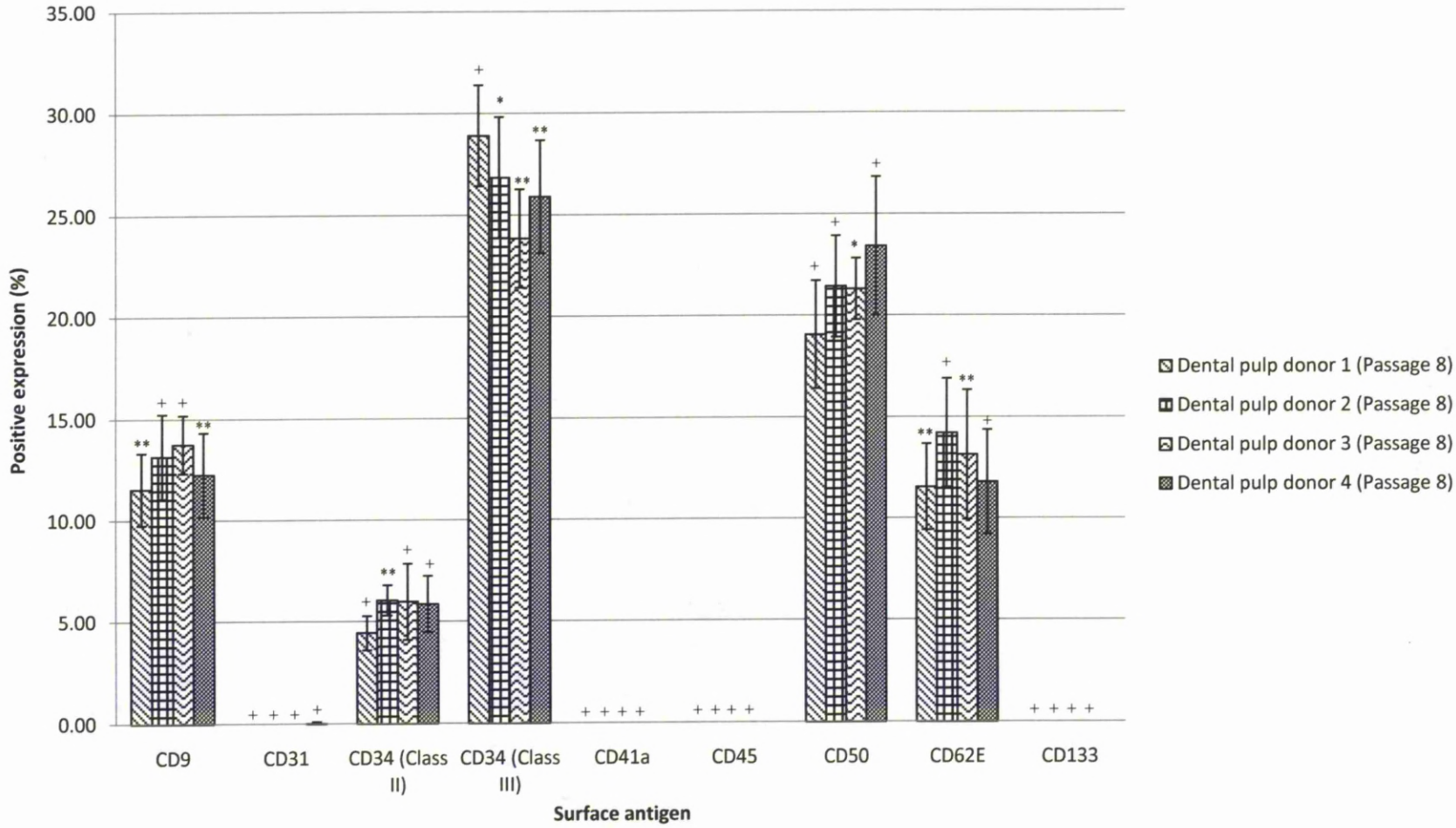

Figure 6.36 **- HSC and endothelial-associated surface marker phenotyping of passage 8 dental pulp cells derived from donors 1-4 cultured in basal commercial media (1 x Freeze-Thaw cycles). Values represent mean positive expression as observed by flow cytometry (n = 4). Error bars correspond to Standard Deviations. Student *t*-test indicated that there were significant (*$p \leq 0.001$) (**$p \leq 0.05$) and non-significant (+$p \geq 0.05$) antigen expression differences when comparing passage 8 cells from each donor which have undergone 1 freeze-thaw cycle with those which have not been freeze-thawed (*Figure 6.27*, Page 210).**

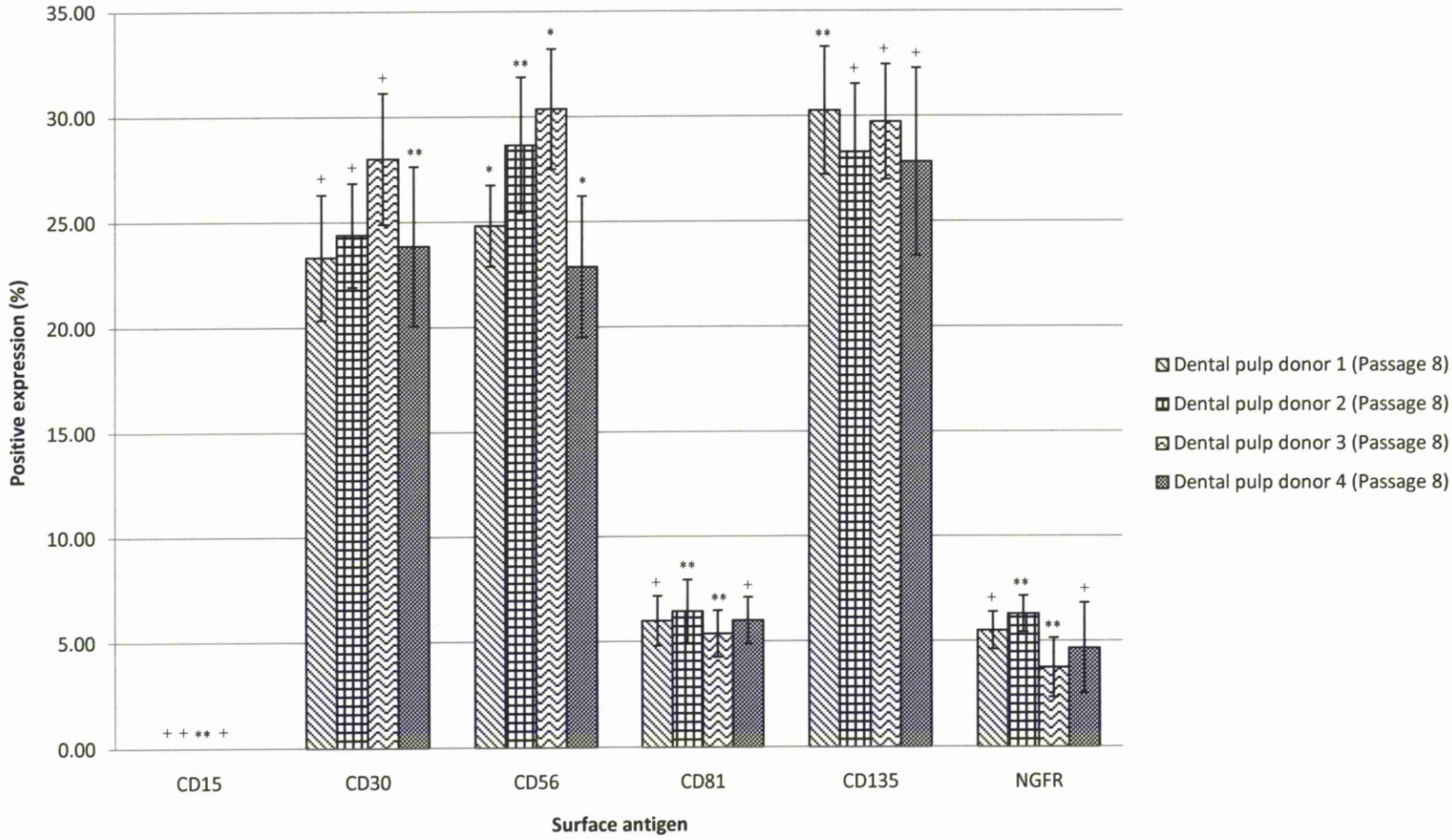

Figure 6.37 **- ES cell and Progenitor-associated surface marker phenotyping of passage 8 dental pulp cells derived from donors 1-4 cultured in basal commercial media (1 x Freeze-Thaw cycles). Values represent mean positive expression as observed by flow cytometry (n = 4). Error bars correspond to Standard Deviations. Student *t*-test indicated that there were significant (*$p \leq 0.001$) (**$p \leq 0.05$) and non-significant (+$p \geq 0.05$) antigen expression differences when comparing passage 8 cells from each donor which have undergone 1 freeze-thaw cycle with those which have not been freeze-thawed (*Figure 6.28*, Page 211).**

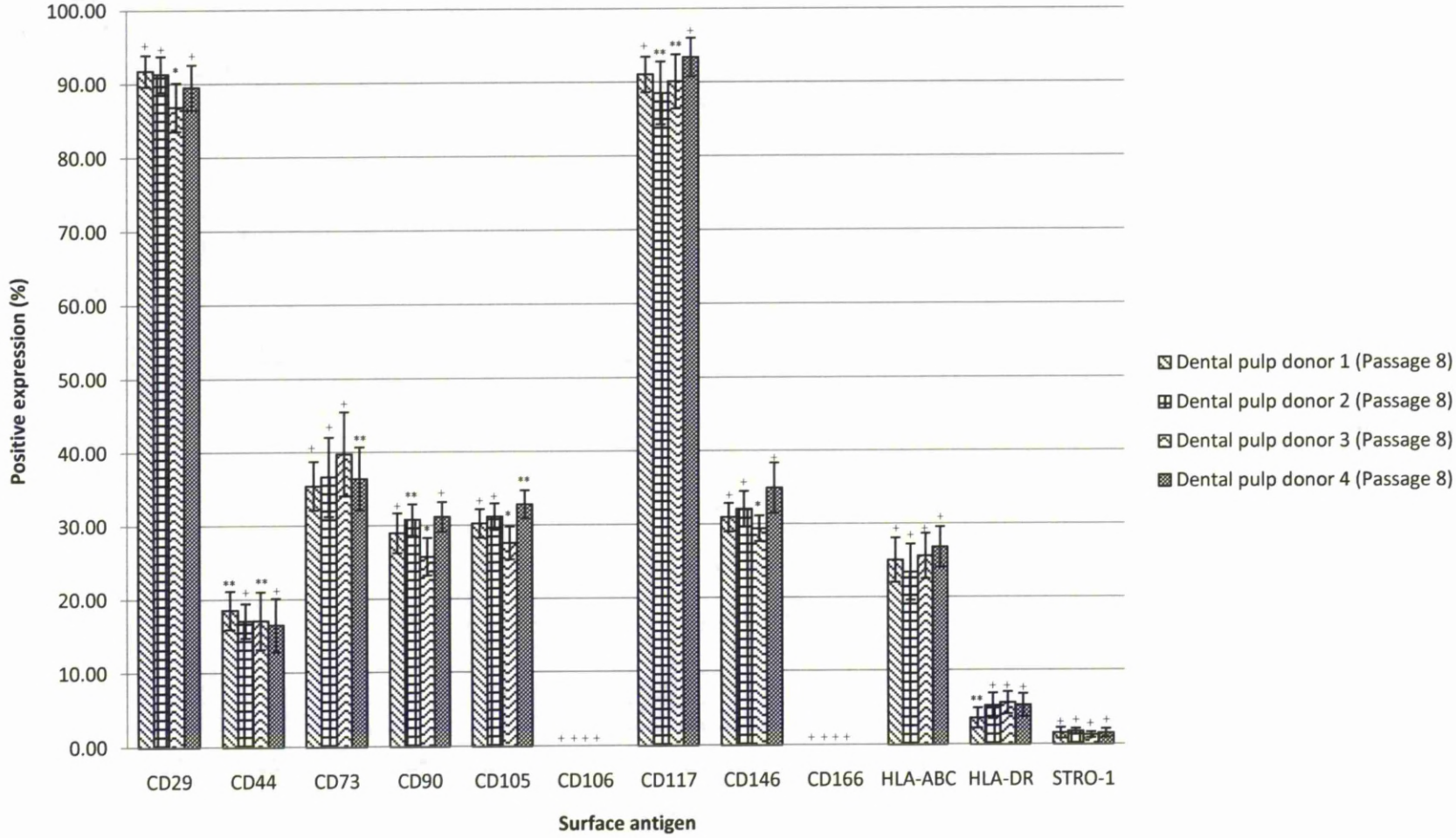

Figure 6.38 - **MSC-associated surface marker phenotyping of passage 8 dental pulp cells derived from donors 1-4 cultured in basal chemically-defined media (1 x Freeze-Thaw cycles). Values represent mean positive expression as observed by flow cytometry (n = 4). Error bars correspond to Standard Deviations. Student *t*-test indicated that there were significant (*$p \leq 0.001$) (**$p \leq 0.05$) and non-significant (+$p \geq 0.05$) antigen expression differences when comparing passage 8 cells from each donor cultured in chemically defined media with those cultured in commercial media (1 x Freeze-Thaw cycles) (*Figure 6.35*, Page 218).**

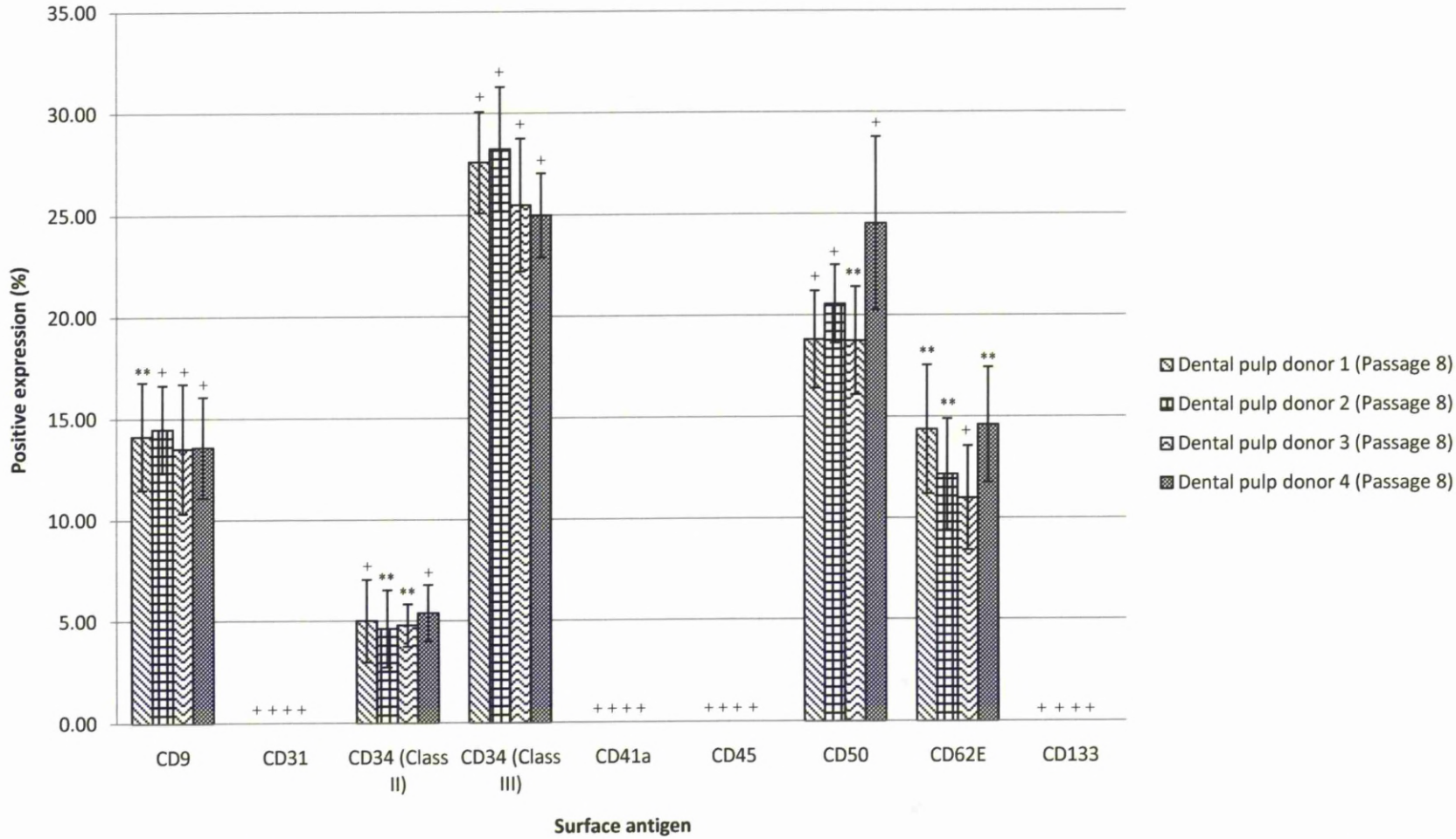

Figure 6.39 - **HSC and endothelial-associated surface marker phenotyping of passage 8 dental pulp cells derived from donors 1-4 cultured in basal chemically-defined media (1 x Freeze-Thaw cycles). Values represent mean positive expression as observed by flow cytometry (n = 4). Error bars correspond to Standard Deviations. Student *t*-test indicated that there were significant (*$p \leq 0.001$) (**$p \leq 0.05$) and non-significant (+$p \geq 0.05$) antigen expression differences when comparing passage 8 cells from each donor cultured in chemically defined media with those cultured in commercial media (1 x Freeze-Thaw cycles) (*Figure 6.36*, Page 219).**

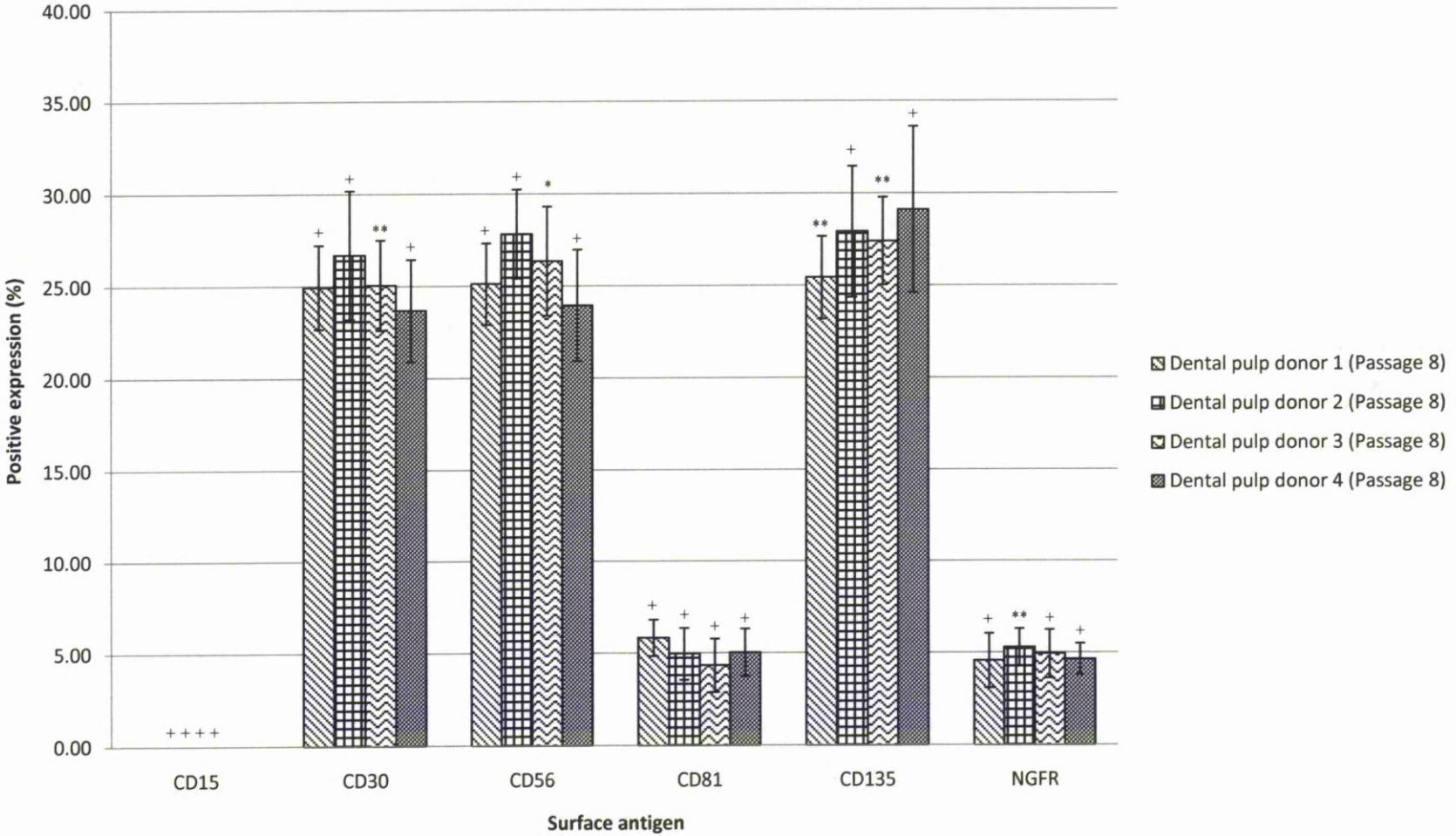

Figure 6.40 **- ES cell and Progenitor-associated surface marker phenotyping of passage 8 dental pulp cells derived from donors 1-4 cultured in basal chemically-defined media (1 x Freeze-Thaw cycles). Values represent mean positive expression as observed by flow cytometry (n = 4). Error bars correspond to Standard Deviations. *t*-test indicated that there were significant (*$p \leq 0.001$) (**$p \leq 0.05$) and non-significant (+$p \geq 0.05$) antigen expression differences when comparing passage 8 cells from each donor cultured in chemically defined media with those cultured in commercial media (1 x Freeze-Thaw cycles) (*Figure 6.37*, Page 220).**

6.3.2 Protein Expression Profiling of Dental Pulp Cells throughout Prolonged *In Vitro* Culture using Immunofluoresence

Unlike bone marrow-, peripheral blood- and umbilical cord-derived cells, isolated dental pulp populations maintained a stable phenotype throughout prolonged *in vitro* culture. However, stable phenotypic expression profiling does not necessarily translate to a conservation of molecular pathways governing plasticity or lineage commitment. Thus it is imperative to establish the ability of the population to maintain a capacity to undertake multilineage differentiation when cultured for prolonged periods *in vitro*. Dental pulp populations were therefore investigated for protein expression over increasing passage, cultured within commercial and chemically-defined basal media, using antibodies complimentary to proteins associated with plasticity or partial lineage commitment.

Fundamental to the maintenance of plasticity is Oct4, a POU-homeodomain transcription factor which is initially expressed as a maternal transcript and is required for the formation of a pluripotent inner cell mass. Moreover, stringent regulation of Oct4 expression is necessary to maintain ES cell identity, with modifications of Oct4 expression generating specified differentiation of ectodermal, endodermal or mesodermal primitive progenitors[92]. Following immunofluorescent staining for Oct4 in isolated dental pulp cells, populations from donors 1 - 4 heterogeneously expressed this protein in approximately 30% of the population. Both nuclear and cytoplasmic expression was observed and, interestingly, cells maintained expression after prolonged *in vitro* culture (*Figures 6.41* and *6.42*).

Oct4 regulates plasticity through a co-operative mechanism with Sox2, forming Oct-Sox heterodimers which bind the Nanog promoter[94,373]. Dental pulp donors 1 - 4 heterogeneously expressed Sox2 in approximately 40% of cells, again maintaining this expression after increasing passage *in vitro*. Expression was both nuclear (*Figure 6.43*) and cytoplasmic (*Figure 6.44*) associated, although expression localisation was heterogeneous within a population and was in no sense attributable to passage number or donor.

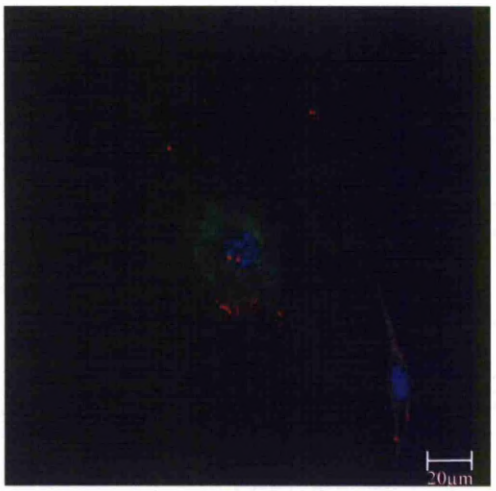

Figure 6.41 - **Dental pulp donor 3 (Passage 3) cultured in commercial basal media stained with Hoechst 33342 (blue), Oregon green (green) and Oct4 antibody (red). Approximately 30% of dental pulp cells exhibited positive Oct4 expression.**

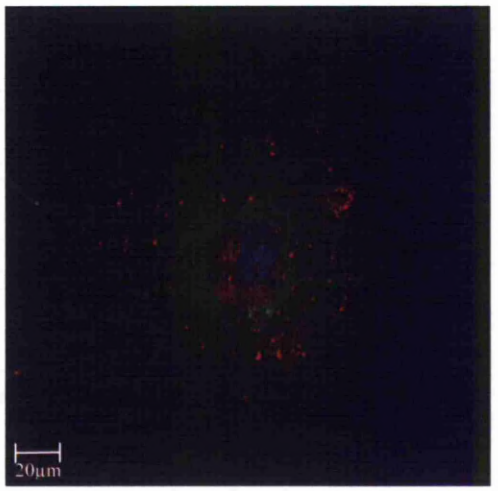

Figure 6.42 - **Dental pulp donor 3 (Passage 30) cultured in commercial basal media stained with Hoechst 33342 (blue), Oregon green (green) and Oct4 antibody (red). Approximately 30% of dental pulp cells exhibited positive Oct4 expression.**

Figure 6.43 - **Dental pulp donor 3 (Passage 3) cultured in commercial basal media stained with Hoechst 33342 (blue), Oregon green (green) and Sox2 antibody (red). Approximately 40% of dental pulp cells exhibited positive Sox2 expression.**

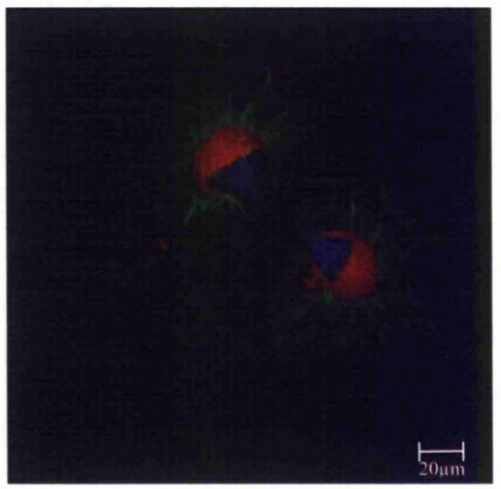

Figure 6.44 - **Dental pulp donor 3 (Passage 30) cultured in commercial basal media stained with Hoechst 33342 (blue), Oregon green (green) and Sox2 antibody (red). Approximately 40% of dental pulp cells exhibited positive Sox2 expression.**

A further proposed regulator of plasticity, Cripto-1, which is hypothesised to function within the Wnt/β-catenin/Tcf signalling pathways and subsequently in stem cell renewal, pluripotency and guided differentiation, was also heterogeneously expressed within approximately 10% of the population throughout increasing passage (*Figures 6.45* and *6.46*), displaying largely cytoplasmic localised expression.

Figure 6.45 - **Dental pulp donor 1 (Passage 3) cultured in commercial basal media stained with Hoechst 33342 (blue), Oregon green (green) and Cripto-1 antibody (red). Approximately 10% of dental pulp cells exhibited positive Cripto-1 expression.**

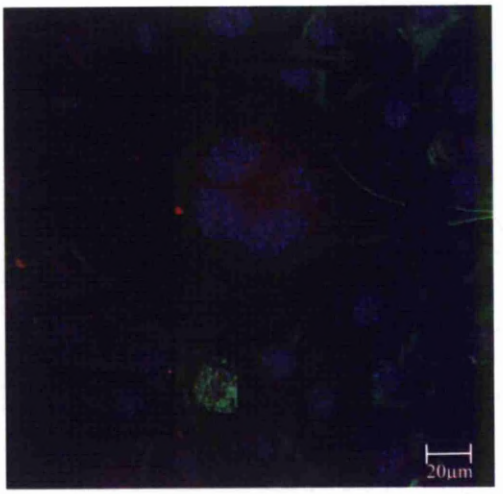

Figure 6.46 - **Dental pulp donor 1 (Passage 3) cultured in commercial basal media stained with Hoechst 33342 (blue), Oregon green (green) and Cripto-1 antibody (red). Approximately 10% of dental pulp cells exhibited positive Cripto-1 expression.**

Tra-1-81 is expressed by human ES, EG and EC cells and, whilst it is generally perceived as a marker of pluripotency, its exact functional role is unknown. Dental pulp-derived populations heterogeneously expressed Tra-1-81 cytoplasmically in approximately 10% of the population in *in vitro* culture (*Figures 6.47* and 6.48), and furthermore maintained expression following freeze-thaw cycling.

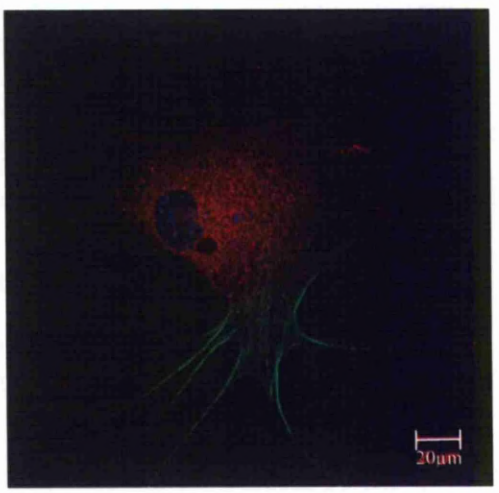

Figure 6.47 - **Dental pulp donor 2 (Passage 3) cultured in commercial basal media stained with Hoechst 33342 (blue), Oregon green (green) and Tra-1-81 antibody (red). Approximately 10% of dental pulp cells exhibited positive Tra-1-81 expression.**

Figure 6.48 - **Dental pulp donor 2 (Passage 30) cultured in commercial basal media stained with Hoechst 33342 (blue), Oregon green (green) and Tra-1-81 antibody (red). Approximately 10% of dental pulp cells exhibited positive Tra-1-81 expression.**

STRO-1 and nucleostemin are currently perceived as markers of cells exhibiting multipotent ability, and cells from all donors demonstrated expression of both markers over time in culture. Nucleostemin was expressed within the nucleus of approximately 60% of the population (*Figure 6.49*), and furthermore cells exhibiting positive nucleostemin expression demonstrated co-expression with STRO-1 (*Figure 6.50*), indicating the presence of proliferative cells with multipotent capacity.

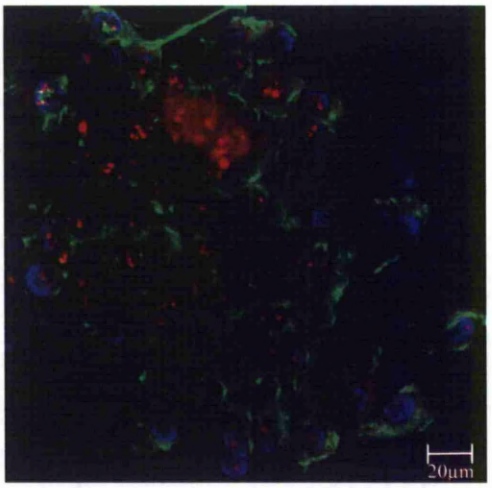

Figure 6.49 **- Dental pulp donor 4 (Passage 5) cultured in commercial basal media stained with Hoechst 33342 (blue), Oregon green (green) and nucleostemin antibody (red). Approximately 60% of dental pulp cells exhibited positive nucleostemin expression.**

Figure 6.50 **- Dental pulp donor 4 (Passage 14) cultured in commercial basal media stained with Hoechst 33342 (blue), STRO-1 antibody (green) and nucleostemin antibody (red). Approximately 60% of dental pulp cells exhibited positive dual nucleostemin and STRO-1 expression.**

The expression of neuronal-associated antigens CD81 and NGFR within the population suggests the presence of a neuronal progenitor subset, which is unsurprising given the developmental origin of the dental pulp niche. REST represents a protein responsible for the silencing of neuronal specific genes in non-neuronal tissues, and is downregulated upon appropriate neuronal stimuli by a truncated version of the protein, REST4, which is hypothesised to silence REST expression via binding of the BDNF promoter. It is interesting, therefore, that dental pulp-derived populations demonstrated approximately 15% positive REST4 expression in basal conditions within subsets of the population (*Figures 6.51* and *6.52*), perhaps suggesting that REST4 is transcribed as to allow basal levels of proteins associated with neuronal progenitors such as nestin (*Figure 6.53*) and TBR2 (*Figure 6.54*), which were expressed by approximately 10% of the populations.

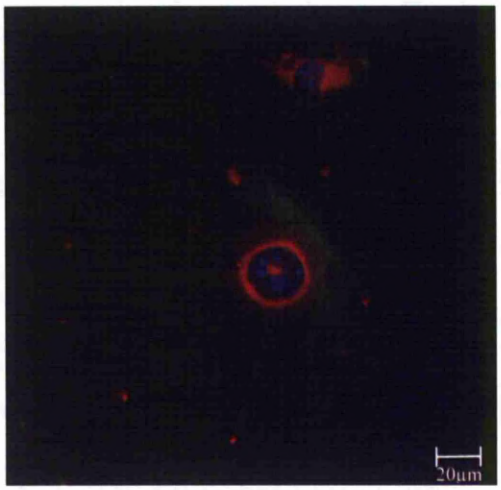

Figure 6.51 - Dental pulp donor 1 (Passage 10) cultured in commercial basal media stained with Hoechst 33342 (blue), Oregon green (green) and REST4 antibody (red). Approximately 15% of dental pulp cells exhibited positive REST4 expression.

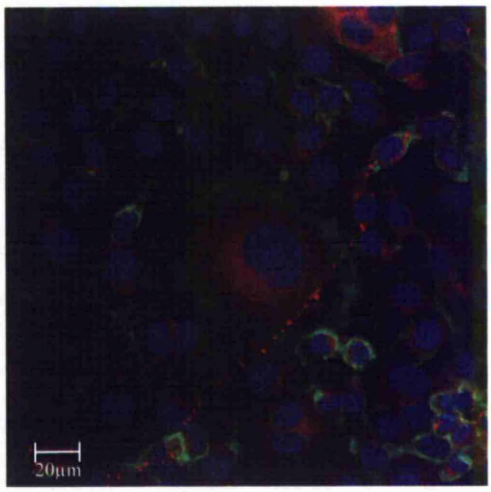

Figure 6.52 - Dental pulp donor 1 (Passage 15) cultured in commercial basal media stained with Hoechst 33342 (blue), Oregon green (green) and REST4 antibody (red). Approximately 15% of dental pulp cells exhibited positive REST4 expression.

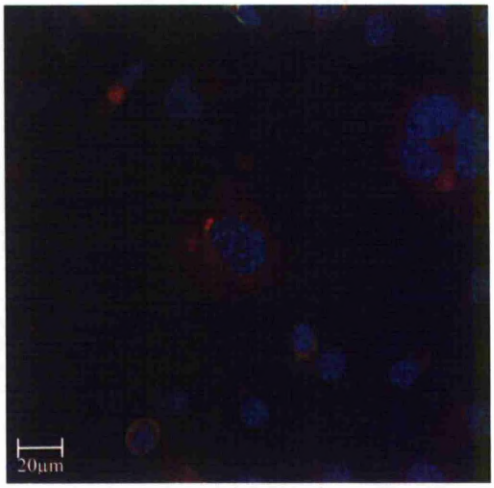

Figure 6.53 - Dental pulp donor 1 (Passage 10) cultured in commercial basal media stained with Hoechst 33342 (blue), Oregon green (green) and nestin antibody (red). Approximately 10% of dental pulp cells exhibited positive nestin expression.

Figure 6.54 - Dental pulp donor 1 (Passage 10) cultured in commercial basal media stained with Hoechst 33342 (blue), Oregon green (green) and TBR2 antibody (red). Approximately 10% of dental pulp cells exhibited positive TBR2 expression.

To further the identification of neuronal progenitors within the population and the developmental origin of the dental pulp, isolated populations were assessed for their expression of proteins associated with the retinal pigment epithelium (RPE) lineage (*Figure 6.55*). The generation of terminally differentiated RPE results from lineage commitment of undifferentiated ES cells towards progressively more committed retinal precursors, finally producing a functional RPE cell type. Progression towards

the RPE phenotype requires a downregulation of Oct4, allowing expression of proteins required for differentiation. Following downregulation of Oct4, cells destined for an RPE lineage express Pax6, a Six3 activated transcription factor essential for normal development of the mammalian lens. $Pax6^+$ cells further commit to RPE precursors which express MiTF, a protein involved in RPE differentiation via modulation of the expression of major melanogenic proteins such as tyrosinase and tyrosinase-related proteins TRP1 and TRP2.

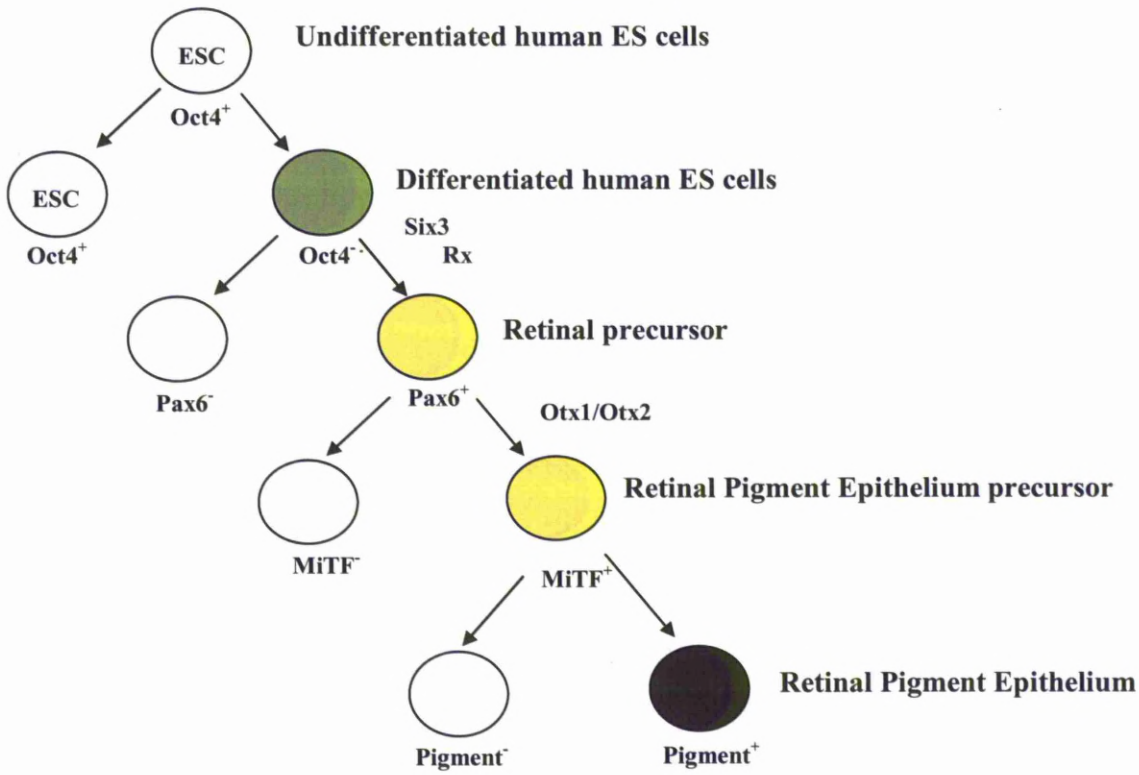

***Figure 6.55* - Progressive RPE lineage commitment.**

Dental pulp-derived populations exhibited maintained expression of both Pax6 (*Figure 6.56*) and MiTF (*Figure 6.57*) within approximately 30% of cells, indicating the presence of a neuronal progenitor subset of RPE lineage commitment. However, it has yet to be established whether $Pax6^+$ cells are in fact co-expressing MiTF, for which a dual stain using these two proteins must be carried out. Nevertheless, the presence of cells transcribing factors associated with retinal and/or RPE precursor cells offers immense therapeutic value for diseases such as macular degeneration,

potentially facilitating the isolation of progenitor subsets capable of regenerating the RPE layer. Further investigations must now concentrate upon the homogeneous isolation of these cells and identify which chemical stimuli enable guided differentiation.

Figure 6.56 **- Dental pulp donor 3 (Passage 15) cultured in commercial basal media stained with Hoechst 33342 (blue), Oregon green (green) and pax6 antibody (red). Approximately 30% of dental pulp cells exhibited positive pax6 expression.**

Figure 6.57 **- Dental pulp donor 3 (Passage 15) cultured in commercial basal media stained with MiTF antibody (red). Approximately 30% of dental pulp cells exhibited positive MiTF expression.**

Intracellular protein expression profiling of dental pulp-derived populations further confirmed flow cytometric observations that the population contains an array of stem and progenitor subpopulations. The maintained expression of Oct4, Sox2, Cripto-1, nucleostemin and STRO-1 suggests the presence of highly plastic stem cell populations capable of undertaking differentiation towards numerous lineages; whilst alternative staining with REST, TBR2, pax6 and MiTF suggests the presence of neuronal progenitors, with these proteins likely to represent cells capable of undertaking neuronal and RPE lineage differentiation. As a whole the population represents an attractive source of stem and progenitor subsets, although it is required that each subpopulation is homogeneously isolated and assessed for their differentiation capacity, potentially allowing their precise application within neuronal and alternative regenerative strategies.

6.4 Proliferation Capacity of Dental Pulp Cells

6.4.1 Proliferation Capacities of Dental Pulp Cells throughout Prolonged *In Vitro* Culture and Freeze-thaw Cycling using CyQUANT Analysis

In order to assess the effects of *in vitro* culture upon dental pulp proliferation capacity, 0.5 x 10^4 cells were cultured in commercial basal conditions throughout 7 day culture and cell numbers assessed at days 1, 3 and 7. Given the maintained phenotypic expression between varying donors over increasing passage demonstrated in 6.3.1, only dental pulp donor 1 cells were assessed.

Continuously cultured dental pulp donor 1 cells (*Figure 6.58*) and equivalent freeze-thawed populations (*Figure 6.59*), frozen following a third passage and thawed following 30 days cryopreservation at -80°C, were assessed for their proliferation rates at passages 4/5 through to 9. Passage 4 cells not subjected to freeze-thawing generated approximately 0.7 x 10^4, 2.7 x 10^4 and 3.9 x 10^4 cells at days 1, 3 and 7 respectively. Interestingly, increasingly cultured populations, whether cryopreserved or continually cultured, maintained this rate of proliferation. Passage 5 to 9 cultures not exposed to cryopreservation demonstrated approximately 0.7 x 10^4, 2.7 x 10^4 and 3.9 x 10^4 cells at days 1, 3 and 7 respectively, whilst freeze-thaw cultures in fact demonstrated slightly greater proliferation rates, with passage 5 to 9 cells generating approximately 0.9 x 10^4, 3.0 x 10^4 and 4.4 x 10^4 cells at days 1, 3 and 7 respectively. However, this increase is likely to be attributable to minimal differences in seeding density or slight modifications to culture conditions.

The ability of dental pulp-derived populations to maintain proliferation following prolonged *in vitro* culture is a significant progression towards their therapeutic utilisation, enabling cryopreservation of isolated cells until required for clinical application. Whilst no quantifiable data was acquired for late passage cultures, no qualitative reduction was observed in proliferative capacity within cells cultured up to 40 passages, and it is likely that such populations will continue to proliferate to the Hayflicks limit of 70 passages[395]. Furthermore, whilst CyQUANT analysis was not utilised to assess cells isolated from different donors, since these cells displayed a comparable ability to maintain phenotype, and similar proliferation rates from a

qualitative perspective, it is hypothesised that they also displayed this capacity to maintain proliferation post prolonged *in vitro* culture and freeze-thawing.

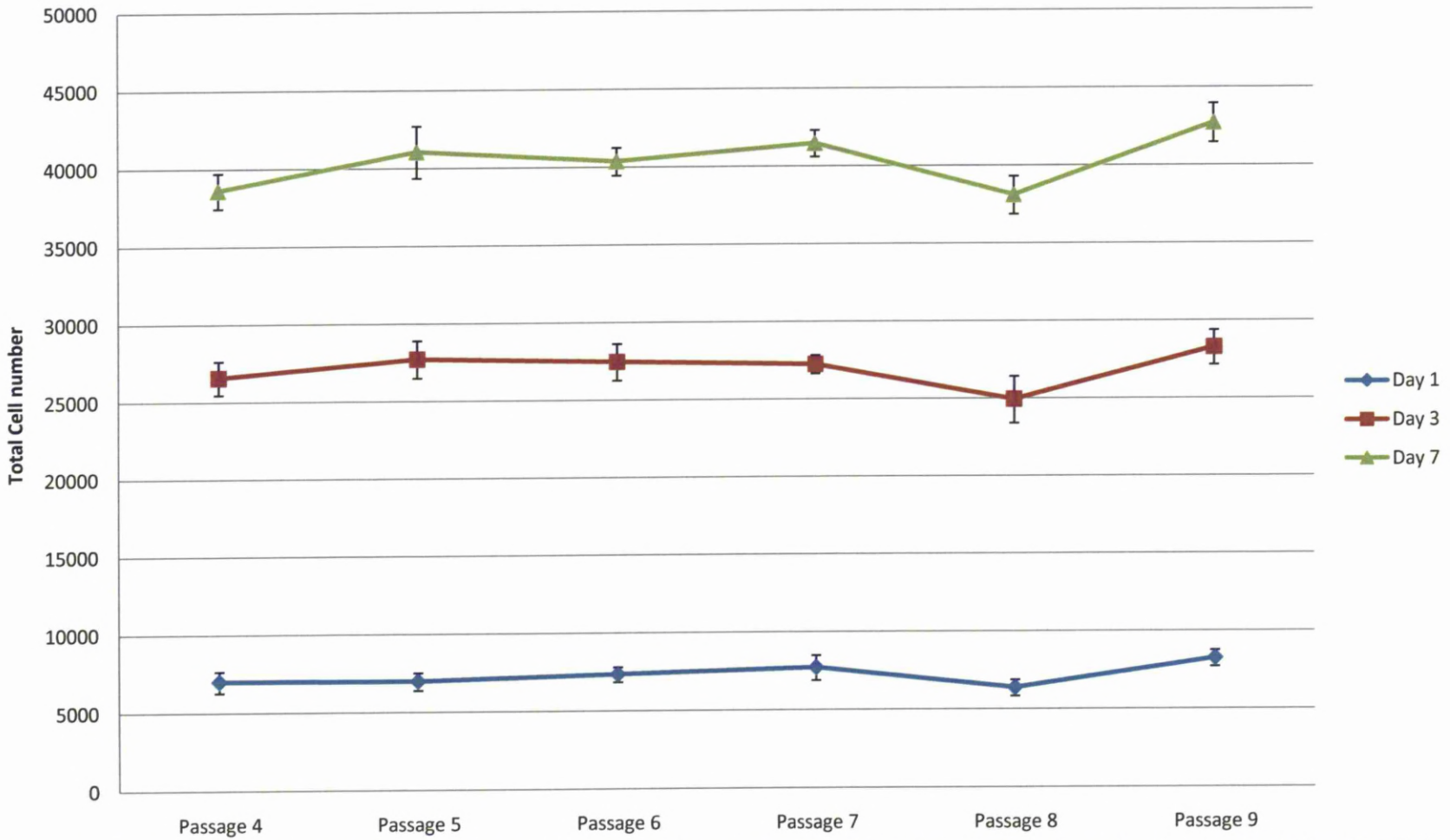

Figure 6.58 - **Proliferation capacity of dental pulp-derived cells from pulp donor 1 passages 4-9 (0 x Freeze-thaw cycle) cultured in commercial basal media for 7 days. Initial seeding density 0.5 x 10^4 cells. Values represent mean numbers of total cells counted at days 1, 3 and 7 for each respective passage (n = 4). Error bars correspond to Standard Deviations.**

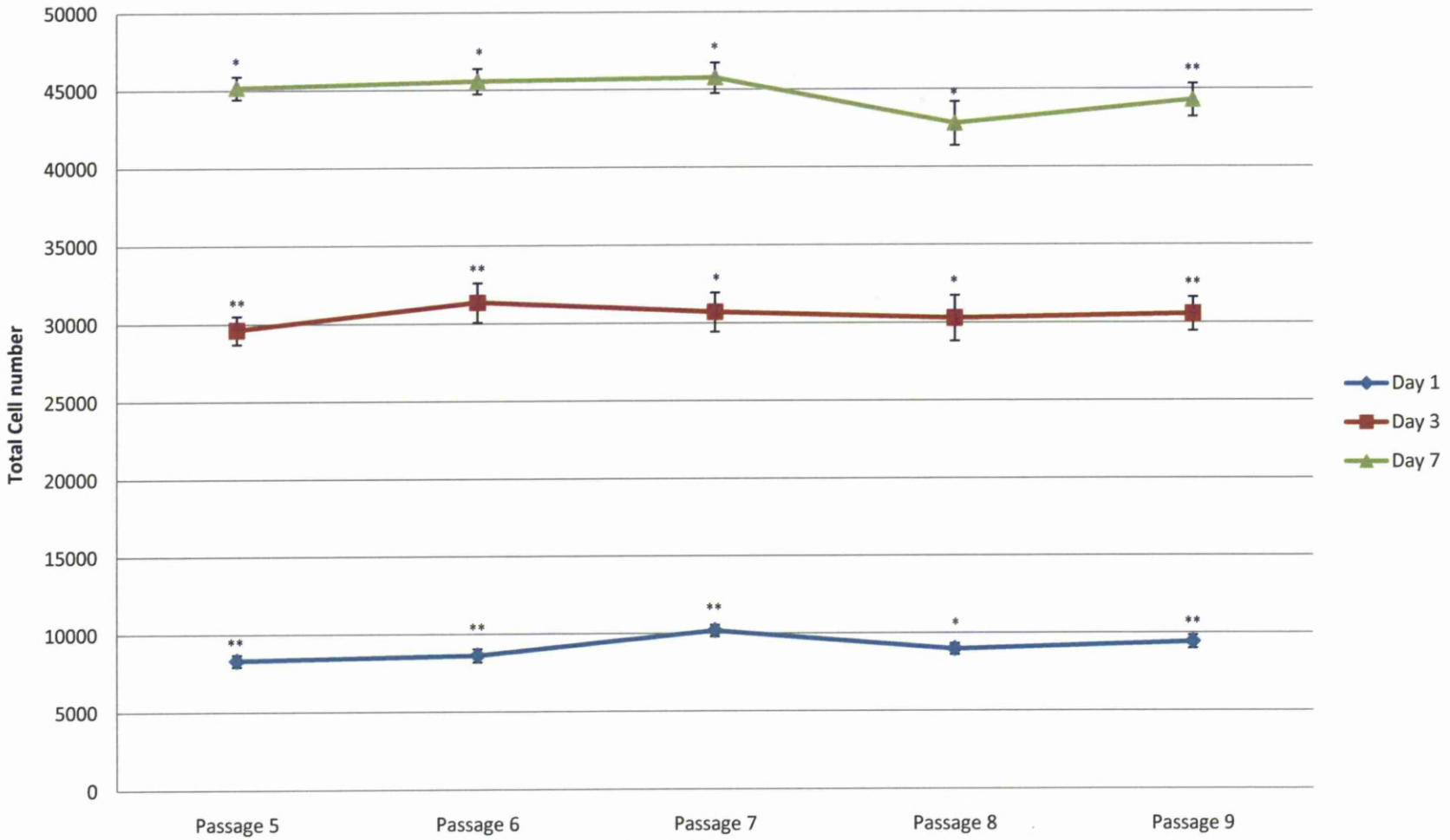

Figure 6.59 - **Proliferation capacity of dental pulp-derived cells from pulp donor 1 passages 4-9 (1 x Freeze-thaw cycle) cultured in commercial basal media for 7 days. Initial seeding density 0.5 x 10^4 cells. Values represent mean numbers of total cells counted at days 1, 3 and 7 for each respective passage (n = 4). Error bars correspond to Standard Deviations. Student *t*-test indicated that there were significant (*$p \leq 0.001$) (**$p \leq 0.05$) differences in proliferation when comparing dental pulp donor 1 cells which had not been freeze-thawed (*Figure 6.58*, Page 233) with those which had undergone 1 freeze-thaw cycle *e.g.* Passage 5 (0 x Freeze-Thaw cycle) total cell number at day 3 of culture compared with Passage 5 (1 x Freeze-Thaw cycle) total cell number at day 3 of culture.**

6.5 Telomere Length Assessment of Dental Pulp Cells

6.5.1 Telomere Length Regulation of Dental Pulp-derived Cells throughout Prolonged *In Vitro* Culture using DAKO Telomere Length Analysis

Reduced proliferation rates observed in bone marrow-derived populations are likely to be attributable to rapid aging of the population when cultured *in vitro*, a hypothesis substantiated by the hastily degrading telomeres observed in 3.4.1. However, given the sustained phenotypic and proliferative capacities of dental pulp populations following prolonged *in vitro* culture, it was hypothesised that the population did not age in the same manner as their bone marrow counterparts when cultured *ex vivo*, with cells instead displaying *in vivo* TTAGG base reductions. Alternatively, it was considered, given the observed expression of telomerase and subsequent telomere maintenance within ES cells, that these phenotypically immature dental pulp cells may in fact sustain telomere lengths *in vitro* via telomerase activity.

Dental pulp donor 1 cells cultured in commercially available basal media were therefore assessed for their telomere lengths at passages 4 through to 9 (*Figure 6.60*), and unlike bone marrow-derived cells, did not exhibit rapid reductions in telomere length. Instead, cells displayed a stable X chromosome telomere length, with an average base length of 13190, 13234, 13189, 13155, 13154 and 13208 at passages 4 to 9 accordingly. However, given the limitations of the assay, it is difficult to confirm with certainty whether cells are in fact maintaining telomere lengths or aging at a comparable *in vivo* rate. However, results do confirm that *in vitro* culture infers minimal impact upon telomere lengths and subsequent aging of these cells, although it must be noted that the assay incorporates a heterogeneous population and subsequently generates an average X chromosome telomere length for the global population. Thus whilst many cells, presumably of a more committed phenotype, may in fact be demonstrating reducing telomere lengths, alternative telomerase-expressing members of the population, presumably more primitive cells, may be maintaining telomere lengths. Thus further studies must ascertain whether telomerase is expressed within the population.

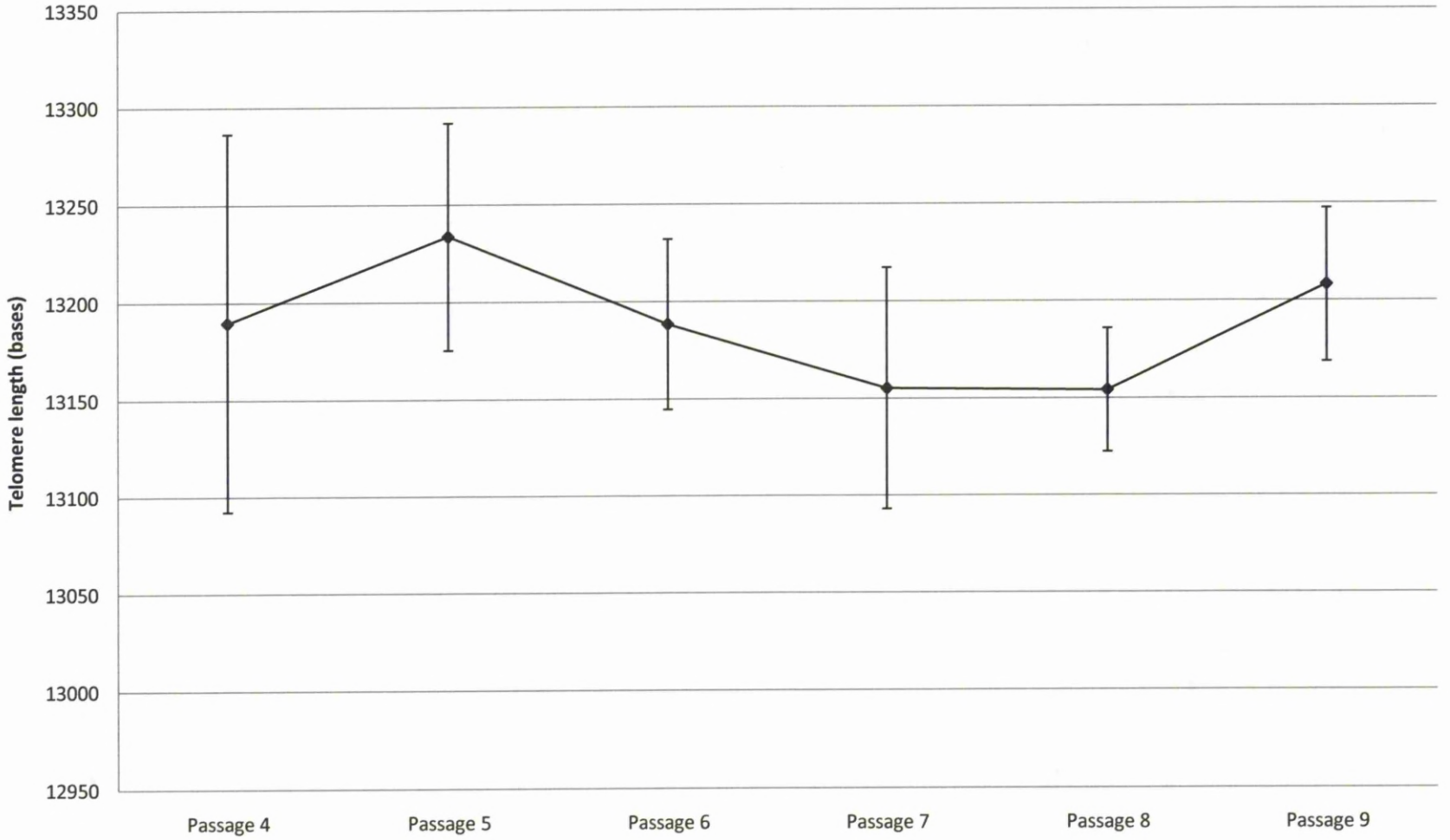

Figure 6.60 **- Mean telomere lengths (n = 4) of dental pulp donor 1 derived cells cultured in basal commercial media (0 x Freeze-thaw cycles) passages 4-9. Error bars correspond to Standard Deviations.**

6.6 CFU Analysis of Dental Pulp Cells

6.6.1 CFU-Fibroblast Analysis of Dental Pulp-derived Cells

Given the surface and intracellular protein expression profiling of dental pulp populations derived from varying donors, it was hypothesised that the population contained progenitors capable of multilineage differentiation and subsequently CFU-F formation. Therefore 0.5 x 10^4 passage 4, 6 and 9 cells derived from donors 1 - 4 were cultured in conditions known to accommodate CFU-F formation within a 35mm^2 culture dish. Following 7 days of culture, distinct colonies were apparent (*Figures 6.61* and *6.62*); seeded cells from each donor at varying passage generated similar average numbers of CFU-Fs (*Figure 6.63*). Passage 4 populations generated 24.8, 21.3, 23.5 and 19.5 average CFU-F formations for donors 1, 2, 3 and 4 respectively. Passage 6 populations from donors 1 - 4 generated similar average CFU-F numbers, producing 18.5, 20.0, 24.0 and 22.3 colonies per 35mm^2 culture dish following 7 days of culture. Passage 9-derived populations from donors 1 - 4 produced CFU-Fs following 7 days of culture, with an average of 28.9, 17.5, 22.0 and 25.5 colonies generated for each respectively.

Results obtained from CFU-F investigations of pulp donor 1 - 4 populations revealed a comparable number of CFU-F formations per 0.5 x 10^4 cells seeded, whilst furthermore maintaining this capacity despite prolonged passage. Interestingly, whilst dental pulp-derived populations displayed relatively low expression of MSC-associated antigens compared with bone marrow-derived cells, they exhibited an innate ability to generate large numbers CFU-Fs, suggesting that CD90 and alternative MSC-associated antigen expressing cells are not necessarily stem or progenitor subsets. In conclusion, dental pulp populations, as surface and intracellular expression profiles would suggest, contain a concentrated number of subpopulations demonstrating CFU-F capacity associated with stem and progenitor subsets, and thereby represent a cell source with significant clinical potential. Should homogeneous isolation of each subpopulation eventually be achieved, the CFU-F assay may represent an attractive technique for assessing multipotent prospects of each respectively isolated population.

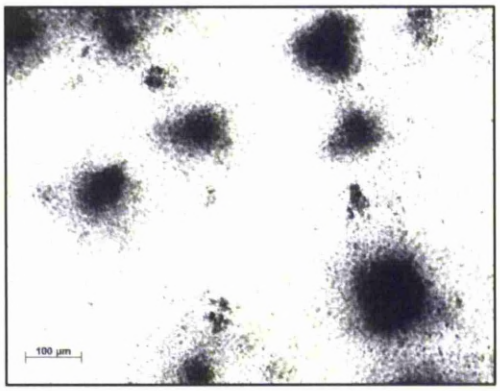

Figure 6.61 - **CFU-F formation from dental pulp donor 1 (Passage 4; 0 x Freeze-thaw) cultured for 7 days in MethoCult media.**

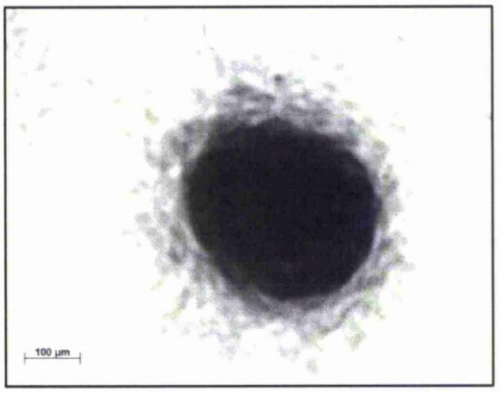

Figure 6.62 - **CFU-F formation from dental pulp donor 1 (Passage 9; 0 x Freeze-thaw) cultured for 7 days in MethoCult media.**

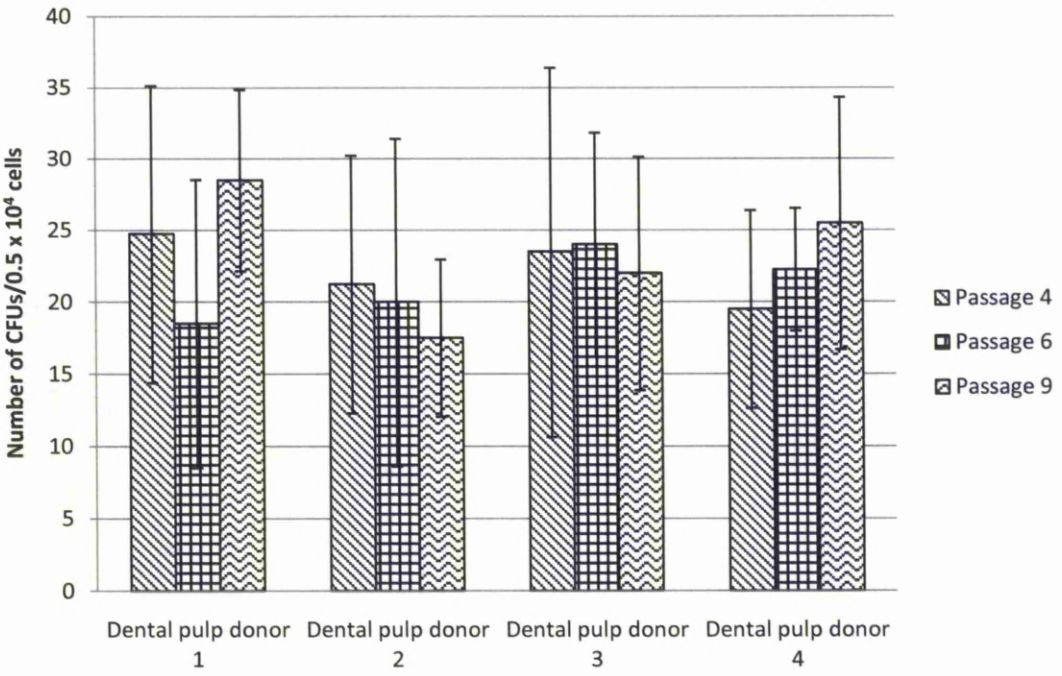

Figure 6.63 - **CFU-F formation per 0.5 x 10^4 cells isolated from human dental pulp donors 1 - 4 (0 x Freeze-thaw) at passages 4, 6 and 9 and cultured for 7 days in MethoCult media. Values represent mean number of cells observed per 35mm^2 culture dish for each donor (n = 4). Error bars correspond to Standard Deviations.**

6.6.2 CFU-Granulocyte/Monocyte Analysis of Dental Pulp-derived Cells

Given expression of HSC-associated antigens CD34 class II and III within all dental pulp populations, 0.5 x 10^4 cells from donors 1 - 4 were cultured in conditions known to induce CFU-GM formation within 35mm^2 culture plates. Following 7 days of culture, distinct colonies were observed (*Figures 6.64* and *6.65*). Passage 4 seeded populations exhibited 5.0, 6.5, 6.8 and 5.5 average CFU-GM formations respectively, passage 6 cells 5.3, 7.8, 5.3 and 7.0 and passage 9 cells 8.8, 4.3, 5.5 and 7.5 (*Figure 6.66*). The capacity of maintained cells to generate CFU-GMs following stimulation would indicate a subpopulation of cells representing hematopoietic progenitors. Given their respective properties, this population is likely to possess a capability to generate mature blood cells, thereby offering immense clinical benefit. Whilst it is unknown which cell type within the population is capable of generating such colonies, CD34$^+$ populations are the most likely given the expression of this antigen in HSC populations. However, given the hypothesised plasticity of the population and the demonstratable expression of plasticity regulators such as Oct4 and Sox2, it could be that these cells, following to appropriate stimulation, differentiate towards hematopoietic progenitor cells and subsequently generate a proportion of observed colonies. Thus the homogeneous isolation and CFU-GM assessment of each subpopulation within human dental pulp must be undertaken.

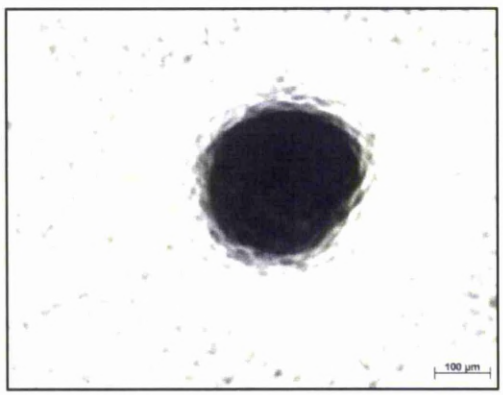

Figure 6.64 - **CFU-GM formation from dental pulp donor 1 (Passage 4; 0 x Freeze-thaw) cultured for 7 days in MethoCult media.**

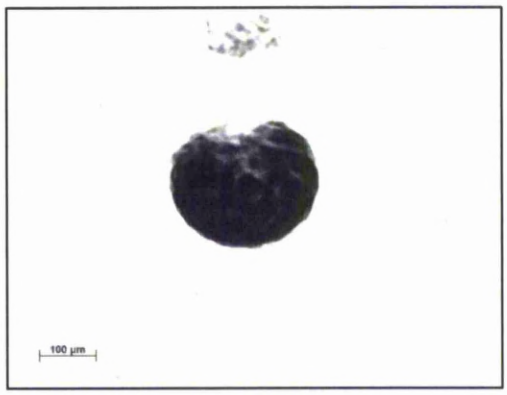

Figure 6.65 - **CFU-GM formation from dental pulp donor 1 (Passage 9; 0 x Freeze-thaw) cultured for 7 days in MethoCult media.**

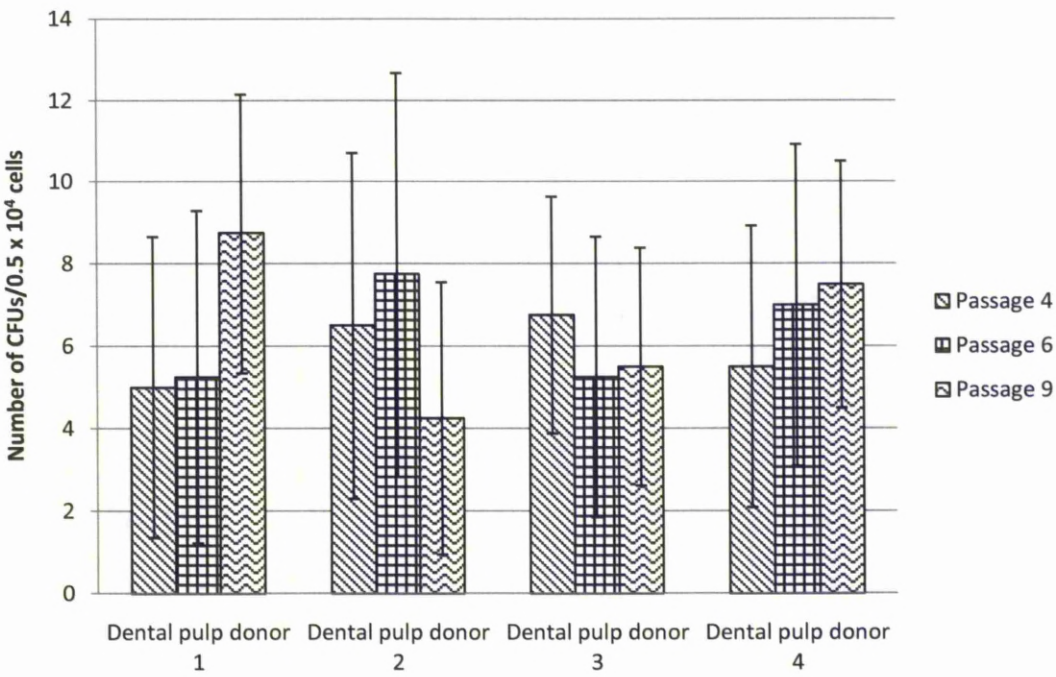

Figure 6.66 - **CFU-GM formation per 0.5 x 10^4 cells isolated from human dental pulp donors 1 - 4 (0 x Freeze-thaw) at passages 4, 6 and 9 and cultured for 7 days in MethoCult media. Values represent mean number of cells observed per 35mm^2 culture dish for each donor (n = 4). Error bars correspond to Standard Deviations.**

6.7 Differentiation of Dental Pulp Cells

6.7.1 Assessment of Pluripotential Ability of Dental Pulp-derived Cells throughout Increasing Passage *In Vitro*

Following the demonstration of maintained expression of factors attributable to the regulation of plasticity, whilst furthermore signifying an ability to generate CFU-Fs and CFU-GMs, dental pulp cells were investigated for their ability to differente towards numerous lineages. Cells of varying passage from donors 1 - 4 were therefore induced with commercially available media and chemically-defined, serum-free alternatives to assess their ability to differentiate.

6.7.2 Adipogenic Differentiation of Pulp-derived Cells using Commercially Available Media

Dental pulp cells were cultured in pre-adipocyte growth media at a seeding density of 3×10^3 cells per well of a 24 well plate for the initial 10 days of culture, followed by exposure to pre-adipocyte differentiation media for 3 days and maintained in adipocyte nutrition media for a further 15 days. Following 7 days of culture, approximately 60% of cells expressed the *in vivo* circulating protein adiponectin. Expression was localised to the cytoplasm (*Figure 6.67*), although following culture in pre-adipocyte differentiation media followed by nutrition media, expression was also detected within the nucleus after 21 days (*Figure 6.68*). It is particularly interesting that adiponectin was expressed after 7 days, since previous reports have attributed adiponectin expression exclusively to mature adipocytes[317], although Oil Red O staining failed to identify lipid formation within the population at this stage of induction. It may therefore be interesting to examine the levels of phosphatidylinositol-3-kinase within adipogenically induced dental pulp cells, since adiponectin secretion is blocked by pharmacological inhibitors of this kinase.

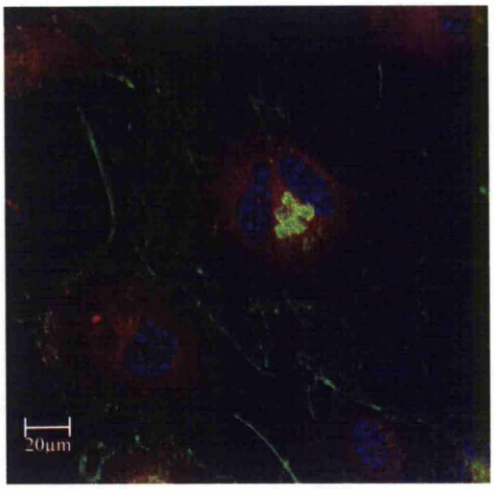

Figure 6.67 **- Dental pulp donor 3 cells (Passage 10) cultured in commercial pre-adipocyte growth media for 7 days stained with Hoechst 33258 (blue), Oregon green (green) and adiponectin antibody (red). Approximately 60% of dental pulp cells exhibited positive adiponectin expression.**

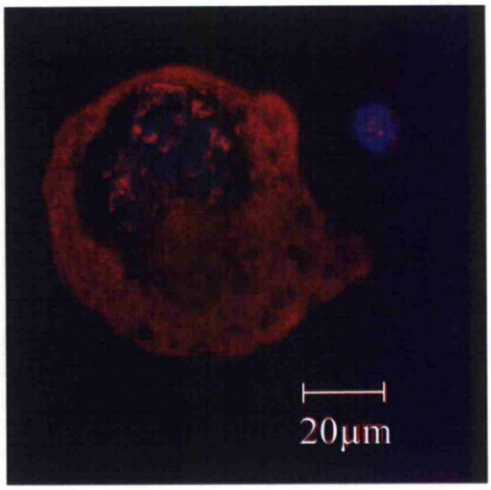

Figure 6.68 **- Dental pulp donor 3 cells (Passage 10) cultured in commercial pre-adipocyte growth media for 10 days, 3 days in pre-adipocyte differentiation media and 8 days in adipocyte nutrition media stained with Hoechst 33258 (blue), Oregon green (green) and adiponectin antibody (red). Approximately 60% of dental pulp cells exhibited positive adiponectin expression.**

Leptin functions as a key regulator of overall body weight via the inhibition of food intake and stimulation of energy expenditure. Following 14 days of adipogenic culture, approximately 60% of cells demonstrated cytoplasmic expression of Leptin (*Figure 6.69*) and maintained this expression throughout the remainder of the 28 day culture. CHOP is a stress induction protein responsible for inhibition of adipogenesis, and was observed within approximately 70% of the population during the initial 7 days of adipogenic culture (*Figure 6.70*), after which the distinct nuclear expression was no longer detected. Down-regulation of CHOP allows the expression of adipocyte specific proteins such as adiponectin and leptin, and other proteins such as PPAR gamma 2 and perilipin, which exhibited cytoplasmic expression within approximately 60% of dental pulp cells following 14 days of adipogenic culture. Regulation of these proteins allow phenotypic and morphological modifications towards a mature adipocyte, with lipid droplets being readily observable within approximately 60% of differentiated dental pulp cells following 28 days culture (*Figures 6.71* and *6.72*). However, it must be noted that dental pulp cells do not homogeneously differentiate into mature adipocytes, with many cells failing to adopt lipid vacuoles typical of the adipogenic phenotype. Whilst conceivably these cells

could still be undertaking differentiation, and with further adipogenic induction would develop such morphological features, it is hypothesised that the non-lipid producing cells may be progenitors of alternative lineages, and are therefore unable to undertake adipogenic differentiation. Nevertheless, the ability of dental pulp cells from donors 1 - 4 to undertake adipogenic differentiation highlights these cells as a potential cell source for clinical treatment following trauma or invasive surgery. Furthermore, their ability to differentiate despite prolonged *in vitro* culture or freeze-thaw cycling increases their potential within the field of fat regeneration.

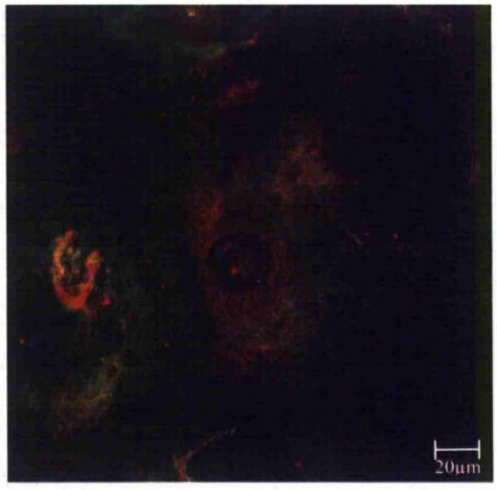

Figure 6.69 **- Dental pulp donor 2 cells (Passage 30) cultured in commercial pre-adipocyte growth media for 10 days, 3 days in pre-adipocyte differentiation media and 1 day in adipocyte nutrition media stained with Hoechst 33258 (blue), Oregon green (green) and leptin antibody (red). Approximately 60% of dental pulp cells exhibited positive leptin expression.**

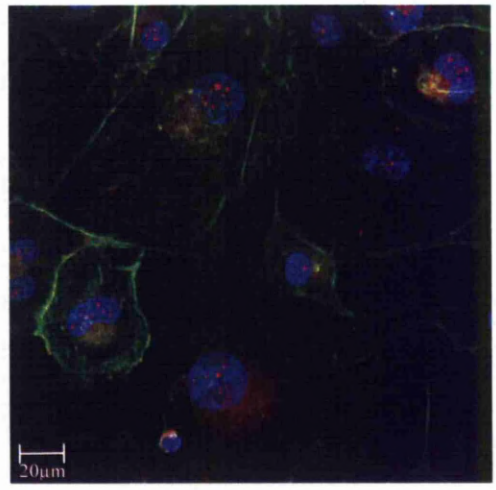

Figure 6.70 **- Dental pulp donor 1 cells (Passage 5) cultured in commercial pre-adipocyte growth media for 7 days stained with Hoechst 33258 (blue), Oregon green (green) and CHOP antibody (red). Approximately 70% of dental pulp cells exhibited positive CHOP expression during the initial 7 days of culture within adipogenic inducting medium, after which no expression was observed.**

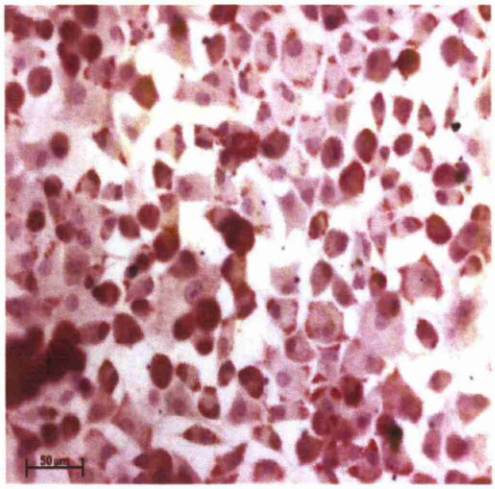

Figure 6.71 - **Dental pulp donor 4 cells (Passage 30) cultured in commercial pre-adipocyte growth media for 10 days, 3 days in pre-adipocyte differentiation media and 15 days in adipocyte nutrition media stained with Oil Red O (Red) and counterstained with Gill's number 1 Hematoxylin (Blue). Approximately 60% of dental pulp cells exhibited positive Oil Red O staining.**

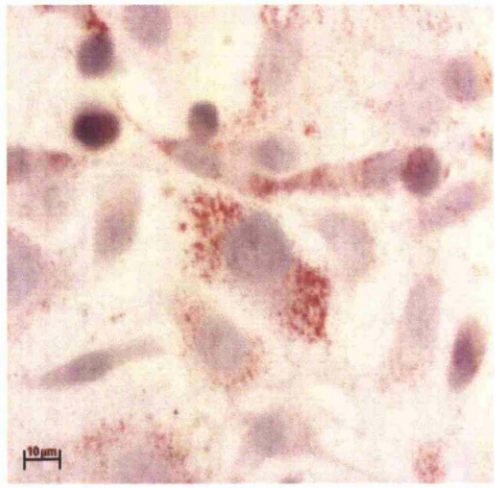

Figure 6.72 - **Dental pulp donor 2 cells (Passage 15) cultured in commercial pre-adipocyte growth media for 10 days, 3 days in pre-adipocyte differentiation media and 15 days in adipocyte nutrition media stained with Oil Red O (Red) and counterstained with Gill's number 1 Hematoxylin (Blue). Approximately 60% of dental pulp cells exhibited positive Oil Red O staining.**

6.7.3 Adipogenic Differentiation of Pulp-derived Cells using Chemically-defined Media

Whilst dental pulp-derived cells demonstrated the ability to differentiate towards an adipogenic lineage when stimulated with commercially available media, the use of serum-containing media may generate concern when used to a clinical setting. Therefore dental pulp cells were differentiated using chemically-defined adipogenic induction media. 3 x 10^3 dental pulp cells per well of a 24 well plate were cultured in chemically-defined media and assessed for their adipogenic associated phenotype as above. As with cells cultured in commercial media, adiponectin expression was detected following 7 days of culture. However, protein expression was both cytoplasmic and nuclear localised, perhaps suggesting an increased commitment towards an adipogenic phenotype. Leptin (*Figure 6.73*), PPAR gamma 2 (*Figure 6.74*) and perilipin were expressed in approximately 60% of the population after 14 days of culture, following the down-regulation of CHOP, which exhibited nuclear localised expression within approximately 70% of cells for the initial 7 days of adipogenic culture (*Figure 6.75*). Whilst upregulation of these adipogenic proteins coincided with those observed following differentiation in adipogenic commercial

media, lipid droplets were formed within approximately 60% of cells after 21 days (*Figure 6.76*), as opposed to commercial induction in which they were observed after 28 days.

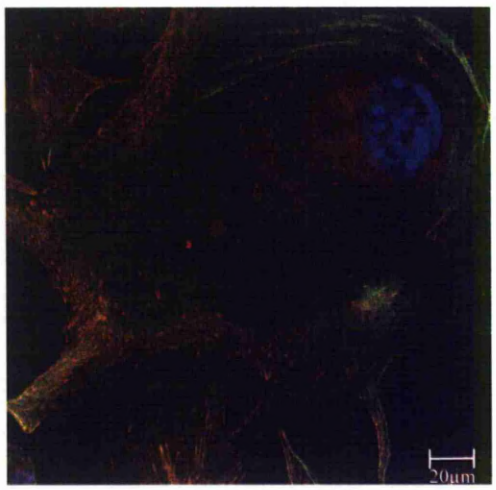

Figure 6.73 **- Dental pulp donor 1 cells (Passage 4) cultured in chemically-defined adipogenic differentiation media for 14 days stained with Hoechst 33258 (blue), Oregon green (green) and leptin antibody (red). Approximately 60% of dental pulp cells exhibited positive leptin expression.**

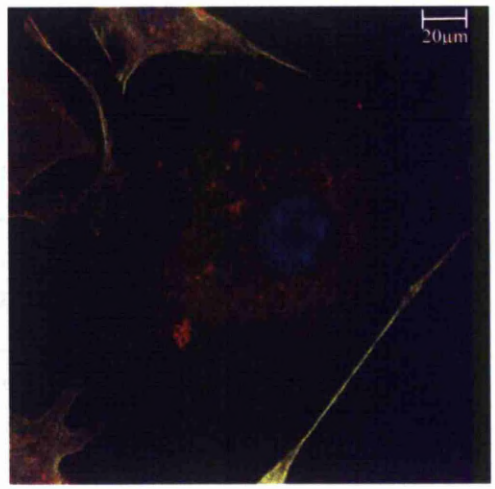

Figure 6.74 **- Dental pulp donor 1 cells (Passage 4) cultured in chemically-defined adipogenic differentiation media for 14 days stained with Hoechst 33258 (blue), Oregon green (green) and PPAR gamma 2 antibody (red). Approximately 60% of dental pulp cells exhibited positive PPAR gamma 2 expression.**

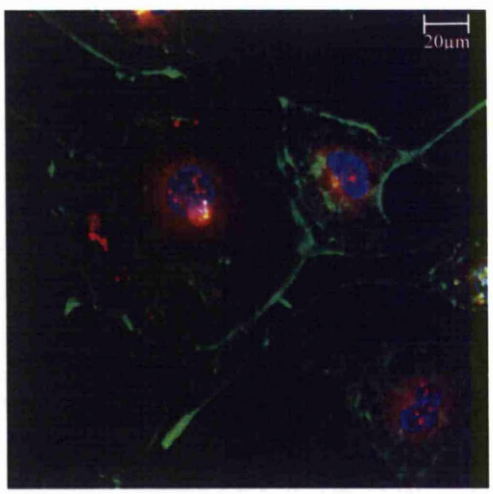

Figure 6.75 **- Dental pulp donor 1 cells (Passage 5) cultured in chemically-defined adipogenic differentiation media for 7 days stained with Hoechst 33258 (blue), Oregon green (green) and CHOP antibody (red). Approximately 70% of dental pulp cells exhibited positive CHOP expression during the initial 7 days of culture within adipogenic inducting medium, after which no expression was observed.**

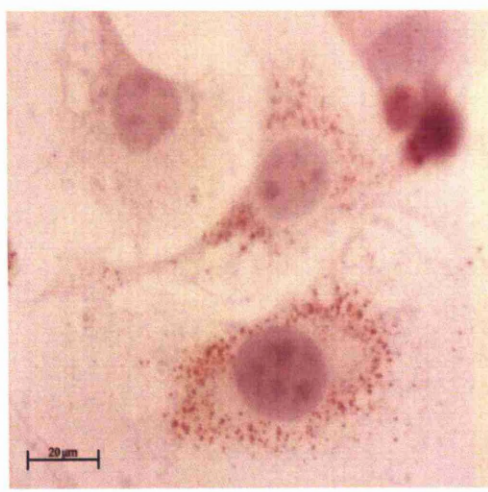

Figure 6.76 **- Dental pulp donor 4 cells (Passage 30) cultured in chemically-defined adipogenic differentiation media for 21 days stained with Oil Red O (Red) and counterstained with Gill's number 1 Hematoxylin (Blue). Approximately 60% of dental pulp cells exhibited positive Oil Red O staining.**

6.7.4 Chondrogenic Differentiation of Pulp-derived Cells using Commercially Available Media

Dental pulp cells were seeded at a concentration of 3 x 10^3 cells per well of a 24 well plate and induced with the TGF-β1 containing chondrogenic differentiation media. Approximately 90% of induced cells expressed collagen I throughout the initial 5 days of culture after which point it no longer transcribed (*Figure 6.77*). Aggrecan, a proteoglycan whose cleavage has been associated with numerous diseases including rheumatoid arthritis and osteoarthritis, was expressed in approximately 70% of cells following 14 days of chondrogenic culture (*Figure 6.78*). Previous investigations mechanistically examining the events during chondrogenic differentiation noted that synthesis of aggrecan and versican core protein signalled an intermediate stage of chondrogenesis, which also involved the small leucine-rich proteoglycans decorin and biglycan. The study also detailed that following aggrecan synthesis, collagen II was synthesised, an event mirrored in approximately 90% of the differentiating dental pulp cells (*Figure 6.79*). Furthermore, Collagen X was also detected within approximately 30% of cells following 21 days of differentiation, a protein largely associated with hypertrophic cartilage[326] (*Figure 6.80*). Differentiating subpopulations of cells exhibited morphological features associated with chondrocytes after 28 days (*Figures 6.81* and *6.82*), and chondrogenic differentiation was further confirmed using Alcian blue to identify the presence of glycosaminoglycans within approximately 60% of the population (*Figure 6.83*). Van Geison staining further confirmed the presence of collagens in approximately 90% of cells following 28 days of differentiation (*Figure 6.84*).

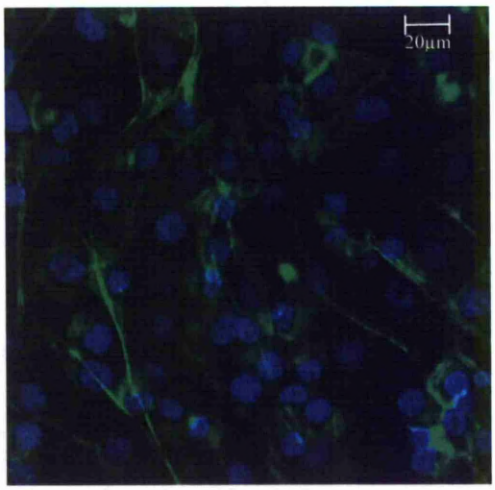

Figure 6.77 - **Dental pulp donor 1 cells (Passage 10) cultured in commercial chondrogenic media for 28 days stained with Hoechst 33258 (blue), Oregon green (green) and collagen I antibody (red). Approximately 90% of dental pulp cells exhibited positive collagen I expression during the initial 5 days of chondrogenic culture, after which no expression was observed.**

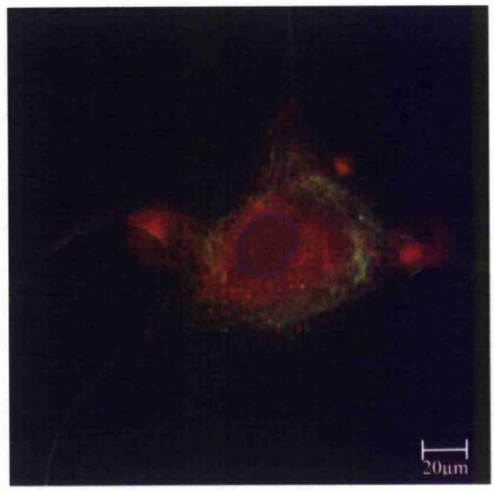

Figure 6.78 - **Dental pulp donor 1 cells (Passage 10) cultured in commercial chondrogenic media for 14 days stained with Hoechst 33258 (blue), Oregon green (green) and aggrecan antibody (red). Approximately 70% of dental pulp cells exhibited positive aggrecan expression.**

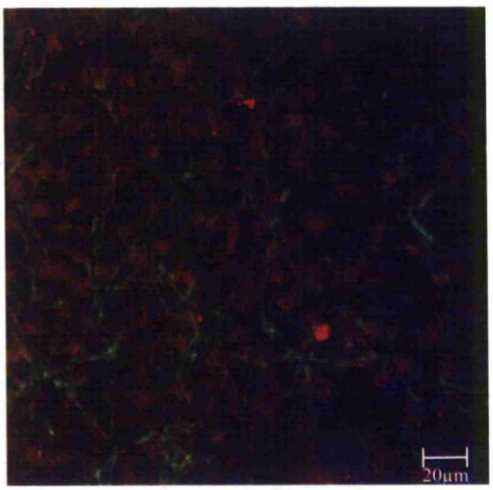

Figure 6.79 - **Dental pulp donor 1 cells (Passage 10) cultured in commercial chondrogenic media for 21 days stained with Hoechst 33258 (blue), Oregon green (green) and collagen II antibody (red). Approximately 90% of dental pulp cells exhibited positive collagen II expression.**

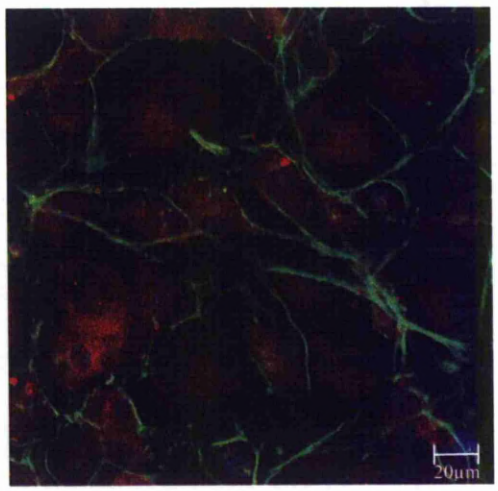

Figure 6.80 - **Dental pulp donor 3 cells (Passage 3) cultured in commercial chondrogenic media for 21 days stained with Hoechst 33258 (blue), Oregon green (green) and collagen X antibody (red). Approximately 30% of dental pulp cells exhibited positive collagen X expression.**

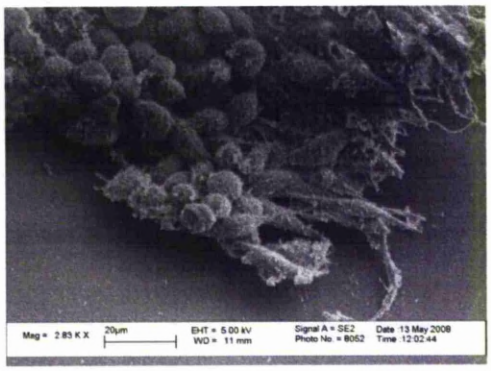

Figure 6.81 - **Dental pulp donor 4 cells (Passage 15) cultured in commercially available chondrogenic differentiation media for 21 days.**

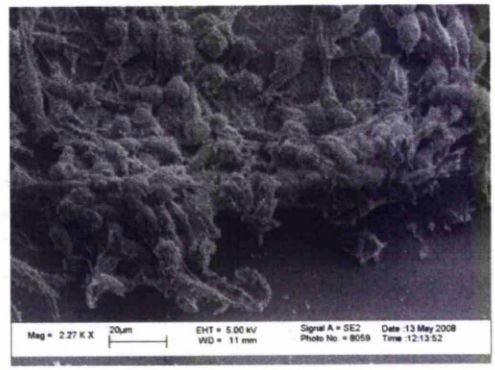

Figure 6.82 - **Dental pulp donor 4 cells (Passage 30) cultured in commercially available chondrogenic differentiation media for 21 days.**

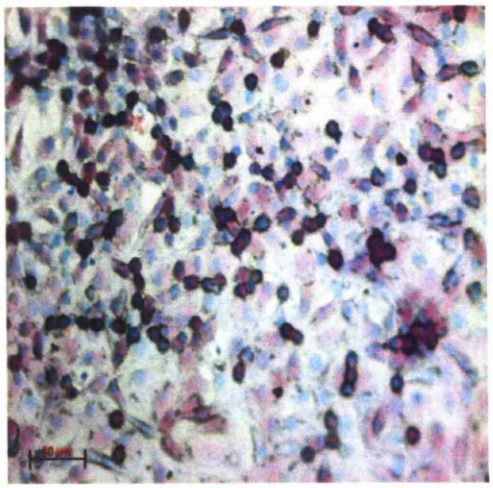

Figure 6.83 - **Dental pulp donor 1 cells (Passage 10) cultured in commercial chondrogenic differentiation media for 28 days stained with Alcian blue (Blue) and counterstained with Nuclear fast red (Pink). Approximately 60% of dental pulp cells exhibited positive Alcian blue staining.**

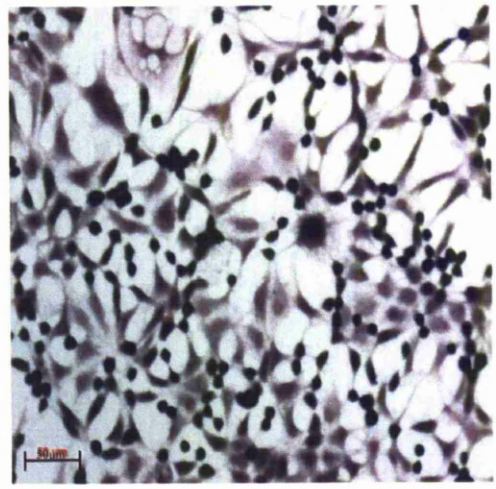

Figure 6.84 - **Dental pulp donor 1 cells (Passage 30) cultured in commercial chondrogenic differentiation media for 28 days stained with Van Geison (Red) and counterstained with Celestine blue (Black). Approximately 90% of dental pulp cells exhibited positive Van Geison staining.**

6.7.5 Chondrogenic Differentiation of Pulp-derived Cells using Chemically-defined Media

In order to further findings describing the chondrogenic lineage potential of dental pulp populations, cells were cultured in chemically-defined chondrogenic media at a concentration of 3 x 10^3 cells per well of a 24 well plate. Cells again committed towards the progressive pathways of chondrogenesis observed using commercial media, though based upon aggrecan production, at an enhanced rate. Collagen I, previously expressed by approximately 90% of cells, ceased production following 3

days of culture (*Figure 6.85*), which coincided with the production of aggrecan in approximately 75% of cells (*Figure 6.86*), a protein which was synthesised following 14 days culture in commercial chondrogenic differentiation media.

Figure 6.85 **- Dental pulp donor 3 cells (Passage 3) cultured in chemically-defined chondrogenic media for 3 days stained with Hoechst 33258 (blue), Oregon green (green) and collagen I antibody (red). Approximately 90% of dental pulp cells exhibited positive collagen I expression during the initial 3 days of chondrogenic culture, after which no expression was observed.**

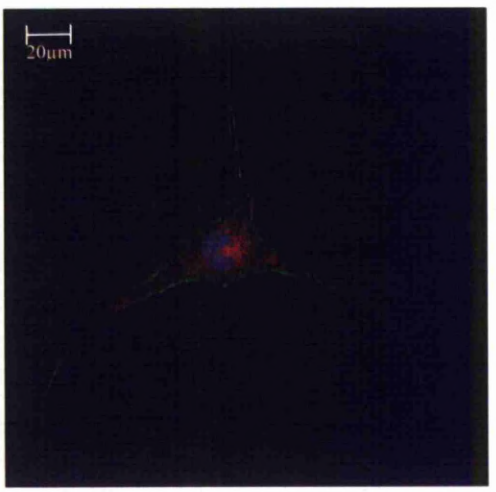

Figure 6.86 **- Dental pulp donor 3 cells (Passage 20) cultured in chemically-defined chondrogenic media for 3 days stained with Hoechst 33258 (blue), Oregon green (green) and aggrecan antibody (red). Approximately 75% of dental pulp cells exhibited positive aggrecan expression.**

Following 21 days of culture collagen II production was identified within approximately 90% of cells, in addition to collagen X, which was expressed by approximately 30% of the population. Differentiating cells appeared morphologically similar to mature chondrocytes following 21 days culture (*Figures 6.87* and *6.88*), and glycosaminoglycan production in approximately 50% of cells was confirmed using Alcian blue staining (*Figures 6.89* and *6.90*), thereby suggesting that chondrogenesis in dental pulp-derived cells is more rapid when induced with chemically-defined media.

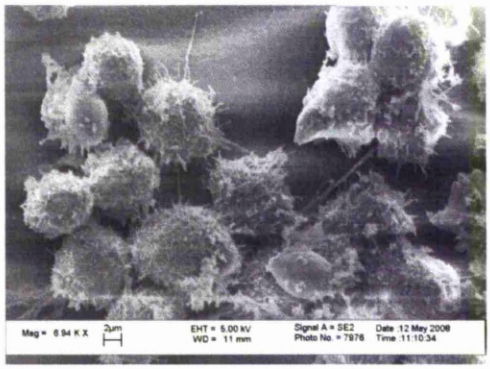

Figure 6.87 - **Dental pulp donor 2 cells (Passage 10) cultured in chemically-defined chondrogenic differentiation media for 21 days.**

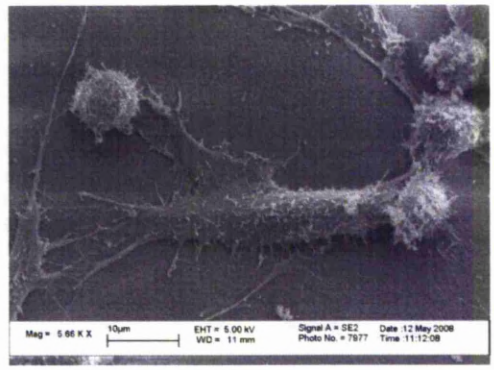

Figure 6.88 - **Dental pulp donor 3 cells (Passage 30) cultured in chemically-defined chondrogenic differentiation media for 21 days.**

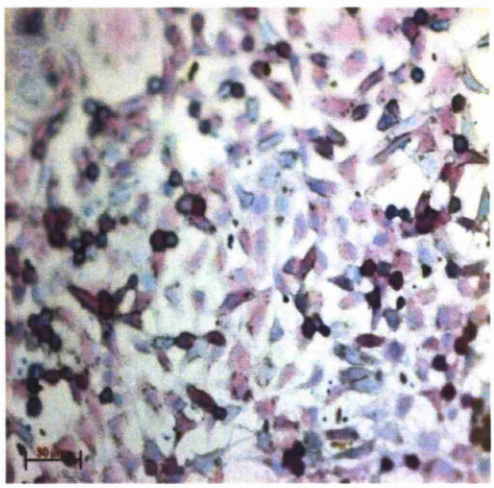

Figure 6.89 - **Dental pulp donor 4 cells (Passage 20) cultured in chemically-defined chondrogenic differentiation media for 21 days stained with Alcian blue (Blue) and counterstained with Nuclear fast red (Pink). Approximately 50% of dental pulp cells exhibited positive Alcian blue staining.**

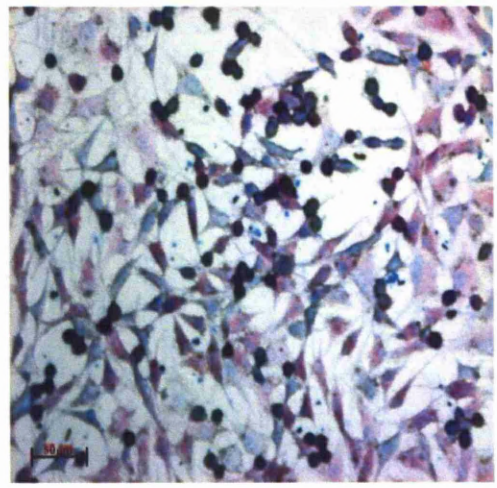

Figure 6.90 - **Dental pulp donor 4 cells (Passage 20) cultured in chemically-defined chondrogenic differentiation media for 21 days stained with Alcian blue (Blue) and counterstained with Nuclear fast red (Pink). Approximately 50% of dental pulp cells exhibited positive Alcian blue staining.**

However, whilst subpopulations of cells clearly demonstrated the ability to undertake chondrogenesis, the heterogeneous manner in which the population differentiated was clearly observed. *Figures 6.87* and *6.88* illustrate the round morphology associated with chondrocytes, although morphologically dissimilar cells appear within the population. Whilst it could be argued that topographical stress impacts significantly on the morphology, *Figures 6.89* and *6.90* clearly demonstrate that many cells were not generating glycosaminoglycans.

6.7.6 Osteogenic Differentiation of Pulp-derived Cells using Commercially Available Media

To investigate the ability of dental pulp-derived cells to differentiate towards an osteogenic lineage, 3 x 10^3 cells per well of a 24 well plate were induced with commercially available osteogenic media. The adipogenic repressor/osteogenic inducer CHOP was initially observed following 7 days of induction within approximately 80% of the population (*Figure 6.91*), allowing the synthesis of nuclear localised CBFA-1 within approximately 80% of the population following 14 days of culture (*Figure 6.92*). CBFA-1 production co-localised with the synthesis of Osteocalcin. Interestingly, the hypertrophic cartilage associated protein Collagen X was observed within approximately 40% of cells following 21 days of culture. Finally, Von Kossa staining confirmed the calcification of the extracellular matrix, a key function of osteogenic cells, within approximately 75% of cells following 28 days differentiation (*Figure 6.93*).

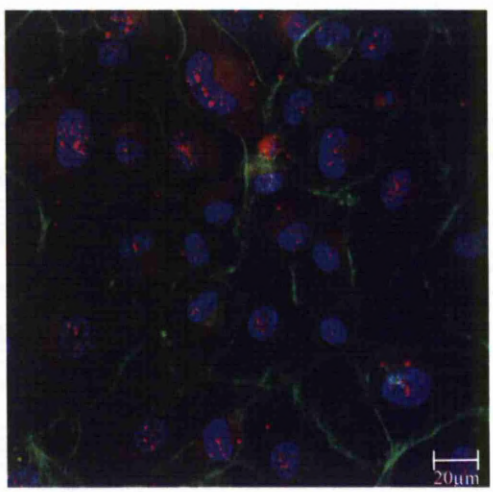

Figure 6.91 **- Dental pulp donor 1 cells (Passage 30) cultured in commercial osteogenic media for 7 days stained with Hoechst 33258 (blue), Oregon green (green) and CHOP antibody (red). Approximately 80% of dental pulp cells exhibited positive CHOP expression.**

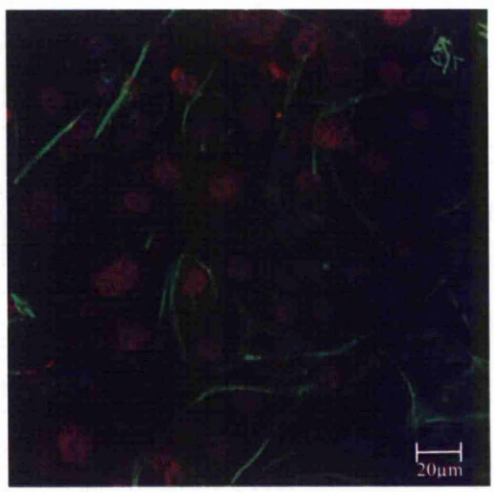

Figure 6.92 **- Dental pulp donor 3 cells (Passage 10) cultured in commercial osteogenic media for 14 days stained with Hoechst 33258 (blue), Oregon green (green) and CBFA-1 antibody (red). Approximately 80% of dental pulp cells exhibited positive CBFA-1 expression.**

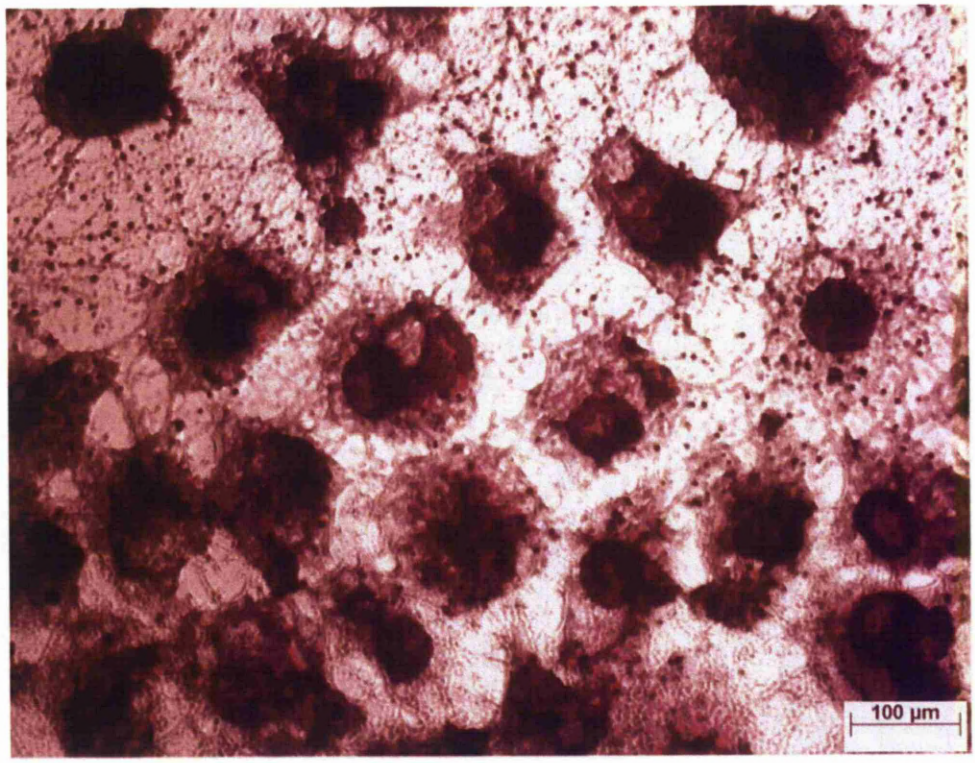

Figure 6.93 **- Dental pulp donor 1 cells (Passage 20) cultured in commercial osteogenic media for 28 days stained with Von Kossa (Dark brown) and counterstained with Harris' Hematoxylin. Approximately 75% of dental pulp cells exhibited positive Von Kossa staining.**

6.7.7 Osteogenic Differentiation of Pulp-derived Cells using Chemically-defined Media

Following the demonstration of dental pulp-derived cells differentiating towards an osteogenic phenotype following commercially available chemical induction, cells were cultured in a chemically-defined osteogenic differentiation alternative. Osteogenic master regulator CHOP protein was expressed in approximately 90% of the population following 7 days of culture (*Figure 6.94*), allowing the expression of CBFA-1 (*Figure 6.95*) and Osteocalcin (*Figure 6.96*) in approximately 80% of cells after 14 days. Collagen X was expressed in 50% of cells following 14 days of differentiation (*Figure 6.97*). Cells demonstrated morphological characteristics associated with osteoblasts (*Figures 6.98* and *6.99*), and calcification of the extracellular matrix was observed in approximately 75% of cells following 21 days of culture.

Figure 6.94 - **Dental pulp donor 1 cells (Passage 28) cultured in chemically-defined osteogenic media for 7 days stained with Hoechst 33258 (blue), Oregon green (green) and CHOP antibody (red). Approximately 90% of dental pulp cells exhibited positive CHOP expression.**

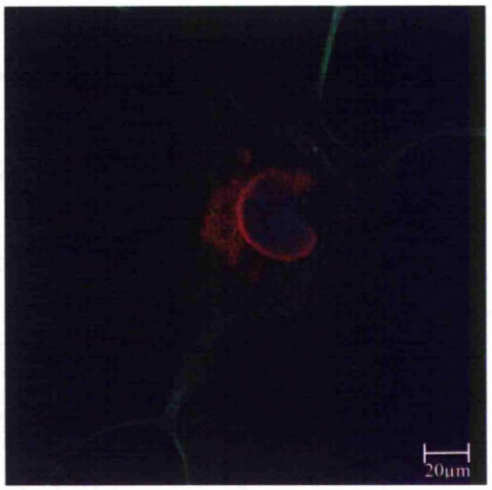

Figure 6.95 - **Dental pulp donor 2 cells (Passage 10) cultured in chemically-defined osteogenic media for 14 days stained with Hoechst 33258 (blue), Oregon green (green) and CBFA-1 antibody (red). Approximately 80% of dental pulp cells exhibited positive CBFA-1 expression.**

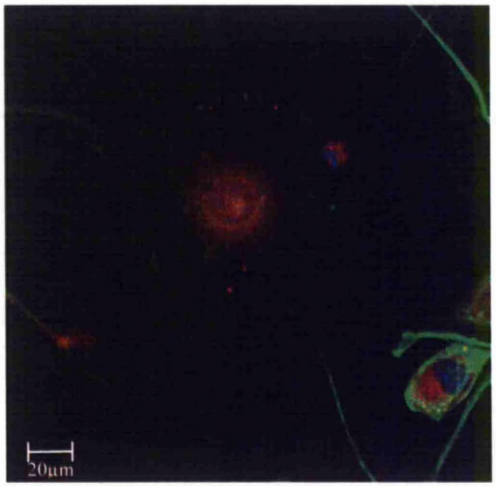

Figure 6.96 - **Dental pulp donor 1 cells (Passage 3) cultured in chemically-defined osteogenic media for 14 days stained with Hoechst 33258 (blue), Oregon green (green) and osteocalcin antibody (red). Approximately 80% of dental pulp cells exhibited positive osteocalcin expression.**

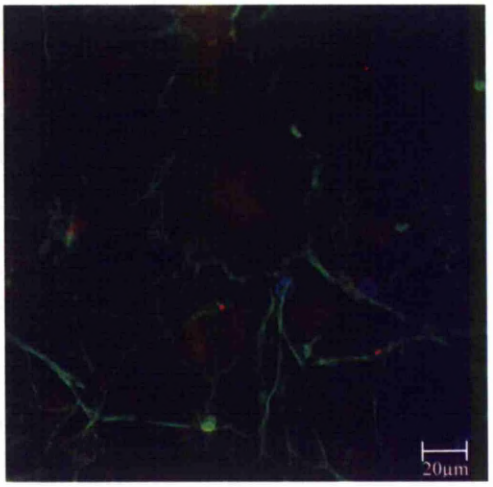

Figure 6.97 - **Dental pulp donor 1 cells (Passage 3) cultured in chemically-defined osteogenic media for 14 days stained with Hoechst 33258 (blue), Oregon green (green) and collagen X antibody (red). Approximately 50% of dental pulp cells exhibited positive collagen X expression.**

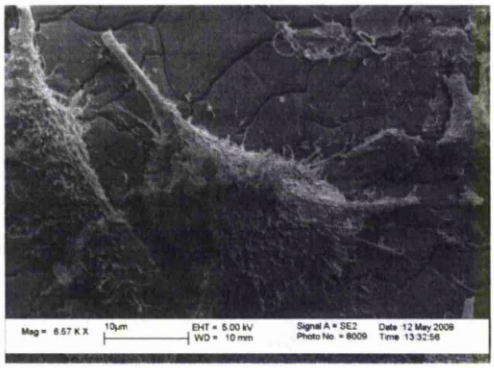

Figure 6.98 - **Dental pulp donor 2 cells (Passage 10) cultured in chemically-defined osteogenic differentiation media for 21 days.**

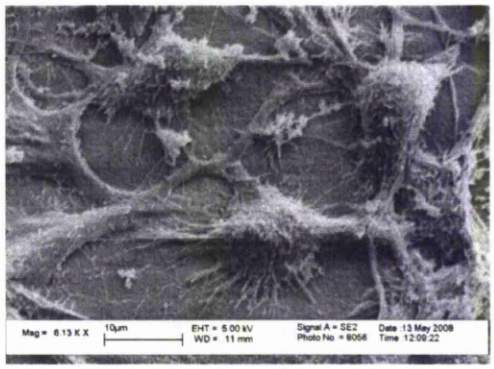

Figure 6.99 - **Dental pulp donor 3 cells (Passage 30) cultured in chemically-defined osteogenic differentiation media for 21 days.**

6.7.8 Neural Differentiation of Pulp-derived Cells using Commercially Available media

To establish the ability of cells within the dental pulp population to commit towards a neuronal lineage, 1% retinoic acid was added to basal culture media. 3 x 10^3 cells were cultured per well of a 24 well plate and exhibited morphological modifications towards the neuronal phenotype after 3 days. Phenotypically, approximately 80% of cells demonstrated production of beta-III-tubulin following 5 days of culture and maintained expression for the remainder of the 28 day culture period *(Figure 6.100)*, whilst thick and thin axon regulatory protein neurofilament was expressed in the nucleus of approximately 90% of cells following 21 days of culture (*Figure 6.101*). NGF functions within the survival and proliferation of neurons whilst furthermore regulating the formation of neurite projections, and was expressed in approximately 80% of the neuronally induced population post 7 days of culture (*Figure 6.102*). The NGF receptor p75 was expressed cytoplasmically within approximately 20% of the population following 21 days of culture (*Figure 6.103*), potentially regulating neuronal growth, migration, differentiation and apoptosis. However, whilst p75 is predominantly expressed by Schwann cells and neurons, this protein has also been detected in non-neuronal tissues, most notably within murine MSCs, and thus expression of this protein is not necessarily an indicator of the neuronal phenotype.

Tachykinin neuropeptide substance P is hypothesised to function as a transmitter of pain signals to the CNS *in vivo*, although has also been proposed to play roles in cellular growth *in vitro*. It is interesting, therefore, that approximately 70% of neuronally differentiated cells exhibited substance P expression following 21 days of culture (*Figure 6.104*), maintaining this expression until day 28.

Synaptic vesicle protein 2, a membrane glycoprotein expressed within the secretory vesicles of neuronal and endocrine cells and proposed to function as a key regulator of complex signalling, was expressed in approximately 60% of cells following 21 days of differentiation (*Figure 6.105*), further proposing a functional aspect of the differentiated population. Coinciding with synaptic vesicle 2 expression, synaptophysin, a synaptic vesicle protein present within almost all neurons in the brain, spinal cord and retina, was expressed within approximately 80% of the population following 21 days (*Figure 6.106*). Whilst the function of synaptophysin is not clearly understood, it is proposed to function through regulation of activity-dependent synapse formation. Of significant interest would now be to undertake dual staining with synaptophysin and synaptic vesicle protein 2 to ascertain whether such vesicles are in fact accommodating the neurotransmitter synaptophysin.

Interestingly, in addition to apparent neuronal differentiation, approximately 10% of cells demonstrated expression of the class III intermediate filament protein GFAP (*Figure 6.107*). GFAP is highly expressed in non-myelinating Schwann cells and functions to synthesise networks alleviating support and strength to neuronal cell axons.

Referring back to neuronal cells, morphological modifications observed following 14 days of culture (*Figures 6.108* to *6.109*) also indicated that neuronal differentiation had occurred.

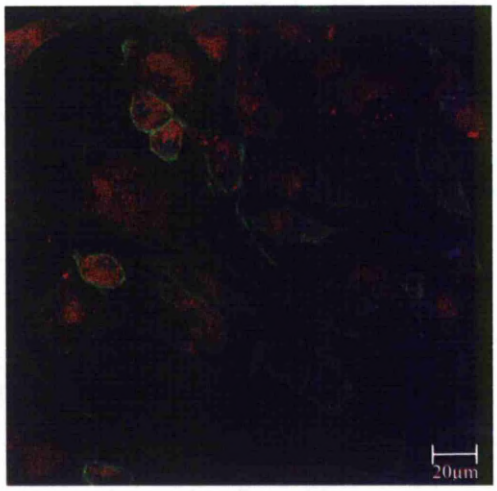

Figure 6.100 - **Dental pulp donor 3 cells (Passage 30) cultured in commercially available neural differentiation media for 21 days stained with Hoechst 33258 (blue), Oregon green (green) and beta-III-tubulin antibody (red). Approximately 80% of dental pulp cells exhibited positive beta-III-tubulin expression.**

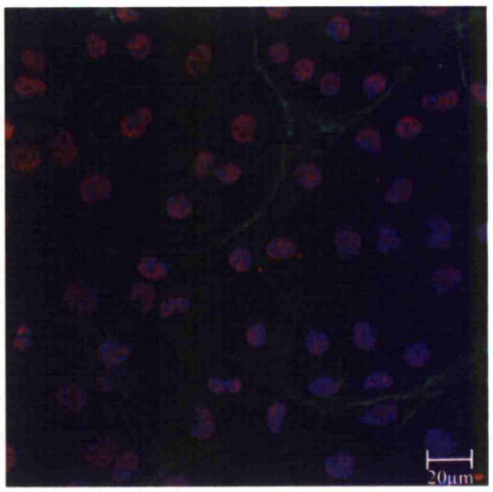

Figure 6.101 - **Dental pulp donor 3 cells (Passage 8) cultured in commercially available neural differentiation media for 21 days stained with Hoechst 33258 (blue), Oregon green (green) and neurofilament antibody (red). Approximately 90% of dental pulp cells exhibited positive neurofilament expression.**

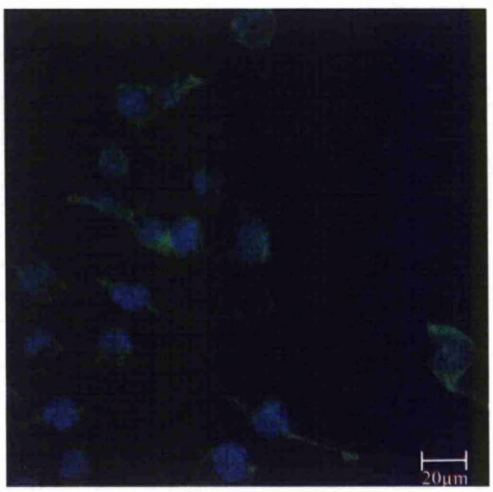

Figure 6.102 - **Dental pulp donor 3 cells (Passage 8) cultured in commercially available neural differentiation media for 7 days stained with Hoechst 33258 (blue) and NGF antibody (green). Approximately 80% of dental pulp cells exhibited positive NGF expression.**

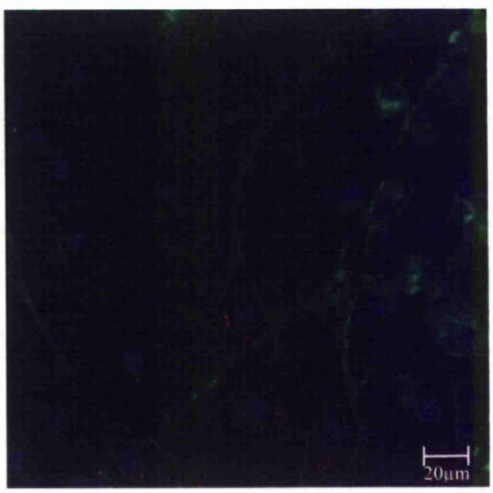

Figure 6.103 - **Dental pulp donor 3 cells (Passage 8) cultured in commercially available neural differentiation media for 21 days stained with Hoechst 33258 (blue), Oregon green (green) and p75 antibody (red). Approximately 20% of dental pulp cells exhibited positive p75 expression.**

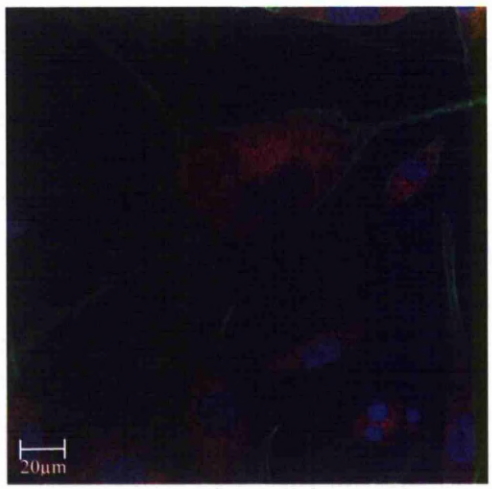

Figure 6.104 - **Dental pulp donor 1 cells (Passage 30) cultured in commercially available neural differentiation media for 21 days stained with Hoechst 33258 (blue), Oregon green (green) and substance P antibody (red). Approximately 70% of dental pulp cells exhibited positive substance expression.**

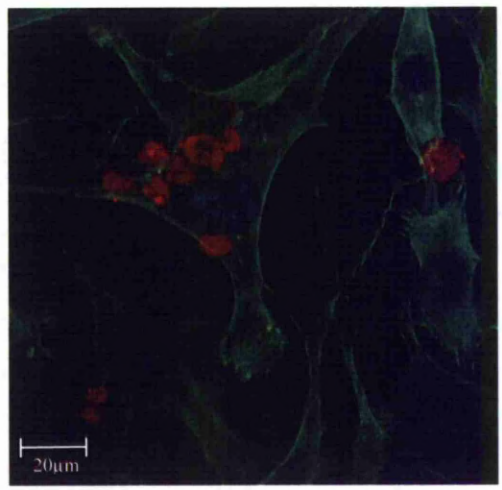

Figure 6.105 - **Dental pulp donor 3 cells (Passage 3) cultured in commercially available neural differentiation media for 21 days stained with Hoechst 33258 (blue), Oregon green (green) and synaptic vesicle protein 2 antibody (red). Approximately 60% of dental pulp cells exhibited positive synaptic vesicle 2 expression.**

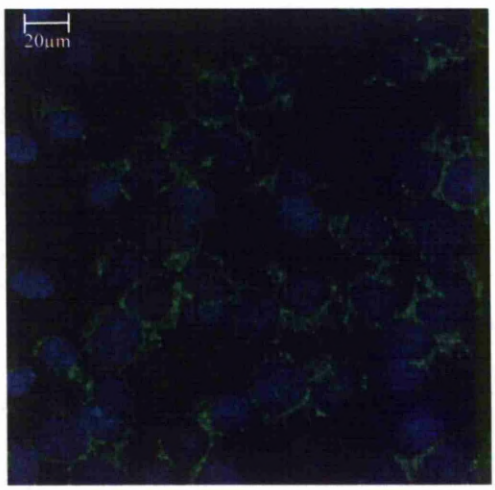

Figure 6.106 - **Dental pulp donor 3 cells (Passage 8) cultured in commercially available neural differentiation media for 21 days stained with Hoechst 33258 (blue) and synaptophysin antibody (green). Approximately 80% of dental pulp cells exhibited positive synaptophysin expression.**

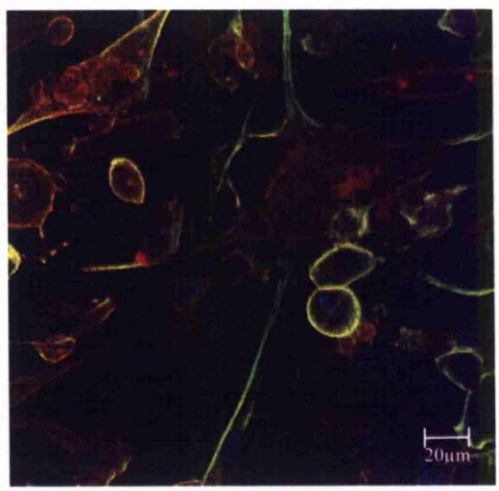

Figure 6.107 - **Dental pulp donor 3 cells (Passage 8) cultured in commercially available neural differentiation media for 21 days stained with Hoechst 33258 (blue) and GFAP antibody (green). Approximately 10% of dental pulp cells exhibited positive GFAP expression.**

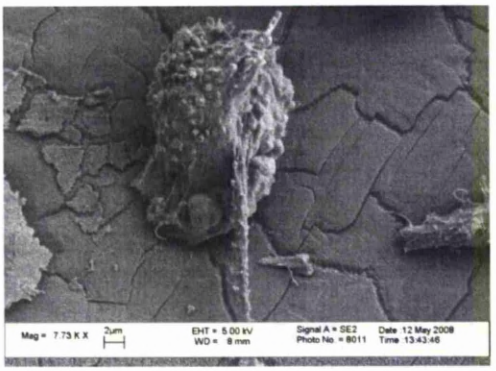

Figure 6.108 - **Dental pulp donor 3 cells (Passage 30) cultured in commercially available differentiation media for 14 days.**

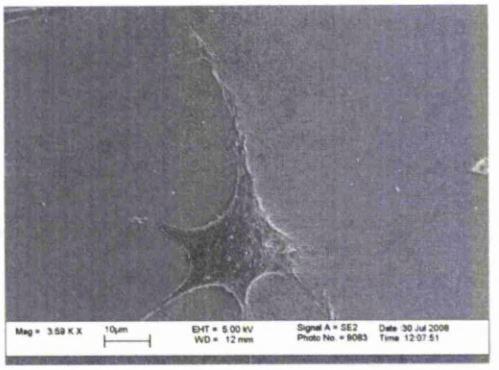

Figure 6.109 - **Dental pulp donor 4 cells (Passage 30) cultured in commercially available differentiation media for 14 days.**

6.7.9 Neural Differentiation of Pulp-derived Cells using Chemically-defined Media

Given the capability of dental pulp-derived populations to undertake neuronal differentiation following exposure to retinoic acid, 3 x 10^3 cells from varying donor and passage were cultured in a chemically-defined, serum-free alternative. Neuronal developmental protein beta-III-tubulin was expressed in approximately 80% of the population following 5 days of neuronal culture and expression was maintained throughout the 28 day period (*Figure 6.110*), comparable with the nuclear-specific expression of axon development regulator neurofilament (*Figure 6.111*). Neuronal reparative protein NGF was expressed in approximately 70% of neuronally induced cells following 21 days (*Figure 6.112*), whilst it's receptor p75 was expressed in approximately 20% of the (*Figure 6.113*).

Proposed pain transmission protein substance P was expressed in approximately 70% of the population following 21 days of culture (*Figure 6.114*) and was maintained until day 28. Functionality of the cells was further confirmed by the presence of synaptic vesicle 2 protein in approximately 60% of cells (*Figure 6.115*), with its hypothesised resident protein synaptophysin expressed by approximately 80% of the population (*Figure 6.116*).

Consistent with commercially-induced neuronal differentiation, chemically-defined stimulus conferred subpopulations comprising approximately 10% of the total population to express the Schwann cell-associated protein GFAP (*Figure 6.117*) following 21 days of differentiation.

Referring to cells expressing neuronal-associated proteins, numerous subpopulations displayed morphological features associated with a neuronal phenotype, procuring an elongated morphology with axon-like projections (*Figures 6.118* and *6.119*).

Figure 6.110 **- Dental pulp donor 3 cells (Passage 8) cultured in chemically-defined neural differentiation media for 21 days stained with Hoechst 33258 (blue), Oregon green (green) and beta-III-tubulin antibody (red). Approximately 80% of dental pulp cells exhibited positive beta-III-tubulin expression.**

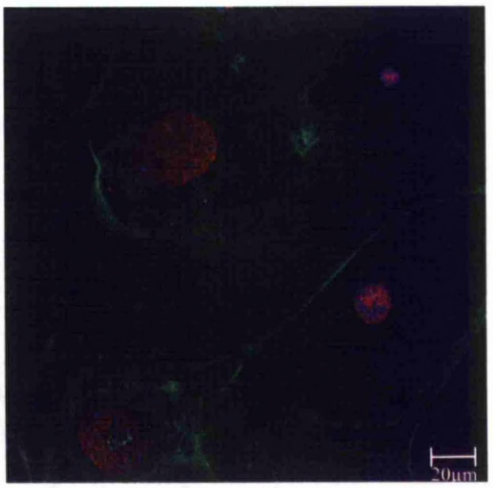

Figure 6.111 **- Dental pulp donor 2 cells (Passage 10) cultured in chemically-defined neural differentiation media for 21 days stained with Hoechst 33258 (blue), Oregon green (green) and neurofilament antiobody (red). Approximately 80% of dental pulp cells exhibited positive neurofilament expression.**

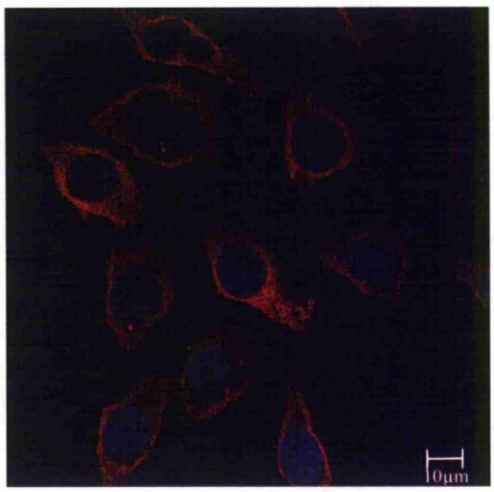

Figure 6.112 - **Dental pulp donor 2 cells (Passage 8) cultured in chemically-defined neural differentiation media for 21 days stained with Hoechst 33258 (blue) and NGF antibody (red). Approximately 70% of dental pulp cells exhibited positive NGF expression.**

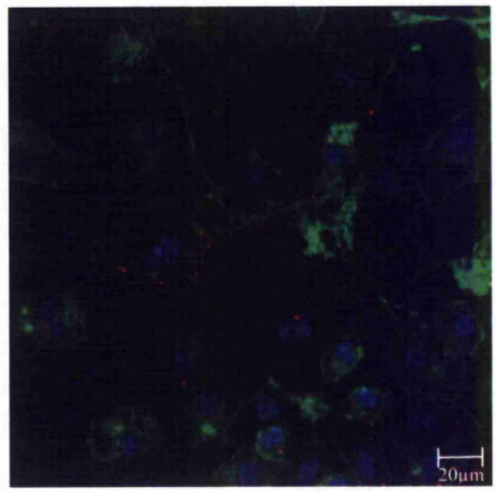

Figure 6.113 - **Dental pulp donor 3 cells (Passage 8) cultured in chemically-defined neural differentiation media for 21 days stained with Hoechst 33258 (blue), Oregon green (green) and p75 antibody (red). Approximately 20% of dental pulp cells exhibited positive p75 expression.**

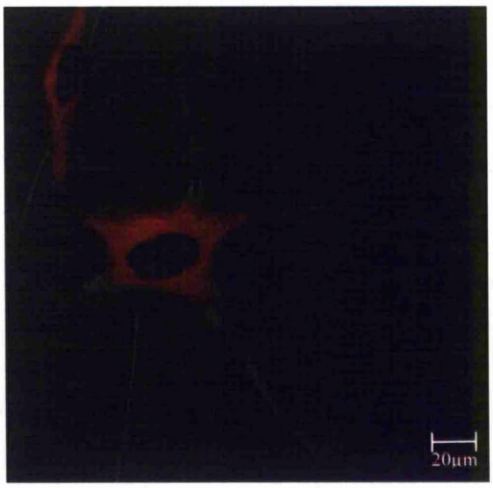

Figure 6.114 - **Dental pulp donor 3 cells (Passage 30) cultured in chemically-defined neural differentiation media for 21 days stained with Hoechst 33258 (blue), Oregon green (green) and substance P antibody (red). Approximately 70% of dental pulp cells exhibited positive substance P expression.**

Figure 6.115 - **Dental pulp donor 4 cells (Passage 15) cultured in chemically-defined neural differentiation media for 21 days stained with Hoechst 33258 (blue), Oregon green (green) and synaptic vesicle protein 2 antibody (red). Approximately 60% of dental pulp cells exhibited positive synaptic vesicle protein 2 expression.**

Figure 6.116 - **Dental pulp donor 3 cells (Passage 30) cultured in chemically-defined neural differentiation media for 21 days stained with Hoechst 33258 (blue), Oregon green (green) and synaptophysin antibody (red). Approximately 80% of dental pulp cells exhibited positive synaptophysin expression.**

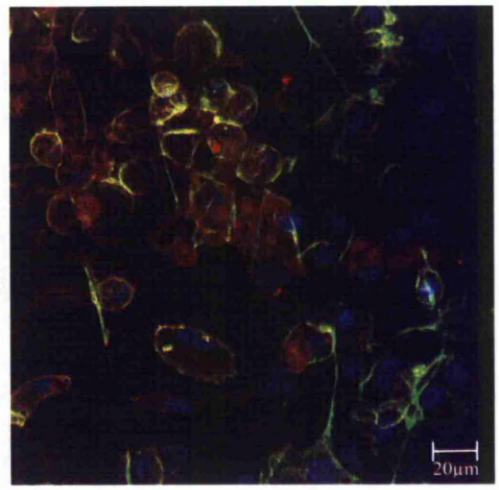

Figure 6.117 - **Dental pulp donor 1 cells (Passage 5) cultured in chemically-defined neural differentiation media for 21 days stained with Hoechst 33258 (blue) and GFAP antibody (red). Approximately 10% of dental pulp cells exhibited positive GFAP expression.**

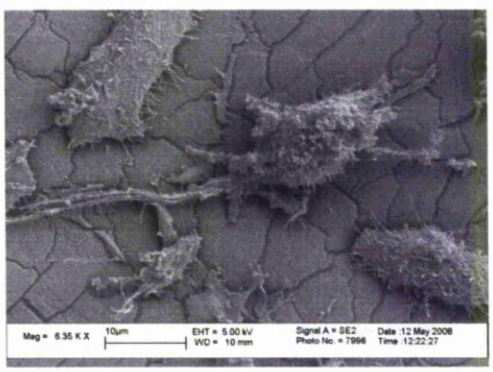

Figure 6.118 - **Dental pulp donor 2 cells (Passage 10) cultured in chemically-defined differentiation media for 14 days.**

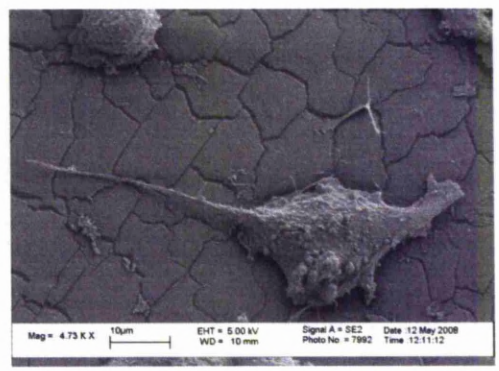

Figure 6.119 - **Dental pulp donor 4 cells (Passage 23) cultured in chemically-defined differentiation media for 14 days.**

6.7.10 Hepatic Differentiation of Pulp-derived Cells using Chemically-defined Media

Whilst the ability to undertake neuronal differentiation after appropriate stimulation would suggest plasticity within the dental pulp population, the relative simplicity of neuronal lineage progression may in fact be due to the presence of neuronal progenitors predisposed to the niche following development of the neural crest. However, given the expression profiling of the population, in particular the

expression of plasticity maintaining proteins such as Oct4 and Sox2, it was hypothesised that the dental pulp contained a primitive population capable of multi- if not pluri- potent differentiation. Therefore, to definitively demonstrate an ability to differentiate towards lineages not associated with the neural crest, pulp-derived populations were induced with chemically-defined hepatic differentiation media.

3 x 10^3 cells were cultured in hepatic chemically-defined differentiation media for 21 days. In this instance, culture media removed at days 1, 3, 5, 7, 14 and 21 was retained for ELISA assaying. The major secretory product of hepatic cells *in vivo* is serum albumin, and cells cultured in hepatic differentiation media secreted increased levels of serum albumin into the culture media compared with basal cultures, whose aspirate were also assessed, over the 21 culture period. (*Figure 6.120*). Furthermore, expression of serum albumin in approximately 70% of hepatically induced cells was observed by immunohistochemistry following 21 days of culture (Figures *6.121* and *6.122*).

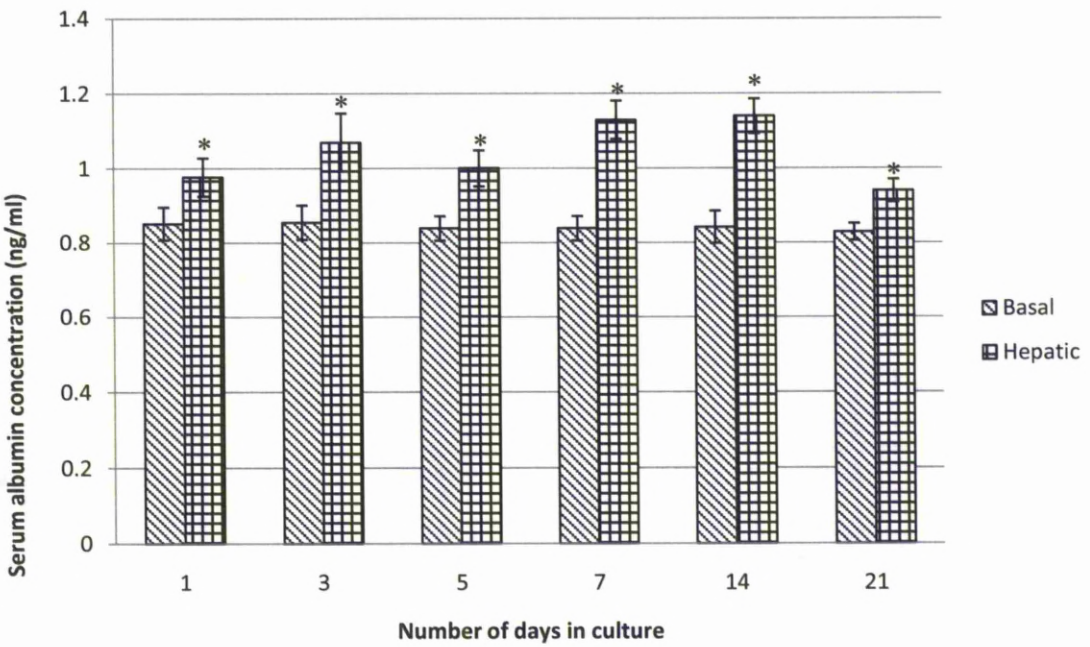

***Figure 6.120* – ELISA quantification of human serum albumin concentration in culture media aspirated from human dental pulp donor 1 cells (Passage 8; 0 x Freeze-thaw cycles) maintained in chemically-defined basal and hepatic conditions. Values represent mean concentrations (n = 4) of serum albumin in each basal and hepatic cultures. Error bars correspond to Standard Deviations. Student *t*-test indicated that increased serum albmin concentrations observed in hepatic cultures were significant compared with basal cultures (*=p≤0.001).**

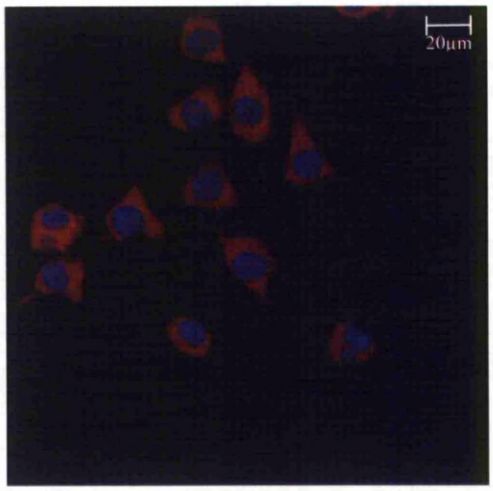

Figure 6.121 **- Dental pulp donor 1 cells (Passage 8) cultured in chemically-defined hepatic differentiation media for 21 days stained with Hoechst 33258 (blue), Oregon green (green) and serum albumin antibody (red). Approximately 70% of dental pulp cells exhibited positive serum albumin expression.**

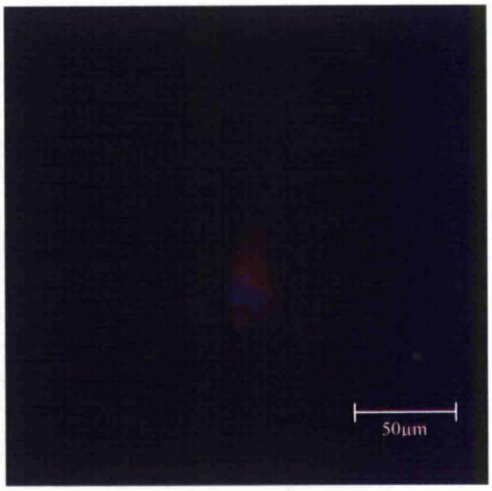

Figure 6.122 **- Dental pulp donor 2 cells (Passage 20) cultured in chemically-defined hepatic differentiation media for 21 days stained with Hoechst 33258 (blue), Oregon green (green) and serum albumin antibody (red). Approximately 70% of dental pulp cells exhibited positive serum albumin expression.**

Approximately 70% of hepatically induced dental pulp populations also expressed the fetal liver developmental-associated α-fetoprotein (*Figure 6.123*), which is hypothesised to function in a similar manner to serum albumin within the developing fetus. *In vivo* α-fetoprotein expression gradually reduces post-natally, although limited expression is maintained within the adult human.

In conclusion chemically-defined hepatic induction of dental pulp-derived populations infers a morphological (*Figure 6.124*) and functional hepatic phenotype in subpopulations of the culture. Furthermore, the expression of α-fetoprotein furthers the hypothesis that a subset of dental pulp-derived cells are of a primitive embryonic like nature.

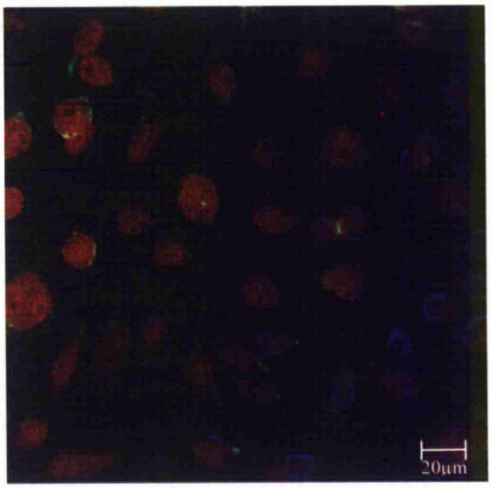

Figure 6.123 - **Dental pulp donor 2 cells (Passage 20) cultured in chemically-defined hepatic differentiation media for 21 days stained with Hoechst 33258 (blue), Oregon green (green) and α-fetoprotein antibody (red). Approximately 70% of dental pulp cells exhibited positive α-fetoprotein expression.**

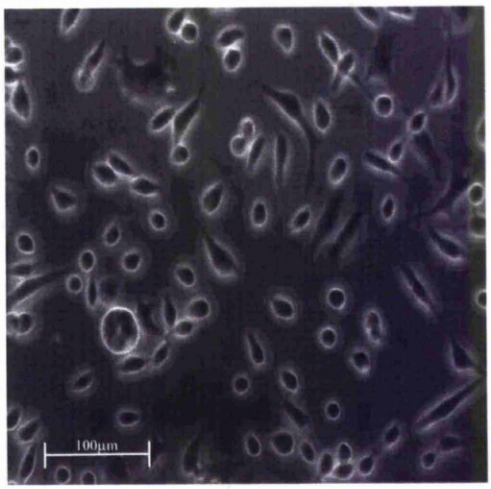

Figure 6.124 - **Dental pulp donor 2 cells (Passage 20) cultured in chemically-defined hepatic differentiation media for 21 days.**

6.8 Antibody-based Purification of Dental Pulp Cells

6.8.1 Purification of Dental Pulp Subpopulations based on Surface Expression Profiling using High Speed Cell Sorting

Whilst dental pulp-derived cell populations demonstrated a maintained proliferative and differentiation capacity throughout prolonged *in vitro* culture, heterogeneity within the population was readily observed. Whilst many studies dismiss the influence of such heterogeneity in a clinical setting, many progenitor cells are pre-committed towards a given lineage, and may therefore spontaneously undertake commitment towards terminal differentiation. Considering a stem cell orientated approach to repair following myocardial infarction, utilisation of cells containing osteogenic-committed cells may result in the formation of mature osteoblasts within regions of the heart, with potentially fatal repercussions given their calcified matrices. It is therefore imperative that isolated cells intended for clinical application are assessed upon a homogeneous subpopulation basis as opposed to global population analysis. Acknowledging the impact of such progenitor subsets, dental

pulp-derived cells were sorted based on positive expression of surface antigens and phenotypically assessed post-sorting.

6.8.2 Purification of Heterogeneous Dental Pulp Populations based upon Differential Efflux of Hoechst 33342

Hoechst stained dental pulp populations from donors 1 and 3 were sorted at passages 8, 15 and 25. Purification of the side population (SP), which is hypothesised to represent a hematopoietic subpopulation of cells, is facilitated by the two binding modes of Hoechst 33342 which subsequently result in different spectral properties, allowing resolution of multiple populations via simultaneous assessment of two respective wavelengths. The SP was discriminated by differential efflux of the Hoechst dye by ABCG2, a multi-drug-like transporter pump, and a property characteristic of HSCs. Cells exhibiting such behaviour, which represented approximately 0.1% of the dental pulp population, were sorted and these $Hoechst^{Dull}$ populations sorted into a separate culture vessel.

$Hoechst^{Dull}$ sorted populations adhered to the TC plastic surface approximately 48 hours post-sorting and spontaneously generated colonies in the absence of erythropoietin stimulation (*Figure 6.125*). Despite purification based on a functional aspect associated with HSCs, colonies exhibited a heterogeneous morphology, containing small rounded cells, endothelial and fibroblastic-like cells, and multi-nuclear cells, suggesting that a number of cells actively regulate a functional ABCG2 pump. Nevertheless, following 12 days of culture independent colonies had proliferated and subsequently joined residing colonies to form a confluent monolayer of cells.

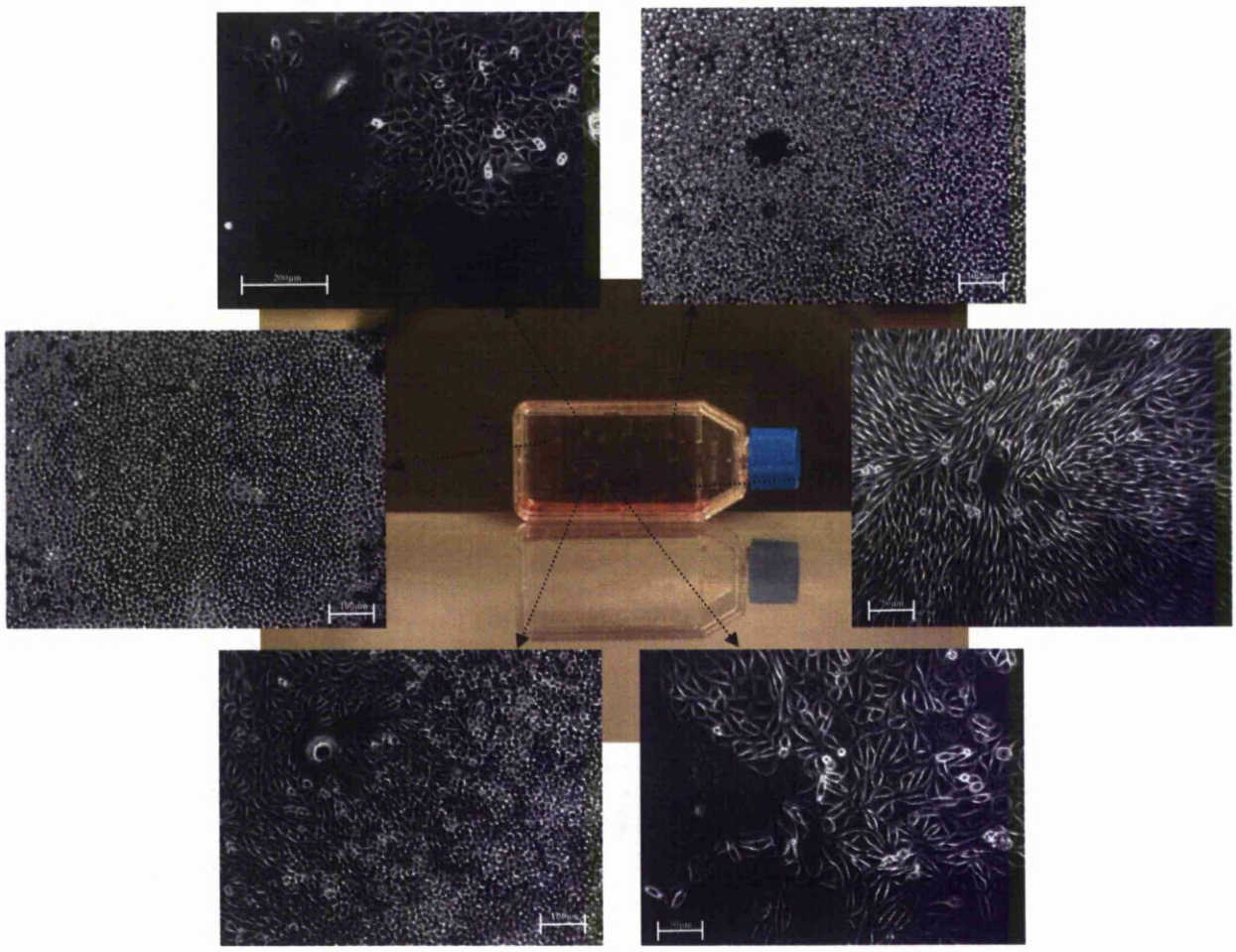

Figure 6.125 **- Pulp donor 1 (Passage 8) cells sorted of the basis of Hoechst^{Dull} efflux seeded in basal media and cultured for 48 hours post-sorting. Images are representive of cells present within the selected colony.**

Following confluence, Hoechst^{Dull} sorted populations were assessed by flow cytometry using an array of surface antigens (*Figure 6.126*). Furthermore, purified cells were seeded within a platelet-poor plasma-derived gel in order to assess their capability to form microvasculature, a further characteristic phenomena of HSCs. 5.0 x 10^{3} Hoechst^{Dull} cells suspended in commercial basal media were introduced onto the surface of the solidified gel and initiated the formation of microtubular-like structures following 5 days of culture (*Figures 6.127* and *6.128*). Following 14 days of culture, previously primitive structures were now densely formed microtubular-like vessels (*Figures 6.129* to *6.134*), an apparent differentiation which did not occur when cells were cultured on tissue culture plastic.

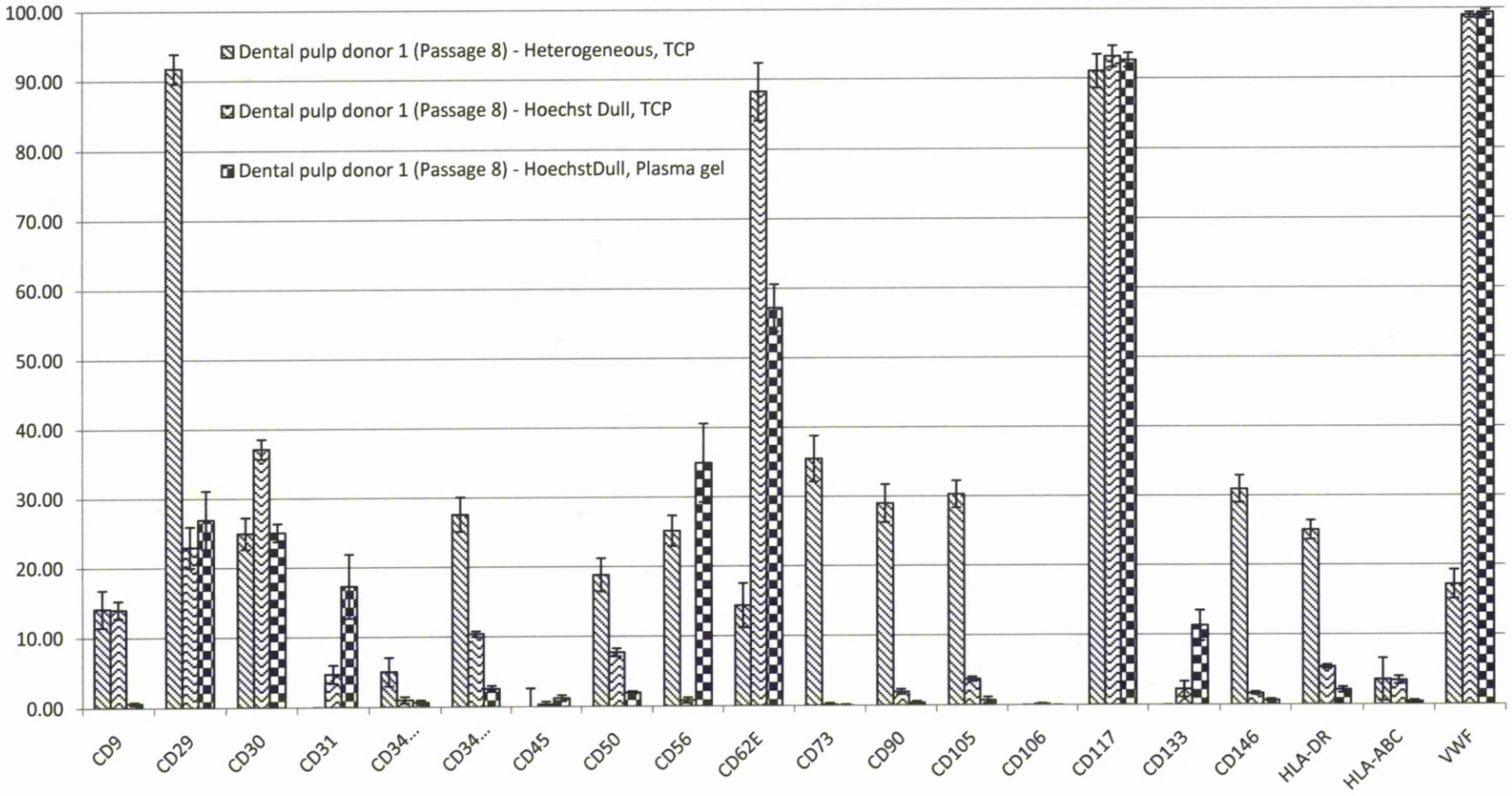

Figure 6.126 - **Flow cytometric analysis of heterogeneous and Hoechst^{Dull} sorted populations derived from pulp donor 1 (Passage 8) cells and cultured on tissue culture plastic (TCP) and platelet-poor plasma derived gel. Values represent mean positive expressions observed by flow cytometry (n = 4). Error bars correspond to Standard Deviations.**

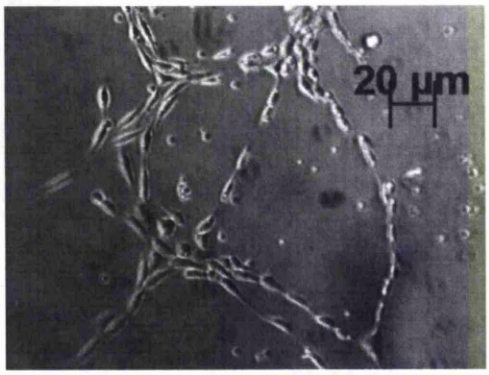

Figure 6.127 - **Hoechst^{Dull} purified dental pulp donor 1 cells (Passage 8) cultured for 5 days on plasma derived gel.**

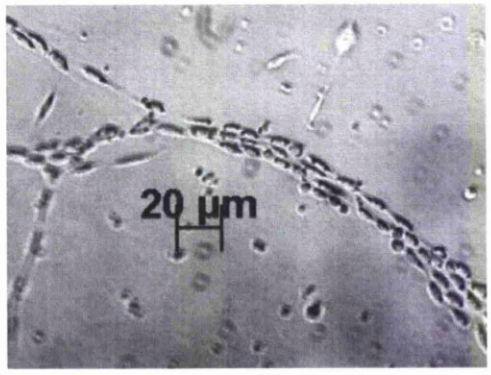

Figure 6.128 - **Hoechst^{Dull} purified dental pulp donor 1 cells (Passage 8) cultured for 5 days on plasma derived gel.**

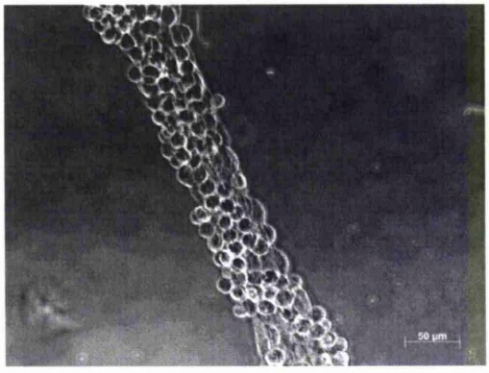

Figure 6.129 - **Hoechst^{Dull} purified dental pulp donor 1 cells (Passage 8) cultured for 14 days on plasma derived gel.**

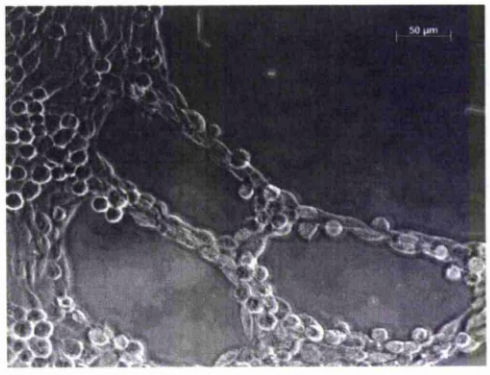

Figure 6.130 - **Hoechst^{Dull} purified dental pulp donor 1 cells (Passage 8) cultured for 14 days on plasma derived gel.**

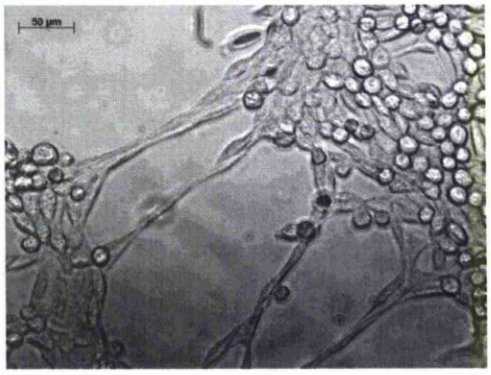

Figure 6.131 - **Hoechst^{Dull} purified dental pulp donor 3 cells (Passage 8) cultured for 14 days on plasma derived gel.**

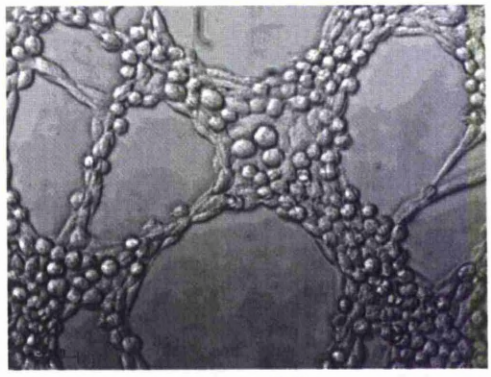

Figure 6.132 - **Hoechst^{Dull} purified dental pulp donor 3 cells (Passage 15) cultured for 14 days on plasma derived gel.**

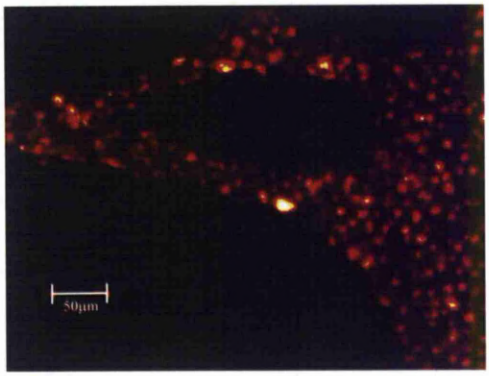

Figure 6.133 **- Hoechst^{Dull} purified dental pulp donor 1 cells (Passage 8) cultured for 14 days on plasma derived gel and stained with fluorescent cell tracking dye.**

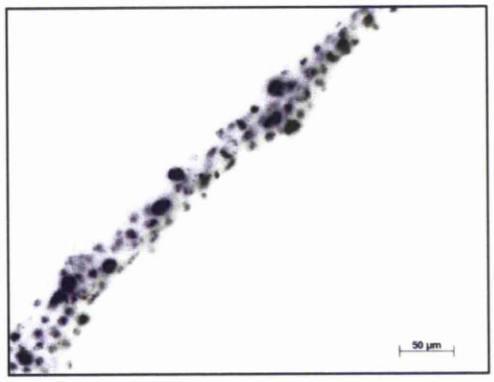

Figure 6.134 **- Hoechst^{Dull} purified dental pulp donor 1 cells (Passage 8) cultured for 14 days on plasma derived gel and stained with fluorescent cell tracking dye.**

Surface phenotyping of the populations revealed reduced upregulation of MSC-associated antigens in Hoechst^{Dull} purified cells but demonstrated an upregulation of endothelial-associated antigens CD31, CD62E, CD133 and VonWillebrand factor in both tissue culture plastic seeded and plasma-gel cultured populations. Both classes of CD34 demonstrated downregulation compared with the heterogeneous phenotype, suggesting that not all CD34^{+} cells represent HSCs and, furthermore, that not all HSCs express class of CD34. Furthermore, approximately 99% of plasma gel-cultured Hoechst^{Dull} cells cytoplasmically expressed VonWillebrand factor, as observed by immunohistochemistry (*Figure 6.135*), whilst this technique also revealed CD31 cytoplasmic and VE-Cadherin peripheral specific expression within approximately 90% of cells (*Figure 6.136*), thereby suggesting that this population of purified cells had differentiated to a mature endothelial phenotype.

However, whilst Hoechst^{Dull} purified populations demonstrated this phenotype immediately following cell sorting, cells cultured to a second passage post-sorting demonstrated a reversion to the heterogeneous phenotype associated with unsorted dental pulp cells. This reversion to a heterogeneous phenotype would suggest either that (i) Hoechst purification failed to adequately discriminate against varying subpopulations, allowing the culture of contaminate cell types not containing actively regulating ABCG2 pumps; (ii) Dental pulp-derived populations are incapable of homogeneous culture and subsequently re-establish the heterogeneic niche with which they reside *in vivo*. Whatever the reason, given the inability of the population to maintain phenotypic stability following sorting based upon Hoechst^{Dull}

discrimination, a small number of cells sorted on this basis were seeded onto TC plastic coverslips immediately post-sorting. Following culture in commercial basal media for 4 hours to allow adherence, cells were fixed and analysed using immunohistochemistry techniques to assess protein expression profiles of a majority subpopulation, thereby facilitating assessment of the Hoechst^{Dull} subpopulation before heterogeneity is re-established. Following rapid post-sort immunohistochemistry of adherent Hoechst^{Dull} cells, results demonstrated that the majority of adherent populations expressed the stem cell proliferation protein nucleostemin within their nucleus, whilst also cytoplasmically expressing the plasticity regulating proteins Oct4 and Sox2. Interestingly, Hoechst^{Dull} cells did not express the stem cell renewal protein Cripto-1; neither did they express the ES cell-associated protein Tra-1-81. RPE-lineage associated proteins MiTF and pax6 were not expressed within the population, nor were alternative neuronal lineage-associated proteins nestin, rest4 and TBR2. The adherent population also failed to express the MSC-associated protein STRO-1 (*Table 6.2* – Page 295).

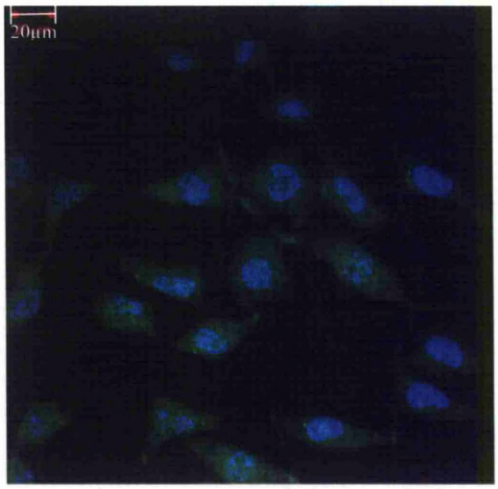

Figure 6.135 **- Hoechst^{Dull} dental pulp donor 1 cells (Passage 8) cultured for 14 days on plasma derived gel and stained with Hoechst 33342 (blue) and VonWillebrand factor antibody (green). Approximately 99% of dental pulp cells exhibited positive VonWillebrand expression.**

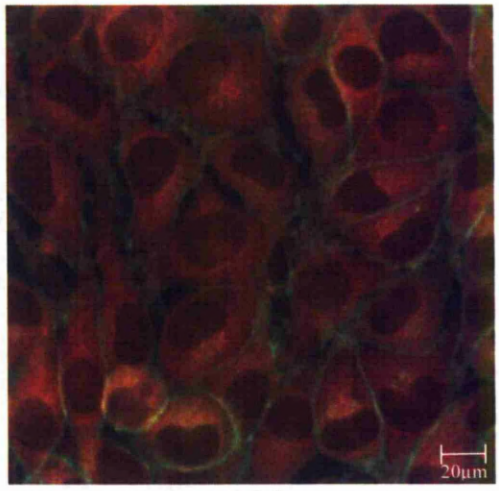

Figure 6.136 **- Hoechst^{Dull} dental pulp donor 1 cells (Passage 8) cultured for 14 days on plasma derived gel and stained with CD31 (red) and VE Cadherin antibody (green). Approximately 90% of dental pulp cells exhibited positive VE Cadherin and CD31 dual expression.**

6.8.3 Purification of Heterogeneous Dental Pulp Populations based upon Differential Expression of CD9

CD9 antigen expression has been reported on endothelial cells and ES cells amongst others. Dental pulp-derived cells exhibited approximately 10% - 20% positive CD9 expression within the population, and were purified on this basis. Cells exhibiting low positive expression of CD9, termed $CD9^{Dull}$, were purified and seeded in commercial basal media. Unlike $Hoechst^{Dull}$ derived cells, $CD9^{Dull}$ purified populations did not generate colonies on the TC plastic surface, exhibiting a heterogeneous morphology (*Figure 6.137*). Furthermore, upon confluence 10 days post-sorting, the population exhibited the heterogeneic phenotype associated with the unsorted pulp population. Purified cells seeded onto TC plastic coverslips were fixed following adherence and assessed using immunohistochemistry for their protein expressions. $CD9^{Dull}$ purified cells exhibited nuclear expression of stem cell renewal protein Cripto-1, with plasticity maintenance protein Sox2 also exhibiting nuclear expression. Stem cell proliferation protein nucleostemin was also expressed within the nucleus, although associated plasticity regulator Oct4 was expressed cytoplasmically. ES cell-associated protein Tra-1-81 was furthermore expressed within the cytoplasm of purified populations, indicating a primitive subpopulation. RPE-associated protein MiTF was expressed within the nucleus, whilst the more primitive RPE protein pax6 was expressed within the cytoplasm. Adherent cells expressed alternative neuronal-lineage associated proteins, rest4 and TBR2 expressed cytoplasmically. Interestingly though, cells did not express the neuronal progenitor-associated protein nestin. MSC-associated protein STRO-1 was also expressed cytoplasmically within the population (*Table 6.2* – Page 295).

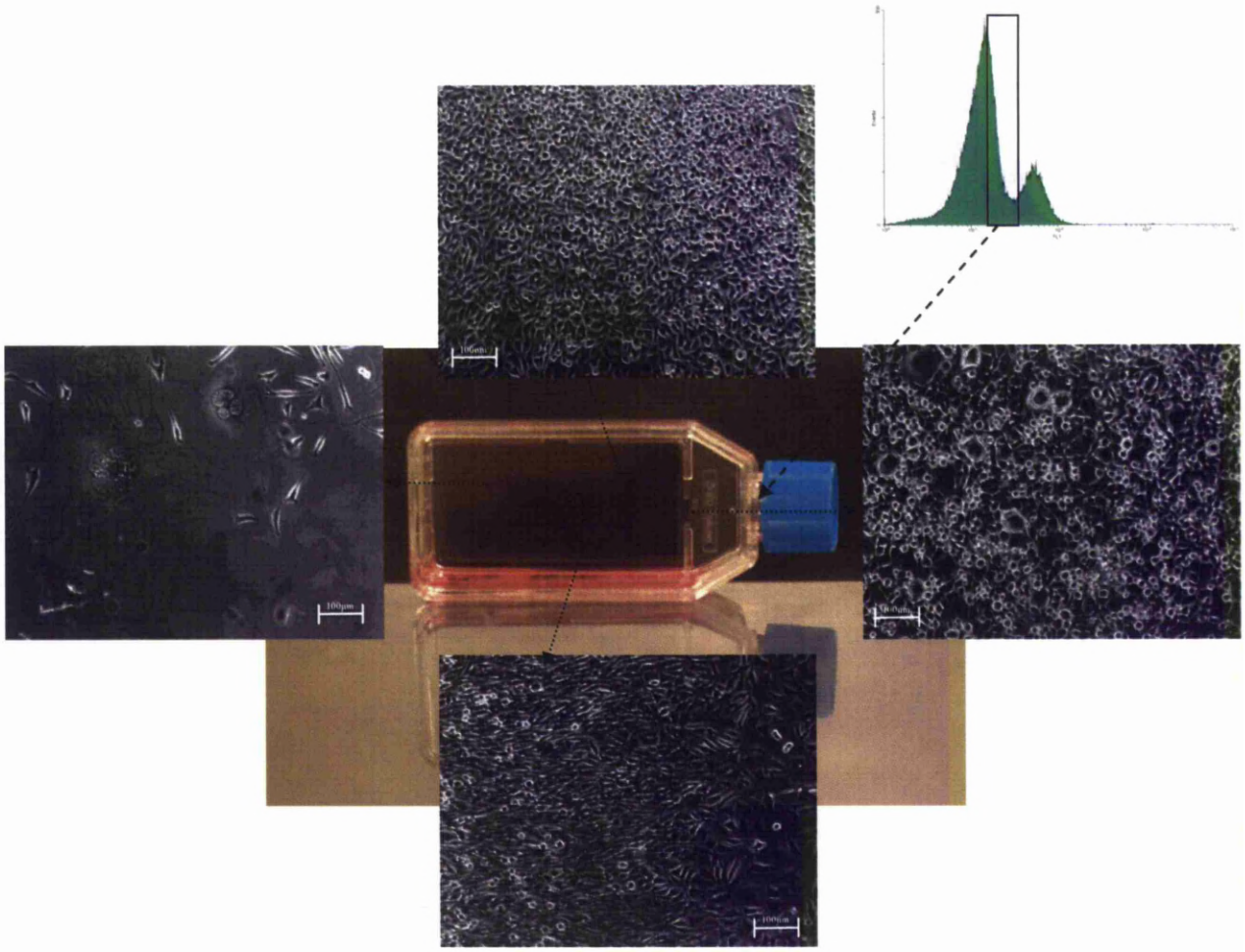

Figure 6.137 **- Pulp donor 1 (Passage 8) cells sorted of the basis of $CD9^{Dull}$ expression seeded in basal media and cultured for 48 hours post-sorting. Images are representive of cells present within the selected region.**

$CD9^{Light}$ expressing cells demonstrated populations exhibiting increased levels of CD9. Purified populations exhibited a heterogeneous morphology on seeding onto TC plastic although they did not form distinct colonies (*Figure 6.138*). Furthermore, upon confluence 14 days post-sorting and subsequent analysis by flow cytometry, the population exhibited the heterogeneous phenotype associated with dental pulp. Following seeding on TC plastic coverslips, $CD9^{Light}$ cells demonstrated the same protein expression profile as that observed with $CD9^{Dull}$ cells (*Table 6.2* – Page 295). In conclusion purification of dental pulp populations based upon CD9 failed to homogeneously purify populations, allowing contaminates which re-establish the heterogeneic phenotype.

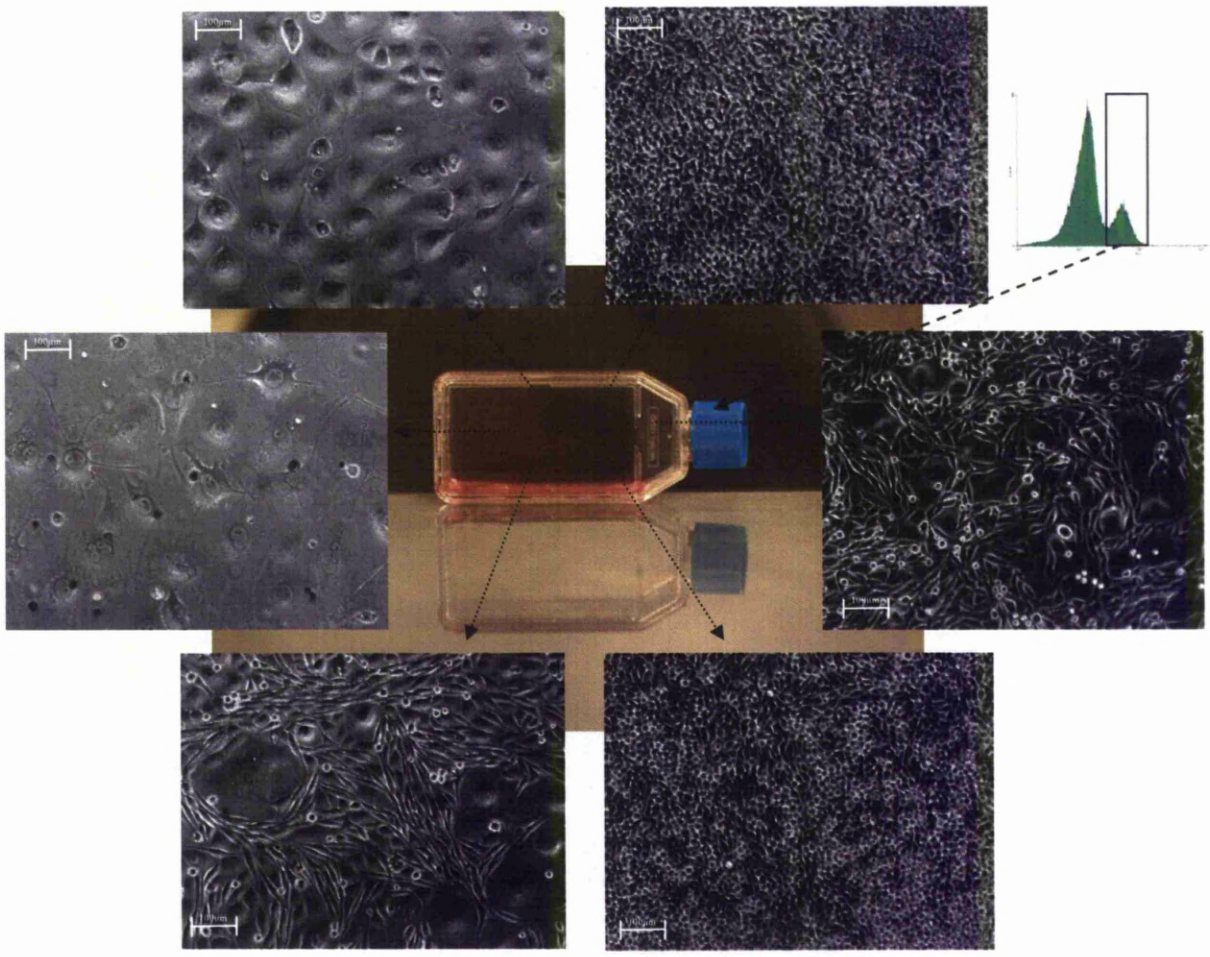

Figure 6.138 - **Pulp donor 1 (Passage 8) cells sorted of the basis of $CD9^{Light}$ expression seeded in basal media and cultured for 48 hours post-sorting. Images are representive of cells present within the selected region.**

6.8.4 Purification of Heterogeneous Dental Pulp Populations based upon Differential Expression of CD30

CD30 was expressed by approximately 25% - 40% of the population and represents a surface antigen predominantly expressed by embryonal carcinoma cells. $CD30^{Dull}$ cells, representing those populations with low expression of CD30, were purified and seeded in basal media on TC plastic. Cells exhibited a heterogeneous morphology and demonstrated the formation of colonies on the TC plastic surface (*Figure 6.139*). Following confluence 17 days post-sorting, surface antigen profile analysis revealed the heterogeneous phenotype associated with dental pulp cells.

Immunohistochemical phenotyping revealed that adherent cells 4 hours post-sorting demonstrated the nuclear expression of pluripotency regulators Oct4 and Sox2, with cells furthermore expressing Cripto-1 and Tra-1-81 within the cytoplasm. RPE progenitor protein pax6 was expressed within the cytoplasm of cells, whilst committed RPE progenitor protein MiTF was also cytoplasmically expressed. Alternative neuronal lineage-associated proteins rest4 and TBR2 were cytoplasmically expressed within the population, although nestin was not expressed. Cells exhibited nuclear expression of the stem cell proliferation protein nucleostemin, whilst furthermore exhibited cytoplasmic expression of the MSC-associated protein STRO-1 (*Table 6.2* – Page 295).

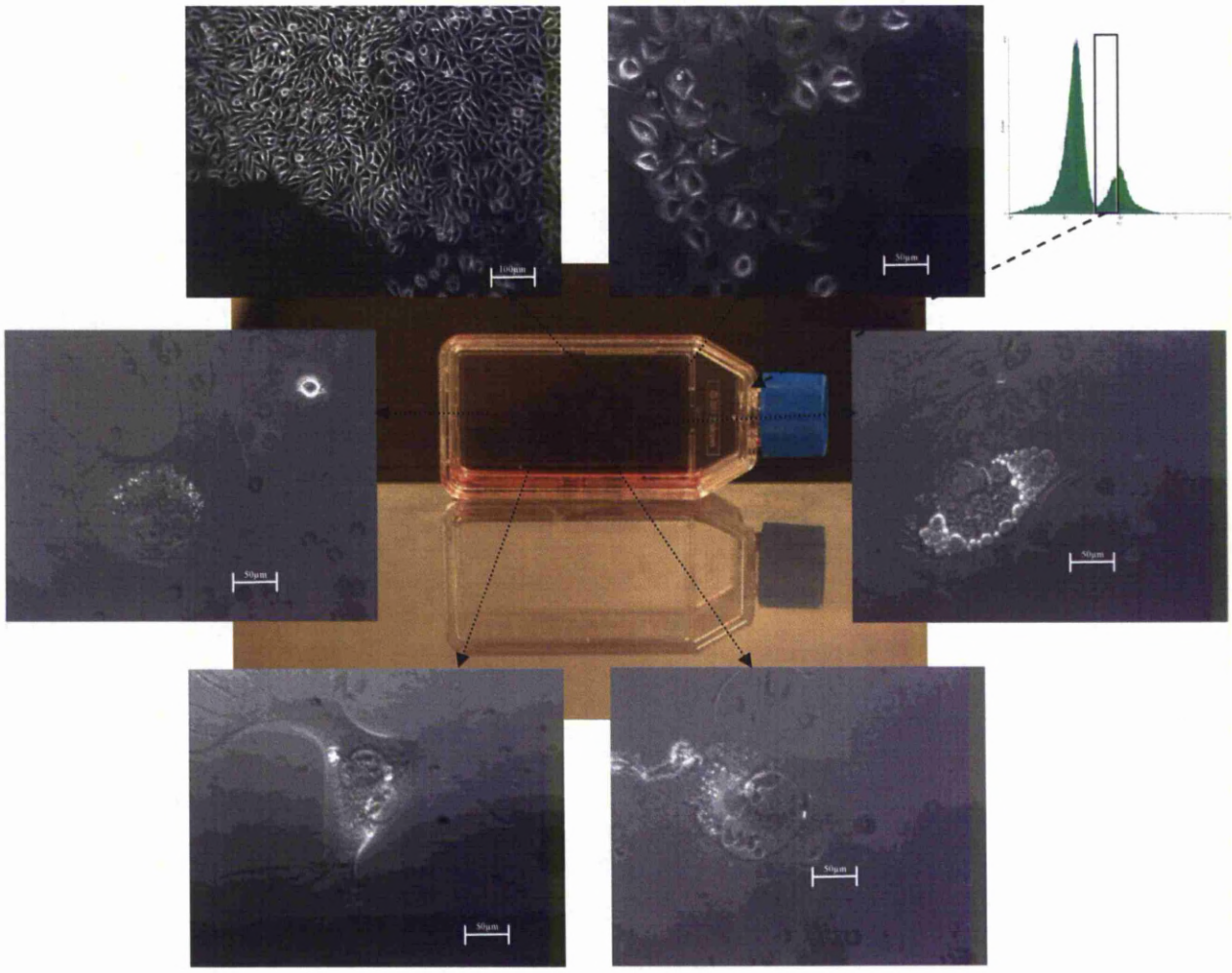

Figure 6.139 **- Pulp donor 1 (Passage 8) cells sorted of the basis of $CD30^{Dull}$ expression seeded in basal media and cultured for 48 hours post-sorting. Images are representive of cells present within the selected colony.**

$CD30^{Light}$ purified populations demonstrated distinct heterogeneity both morphologically (*Figure 6.140*) and phenotypically when observed using flow cytometry upon confluence 18 days post-sorting. Cells fixed following adherence demonstrated almost identical protein expression profiling compared with that observed within $CD30^{Dull}$ purified populations, the exception being the cytoplasmic expression of nestin within the population (*Table 6.2* – Page 295).

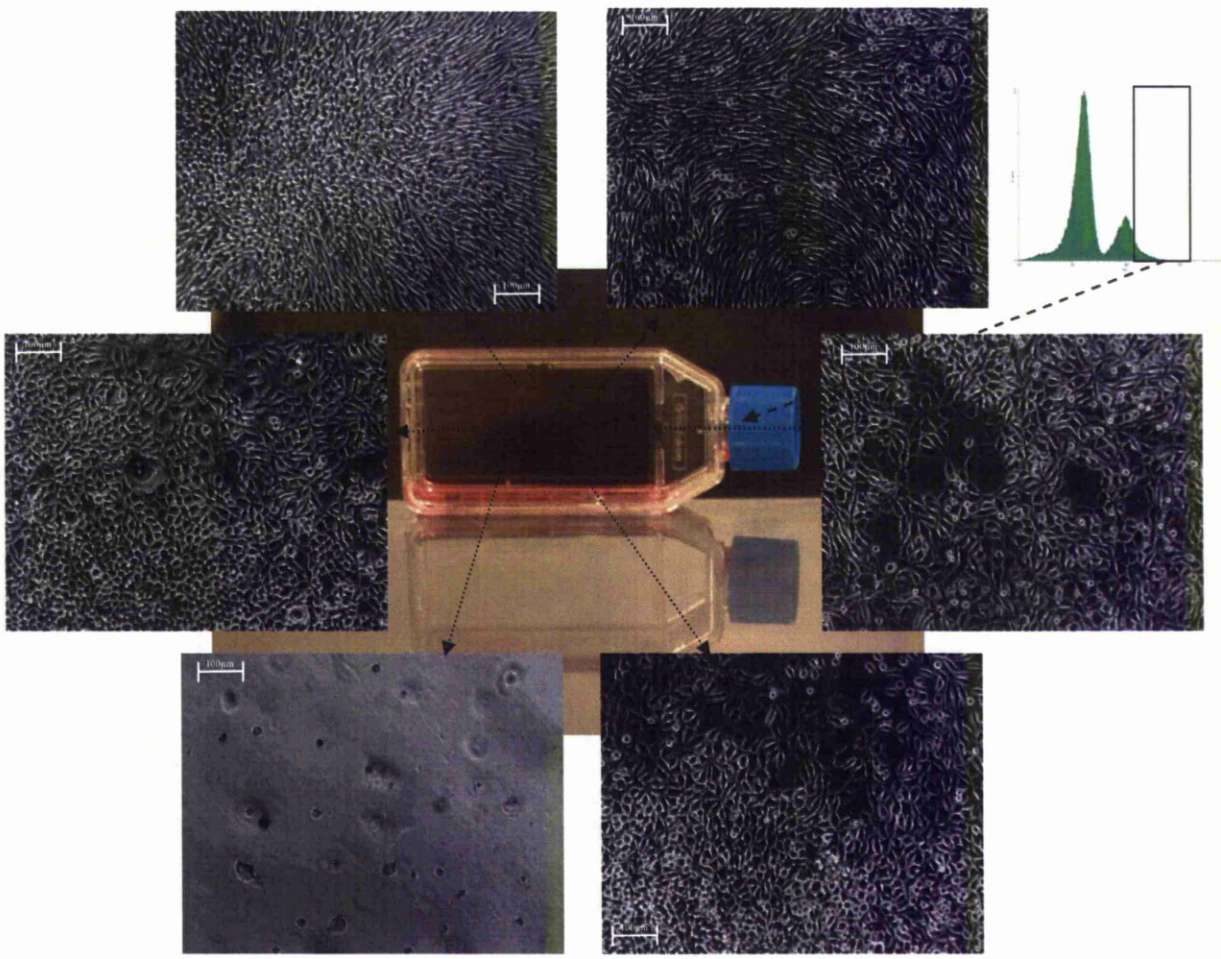

***Figure 6.140* - Pulp donor 1 (Passage 8) cells sorted of the basis of $CD30^{Light}$ expression seeded in basal media and cultured for 48 hours post-sorting. Images are representive of cells present within the selected region.**

6.8.5 Purification of Heterogeneous Dental Pulp Populations based upon Differential Expression of CD34 (Class III)

CD34 (Class III) represents an antigen largely associated with HSCs and was expressed by approximately 20% - 30% of dental pulp cells. $CD34^{Dull}$ purified populations did not form colonies on TC plastic adherence, with the cells demonstrating a heterogeneous morphology (*Figure 6.141*). This heterogeneity was further highlighted when the population was assessed using flow cytometry upon confluency 14 days post-sorting, with cells displaying the heterogeneous phenotype previously identified for dental pulp cells. Immunohistochemistry 4 hours post-sorting demonstrated that purified $CD34^{Dull}$ populations did not express proteins associated with plasticity or primitive ES cells, although the population did exhibit nuclear expression of nucleostemin and cytoplasmic expression of STRO-1. Interestingly, neural progenitor protein rest4 was expressed within the cytoplasm of the cells, although no expression of nestin or TBR2 could be detected (*Table 6.2* – Page 295).

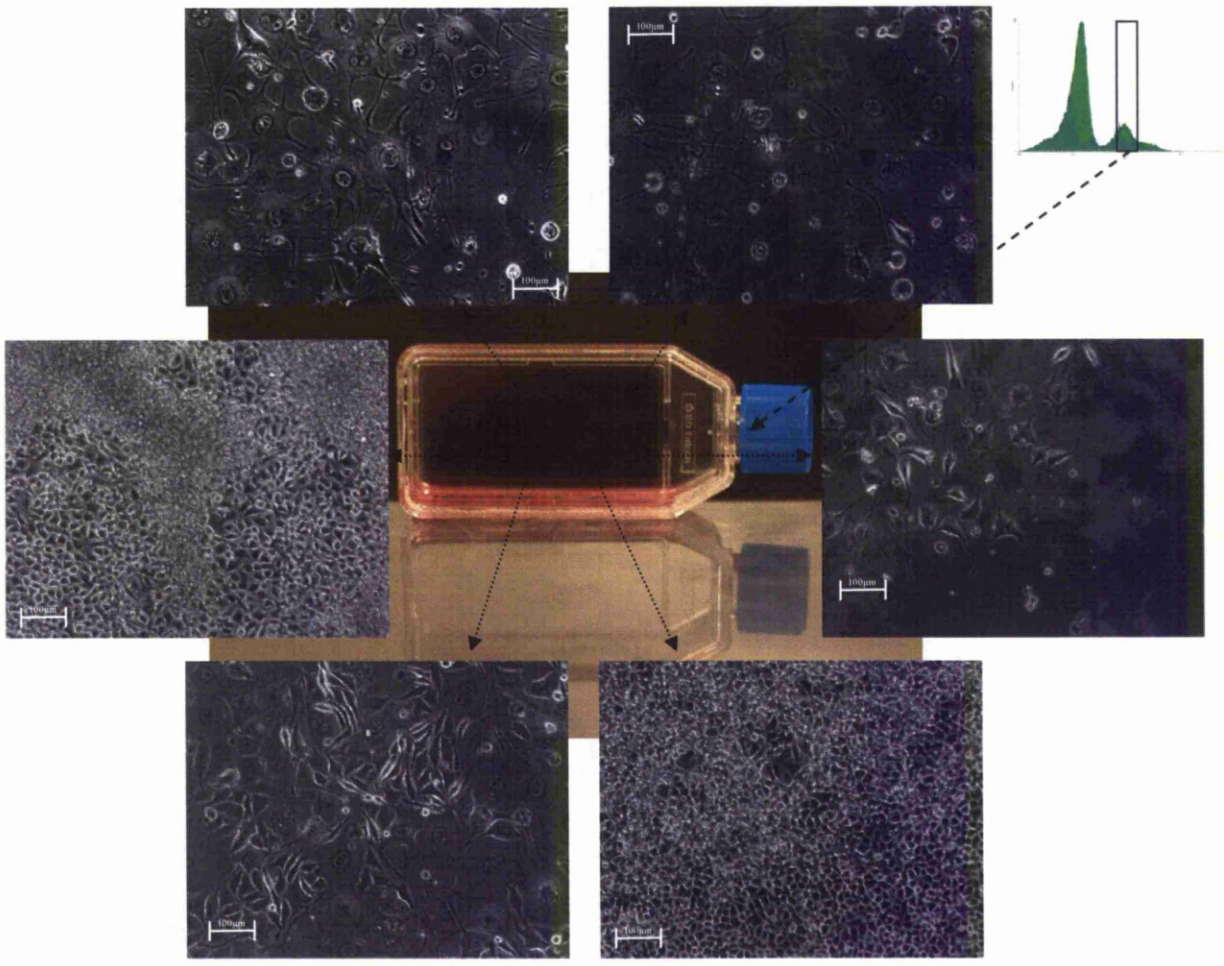

Figure 6.141 **- Pulp donor 1 (Passage 8) cells sorted of the basis of $CD34^{Dull}$ expression seeded in basal media and cultured for 48 hours post-sorting. Images are representive of cells present within the selected region.**

$CD34^{Light}$ purified populations generated numerous small heterogeneic colonies on adherence with the TC plastic substrate (*Figure 6.142*), although theyy demonstrated the heterogeneic phenotype associated with unsorted dental pulp cells when assessed using flow cytometry 14 days post-sorting. Immunohistochemical assessment 4 hours post-sorting revealed a similar expression profile to that observed within $CD34^{Dull}$ purified populations, although $CD34^{Light}$ populations exhibited nucleolar expression of the RPE protein MiTF and the cytoplasmic expression of the ES cell-associated protein Tra-1-81 (*Table 6.2* – Page 295).

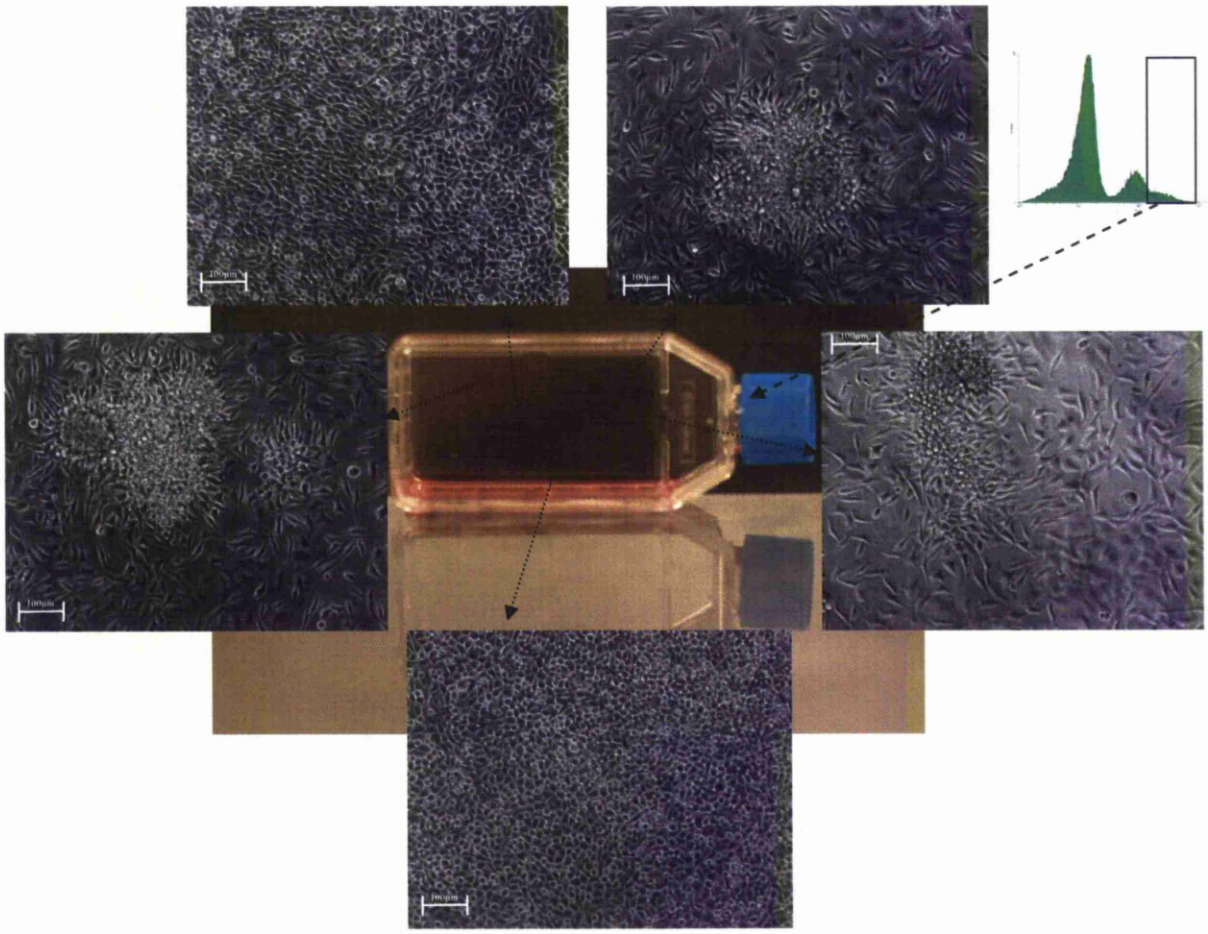

Figure 6.142 **- Pulp donor 1 (Passage 8) cells sorted of the basis of CD34^{Light} expression seeded in basal media and cultured for 48 hours post-sorting. Images are representive of cells present within the selected colony.**

6.8.6 Purification of Heterogeneous Dental Pulp Populations based upon Differential Expression of CD50

Leukocyte adhesion antigen CD50 was expressed by approximately 10% - 20% of dental pulp cells which were subsequently purified. CD50^{Dull} populations generated distinct colonies on adherence to the TC plastic substrate, although the colonies demonstrated distinct heterogeneity (*Figure 6.143*), with further confirmed when the population was assessed using flow cytometry upon of confluence 11 days post-sorting. Whilst cells displayed the heterogeneic phenotype associated with non-purified dental pulp cells, immunohistochemistry of adherent cells 4 hours post-sorting demonstrated cytoplasmic expression of MiTF and pax6, indicating an RPE-

associated cell type. Furthermore, neuronal proteins rest4 and TBR2 were cytoplasmically expressed, although nestin was not detected. Interestingly, whilst STRO-1 and nucleostemin were observed in the cytoplasm and nucleus respectively, plasticity regulatory proteins Cripto-1, Oct4 and Sox2 were not expressed (*Table 6.2* – Page 295).

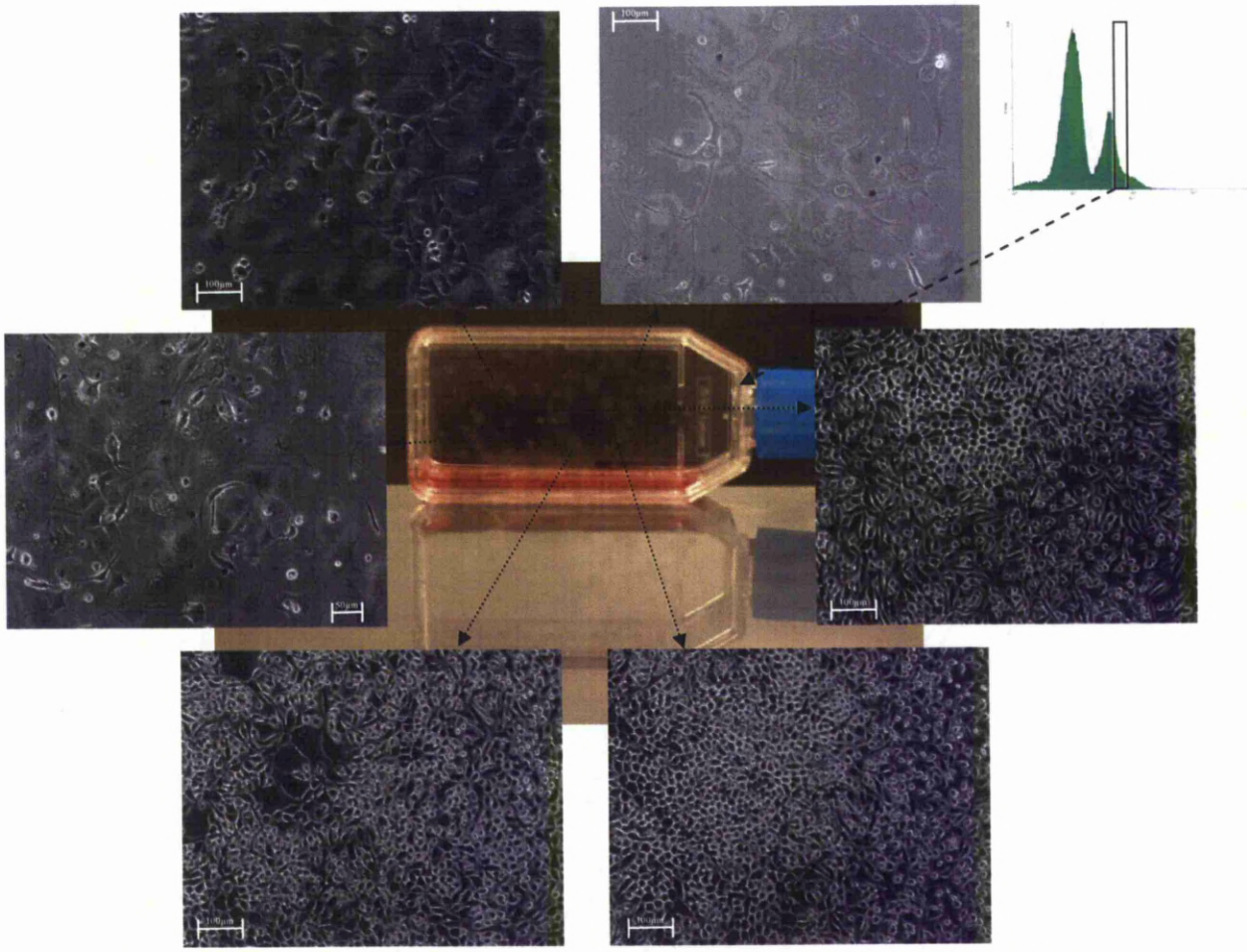

Figure 6.143 **- Pulp donor 1 (Passage 8) cells sorted of the basis of $CD50^{Dull}$ expression seeded in basal media and cultured for 48 hours post-sorting. Images are representive of cells present within the selected colony.**

$CD50^{Light}$ purified cells generated 3 distinct colonies following purification and demonstrated global heterogeneic morphology (*Figure 6.144*). However, on confluence 13 days post-sorting, flow cytometry revealed the heterogeneous phenotype associated with non-purified dental pulp cells. Immunohistochemistry of cells 4 hours post-sorting revealed a similar expression profile with that observed in $CD50^{Dull}$ purified populations, the exception being the nucleolar as opposed to cytoplasmic-specific expression of MiTF (*Table 6.2* – Page 295).

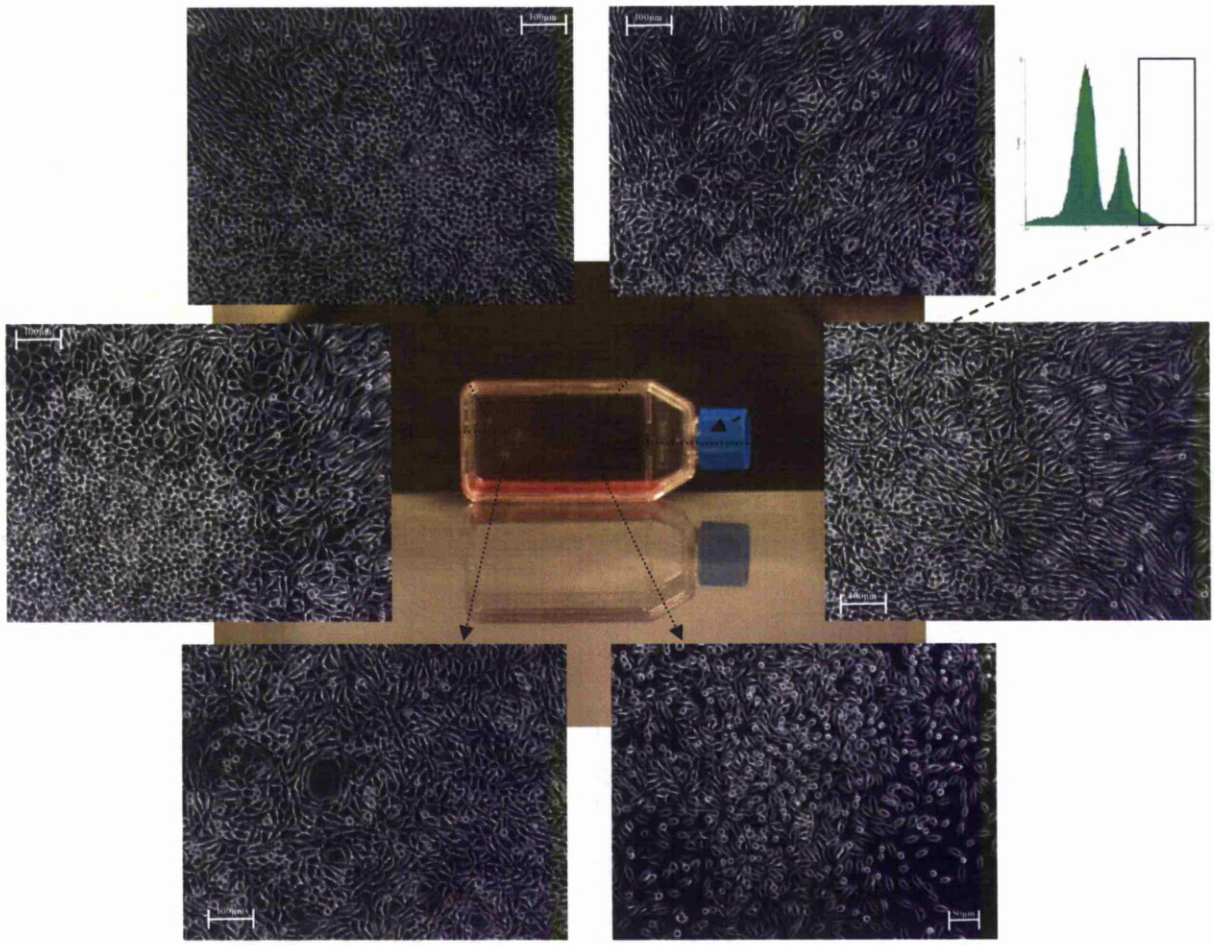

Figure 6.144 **- Pulp donor 1 (Passage 8) cells sorted of the basis of $CD50^{Light}$ expression seeded in basal media and cultured for 48 hours post-sorting. Images are representive of cells present within the selected colony/region.**

6.8.7 Purification of Heterogeneous Dental Pulp Populations based upon Differential Expression of CD56

Leukocyte-associated antigen CD56 was expressed by 20% - 40% of dental pulp-derived cells, and populations were subsequently sorted upon the basis of $CD56^{Dull}$ and $CD56^{Light}$ expression. $CD56^{Dull}$ populations generated small heterogeneous colonies on adherence to the TC plastic substrate (*Figure 6.145*), and exhibited a heterogeneous dental pulp phenotype upon confluence 11 days post-sorting, as observed by flow cytometry. Cells fixed 4 hours post-sorting demonstrated cytoplasmic expression of plasticity regulation proteins Oct4 and Sox2, and although Cripto-1 expression was not observed, the ES cell-associated protein Tra-1-81 was

also expressed within the cytoplasm. STRO-1 was also expressed within the cytoplasm of adherent cells, whilst stem cell proliferation protein nucleostemin was expressed in the nucleus. RPE-associated proteins pax6 and MiTF were expressed within the cytoplasm of adherent populations, whilst neuronal-associated proteins nestin, rest4 and TBR2 were expressed within the cytoplasm (*Table 6.2* – Page 295).

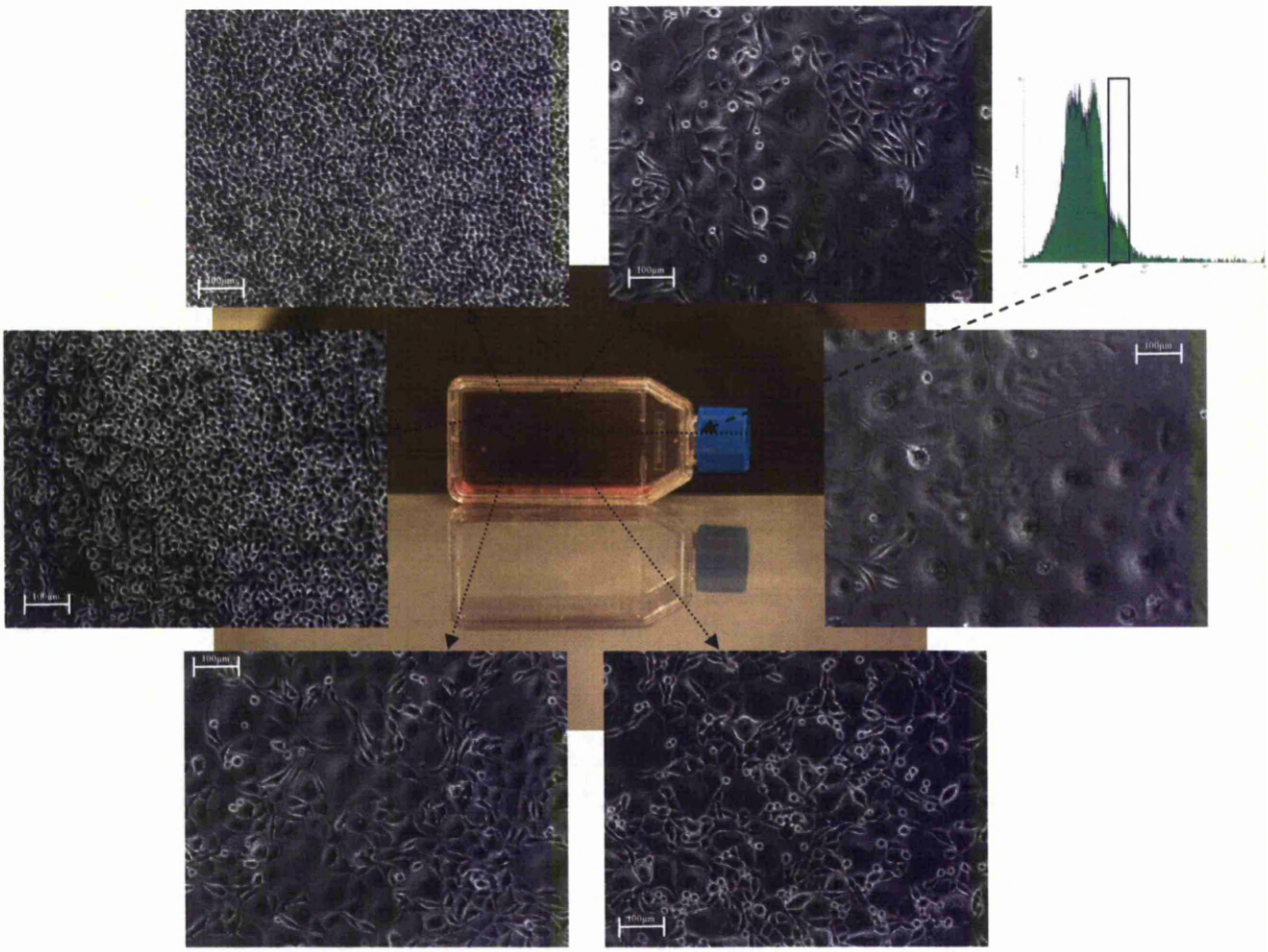

Figure 6.145 **- Pulp donor 1 (Passage 8) cells sorted of the basis of $CD56^{Dull}$ expression seeded in basal media and cultured for 48 hours post-sorting. Images are representive of cells present within the selected colony.**

$CD56^{Light}$ purified populations did not generate colonies when interacting with the TC plastic surface, although did exhibit a heterogeneous morphology (*Figure 6.146*). However, upon confluence 13 days post-sorting, flow cytometry and immunohistochemistry revealed an identical protein expression profile to that observed within $CD56^{Dull}$ purified populations (*Table 6.2* – Page 295).

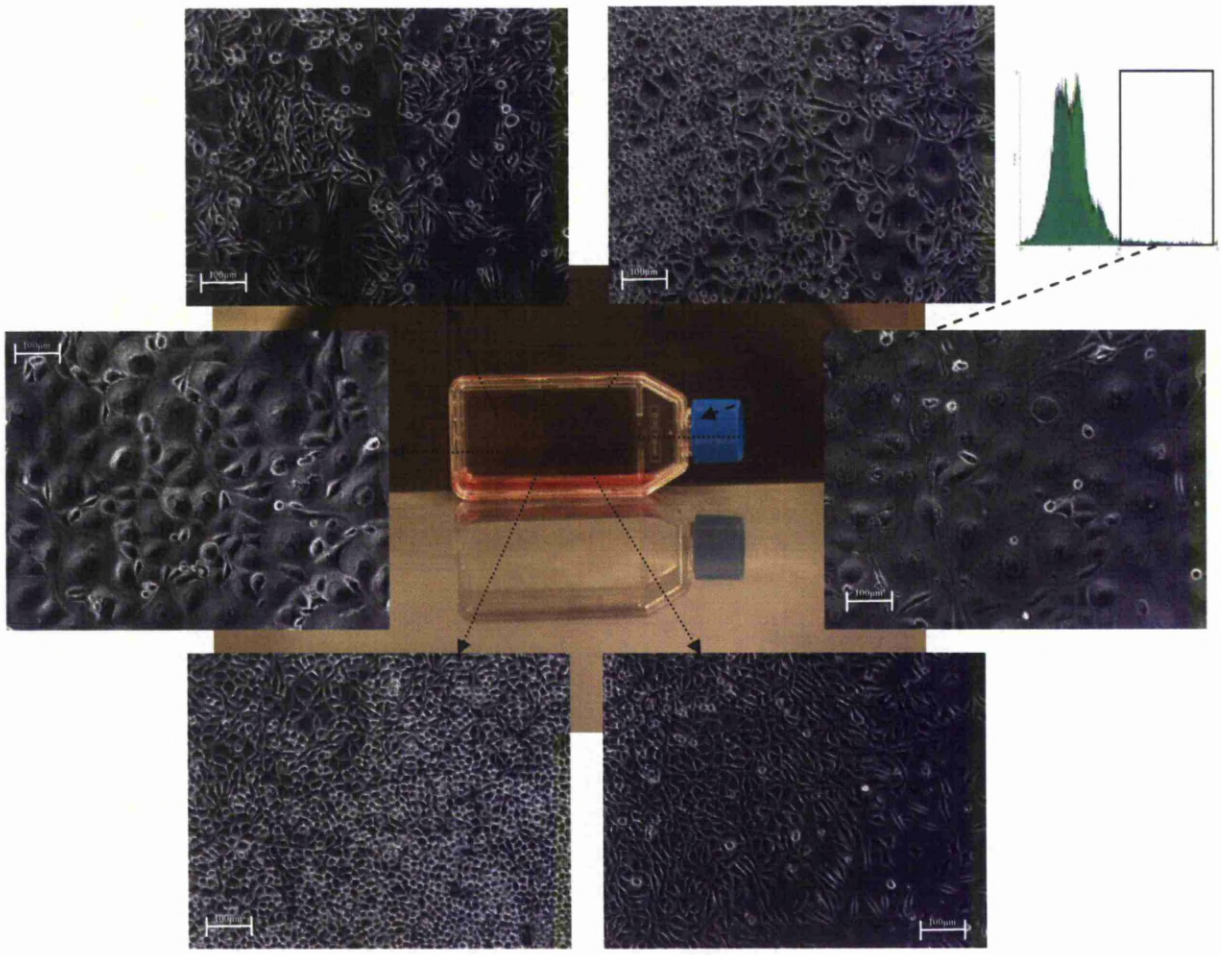

Figure 6.146 **- Pulp donor 1 (Passage 8) cells sorted of the basis of $CD56^{Light}$ expression seeded in basal media and cultured for 48 hours post-sorting. Images are representive of cells present within the selected region.**

6.8.8 Purification of Heterogeneous Dental Pulp Populations based upon Differential Expression of CD62E

Endothelial-associated antigen CD62E was expressed by approximately 5% - 20% of dental pulp cells, and thus $CD62E^{Dull}$ and $CD62E^{Light}$ populations were isolated. $CD62E^{Dull}$ purified cells spontaneously generated colonies on the TC plastic surface (*Figure 6.147*). However, colonies were morphologically heterogeneous and, upon confluence 9 days post-sorting, flow cytometry further confirmed a heterogeneic pulp phenotype. Immunohistochemistry of adherent cells 4 hours following antibody-based purification revealed cytoplasmic expression of pax6 and MiTF, with alternative neuronal proteins rest4 and TBR2 also exhibiting cytoplasmic expression. Interestingly nestin was not expressed. Whilst cells exhibited cytoplasmic and

nuclear expression of STRO-1 and nucleostemin, no Oct4, Sox2 or Cripto-1 expression was detected (*Table 6.2* – Page 295).

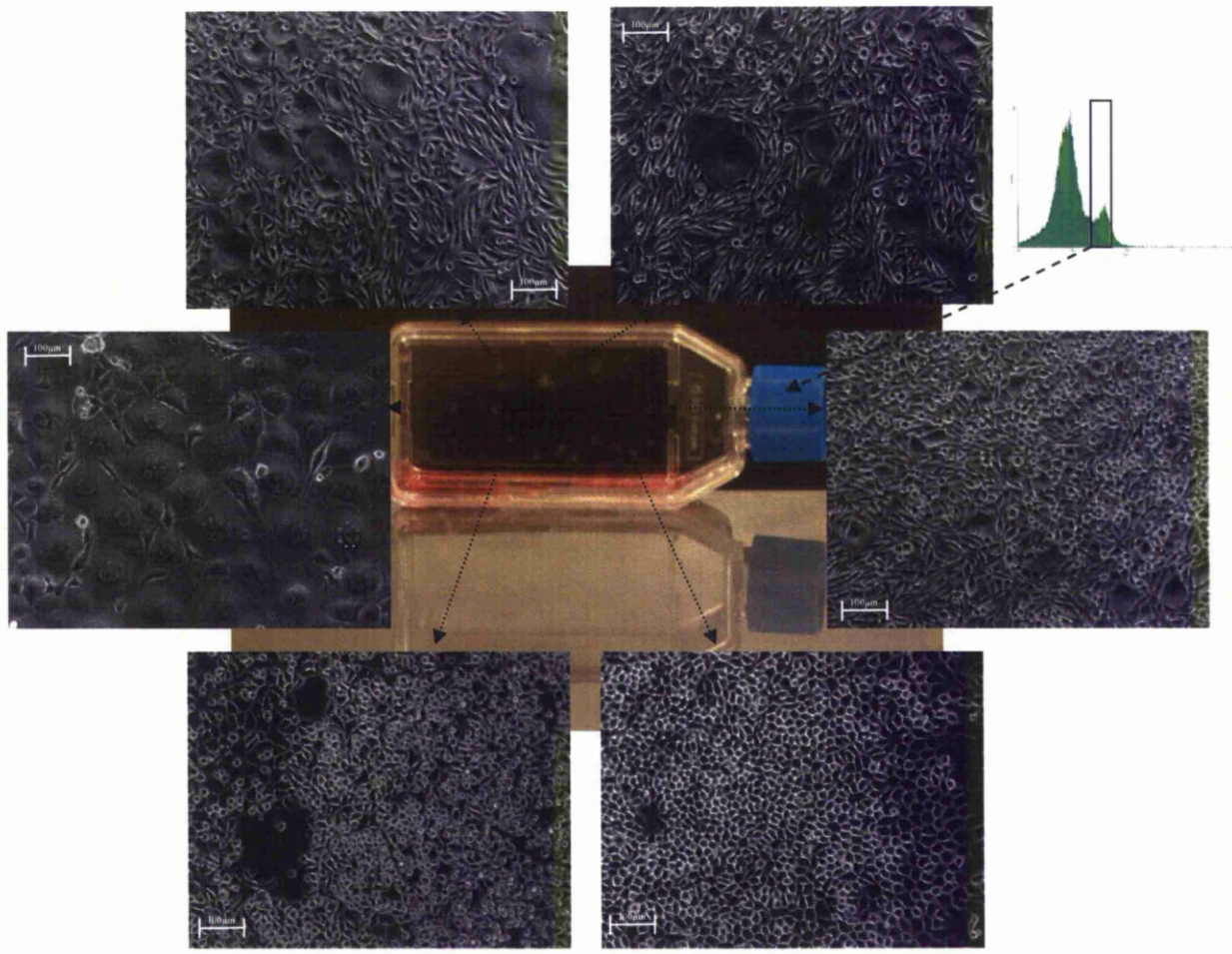

***Figure 6.147* - Pulp donor 1 (Passage 8) cells sorted of the basis of CD62E^{Dull} expression seeded in basal media and cultured for 48 hours post sorting. Images are representive of cells present within the selected colony.**

CD62^{Light} purified populations also generated colonies when seeded onto TC plastic (*Figure 6.148*), and furthermore exhibited morphological and phenotypic heterogeneity, as observed by flow cytometric analysis of confluent cells confluence 9 days post-sorting. Cells fixed 4 hours post-sorting demonstrated a similar expression profile to that observed in CD62^{Dull} purified cells (*Table 6.2* – Page 295).

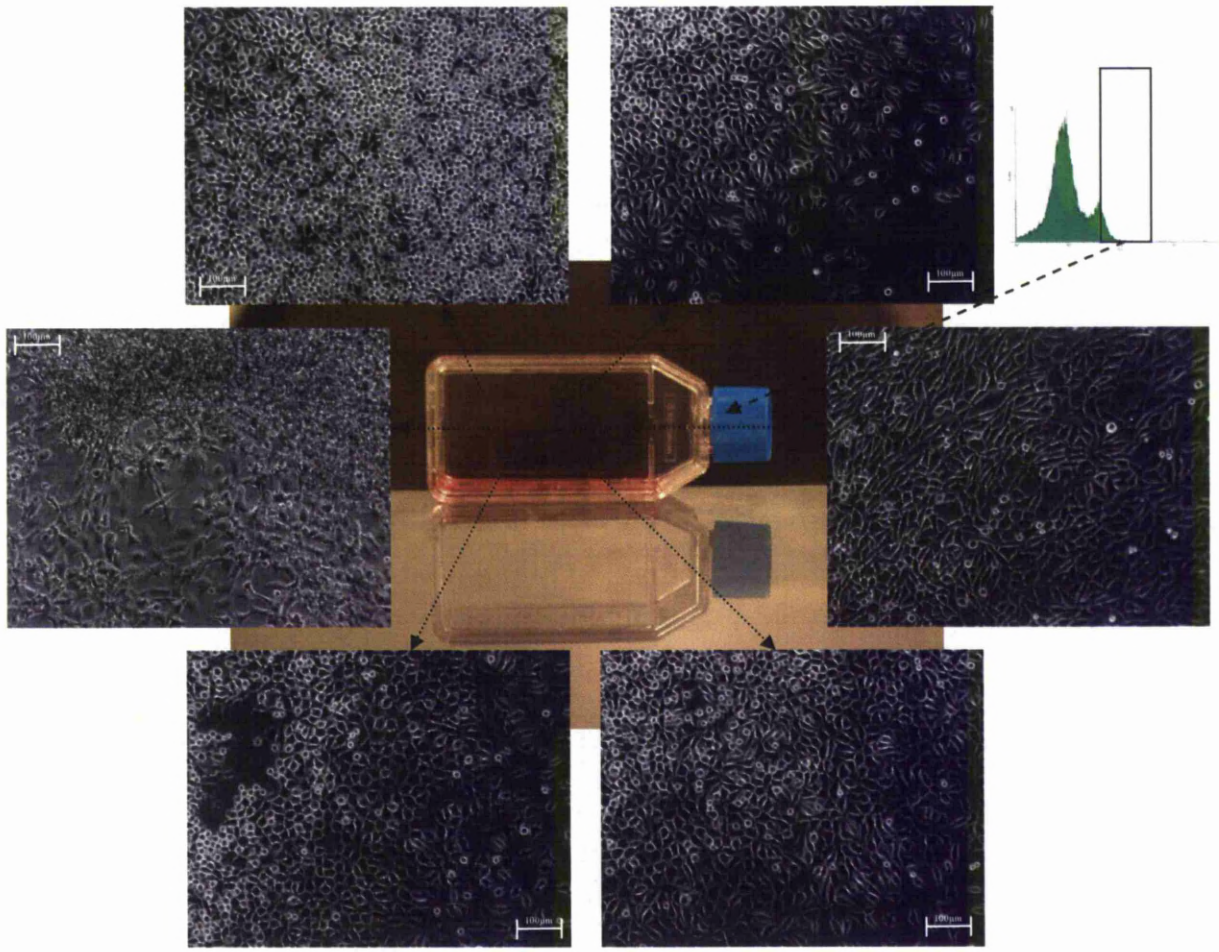

Figure 6.148 **- Pulp donor 1 (Passage 8) cells sorted of the basis of CD62E^{Light} expression seeded in basal media and cultured for 48 hours post-sorting. Images are representive of cells present within the selected colony.**

6.8.9 Purification of Heterogeneous Dental Pulp Populations based upon Differential Expression of CD73

MSC-associated antigen CD73 was expressed by 30% - 50% of dental pulp-derived populations and was purified on the basis of CD73^{Dull} and CD73^{Light} expression. CD73^{Dull} populations produced colony formation on TC plastic adherence, whilst CD73^{Light} in fact did not form distinct colonies (*Figure 6.149*). However, heterogeneic morphology was observed within both populations, and phenotypic analysis of confluent purified populations 14 days post-sorting revealed a heterogeneic surface antigen profile. Regarding immunofluorescent staining of cells 4 hours post-adherence, differently purified populations exhibited similar protein expression profiles as observed by immunohistochemistry. Both populations

demonstrated cytoplasmic expression of pluripotent maintaining proteins Oct4, Sox2 and Cripto-1, whilst Tra-1-81 was also expressed within the cytoplasm of cells. MiTF and Pax6 further exhibited cytoplasmic expression, as did alternative neuronal proteins nestin, rest4 and TBR2. Nucleostemin exhibited nuclear-specific expression within each population, whilst MSC-associated protein STRO-1 was cytoplasmically expressed (*Table 6.2* – Page 295).

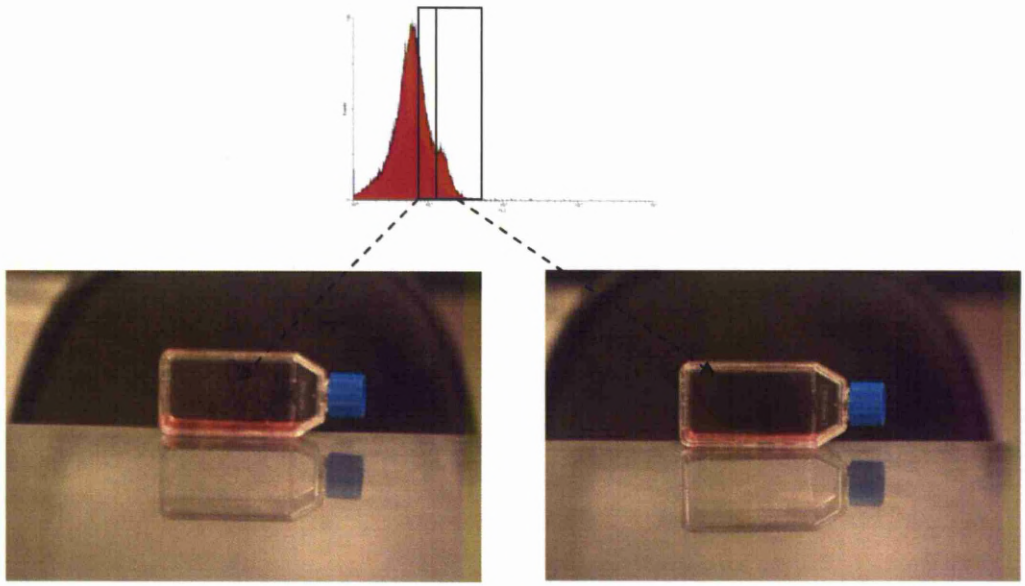

Figure 6.149 **- Pulp donor 1 (Passage 8) cells sorted of the basis of $CD73^{Dull}$ and $CD73^{Light}$ expression seeded in basal media and cultured for 48 hours post-sorting.**

6.8.10 Purification of Heterogeneous Dental Pulp Populations based upon Differential Expression of CD81

Neural progenitor-associated antigen CD81 was expressed by approximately 5% of the dental pulp population and was subsequently purified based on this positive expression. $CD81^{Dull}$ purified cells generated one distinct colony on TC plastic adherence and displayed both morphological (*Figure 6.150*) and phenotypic heterogeneity, as observed by flow cytometry following attainment of confluence 20 days post-sorting. Immunohistochemical assessment of adherent cells 4 hours post-sorting demonstrated the cytoplasmic expression of plasticity maintaining proteins Cripto-1 and Sox2, whilst Oct4 was expressed within the nucleus of cells. ES-cell-associated protein Tra-1-81 was also expressed within the cytoplasm of cells. Whilst cells cytoplasmically expressed RPE progenitor-associated protein pax6, the

committed progenitor protein MiTF was not detected within the culture. Neural-associated proteins nestin and TBR2 were also expressed cytoplasmically, whilst neuronal differentiation regulator rest4 exhibited nucleolar specific expression. Stem cell proliferation protein nucleostemin was expressed within the nucleus, whilst MSC-associated protein STRO-1 was expressed in the cytoplasm of purified cells (*Table 6.2* – Page 295).

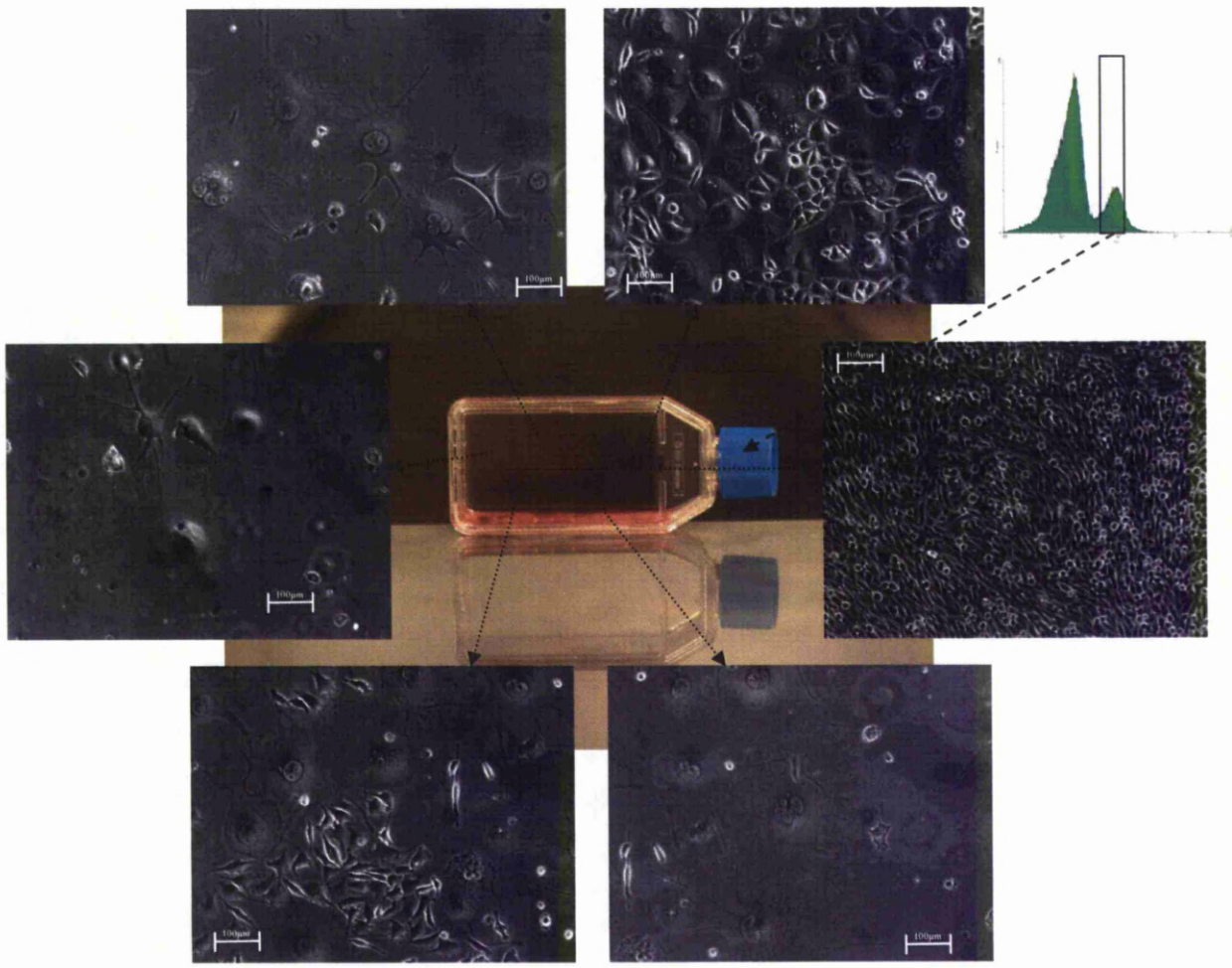

Figure 6.150 **- Pulp donor 1 (Passage 8) cells sorted of the basis of CD81^{Dull} expression seeded in basal media and cultured for 48 hours post-sorting. Images are representive of cells present within the selected colony/region.**

CD81^{Light} purified cells spontaneously generated colonies on the TC plastic surface, although cells exhibited both morphological (*Figure 6.151*) and phenotypic heterogeneity, as observed by flow cytometric analysis of confluent cells 24 days post-sorting. Immunohistochemistry of cells 4 hours post-sorting exhibited

cytoplasmic expression of Oct4, Sox2 and Cripto-1, whilst also demonstrating nucleolar localised expression of Tra-1-81. Cells cytoplasmically expressed the RPE-associated protein pax6, whilst MiTF was also detected. Neural progenitor protein nestin was cytoplasmically expressed, as were associated proteins rest4 and TBR2. Nucleostemin was expressed within the nucleus of cells, and STRO-1 exhibited cytoplasmic-specific expression (*Table 6.2* – Page 295).

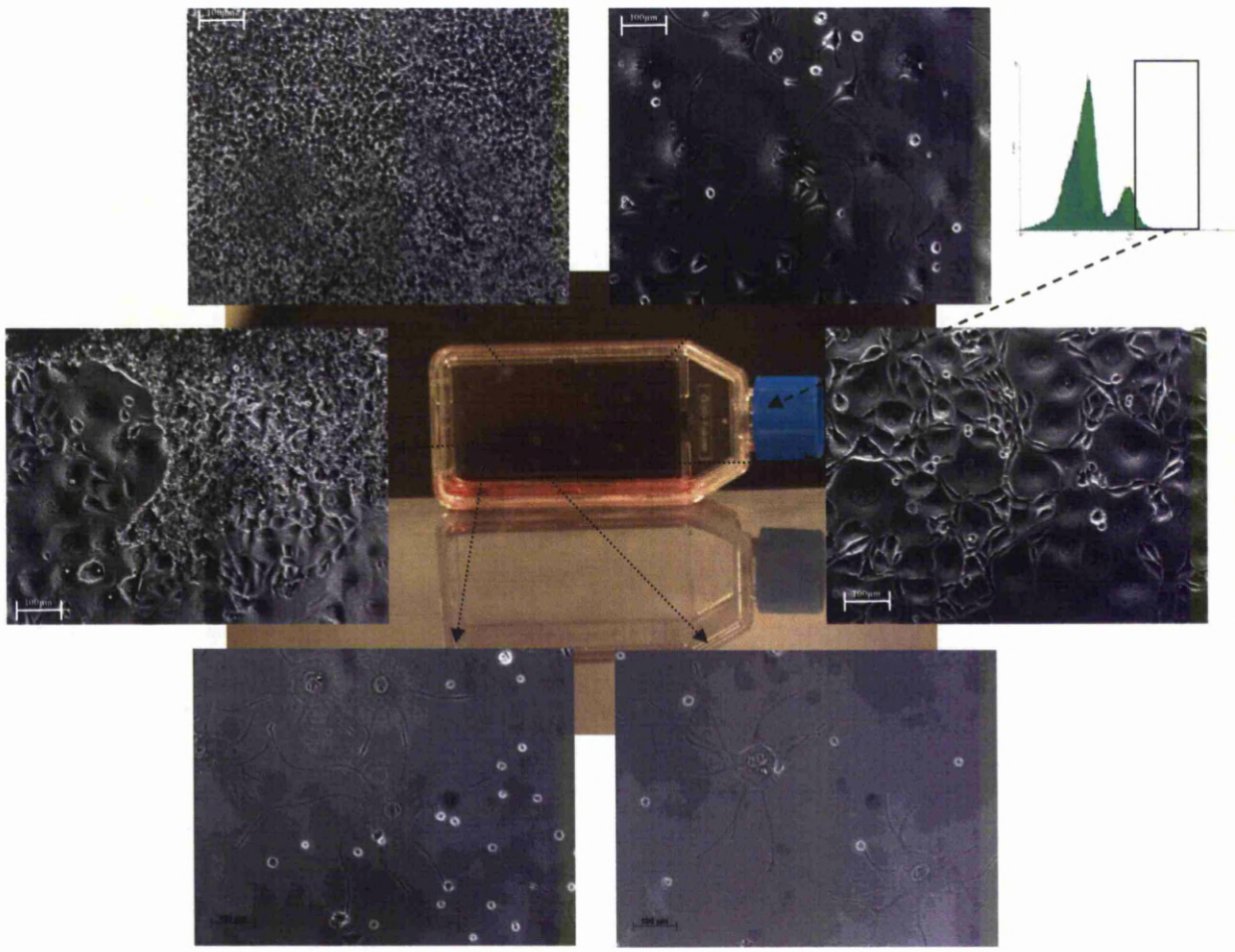

Figure 6.151 **- Pulp donor 1 (Passage 8) cells sorted of the basis of CD81^{Light} expression seeded in basal media and cultured for 48 hours post-sorting. Images are representive of cells present within the selected colony.**

6.8.11 Purification of Heterogeneous Dental Pulp Populations based upon Differential Expression of CD90

MSC-associated antigen CD90 was expressed by approximately 25% - 30% of the dental pulp population, and CD90^{Dull} purified cells generated one distinct colony

when interacting with the TC plastic substrate (*Figure 6.152*). The global population displayed a morphological and, as demonstrated by flow cytometric analysis of confluent cells 17 days post-sorting, phenotypic heterogeneity as that observed in non-purified populations. Adherent populations assessed 4 hours post-sorting exhibited cytoplasmic expression of plasticity-maintainers Sox2 and Cripto-1, whilst furthermore exhibiting nuclear expression of Oct4. ES cell-associated protein Tra-1-81 also demonstrated cytoplasmic expression. RPE progenitor-associated protein pax6 was expressed within the nucleus of cells, whilst the RPE progression protein MiTF was cytoplasmically expressed. Neuronal proteins rest4 and TBR2 exhibited cytoplasmic expression, although nestin was not detected. Stem cell proliferation protein was detected within the nucleus of cells, whilst MSC-associated protein STRO-1 was expressed within the cytoplasm (*Table 6.2* – Page 295).

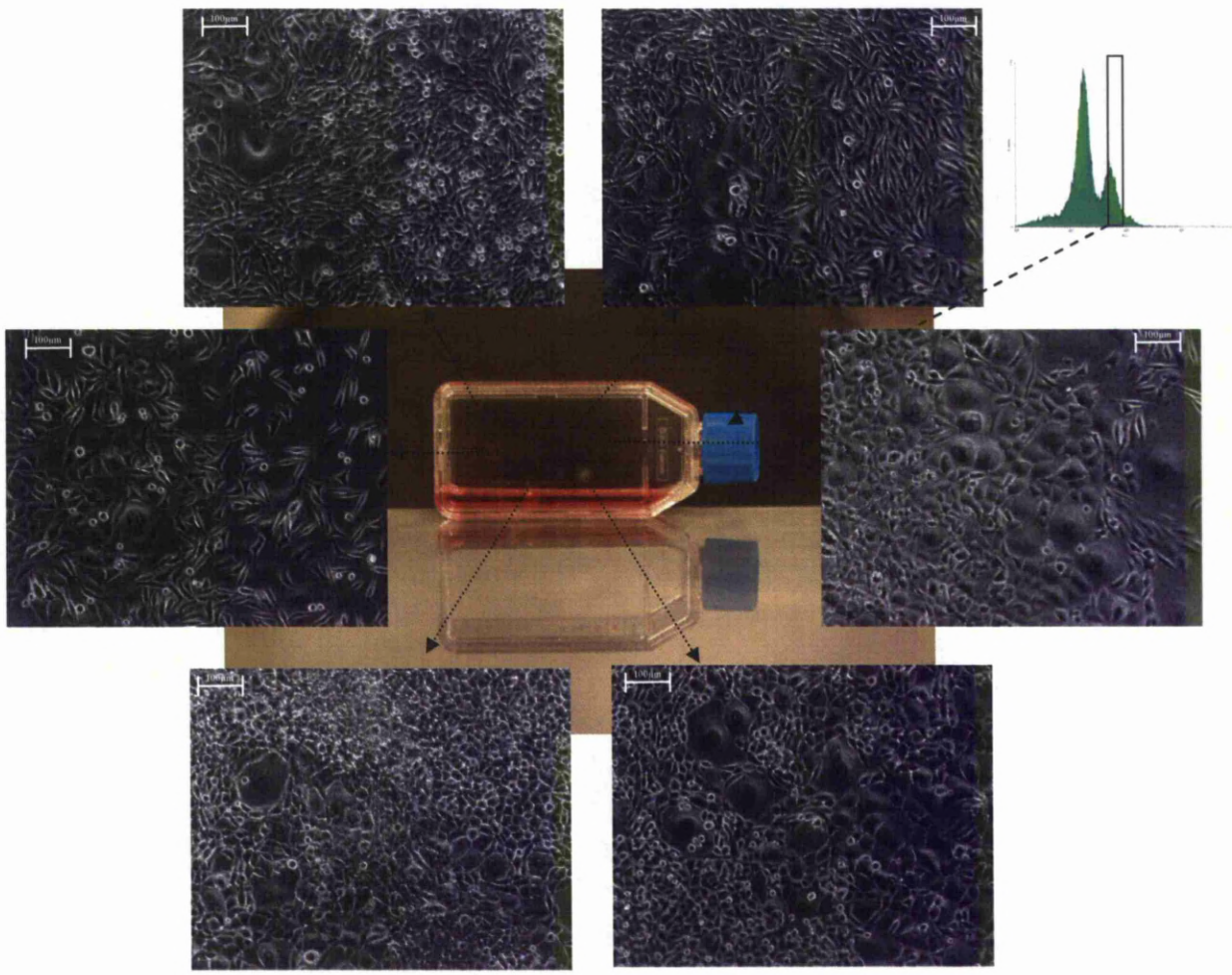

***Figure 6.152* - Pulp donor 1 (Passage 8) cells sorted of the basis of $CD90^{Dull}$ expression seeded in basal media and cultured for 48 hours post-sorting. Images are representive of cells present within the selected colony/region.**

$CD90^{Light}$ purified populations generated multiple colonies on adherence to TC plastic surface, although morphological (*Figure 6.153*) and phenotypic characteristics, as observed by flow cytometric studies of confluent cells 16 days post-sorting, were heterogeneous. Immunohistochemical analysis of adherent cells demonstrated nuclear expression of Oct4 and Sox2, whilst Cripto-1 exhibited nucleolar expression within cells. Furthermore, Tra-1-81 exhibited cytoplasmic expression. Pax6 exhibited nuclear expression, whilst associated protein MiTF was expressed within the cytoplasm. Whilst neural progenitor protein nestin was not detected, neuronal-associated proteins rest4 and TBR2 were expressed within the cytoplasm of cells. Nucleostemin was expressed within the nucleus, whilst STRO-1 demonstrated cytoplasmic expression (*Table 6.2* – Page 295).

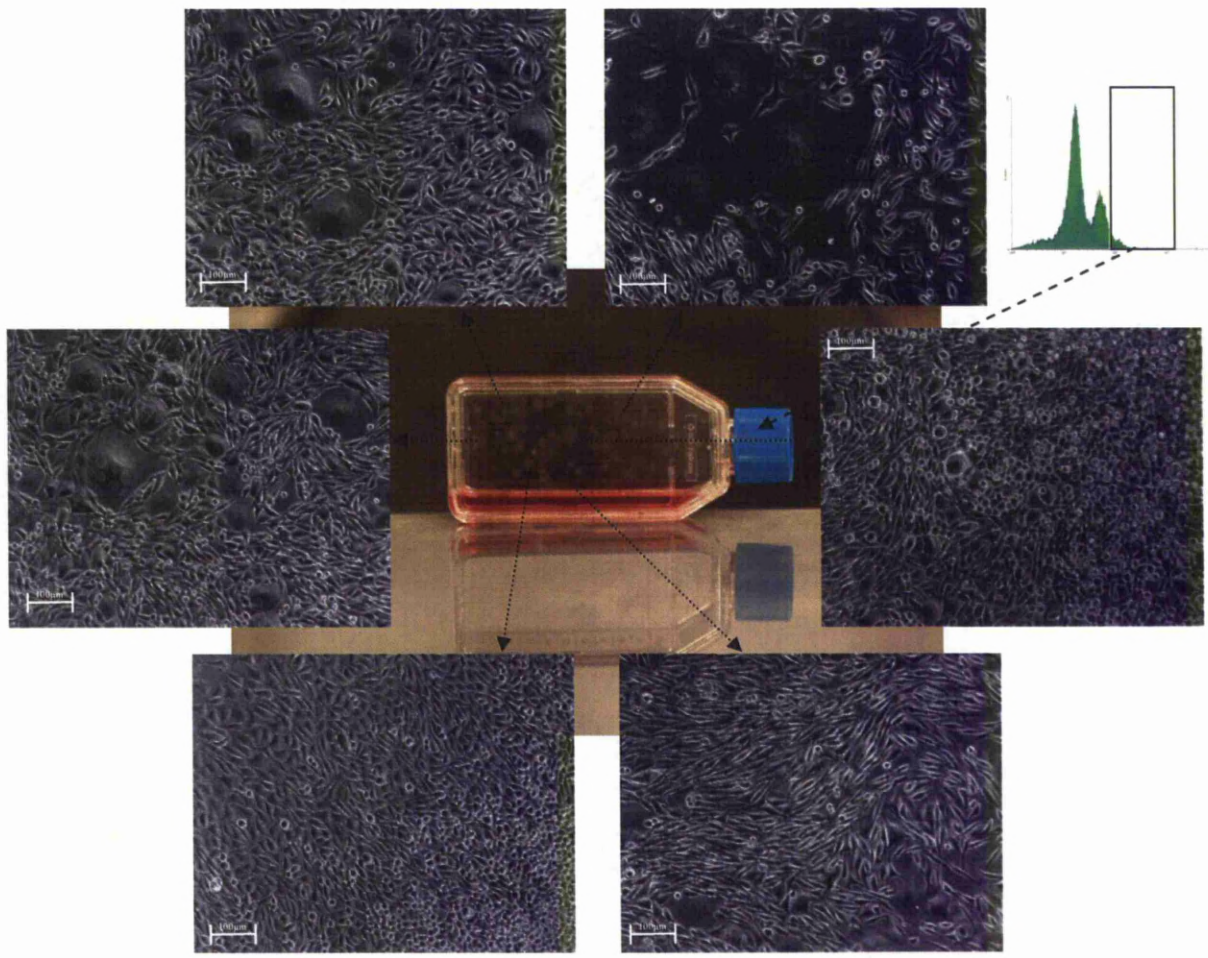

***Figure 6.153* - Pulp donor 1 (Passage 8) cells sorted of the basis of $CD90^{Light}$ expression seeded in basal media and cultured for 48 hours post-sorting. Images are representive of cells present within the selected colony. Images are representive of cells present within the selected colony.**

6.8.12 Purification of Heterogeneous Dental Pulp Populations based upon Differential Expression of CD105

CD105 is expressed by both endothelial cells and MSCs and was furthermore expressed by approximately 25% - 35% of dental pulp cells. $CD105^{Dull}$ purified cells demonstrated colony formation on adherence to the TC plastic surface, although they exhibited morphological (*Figure 6.154*) and phenotypic heterogeneity, as observed by flow cytmetric analysis of confluent cells 12 days post-sorting. Adherent cells analysed using immunohistochemistry 4 hours post-sorting demonstrated cytoplasmic expression of Oct4 and Sox2, although they did not express primitive-associated proteins Cripto-1 or Tra-1-81. Whilst RPE progenitor protein pax6 was expressed within the cytoplasm of cells, the progressive protein MiTF was not detected. Alternative neuronal proteins rest4 and TBR2 were cytoplasmically expressed within the population, although neural progenitor protein nestin was not expressed. Nucleostemin and STRO-1 were expressed within the nucleus and cytoplasm of cells respectively. Interestingly, $CD105^{Light}$ purified populations did not generate colonies upon the surface of the TC plastic substrate; instead the heterogeneous cell population formed a monolayer population, becoming confluent 10 days post-sorting. However, whilst not generating colonies, $CD105^{Light}$ populations exhibited an identical phenotype compared with $CD105^{Dull}$ populations, as observed by flow cytometry and immunohistochemistry (*Table 6.2* – Page 295).

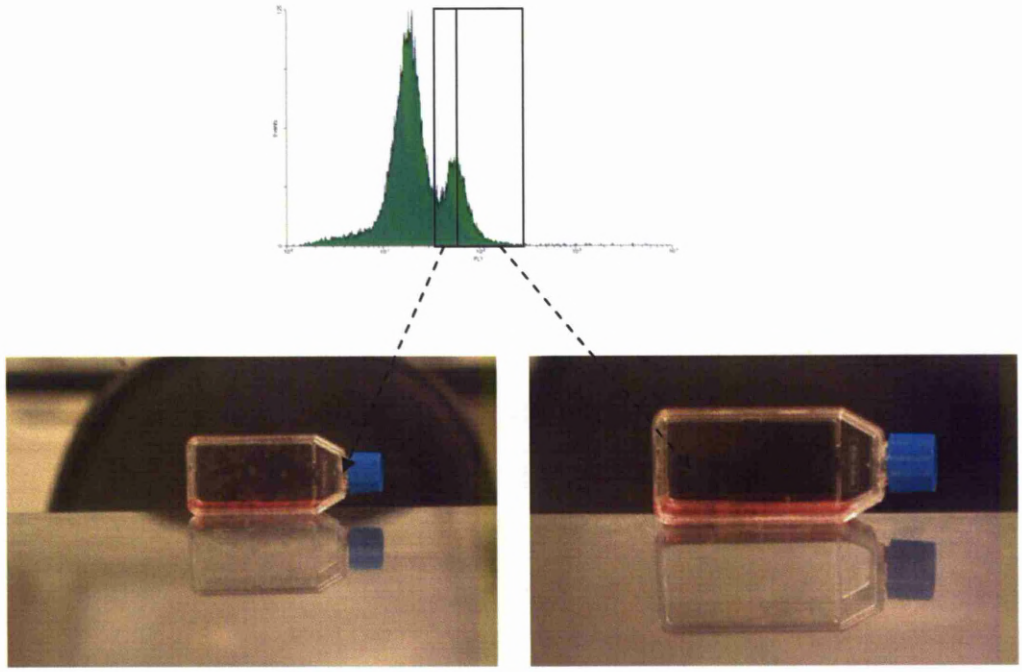

Figure 6.154 **- Pulp donor 1 (Passage 8) cells sorted of the basis of $CD105^{Dull}$ and $CD105^{Light}$ expression seeded in basal media and cultured for 48 hours post-sorting.**

6.8.13 Purification of Heterogeneous Dental Pulp Populations based upon Differential Expression of STRO-1

STRO-1 was expressed by approximately 0.5% - 1% of heterogeneous dental pulp cells, and was subsequently purified to assess phenotypic capacity of the population. STRO-1^{Dull} cells generated only one distinct colony on the surface of the TC plastic and became confluent 18 days post-sorting, with the population exhibiting morphological (*Figure 6.155*) and phenotypic characteristics associated with non-purified dental pulp populations. Immunohistochemistry of adherent populations 4 hours post-sorting revealed cytoplasmic expression of the RPE-protein MiTF, although interestingly the primitive RPE protein pax6 was not expressed. Strikingly given the proposed cell phenotype STRO-1 is hypothesised to purify, no expression of Sox2 was detected within the population, although co-regulator Oct4 was detected within the nucleus of cells. Whilst embryonic-associated proteins Cripto-1 and Tra-1-81 were not expressed within the population, nucleostemin and STRO-1 were expressed within the nucleus and cytoplasm respectively. Interestingly, neural-

associated proteins nestin, rest4 and TBR2 were expressed within the cytoplasm of the population (*Table 6.2* – Page 295).

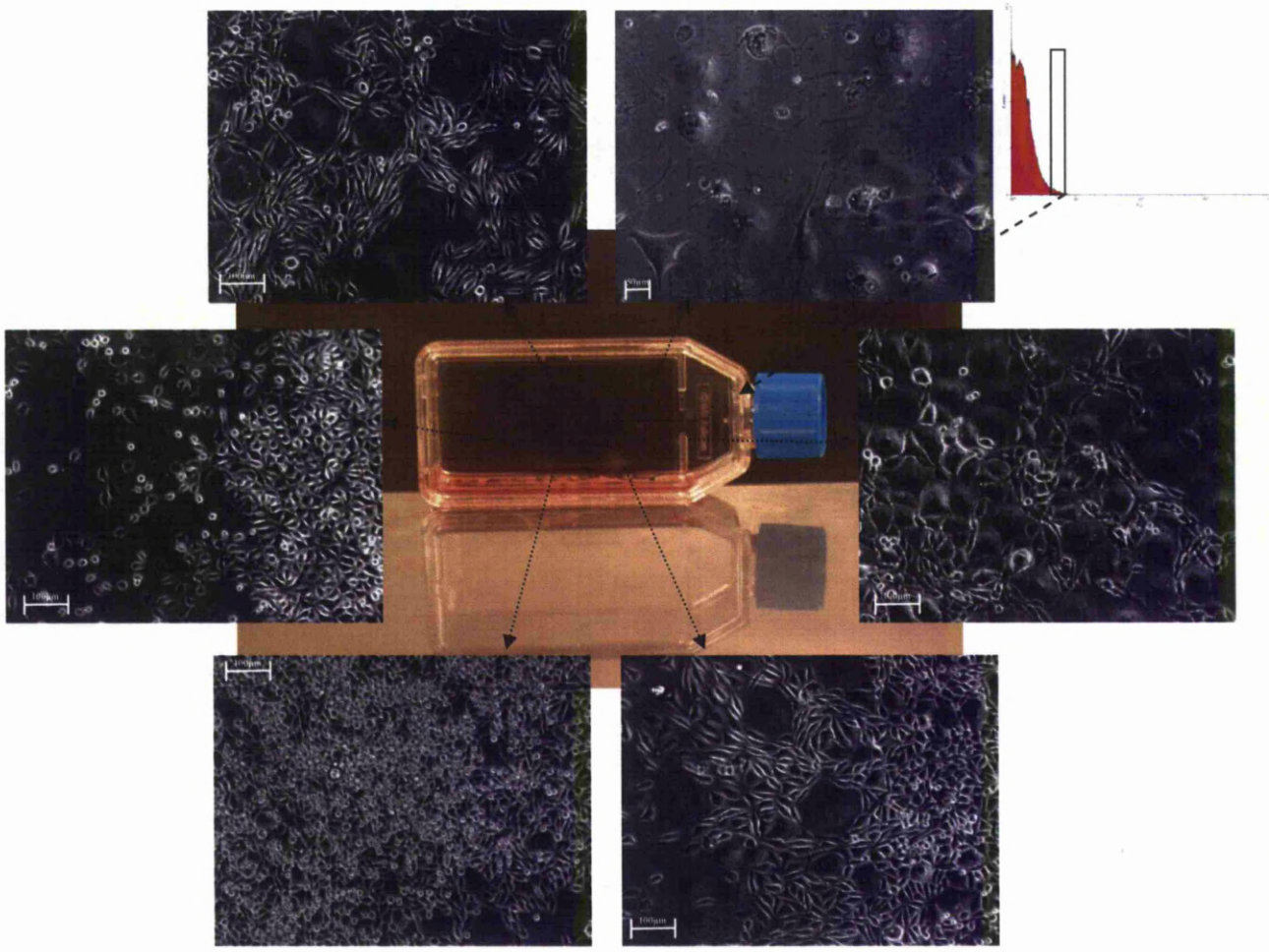

Figure 6.155 **- Pulp donor 1 (Passage 8) cells sorted of the basis of STRO-1^{Dull} expression seeded in basal media and cultured for 48 hours post-sorting. Images are representive of cells present within the selected colony.**

STRO-1^{Light} purified populations generated colonies upon adherence to the TC plastic, although demonstrated a similar morphological (*Figure 6.166*) and phenotypic heterogeneity, as observed by flow cytometric analysis of confluent cells 22 days post-sorting, compared with STRO-1^{Dull} positive cells. Furthermore, immunohistochemistry assaying of adherent cells 4 hours post-sorting demonstrated an identical expression to that observed in STRO-1^{Dull} populations (*Table 6.2* – Page 295).

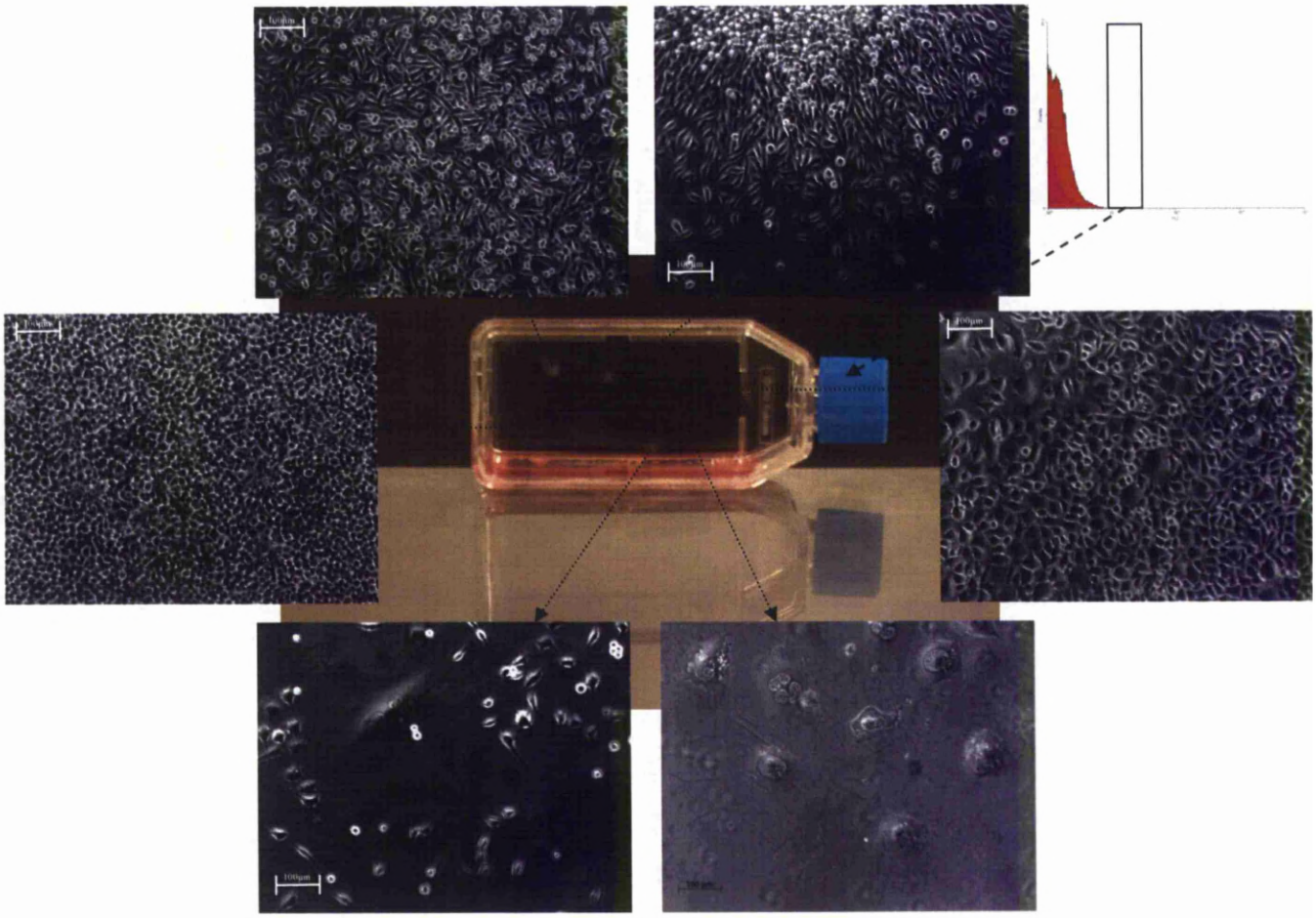

Figure 6.156 **- Pulp donor 1 (Passage 8) cells sorted of the basis of STRO-1^{Light} expression seeded in basal media and cultured for 48 hours post-sorting. Images are representive of cells present within the selected colony.**

6.8.14 Antibody-based Techniques for the Purification of Heterogeneous Dental Pulp populations

At present antibody-related techniques, and in particular the STRO-1 surface antigen, represent the most widely used method for the purification of homogeneous stem cell populations. However, attempted purification of dental pulp-derived populations using an array of surface antigens failed to ascertain a homogeneous subpopulation, with cells re-establishing a heterogeneic-associated phenotype upon confluence. Whilst Hoechst purified populations retain an alternative phenotype until second passage post-sort confluence, they too demonstrated a reversion to the heterogeneous dental pulp population at this point. This would suggest that by sorting on the basis

of a functional cell aspect *i.e.* the presence of an ABCG2 transporter pump, cell populations of a greater purity than antibody related discrimination can be formed, but contaminates capable of re-establishing the heterogeneic phenotype still remain. And whilst adherent cells were assessed using immunohistochemistry 4 hours post-sorting to allow probing of protein expression within each purified subpopulation (*Table 6.2*), their inability to maintain homogeneity subsequent to further proliferation is detrimental from a clinical perspective. It is therefore required that alternative techniques are devised capable of homogeneously discriminating against subpopulations of varying characteristics. However, whilst attainment of homogeneous subpopulations of cells from dental pulp would undoubtedy prove clinically significant, given the aforementioned results, it may be that this is not plausible; whilst we have initially attributed the re-establishment of heterogeneity to rogue progenitor impurities, it may be that the population as a whole in fact strives to remain in a heterogeneic state, maintaining standard numbers of each subpopulation that make up the niche. This is a plausible hypothesis given that purified populations exhibited increased cycling times compared with the heterogeneous, unpurified pulp populations, requiring greater culture time to obtain confluence. Given that that primitive cells exhibit a more quiescent state than committed cells, these results would therefore suggest that Hoechst and antigen purified populations were in fact stem or progenitor subsets. Further investigations are therefore required to establish whether this may be the case, a result with significant relevance for all future regenerative strategies.

Surface antigen Purification	Protein expression										
	Cripto-1	MiTF	Nestin	Nucleostemin	Oct4	Pax6	REST4	Sox2	STRO-1	Tbr2	Tra-1-81
$Hoechst^{Dull}$	X	X	X	NU	CY	X	X	CY	X	X	X
$CD9^{Dull}$	NU	NU	X	NU	CY	CY	CY	NU	CY	CY	CY
$CD9^{Light}$	NU	NU	X	NU	CY	CY	CY	NU	CY	CY	CY
$CD30^{Dull}$	CY	CY	X	NU	NU	CY	CY	NU	CY	CY	CY
$CD30^{Light}$	CY	CY	CY	NU	NU	CY	CY	NU	CY	CY	CY
$CD34\ (III)^{Dull}$	X	X	X	NU	X	X	CY	X	CY	X	X
$CD34\ (III)^{Light}$	X	N/O	X	NU	X	X	CY	X	CY	X	CY
$CD50^{Dull}$	X	CY	X	NU	X	CY	CY	X	CY	CY	X
$CD50^{Light}$	X	N/O	X	NU	X	CY	CY	X	CY	CY	X
$CD56^{Dull}$	X	CY	CY	NU	CY	CY	CY	CY	CY	CY	CY
$CD56^{Light}$	X	CY	CY	NU	CY	CY	CY	CY	CY	CY	CY
$CD62E^{Dull}$	X	CY	X	NU	X	CY	CY	X	CY	CY	X
$CD62E^{Light}$	X	CY	X	NU	X	CY	CY	X	CY	CY	X
$CD73^{Dull}$	CY	CY	CY	NU	CY	CY	CY	CY	CY	CY	CY
$CD73^{Light}$	CY	CY	CY	NU	CY	CY	CY	CY	CY	CY	CY
$CD81^{Dull}$	CY	X	CY	NU	NU	CY	N/O	CY	CY	CY	CY
$CD81^{Light}$	CY	CY	CY	NU	CY	CY	N/O	CY	CY	CY	N/O
$CD90^{Dull}$	CY	CY	X	NU	NU	NU	CY	CY	CY	CY	CY

$CD90^{Light}$	N/O	CY	X	NU	NU	NU	CY	NU	CY	CY	CY
$CD105^{Dull}$	X	X	X	NU	CY	CY	CY	CY	CY	CY	X
$CD105^{Light}$	X	X	X	NU	CY	CY	CY	CY	CY	CY	X
$STRO\text{-}1^{Dull}$	X	CY	CY	NU	NU	X	CY	X	CY	CY	X
$STRO\text{-}1^{Light}$	X	CY	CY	NU	NU	X	CY	X	CY	CY	X

Table 6.2 **- Immunohistochemistry protein expression profiling of Hoechst/surface antigen purified dental pulp populations fixed 4 hours post-sorting. X = no expression; CY = cytoplasmic expression; NU = nuclear expression; N/O = nucleolar expression.**

6.9 Conclusion

6.9.1 Dental Pulp as a Niche for the Isolation of Clinically Desirable Cells

Dental pulp represents an attractive niche from which to isolate cells for therapeutic strategies given the relative ease with which it can be obtained, especially with regards deciduous teeth from which cells could be isolated and cryopreserved following natural loss of the tooth. Isolation of cells from dental pulp was a relatively straightforward procedure, with isolated cells readily adhering and undertaking rapid proliferation. The maintenance of *in vitro* expression regardless of donor age or sex overcomes many therapeutic boundaries encountered with bone marrow, peripheral blood and umbilical cord-derived populations, and their ability to undertake multilineage differentiation further enhances their therapeutic value. Whilst dental pulp-derived populations were only induced towards adipogenic, chondrogenic, osteogenic, neuronal and hepatic lineages, their expression of plasticity regulating proteins Oct4 and Sox2 suggests a pluripotent capability comparable with that of ES cells, a hypothesis further enhanced by the expression of primitive proteins Cripto-1 and Tra-1-81. The expression of pax6 and MiTF within the population suggests the presence of cells of an RPE committed lineage, thereby representing a potential source for regenerative approaches to macular degenerative diseases. However, given that pulp-derived cells display many characteristics associated with ES cells, it is required that they are assessed further for ES cell-associated traits such as karyotypic instability and spontaneous differentiation.

Assuming, however, that dental pulp-derived cells maintain a normal karyotype, it would be therapeutically beneficial if individual subpopulations were homogeneously isolated and assessed for their proliferative and differentiation capacity. However, Hoechst and antibody based purification strategies failed to homogeneously isolate differing subpopulations, with a heterogeneous phenotype maintained following culture. Whilst it is plausible that dental pulp cells diifferentiate to maintain the heterogeneity of the *in vivo* niche and, following purification, undergo numerous differentiations to re-establish this, it is also perceivable that current purification strategies fail to homogeneously exclude cell impurities which subsequently re-establish heterogeneity. Given that such an issue

would have a significant impact on all regenerative strategies this is an issue which must be investigated.

In conclusion, dental pulp-derived populations heterogeneously expressed antigens associated with MSCs, HSCs and EPCs, and ES cells and alternative progenitors. It was of significant interest that this phenotype was maintained throughout prolonged *in vitro* culture, whilst this was also accompanied by consistant proliferation rates. Furthermore, following immunofluorescent probing of the population, stem and progenitor subpopulations became more apparent: the expression of Oct4, Sox2, Cripto-1 and Tra-1-81 indicated the presence of a highly immature, plastic population; rest4 and TBR2 suggested the presence of neuronal progenitors; and pax6 and MiTF those of the RPE lineage. The presence of large numbers of both hematopoietic and non-hematopoietic progenitors were demonstrated by CFU-GM and CFU-F assays, with such cells likely responsible for the observed adipogenic, chondrogenic, osteogenic, neuronal and hepatic differentiation. However, purification based upon differing Hoechst emission or variation in antigen expression failed to homogeneously isolate different subpopulations, although protein expression variance within initially adherent cells and the slow cycling times of sorted cells suggested that stem and progenitor subsets had been isolated. However, either through instated re-establishment of heterogeneity by the homogeneously sorted cells or inclusion of progenitor impurities post-purification, the population failed to maintain a homogeneous phenotype, an issue which needs to be addressed.

6.9.2 Response to Chapter Aims

Results presented within this chapter did address the aims detailed in 6.1.1, with cells isolated from the dental pulp of donors of varying age, sex and tooth condition being characterised. Flow cytometry analysis revealed similar phenotypic characteristics of isolated populations and this phenotype, along with proliferation rates, was maintained throughout *in vitro* culture and following freeze-thaw cycling. This was also the case with regards expression of plasticity regulating proteins, with Sox2, Oct4, Cripto-1 and Tra-1-81 expressed throughout *in vitro* culture. The maintained expression of rest4 and TBR2 suggested the presence of neuronal progenitors derived from the CNC, whilst cells expressing pax6 and MiTF were hypothesised to

represent RPE progenitor cells. Isolated cells demonstrated a consistent ability to generate similar numbers of CFU-Fs and CFU-GMs and cells were successfully differentiated towards adipogenic, chondrogenic, osteogenic, neuronal and hepatic lineages at different passages as to demonstrate a maintained ability of populations to undertake multilineage differentiation. Given the phenotypic stability of the cells, telomere length studies were carried out and subsequently demonstrated that the rapid *in vitro* aging of cells, as observed in bone marrow-derived MSCs, had not taken place and is likely the reason for this stability. Finally, cells were purified using antibody-based methods and characterised as above. However, whether because of impurities following sorting or an inbuilt predisposition of cells to re-establish heterogeneity, purified populations cultured to confluence re-established the heterogeneic phenotype.

7. Stem Cell Conserved Domains as Novel Markers for Homogeneous Isolation of Stem and Progenitor Subpopulations

7.1 Introduction

7.1.1 Requirement for the Development of Novel Methods to Isolate Homogeneous Stem and Progenitor Subpopulations of High Purity from Tissues

Investigations assessing the potential of cells derived from numerous adult tissues have yielded interesting results with respect to their ability to undertake lineage differentiation not associated with their residing niche or trophic germ layer. However, at present the majority of studies fail to identify subpopulations responsible for observed differentiation events, neglecting to distinguish whether a stem cell and/or more committed progenitor counterpart undertakes lineage commitment. Whilst partial homogeneity has been achieved through sorting on the basis of surface expression markers, and in particular STRO-1, such sorting techniques fail to purify cells of varying plasticity. This is particularly evident with regards data obtained from dental pulp studies both in heterogeneous and antigen-purified populations, in particular the incapacity of purified cells to maintain the homogeneously selected phenotype *in vitro*. Whilst this could conceivably be attributed to a phenomenon maintaining a pre-programmed global niche, it is also possible that surface antigen-based sorting techniques fail to homogeneously isolate individual subpopulations, subsequently resulting in single or multiple subpopulation impurities which, following *in vitro* culture, re-establish the global heterogeneous phenotype.

Whatever the reason, however, with which this heterogeneity is re-estbalished, it is likely that antigen-based purification fails to homogeneously select cells based on plasticity or lineage potential, and thus alternative methods based on the lineage capacity of the cell must be designed to allow purification. Should this be achieved, it may allow for investigations confirming the mechanisms responsible for re-establishing the heterogeneic phenotype. Interestingly, many investigations have dismissed such issues of heterogeneity as inconsequential; suggesting that rogue

progenitor subpopulations will exert minimum impact within a clinical setting. However, results of recent clinical studies have cast doubts on such theories, in particular with respect to clinical trials utilising bone marrow-derived stem cells for myocardial repair[415]. Following implantation many studies have reported the formation of calcified tissue within the myocardium, presumably resulting from subpopulations of osteogenic committed cells which have differentiated to a functional osteoblast. Such superfluous differentiation events could, in many clinical applications, prevent anticipated regeneration or prove potentially fatal. Thus, if tissue engineering approaches to medicine are to generate numerous clinical devices to accommodate a range of diseases, it is imperative that homogeneous cell populations are implanted. If it does, however, conspire that purified cells do in fact re-establish the heterogeneic niche with which they are associated, studies must be undertaken to assess the impact of progenitor subpopulations isolated from numerous tissues have within a clinical setting and, assuming a negative impact, to modify *in vitro* culture conditions to maintain the homogeneously selected phenotype.

7.1.2 Stem Cell Conserved Domains as Novel Markers for Homogeneous Isolation of Stem and Progenitor Subpopulations

Initial understanding of DNA structure and its role within translational events depicted a scenario in which intron coding regions represent redundant bases, essentially serving as a buffering system to protect transcribed exons. Whilst in some senses this interpretation is correct in that introns are not transcribed per se, investigations over recent years have illustrated their fundamental role within the genome. In fact introns serve as regulators of exon, and therefore gene, transcription, acting as binding sites for transcriptional machinery to enable genes to be transcribed and subsequently translated. In addition to allowing binding of RNA polymerase II, intron promoter regions adjacent to genes allow binding of both general transcription factors (GTFs) such as TFIIA, TFIIB, TFIID, TFIIE, TFIIF and TFIIH, and consequently specific transcription factors such as those related to Oct and Sox transcription factor families. GTFs sequentially assemble on the core promoter thereby forming stable nucleoprotein complexes, which subsequently allows for the recruitment of RNA polymerase II to form the pre-initiation complex (PIC). Three divergent classes of DNA sequence elements direct RNA polymerase II transcription.

The first includes DNA sequences within the core promoter; a pyrimidine-rich initiator motif and generally a TATA-box (consensus TATAAA) located approximately 25-35 base pair (bp) upstream of the transcription start site. Both of these DNA elements are recognised by the GTF machinery to initiate transcription. There are two other classes of *cis*-regulatory elements: proximal-promoter and distal-promoter elements (enhancers). Specific transcription factors bind to these *cis*-regulatory elements, regulating transcription rates and expression patterns either by activating or inhibiting the recruitment and assembly of the PIC (*Figure 7.1*)[416].

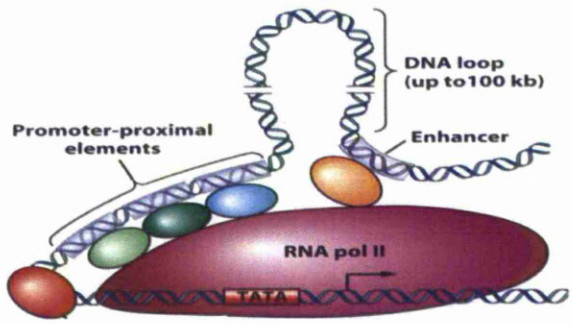

***Figure 7.1* - Association of RNA polymerase II and GTFs to core promoter for transcription initiation. Core promoter elements shown are the TATA-box, promoter-proximal elements and promoter-distal elements (enhancers) (modified from B. Lewin, Genes IX).**

Evolution strives to retain advantageous genetic modifications over increasing time, with many important developmental traits conserved throughout species development. Such genetic conservation can now be readily observed following the complete sequencing of numerous genomes within recent years, with the study of evolutionary conserved regions (ECRs) becoming an area of intensive research as a direct consequence. Conservation of genetic information implies a degree of importance towards the survival of the organism, with advantageous genes demonstrating high levels of conservation across species of increasing evolutionary stature. In addition to the conservation of advantageous coding regions, *cis*-regulatory elements responsible for transcriptional maintenance are also conserved. Many investigations have studied such ECRs and their residing polymorphisms and mutations and have suggested relationships with respect to various neurological disorders[417], cocaine addiction[418], and developmental progression[376].

Interestingly, identification of highly conserved genes fundamentally associated with maintenance of plasticity and control of differentiation revealed associated highly conserved *cis*-regulatory flanking regions. Upon identification it was acknowledged that such areas could represent functional characteristics on which to base homogeneous cell purification strategies, and as such regions were interrogated for their residing transcription factor binding sites and subsequently tested for their specific activity within populations of varying plasticity and differentiation commitment. *Cis*-regulatory regions of high conservation and potential lineage identification were designated Stem Cell Conserved Domains (SCCDs).

SCCDs associated with desired phenotypic characteristics were selected and corresponding synthetically engineered sequences subsequently inserted into a pGL3p vector containing a Luciferase reporter gene with an SV40 minimal promoter. Constructs were transfected into both lineage induced and non-induced cells isolated from various tissues and assessed for their regulatory impacts via comparing fold increase or decrease of luciferase expression generated by SCCD containing reporters over the basal pGL3p vector expression. Whilst initial investigations detailed below have identified potential SCCDs for the isolation of varyingly plastic cells, pre-adipocytes and neuronal progenitor cells, bioinformatic studies have identified numerous SCCDs with potential for purifying numerous lineage committed progenitors (*Table 7.1*). Whilst initial investigations have attempted to generate proof of concept data regarding functions of selected SCCDs, domains signifying a regulatory function can subsequently be inserted into a vector containing a GFP reporter gene and thereby facilitate the homogeneous purification of cells based upon regulatory capacity associated with a given phenotype using high speed cell sorting (*Figure 7.2*).

Cell type	Gene neighbouring a potential SCCD
Pre-adipocyte	Dlk-1, Fabp4, Fabp5, GATA2, GATA3, Irs1, Irs2, NDN
Pre-cardiomyocyte	NPPA, TEAD1
Pre-chondrocyte	CDH2, FGFR2, IGFL1, IGFL3, Sox9
Pre-endothelial	CD34, CSF1, CSF2, CSF3, GATA1, IL7, IL7R
Pre-hematopoietic	ANP32C, β-globin, CDX4, EPO, GYPA, Hoxb4, TNT

Pre-hepatocyte	CD24, CTLA4, Epha4, ITGB1, KRT8, NT5E, TCF1, Vcam1
Pre-islets langerhan	CX3CL1, HAND-1, Hlxb-9, INSM1, MixL1, SLC2A2
Pre-metanephric	CALCRL, CDH6, DUSP6, Jag1, MMP10, MSX1, Pax2
Pre-neuron	ASCL1, FGF8, FGFR2, MAP2, PROM1, REST, Sox2
Pre-osteoblast	AAK1, CDH11, MEPE
Pluripotent stem cell	BEST1, EOMES, FOXD3, HLA-DRA, Oct4, Sox2
Pre-RPE	KRT7, RBP1, RBP2, RPE65
Pre-skeletal muscle	DMD, Msx1, MYH13, Nkx2-5, Pax3

***Table 7.1* - SCCDs neighbouring known regulatory genes fundamental to guidance/maintenance of given phenotypes: Potential regions for homogeneous purification of stem/progenitors subsets.**

7.1.3 Aims of this Chapter

This investigation aims to provide proof of concept data for SCCDs flanking the (i) *Sox2* gene to demonstrate a transcriptional role in regulating plasticity. Luciferase reporter constructs will be transfected into bone marrow-, dental pulp- and umbilical cord-derived cells cultured in basal conditions and adipogenic and neural differentiation media; (ii) *NRSF* gene to demonstrate a regulatory capacity with neurogenesis. Luciferase reporter constructs will be transfected into bone marrow- and dental pulp-derived cells cultured in basal and neuronal induction media; (iii) *Dlk-1* gene to demonstrate a role within adipogenic lineage commitment. Luciferase reporter constructs will be transfected into bone marrow- and dental pulp-derived cells cultured in basal and adipogenic media. Obtained luciferase values will allow calculation of transcription factor binding, and therefore transcriptional regulatory capacity, of the selected SCCD. Should the selected regions prove to have a functional regulatory capacity, GFP reporter constructs containing the selected regions will be constructed to allow purification of cells displaying up-/down-regulations using high speed cell sorting.

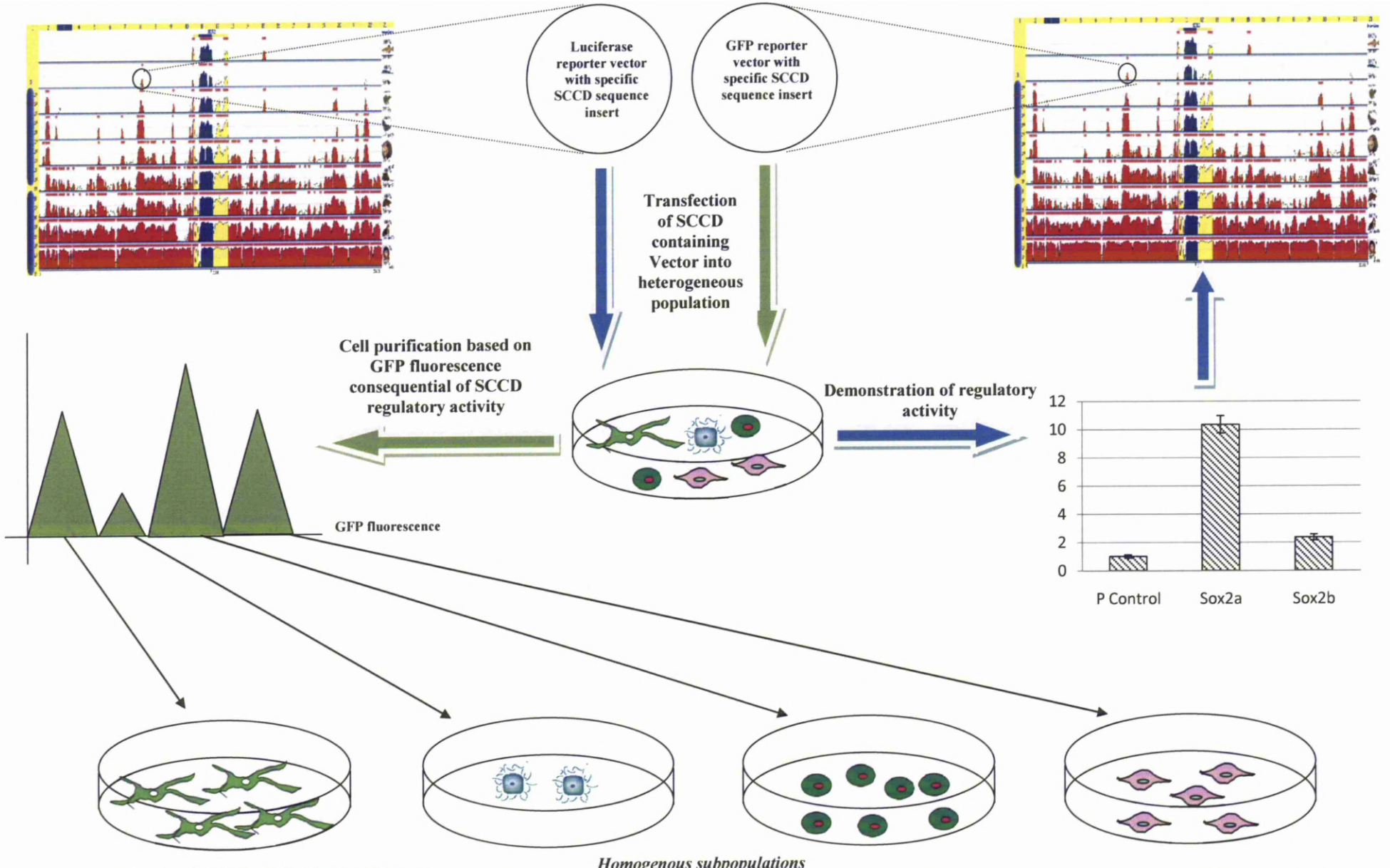

Figure 7.2 - **SCCD Cell Purification Strategy**

7.2 Sox2 SCCDs

7.2.1 Utilisation of Sox2 SCCDs for the Purification of Stem Cells Exhibiting Varying Levels of Plasticity

Sox2 is highly expressed in ES cells and debatably within adult-derived cells, interacting with Oct4 and Nanog to facilitate downregulation of lineage specific transcription and thereby maintain the cell in an undifferentiated state, a fundamental property of the developing embryo[93,96]. The demonstration of Sox2 influence with regards maintenance of plasticity highlighted the region as a potential target for bioinformatics, and unsurprisingly the Sox2 gene is highly conserved throughout evolution, indicating that it may be fundamentally required to maintain plasticity during development. Further bioinformatic probing of regions surrounding the Sox2 gene revealed a highly conserved *cis*-regulatory SCCD approximately 3kb upstream of the Sox2 exon region, which contained binding sites for plasticity-associated transcription factors such as Oct4, HOXA4 and NF-κB, thereby suggesting a functional role for the SCCD. Synthetic sequences mimicking this SCCD were cloned into a pGL3p vector with an SV40 minimal promoter; Sox2a representing a short replicate and Sox2b a longer sequence. Plasmids containing these constructs were transfected into cells isolated from bone marrow, dental pulp and umbilical cord in both basal and induction media to assess the regulatory capacity of this SCCD.

7.2.2 Demonstration of a Regulatory Capacity of a Sox2 SCCD in Bone Marrow-derived MSCs Cultured in Basal and Differentiation Media

To asses the regulatory capacity of the Sox2 SCCD, synthetically generated plasmids, Sox2a and Sox2b, were transfected into Lonza passage 5 bone marrow-derived MSCs using Qiagen Effectene technology. Cells cultured in commercially synthesised basal, adipogenic and neuronal media were transfected 48 hours prior to regulatory analysis. Sox2a (*Figure 7.3*) was upregulated between 6- and 11- fold in basal conditions over the 28 day culture period, indicating a fundamental regulatory role with within the population. Upon introduction into adipogenic and neuronal differentiation media, Sox2a demonstrated a reduced upregulation following 3 days

of culture, with only a 1.82 fold upregulation in adipogenic media and a 1.55 fold upregulation in neuronal media. Following 7 days of differentiation, Sox2a was downregulated within the population, exhibiting a 0.31 fold decrease in adipogenic media and a 0.52 fold decrease in neuronal media. MSCs cultured in adipogenic media demonstrated further downregulation for the remainder of the culture period; exhibiting 0.54-, 0.65-, and 0.54- fold downregulations at 14, 21 and 28 days respectively. No regulatory data was obtained for MSCs cultured in neuronal media at 14 and 21 days, with infection of the culture preventing acquisition of data. However, the 0.8 fold downregulation following 28 days of neuronal culture would indicate that Sox2a remained downregulated for the duration of the culture. Sox2b (*Figure 7.4*) represented a sequence incorporating a greater length of the Sox2 SCCD sequence compared with Sox2a, although interestingly did not demonstrate as greater regulatory capacity. In basal conditions Sox2b exhibited a 1- to 2.5- fold upregulation over the 28 day culture period, indicating a reduced functional capacity compared with the Sox2a plasmid. Upon introduction into chemically-defined adipogenic media, cells exhibited a reduced 1.06 fold upregulation following 3 days of differentiation. Following further adipogenic differentiation, Sox2b was further downregulated; demonstrating 0.15-, 0.5-, 0.46-, and 0.47- fold downregulations at days 7, 14, 21 and 28 respectively. MSCs cultured in neural differentiation media demonstrated a similar regulatory capacity, exhibiting a reduced upregulation of 1.13 fold following 3 days of differentiation, with 0.47- and 0.54- fold downregulation at days 7 and 28 respectively. No data was noted for days 14 and 21 due to infection of culture.

To assess the regulatory capacity of MSCs cultured for prolonged periods *in vitro*, passage 8 MSCs cultured in basal media were compared with passage 5 results obtained previously (*Figure 7.5*). Cells cultured for 7 days exhibited significant differences with regards Sox2a regulation, with passage 5 cells demonstrating a 9.58 fold upregulation compared with 2.10 fold observed in passage 8 cells. Passage 8 cells also demonstrated a reduced upregulation with regards Sox2b, generating a 1.04 fold upregulation compared with 1.67 fold observed in passage 5 cells. This reduced upregulation is consistent with the labouring proliferative and differentiation capacities observed *in vitro*, suggesting that prolonged tissue culture either modifies transcriptional regulation responsible for maintenance of cellular plasticity, or

alternatively, MSCs differentiate towards terminally differentiated cells which demonstrate downregulation of the Sox2 SCCD.

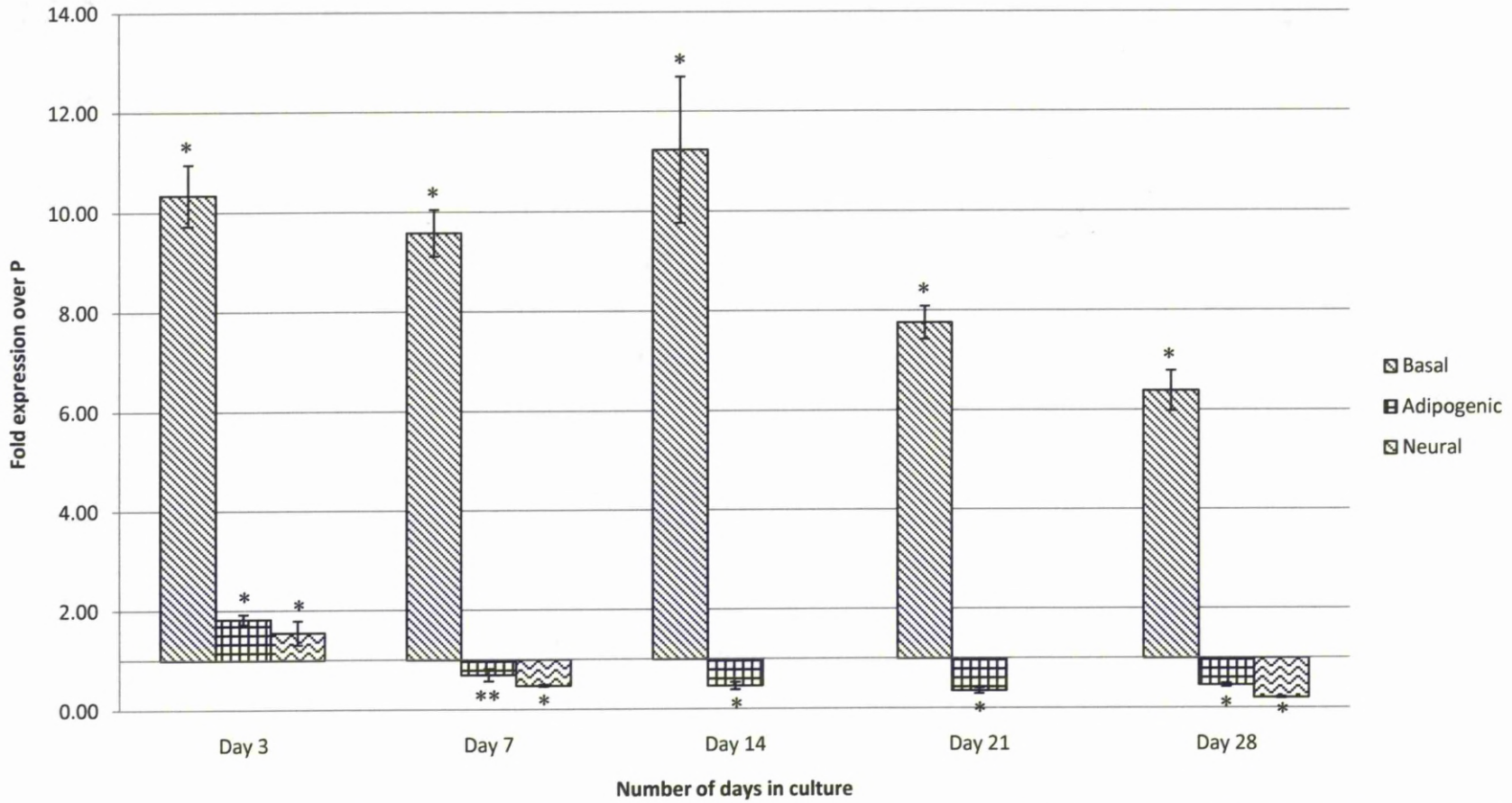

Figure 7.3 - **Sox2a regulation in bone marrow-derived MSCs (Passage 5, 1 x Freeze-thaw) cultured in chemically-defined basal, adipogenic and neural media for 28 days. Data for Sox2a regulation in MSCs cultured in neural media at days 14 and 21 were not obtained due to infection of culture. Values represent mean up-/down-regulation over the pGL3p control (pGL3p control = 1) (n = 4). Error bars correspond to Standard Deviations. Student *t*-test indicated that (i) Sox2a up-regulation over pGL3p in basal culture was significant at days 3, 7, 14, 21 and 28 (*$p \leq 0.001$); (ii) Sox2a up- and down- regulation over pGL3p in adipogenic culture was significant at days 3, 7, 14, 21 and 28 (*$p \leq 0.001$) (**$p \leq 0.05$); (iii) Sox2a up- and down- regulation over pGL3p in neural culture was significant at days 3, 7, and 28 (*$p \leq 0.001$).**

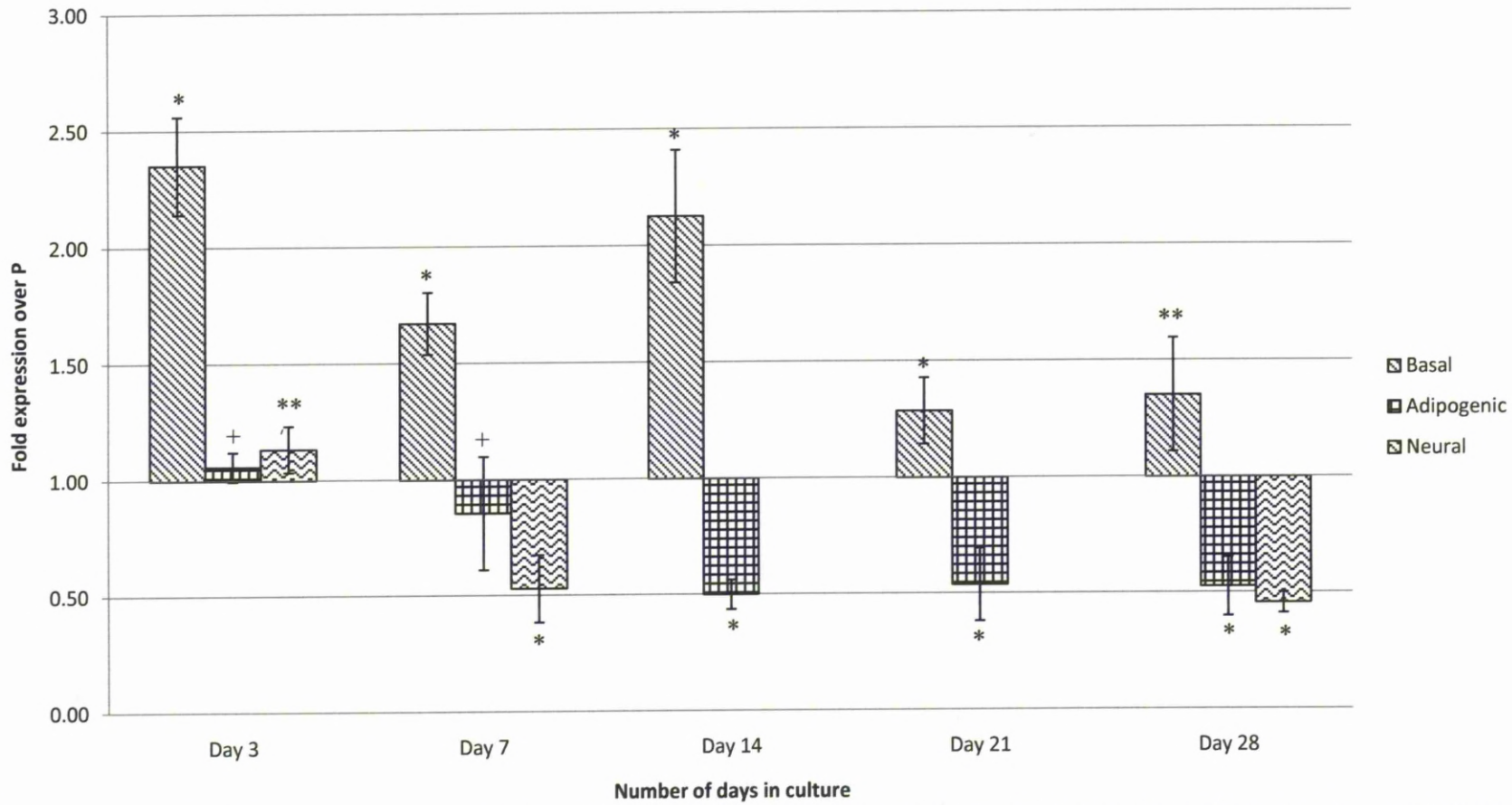

Figure 7.4 - **Sox2b regulation in bone marrow-derived MSCs (Passage 5, 1 x Freeze-thaw) cultured in chemically-defined basal, adipogenic and neural media for 28 days. Data for Sox2b regulation in MSCs cultured in neural media at days 14 and 21 were not obtained due to infection of culture. Values represent mean up-/down-regulation over the pGL3p control (pGL3p control = 1) (n = 4). Error bars correspond to Standard Deviations. Student *t*-test indicated that (i) Sox2b up-regulation over pGL3p in basal culture was significant at days 3, 7, 14, 21 and 28 (*$p \leq 0.001$) (**$p \leq 0.05$); (ii) Sox2b up- and down- regulation over pGL3p in adipogenic culture was significant at days 14, 21 and 28 (*$p \leq 0.001$) but not at days 3 and 7 (+$p \geq 0.05$); (iii) Sox2b up- and down- regulation over pGL3p in neural culture was significant at days 3, 7, and 28 (*$p \leq 0.001$) (**$p \leq 0.05$).**

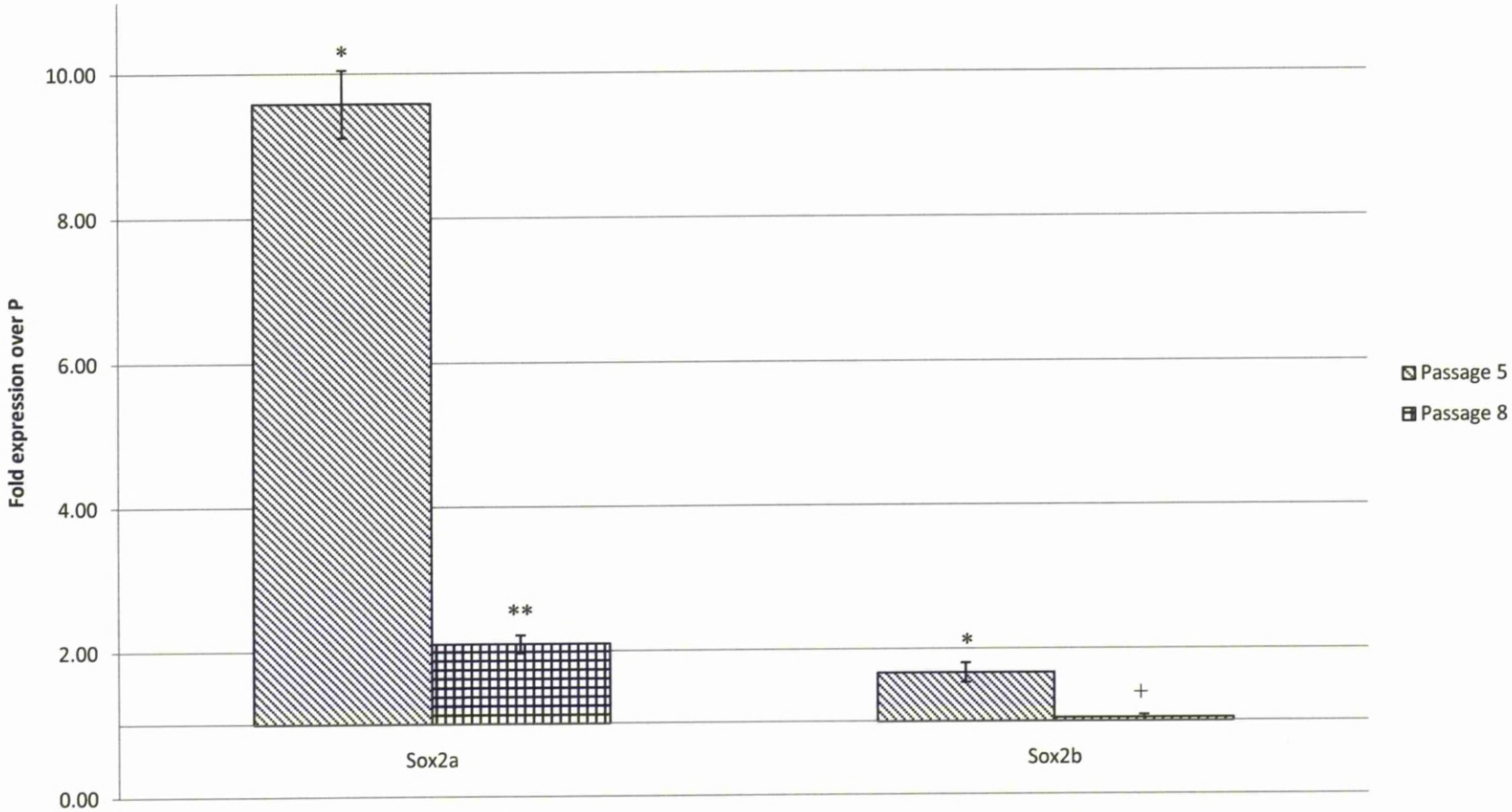

Figure 7.5 - **Sox2a and Sox2b regulation in bone marrow-derived MSCs at *in vitro* passage 5 and 8 (1 x Freeze-thaw) cultured in chemically-defined basal media for 7 days. Values represent mean up-/down-regulation over the pGL3p control (pGL3p control = 1) (n = 4). Error bars correspond to Standard Deviations. Student *t*-test indicated that (i) Sox2a up-regulation over pGL3p was significant at passage 5 and 8 (*$p \leq 0.001$) (**$p \leq 0.05$); (ii) Sox2b up-regulation over pGL3p was significant at passage 5 (*$p \leq 0.001$) but not passage 8 (+$p \geq 0.05$).**

7.2.3 Demonstration of a Regulatory Capacity of a Sox2 SCCD in Dental pulp-derived Populations Cultured in Basal and Differentiation Media

To assess the regulatory capacity of the Sox2 SCCD in dental pulp-derived populations, Sox2a and Sox2b were transfected into passage 5 pulp donor 3 cells cultured in chemically-defined basal, adipogenic and neuronal media. However, due to the reduced differentiation period required for lineage commitment of dental pulp cells in comparison with bone marrow-derived MSCs, as detailed in Chapter 6, cells were transfected at days 3, 7, 14 and 21, neglecting transfection at day 28.

Sox2a (*Figure 7.6*) transfected using Effectene transfection methods maintained a 2.7- to 3.5- fold upregulation in basal conditions, demonstrating a regulatory role within the population. Following introduction into chemically-defined adipogenic media, the Sox2a SCCD was immediately downregulated; demonstrating 0.47-, 0.47, 0.45- and 0.48- fold downregulation at days 3, 7, 14 and 21 respectively. Chemical induction towards a neuronal phenotype generated similar results, with the Sox2a SCCD downregulated 0.40-, 0.45-, 0.47- and 0.51- fold at days 3, 7, 14 and 21 respectively. Sox2b (*Figure 7.7*) construct was transfected using Effectene methodologies. Cells cultured in basal media demonstrated a 1.5- to 2.0- fold upregulation of Sox2b over the 21 day culture, although this was downregulated after introduction of differentiation stimulation. Adipogenic differentiation resulted in 0.44-, 0.50-, 0.44- and 0.46- fold downregulation at days 3, 7, 14 and 21 respectively. Conversely, neuronally induced cells demonstrated significantly reduced downregulation of Sox2b, with 0.19-, 0.08-, 0.19- and 0.0- fold downregulation at days 3, 7, 14 and 21 respectively. This apparently reduced downregulation following neuronal induction is interesting since the transfection efficiency was comparable with other transfections, suggesting that the results were an accurate reflection of regulatory function. It would therefore be interesting to probe cells exhibiting this partial downregulation to assess their phenotypic properties with regards neuronally associated markers, with homogenous characterisation potentially yielding highly proliferative neuronal progenitors.

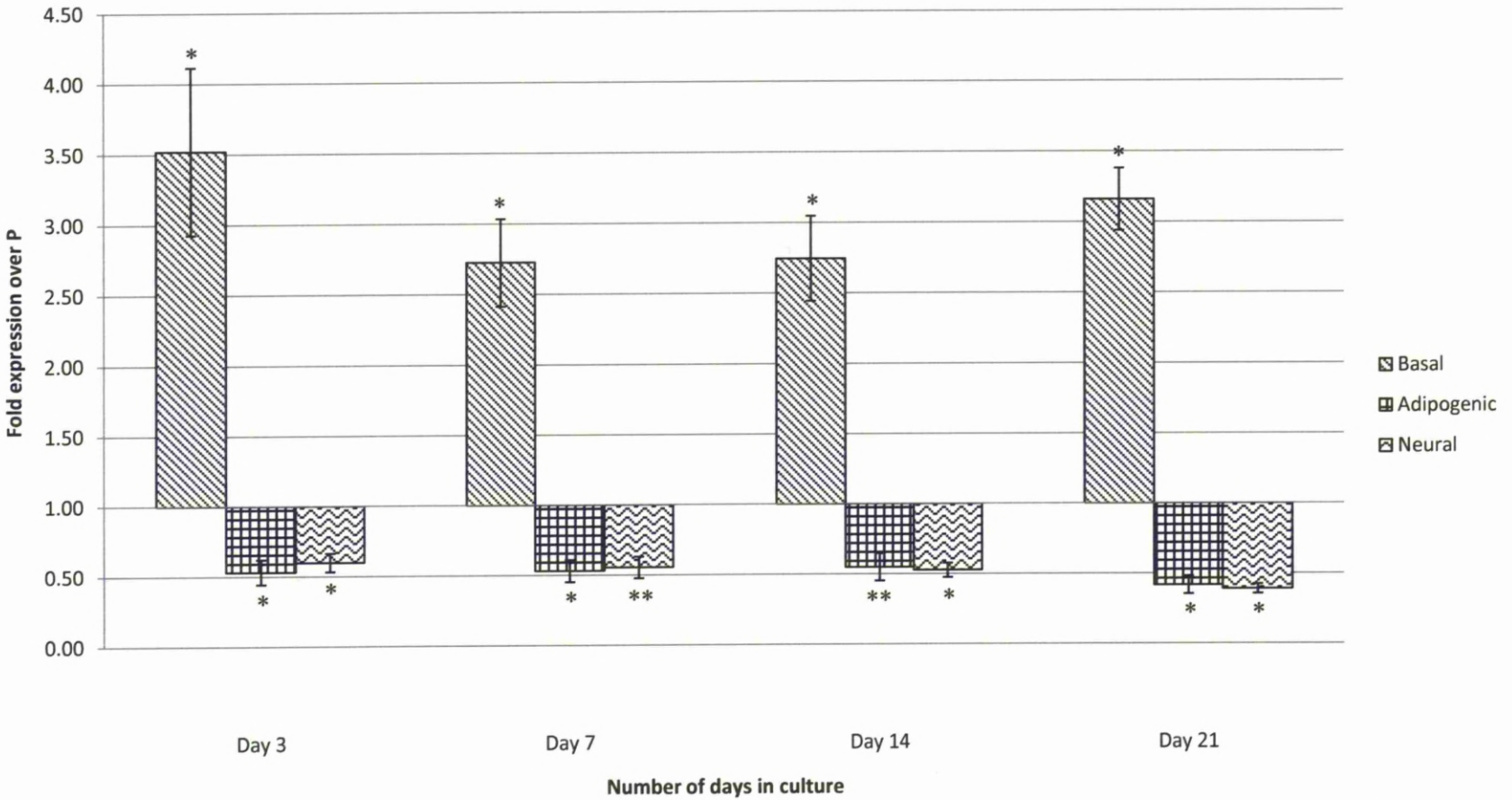

Figure 7.6 - **Sox2a regulation in dental pulp-derived cells (Passage 5, 1 x Freeze-thaw) cultured in chemically-defined basal, adipogenic and neural media for 21 days. Values represent mean up-/down-regulation over the pGL3p control (pGL3p control = 1) (n = 4). Error bars correspond to Standard Deviations. Student *t*-test indicated that (i) Sox2a up-regulation over pGL3p in basal culture was significant at days 3, 7, 14 and 21 (*p≤0.001); (ii) Sox2a down-regulation over pGL3p in adipogenic culture was significant at days 3, 7, 14 and 21 (*p≤0.001) (**p≤0.05); (iii) Sox2a down-regulation over pGL3p in neural culture was significant at days 3, 7, 14 and 21 (*p≤0.001) (**p≤0.05).**

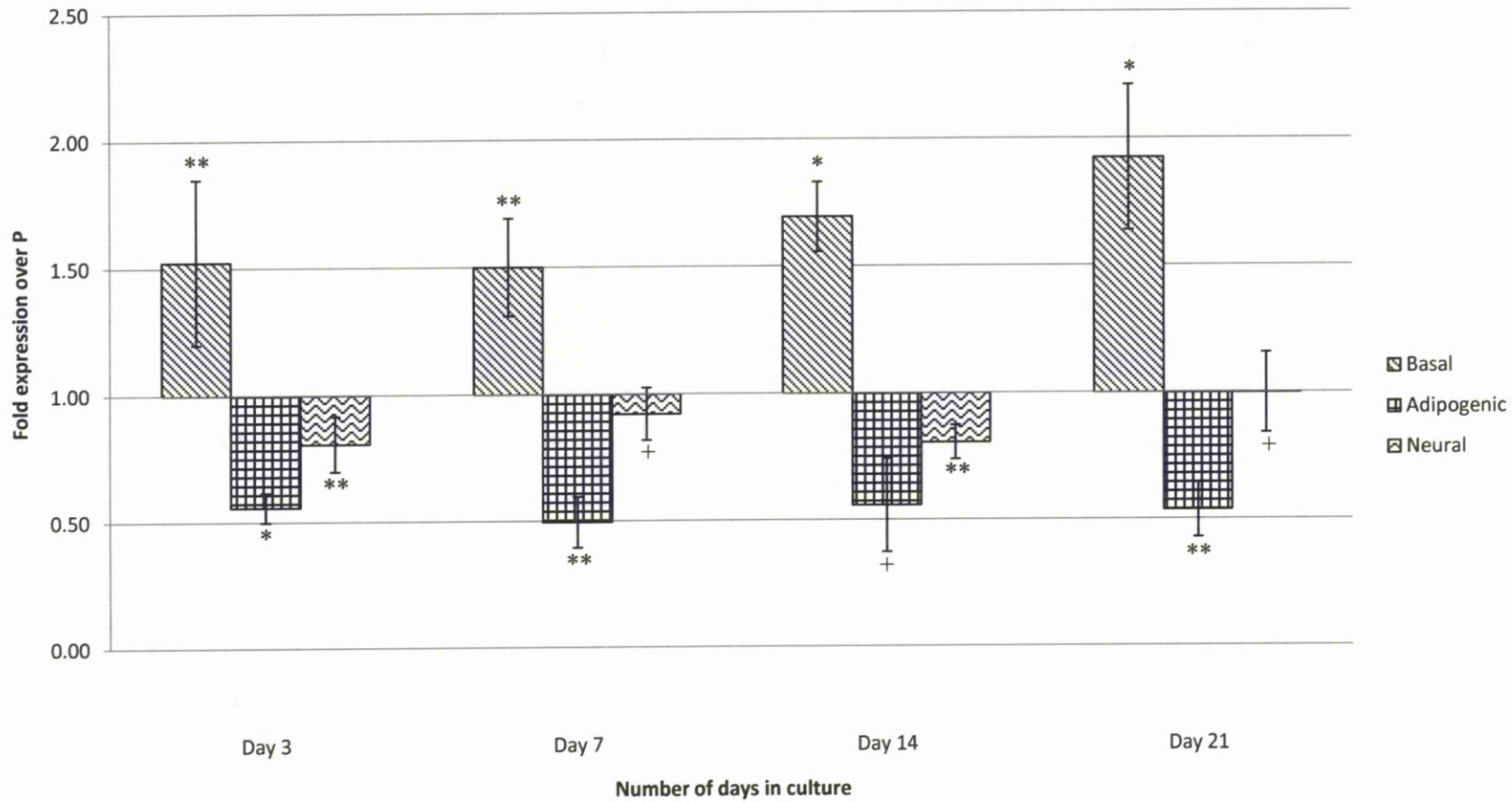

Figure 7.7 **- Sox2b regulation in dental pulp-derived cells (Passage 5, 1 x Freeze-thaw) cultured in chemically-defined basal, adipogenic and neural media for 21 days. Values represent mean up-/down-regulation over the pGL3p control (pGL3p control = 1) (n = 4). Error bars correspond to Standard Deviations. Student *t*-test indicated that (i) Sox2b up-regulation over pGL3p in basal culture was significant at days 3, 7, 14 and 21 (*$p \leq 0.001$) (**$p \leq 0.05$); (ii) Sox2b down-regulation over pGL3p in adipogenic culture was significant at days 3, 7 and 21 (*$p \leq 0.001$) (**$p \leq 0.05$) but not day 14 (+$p \geq 0.05$); (iii) Sox2b down-regulation over pGL3p in neural culture was significant at days 3 and 14 (**$p \leq 0.05$) but not days 7 and 21 (+$p \geq 0.05$).**

7.2.4 Demonstration of a Regulatory Capacity of a Sox2 SCCD in Whole Umbilical Cord-derived Populations Cultured in Basal Media

Cells derived following enzymatic digestion of whole umbilical cord displayed many properties associated with bone marrow-derived populations, including similar phenotypic and proliferative characteristics. Passage 5 umbilical cords were therefore transfected with Sox2a and Sox2b reporter constructs to assess the regulatory impact of the Sox2 SCCD under basal conditions in comparison with the activity demonstrated in bone marrow-derived cells.

Sox2a and Sox2b reporter constructs were transfected using Effectene into cord cultured for 7 days in chemically-defined basal media (*Figure 7.8*). Sox2a demonstrated a 10.3 fold upregulation, marginally higher than the 9.58 fold upregulation observed in bone marrow-derived cells of the same passage. Sox2b generated a 2.59 fold upregulation in umbilical cord cells, again insignificantly higher than the 2.10 fold upregulation achieved in bone marrow-derived cells. Thus, whilst umbilical cord-derived cells exhibited slight increases with regards upregulation of the Sox2 SCCD, the insignificance of the regulatory differences are likely to be attributable to slightly varying numbers of alternatively transcribing progenitor cells or differing transfection efficiencies. It is therefore likely that both umbilical cord and bone marrow-derived heterogeneous populations globally regulate the Sox2 SCCD in a similar manner, and from further similarities observed with regards phenotypic and proliferative capacity, it could be suggested that populations derived from these two tissues contain subpopulations of stem, progenitor and terminally differentiated cells in similar quantities. Alternatively, however, the increased regulatory function of both Sox2 SCCDs exhibited by cord cells could be attrubuted to a small number of primitive cells derived from the developing embryo, populations which could represent highly plastic cells.

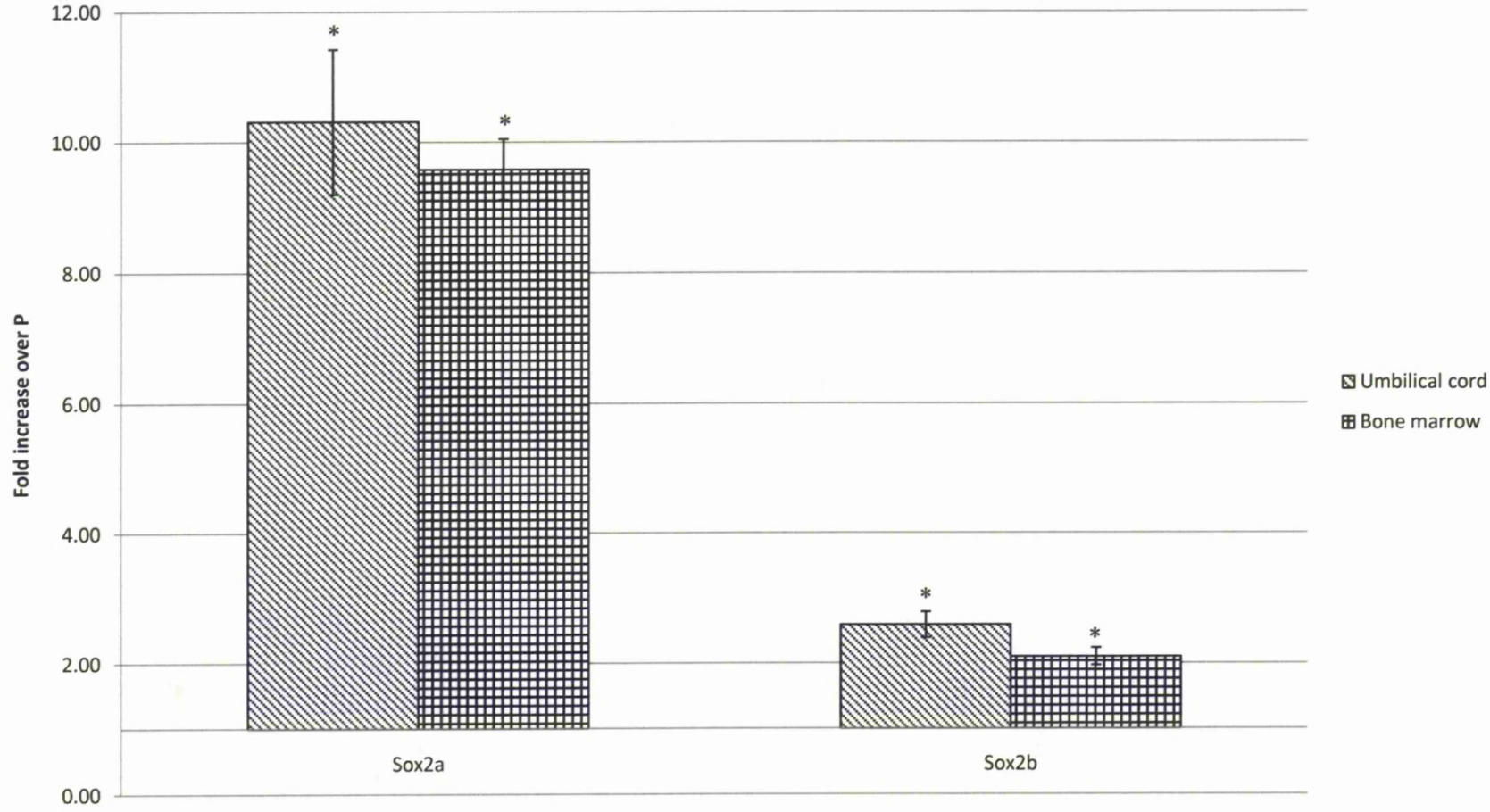

Figure 7.8 - **Sox2a and Sox2b regulatory capacity in cells derived from (i) enzymatically digested whole umbilical cord (Passage 5, 1 x Freeze-thaw); (ii) bone marrow-derived MSCs (Passage 5, 1 x Freeze-thaw) cultured in chemically-defined basal media for 7 days. Values represent mean up-/down- regulation over the pGL3p control (pGL3p control = 1) (n = 4). Error bars correspond to Standard Deviations. Student *t*-test indicated that (i) Sox2a and Sox2b up-regulation over pGL3p in umbilical cord cells in basal culture were significant (*$p \leq 0.001$); (ii) Sox2a and Sox2b up-regulation over pGL3p in bone marrow cells in basal culture were significant (*$p \leq 0.001$).**

7.2.5 Regulatory Capacity of Sox2 SCCD Represents Criteria on which to Purify Homogenous Stem Cell Populations

Constructs designed to assess the regulatory capacity of the Sox2 SCCD demonstrated a key regulatory function in undifferentiated cells which is rapidly downregulated following differentiation. It is therefore suggested that the Sox2 SCCD functions to maintain plasticity within cells, facilitating binding of transcription factors such as Oct4 which maintain cells in an undifferentiated state. Sox2a demonstrated a greater potential for assessing regulation in bone marrow, dental pulp and umbilical cord-derived cells, and therefore represents a potential target for the purification of multipotent stem cells cultured under basal conditions. With respect to the isolation of cells exhibiting varying levels of plasticity, cloning of the Sox2a SCCD into a GFP reporter construct can allow for the homogeneous isolation of cells based upon Sox2a upregulation, hypothesising that cells exhibiting greater upregulation of Sox2a represent a more potent phenotype with regards differentiation potential. This homogeneous characterisation of such multipotent subpopulations could finally allow assessment of differentiation capacity of adult stem cells and subsequently the development of regenerative techniques using homogeneous populations. Furthermore, cells exhibiting lesser upregulations could represent progenitors of varying lineage commitment, with their homogenous characterisation potentially allowing their application in numerous clinical applications.

Whilst homogeneous cell purification is the primary purpose of this novel technology, it could also represent a marker to allow tailoring of media to maintain isolated populations in an undifferentiated, homogeneous state for prolonged periods *in vitro*. Given the inability of antigen putified cells to maintain the homogeneous phenotype following proliferation, and furthermore the significantly reduced upregulation of Sox2a observed in passage 8 bone marrow cells compared with those cultured for only 5 passages, Sox2a can represent a marker on which to firstly purify subpopulations based upon a functional capacity and subsequently assess global cellular phenotype, providing investigators attempting to synthesise defined media to maintain cells for prolonged periods *ex vivo* with an invaluable tool to assess effects of the media with regards transcriptional regulation. Whilst antibody based

phenotype profiling using flow cytometry allows investigators to assess maintenance of phenotype, it fails to identify whether desired stem or progenitor cell populations are being maintained. Media can therefore be tailored to generate maintained upregulation of Sox2a, potentially allowing for the culture of populations representing high levels of plasticity which can be proliferated for a prolonged period *in vitro*, generating large numbers of highly desirable cells for clinical application.

7.3 NRSF SCCDs

7.3.1 Utilisation of NRSF SCCDs for the Purification of Neural Progenitors

REST, also known as Neuronal Restrictive Silencer Factor (NRSF), is proposed to act as a key regulator of neuronal differentiation, essentially acting as a repressor of neuron-associated genes in non-neuronal tissue. Bioinformatic profiling of this region revealed high conservation of the NRSF gene and, from a perspective SCCD viewpoint, two highly conserved cis-regulatory regions upstream of the NRSF exon region. The first resides approximately 40kb upstream of the NRSF exon, and accommodates conserved binding sites for neurogenesis associated transcription factors Pax6 and Sox9. Short (NRSF1a) and long (NRSF1b) sequences incorporating this SCCD region were cloned into a pGL3p vector. The second SCCD resides approximately 40kb upstream of the SPINK gene, and 110kb upstream of the NRSF exon. SPINK is a serine protease inhibitor and mutations of this region are hypothesised to be responsible for a loss of tyrosine inhibitor function[419]. However, due to the high conservation of the SCCD and the presence of a HOXA4 transcription factor binding site, a transcription factor integral to neurogenesis, a sequence incorporating this region (NRSF2a) was cloned into a pGL3p vector. Plasmids containing NRSF-associated SCCDs were transfected into bone marrow and dental pulp-derived cells cultured in chemically-defined basal and neuronal media.

7.3.2 Demonstration of Regulatory Capacity of a NRSF SCCD in Bone Marrow-derived MSCs Cultured in Basal and Neuronal Differentiation Media

Attempting to demonstrate regulatory capacity for one or both of the NRSF SCCDs in bone marrow-derived populations, NRSF constructs 1a, 1b and 2a were transfected using Effectene into passage 5 bone marrow-derived MSCs cultured in chemically-defined basal and neuronal media at days 3, 7, 14, 21 and 28.

NRSF1a reporter construct representing a short version of the SCCD approximately 40kb upstream of the NRSF exon, demonstrated upregulation of 5.3- to 8.5- fold in basal conditions, suggesting a functional role within non-neuronal differentiating cells (*Figure 7.9*). No data was obtained for day 21 transfections in basal conditions due to infection of the culture media. However, following exposure to neuronal induction, cells exhibited lessened upregulation of NRSF1a, demonstrating 4.96-, 2.51-, 1.83- and 1.08- fold upregulations at days 3, 7, 14 and 21 respectively. Following 28 days of neuronal differentiation, corresponding to a time point at which neural associated markers such as beta-III-tubulin and neurofilament are, from the literature, observed within the differentiating population; NRSF1a demonstrated a 0.56 fold downregulation within the population, suggesting that this downregulation was required for the expression of neuronal genes. It is therefore suggested that the NRSF1a SCCD regulates NRSF gene expression, conversely acting as a regulator of neurogenesis by modifying transcription rates of NRSF. Under basal conditions the NRSF SCCD is highly upregulated, resulting in abundant production of the NRSF protein, which subsequently represses neuronal-associated genes under basal conditions. Upon detection of appropriate stimulation, in this case chemically synthesised neural differentiation media, the NRSF SCCD is downregulated, subsequently resulting in reduced levels of transcribed NRSF and thereby allowing expression of genes required for neuronal differentiation.

NRSF1b encompasses a greater proportion of the SCCD region and was transfected into passage 5 bone marrow-derived cells using Effectene. NRSF1b demonstrated a reduced upregulation in basal conditions compared with NRSF1a, yielding upregulation of 1.8- to 2.3- fold over the 28 day culture period (*Figure 7.10*). No data

was obtained for day 21 transfections in basal conditions due to infection of the culture media. As with NRSF1a, NRSF1b upregulation was reduced upon exposure to neural differentiation media, generating upregulation of 1.28-, 1.14-, 1.45-, 1.27- and 1.39- fold at days 3, 7, 14, 21 and 28 respectively. However, at no point during neurogenic differentiation was NRSF1b downregulated, perhaps indicating that the construct is less applicable for purification of neuronal progenitors.

In terms of genetic location, NRSF2a is more likely to be a regulator of the SPINK gene that NRSF. However, due its high conservation in comparison with that of the SPINK exon region, and furthermore the presence of a HOXA4 transcription factor binding site, NRSF2a was assessed for its regulatory activity in basal and neurogenic conditions. In basal conditions NRSF2a was upregulated 2.6- to 5.4- fold during the 28 day culture period, suggesting a functional capacity within the MSC population. No data was obtained for day 21 transfections due to infection. Upon neuronal induction, NRSF2a demonstrated progressively reduced upregulations of 2.49-, 1.54- and 1.21- fold at days 3, 7 and 14 respectively. Following 21 days of culture NRSF2a was downregulated 0.08 fold, further downregulating to 0.17 fold following terminal differentiation. Whilst the downregulation at day 28 (and terminal differentiation) was less dramatic than encountered with NRSF1a, the results nevertheless suggest a functional if less central role for the NRSF2a SCCD during neurogenesis (*Figure 7.11*).

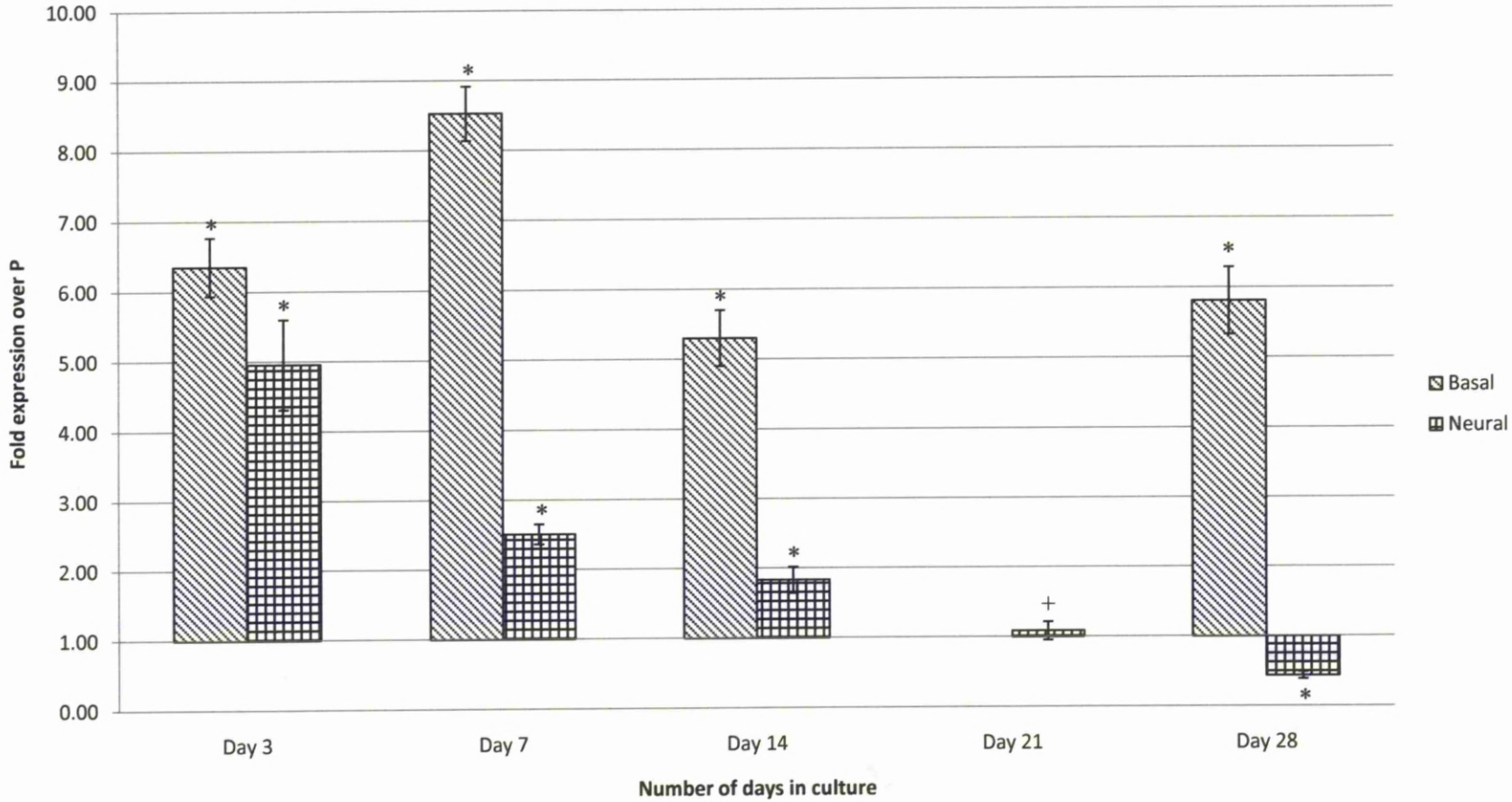

Figure 7.9 - **NRSF1a regulation in bone marrow-derived MSCs (Passage 5, 1 x Freeze-thaw) cultured in chemically-defined basal and neural media for 28 days. Data for NRSF1a regulation in MSCs cultured in basal media at day 21 were not obtained due to infection of culture. Values represent mean up-/down-regulation over the pGL3p control (pGL3p control = 1) (n = 4). Error bars correspond to Standard Deviations. Student *t*-test indicated that (i) NRSF1a up-regulation over pGL3p in basal culture was significant at days 3, 7, 14 and 28 (*$p \leq 0.001$); (ii) NRSF1a up- and down- regulation over pGL3p in neural culture was significant at days 3, 7, 14 and 28 (*$p \leq 0.001$) but not day 21 (+$p \geq 0.05$).**

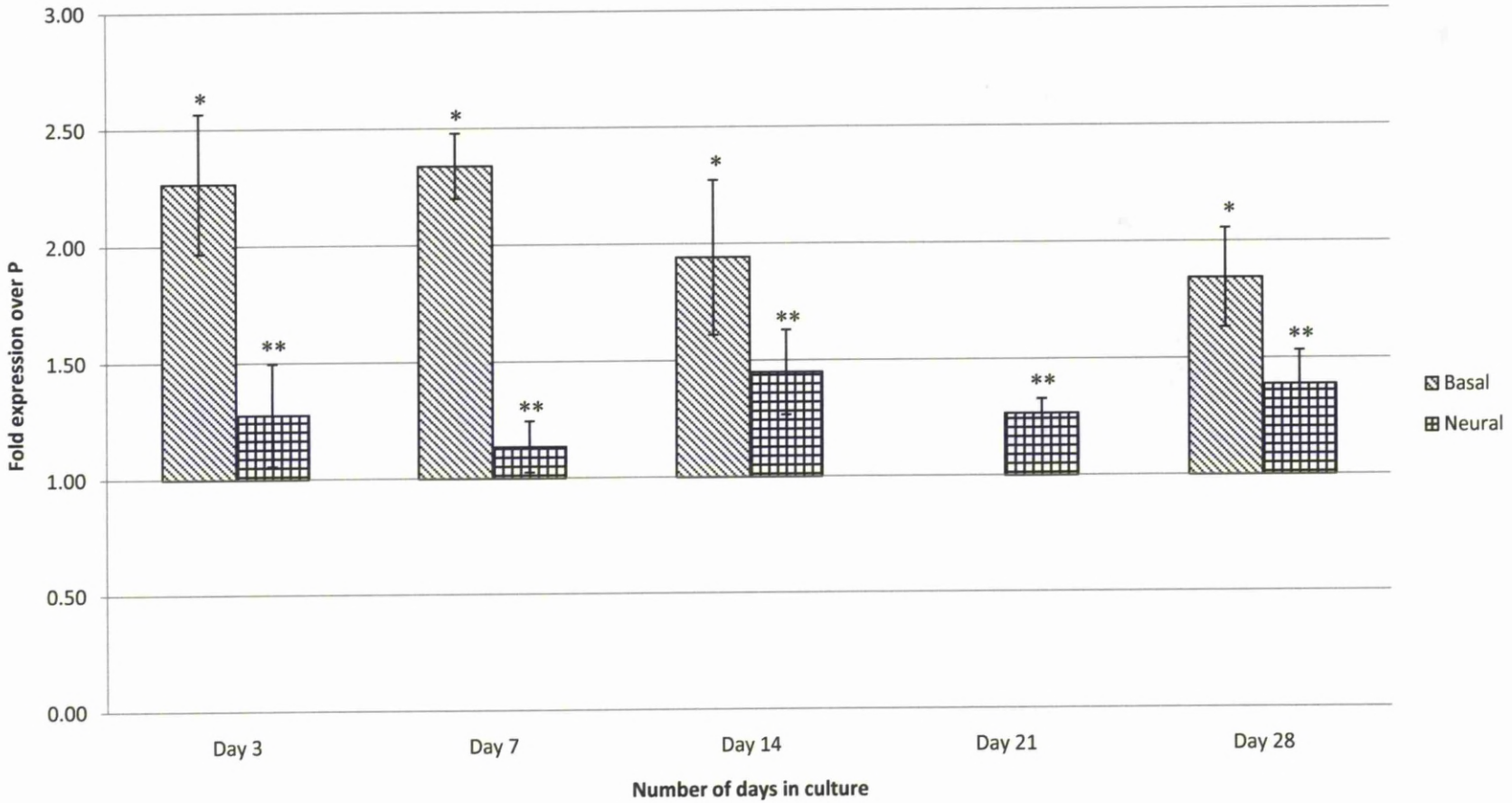

Figure 7.10 - **NRSF1b regulation in bone marrow-derived MSCs (Passage 5, 1 x Freeze-thaw) cultured in chemically-defined basal neural and media for 28 days. Data for NRSF1b regulation in MSCs cultured in basal media at day 21 were not obtained due to infection of culture. Values represent mean up-/down-regulation over the pGL3p control (pGL3p control = 1) (n = 4). Error bars correspond to Standard Deviations. Student *t*-test indicated that (i) NRSF1b up-regulation over pGL3p in basal culture was significant at days 3, 7, 14 and 28 (*$p \leq 0.001$); (ii) NRSF1b up-regulation over pGL3p in neural culture was significant at days 3, 7, 14, 21 and 28 (**$p \leq 0.05$).**

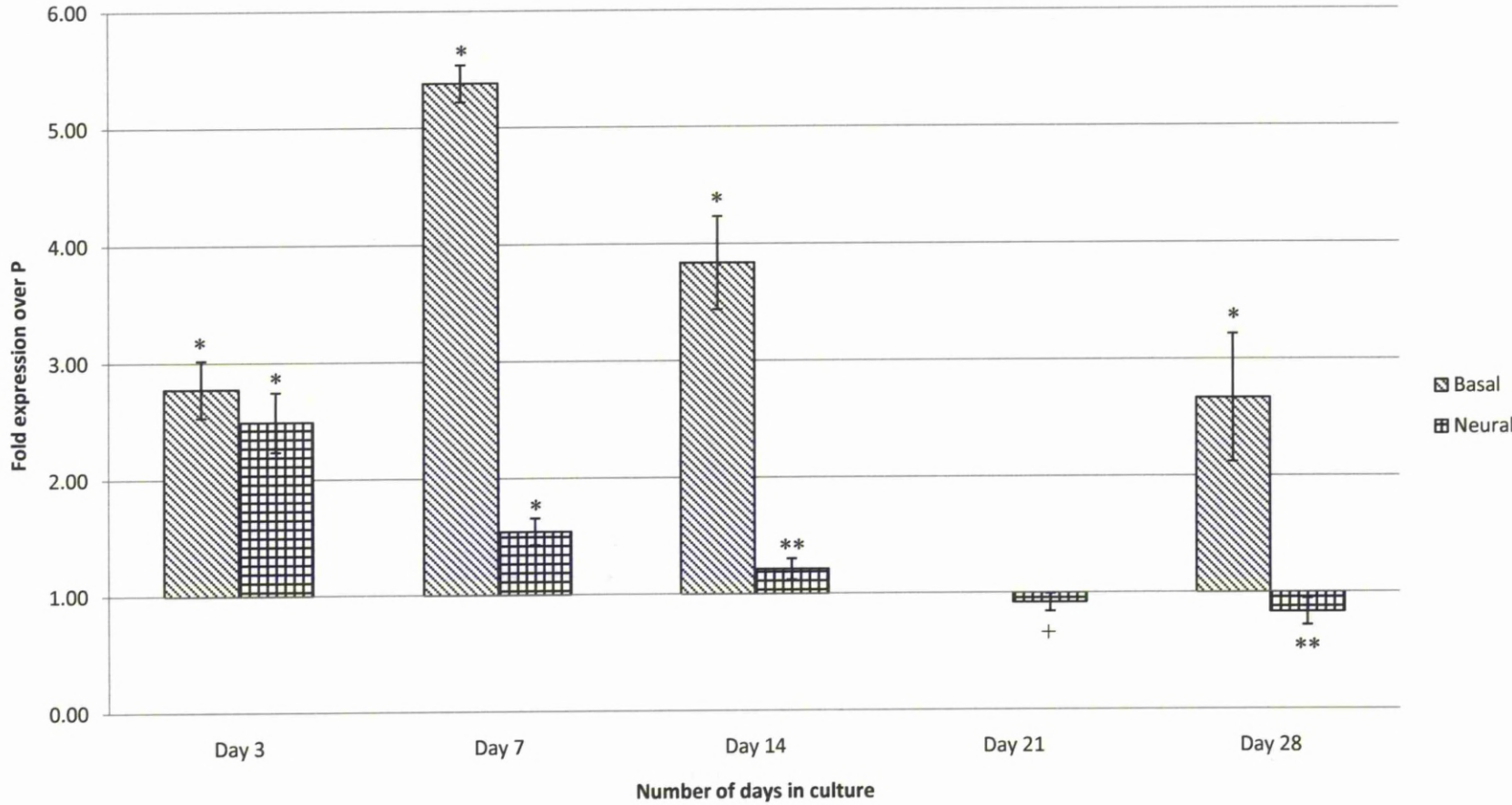

Figure *7.11* - NRSF2a regulation in bone marrow-derived MSCs (Passage 5, 1 x Freeze-thaw) cultured in chemically-defined basal and neural media for 28 days. Data for NRSF2a regulation in MSCs cultured in basal media at day 21 were not obtained due to infection of culture. Values represent mean up-/down-regulation over the pGL3p control (pGL3p control = 1) (n = 4). Error bars correspond to Standard Deviations. Student *t*-test indicated that (i) NRSF2a up-regulation over pGL3p in basal culture was significant at days 3, 7, 14 and 28 (*$p \leq 0.001$); (ii) NRSF2a up- and down- regulation over pGL3p in neural culture was significant at days 3, 7, 14 and 28 (*$p \leq 0.001$) ($p \leq 0.05$) but not day 21 (+$p \geq 0.05$).**

7.3.3 Demonstration of Regulatory Capacity of a NRSF SCCD in Dental Pulp-derived Cells Cultured in Basal and Neuronal Differentiation Media

Cells from pulp donor 3 cultured for 5 passages *in vitro* were assessed for the regulatory expression of the two NRSF SCCDs within the population. NRSF1a was transfected into the cells using Effectene transfection techniques and, contrastingly to regulatory activity observed in bone marrow-derived cells, it was downregulated in basal conditions, with repressive activities comprising 0.2-, 0.09-, 0.34- and 0.07-fold downregulations observed at days 3, 7, 14 and 21 respectively (*Figure 7.12*). This consistent downregulation in basal conditions may initially cause concern, though when the hypothesised developmental origin of dental pulp-derived cells is considered, the downregulation is predictable. In essence it is perceived that dental pulp represents a niche comprising numerous subpopulations, amongst them residing neural progenitor cells which are likely to express numerous neuronal associated genes, thus requiring a downregulation of NRSF gene expression, which it is suggested is regulated by the NRSF1a SCCD. Upon introduction into neural differentiation media, NRSF1a is further downregulated, yielding repression of 0.59-, 0.58-, 0.58- and 0.67- fold at days 3, 7, 14 and 21 respectively. It is therefore hypothesised that NRSF1a represents a candidate SCCD for the identification of neural progenitor subsets of varying commitment, with translation of the technology to a GFP based vector potentially circumventing the isolation of neural progenitors from induced and non-induced cell populations using high speed cell sorting post-transfection.

NRSF1b, representing a longer version of NRSF1a, was transfected in passage 5 cells cultured in basal media and demonstrated downregulation of 0.04-, 0.29- and 0.21- fold at days 3, 14 and 21 respectively (*Figure 7.13*). Unexpectedly, non-induced cells cultured for 7 days demonstrated a minimal upregulation encompassing a 1.09 fold increase, although this was attributed to a poor transfection efficiency achieved in one experimental repeat. Upon neuronal induction NRSF1b continued to be downregulated although did not appear to increase repression, generating 0.11-, 0.14-, 0.29- and 0.21- fold decrease at days 3, 7, 14 and 21 respectively. Due to the reduced volatility in terms of regulatory repression, NRSF1b represents a less

suitable tool for the purification of neural progenitor cells from dental pulp in comparison to NRSF1a.

The SPINK gene flanking SCCD NRSF2a also demonstrated downregulation when transfected into passage 5 dental pulp-derived cells, generated 0.23-, 0.19-, 0.35- and 0.06 fold repressions at days 3, 7, 14 and 21 respectively (*Figure 7.14*). Post-neuronal induction NRSF2a continued to be downregulated, yielding repression of 0.39-, 0.37-, 0.34- and 0.49- fold at days 3, 7, 14 and 21 respectively. However, as with results obtained with NRSF1b, the limited variation with regards observed regulatory expression subsequently limits its capacity for the purification of homogenous subpopulations of neuronal precursors.

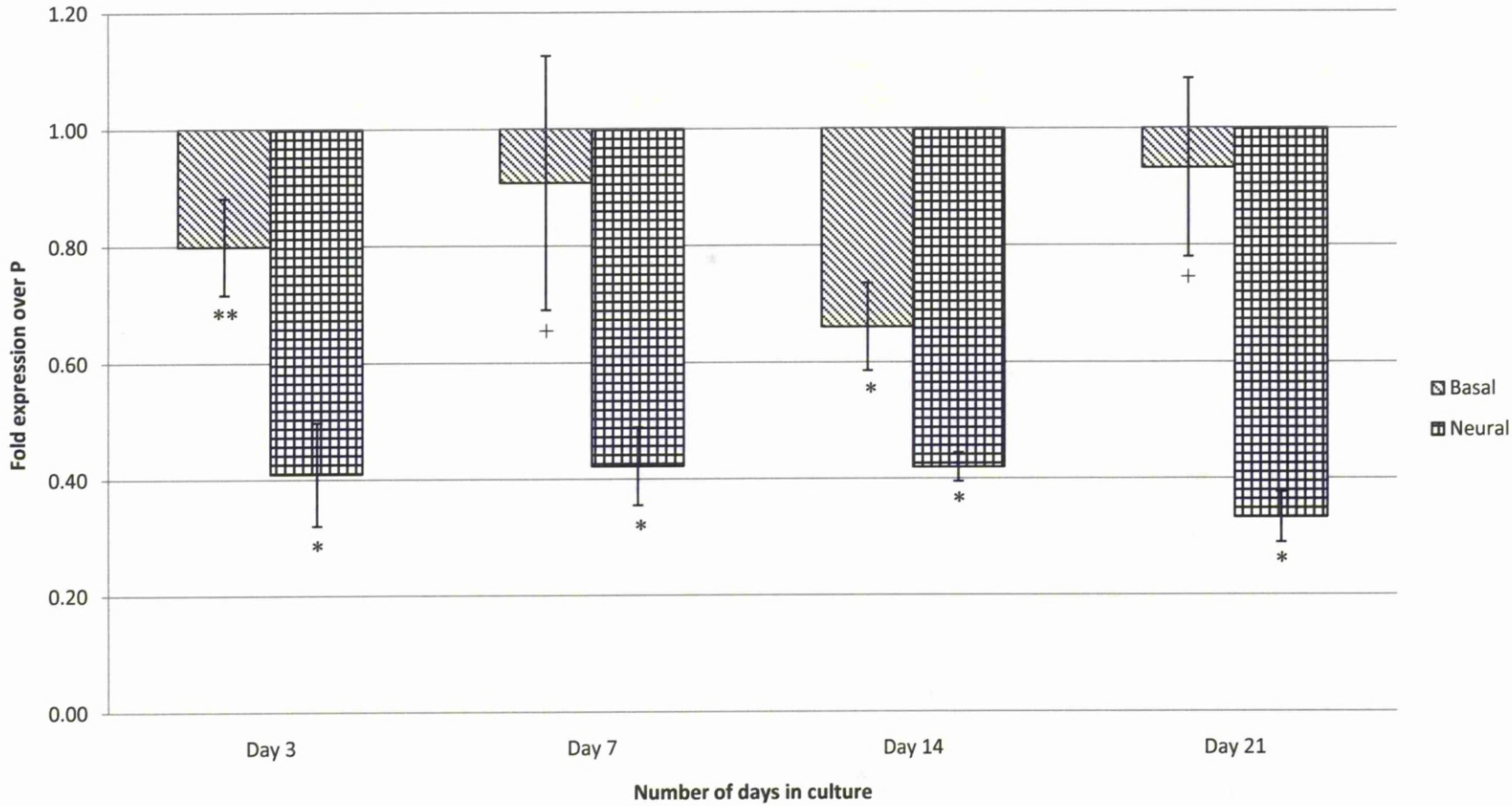

Figure 7.12 - **NRSF1a regulation in dental pulp-derived cells (Passage 5, 1 x Freeze-thaw) cultured in chemically-defined basal neural and media for 28 days. Values represent mean up-/down-regulation over the pGL3p control (pGL3p control = 1) (n = 4). Error bars correspond to Standard Deviations. Student *t*-test indicated that (i) NRSF1a down-regulation over pGL3p in basal culture was significant at days 3 and 14 (*$p \leq 0.001$) (**$p \leq 0.05$) but not days 7 and 21 (+$p \geq 0.05$); (ii) NRSF1a down-regulation over pGL3p in neural culture was significant at days 3, 7, 14 and 21 (*$p \leq 0.001$).**

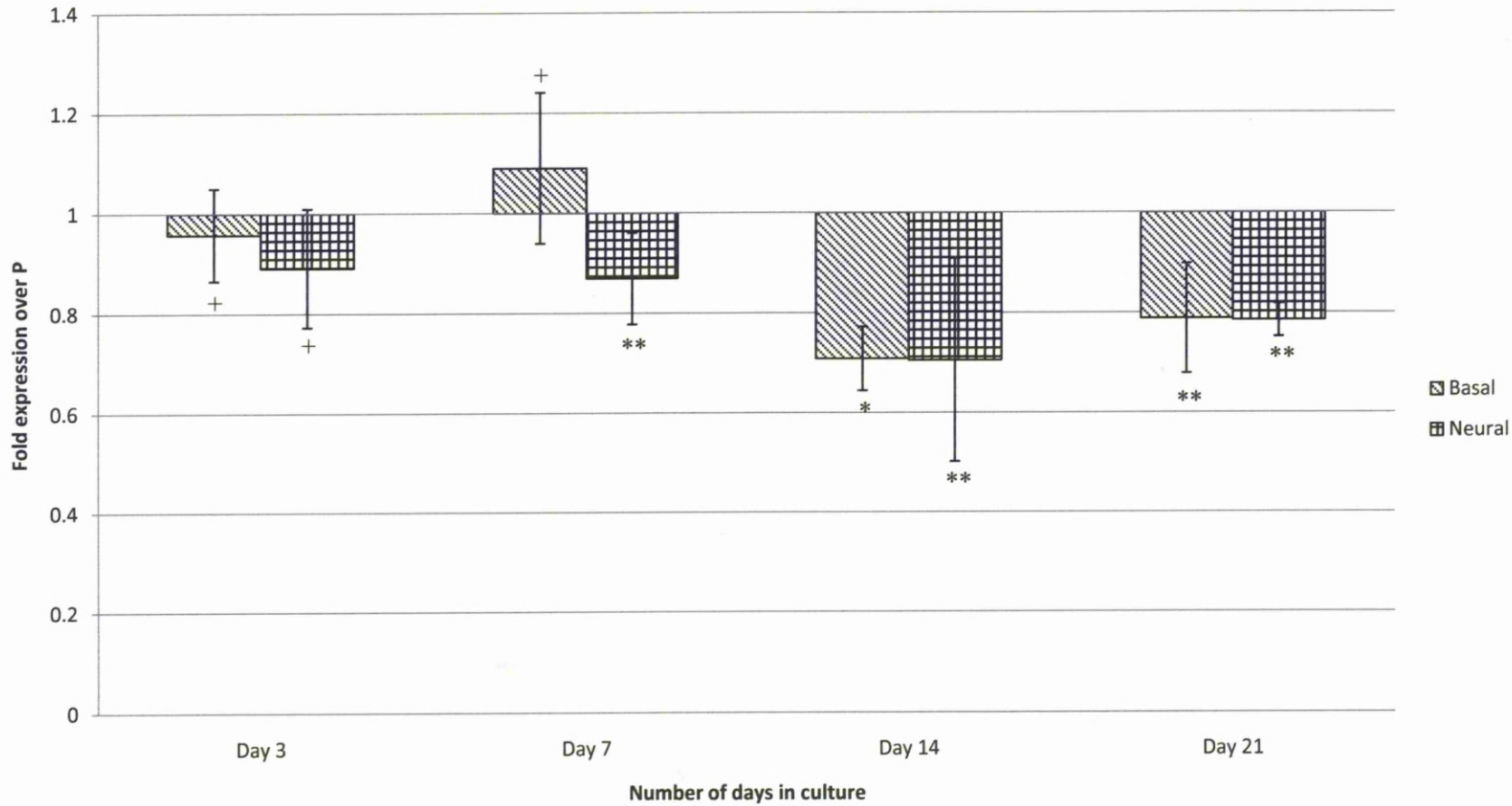

Figure 7.13 - **NRSF1b regulation in dental pulp-derived cells (Passage 5, 1 x Freeze-thaw) cultured in chemically-defined basal and neural media for 28 days. Values represent mean up-/down-regulation over the pGL3p control (pGL3p control = 1) (n = 4). Error bars correspond to Standard Deviations. Student *t*-test indicated that (i) NRSF1b up- and down- regulation over pGL3p in basal culture was significant at days 14 and 21 (*$p \leq 0.001$) (**$p \leq 0.05$) but not days 3 and 7 (+$p \geq 0.05$); (ii) NRSF1b down-regulation over pGL3p in neural culture was significant at days 7, 14 and 21 (**$p \leq 0.05$) but not day 3 (**$p \geq 0.05$).**

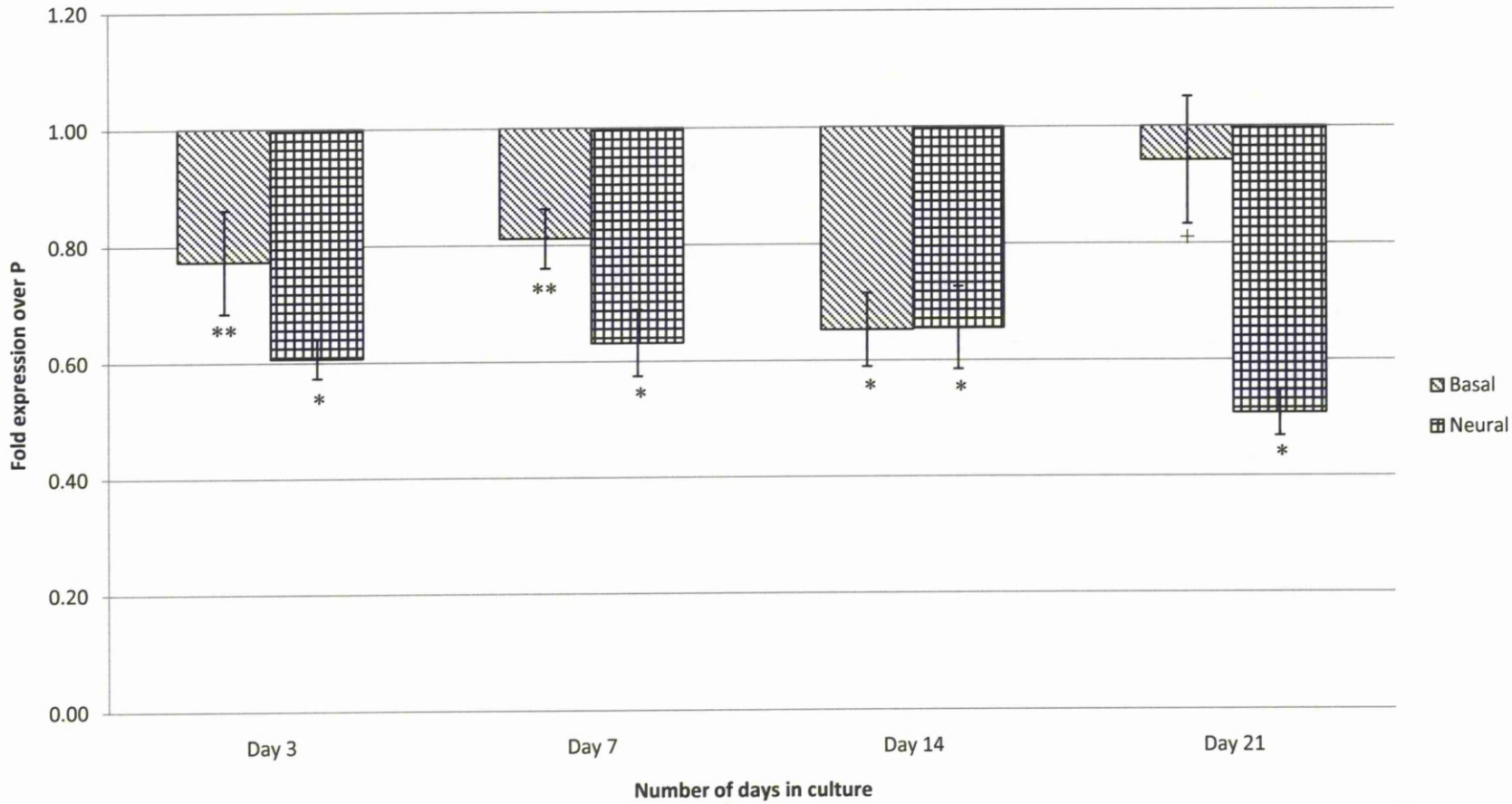

Figure 7.14 - **NRSF2a regulation in dental pulp-derived cells (Passage 5, 1 x Freeze-thaw) cultured in chemically-defined basal and neural media for 28 days. Values represent mean up-/down-regulation over the pGL3p control (pGL3p control = 1) (n = 4). Error bars correspond to Standard Deviations. Student *t*-test indicated that (i) NRSF2a down-regulation over pGL3p in basal culture was significant at days 3, 7 and 14 (*$p \leq 0.001$) (**$p \leq 0.05$) but not day 21 (**$p \geq 0.05$); (ii) NRSF2a down-regulation over pGL3p in neural culture was significant at days 3, 7, 14 and 21 (*$p \leq 0.001$).**

7.3.4 Regulatory Capacity of NRSF SCCD Represents Criteria on which to Purify Homogenous Neuronal Progenitor Populations

NRSF SCCDs and NRSF1a in particular, demonstrated extensive functional capacity of regulatory activity in basal and neuronal conditions within bone marrow and dental pulp-derived populations. With regards bone marrow-derived cells, further investigations examining NRSF1a regulation during days 21-28 of differentiation will elucidate days on which to transfect and subsequently isolate cells of a neuronal precursor phenotype, since cells differentiated for 21 days failed to downregulate NRSF1a sufficiently to allow selection and at 28 days are likely to be terminally differentiated and of reduced clinical value. Considering NRSF1a for purification of dental pulp cells, it is likely that it can be utilised to purify neuronal precursor cells from both induced and non-induced populations, potentially allowing for the selection of progressively more committed phenotypes depending on clinical requirement. Isolation of non-induced cells and cells exhibiting progressively more committed neuronal phenotypes can be homogeneously characterised and their ability to generate varying types of functional neuronal phenotype assessed. Furthermore, given that previously hypothesised purification of neuronal progenitor subsets based upon $CD81^+$ and $NGFR^+$ selection resulted in populations which demonstrated a heterogeneic phenotype following attainment of confluency, selection based upon this functional transcriptional capacity can homogeneously discriminate against potential progenitor impurities and thereby assess whether dental pulp-derived populations do in fact strive to remain within the heterogeneic niche, and subsequently re-establish heterogeneity through a series of specific differentiation events. If this is the case, further studies can assess the effects of heterogeneity from a clinical perspective and, should it prove to be detrimental, investigate *in vitro* conditions capable of programming cells to maintain a homogeneous phenotype.

7.4 Dlk-1 SCCD

7.4.1 Utilisation of Dlk-1 SCCD for the Purification of Adipogenic Progenitors

Genetically based approaches using the 3T3-L1 pre-adipocyte cell line have facilitated the identification of key transcription factors key to the complex transcriptional cascade that is activated during adipogenesis. Such factors include PPAR gamma 2, C/EBP, and ADD1-sterol regulatory element binding protein 1c, whose combined sequential activation induce expression of adipocyte-specific genes, subsequently resulting in the activation of enzymes, structural proteins, hormone receptors, and a variety of secreted factors involved in the regulation of energy homeostasis[420]. Identification of these factors within differentiating stem and progenitor populations has illustrated their ability to differentiate to an adipogenic phenotype. However, the utilisation of cycling adipogenic precursors *in vivo* has been plagued by controversial phenomena detailing the dedifferentiation of preadipocytes to macrophages[421]. The phenomena has however, proved difficult to confirm given the heterogeneity of implanted cells. Furthermore, should the phenomena prove to be correct, evidence of its existence fails to generate a solution to the issue given that the mechanisms underlying their hypothesised dedifferentiation are vague. From both a scientific and clinical perspective therefore, the homogeneous implantation of adipogenic precursors would yield both conclusive scientific answers and consequently plausible clinical benefits. Understanding the homogeneous dedifferentiation, if indeed it does occur, would allow tailoring of the pre-implantation culture conditions to retain the pre-adipogenic phenotype. In fact the purification of pre-adipocytes alone may be sufficient to prevent dedifferentiation, removing the array of chemokines and growth factors present within the heterogeneous populations, factors which may have a significant role in pre-adipocyte dedifferentiation.

In an attempt to identify a functional SCCD associated with adipogenesis, bioinformatics were employed to assess genes and their surrounding regions associated with adipogenic differentiation. Following examination, Dlk-1, an *in vitro* inhibitor of adipogenesis[422], was identified as having a highly conserved region approximately 18kb upstream of the exon region, furthermore containing a binding

site for the adipogenesis-associated transcription factor FREAC-2. Synthetic sequences mimicking this SCCD region were constructed and the resulting product cloned into a pGL3p vector.

7.4.2 Demonstration of a Dlk-1 SCCD Regulatory Capacity in Bone Marrow-derived MSCs Cultured in Basal and Adipogenic Differentiation Media

In an attempt to demonstrate a regulatory function of the Dlk-1 SCCD during *in vitro* adipogenesis, passage 5 bone marrow-derived MSCs were transfected using Effectene methodologies. Cells cultured in basal media demonstrated upregulation of 1.5- to 3.3- fold during the 28 day culture period (*Figure 7.15*). Upon initial introduction of chemically-defined adipogenic stimulation, Dlk-1 remained upregulated within the cells, generating 2.77-, 2.48- and 1.40- fold increase at days 3, 7, and 14 respectively. However, following 21 days of differentiation, Dlk-1 was downregulated 0.24 fold, and exhibited a further downregulation of 0.37-fold following 28 days and terminal differentiation of cells, as observed by Oil Red O staining.

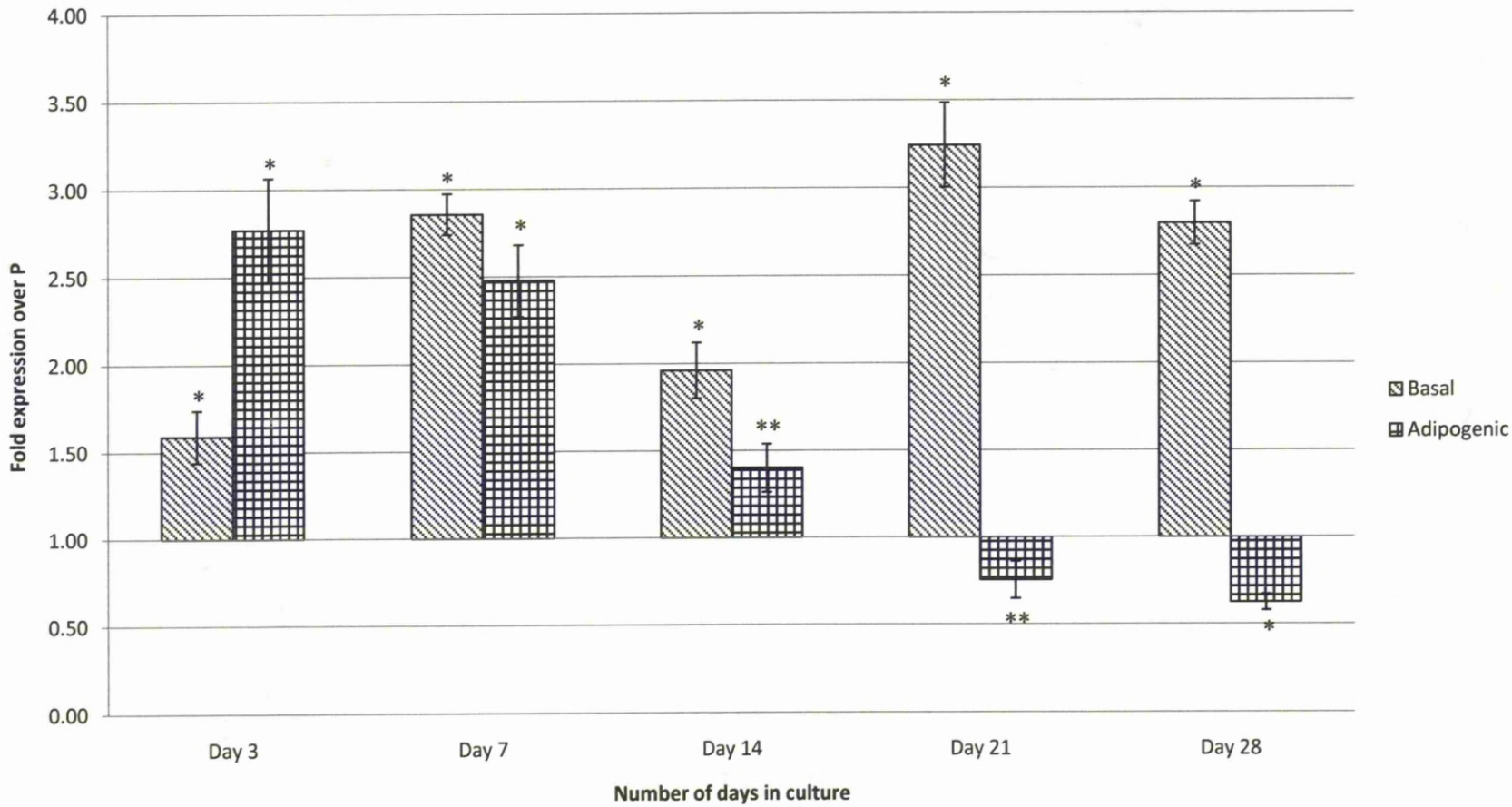

Figure 7.15 - **Dlk-1 regulation in bone marrow-derived MSCs (Passage 5, 1 x Freeze-thaw) cultured in chemically-defined basal and adipogenic media for 28 days. Values represent mean up-/down-regulation over the pGL3p control (pGL3p control = 1) (n = 4). Error bars correspond to Standard Deviations. Student *t*-test indicated that (i) Dlk-1 up-regulation over pGL3p in basal culture was significant at days 3, 7, 14, 21 and 28 (*$p \leq 0.001$); (ii) Dlk-1 up- and down- regulation over pGL3p in adipogenic culture was significant at days 3, 7, 14, 21 and 28 (*$p \leq 0.001$) (**$p \leq 0.05$).**

7.4.3 Demonstration of a Dlk-1 SCCD Regulatory Capacity in Dental Pulp-derived MSCs Cultured in Basal and Adipogenic Differentiation Media

The pGL3p-Dlk-1 SCCD containing construct was transfected into passage 5 pulp donor 3 cells in order to assess its regulatory impact during *in vitro* adipogenesis within the population. Post-Effectene transfection, cells cultured in basal media displayed an upregulation of the Dlk-1 SCCD, as demonstrated by 4.74-, 3.77-, 3.08- and 2.91- fold upregulation at days 3, 7, 14 and 21 respectively (*Figure 7.16*). Following induction with chemically-defined adipogenic media, Dlk-1 remained upregulated during the initial 7 days of differentiation, generating upregulation of 4.31- and 1.28- fold at days 3 and 7 respectively. However, after 14 days of adipogenic induction, Dlk-1 was downregulated 0.16 fold, with 0.54 fold repression after 21 days and terminal differentiation.

7.4.4 Regulatory Capacity of Dlk-1 SCCD Represents Criteria on which to Purify Homogenous Adipogenic Progenitor Populations

Results obtained with bone marrow and dental pulp-derived cells suggest that the Dlk-1 SCCD functions as a key regulator of adipogenesis, inducing transcription of the Dlk-1 gene which subsequently represses genes required for adipogenesis. Upon appropriate adipogenic stimulation, the Dlk-1 SCCD is downregulated, consequentially reducing transcriptional levels at the Dlk-1 gene and allowing expression of genes required for adipogenesis. This functional capacity represents an attractive target for the isolation of adipogenic precursors, sorting Dlk-1-GFP transfected cells exhibiting downregulation of Dlk-1. Cells exhibiting varying levels of Dlk-1 downregulation can be subsequently purified and assessed for their phenotypic properties, thereby allowing homogeneous selection of pre-adipocytes demonstrating a stage of lineage commitment for implantation. Utilisation of such a homogeneous population pre-implantation will allow definitive assessment and subsequently further understanding of dedifferentiation mechanisms should this phenomena prove correct, although the elimination of undesirable cells and their accompanying chemokines and growth factors may prevent such dedifferentiation occurring. However, given that it is plausible that cells may in fact re-establish

heterogeneity following purification, it may be that, following proof of this theory and assessment of heterogeneic impact from a clinical setting, *in vitro* manipulation is required to maintain Dlk-1 SCCD purified cells in a homogeneous manner.

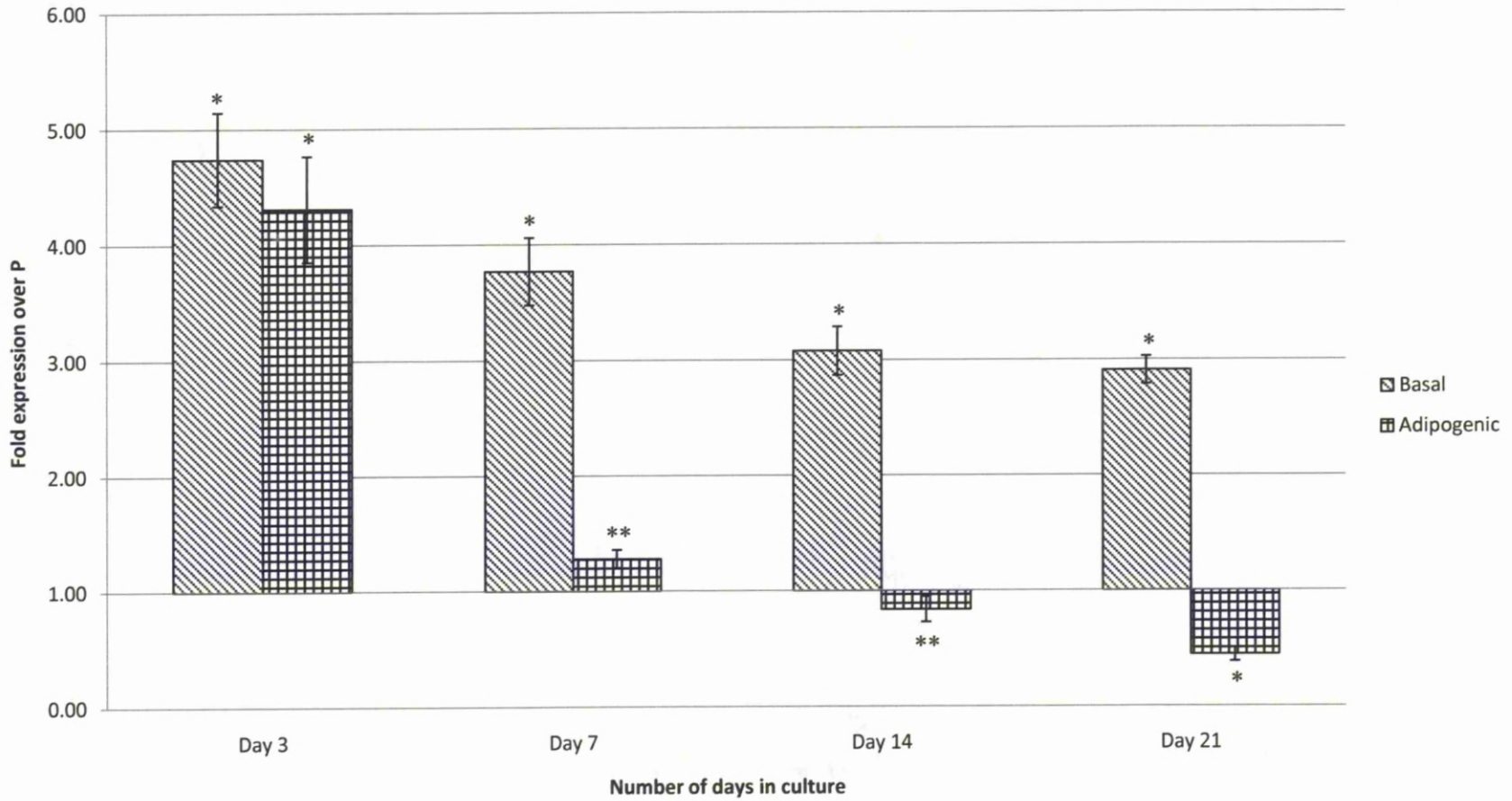

Figure 7.16 - **Dlk-1 regulation in dental pulp-derived cells (Passage 5, 1 x Freeze-thaw) cultured in chemically-defined basal and adipogenic media for 28 days. Values represent mean up-/down- regulations over the pGL3p control (pGL3p control = 1) (n = 4). Error bars correspond to Standard Deviations. . Student *t*-test indicated that (i) Dlk-1 up-regulation over pGL3p in basal culture was significant at days 3, 7, 14 and 21 (*$p \leq 0.001$); (ii) Dlk-1 up- and down- regulation over pGL3p in adipogenic culture was significant at days 3, 7, 14 and 21 (*$p \leq 0.001$) (**$p \leq 0.05$).**

7.5 Conclusion

7.5.1 Stem Cell Conserved Domains as Markers for the Purification of Stem Cells and Progenitors of Varying Lineage

Current antibody-based methods for the purification of cells fail to homogeneously isolate stem and progenitor subpopulations based upon their functional characteristics. SCCDs flanking genes known to regulate a desired phenotype offer a novel marker on which to purify cells exhibiting desired proliferative or differentiation capacities. Thus far, regulatory activities for Sox2, NRSF and Dlk-1 SCCDs have been demonstrated using luciferase-based reporter constructs with an SV40 minimal promoter. Cells were transfected using Effectene, providing a transfection efficiency of between 60-70%. Whilst Amaxa transfections yielded greater efficiencies, up to 90% in many cases, the number of cells required per transfection (5×10^5) was unfeasible when experiments were required to confirm a regulatory function. However, upon cloning a selected SCCD region into a GFP vector to allow homogeneous isolation of a desired subpopulation, Amaxa transfections may instead be utilised as screening larger numbers of cells to allow purification of a greater number of the desired subpopulation. Thus far, regulatory impacts observed for Sox2, NRSF and Dlk-1 SCCD using luciferase reporter constructs generate a global regulatory value, with phenotypically dissimilar cells producing different luciferase values for each construct. Thus, whilst many cells may demonstrate upregulation of the given construct, the value attained may be lower due to repression of the construct by alternative subpopulations (*Figure 7.17*). GFP assessment using flow cytometry circumvents this problem, allowing individual assessment of a cells regulatory capacity, facilitating its purification.

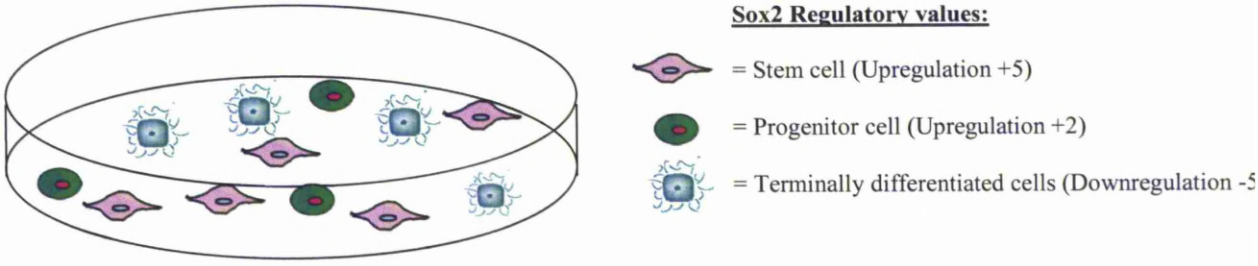

Heterogeneous cell population: Global upregulation of luciferase (and therefore SCCD) = +11

Figure 7.17 **- Global regulatory analysis of a given SCCD using luciferase reporter constructs.**

Cloning of given SCCDs into a GFP vector with a minimal promoter will provide an invaluable tool to facilitate the generation of homogeneous subpopulations for scientific assessment or clinical application. Further specificity of desired subpopulations can be attained by cloning SCCDs of varying properties into alternative reporter constructs. For example, dual transfection of a population with a Sox2a-GFP/NRSF1a-YFP combination will allow purification of highly primitive neuronal progenitors.

In conclusion, evolution of these SCCDs into a GFP reporter construct will allow the homogeneous purification of desired stem and progenitor subsets based upon a functional transcriptional capacity. Definitive homogeneous isolation using this technology will allow the hypothesised phenomena describing the capability of purified cells to re-establishment heterogeneity to be assessed. Furthermore, if this hypothesis proves correct, further studies can assess the impacts of heterogeneity from a clinical perspective and, should it prove to be detrimental, studies attempting to modify *in vitro* conditions capable of reprogramming SCCD purified populations to maintain the homogeneously selected phenotype can be undertaken.

7.5.2 Response to Chapter Aims

Results detailed within this chapter largely addressed the aims set out in 7.1.2 by confirming the binding of transcription factors, and subsequently a regulatory function, at SCCDs flanking the *Sox2*, *NRSF* and *Dlk-1* genes. Whilst some of the SCCDs tested failed to demonstrate a functional role, Sox2a, NRSF1a and Dlk-1 were of significant interest for the purification of multipotent stem/progenitor cells, neuronal progenitors, and adipogenic progenitor cells, respectively. However, whilst data obtained using a luciferase reporter construct allowed for the identification of functional SCCDs, it is now required that such regions are cloned into a GFP reporter construct in order to allow homogeneous purification using high speed cell sorting. Unfortunately, this task was not achieved within the timeframe of this project.

8. Discussion and Conclusions

8.1 Discussion

8.1.1 Bone Marrow-, Peripheral Blood, Umbilical Cord- and Dental Pulp-derived cells for use in Tissue Engineering

For many years both medical and public sectors have envisaged radical off-the-shelf therapies for a diverse range of debilitating illnesses, essentially allowing autologous replacement of compromised tissues or organs. Whilst at first such concepts appeared fanciful, progressive advances within the synonymous fields of tissue engineering and regenerative medicine throughout the previous half century have raised hopes that such therapies can become available. Conceptual understandings of developmental lineage commitments have allowed tailoring of *in vitro* culture conditions to essentially mimic those encountered *in vivo*, resulting in the isolation, limited *ex vivo* expansion and, in some cases, guided lineage differentiation of stem and progenitor subsets isolated from numerous tissues.

Whilst ES cells have generated much excitement with regards their pluripotent capability, their erratic behaviour concerning spontaneous differentiation and karyotype in stability raises key issues from a technical perspective, whilst the destruction of embryos required for their isolation raises a minefield of ethical dilemmas. Novel iPS cell technologies have attempted to overcome these issues, though much concern has been voiced regarding the oncogenicity of factors required to induce reprogramming and the potential for insertional mutagenesis as a consequence of integrating retroviral or lentiviral vectors. Furthermore, current iPS cell technologies induce only a limited number of cells within given populations to undertake reprogramming, and it is therefore plausible that cells which have maintained a limited capacity to undertake differentiation *i.e.* stem or progenitor cells, can be more readily induced to undertake complete reprogramming following appropriate stimulation. Therefore iPS cell technologies may benefit considerably from the utilisation of homogeneous stem or progenitor cells as a starting material, allowing investigators to comprehensively identify factors required to homogeneously reprogram given stem or progenitor subsets. The results detailed

within this study may therefore be applicable to investigators attempting to optimise future iPS cell induction techniques, allowing selection of populations at an optimum passage or following SCCD-based purification to increase reprogramming efficiency.

In addition to furthering future iPS cell reprogramming attempts, results obtained within this investigation detail *in vitro* characteristics of isolated populations which must be considered when undertaking future biomaterial design. Current potential therapeutics at the forefront of research involves the combination of hypothesised multipotent cell populations with topographically or chemically modified biomaterials, potentially generating functional organ or tissue replacements. However, whilst the field of biomaterial development continues to progress at a rapid pace, it may be that materials currently being devised subsequently prove redundant given the cell types being seeded.

Bone marrow-derived cells currently represent the most utilised cell source with respect to seeding on varyious biomaterials, although the multipotentiality of cells seeded remains heterogeneous. Bone marrow-derived cells exhibit an inability to maintain an MSC-associated phenotype following a sixth *in vitro* passage, and whilst numerous antigens are questionable with regards their functional representation, the downregulation of chondrogenesis-requiring antigen CD105 suggests that the population exhibited a reduced capacity to differentiate following increasing culture. This downregulation of MSC-associated antigens coincided with a dramatic reduction in proliferation, a considerable problem if these cells are to be utilised clinically. It is likely that this downregulation of MSC-associated antigens and proliferative capacity following *in vitro* culture can be attributed to rapid aging of the cells, a hypothesis substantiated by the fact that MSC populations exhibited significantly greater telomere length degradation *in vitro* compared with those observed in previous *in vivo* studies. Since tissue engineering applications are likely to require large numbers of cells, it is suggested that further studies are required to optimise *in vitro* culture conditions and thereby prevent such rapid aging, allowing cells to proliferate to Hayflicks limit of 70 passages[395]. However, until this is acieved, it is recommended that biomaterials are seeded with bone marrow-derived cells cultured for no more than 4 passages *in vitro* prior to seeding, thereby introducing to the materials populations exhibiting higher expression of MSC-

associated antigens with a greater capacity for proliferation and almost certainly differentiation. However, whilst this may allow partial tailoring of biomaterials, the inability of current culture methods to yield large numbers of bone marrow-derived cells which have not undertaken rapid aging, and subsequently phenotypic and proliferation demise, are likely to prevent incorporation of these cells into a tissue engineered construct.

Peripheral blood represents an attractive source for the isolation of clinically desirable cells given the non-invasive procedures required for attainment, an additional drawback of bone marrow-derived cells. Adherent populations isolated from peripheral blood of four donors using Histopaque and RosetteSep exhibited no morphological or phenotypic differences, with each population heterogeneously expressing antigens associated with MSCs, HSCs, EPCs and alternative progenitor subsets. CFU assays further indicated the presence of hematopoietic and non-hematopoietic progenitors within each population isolated, with each isolation method and donor generating similar numbers of CFUs. It was not surprising therefore that isolated populations were able to undertake adipogenic, chondrogenic and osteogenic differentiation. However, adherent populations displayed a severe limitation to undertake proliferation, with cells unable to sustain mitosis post initial confluence. This inability to undertake proliferation is obviously significant with regards the utilisation of such cells in a clinical application, and thus culture conditions must be addressed in order to facilitate continued cell division. However, given the similar phenotypic expression with bone marrow-derived populations, it may be that blood-derived cells display the same phenotypic instability restricting the clinical utilisation of their bone marrow-derived counterparts.

The phenotypic instability of bone marrow and peripheral blood-derived populations represents a severe limitation with regards their prospective use in tissue engineering applications. It was therefore hoped that umbilical cords, given their functional capacity within development, may allow for the isolation of primitive cells capable of maintained proliferation and multilineage differentiation. Adherent cells obtained by plating of Wharton's jelly and whole cord digestions yielded morphologically dissimilar cells describing fibroblastic- and smooth muscle- like morphologies respectively. However, both populations demonstrated a similar phenotypic

expression profile to that observed in bone marrow-derived cells, and furthermore suffered the same phenotypic instability. Furthermore, umbilical cord-derived populations demonstrated a downregulation of MSC-associated surface antigens following cryopreservation, limiting their ability to be banked for future use. Following a fifth passage each isolated population also demonstrated a reduced capacity to undertake proliferation, a significant restriction with regards clinical potential. This reduced proliferation was also characterised by the ceasing of nucleostemin expression, which terminated following a sixth passage. And whilst it is of significant clinical potential that cord populations were able to neuronally differentiate, their inability to generate large cell numbers for clinical application require that corresponding issues required to evolve bone marrow-derived cell therapeutics are addressed.

Whilst bone marrow, peripheral blood and umbilical cord-derived populations displayed the ability to differentiate within subsets of the population, their inability to maintain stable *in vitro* phenotypes and coinciding reduction of proliferation cause significant reason for concern from a therapeutic viewpoint given that large numbers of cells, and thus prolonged *in vitro* culture, are likely to be required for clinical application. In the instance of bone marrow-derived cells, the downregulation of MSC-associated antigens and coinciding reduction in proliferation appears to be due to the rapid *in vitro* aging of the population, a phenomena confirmed by their rapidly reducing telomeres in comparison with that observed *in vivo*. Thus it is imperative that culture conditions are modified to limit this aging of bone marrow, and presumably peripheral blood and umbilical cord cells, if they are to be utilised clinically.

However, whilst cells derived from bone marrow, peripheral blood and umbilical cord demonstrated severe limitations from a clinical perspective, dental pulp cells overcome many of these problems. Isolated dental pulp cells retained the ability to proliferate, a feat probably attributable to their maintained or *in vivo*-like reducing telomere lengths. Furthermore, their ability to undertake adipogenic, chondrogenic, osteogenic, neuronal and hepatic lineages offers immense clinical value. This could, however, represent the tip of their differentiation iceberg given the high number of CFU-forming cells within the population and heterogeneous expression of proteins

such as Oct4 and Sox2, indicating pluripotent capability comparable to ES cells. If through further study this proves to be the case, dental pulp could represent a highly valuable clinical source, overcoming many of the ethical and technical dilemmas associated with ES cells, although given their similar characteristics, it is essential that issues of karyotypic stability within the population are addressed.

Nevertheless, whilst overcoming numerous ES cell-related issues, the heterogeneity of dental pulp populations compared with ES cells is problematic. Despite purification based upon a number of surface antigens, the re-establishment of a heterogeneic phenotype suggests the presence of a highly proliferative subpopulation for which current antibodies are unable discriminate. Interestingly, upon purification based upon Hoechst dye emission, phenomena associated with a functional HSC-associated transporter pump, adherent populations maintained a stable phenotype until acquiring confluence and furthermore demonstrated the ability to form microtubule-like structures when cultured in a semi-solid matrix. Moreover, given that the population re-established a heterogeneic phenotype following a second passage post-purification, it would suggest that purification based upon functional aspects of a given cell phenotype yield populations of greater homogeneity, although Hoechst emission fails to completely exclude the highly proliferative impurity. However, whilst cell impurities would appear a likely explanation for this re-establishment of heterogeneity, it could be that homogeneously purified progenitors, which were likely purified given the slower cycling times of sorted cells, strive to maintain the heterogeneic niche, with homogeneous stem cell populations undergoing differentiation in order to re-establish this post-sorting. This data complements previous studies describing the *in vitro* heterogeneity of clonal neurospheres[423], and it may be that populations are capable of flexible and regulated tissue self-organisation based on cell-cell and cell-environment interactions[424].

Further adding to the likelihood that stem and progenitor subsets were predominantly isolated following antibody-based purification, studies examining protein expression profiles of cells immediately post-sorting revealed expression of proteins associated with primitive cells including those of the RPE lineage, thereby highlighting dental pulp as possessing numerous subpopulations of diverse clinical potential. Thus, given that antibody-based purification strategies are acknowledged to incorporate

impurities, it is essential that homogeneous subpopulations be attained as to ascertain whether this phenomena concerning re-establishment of heterogeneity is due to progenitor impurities or is a result of populations striving to re-establish the heterogeneic niche. As such, a novel SCCD-based cell purification strategy was devised.

SCCD technologies are based on the conservation of advantageous genetic modifications throughout species development, utilising such regions as criteria upon which to base cell purification. The Sox2 gene represents a key regulator within the maintenance of plasticity, and neighbouring SCCDs, in particular Sox2a, demonstrated an upregulation within bone marrow, dental pulp and umbilical cord populations under basal conditions. However, following chemical lineage induction the Sox2a SCCD was downregulated, and interestingly also exhibited reduced expression in eighth passage bone marrow populations compared with their passage 5 counterparts. It is therefore suggested that Sox2 SCCD functions to maintain plasticity within cells, facilitating the binding of transcription factors fundamental for maintenance of a primitive phenotype. Sox2a thus represents a criterion upon which to purify cells exhibiting varying levels of upregulation and, therefore, plasticity. Progression of this current technology towards a GFP-based reporter construct can facilitate its use in the purification of stem and progenitor subsets exhibiting such regulatory differences, finally allowing for the homogeneous culture of cells exhibiting varying lineage potential. This would also answer questions of the capability of purified cells to re-establish heterogeneity, an issue which must be addressed if it conspires to be the case.

Translating to the field of iPS cell technologies, this technology can provide a base cell culture on which to optimise reprogramming strategies, with the hypothesis that cells which have not terminally differentiated proving more cooperative to subsequent re-establishment of plasticity.

Given the downregulation of MSC-associated antigens and coinciding reduced proliferation, likely due to the rapid *in vitro* aging of the population, the homogeneous isolation of a stem cell population can provide a base upon which to tailor culture conditions to prevent degradation. Given the hastily reducing telomere

lengths *in vitro* compared with those observed within the bone marrow niche, it is apparent that culture conditions do not replicate those present *in vivo*. Utilising a homogeneous stem cell population as a starting culture will exclude superfluous progenitor and terminally differentiated cell types which, given their likely emission of numerous growth factors which could have unknown effects upon the stem cell subset, will allow greater optimisation of cultures.

From a biomaterial construction perspective, the purification of homogeneous stem cell populations will allow for the seeding of known cell populations and subsequent assessment of material success. At present, given the heterogeneity of populations being seeded, biomaterial design experts face an almost impossible task of generating chemical or topographically specific materials cable of guided lineage specific differentiation. Thus current blueprints for biomaterials are likely to prove redundant until homogeneous populations can be seeded. However, whilst purification based upon the Sox2 SCCD can yield undifferentiated populations for material seeding, it may prove prudent to utilise progenitor subsets, sorted upon the basis of SCCDs such as Dlk-1 or NRSF in the respective cases of adipogenic and neuronal precursors, as homogeneous seeding materials. If we consider that tissue engineering and regenerative approaches strive to regenerate a functional organ or tissue composed of terminally differentiated cells, it seems of little value seeding cells of a completely undifferentiated state only to direct them towards a given lineage, since this is likely to greatly increase intricacy of the biomaterial design. However, isolation of committed proliferative precursors will require far less manipulation from the material, and may therefore represent a more attractive cell type for tissue regeneration.

In conclusion, this technology represents a powerful tool within the field, allowing for the isolation of homogeneous stem and progenitor subsets of immense clinical potential. Whilst SCCD purified populations from bone marrow, peripheral blood and umbilical cord are likely to represent populations upon which further tailoring of culture conditions are required to prevent hypothesised *in vitro* aging, dental pulp purified populations, many of which appear to represent exciting progenitor subsets given their protein expression profiles and differentiation capacity, can represent a cell source upon which to base numerous SCCD purification and future regenerative

strategies. Thus the simultaneous development of novel cell purification strategies based upon SCCDs is likely complement this interesting cell source, yielding stem and progenitor subsets of varying lineage, and therefore clinical, potential. Prior to this, however, we must establish whether SCCD purified cells are capable of maintaining this homogeneously selected phenotype following *in vitro* culture and, if it conspires that cells do in fact differentiate to recreate the heterogeneic niche, the issues of heterogeneity within clinical applications must be more rigourously studied. If following such assessment it is demonstrated that homogeneity is required to achieve tissue regeneration, *in vitro* culture conditions must be tailored in order to re-program cells to maintain a homogeneous phenotype.

8.2 Conclusions

8.2.1 Concluding remarks of the investigation

Given the informative characterisation of each cell type gathered within this study, it is essential to compiled findings in a straightforward manner. Following the aims of the study detailed in section 1.5.1, the conclusive findings of this study are:-

1. Optimisation of techniques for the isolation of cells from various niches yielded adherent populations of similar phenotypic properties:
    - In the case of human peripheral blood, Histopaque and RosetteSep isolated, regardless of donor variation, adherent cells of similar morphological and phenotypic characteristics, likely incorporating MSC-like cells, HSC and EPCs, and progenitor subsets of different lineage potential.
    - Acquisition of adherent populations following the direct plating of umbilical cord-derived Wharton's jelly yielded cells exhibiting a fibroblastic-like morphology. Conversely, however, cells isolated from whole cord digestion exhibited a smooth muscle-like morphology. Nonetheless, despite such apparent morphological differences, each population exhibited similar phenotypic

characteristics, likely incorporating MSC-like cells, HSCs and EPCs, and ES cell-like and progenitor subsets.

- Populations isolated following the mechanical and enzymatic digestions of human dental pulp exhibited a fibroblastic morphology, with adherent populations from different donors displaying similar morphological and phenotypic characteristics, likely incorporating hematopoietic and non-hematopoietic cells of primitive and more mature phenotypes.

2. Isolated populations were assessed for their phenotype and subsequent *in vitro* maintenance:
    - Bone marrow-derived populations purchased from Lonza exhibited expression of MSC-associated surface antigens throughout passages 3 and 4. However, subsequent passages exhibited downregulation of such antigens. Furthermore, this downregulation coincided with upregulation of antigens hypothesised to be associated with terminally differentiated cells such as endothelial cells, suggesting spontaneous terminal differentiation within the population.
    - Histopaque and RosetteSep purified cells exhibited similar phenotypic profiles regardless of donor. Primary passage adherent populations demonstrated, with the exception of CD166, similar expression of MSC-associated antigens with that observed in bone marrow-derived populations. Isolated peripheral blood populations also exhibited expression of antigens associated with EPCs, HSCs and ES cells. However, given their significant lack of proliferative capacity, peripheral blood cell phenotypes could only be assessed for a primary passage.
    - Umbilical cord cells isolated via plating of Wharton's jelly or whole cord digestion displayed, with the exception of antigens CD166, HLA-ABC and HLA-DR, similar

phenotypic profiles. Furthermore, phenotypic characteristics were similar to those observed within bone marrow-derived cells, including the inability to maintain this phenotype following progressive *in vitro* culture. Additionally, cryopreservation and subsequent thawing of each isolated cord population induced similar phenotypic modifications to those observed following prolonged *in vitro* culture.

- Dental pulp-derived populations similar phenotypic profiles; exhibiting antigens associated with MSCs, HSCs, ES cells and alternative progenitor subsets, in particular those of the neuronal developmental lineage. Of particular interest was the ability of each dental pulp-derived population to maintain this phenotype throughout prolonged *in vitro* culture, in this case up to 40 passages, and also cryopreservation, with no apparent phenotypic modification.

3. Following investigation of phenotypic profiles, umbilical cord and dental pulp-derived populations were assessed for their protein expression:
    - Umbilical cord-derived cells exhibited nuclear-localised expression of the stem cell proliferation marker nucleostemin throughout passages 3 - 5, after which no expression was observed. Given the downregulation of MSC-associated antigens following similar periods of prolonged culture, it is suggested that cord populations differentiate to a phenotype incorporating significantly reduced plasticity and possible terminal differentiation.
    - Dental pulp populations from each donor maintained protein expression, demonstrating expression of plasticity regulators Oct4 and Sox2. Further to the continued expression of STRO-1 and nucleostemin, dental pulp cells exhibited expression of embryonic development-associated proteins Cripto-1 and Tra-1-81. Given the developmental

origin of this niche, the expression of neural progenitor-associated proteins within subsets of the population implies a potential for future neuronal regeneration strategies. Furthermore, the expression of RPE lineage-associated proteins pax6 and MiTF implies a potential for the regeneration of macular disease.

4. If isolated multipotent populations are to be utilised clinically, it is likely that large numbers of cells, and hence prolonged *in vitro* culture, are likely to be required:
    - Bone marrow-derived populations exhibited severe limitations regarding their ability to maintain proliferation, with cells post passage 5 demonstrating greatly reduced proliferative capacity, a property which further diminished following further culture, with passage 9 cells failing to proliferate to confluency.
    - Quantitative proliferation analysis of Histopaque and RosetteSep blood-derived cells was unable to be undertaken given their proliferative limitations. Extensive work is therefore required if blood-derived populations are to be utilised clinically, endeavouring to establish *in vitro* conditions capable of maintaining mitosis.
    - Umbilical cord populations exhibited similar proliferative limitations to those observed within bone marrow-derived cells, with increasing *in vitro* culture reducing their capacity to undertake mitosis.
    - Dental pulp-derived populations, regardless of donor, exhibited exaggerated capacity to undertake proliferation compared with bone marrow and umbilical cord-derived populations. Furthermore, cells were able to maintain proliferation throughout prolonged *in vitro* culture and also following cryopreservation.

5. CFU analysis represents an attractive assay for the quantification of progenitor subsets within a given isolated cell type, thereby indicating potential clinical value of isolated populations:
    - Histopaque and RosetteSep peripheral blood-derived populations from different donors displayed similar numbers of CFU-Fs and CFU-GMs within the population, generating approximately 70 colonies/10^6 cells for each assay.
    - Dental pulp-derived populations from each donor demonstrated CFU-forming capabilities, and furthermore retained this capability throughout prolonged *in vitro* culture, indicating a maintained presence of progenitor subpopulations. Concerning CFU-F assays, dental pulp-derived populations continually generated approximately 25 CFU-Fs/0.5 x 10^4 cells, whilst furthermore forming approximately 8 CFU-GMs/0.5 x 10^4 seeded cells.

6. Given the phenotypic instability of bone marrow-derived populations following prolonged *in vitro* passage, attempts were undertaken to gain a mechanistic understanding of events responsible. Rapid aging of cells, as quantified by rapidly reducing telomeres, has been suggested as a possible underlying reason. Bone marrow populations were therefore compared with dental pulp-derived populations, which exhibited no surface antigen or proliferation failure:
    - *In vivo* bone marrow cells exhibit a consistent telomere shortening of approximately 17 bases per annum. However, *in vitro* bone-marrow derived populations exhibited reductions of approximately 100-150 bases per passage, indicating rapid *in vitro* aging. This is likely to be responsible for reduced proliferation and downregulation of surface antigens, and thus culture conditions need to be addressed in order to prevent this pronounced aging process.

- Dental pulp-derived populations displayed no surface antigen or proliferative modifications despite *in vitro* culture, and thus it was not surprising that they maintained a telomere length of approximately 1.3 x 10^4 bases in donor 1 isolated cells.

7. Guided lineage differentiation following exposure to appropriate stimulation is the basis of numerous regenerative applications. Early passage bone marrow-derived cells have previously demonstrated the capacity to undertake adipogenic, chondrogenic and osteogenic differentiation, although their ability to do this was compromised following increasing passage, likely due to rapid aging within the population. Populations isolated from differing niches were therefore assessed for their differentiation potential:
    - Following appropriate stimulation, blood-derived populations demonstrated the capacity to differentiate to adipogenic, chondrogenic and osteogenic phenotypes following appropriate commercially available stimulation. However, their inability to proliferate and attain significant cell numbers prior to differentiation is a restriction for their clinical utilisation.
    - Previous studies have demonstrated the ability of umbilical cord-derived populations to differentiate to adipogenic, chondrogenic and osteogenic lineages. After introduction into commercially available neural induction media, cells isolated from Wharton's jelly and whole cord digestions heterogeneously demonstrated morphological and phenotypic characteristics associated with a neuronal phenotype, which could potentially prove therapeutically useful. However, given their phenotypic instability following prolonged *in vitro* culture, it is necessary that this issue be addressed prior to further investigations with this cell source.
    - Dental pulp-derived cells from each donor exhibited an innate ability to heterogeneously undertake adipogenic,

chondrogenic, osteogenic, neuronal and hepatic lineages following stimulation with both commercially available and chemically-defined media. Furthermore, following the demonstration that subpopulations within the culture exhibited expression of plasticity-associated proteins Oct-4 and Sox2, it may be that such cells are able to fulfil further differentiation commitment following appropriate stimulation. Additionally, given their retained phenotype following *in vitro* culture, these cells could represent a clinically valuable cell source for numerous regenerative applications.

8. Despite the overwhelming ability demonstrated by dental pulp-derived populations, it is imperative that, if they are to be utilised within a clinical setting, each subpopulation is homogeneously isolated and characterised for their respective characteristics and potential:
    - Dental pulp-derived populations isolated upon the basis of surface antigen expression initially demonstrated differing protein expression profiles. However, when allowed to proliferate to confluence these populations resumed the heterogeneous phenotype associated with this population, suggesting that impurities not fulfilling the selection criteria had been incorporated within the culture. This was further substantiated when purification based upon emission of Hoechst 33342 dye, hypothesised to allow the homogeneous sorting of EPCs. Such cells retained a differing phenotype following initial confluence, although following a second passage re-established the heterogeneous phenotype, suggesting that purification upon the basis of a functional aspect within the population allows for greater purification. Hoechst-isolated populations seeded within a semi-solid matrix demonstrated the spontaneous formation of microtubular-like structures which expressed VWF and CD31, proteins

associated with EPCs. Such populations could therefore represent an attractive source for future myocardial engineering attempts. However, whilst progenitor impurities offer a plausible explanation for this re-establishment of heterogeneity, it could be that purified stem and progenitor subsets strive to maintain the heterogeneic niche. And whilst it is acknowledged that impurities are ncorporated following antibody-based cell sorting, given the primitive protein expressions observed within initially adherent cells and furthermore the slow cycling time of sorted populations, this explanation offers an alternative theory which must be addressed, although the homogeneous purification of cells based upon functional capacity will be required to assess this hypothesis.

- Given the limitations of antigen-based cell sorting, novel SCCD purification strategies were developed. Initial investigations utilising a luciferase reporter construct enabled proof of concept studies to be undertake. Resulting data indicated the potential utilisation of the Sox2a SCCD for the purification of stem and progenitor cell subsets exhibiting varying levels of plasticity from heterogeneous populations. Furthermore, NRSF and Dlk-1 residing SCCDs and their associated transcription factor binding properties could represent attractive criteria for the isolation of neuronal and adipogenic progenitor subsets, both of which represent attractive cell types within the field of tissue engineering.

8.3 Future work

8.3.1 Further Work Required to Advance Current Understandings towards a Clinical Setting

Despite the findings of this study, further investigations on numerous fronts are required to progress the utilisation of respective cell types within this exciting and rapidly progressing field. It is envisaged that characterisation experiments undertaken within this study will not only shed light upon the cell types covered, but also represent a basis on which to undertake future cell characterisation. Furthermore, whilst initial proof of concept studies utilising SCCD purification strategies are interesting, research now must focus upon progressing this technology to a GFP based vector in order to facilitate homogeneous purification of desired subpopulations. It is therefore suggested that, in order to progress the field of tissue engineering towards a clinical endpoint, the following issues and corresponding investigations are addressed:

1. Given the phenotypic and proliferative instability of bone marrow and umbilical cord-derived populations of increasing passage, a detrimental issue from a clinical perspective given the likely requirement for large numbers of unmodified cells, tailoring of current *in vitro* culture conditions is obviously required to allow proliferation to Hayflicks limit. Furthermore, given that this instability is likely due to the rapid aging of cells *in vitro*, it is suggested that culture optimisations use telomere lengths as a guide to success.

2. Whilst quantitative assessment of phenotype and proliferation of blood-derived cells proved difficult given their severe proliferative incapacity, it is likely that such populations undergo *in vitro* aging similar to that observed within bone marrow-derived cells. However, given their non-invasive isolation and spontaneous *in vivo* regenerative capacity, combined with their ability to undertake adipogenic, chondrogenic and osteogenic lineages, they represent an attractive cell source if culture conditions can be devised to allow their maintained growth.

3. A fundamental prerequisite of regenerative approaches to medicine permits that cells, in particular those gathered from redundant tissues such as dental pulp of deciduous teeth and umbilical cords, are able to be cryopreserved until required for a given restorative strategy in later life. Whilst dental pulp-derived cells displayed no instability subsequent to freeze-thawing, umbilical cord-derived populations demonstrated a phenotype similar to that of late passage cells. Thus, if umbilical cord-derived cells are to be therapeutically viable, it is necessary that they can be stored for prolonged periods with no phenotypic modification, and thus current cryopreservation protocols need to be addressed.
4. Given the innate ability of dental pulp-derived cells to differentiate to adipogenic, chondrogenic, osteogenic, neuronal and hepatic lineages, and furthermore their heterogeneous expression of proteins responsible for regulation plasticity, it is of significant interest to observe alternative lineages they are able to differentiate into. Optimisation of stimulatory media and biomaterials will therefore be devised in order to further assess their differentiation potential.

5. Whilst it is of significant interest to ascertain the full capability of dental pulp-derived populations, their homogeneous isolation and characterisation prior to utilisation is essential. Progression of Sox2 SCCD technologies to a GFP-based reporter construct will facilitate the isolation of cells exhibiting varying levels of plasticity, whilst NRSF and Dlk-1 SCCDs can allow the homogeneous isolation of neuronal and adipogenic progenitors.

6. Following to the homogeneous isolation of stem and progenitor subsets based on SCCD selection criteria, numerous *in vitro* and *in vivo* characterisation studies will be undertaken. Initial studies must investigate the theory indicating the potential of purified stem and progenitor subpopulations to re-establish heterogeneity, an issue which, if true, must be rigourously studied. Primarily the impact of such heterogeneity must be established on the clinical application and, should it prove to be inhibitory to regeneration, *in vitro* tailoring of conditions reprogramming cells to maintain homogeneity must be addressed. Following such investigations, of particular interest may be the *in*

vivo implantation of adipogenic precursors which, given the homogeneity of the implanted population, will conclusively provide evidence concerning pre-adipocyte dedifferentiation to macrophages. Furthermore, understanding the homogeneous dedifferentiation, if indeed it does occur, would allow tailoring of pre-implantation culture conditions to retain the pre-adipogenic phenotype. In fact the purification of pre-adipocytes alone may be sufficient to prevent dedifferentiation, removing the array of chemokines and growth factors present within the heterogeneous populations, factors which may have significant impact on pre-adipocyte dedifferentiation.

9. References

1. Meijer, G.J., de Bruijn, J.D., Koole, R. & van Blitterswijk, C.A. Cell-Based Bone Tissue Engineering. *PLoS Med* **4**, e9 (2007).
2. Muschler, G.F., Nakamoto, C. & Griffith, L.G. Engineering principles of clinical cell-based tissue engineering. *J Bone Joint Surg Am* **86-A**, 1541-1558 (2004).
3. Petit-Zeman, S. Regenerative medicine. *Nat Biotechnol* **19**, 201-206 (2001).
4. Griffith, L.G. & Naughton, G. Tissue engineering--current challenges and expanding opportunities. *Science* **295**, 1009-1014 (2002).
5. Rice, M.A., Dodson, B.T., Arthur, J.A. & Anseth, K.S. Cell-based therapies and tissue engineering. *Otolaryngol Clin North Am* **38**, 199-214, v (2005).
6. Smith, K.D. & Angus McGrouther, D. Strategies for cell engineering in tissue repair. *Wound Repair Regen* **5**, 212 (1997).
7. Alsberg, E., Anderson, K.W., Albeiruti, A., Rowley, J.A. & Mooney, D.J. Engineering growing tissues. *Proc Natl Acad Sci U S A* **99**, 12025-12030 (2002).
8. Zandstra, P.W. The opportunity of stem cell bioengineering. *Biotechnol Bioeng* **88**, 263 (2004).
9. Zandstra, P.W. & Nagy, A. Stem cell bioengineering. *Annu Rev Biomed Eng* **3**, 275-305 (2001).
10. Cancedda, R., Dozin, B., Giannoni, P. & Quarto, R. Tissue engineering and cell therapy of cartilage and bone. *Matrix Biol* **22**, 81-91 (2003).
11. Schek, R.M., Taboas, J.M., Hollister, S.J. & Krebsbach, P.H. Tissue engineering osteochondral implants for temporomandibular joint repair. *Orthod Craniofac Res* **8**, 313-319 (2005).
12. Hart, D.A., Kydd, A.S., Frank, C.B. & Hildebrand, K.A. Tissue repair in rheumatoid arthritis: challenges and opportunities in the face of a systemic inflammatory disease. *Best Pract Res Clin Rheumatol* **18**, 187-202 (2004).
13. Gu, Y., Yu, J., Lum, L.G. & Lee, R.J. Tissue engineering and stem cell therapy for myocardial repair. *Front Biosci* **12**, 5157-5165 (2007).
14. Levenberg, S. Engineering blood vessels from stem cells: recent advances and applications. *Curr Opin Biotechnol* **16**, 516-523 (2005).
15. Gomillion, C.T. & Burg, K.J. Stem cells and adipose tissue engineering. *Biomaterials* **27**, 6052-6063 (2006).
16. Patrick, C.W., Jr. Tissue engineering strategies for adipose tissue repair. *Anat Rec* **263**, 361-366 (2001).
17. Patrick, C.W., Jr. Adipose tissue engineering: the future of breast and soft tissue reconstruction following tumor resection. *Semin Surg Oncol* **19**, 302-311 (2000).
18. Andrade, C.F., Wong, A.P., Waddell, T.K., Keshavjee, S. & Liu, M. Cell-based tissue engineering for lung regeneration. *Am J Physiol Lung Cell Mol Physiol* **292**, L510-518 (2007).
19. MacNeil, S. Progress and opportunities for tissue-engineered skin. *Nature* **445**, 874-880 (2007).
20. Kubota, A., *et al.* Transplantable retinal pigment epithelial cell sheets for tissue engineering. *Biomaterials* **27**, 3639-3644 (2006).

21. Bartold, P.M., McCulloch, C.A., Narayanan, A.S. & Pitaru, S. Tissue engineering: a new paradigm for periodontal regeneration based on molecular and cell biology. *Periodontol 2000* **24**, 253-269 (2000).
22. Nakashima, M. & Akamine, A. The application of tissue engineering to regeneration of pulp and dentin in endodontics. *J Endod* **31**, 711-718 (2005).
23. Cross, W.R., Thomas, D.F. & Southgate, J. Tissue engineering and stem cell research in urology. *BJU Int* **92**, 165-171 (2003).
24. Kingham, P.J., Terenghi, G. & Birchall, M.A. Tissue engineering strategies for reinnervation of the larynx. *Clin Otolaryngol* **31**, 245 (2006).
25. Humes, H.D. Cell therapy and tissue engineering for renal replacement therapy. *Am J Kidney Dis* **32**, xlii-xliv (1998).
26. Joraku, A., Sullivan, C.A., Yoo, J.J. & Atala, A. Tissue engineering of functional salivary gland tissue. *Laryngoscope* **115**, 244-248 (2005).
27. Ding, D.C., Shyu, W.C., Lin, S.Z. & Li, H. Current concepts in adult stem cell therapy for stroke. *Curr Med Chem* **13**, 3565-3574 (2006).
28. Wallace, V.A. Stem cells: a source for neuron repair in retinal disease. *Can J Ophthalmol* **42**, 442-446 (2007).
29. Yannas, I.V. Facts and theories of induced organ regeneration. *Adv Biochem Eng Biotechnol* **93**, 1-38 (2005).
30. Yannas, I.V. Similarities and differences between induced organ regeneration in adults and early foetal regeneration. *J R Soc Interface* **2**, 403-417 (2005).
31. Yannas, I.V., Kwan, M.D. & Longaker, M.T. Early fetal healing as a model for adult organ regeneration. *Tissue Eng* **13**, 1789-1798 (2007).
32. Goessler, U.R., Riedel, K., Hormann, K. & Riedel, F. Perspectives of gene therapy in stem cell tissue engineering. *Cells Tissues Organs* **183**, 169-179 (2006).
33. Daley, G.Q., Goodell, M.A. & Snyder, E.Y. Realistic prospects for stem cell therapeutics. *Hematology Am Soc Hematol Educ Program*, 398-418 (2003).
34. Stoltz, J.F., *et al.* Cell and tissue engineering and clinical applications: an overview. *Biomed Mater Eng* **16**, S3-S18 (2006).
35. Myckatyn, T.M., Mackinnon, S.E. & McDonald, J.W. Stem cell transplantation and other novel techniques for promoting recovery from spinal cord injury. *Transpl Immunol* **12**, 343-358 (2004).
36. Fodor, W.L. Tissue engineering and cell based therapies, from the bench to the clinic: the potential to replace, repair and regenerate. *Reprod Biol Endocrinol* **1**, 102 (2003).
37. Sanmartin, A., English, D. & Sanberg, P.R. Stem cells in cell transplantation. *Stem Cells Dev* **15**, 963-966 (2006).
38. SanMartin, A. & Borlongan, C.V. Cell transplantation: toward cell therapy. *Cell Transplant* **15**, 665-673 (2006).
39. Koh, C.J. & Atala, A. Tissue engineering, stem cells, and cloning: opportunities for regenerative medicine. *J Am Soc Nephrol* **15**, 1113-1125 (2004).
40. Lutolf, M.P., *et al.* Synthetic matrix metalloproteinase-sensitive hydrogels for the conduction of tissue regeneration: engineering cell-invasion characteristics. *Proc Natl Acad Sci U S A* **100**, 5413-5418 (2003).
41. Hattori, H., *et al.* Bone formation using human adipose tissue-derived stromal cells and a biodegradable scaffold. *J Biomed Mater Res B Appl Biomater* **76**, 230-239 (2006).

42. Simpson, D., Liu, H., Fan, T.H., Nerem, R. & Dudley, S.C., Jr. A Tissue Engineering Approach to Progenitor Cell Delivery Results in Significant Cell Engraftment and Improved Myocardial Remodeling. *Stem Cells* (2007).
43. Fox, J.M., Chamberlain, G., Ashton, B.A. & Middleton, J. Recent advances into the understanding of mesenchymal stem cell trafficking. *Br J Haematol* **137**, 491-502 (2007).
44. Chen, S.L., *et al.* Improvement of cardiac function after transplantation of autologous bone marrow mesenchymal stem cells in patients with acute myocardial infarction. *Chin Med J (Engl)* **117**, 1443-1448 (2004).
45. Miyahara, Y., *et al.* Monolayered mesenchymal stem cells repair scarred myocardium after myocardial infarction. *Nat Med* **12**, 459-465 (2006).
46. Shiota, M., *et al.* Isolation and characterization of bone marrow-derived mesenchymal progenitor cells with myogenic and neuronal properties. *Exp Cell Res* **313**, 1008-1023 (2007).
47. Wiehe, J.M., *et al.* Labeling of adult stem cells for in vivo-application in the human heart. *Histol Histopathol* **20**, 901-906 (2005).
48. Le Blanc, K., *et al.* Treatment of severe acute graft-versus-host disease with third party haploidentical mesenchymal stem cells. *Lancet* **363**, 1439-1441 (2004).
49. Fang, B., Song, Y., Zhao, R.C., Han, Q. & Lin, Q. Using human adipose tissue-derived mesenchymal stem cells as salvage therapy for hepatic graft-versus-host disease resembling acute hepatitis. *Transplant Proc* **39**, 1710-1713 (2007).
50. Fang, B., Song, Y.P., Liao, L.M., Han, Q. & Zhao, R.C. Treatment of severe therapy-resistant acute graft-versus-host disease with human adipose tissue-derived mesenchymal stem cells. *Bone Marrow Transplant* **38**, 389-390 (2006).
51. Audet, J. Stem cell bioengineering for regenerative medicine. *Expert Opin Biol Ther* **4**, 631-644 (2004).
52. Raghunath, J., Salacinski, H.J., Sales, K.M., Butler, P.E. & Seifalian, A.M. Advancing cartilage tissue engineering: the application of stem cell technology. *Curr Opin Biotechnol* **16**, 503-509 (2005).
53. Mauney, J.R., Volloch, V. & Kaplan, D.L. Matrix-mediated retention of adipogenic differentiation potential by human adult bone marrow-derived mesenchymal stem cells during ex vivo expansion. *Biomaterials* **26**, 6167-6175 (2005).
54. Yoshimoto, H., Shin, Y.M., Terai, H. & Vacanti, J.P. A biodegradable nanofiber scaffold by electrospinning and its potential for bone tissue engineering. *Biomaterials* **24**, 2077-2082 (2003).
55. PP, B.M., *et al.* Chitosan particles agglomerated scaffolds for cartilage and osteochondral tissue engineering approaches with adipose tissue derived stem cells. *J Mater Sci Mater Med* **16**, 1077-1085 (2005).
56. Lechner, S. & Huss, R. Bone engineering: combining smart biomaterials and the application of stem cells. *Artif Organs* **30**, 770-774 (2006).
57. Mao, J.J., *et al.* Craniofacial tissue engineering by stem cells. *J Dent Res* **85**, 966-979 (2006).
58. Blau, H.M., Brazelton, T.R. & Weimann, J.M. The evolving concept of a stem cell: entity or function? *Cell* **105**, 829-841 (2001).
59. Alison, M.R., Poulsom, R., Forbes, S. & Wright, N.A. An introduction to stem cells. *J Pathol* **197**, 419-423 (2002).

60. Crick, F. Central dogma of molecular biology. *Nature* **227**, 561-563 (1970).
61. Lakshmipathy, U. & Verfaillie, C. Stem cell plasticity. *Blood Rev* **19**, 29-38 (2005).
62. Horwitz, E.M. Stem cell plasticity: a new image of the bone marrow stem cell. *Curr Opin Pediatr* **15**, 32-37 (2003).
63. Kohyama, J., *et al.* Brain from bone: efficient "meta-differentiation" of marrow stroma-derived mature osteoblasts to neurons with Noggin or a demethylating agent. *Differentiation* **68**, 235-244 (2001).
64. Frisen, J. Stem cell plasticity? *Neuron* **35**, 415-418 (2002).
65. Wulf, G.G., Jackson, K.A. & Goodell, M.A. Somatic stem cell plasticity: current evidence and emerging concepts. *Exp Hematol* **29**, 1361-1370 (2001).
66. Forbes, S.J., Vig, P., Poulsom, R., Wright, N.A. & Alison, M.R. Adult stem cell plasticity: new pathways of tissue regeneration become visible. *Clin Sci (Lond)* **103**, 355-369 (2002).
67. Almeida-Porada, G., Porada, C. & Zanjani, E.D. Adult stem cell plasticity and methods of detection. *Rev Clin Exp Hematol* **5**, 26-41 (2001).
68. Alsberg, E., von Recum, H.A. & Mahoney, M.J. Environmental cues to guide stem cell fate decision for tissue engineering applications. *Expert Opin Biol Ther* **6**, 847-866 (2006).
69. Benayahu, D., Akavia, U.D. & Shur, I. Differentiation of bone marrow stroma-derived mesenchymal cells. *Curr Med Chem* **14**, 173-179 (2007).
70. Mertelsmann, R. Plasticity of bone marrow-derived stem cells. *J Hematother Stem Cell Res* **9**, 957-960 (2000).
71. Colter, D.C., Class, R., DiGirolamo, C.M. & Prockop, D.J. Rapid expansion of recycling stem cells in cultures of plastic-adherent cells from human bone marrow. *Proc Natl Acad Sci U S A* **97**, 3213-3218 (2000).
72. Martin-Rendon, E. & Watt, S.M. Exploitation of stem cell plasticity. *Transfus Med* **13**, 325-349 (2003).
73. Poulsom, R., Alison, M.R., Forbes, S.J. & Wright, N.A. Adult stem cell plasticity. *J Pathol* **197**, 441-456 (2002).
74. Goodell, M.A., *et al.* Stem cell plasticity in muscle and bone marrow. *Ann N Y Acad Sci* **938**, 208-218; discussion 218-220 (2001).
75. Pittenger, M.F., *et al.* Multilineage potential of adult human mesenchymal stem cells. *Science* **284**, 143-147 (1999).
76. Planat-Benard, V., *et al.* Plasticity of human adipose lineage cells toward endothelial cells: physiological and therapeutic perspectives. *Circulation* **109**, 656-663 (2004).
77. Wislet-Gendebien, S., *et al.* Plasticity of cultured mesenchymal stem cells: switch from nestin-positive to excitable neuron-like phenotype. *Stem Cells* **23**, 392-402 (2005).
78. Zuk, P.A., *et al.* Multilineage cells from human adipose tissue: implications for cell-based therapies. *Tissue Eng* **7**, 211-228 (2001).
79. Makino, S., *et al.* Cardiomyocytes can be generated from marrow stromal cells in vitro. *J Clin Invest* **103**, 697-705 (1999).
80. Sanchez-Ramos, J.R. Neural cells derived from adult bone marrow and umbilical cord blood. *J Neurosci Res* **69**, 880-893 (2002).
81. Harris, J.R., *et al.* Bone marrow-derived cells home to and regenerate retinal pigment epithelium after injury. *Invest Ophthalmol Vis Sci* **47**, 2108-2113 (2006).

82. Strem, B.M., *et al.* Multipotential differentiation of adipose tissue-derived stem cells. *Keio J Med* **54**, 132-141 (2005).
83. Jiang, Y., *et al.* Pluripotency of mesenchymal stem cells derived from adult marrow. *Nature* **447**, 880-881 (2007).
84. Takahashi, K. & Yamanaka, S. Induction of pluripotent stem cells from mouse embryonic and adult fibroblast cultures by defined factors. *Cell* **126**, 663-676 (2006).
85. Gurdon, J.B. From nuclear transfer to nuclear reprogramming: The reversal of cell differentiation. *Annual Review Of Cell And Developmental Biology* **22**, 1-22 (2006).
86. Gurdon, J.B. Nuclear transplantation in eggs and oocytes. *J Cell Sci Suppl* **4**, 287-318 (1986).
87. Tada, M., Takahama, Y., Abe, K., Nakatsuji, N. & Tada, T. Nuclear reprogramming of somatic cells by in vitro hybridization with ES cells. *Curr Biol* **11**, 1553-1558 (2001).
88. Perry, A.C. Induced pluripotency and cellular alchemy. *Nat Biotechnol* **24**, 1363-1364 (2006).
89. Hochedlinger, K. & Jaenisch, R. Nuclear reprogramming and pluripotency. *Nature* **441**, 1061-1067 (2006).
90. Hansis, C., Barreto, G., Maltry, N. & Niehrs, C. Nuclear reprogramming of human somatic cells by xenopus egg extract requires BRG1. *Curr Biol* **14**, 1475-1480 (2004).
91. Kikyo, N., Wade, P.A., Guschin, D., Ge, H. & Wolffe, A.P. Active remodeling of somatic nuclei in egg cytoplasm by the nucleosomal ATPase ISWI. *Science* **289**, 2360-2362 (2000).
92. Campbell, P.A., Perez-Iratxeta, C., Andrade-Navarro, M.A. & Rudnicki, M.A. Oct4 targets regulatory nodes to modulate stem cell function. *PLoS ONE* **2**, e553 (2007).
93. Masui, S., *et al.* Pluripotency governed by Sox2 via regulation of Oct3/4 expression in mouse embryonic stem cells. *Nat Cell Biol* **9**, 625-635 (2007).
94. Wang, J., *et al.* A protein interaction network for pluripotency of embryonic stem cells. *Nature* **444**, 364-368 (2006).
95. Hatano, S.Y., *et al.* Pluripotential competence of cells associated with Nanog activity. *Mech Dev* **122**, 67-79 (2005).
96. Wang, Z.X., *et al.* Oct4 and sox2 directly regulate expression of another pluripotency transcription factor, Zfp206, in embryonic stem cells. *Journal Of Biological Chemistry* **282**, 12822-12830 (2007).
97. Loh, Y.H., *et al.* The Oct4 and Nanog transcription network regulates pluripotency in mouse embryonic stem cells. *Nat Genet* **38**, 431-440 (2006).
98. Kaji, K., *et al.* The NuRD component Mbd3 is required for pluripotency of embryonic stem cells. *Nat Cell Biol* **8**, 285-292 (2006).
99. Byrne, J.A., Simonsson, S., Western, P.S. & Gurdon, J.B. Nuclei of adult mammalian somatic cells are directly reprogrammed to oct-4 stem cell gene expression by amphibian oocytes. *Curr Biol* **13**, 1206-1213 (2003).
100. Mitsui, K., *et al.* The homeoprotein Nanog is required for maintenance of pluripotency in mouse epiblast and ES cells. *Cell* **113**, 631-642 (2003).
101. Chambers, I., *et al.* Functional expression cloning of Nanog, a pluripotency sustaining factor in embryonic stem cells. *Cell* **113**, 643-655 (2003).
102. Pan, G. & Thomson, J.A. Nanog and transcriptional networks in embryonic stem cell pluripotency. *Cell Res* **17**, 42-49 (2007).

103. Nichols, J., *et al.* Formation of pluripotent stem cells in the mammalian embryo depends on the POU transcription factor Oct4. *Cell* **95**, 379-391 (1998).
104. Avilion, A.A., *et al.* Multipotent cell lineages in early mouse development depend on SOX2 function. *Genes Dev* **17**, 126-140 (2003).
105. Solter, D. From teratocarcinomas to embryonic stem cells and beyond: a history of embryonic stem cell research. *Nat Rev Genet* **7**, 319-327 (2006).
106. Lavine, M., Roberts, L. & Smith, O. If I Only Had a. *Science* **295**, 995- (2002).
107. Ding, S. & Schultz, P.G. A role for chemistry in stem cell biology. *Nat Biotechnol* **22**, 833-840 (2004).
108. Thomson, J.A., *et al.* Embryonic stem cell lines derived from human blastocysts. *Science* **282**, 1145-1147 (1998).
109. Choong, C. & Rao, M.S. Human embryonic stem cells. *Neurosurg Clin N Am* **18**, 1-14, vii (2007).
110. Geijsen, N., *et al.* Derivation of embryonic germ cells and male gametes from embryonic stem cells. *Nature* **427**, 148-154 (2004).
111. Hubner, K., *et al.* Derivation of oocytes from mouse embryonic stem cells. *Science* **300**, 1251-1256 (2003).
112. Toyooka, Y., Tsunekawa, N., Akasu, R. & Noce, T. Embryonic stem cells can form germ cells in vitro. *Proc Natl Acad Sci U S A* **100**, 11457-11462 (2003).
113. Fischbach, G.D. & Fischbach, R.L. Stem cells: science, policy, and ethics. *J Clin Invest* **114**, 1364-1370 (2004).
114. Costa, F.F., Le Blanc, K. & Brodin, B. Concise review: cancer/testis antigens, stem cells, and cancer. *Stem Cells* **25**, 707-711 (2007).
115. Bobrow, J.C. The ethics and politics of stem cell research. *Trans Am Ophthalmol Soc* **103**, 138-141; discussion 141-132 (2005).
116. Balint, J.A. Ethical issues in stem cell research. *Albany Law Rev* **65**, 729-742 (2002).
117. Bruce, A. The search for truth and freedom: ethical issues surrounding human cloning and stem cell research. *J Law Med* **9**, 323-335 (2002).
118. Childress, J.F. Human stem cell research: some controversies in bioethics and public policy. *Blood Cells Mol Dis* **32**, 100-105 (2004).
119. Chin, J.J. Ethical issues in stem cell research. *Med J Malaysia* **58 Suppl A**, 111-118 (2003).
120. Cohen, C.B. Ethical issues in embryonic stem cell research. *Jama* **285**, 1439; author reply 1440 (2001).
121. de, S.C.N.M. Research ethics, science policy, and four contexts for the stem cell debate. *J Investig Med* **54**, 38-42 (2006).
122. de Wert, G. The use of human embryonic stem cells for research: an ethical evaluation. *Prog Brain Res* **138**, 465-470 (2002).
123. Vicini, A. Ethical issues and approaches in stem cell research: from international insights to a proposal. *J Soc Christ Ethics* **23**, 71-98 (2003).
124. Wainwright, S.P., Williams, C., Michael, M., Farsides, B. & Cribb, A. Ethical boundary-work in the embryonic stem cell laboratory. *Sociol Health Illn* **28**, 732-748 (2006).
125. Welin, S. Ethical issues in human embryonic stem cell research. *Acta Obstet Gynecol Scand* **81**, 377-382 (2002).

126. Wertz, D.C. Embryo and stem cell research in the United States: history and politics. *Gene Ther* **9**, 674-678 (2002).
127. Solter, D. & Knowles, B.B. Immunosurgery of mouse blastocyst. *Proc Natl Acad Sci U S A* **72**, 5099-5102 (1975).
128. Balbach, S.T., *et al.* Chromosome stability differs in cloned mouse embryos and derivative ES cells. *Dev Biol* **308**, 309-321 (2007).
129. Matveeva, N.M., *et al.* Unequal segregation of parental chromosomes in embryonic stem cell hybrids. *Mol Reprod Dev* **71**, 305-314 (2005).
130. Ljubuncic, P. & Reznick, A.Z. The evolutionary theories of aging revisited--a mini-review. *Gerontology* **55**, 205-216 (2009).
131. Shamblott, M.J., *et al.* Derivation of pluripotent stem cells from cultured human primordial germ cells. *Proc Natl Acad Sci U S A* **95**, 13726-13731 (1998).
132. Gurdon, J.B., Laskey, R.A. & Reeves, O.R. The developmental capacity of nuclei transplanted from keratinized skin cells of adult frogs. *J Embryol Exp Morphol* **34**, 93-112 (1975).
133. Gurdon, J.B. Nuclear transplantation and the analysis of gene activity in early amphibian development. *Adv Exp Med Biol* **62**, 35-44 (1975).
134. Quinlivan, T.D., Martin, C.A., Taylor, W.B. & Cairney, I.M. Estimates of pre- and perinatal mortality in the New Zealand Romney Marsh ewe. I. Pre- and perinatal mortality in those ewes that conceived to one service. *J Reprod Fertil* **11**, 379-390 (1966).
135. Nash, M.L., Hungerford, L.L., Nash, T.G. & Zinn, G.M. Risk factors for perinatal and postnatal mortality in lambs. *Vet Rec* **139**, 64-67 (1996).
136. Wilmut, I., Schnieke, A.E., McWhir, J., Kind, A.J. & Campbell, K.H. Viable offspring derived from fetal and adult mammalian cells. *Cloning Stem Cells* **9**, 3-7 (2007).
137. Ready, T. Scientists resign over stem-cell study. *Nat Med* **8**, 200 (2002).
138. Wilmut, I. Are there any normal cloned mammals? *Nat Med* **8**, 215-216 (2002).
139. Tamashiro, K.L., *et al.* Cloned mice have an obese phenotype not transmitted to their offspring. *Nat Med* **8**, 262-267 (2002).
140. Maherali, N., *et al.* Directly reprogrammed fibroblasts show global epigenetic remodeling and widespread tissue contribution. *Cell Stem Cell* **1**, 55-70 (2007).
141. Okita, K., Ichisaka, T. & Yamanaka, S. Generation of germline-competent induced pluripotent stem cells. *Nature* **448**, 313-317 (2007).
142. Liu, H., *et al.* Generation of induced pluripotent stem cells from adult rhesus monkey fibroblasts. *Cell Stem Cell* **3**, 587-590 (2008).
143. Yu, J., *et al.* Induced pluripotent stem cell lines derived from human somatic cells. *Science* **318**, 1917-1920 (2007).
144. Muller, L.U., Daley, G.Q. & Williams, D.A. Upping the Ante: Recent Advances in Direct Reprogramming. *Mol Ther* (2009).
145. Nakagawa, M., *et al.* Generation of induced pluripotent stem cells without Myc from mouse and human fibroblasts. *Nat Biotechnol* **26**, 101-106 (2008).
146. Okita, K., Nakagawa, M., Hyenjong, H., Ichisaka, T. & Yamanaka, S. Generation of mouse induced pluripotent stem cells without viral vectors. *Science* **322**, 949-953 (2008).

147. Stadtfeld, M., Nagaya, M., Utikal, J., Weir, G. & Hochedlinger, K. Induced pluripotent stem cells generated without viral integration. *Science* **322**, 945-949 (2008).
148. Huangfu, D., *et al.* Induction of pluripotent stem cells by defined factors is greatly improved by small-molecule compounds. *Nat Biotechnol* **26**, 795-797 (2008).
149. Kim, J.B., *et al.* Oct4-induced pluripotency in adult neural stem cells. *Cell* **136**, 411-419 (2009).
150. Park, I.H., *et al.* Reprogramming of human somatic cells to pluripotency with defined factors. *Nature* **451**, 141-146 (2008).
151. Takahashi, K., *et al.* Induction of pluripotent stem cells from adult human fibroblasts by defined factors. *Cell* **131**, 861-872 (2007).
152. Alison, M.R., *et al.* Recipes for adult stem cell plasticity: fusion cuisine or readymade? *J Clin Pathol* **57**, 113-120 (2004).
153. Brzoska, M., Geiger, H., Gauer, S. & Baer, P. Epithelial differentiation of human adipose tissue-derived adult stem cells. *Biochem Biophys Res Commun* **330**, 142-150 (2005).
154. Chen, Y., Teng, F.Y. & Tang, B.L. Coaxing bone marrow stromal mesenchymal stem cells towards neuronal differentiation: progress and uncertainties. *Cell Mol Life Sci* **63**, 1649-1657 (2006).
155. Gimble, J. & Guilak, F. Adipose-derived adult stem cells: isolation, characterization, and differentiation potential. *Cytotherapy* **5**, 362-369 (2003).
156. Grove, J.E., Bruscia, E. & Krause, D.S. Plasticity of bone marrow-derived stem cells. *Stem Cells* **22**, 487-500 (2004).
157. Kim, S., *et al.* Neural differentiation potential of peripheral blood- and bone-marrow-derived precursor cells. *Brain Res* **1123**, 27-33 (2006).
158. Quesenberry, P.J., *et al.* Stem cell plasticity: an overview. *Blood Cells Mol Dis* **32**, 1-4 (2004).
159. Sekiya, I., Larson, B.L., Vuoristo, J.T., Cui, J.G. & Prockop, D.J. Adipogenic differentiation of human adult stem cells from bone marrow stroma (MSCs). *J Bone Miner Res* **19**, 256-264 (2004).
160. Spyridonidis, A., Zeiser, R., Follo, M., Metaxas, Y. & Finke, J. Stem cell plasticity: the debate begins to clarify. *Stem Cell Rev* **1**, 37-43 (2005).
161. Verfaillie, C.M. Adult stem cells: assessing the case for pluripotency. *Trends Cell Biol* **12**, 502-508 (2002).
162. Yang, X., *et al.* Plasticity of epidermal adult stem cells derived from adult goat ear skin. *Mol Reprod Dev* **74**, 386-396 (2007).
163. Young, H.E. & Black, A.C., Jr. Adult stem cells. *Anat Rec A Discov Mol Cell Evol Biol* **276**, 75-102 (2004).
164. Hong, L., Peptan, I.A., Colpan, A. & Daw, J.L. Adipose tissue engineering by human adipose-derived stromal cells. *Cells Tissues Organs* **183**, 133-140 (2006).
165. Bruder, S.P. & Fox, B.S. Tissue engineering of bone. Cell based strategies. *Clin Orthop Relat Res*, S68-83 (1999).
166. Marcacci, M., *et al.* New cell-based technologies in bone and cartilage tissue engineering. II. Cartilage regeneration. *Chir Organi Mov* **88**, 42-47 (2003).
167. Lietz, M., Dreesmann, L., Hoss, M., Oberhoffner, S. & Schlosshauer, B. Neuro tissue engineering of glial nerve guides and the impact of different cell types. *Biomaterials* **27**, 1425-1436 (2006).

168. Yen, A.H. & Sharpe, P.T. Stem cells and tooth tissue engineering. *Cell Tissue Res* **331**, 359-372 (2008).
169. Dieterlen-Lievre, F. On the origin of haemopoietic stem cells in the avian embryo: an experimental approach. *J Embryol Exp Morphol* **33**, 607-619 (1975).
170. Turpen, J.B., Knudson, C.M. & Hoefen, P.S. The early ontogeny of hematopoietic cells studied by grafting cytogenetically labeled tissue anlagen: localization of a prospective stem cell compartment. *Dev Biol* **85**, 99-112 (1981).
171. Ciau-Uitz, A., Walmsley, M. & Patient, R. Distinct origins of adult and embryonic blood in Xenopus. *Cell* **102**, 787-796 (2000).
172. Moore, M.A. & Metcalf, D. Ontogeny of the haemopoietic system: yolk sac origin of in vivo and in vitro colony forming cells in the developing mouse embryo. *Br J Haematol* **18**, 279-296 (1970).
173. Muller, A.M., Medvinsky, A., Strouboulis, J., Grosveld, F. & Dzierzak, E. Development of hematopoietic stem cell activity in the mouse embryo. *Immunity* **1**, 291-301 (1994).
174. Medvinsky, A. & Dzierzak, E. Definitive hematopoiesis is autonomously initiated by the AGM region. *Cell* **86**, 897-906 (1996).
175. de Bruijn, M.F., Speck, N.A., Peeters, M.C. & Dzierzak, E. Definitive hematopoietic stem cells first develop within the major arterial regions of the mouse embryo. *EMBO J* **19**, 2465-2474 (2000).
176. Dzierzak, E. The emergence of definitive hematopoietic stem cells in the mammal. *Curr Opin Hematol* **12**, 197-202 (2005).
177. Flake, A.W., Harrison, M.R., Adzick, N.S. & Zanjani, E.D. Transplantation of fetal hematopoietic stem cells in utero: the creation of hematopoietic chimeras. *Science* **233**, 776-778 (1986).
178. Kondo, M., *et al.* Biology of hematopoietic stem cells and progenitors: implications for clinical application. *Annu Rev Immunol* **21**, 759-806 (2003).
179. Giebel, B., *et al.* Primitive human hematopoietic cells give rise to differentially specified daughter cells upon their initial cell division. *Blood* **107**, 2146-2152 (2006).
180. Barzilay, R., *et al.* Induction of human mesenchymal stem cells into dopamine-producing cells with different differentiation protocols. *Stem Cells Dev* **17**, 547-554 (2008).
181. Sheng, H., *et al.* A critical role of IFNgamma in priming MSC-mediated suppression of T cell proliferation through up-regulation of B7-H1. *Cell Res* **18**, 846-857 (2008).
182. Keating, A. How do mesenchymal stromal cells suppress T cells? *Cell Stem Cell* **2**, 106-108 (2008).
183. Baal, N., *et al.* Expression of transcription factor Oct-4 and other embryonic genes in CD133 positive cells from human umbilical cord blood. *Thromb Haemost* **92**, 767-775 (2004).
184. Voelkel, T., *et al.* Highly efficient neural differentiation of peripheral blood human hematopoietic stem cells. *FASEB J.* **22**, 30- (2008).
185. Ebihara, Y., *et al.* Hematopoietic origins of fibroblasts: II. In vitro studies of fibroblasts, CFU-F, and fibrocytes. *Exp Hematol* **34**, 219-229 (2006).
186. Chen, N., *et al.* Human umbilical cord blood progenitors: the potential of these hematopoietic cells to become neural. *Stem Cells* **23**, 1560-1570 (2005).

187. Gomez-Ochoa, P., *et al.* Isolation and development of haematopoietic progenitor cells from peripheral blood of adult and newborn pigs. *Acta Vet Hung* **55**, 171-180 (2007).
188. Shizuru, J.A., Negrin, R.S. & Weissman, I.L. Hematopoietic stem and progenitor cells: clinical and preclinical regeneration of the hematolymphoid system. *Annu Rev Med* **56**, 509-538 (2005).
189. Antin, J.H. Graft-versus-leukemia: no longer an epiphenomenon. *Blood* **82**, 2273-2277 (1993).
190. Ferrara, J.L., Levy, R. & Chao, N.J. Pathophysiologic mechanisms of acute graft-vs.-host disease. *Biol Blood Marrow Transplant* **5**, 347-356 (1999).
191. Friedenstein, A.J., Chailakhjan, R.K. & Lalykina, K.S. The development of fibroblast colonies in monolayer cultures of guinea-pig bone marrow and spleen cells. *Cell Tissue Kinet* **3**, 393-403 (1970).
192. Alhadlaq, A. & Mao, J.J. Tissue-engineered neogenesis of human-shaped mandibular condyle from rat mesenchymal stem cells. *J Dent Res* **82**, 951-956 (2003).
193. Thomson, B.M., *et al.* Preliminary characterization of porcine bone marrow stromal cells: skeletogenic potential, colony-forming activity, and response to dexamethasone, transforming growth factor beta, and basic fibroblast growth factor. *J Bone Miner Res* **8**, 1173-1183 (1993).
194. Meirelles Lda, S. & Nardi, N.B. Murine marrow-derived mesenchymal stem cell: isolation, in vitro expansion, and characterization. *Br J Haematol* **123**, 702-711 (2003).
195. Jiang, Y., *et al.* Pluripotency of mesenchymal stem cells derived from adult marrow. *Nature* **418**, 41-49 (2002).
196. Alhadlaq, A., *et al.* Adult stem cell driven genesis of human-shaped articular condyle. *Ann Biomed Eng* **32**, 911-923 (2004).
197. Wakitani, S., *et al.* Mesenchymal cell-based repair of large, full-thickness defects of articular cartilage. *J Bone Joint Surg Am* **76**, 579-592 (1994).
198. Kadiyala, S., Young, R.G., Thiede, M.A. & Bruder, S.P. Culture expanded canine mesenchymal stem cells possess osteochondrogenic potential in vivo and in vitro. *Cell Transplant* **6**, 125-134 (1997).
199. Shang, Q., *et al.* Tissue-engineered bone repair of sheep cranial defects with autologous bone marrow stromal cells. *J Craniofac Surg* **12**, 586-593; discussion 594-585 (2001).
200. Ringe, J., *et al.* Porcine mesenchymal stem cells. Induction of distinct mesenchymal cell lineages. *Cell Tissue Res* **307**, 321-327 (2002).
201. Worster, A.A., Nixon, A.J., Brower-Toland, B.D. & Williams, J. Effect of transforming growth factor beta1 on chondrogenic differentiation of cultured equine mesenchymal stem cells. *Am J Vet Res* **61**, 1003-1010 (2000).
202. Niku, M., Ilmonen, L., Pessa-Morikawa, T. & Iivanainen, A. Limited contribution of circulating cells to the development and maintenance of nonhematopoietic bovine tissues. *Stem Cells* **22**, 12-20 (2004).
203. Simmons, P.J. & Torok-Storb, B. Identification of stromal cell precursors in human bone marrow by a novel monoclonal antibody, STRO-1. *Blood* **78**, 55-62 (1991).
204. Seshi, B., Kumar, S. & Sellers, D. Human bone marrow stromal cell: coexpression of markers specific for multiple mesenchymal cell lineages. *Blood Cells Mol Dis* **26**, 234-246 (2000).

205. Haynesworth, S.E., Baber, M.A. & Caplan, A.I. Cell surface antigens on human marrow-derived mesenchymal cells are detected by monoclonal antibodies. *Bone* **13**, 69-80 (1992).
206. Modderman, W.E., Vrijheid-Lammers, T., Lowik, C.W. & Nijweide, P.J. Removal of hematopoietic cells and macrophages from mouse bone marrow cultures: isolation of fibroblastlike stromal cells. *Exp Hematol* **22**, 194-201 (1994).
207. Van Vlasselaer, P., Falla, N., Snoeck, H. & Mathieu, E. Characterization and purification of osteogenic cells from murine bone marrow by two-color cell sorting using anti-Sca-1 monoclonal antibody and wheat germ agglutinin. *Blood* **84**, 753-763 (1994).
208. Rickard, D.J., *et al.* Isolation and characterization of osteoblast precursor cells from human bone marrow. *J Bone Miner Res* **11**, 312-324 (1996).
209. Gronthos, S., Simmons, P.J., Graves, S.E. & Robey, P.G. Integrin-mediated interactions between human bone marrow stromal precursor cells and the extracellular matrix. *Bone* **28**, 174-181 (2001).
210. Gronthos, S., *et al.* Molecular and cellular characterisation of highly purified stromal stem cells derived from human bone marrow. *J Cell Sci* **116**, 1827-1835 (2003).
211. Hinds, K.A., *et al.* Highly efficient endosomal labeling of progenitor and stem cells with large magnetic particles allows magnetic resonance imaging of single cells. *Blood* **102**, 867-872 (2003).
212. Alison, M.R., Brittan, M., Lovell, M.J. & Wright, N.A. Markers of adult tissue-based stem cells. *Handb Exp Pharmacol*, 185-227 (2006).
213. Tseng, P.Y., Chen, C.J., Sheu, C.C., Yu, C.W. & Huang, Y.S. Spontaneous differentiation of adult rat marrow stromal cells in a long-term culture. *J Vet Med Sci* **69**, 95-102 (2007).
214. Zannettino, A.C., *et al.* Human mulipotential mesenchymal/stromal stem cells are derived from a discrete subpopulation of STRO-1bright/CD34 /CD45(-)/glycophorin-A-bone marrow cells. *Haematologica* **92**, 1707-1708 (2007).
215. Gronthos, S. & Zannettino, A.C. A method to isolate and purify human bone marrow stromal stem cells. *Methods Mol Biol* **449**, 45-57 (2008).
216. Tsai, R.Y. & McKay, R.D. A nucleolar mechanism controlling cell proliferation in stem cells and cancer cells. *Genes Dev* **16**, 2991-3003 (2002).
217. Baddoo, M., *et al.* Characterization of mesenchymal stem cells isolated from murine bone marrow by negative selection. *J Cell Biochem* **89**, 1235-1249 (2003).
218. Lengner, C.J., Welstead, G.G. & Jaenisch, R. The pluripotency regulator Oct4: a role in somatic stem cells? *Cell Cycle* **7**, 725-728 (2008).
219. Liedtke, S., Stephan, M. & Kogler, G. Oct4 expression revisited: potential pitfalls for data misinterpretation in stem cell research. *Biol Chem* **389**, 845-850 (2008).
220. Zuk, P.A. The intracellular distribution of the ES cell totipotent markers OCT4 and Sox2 in adult stem cells differs dramatically according to commercial antibody used. *J Cell Biochem* **106**, 867-877 (2009).
221. Lengner, C.J., *et al.* Oct4 expression is not required for mouse somatic stem cell self-renewal. *Cell Stem Cell* **1**, 403-415 (2007).
222. Greco, S.J., Liu, K. & Rameshwar, P. Functional similarities among genes regulated by OCT4 in human mesenchymal and embryonic stem cells. *Stem Cells* **25**, 3143-3154 (2007).

223. Izadpanah, R., *et al.* Characterization of multipotent mesenchymal stem cells from the bone marrow of rhesus macaques. *Stem Cells Dev* **14**, 440-451 (2005).
224. Ulloa-Montoya, F., *et al.* Comparative transcriptome analysis of embryonic and adult stem cells with extended and limited differentiation capacity. *Genome Biol* **8**, R163 (2007).
225. Prockop, D.J. Marrow stromal cells as stem cells for nonhematopoietic tissues. *Science* **276**, 71-74 (1997).
226. Mets, T. & Verdonk, G. In vitro aging of human bone marrow derived stromal cells. *Mech Ageing Dev* **16**, 81-89 (1981).
227. D'Ippolito, G., Schiller, P.C., Ricordi, C., Roos, B.A. & Howard, G.A. Age-related osteogenic potential of mesenchymal stromal stem cells from human vertebral bone marrow. *J Bone Miner Res* **14**, 1115-1122 (1999).
228. Bruder, S.P., Jaiswal, N. & Haynesworth, S.E. Growth kinetics, self-renewal, and the osteogenic potential of purified human mesenchymal stem cells during extensive subcultivation and following cryopreservation. *J Cell Biochem* **64**, 278-294 (1997).
229. Digirolamo, C.M., *et al.* Propagation and senescence of human marrow stromal cells in culture: a simple colony-forming assay identifies samples with the greatest potential to propagate and differentiate. *Br J Haematol* **107**, 275-281 (1999).
230. Banfi, A., *et al.* Proliferation kinetics and differentiation potential of ex vivo expanded human bone marrow stromal cells: Implications for their use in cell therapy. *Exp Hematol* **28**, 707-715 (2000).
231. Stenderup, K., Justesen, J., Clausen, C. & Kassem, M. Aging is associated with decreased maximal life span and accelerated senescence of bone marrow stromal cells. *Bone* **33**, 919-926 (2003).
232. Rombouts, W.J. & Ploemacher, R.E. Primary murine MSC show highly efficient homing to the bone marrow but lose homing ability following culture. *Leukemia* **17**, 160-170 (2003).
233. Baxter, M.A., *et al.* Study of telomere length reveals rapid aging of human marrow stromal cells following in vitro expansion. *Stem Cells* **22**, 675-682 (2004).
234. Raposio, E., *et al.* Characterization of multipotent cells from human adult hair follicles. *Toxicol In Vitro* **21**, 320-323 (2007).
235. Gage, F.H. Mammalian neural stem cells. *Science* **287**, 1433-1438 (2000).
236. Jiao, J. & Chen, D.F. Induction of neurogenesis in nonconventional neurogenic regions of the adult central nervous system by niche astrocyte-produced signals. *Stem Cells* **26**, 1221-1230 (2008).
237. Bentley, A.J., *et al.* Characterization of human corneal stem cells by synchrotron infrared micro-spectroscopy. *Mol Vis* **13**, 237-242 (2007).
238. German, M.J., *et al.* Characterization of putative stem cell populations in the cornea using synchrotron infrared microspectroscopy. *Invest Ophthalmol Vis Sci* **47**, 2417-2421 (2006).
239. Kim, H.S., *et al.* Phenotypic characterization of human corneal epithelial cells expanded ex vivo from limbal explant and single cell cultures. *Exp Eye Res* **79**, 41-49 (2004).
240. Revoltella, R.P., Papini, S., Rosellini, A. & Michelini, M. Epithelial stem cells of the eye surface. *Cell Prolif* **40**, 445-461 (2007).

241. Ahmad, I., Das, A.V., James, J., Bhattacharya, S. & Zhao, X. Neural stem cells in the mammalian eye: types and regulation. *Semin Cell Dev Biol* **15**, 53-62 (2004).
242. Ahmad, I., Tang, L. & Pham, H. Identification of neural progenitors in the adult mammalian eye. *Biochem Biophys Res Commun* **270**, 517-521 (2000).
243. Amato, M.A., Arnault, E. & Perron, M. Retinal stem cells in vertebrates: parallels and divergences. *Int J Dev Biol* **48**, 993-1001 (2004).
244. Sun, G., Asami, M., Ohta, H., Kosaka, J. & Kosaka, M. Retinal stem/progenitor properties of iris pigment epithelial cells. *Dev Biol* **289**, 243-252 (2006).
245. Arthur, A., Rychkov, G., Shi, S., Koblar, S.A. & Gronthos, S. Adult human dental pulp stem cells differentiate toward functionally active neurons under appropriate environmental cues. *Stem Cells* **26**, 1787-1795 (2008).
246. Jo, Y.Y., *et al.* Isolation and characterization of postnatal stem cells from human dental tissues. *Tissue Eng* **13**, 767-773 (2007).
247. Liu, X., Driskell, R.R. & Engelhardt, J.F. Stem cells in the lung. *Methods Enzymol* **419**, 285-321 (2006).
248. Abuljadayel, I.S., *et al.* SCID repopulating cells derived from unmobilised adult human peripheral blood. *Curr Med Res Opin* **20**, 87-100 (2004).
249. Kuwana, M., *et al.* Human circulating CD14+ monocytes as a source of progenitors that exhibit mesenchymal cell differentiation. *J Leukoc Biol* **74**, 833-845 (2003).
250. Roufosse, C.A., Direkze, N.C., Otto, W.R. & Wright, N.A. Circulating mesenchymal stem cells. *Int J Biochem Cell Biol* **36**, 585-597 (2004).
251. Zhao, Y., *et al.* A unique human blood-derived cell population displays high potential for producing insulin. *Biochem Biophys Res Commun* **360**, 205-211 (2007).
252. Barile, L., Messina, E., Giacomello, A. & Marban, E. Endogenous Cardiac Stem Cells. *Prog Cardiovasc Dis* **50**, 31-48 (2007).
253. Booth, C., O'Shea, J.A. & Potten, C.S. Maintenance of functional stem cells in isolated and cultured adult intestinal epithelium. *Exp Cell Res* **249**, 359-366 (1999).
254. Potten, C.S. Stem cells in gastrointestinal epithelium: numbers, characteristics and death. *Philos Trans R Soc Lond B Biol Sci* **353**, 821-830 (1998).
255. Stappenbeck, T.S., Mills, J.C. & Gordon, J.I. Molecular features of adult mouse small intestinal epithelial progenitors. *Proc Natl Acad Sci U S A* **100**, 1004-1009 (2003).
256. Wong, M.H. Regulation of intestinal stem cells. *J Investig Dermatol Symp Proc* **9**, 224-228 (2004).
257. Banas, A., *et al.* Adipose tissue-derived mesenchymal stem cells as a source of human hepatocytes. *Hepatology* **46**, 219-228 (2007).
258. Boquest, A.C., Shahdadfar, A., Brinchmann, J.E. & Collas, P. Isolation of stromal stem cells from human adipose tissue. *Methods Mol Biol* **325**, 35-46 (2006).
259. Casteilla, L. & Dani, C. Adipose tissue-derived cells: from physiology to regenerative medicine. *Diabetes Metab* **32**, 393-401 (2006).
260. Casteilla, L., *et al.* Plasticity of adipose tissue: a promising therapeutic avenue in the treatment of cardiovascular and blood diseases? *Arch Mal Coeur Vaiss* **98**, 922-926 (2005).

261. Choi, Y.S., *et al.* Adipogenic differentiation of adipose tissue derived adult stem cells in nude mouse. *Biochem Biophys Res Commun* **345**, 631-637 (2006).
262. Dicker, A., *et al.* Functional studies of mesenchymal stem cells derived from adult human adipose tissue. *Exp Cell Res* **308**, 283-290 (2005).
263. Gimble, J.M., Katz, A.J. & Bunnell, B.A. Adipose-derived stem cells for regenerative medicine. *Circ Res* **100**, 1249-1260 (2007).
264. Hausman, G.J. & Hausman, D.B. Search for the preadipocyte progenitor cell. *J Clin Invest* **116**, 3103-3106 (2006).
265. Deasy, B.M., Jankowski, R.J. & Huard, J. Muscle-derived stem cells: characterization and potential for cell-mediated therapy. *Blood Cells Mol Dis* **27**, 924-933 (2001).
266. O'Brien, K., Muskiewicz, K. & Gussoni, E. Recent advances in and therapeutic potential of muscle-derived stem cells. *J Cell Biochem Suppl* **38**, 80-87 (2002).
267. Tajbakhsh, S. Skeletal muscle stem and progenitor cells: reconciling genetics and lineage. *Exp Cell Res* **306**, 364-372 (2005).
268. Vourc'h, P., *et al.* Isolation and characterization of cells with neurogenic potential from adult skeletal muscle. *Biochem Biophys Res Commun* **317**, 893-901 (2004).
269. Belicchi, M., *et al.* Human skin-derived stem cells migrate throughout forebrain and differentiate into astrocytes after injection into adult mouse brain. *J Neurosci Res* **77**, 475-486 (2004).
270. Cotsarelis, G. Epithelial stem cells: a folliculocentric view. *J Invest Dermatol* **126**, 1459-1468 (2006).
271. Kawase, Y., Yanagi, Y., Takato, T., Fujimoto, M. & Okochi, H. Characterization of multipotent adult stem cells from the skin: transforming growth factor-beta (TGF-beta) facilitates cell growth. *Exp Cell Res* **295**, 194-203 (2004).
272. Meindl, S., Schmidt, U., Vaculik, C. & Elbe-Burger, A. Characterization, isolation, and differentiation of murine skin cells expressing hematopoietic stem cell markers. *J Leukoc Biol* **80**, 816-826 (2006).
273. Watt, F.M. Epidermal stem cells: markers, patterning and the control of stem cell fate. *Philos Trans R Soc Lond B Biol Sci* **353**, 831-837 (1998).
274. Gimble, J.M. & Guilak, F. Differentiation potential of adipose derived adult stem (ADAS) cells. *Curr Top Dev Biol* **58**, 137-160 (2003).
275. Corti, S., *et al.* Identification of a primitive brain-derived neural stem cell population based on aldehyde dehydrogenase activity. *Stem Cells* **24**, 975-985 (2006).
276. Sosnova, M., Bradl, M. & Forrester, J.V. CD34+ corneal stromal cells are bone marrow-derived and express hemopoietic stem cell markers. *Stem Cells* **23**, 507-515 (2005).
277. Kerkis, I., *et al.* Isolation and characterization of a population of immature dental pulp stem cells expressing OCT-4 and other embryonic stem cell markers. *Cells Tissues Organs* **184**, 105-116 (2006).
278. Nowak, J.A., Polak, L., Pasolli, H.A. & Fuchs, E. Hair follicle stem cells are specified and function in early skin morphogenesis. *Cell Stem Cell* **3**, 33-43 (2008).
279. Montgomery, R.K. & Breault, D.T. Small intestinal stem cell markers. *J Anat* **213**, 52-58 (2008).

280. Kim, C.F. Paving the road for lung stem cell biology: bronchioalveolar stem cells and other putative distal lung stem cells. *Am J Physiol Lung Cell Mol Physiol* **293**, L1092-1098 (2007).
281. Porat, Y., *et al.* Isolation of an adult blood-derived progenitor cell population capable of differentiation into angiogenic, myocardial and neural lineages. *Br J Haematol* **135**, 703-714 (2006).
282. Delo, D.M., De Coppi, P., Bartsch, G., Jr. & Atala, A. Amniotic fluid and placental stem cells. *Methods Enzymol* **419**, 426-438 (2006).
283. Fauza, D. Amniotic fluid and placental stem cells. *Best Pract Res Clin Obstet Gynaecol* **18**, 877-891 (2004).
284. Kaviani, A., *et al.* The placenta as a cell source in fetal tissue engineering. *J Pediatr Surg* **37**, 995-999; discussion 995-999 (2002).
285. Matikainen, T. & Laine, J. Placenta-an alternative source of stem cells. *Toxicol Appl Pharmacol* **207**, 544-549 (2005).
286. Coles, B.L., *et al.* Facile isolation and the characterization of human retinal stem cells. *Proc Natl Acad Sci U S A* **101**, 15772-15777 (2004).
287. Engelhardt, M., Bogdahn, U. & Aigner, L. Adult retinal pigment epithelium cells express neural progenitor properties and the neuronal precursor protein doublecortin. *Brain Res* **1040**, 98-111 (2005).
288. Toma, J.G., *et al.* Isolation of multipotent adult stem cells from the dermis of mammalian skin. *Nat Cell Biol* **3**, 778-784 (2001).
289. Carlin, R., Davis, D., Weiss, M., Schultz, B. & Troyer, D. Expression of early transcription factors Oct4, Sox2 and Nanog by porcine umbilical cord (PUC) matrix cells. *Reprod Biol Endocrinol* **4**, 8 (2006).
290. Wang, H.S., *et al.* Mesenchymal stem cells in the Wharton's jelly of the human umbilical cord. *Stem Cells* **22**, 1330-1337 (2004).
291. Alvarado-Moreno, A., Chavez-Gonzalez, A., Cerbulo, A., Arriaga, L. & Mayani, H. Cell cycle differences in vitro between primitive hematopoietic cell populations from adult and umbilical cord blood. *Stem Cells Dev* **16**, 223-230 (2007).
292. Aoki, M., Yasutake, M. & Murohara, T. Derivation of functional endothelial progenitor cells from human umbilical cord blood mononuclear cells isolated by a novel cell filtration device. *Stem Cells* **22**, 994-1002 (2004).
293. Cicuttini, F.M., Welch, K. & Boyd, A.W. Characterization of CD34+HLA-DR-CD38+ and CD34+HLA-DR-CD38- progenitor cells from human umbilical cord blood. *Growth Factors* **10**, 127-134 (1994).
294. Oka, M., *et al.* CD9 is associated with leukemia inhibitory factor-mediated maintenance of embryonic stem cells. *Mol Biol Cell* **13**, 1274-1281 (2002).
295. Viriyakosol, S., Mathison, J.C., Tobias, P.S. & Kirkland, T.N. Structure-function analysis of CD14 as a soluble receptor for lipopolysaccharide. *J Biol Chem* **275**, 3144-3149 (2000).
296. Gadhoum, S.Z. & Sackstein, R. CD15 expression in human myeloid cell differentiation is regulated by sialidase activity. *Nat Chem Biol* **4**, 751-757 (2008).
297. Jimenez-Marin, A., *et al.* Molecular cloning and characterization of the pig homologue to human CD29, the integrin beta1 subunit. *Transplantation* **70**, 649-655 (2000).
298. Herszfeld, D., *et al.* CD30 is a survival factor and a biomarker for transformed human pluripotent stem cells. *Nat Biotechnol* **24**, 351-357 (2006).

299. DeLisser, H.M., *et al.* Involvement of endothelial PECAM-1/CD31 in angiogenesis. *Am J Pathol* **151**, 671-677 (1997).
300. Steen, R., Tjonnfjord, G.E., Groseth, L.A. & Egeland, T. Characteristics of haemopoietic progenitor cells related to CD34 epitope class expression. *Eur J Haematol* **64**, 245-251 (2000).
301. Bourguignon, L.Y., Peyrollier, K., Xia, W. & Gilad, E. Hyaluronan-CD44 interaction activates stem cell marker Nanog, Stat-3-mediated MDR1 gene expression, and ankyrin-regulated multidrug efflux in breast and ovarian tumor cells. *J Biol Chem* **283**, 17635-17651 (2008).
302. Hermiston, M.L., Xu, Z. & Weiss, A. CD45: a critical regulator of signaling thresholds in immune cells. *Annu Rev Immunol* **21**, 107-137 (2003).
303. Kos, F.J. & Chin, C.S. Costimulation of T cell receptor-triggered IL-2 production by Jurkat T cells via fibroblast growth factor receptor 1 upon its engagement by CD56. *Immunol Cell Biol* **80**, 364-369 (2002).
304. Barry, F., Boynton, R., Murphy, M., Haynesworth, S. & Zaia, J. The SH-3 and SH-4 antibodies recognize distinct epitopes on CD73 from human mesenchymal stem cells. *Biochem Biophys Res Commun* **289**, 519-524 (2001).
305. Airas, L., Niemela, J. & Jalkanen, S. CD73 engagement promotes lymphocyte binding to endothelial cells via a lymphocyte function-associated antigen-1-dependent mechanism. *J Immunol* **165**, 5411-5417 (2000).
306. Klassen, H., Schwartz, M.R., Bailey, A.H. & Young, M.J. Surface markers expressed by multipotent human and mouse neural progenitor cells include tetraspanins and non-protein epitopes. *Neurosci Lett* **312**, 180-182 (2001).
307. Nakamura, Y., *et al.* Expression of CD90 on keratinocyte stem/progenitor cells. *Br J Dermatol* **154**, 1062-1070 (2006).
308. Cho, S.K., Bourdeau, A., Letarte, M. & Zuniga-Pflucker, J.C. Expression and function of CD105 during the onset of hematopoiesis from Flk1(+) precursors. *Blood* **98**, 3635-3642 (2001).
309. Fu, X., *et al.* Migration of bone marrow-derived mesenchymal stem cells induced by tumor necrosis factor-alpha and its possible role in wound healing. *Wound Repair Regen* **17**, 185-191 (2009).
310. Monsef, N., Soller, M., Isaksson, M., Abrahamsson, P.A. & Panagopoulos, I. The expression of pluripotency marker Oct 3/4 in prostate cancer and benign prostate hyperplasia. *Prostate* (2009).
311. Peh, G.S., Lang, R.J., Pera, M.F. & Hawes, S.M. CD133 expression by neural progenitors derived from human embryonic stem cells and its use for their prospective isolation. *Stem Cells Dev* **18**, 269-282 (2009).
312. Sorrentino, A., *et al.* Isolation and characterization of CD146+ multipotent mesenchymal stromal cells. *Exp Hematol* **36**, 1035-1046 (2008).
313. Varma, M.J., *et al.* Phenotypical and functional characterization of freshly isolated adipose tissue-derived stem cells. *Stem Cells Dev* **16**, 91-104 (2007).
314. Kim, J., *et al.* Ex vivo characteristics of human amniotic membrane-derived stem cells. *Cloning Stem Cells* **9**, 581-594 (2007).
315. De Meyer, S.F., Deckmyn, H. & Vanhoorelbeke, K. Von Willebrand factor to the rescue. *Blood* (2009).
316. Kumar, S., Coenen, M.J., Scherer, P.E. & Bahn, R.S. Evidence for enhanced adipogenesis in the orbits of patients with Graves' ophthalmopathy. *J Clin Endocrinol Metab* **89**, 930-935 (2004).

317. Rodriguez, A.M., *et al.* Adipocyte differentiation of multipotent cells established from human adipose tissue. *Biochem Biophys Res Commun* **315**, 255-263 (2004).
318. Ryden, M., *et al.* Functional characterization of human mesenchymal stem cell-derived adipocytes. *Biochem Biophys Res Commun* **311**, 391-397 (2003).
319. Zvonic, S., *et al.* Secretome of primary cultures of human adipose-derived stem cells: modulation of serpins by adipogenesis. *Mol Cell Proteomics* **6**, 18-28 (2007).
320. David, J.J., Tullu, M.S., Rathi, P., Sawalakhe, N. & Ghildiyal, R.G. Neonatal presentation of a rare metabolic liver disease. *Trop Gastroenterol* **29**, 229-231 (2008).
321. Jelliffe-Pawlowski, L.L., Walton-Haynes, L. & Currier, R.J. Identification of second trimester screen positive pregnancies at increased risk for congenital heart defects. *Prenat Diagn* (2009).
322. Kaibori, M., Matsui, K., Saito, T. & Kamiyama, Y. Risk factors for early death due to recurrence after resection of large hepatocellular carcinomas. *Hepatogastroenterology* **55**, 2151-2156 (2008).
323. Warren, M. & Karen, T.S. Two cases of primary yolk sac tumor of the liver in childhood; case reports and literature review. *Pediatr Dev Pathol*, 1 (2009).
324. Wu, F.X., *et al.* Identifying serological biomarkers of hepatocellular carcinoma using surface-enhanced laser desorption/ionization-time-of-flight mass spectroscopy. *Cancer Lett* (2009).
325. Cai, Y.F., Chen, J.S., Su, S.Y., Zhen, Z.J. & Chen, H.W. Passage of bone-marrow-derived liver stem cells in a proliferating culture system. *World J Gastroenterol* **15**, 1630-1635 (2009).
326. Barry, F., Boynton, R.E., Liu, B. & Murphy, J.M. Chondrogenic differentiation of mesenchymal stem cells from bone marrow: differentiation-dependent gene expression of matrix components. *Exp Cell Res* **268**, 189-200 (2001).
327. Chen, J.R., *et al.* Transplanted bone marrow stromal cells migrate, differentiate and improve motor function in rats with experimentally induced cerebral stroke. *J Anat* **213**, 249-258 (2008).
328. Yu, L.M., Wosnick, J.H. & Shoichet, M.S. Miniaturized system of neurotrophin patterning for guided regeneration. *J Neurosci Methods* **171**, 253-263 (2008).
329. Joe, P.A., Banerjee, A. & Luduena, R.F. The roles of cys124 and ser239 in the functional properties of human betaIII tubulin. *Cell Motil Cytoskeleton* **65**, 476-486 (2008).
330. Draberova, E., *et al.* Class III beta-tubulin is constitutively coexpressed with glial fibrillary acidic protein and nestin in midgestational human fetal astrocytes: implications for phenotypic identity. *J Neuropathol Exp Neurol* **67**, 341-354 (2008).
331. Bostrom, M., *et al.* Neural network and "ganglion" formations in vitro: a video microscopy and scanning electron microscopy study on adult cultured spiral ganglion cells. *Otol Neurotol* **28**, 1109-1119 (2007).
332. Ning, H., *et al.* Insulin growth factor signaling mediates neuron-like differentiation of adipose-tissue-derived stem cells. *Differentiation* **76**, 488-494 (2008).

333. Curran, J.M., Chen, R. & Hunt, J.A. Controlling the phenotype and function of mesenchymal stem cells in vitro by adhesion to silane-modified clean glass surfaces. *Biomaterials* **26**, 7057-7067 (2005).
334. Phillips, J.E., Guldberg, R.E. & Garcia, A.J. Dermal Fibroblasts Genetically Modified to Express Runx2/Cbfa1 as a Mineralizing Cell Source for Bone Tissue Engineering. *Tissue Eng* (2007).
335. Schutze, N., Noth, U., Schneidereit, J., Hendrich, C. & Jakob, F. Differential expression of CCN-family members in primary human bone marrow-derived mesenchymal stem cells during osteogenic, chondrogenic and adipogenic differentiation. *Cell Commun Signal* **3**, 5 (2005).
336. Isenmann, S., Cakouros, D., Zannettino, A., Shi, S. & Gronthos, S. hTERT transcription is repressed by Cbfa1 in human mesenchymal stem cell populations. *J Bone Miner Res* **22**, 897-906 (2007).
337. Pereira, R.C., Stadmeyer, L., Marciniak, S.J., Ron, D. & Canalis, E. C/EBP homologous protein is necessary for normal osteoblastic function. *J Cell Biochem* **97**, 633-640 (2006).
338. Heckmann, L., *et al.* Human mesenchymal progenitor cell responses to a novel textured poly(L-lactide) scaffold for ligament tissue engineering. *J Biomed Mater Res B Appl Biomater* **81**, 82-90 (2007).
339. Wei, Y., Hu, Y., Lv, R. & Li, D. Regulation of adipose-derived adult stem cells differentiating into chondrocytes with the use of rhBMP-2. *Cytotherapy* **8**, 570-579 (2006).
340. Lee, J.W., Kim, Y.H., Kim, S.H., Han, S.H. & Hahn, S.B. Chondrogenic differentiation of mesenchymal stem cells and its clinical applications. *Yonsei Med J* **45 Suppl**, 41-47 (2004).
341. Raghunath, J., *et al.* Chondrogenic potential of blood-acquired mesenchymal progenitor cells. *J Plast Reconstr Aesthet Surg* (2009).
342. Shoulders, M.D. & Raines, R.T. Collagen Structure and Stability. *Annu Rev Biochem* (2009).
343. Li, J., *et al.* A minimal common osteochondrocytic differentiation media for the osteogenic and chondrogenic differentiation of bone marrow stromal cells in the construction of osteochondral graft. *Tissue Eng Part A* (2009).
344. Strizzi, L., Bianco, C., Normanno, N. & Salomon, D. Cripto-1: a multifunctional modulator during embryogenesis and oncogenesis. *Oncogene* **24**, 5731-5741 (2005).
345. Guo, G., *et al.* Klf4 reverts developmentally programmed restriction of ground state pluripotency. *Development* **136**, 1063-1069 (2009).
346. Park, I.H. & Daley, G.Q. Human iPS cell derivation/reprogramming. *Curr Protoc Stem Cell Biol* **Chapter 4**, Unit 4A 1 (2009).
347. Levin, B.E. Synergy of nature and nurture in the development of childhood obesity. *Int J Obes (Lond)* **33 Suppl 1**, S53-56 (2009).
348. Ziylan, Y.Z., Baltaci, A.K. & Mogulkoc, R. Leptin transport in the central nervous system. *Cell Biochem Funct* **27**, 63-70 (2009).
349. Villanueva, E.C. & Myers, M.G., Jr. Leptin receptor signaling and the regulation of mammalian physiology. *Int J Obes (Lond)* **32 Suppl 7**, S8-12 (2008).
350. Fantuzzi, G. Three questions about leptin and immunity. *Brain Behav Immun* **23**, 405-410 (2009).
351. Park, H.Y. & Gilchrest, B.A. More on MITF. *J Invest Dermatol* **119**, 1218-1219 (2002).

352. Tsukiji, N., *et al.* Mitf functions as an in ovo regulator for cell differentiation and proliferation during development of the chick RPE. *Dev Biol* **326**, 335-346 (2009).
353. Covaceuszach, S., *et al.* Development of a non invasive NGF-based therapy for Alzheimer's disease. *Curr Alzheimer Res* **6**, 158-170 (2009).
354. Nomura, J., *et al.* Differential Requirement for Nucleostemin in Embryonic Stem Cell and Neural Stem Cell Viability. *Stem Cells* **27**, 1066-1076 (2009).
355. Ma, H. & Pederson, T. Nucleostemin: a multiplex regulator of cell-cycle progression. *Trends Cell Biol* **18**, 575-579 (2008).
356. Ma, H. & Pederson, T. Depletion of the nucleolar protein nucleostemin causes G1 cell cycle arrest via the p53 pathway. *Mol Biol Cell* **18**, 2630-2635 (2007).
357. Prusa, A.R., Marton, E., Rosner, M., Bernaschek, G. & Hengstschlager, M. Oct-4-expressing cells in human amniotic fluid: a new source for stem cell research? *Hum Reprod* **18**, 1489-1493 (2003).
358. Lee, N.K., *et al.* Endocrine regulation of energy metabolism by the skeleton. *Cell* **130**, 456-469 (2007).
359. Furuno, T. & Nakanishi, M. Neurotrophic factors increase tumor necrosis factor-alpha-induced nuclear translocation of NF-kappaB in rat PC12 cells. *Neurosci Lett* **392**, 240-244 (2006).
360. Burke, M.A. & Bothwell, M. p75 neurotrophin receptor mediates neurotrophin activation of NF-kappa B and induction of iNOS expression in P19 neurons. *J Neurobiol* **55**, 191-203 (2003).
361. Hamanoue, M., *et al.* p75-mediated NF-kappaB activation enhances the survival response of developing sensory neurons to nerve growth factor. *Mol Cell Neurosci* **14**, 28-40 (1999).
362. Cragnolini, A.B., Huang, Y., Gokina, P. & Friedman, W.J. Nerve growth factor attenuates proliferation of astrocytes via the p75 neurotrophin receptor. *Glia* (2009).
363. Cvekl, A. & Duncan, M.K. Genetic and epigenetic mechanisms of gene regulation during lens development. *Prog Retin Eye Res* **26**, 555-597 (2007).
364. Liu, W., Lagutin, O.V., Mende, M., Streit, A. & Oliver, G. Six3 activation of Pax6 expression is essential for mammalian lens induction and specification. *EMBO J* **25**, 5383-5395 (2006).
365. Brasaemle, D.L., *et al.* Perilipin A increases triacylglycerol storage by decreasing the rate of triacylglycerol hydrolysis. *J Biol Chem* **275**, 38486-38493 (2000).
366. Bruce, A.W., *et al.* Genome-wide analysis of repressor element 1 silencing transcription factor/neuron-restrictive silencing factor (REST/NRSF) target genes. *Proc Natl Acad Sci U S A* **101**, 10458-10463 (2004).
367. Pinnoji, R.C., *et al.* Repressor element-1 silencing transcription factor/neuronal restrictive silencer factor (REST/NRSF) can regulate HSV-1 immediate-early transcription via histone modification. *Virol J* **4**, 56 (2007).
368. Tabuchi, A., *et al.* REST4-mediated modulation of REST/NRSF-silencing function during BDNF gene promoter activation. *Biochem Biophys Res Commun* **290**, 415-420 (2002).
369. Caddick, J., Kingham, P.J., Gardiner, N.J., Wiberg, M. & Terenghi, G. Phenotypic and functional characteristics of mesenchymal stem cells differentiated along a Schwann cell lineage. *Glia* **54**, 840-849 (2006).

370. Hachem, S., *et al.* Spatial and temporal expression of S100B in cells of oligodendrocyte lineage. *Glia* **51**, 81-97 (2005).
371. Zimmer, D.B., Cornwall, E.H., Landar, A. & Song, W. The S100 protein family: history, function, and expression. *Brain Res Bull* **37**, 417-429 (1995).
372. Katoh, Y. & Katoh, M. Comparative genomics on SOX2 orthologs. *Oncol Rep* **14**, 797-800 (2005).
373. Rodda, D.J., *et al.* Transcriptional regulation of nanog by OCT4 and SOX2. *J Biol Chem* **280**, 24731-24737 (2005).
374. Stadtfeld, M., Brennand, K. & Hochedlinger, K. Reprogramming of pancreatic beta cells into induced pluripotent stem cells. *Curr Biol* **18**, 890-894 (2008).
375. Stadtfeld, M., Maherali, N., Breault, D.T. & Hochedlinger, K. Defining molecular cornerstones during fibroblast to iPS cell reprogramming in mouse. *Cell Stem Cell* **2**, 230-240 (2008).
376. Uchikawa, M., Ishida, Y., Takemoto, T., Kamachi, Y. & Kondoh, H. Functional analysis of chicken Sox2 enhancers highlights an array of diverse regulatory elements that are conserved in mammals. *Dev Cell* **4**, 509-519 (2003).
377. Gronthos, S., *et al.* Differential cell surface expression of the STRO-1 and alkaline phosphatase antigens on discrete developmental stages in primary cultures of human bone cells. *J Bone Miner Res* **14**, 47-56 (1999).
378. Tuli, R., *et al.* Characterization of multipotential mesenchymal progenitor cells derived from human trabecular bone. *Stem Cells* **21**, 681-693 (2003).
379. Brown, S.M., Lamberts, D.W., Reid, T.W., Nishida, T. & Murphy, C.J. Neurotrophic and anhidrotic keratopathy treated with substance P and insulinlike growth factor 1. *Arch Ophthalmol* **115**, 926-927 (1997).
380. Reid, T.W., Murphy, C.J., Iwahashi, C.K., Foster, B.A. & Mannis, M.J. Stimulation of epithelial cell growth by the neuropeptide substance P. *J Cell Biochem* **52**, 476-485 (1993).
381. Cho, K.J., *et al.* Neurons derived from human mesenchymal stem cells show synaptic transmission and can be induced to produce the neurotransmitter substance P by interleukin-1 alpha. *Stem Cells* **23**, 383-391 (2005).
382. Millward-Sadler, S.J., *et al.* Tachykinin expression in cartilage and function in human articular chondrocyte mechanotransduction. *Arthritis Rheum* **48**, 146-156 (2003).
383. Tarsa, L. & Goda, Y. Synaptophysin regulates activity-dependent synapse formation in cultured hippocampal neurons. *Proc Natl Acad Sci U S A* **99**, 1012-1016 (2002).
384. Hodge, R.D., *et al.* Intermediate progenitors in adult hippocampal neurogenesis: Tbr2 expression and coordinate regulation of neuronal output. *J Neurosci* **28**, 3707-3717 (2008).
385. Bach, T.L., Barsigian, C., Yaen, C.H. & Martinez, J. Endothelial cell VE-cadherin functions as a receptor for the beta15-42 sequence of fibrin. *J Biol Chem* **273**, 30719-30728 (1998).
386. Ali, F.R., Haddley, K. & Quinn, J.P. Assessing the impact of genetic variation on transcriptional regulation in vitro. *Methods Mol Biol* **628**, 195-214.
387. Alhadlaq, A. & Mao, J.J. Mesenchymal stem cells: isolation and therapeutics. *Stem Cells Dev* **13**, 436-448 (2004).

388. Arthur, A., Zannettino, A. & Gronthos, S. The therapeutic applications of multipotential mesenchymal/stromal stem cells in skeletal tissue repair. *J Cell Physiol* (2008).
389. Barry, F.P. & Murphy, J.M. Mesenchymal stem cells: clinical applications and biological characterization. *Int J Biochem Cell Biol* **36**, 568-584 (2004).
390. Grayson, W.L., Zhao, F., Izadpanah, R., Bunnell, B. & Ma, T. Effects of hypoxia on human mesenchymal stem cell expansion and plasticity in 3D constructs. *J Cell Physiol* **207**, 331-339 (2006).
391. Neuhuber, B., Swanger, S.A., Howard, L., Mackay, A. & Fischer, I. Effects of plating density and culture time on bone marrow stromal cell characteristics. *Exp Hematol* **36**, 1176-1185 (2008).
392. Bensidhoum, M., *et al.* Homing of in vitro expanded Stro-1- or Stro-1+ human mesenchymal stem cells into the NOD/SCID mouse and their role in supporting human CD34 cell engraftment. Vol. 103 3313-3319 (2004).
393. Beyer Nardi, N. & da Silva Meirelles, L. Mesenchymal stem cells: isolation, in vitro expansion and characterization. *Handb Exp Pharmacol*, 249-282 (2006).
394. Rhodes, N.P., Shortland, A.P., Rattray, A. & Williams, D.F. Platelet reactions to modified surfaces under dynamic conditions. *J Mater Sci Mater Med* **9**, 767-772 (1998).
395. Hayflick, L. The Limited in Vitro Lifetime of Human Diploid Cell Strains. *Exp Cell Res* **37**, 614-636 (1965).
396. Asahara, T., *et al.* Isolation of putative progenitor endothelial cells for angiogenesis. *Science* **275**, 964-967 (1997).
397. Kalka, C., *et al.* Transplantation of ex vivo expanded endothelial progenitor cells for therapeutic neovascularization. *Proc Natl Acad Sci U S A* **97**, 3422-3427 (2000).
398. Kawamoto, A., *et al.* Intramyocardial transplantation of autologous endothelial progenitor cells for therapeutic neovascularization of myocardial ischemia. *Circulation* **107**, 461-468 (2003).
399. Harraz, M., Jiao, C., Hanlon, H.D., Hartley, R.S. & Schatteman, G.C. CD34-blood-derived human endothelial cell progenitors. *Stem Cells* **19**, 304-312 (2001).
400. Nakul-Aquaronne, D., Bayle, J. & Frelin, C. Coexpression of endothelial markers and CD14 by cytokine mobilized CD34+ cells under angiogenic stimulation. *Cardiovasc Res* **57**, 816-823 (2003).
401. Lin, Y., Weisdorf, D.J., Solovey, A. & Hebbel, R.P. Origins of circulating endothelial cells and endothelial outgrowth from blood. *J Clin Invest* **105**, 71-77 (2000).
402. Gulati, R., *et al.* Diverse origin and function of cells with endothelial phenotype obtained from adult human blood. *Circ Res* **93**, 1023-1025 (2003).
403. Zhang, S.J., *et al.* Adult endothelial progenitor cells from human peripheral blood maintain monocyte/macrophage function throughout in vitro culture. *Cell Res* **16**, 577-584 (2006).
404. Cesselli, D., *et al.* Multipotent progenitor cells are present in human peripheral blood. *Circ Res* **104**, 1225-1234 (2009).
405. Kliman, H.J. The placenta revealed. *Am J Pathol* **143**, 332-336 (1993).
406. Kobayashi, K., Kubota, T. & Aso, T. Study on myofibroblast differentiation in the stromal cells of Wharton's jelly: expression and localization of alpha-smooth muscle actin. *Early Hum Dev* **51**, 223-233 (1998).

407. Schroder, J. Fetal cells in the blood of pregnant mothers. *J Med Genet* **18**, 321-322 (1981).
408. Kang, X.Q., *et al.* Differentiating characterization of human umbilical cord blood-derived mesenchymal stem cells in vitro. *Cell Biol Int* **30**, 569-575 (2006).
409. Kern, S., Eichler, H., Stoeve, J., Kluter, H. & Bieback, K. Comparative analysis of mesenchymal stem cells from bone marrow, umbilical cord blood, or adipose tissue. *Stem Cells* **24**, 1294-1301 (2006).
410. Romanov, Y.A., Svintsitskaya, V.A. & Smirnov, V.N. Searching for alternative sources of postnatal human mesenchymal stem cells: candidate MSC-like cells from umbilical cord. *Stem Cells* **21**, 105-110 (2003).
411. Weiss, M.L. & Troyer, D.L. Stem cells in the umbilical cord. *Stem Cell Rev* **2**, 155-162 (2006).
412. Cho, S.W., *et al.* Lineage of non-cranial neural crest cell in the dental mesenchyme: using a lacZ reporter gene during early tooth development. *J Electron Microsc (Tokyo)* **52**, 567-571 (2003).
413. Chai, Y., *et al.* Fate of the mammalian cranial neural crest during tooth and mandibular morphogenesis. *Development* **127**, 1671-1679 (2000).
414. Miletich, I. & Sharpe, P.T. Neural crest contribution to mammalian tooth formation. *Birth Defects Res C Embryo Today* **72**, 200-212 (2004).
415. Yoon, Y.S., Park, J.S., Tkebuchava, T., Luedeman, C. & Losordo, D.W. Unexpected severe calcification after transplantation of bone marrow cells in acute myocardial infarction. *Circulation* **109**, 3154-3157 (2004).
416. Orphanides, G., Lagrange, T. & Reinberg, D. The general transcription factors of RNA polymerase II. *Genes Dev* **10**, 2657-2683 (1996).
417. MacKenzie, A. & Quinn, J.P. Post-genomic approaches to exploring neuropeptide gene mis-expression in disease. *Neuropeptides* **38**, 1-15 (2004).
418. Guindalini, C., *et al.* A dopamine transporter gene functional variant associated with cocaine abuse in a Brazilian sample. *Proc Natl Acad Sci U S A* **103**, 4552-4557 (2006).
419. Gomez-Lira, M., *et al.* Mutations in the SPINK1 gene in idiopathic pancreatitis Italian patients. *Eur J Hum Genet* **11**, 543-546 (2003).
420. Atiar Rahman, M., *et al.* Proteome analysis for 3T3-L1 adipocyte differentiation. *J Microbiol Biotechnol* **18**, 1895-1902 (2008).
421. Charriere, G., *et al.* Preadipocyte conversion to macrophage. Evidence of plasticity. *J Biol Chem* **278**, 9850-9855 (2003).
422. Moon, Y.S., *et al.* Mice lacking paternally expressed Pref-1/Dlk1 display growth retardation and accelerated adiposity. *Mol Cell Biol* **22**, 5585-5592 (2002).
423. Suslov, O.N., Kukekov, V.G., Ignatova, T.N. & Steindler, D.A. Neural stem cell heterogeneity demonstrated by molecular phenotyping of clonal neurospheres. *Proc Natl Acad Sci U S A* **99**, 14506-14511 (2002).
424. Loeffler, M. & Roeder, I. Tissue stem cells: definition, plasticity, heterogeneity, self-organization and models--a conceptual approach. *Cells Tissues Organs* **171**, 8-26 (2002).